



Morgan, Timaeus Edmund Francis (2019) *Molecular probes for understanding disease using PET and fluorescence imaging*. PhD thesis.

<http://theses.gla.ac.uk/76760/>

Copyright and moral rights for this work are retained by the author

A copy can be downloaded for personal non-commercial research or study, without prior permission or charge

This work cannot be reproduced or quoted extensively from without first obtaining permission in writing from the author

The content must not be changed in any way or sold commercially in any format or medium without the formal permission of the author

When referring to this work, full bibliographic details including the author, title, awarding institution and date of the thesis must be given

Enlighten: Theses

<https://theses.gla.ac.uk/>  
[research-enlighten@glasgow.ac.uk](mailto:research-enlighten@glasgow.ac.uk)

# **Molecular Probes for Understanding Disease Using PET and Fluorescence Imaging**

**Timaeus E. F. Morgan MChem**

A thesis submitted in part fulfilment of the requirements of the  
degree of Doctor of Philosophy



**University  
of Glasgow**

School of Chemistry

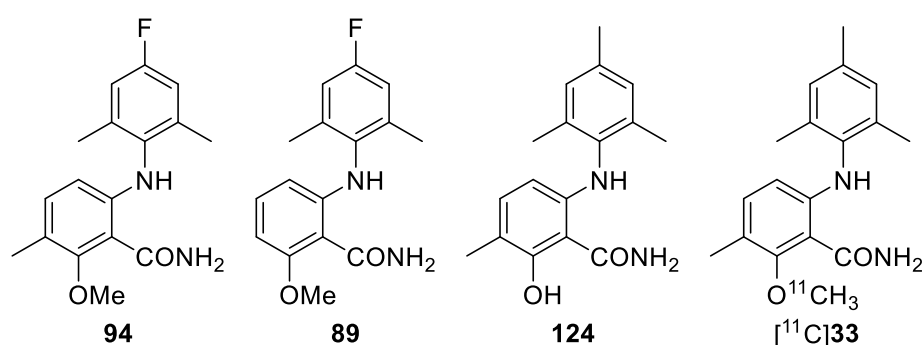
College of Science & Engineering

University of Glasgow

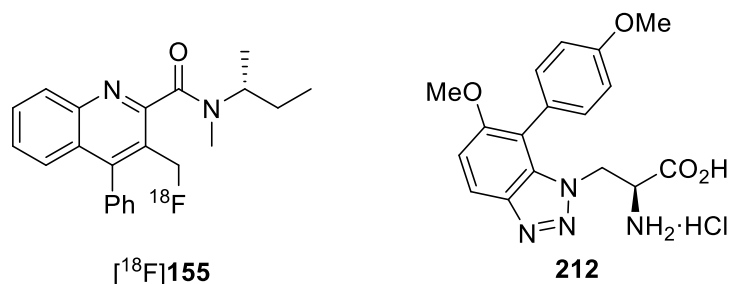
September 2019

## Abstract

During the course of this PhD, several libraries of potential PET imaging agents were synthesised for testing their affinity and selectivity for sphingosine-1-phosphate 5 receptors (S1P<sub>5</sub>). These receptors are located within oligodendrocytes and are proposed to have a major role in the re-myelination of neurons. Imaging of these receptors could lead to new treatments and diagnostic tools for the management of demyelinating disorders, such as multiple sclerosis (MS). The libraries of compounds were subject to biological evaluation and two lead compounds, fluorobenzamides **89** and **94**, were identified as being the most potent and selective for S1P<sub>5</sub> receptors. The synthesis of a further compound that was described in the literature as having high affinity for S1P<sub>5</sub> was adapted to allow for the preparation of precursor **124** for <sup>11</sup>C-labelling. The radiosynthesis of compound [<sup>11</sup>C]**33** was then optimised.



An improved synthesis of AB5186, an imaging agent for the translocator protein (TSPO), was developed. TSPO has been shown to be involved in inflammatory processes and is a biomarker for many inflammatory diseases. Evaluation of AB5186 led to the synthesis of a higher affinity compound LW223 (**155**), which was not sensitive to the single nucleotide polymorphism present in TSPO. A synthesis of LW223 (**155**) was developed that allowed for the production of two potential precursors for radiofluorination. Investigation of the radiochemistry showed a chloro-precursor was the most efficient for <sup>18</sup>F-labelling.



Finally, an investigation into a polymer-supported nitrite reagent approach for the synthesis of benzotriazole derived  $\alpha$ -amino acids allowed the preparation of a variety of functionalised compounds in relatively few steps. Further derivatisation of these compounds led to the discovery of a benzotriazole derived  $\alpha$ -amino acid **212** with strong fluorescence in the visible region.

# Table of Contents

Abstract .....	1
Table of Contents .....	2
Acknowledgements.....	4
Author's Declaration .....	6
Abbreviations.....	7
1 Introduction .....	12
1.1 Molecular Imaging .....	12
1.2 Positron Emission Tomography .....	12
1.2.1 Principles of Positron Emission Tomography.....	12
1.2.2 Types of PET Imaging Systems.....	14
1.2.3 Radionuclides Used in PET Imaging.....	15
1.2.4 Production of Radionuclides .....	17
1.2.5 Radiolabelling Methods .....	19
1.2.6 Clinical Applications of Radiotracers.....	27
1.3 Sphingosine-1-Phosphate 5 Receptor (S1P <sub>5</sub> ).....	31
1.3.1 Multiple Sclerosis.....	31
1.3.2 Sphingosine-1-Phosphate Receptors .....	33
1.3.3 S1P Receptor Agonists.....	33
1.3.4 S1P Receptor Imaging Using PET.....	36
1.4 The Translocator Protein (TSPO) .....	38
1.4.1 Function and Distribution of TSPO.....	38
1.4.2 Imaging agents for TSPO .....	39
2 Results and Discussion.....	42
2.1 New Selective PET Imaging Agents for the .....	42
Sphingosine-1-Phosphate 5 Receptor .....	42
2.1.1 Project Aims .....	42
2.1.2 Synthesis of Fluoro-Benzamide Library .....	43
2.1.3 Synthesis of 3-Substituted Benzamide Library.....	55
2.1.4 Synthesis of Fluorophthalazinone Library .....	58
2.1.5 Investigation of Physicochemical Properties .....	62
2.1.6 Synthesis of a Carbon-11 Precursor .....	69
2.1.7 Radiochemistry.....	75
2.1.8 Biological Evaluation .....	80
2.1.9 Lead Compound Fluorination.....	88
2.1.10 Conclusions.....	92
2.1.11 Future Work.....	93

2.2	Synthesis of LW223: A PET Imaging Agent for TSPO .....	95
2.2.1	Project Aims .....	95
2.2.2	Synthesis and Evaluation of AB5186 .....	96
2.2.3	Synthesis and Evaluation of LW223 .....	101
2.2.4	Radiosynthesis of [ <sup>18</sup> F]LW223 .....	115
2.2.5	Preclinical Studies .....	120
2.2.6	Conclusions .....	121
2.2.7	Future Work .....	122
2.3	Novel Benzotriazole Derived $\alpha$ -Amino Acids .....	123
2.3.1	Project Aims .....	123
2.3.2	Synthesis of Benzotriazole Derived $\alpha$ -Amino Acids .....	124
2.3.3	Further Functionalisation and Analysis .....	132
2.3.4	Synthesis of More Conjugated Benzotriazole $\alpha$ -Amino Acids .....	135
2.3.5	Conclusions .....	143
2.3.6	Future work .....	144
3	Experimental .....	146
3.1	General .....	146
3.2	S1P <sub>5</sub> Experimental .....	146
3.3	HPLC Methods for Physicochemical Analysis .....	199
3.4	Procedure for the [ <sup>35</sup> S]GTP $\gamma$ S Binding Assay .....	202
3.5	TSPO Experimental .....	203
3.6	Benzotriazoles Experimental .....	220
4	References .....	244
	Appendix I .....	260
	Appendix II .....	261
	Appendix III .....	262

## Acknowledgements

First and foremost, I must thank my supervisor Dr Andy Sutherland for allowing me to undertake a PhD in his group. I can't imagine the pain I've put him through these past four years, but his assistance has always been abundant and valuable. I couldn't have had a more helpful supervisor. I would not be in this position if it wasn't for my beautiful wife Poppy who has always been my cheerleader. I couldn't have got this far if it wasn't for her patience and kindness. I owe so much to my own parents for encouraging my education and also to my brother Dewi for reminding me there are always other things to do!

I would like to thank all of the technical staff in the Joseph Black Building for their assistance throughout my PhD studies. Frank McGeoch has been fantastic and was always there to help before you even knew you needed it. A big thanks to Jim and Andy (MS), David Adam (NMR) and everyone at stores, not least to Ted. Thank you to Stuart and Arlene in IT for keeping my computer ticking over and to Claire Wilson for the crystallography studies. I owe a debt of gratitude to everyone over at Glasgow PET Centre, but especially to Dmitry for his ever enthusiastic and positive attitude that I can only hope has rubbed-off at least a little bit. A big thanks to Sue and Gavin for their continued assistance in all things radiochemistry.

It can be difficult starting a new job, but everyone in the PET is Wonderful (PiW) group have been so welcoming and appreciative of the task ahead of me. Thank you Adriana for help with the biology and for your assistance in my first few month in Edinburgh. A huge thanks to Wendy for the talks about physics and for the diagrams and also to Mark who has been invaluable for helping with biology and for providing figures.

Everybody in the Sutherland group has been so much fun to work with over the last few years, especially Jonathan. There are too many now to mention all by name, but everybody has helped me one way or another over the course of my PhD. Réka and Jonathan were the best students to start off my PhD with and how could we forget sweet Mr Martyn! Five o'clock prog will always be a fond memory. I miss the mid-week trips to the pub with Kerry, followed by the inevitable spicy grill, but my health probably doesn't. Nikki and Alex were always happy to help from my first day and Holly and Mohamed have made worthy fumehood buddies. Huge thanks also to my Masters student Emma for her work on the S1P project, Ned for his pioneering work on the benzotriazole project and to Lewis Williams for his assistance on the TSPO project.

I must thank the whole of the Loudon lab and Hartley group, not least BSL, but also to Stuart for sharing wisdom beyond his years. The Neurosciences Foundation and the EPSRC are gratefully acknowledged for their funding and support.

It is no exaggeration that my proudest achievement has been the establishment of Milk Club. There was much hardship, but we persevered. My years in charge have been some of the best of my life, but now I leave it in the capable hands of Martyn and I can finally retire. *Ab ubere bonum est*; may it live for another thousand years.

## Author's Declaration

I declare that, except where explicit reference is made to the contribution of others, this thesis represents the original work of Timaeus E. F. Morgan and has not been submitted for any other degree at the University of Glasgow or any other institution. The research was carried out at the University of Glasgow in the Loudon Laboratory under the supervision of Dr Andrew Sutherland between October 2015 to April 2019. Aspects of the work described herein have been published elsewhere as listed below.

M. G. MacAskill, T. Walton, L. Williams, T. E. F. Morgan, C. J. Alcaide-Corral, M. R. Dweck, G. A. Gray, D. E. Newby, C. Lucatelli, A. Sutherland, S. L. Pimlott and A. A. S. Tavares, *PLOS ONE*, 2019, **14**, e0217515.

J. D. Bell, T. E. F. Morgan, N. Buijs, A. H. Harkiss, C. R. Wellaway and A. Sutherland, *J. Org. Chem.*, 2019, **84**, 10436–10448.

## Abbreviations

Ac	Acetyl
AD	Alzheimer's disease
AHCN	1,1'-Azobis(cyclohexanecarbonitrile)
AIBN	Azobisisobutyronitrile
$A_m$	Molar activity
Ar	Aromatic
$A_s$	Specific activity
BBB	Blood-brain barrier
Bn	Benzyl
br	Broad
Bt	Benzotriazole
Cbz	Carboxybenzyl
CI	Chemical ionisation
CNS	Central nervous system
CT	Computed tomography
dba	Dibenzylideneacetone
dppf	1,1'-Bis(diphenylphosphino)ferrocene
CDMT	2-Chloro-4,6-dimethoxy-1,3,5-triazine
COSY	Correlated spectroscopy
Cy	Cyclohexyl
d	Doublet
DEPT	Distortionless enhancement polarisation transfer
DIPEA	Diisopropylethylamine
DMAP	4-Dimethylaminopyridine
DMF	Dimethylformamide
DMSO	Dimethyl sulfoxide
DMTMM	4-(4,6-Dimethoxy-1,3,5-triazin-2-yl)-4-methylmorpholinium chloride
DTBZ	Dihydrotetrabenazine

EC <sub>50</sub>	Half maximal effective concentration
EI	Electron impact
ESI	Electrospray ionisation
Et	Ethyl
FDG	Fluorodeoxyglucose
FOV	Field of view
g	Grams
GBq	Gigabecquerel
GDP	Guanosine diphosphate
GM	Geiger-Muller
GPCR	G protein coupled receptor
GTP	Guanosine triphosphate
h	Hour
HAB	High affinity binders
HBTU	O-(Benzotriazol-1-yl)-N,N,N',N'-tetramethyluronium hexafluorophosphate
HPLC	High performance liquid chromatography
HSA	Human serum albumin
HSQC	Heteronuclear single quantum coherence
Hz	Hertz
IAM	Immobilised artificial membrane
<sup>i</sup> Bu	Isobutyl
<sup>i</sup> Pr	Isopropyl
K <sub>222</sub>	Kryptofix <sup>®</sup> 222
K <sub>m</sub>	Membrane partition coefficient
LAB	Low affinity binders
LAH	Lithium aluminium hydride
LDA	Lithium diisopropylamide
LiHMDS	Lithium hexamethyldisilazide
lit.	Literature

Log <i>P</i>	Partition coefficient
LOR	Line of response
M	Molar
m	Multiplet
<i>m</i> -	<i>meta</i>
MAB	Mixed affinity binders
MBq	Megabecquerels
<i>m</i> -CPBA	<i>meta</i> -Chloroperoxybenzoic acid
mCRPC	Metastatic castration resistant prostate cancer
Me	Methyl
MeCN	Acetonitrile
MeV	Megaelectronvolts
min	Minutes
mL	Millilitres
MMI	Multi-modality imaging
Mol	Moles
MOM	Methoxymethyl
Mp	Melting point
MRI	Magnetic resonance imaging
MS	Multiple Sclerosis
Ms	Mesyl
<i>m/z</i>	Mass to charge ratio
NBS	<i>N</i> -Bromosuccinimide
<sup>n</sup> Bu	<i>n</i> -Butyl
NCS	<i>N</i> -Chlorosuccinimide
NIS	<i>N</i> -Iodosuccinimide
NMM	<i>N</i> -Methylmorpholine
NMR	Nuclear magnetic resonance
NOE	Nuclear Overhauser effect
NOTA	2-[4,7-Bis(carboxymethyl)-1,4,7-triazonan-1-yl]acetic acid

<i>o</i> -	<i>ortho</i>
<i>p</i> -	<i>para</i>
PBR	Peripheral benzodiazepine receptor
PBS	Phosphate-buffered saline
PET	Positron emission tomography
Ph	Phenyl
PhMe	Toluene
PiB	Pittsburgh compound B
Pin	Pinacol
$P_m$	Permeability
PMB	<i>para</i> -Methoxybenzyl
PPA	Polyphosphoric acid
PPB	Plasma protein binding
RCY	Radiochemical yield
rt	Room temperature
s	Singlet
SAR	Structure activity relationship
sept	Septet
$S_NAr$	Nucleophilic aromatic substitution
SPE	Solid-phase extraction
SPECT	Single-photon emission computed tomography
SphK2	Sphingosine kinase 2
S1P	Sphingosine-1-phosphate
t	Triplet
TBAF	Tetra- <i>n</i> -butylammonium fluoride
TBAOH	Tetra- <i>n</i> -butylammonium hydroxide
TBDMS	<i>tert</i> -Butyldimethylsilyl
Tf	Triflyl
TFA	Trifluoroacetic acid
THF	Tetrahydrofuran

TLC	Thin-layer chromatography
TMS	Trimethylsilyl
Ts	Tosyl
TSPO	Translocator protein
UV	Ultraviolet
VMAT2	Vesicular monoamine transporter 2
°C	Degrees centigrade
Δ	Reflux

# 1 Introduction

## 1.1 Molecular Imaging

Molecular imaging describes a wide range of medical imaging techniques including magnetic resonance imaging (MRI), optical imaging and nuclear imaging. These techniques provide different methods to produce an image: magnetism, sound, and in the case of nuclear imaging, radiolabelled molecules that decay to produce signals. The term molecular imaging is often broadly used and can be interpreted in one of two ways: imaging using molecules or the imaging of molecules.<sup>1</sup> A more precise definition would be the non-invasive visualisation and measurement of *in vivo* biological processes at the cellular and molecular level *via* specific imaging probes.<sup>2</sup>

Molecular imaging has the ability to produce 'real time' images, useful for monitoring the progression of disease or for measuring the efficacy of a drug. Nuclear imaging approaches, such as positron emission tomography (PET) and single photon emission computed tomography (SPECT) are the most sensitive techniques used for molecular imaging and benefit from an unlimited depth penetration.<sup>3</sup> These methods require the use of a radiolabelled molecule to measure the *in vivo* distribution of a radiotracer *via* the external detection of high energy light in the form of gamma radiation from the decay of the radionuclide.

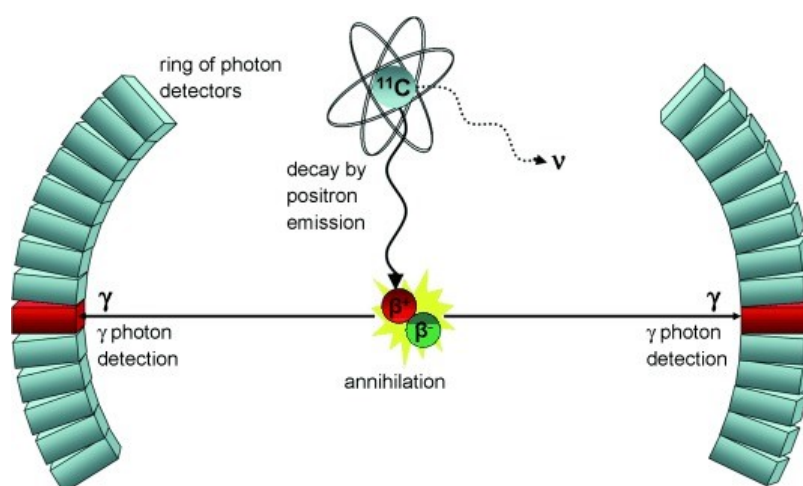
In planar imaging, the radiation from a patient is collected and the data shown as if the radiation had been emitted from a single plane.<sup>3</sup> However, contrast of the image is reduced and images of interest at a particular depth are obscured by images above and below that area. Computed tomography overcomes this problem by using mathematical algorithms to convert the data; the term tomography is used to describe the image of a slice and so a tomographic image is a two-dimensional representation of an image within a particular plane of a three-dimensional object.

## 1.2 Positron Emission Tomography

### 1.2.1 Principles of Positron Emission Tomography

PET is a nuclear medicine imaging technology that is based on the positron decay process.<sup>4</sup> This type of radioactive decay occurs in radionuclides that have an excess of protons: the nucleus becomes more stable by the transformation of a proton into a neutron through the loss of an anti-electron called a positron ( $\beta^+$ ) and a neutrino ( $\nu$ ). A consequence of the matter-antimatter relationship between the positron and the electron

is that the emitted positron will soon encounter an 'ordinary' electron. On emission from the nucleus, the positron travels a short distance in the surrounding tissue, expending its kinetic energy in inelastic collisions, before annihilating by combining with an electron.<sup>4</sup> This distance travelled is referred to as the positron range. After annihilation, 511 keV of energy for each particle in the form of gamma radiation is released. The two gamma rays are equal in energy and emitted simultaneously in opposite directions. The PET apparatus utilises this decay process by injecting a patient with a radioactive tracer and surrounding them with a ring of scintillations detectors (Figure 1). These detectors have the ability to absorb the incoming photons and convert the energy into an electric signal. When simultaneous arrival of gamma rays is detected, the point of origin of this annihilation is assumed to lie on a line connecting the two signals, known as the line of response (LOR). Measurements of multiple sets of LORs allow for reconstruction of an image showing the distribution of the radionuclide.<sup>5</sup>

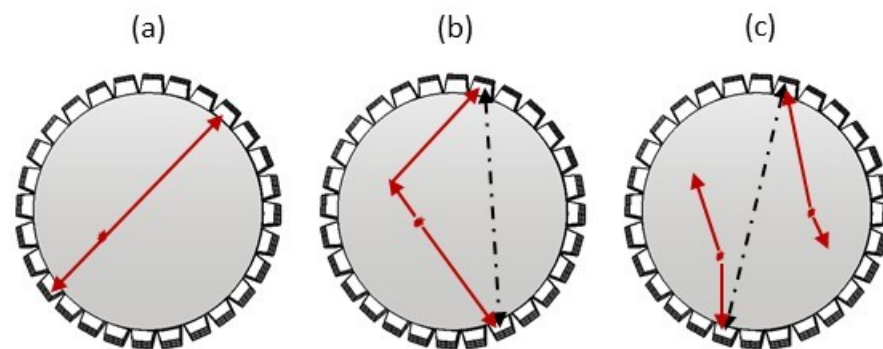


**Figure 1: Positron decay and annihilation processes in PET**

(Reprinted with permission from *Angew. Chem. Int. Ed.*, 2008, **47**, 8998–9033. Copyright 2008 John Wiley and Sons)<sup>6</sup>

A major challenge in the reconstruction of the PET image is the location of the origin of decay. Two fundamental sources of error exist.<sup>5</sup> The first is that the reconstructed image is based on the location of the positronium ( $\beta^+ - \beta^-$  complex) and, thus, does not take into account the positron range. The second is that, depending on the energy of the positron upon annihilation, the two gamma rays emitted will not be exactly  $180^\circ$  to one another due to conservation of momentum; this error can be as much as  $\pm 6^\circ$ . These processes are fundamental to PET methodology and limit the spatial resolution of this technique to between 1.5–3.0 mm, independent of any new PET apparatus and detection methods. Notwithstanding, this resolution is substantially better than that accomplished on a SPECT imaging system.

Another factor that has to be taken into account when locating the origin of decay is the type of coincidence that is detected by the PET apparatus. True coincidence (Figure 2a) is the desired detection event, whereby a positronium annihilates to form two non-collinear gamma rays. This can be complicated by Compton scattering of one of the gamma rays causing an incorrect LOR to be calculated (Figure 2b). Accidental or random coincidences can also be detected, in which the LOR is incorrectly calculated due to two separate disintegrations (Figure 2c). Only true coincidences will provide accurate spatial information and, in practice, different practical and mathematical techniques are used to reduce the scattered and accidental coincidences.<sup>5</sup> A further source of error comes from the gamma ray penetrating into the detector ring before interacting. Although not a problem when arriving along the diameter from the middle of the detector ring, if the annihilation event occurs at an acute angle, it may travel through several detection crystals before being absorbed. This phenomenon is referred to as ‘radial astigmatism’ and can become more of a challenge to overcome in preclinical microPET systems.<sup>7</sup>



**Figure 2: Types of coincidences detected by a PET apparatus: (a) True coincidences; (b) scatter; (c) accidental coincidences.**

### 1.2.2 Types of PET Imaging Systems

Although it is extremely useful at providing a detailed image of the target and the physiological process at the molecular level, PET does not afford any anatomical information. For this reason PET is often combined with other types of imaging in a technique known as multi-modality imaging (MMI).<sup>8</sup> PET is often combined with X-ray computed tomography (CT), as this is an operationally simple process where the two machines can be placed beside one another. These scans can be performed sequentially and on a single patient bed, allowing for quick collection and analysis of physiological and anatomical data. The limitations of this technique are the poor soft tissue contrast and attenuation correction, which can cause error due to patient movement.<sup>9</sup>

Combination of PET with magnetic resonance imaging (MRI) has been highly desirable due to the superiority of MRI for the acquisition of soft tissue analysis. This MMI technique can also considerably reduce the dose of ionising radiation administered to a patient, as the CT scan constitutes 60–80% of the radiation dose.<sup>10</sup> However, the major challenge in this technology is the development of a PET scanner that can operate in close proximity to a strong magnetic field.<sup>11</sup> With recent improvements in PET and MRI equipment, this MMI technology is becoming more widely used, but more studies into improving the attenuation correction are required.<sup>12</sup>

Both PET/CT and PET/MRI systems are currently used in smaller preclinical scanners known as microPET. These scanners are capable of small animal imaging in the field of radiotracer development.<sup>13</sup> As the system is more compact, the whole of the animal can be scanned at once, rather than just a small section and this also improves the spatial resolution. As mentioned previously, it should be noted that the incidence of radial-astigmatism increases due to the disintegrations occurring closer to the detection ring.<sup>7</sup>

One of the current drawbacks of the PET scanner is that photon detection is an inefficient process, with only 1% of the photons emitted from a patient being detected. This is due to the axial field of view (FOV) in current scanners being less than 25 cm. This limitation means that a 'full-body' scan requires several scans and radiotracer distribution can only be measured from one position at a time. A recent development in the field of PET is the construction of the first 'total-body' PET/CT scanner by the EXPLORER Consortium.<sup>14</sup> In total-body PET, the FOV is extended to cover the entire length of the body and allows for simultaneous distribution data to be acquired. Also, unlike current PET scanners, the majority of emitted photons would be collected resulting in high sensitivity and signal to noise ratio of a radiotracer.<sup>15</sup> In such a system, the administered dose of radiotracer could be much lower and this would enable the imaging of short half-life radionuclides without the necessity for an on-site cyclotron. Recently, the first human imaging studies have been carried out with a total-body PET scanner; however, this technology is currently limited by high cost of manufacture.<sup>14</sup>

### **1.2.3 Radionuclides Used in PET Imaging**

There are many different radionuclides used in PET imaging. Ideally the radioisotope chosen would decay by mostly positron emission and not by electron capture as well as having a half-life comparable to that of the process being imaged. A short half-life radionuclide might not be around long enough for sufficient data to be collected; however, those with a long half-life would linger in the patient for too long. Some of the more common radionuclides for PET imaging are shown below (Table 1).<sup>4</sup> The most common

radionuclides used in PET imaging are carbon-11 and fluorine-18. Since carbon is the main constituent in most organic molecules, replacement of carbon-12 with carbon-11 produces only an isotope effect as a radiolabelled imaging agent. The shorter half-life of carbon-11 currently limits its use to centres and hospitals with an on-site cyclotron. However, this may change as PET technology becomes more advanced. The short half-life of carbon-11 can be an advantage, allowing for several automated productions in a single day, whereas fluorine-18 usually requires a 24 h wait for the radioactivity to decay.

Although fluorine is not as common in naturally occurring compounds as carbon, replacement of a hydroxyl group or hydrogen atom with fluorine-18 is common. The fluorine atom is similar in size to a hydrogen atom and it has the added advantage that the carbon–fluorine bond is the strongest in organic chemistry and is, therefore, unlikely to be metabolised resulting in the loss of the radiolabel.<sup>4</sup> Fluorine-18 benefits from a longer half-life of 110 minutes which in turn allows for a more complex synthesis and longer *in vivo* studies. However, a common misconception exists surrounding fluorine-18 that states: the low positron energy produced (0.64 MeV) results in higher resolution images since the positron range will be decreased. Although the positron range is decreased for the positron from fluorine-18 decay, this does not affect the spatial resolution in PET. Instead, the errors previously described (see section 1.2) account for the current limit of spatial resolution in PET technology.<sup>7</sup> Nevertheless, the positron range may play a more important role in radionuclide selection as the photon detector crystals and PET imaging systems become more advanced.

**Table 1: Commonly used radionuclides for PET imaging**

Nuclide	Half-life (min)	Type of Emission	Max. Energy (MeV)
<sup>11</sup> C	20.3	$\beta^+$	0.97
<sup>18</sup> F	110	$\beta^+$	0.64
<sup>13</sup> N	10	$\beta^+$	1.20
<sup>15</sup> O	2	$\beta^+$	1.74
<sup>64</sup> Cu	762	$\beta^+$ / electron capture	0.66
<sup>68</sup> Ga	68.1	$\beta^+$ / electron capture	1.90
<sup>76</sup> Br	972	$\beta^+$ / electron capture	4.00
<sup>124</sup> I	60192	$\beta^+$ / electron capture	2.14

## 1.2.4 Production of Radionuclides

### 1.2.4.1 The cyclotron

The cyclotron is a type of particle accelerator, first developed by Ernest Lawrence at the beginning of the 1930s.<sup>16</sup> Cyclotrons are capable of accelerating a charged particle beam to a high enough energy to initiate nuclear reactions and are responsible for the discovery and generation of many radionuclides used in nuclear medicine. The acceleration chamber of the cyclotron consists of two hollow D-shaped electrodes ('dees') located between the poles of an electromagnet with a magnetic field applied perpendicular to the plane of the electrodes.<sup>17</sup> Ions are produced from an ion source at the centre of the acceleration chamber and the magnetic field influences a Lorentz force causing them to travel in circular orbits. These ions are accelerated by an oscillating electric field between the 'dees'. The diameter of the orbit increases as the speed of the ions increases, which causes the ion beam to travel in a spiral. This allows for the production of a high energy ion beam, with proton energies of the most powerful cyclotrons in the region of 70 MeV. However, for the routine production of most radionuclides for medical imaging, proton beam energies below 30–40 MeV are more than sufficient. As it exits the cyclotron, this beam can be directed at a target containing a gas or liquid that will take part in the nuclear reaction, producing the desired radionuclide.

### 1.2.4.2 Production of the fluorine-18 nuclide

Production of fluorine-18 can be brought about by a variety of different nuclear reactions, the most effective of which is the  $^{18}\text{O}(p,n)^{18}\text{F}$  reaction of  $^{18}\text{O}$ -enriched water (Table 2).<sup>18</sup> This method produces aqueous [ $^{18}\text{F}$ ]fluoride, which can be used for nucleophilic radiolabelling procedures. The high molar activity can be easily achieved even with low energy cyclotrons, requiring short irradiation times. For electrophilic radiofluorinations, [ $^{18}\text{F}$ ]F<sub>2</sub> is required and can be produced *via* two methods from different gas targets. These processes are hindered due to adsorption of [ $^{18}\text{F}$ ]F<sub>2</sub> on the walls of the target, so to circumvent this, [ $^{19}\text{F}$ ]F<sub>2</sub> is added to the target. This affects the molar activity of the [ $^{18}\text{F}$ ]F<sub>2</sub> due to higher concentrations of non-radioactive fluorine and is referred to as carrier-added (c.a.). The  $^{20}\text{Ne}(d,\alpha)^{18}\text{F}$  reaction produces c.a. [ $^{18}\text{F}$ ]F<sub>2</sub> in low molar activities, however, Hess *et al.* reported an improved target system involving a two-step irradiation.<sup>19</sup> Firstly, oxygen-18 gas is irradiated with a proton beam to form fluorine-18, which is deposited on the target inner surface. After cryogenic recovery of the oxygen-18, elemental fluorine gas and krypton are added and a short proton irradiation enables isotopic exchange of the deposited [ $^{18}\text{F}$ ]F<sub>2</sub>. This method can produce up to 0.6 GBq  $\mu\text{mol}^{-1}$  activities and enables recovery of the valuable oxygen-18 gas for further productions.

**Table 2: Different approaches for the production of  $^{18}\text{F}$** 

Reaction	$^{18}\text{O}(\text{p},\text{n})^{18}\text{F}$	$^{16}\text{O}(^3\text{He},\text{p})^{18}\text{F}$	$^{20}\text{Ne}(\text{d},\alpha)^{18}\text{F}$	$^{18}\text{O}(\text{p},\text{n})^{18}\text{F}$
Target	$[^{18}\text{O}]\text{H}_2\text{O}$	$\text{H}_2\text{O}$	Ne (200 $\mu\text{mol}$ $\text{F}_2$ )	$[^{18}\text{O}]\text{O}_2$ , Kr (50 $\mu\text{mol}$ $\text{F}_2$ )
Product	$[^{18}\text{F}]\text{F}^-_{(\text{aq})}$	$[^{18}\text{F}]\text{F}^-_{(\text{aq})}$	$[^{18}\text{F}]\text{F}_2$	$[^{18}\text{F}]\text{F}_2$
Yield (GBq $\mu\text{Ah}^{-1}$ )	2.22	0.26	0.40	1.0
Molar Activity (GBq $\mu\text{mol}^{-1}$ )	$\approx 600$	$\approx 50$	$\approx 0.1$	$\approx 0.6$

### 1.2.4.3 Production of the carbon-11 nuclide

Due to the short half-life of carbon-11, production of this nuclide and its reactive forms generates added challenges. The most commonly used process for the production of carbon-11 is the  $^{14}\text{N}(\text{p},\alpha)^{11}\text{C}$  nuclear reaction. Addition of small quantities of hydrogen or oxygen gas to the target enables the production of  $[^{11}\text{C}]\text{CH}_4$  or  $[^{11}\text{C}]\text{CO}_2$ , respectively. Although, in the case of the latter, trace quantities of oxygen present in the  $\text{N}_2$  have been shown to be sufficient without further addition of  $\text{O}_2$  gas.<sup>20</sup> Irradiation to form  $[^{11}\text{C}]\text{CO}_2$  often results in simultaneous production of  $[^{11}\text{C}]\text{CO}$ , however, this can easily be cryogenically separated. Since the nuclear reaction involves irradiation of a nitrogen gas target (a non-carbon containing material), this process is capable of producing  $[^{11}\text{C}]\text{CH}_4$  and  $[^{11}\text{C}]\text{CO}_2$  in high specific activities. However, a challenge in the production of high specific activity carbon-11 is preventing the introduction of naturally abundant carbon-12. This can be introduced from impurities in the target gas or even from the valves and seals within the target.

Of the forms of carbon-11 produced from the cyclotron,  $[^{11}\text{C}]\text{CO}_2$  is the most versatile, owing to its ease of separation and high production yield.<sup>21</sup> Another advantage is the prospect for chemical transformations, with  $[^{11}\text{C}]\text{CO}_2$  being the source of a variety of different secondary precursors, the most commonly used is  $[^{11}\text{C}]\text{MeI}$ .<sup>22</sup> Production of  $[^{11}\text{C}]\text{MeI}$  can be carried out using two different methods from  $[^{11}\text{C}]\text{CO}_2$ , known as the 'wet' method and the 'gas phase' method (Figure 3). In the 'wet' method, reduction of  $[^{11}\text{C}]\text{CO}_2$  takes place using lithium aluminium hydride (LAH) in organic solvent to form  $[^{11}\text{C}]\text{methanol}$  and conversion to  $[^{11}\text{C}]\text{MeI}$  takes place using hydrogen iodide. Although this method returns high radiochemical yields, the specific activity is low due to trace amounts of organic solvent and LAH absorbing  $\text{CO}_2$  from the atmosphere and carrying this into the reaction mixture.<sup>23</sup> The 'gas phase' method avoids the use of LAH and instead produces  $[^{11}\text{C}]\text{methane}$  *via* reduction with  $\text{H}_2$  and free radical iodination with  $\text{I}_2$  in a

circulating gas phase. This also avoids the use of hydrogen iodide and prevents tubing deterioration within the apparatus. This method is capable of producing specific activities of [ $^{11}\text{C}$ ]MeI up to  $4,700 \text{ GBq } \mu\text{mol}^{-1}$ .<sup>24</sup>

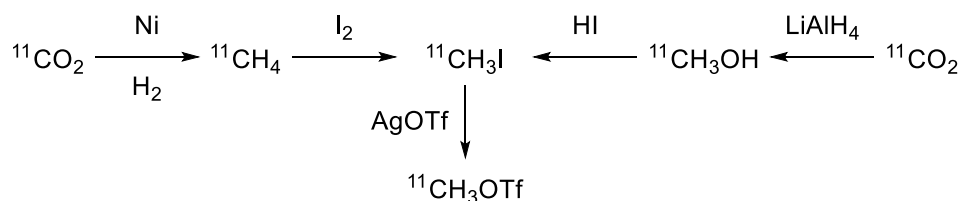
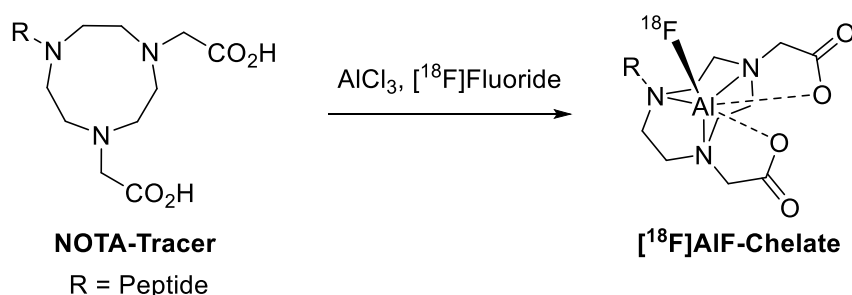


Figure 3: Production of [ $^{11}\text{C}$ ]MeI and [ $^{11}\text{C}$ ]MeOTf

## 1.2.5 Radiolabelling Methods

### 1.2.5.1 Radiochemistry Techniques

The incorporation of a radionuclide into a small molecule or peptide is important for imaging physiological processes using PET.<sup>25</sup> The non-radioactive form of the compound can be independently tested to confirm affinity for a particular target or, in the case of carbon-11, modifying the synthesis of an existing drug or tracer allows for a [ $^{11}\text{C}$ ]methylation. Incorporation of a radionuclide can take place using a variety of different methods, but these can be grouped into two main categories: covalent attachment and chelation of a radionuclide. Covalent attachment is the most common method for incorporation of carbon-11 or fluorine-18 and for small molecules. This has the advantage that the carbon–fluorine and carbon–carbon bonds are strong and unlikely to be metabolised. However, this method requires the synthesis of an appropriate precursor for labelling, longer reaction times at higher temperatures and can be a challenge if trying to label a large biomolecule such as a peptide.<sup>26</sup> Previously, chelation of the PET nuclide gallium-68 using a 1,4,7-triazacyclononane-1,4,7-triacetic acid (NOTA) chelator allowed for quick radiolabelling of NOTA-peptides.<sup>27</sup> Further work in this field expanded the use of NOTA for the chelation of [ $^{18}\text{F}$ ]AlF (Scheme 1).<sup>28</sup>



Scheme 1: [ $^{18}\text{F}$ ]AlF chelation attachment

The radiolabelling of any compound has practical challenges due to the presence of radiation from the positron decay process.<sup>6</sup> As such, these reactions have to take place behind appropriate shielding, usually several inches of lead. Production of a radiotracer can be performed using two practical methods: a manual or an automated synthesis. In manual synthesis, the reaction is carried out in the same way as a standard organic chemistry reaction, but with the operator standing behind lead shielding and limiting the time they spend manipulating the radioactivity to reduce their overall dose. This method has the advantage that a reaction can be carried out in the same manner as the non-radioactive synthesis and, therefore, should require little optimisation. The disadvantage is that, in order to protect the safety of the operator, only low levels of radiation should be used. Another shortcoming is that, as with many non-radioactive syntheses, the operator requires a certain level of skill and knowledge in order to carry out a successful production of the radiotracer. Therefore, for the routine production of radiotracers in a clinical setting, most radiosyntheses are carried out on automated systems.<sup>29</sup> These synthesisers benefit from the ability to be controlled remotely and so an operator can perform a reaction using high levels of radiation without any risk to health. Once a synthesis is optimised, this process is highly reproducible and requires minimal input from the operator. Indeed, many synthesisers exist that employ a cassette-based system that allows for routine production by trained technical staff. Since this automation is intrinsic to the production of PET radiotracers for the clinic, it is highly desirable for optimisation of a radiotracer still undergoing preclinical evaluation to be produced in this way. This can aid the translation of a radiotracer to a clinical setting.

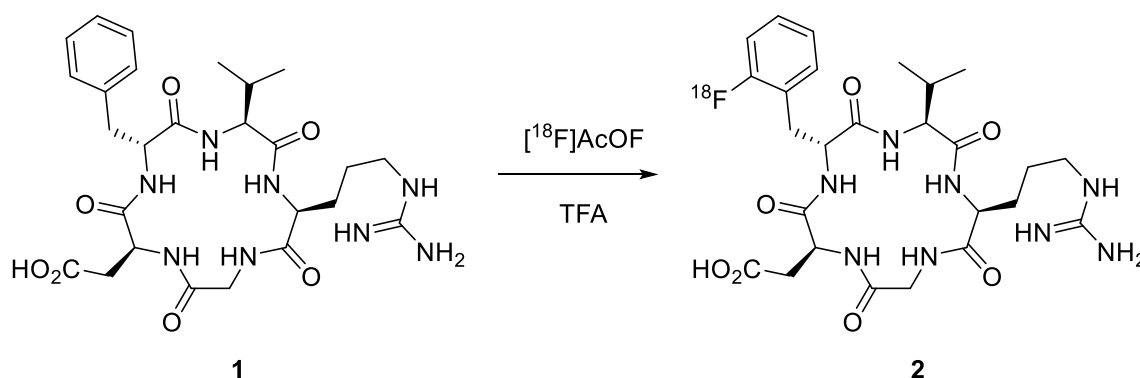
#### **1.2.5.2 Preparation of radiotracers**

An added challenge in the preparation of radiotracers is in the quantity of radionuclide produced by the cyclotron. Even for very large quantities of radiation, this is in the nanomolar to picomolar range.<sup>6</sup> As the non-radioactive components of the reaction are often in such high stoichiometric excess, this gives the reaction pseudo-first-order kinetics with respect to the radionuclide. This has the advantage that reactions that would generally require days to go to completion can be complete within minutes. The consequence of this is that trace impurities in reagents and solvent can greatly affect the reaction; if a reaction with a trace impurity is faster than that of a desired precursor then no product may be formed.<sup>6</sup> Since the product is formed in such small quantities, traditional methods of characterisation, such as nuclear magnetic resonance (NMR) spectroscopy cannot be used. Instead, high performance liquid chromatography (HPLC) and thin-layer chromatography (TLC), using radioactivity detectors is employed. The radiotracer is quantified by its radiochemical yield (RCY): the radioactivity of product expressed as a percentage of the starting radioactivity, which is decay corrected to the

start of synthesis and is identical to the concept of chemical yield.<sup>30</sup> Another important value is the specific activity ( $A_s$ ), which is defined as the measured activity per gram of compound, usually expressed in GBq mg<sup>-1</sup>. The theoretical maximum value of  $A_s$  is never reached due to isotopic dilution by the naturally occurring isotope.<sup>6</sup> However, a particularly low specific activity would imply a high level of isotopic dilution and, thus, the toxicological effect of any administered radioisotope would be greater. However, most radiotracers fall into the <1.5  $\mu$ g level of administration and pose no toxicological threat to the patient.<sup>31</sup>

### 1.2.5.3 Common labelling methods for fluorine-18

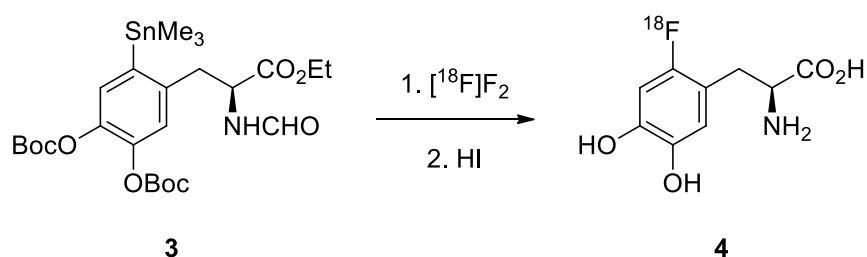
There are two broad categories of reactions to incorporate fluorine-18: direct fluorination using [<sup>18</sup>F]fluoride or [<sup>18</sup>F]F<sub>2</sub> from the cyclotron and indirect fluorination, which requires a multi-step approach. Direct fluorination can be further split into electrophilic fluorination methods using [<sup>18</sup>F]F<sub>2</sub> and nucleophilic reactions using [<sup>18</sup>F]fluoride. As mentioned previously (see section 1.2.4.2), electrophilic methods suffer from poor specific activity due to the presence of a fluorine-19 carrier. Since this means that the maximum possible RCY for the radiofluorination would be 50%, these methods are not as popular. Notwithstanding, electrophilic aromatic substitution of electron-rich aryl systems has been shown to be effective, but can suffer from poor regioselectivity due to their high reactivity.<sup>32</sup> Conversion of [<sup>18</sup>F]F<sub>2</sub> into the less reactive [<sup>18</sup>F]AcOF enables a more regioselective reaction to take place and this has been used for the synthesis of cyclic RGD peptide **2** for *in vivo* studies of  $\alpha_v\beta_3$  integrin (Scheme 2). This radiotracer is used for the study of tumour status.<sup>33</sup> The lower reactivity prevents the di-fluorination of peptide **1** and enables separation of the desired *ortho*-substituted product in 27% RCY and specific activity of 32.8 GBq  $\mu$ mol<sup>-1</sup>.



**Scheme 2: Radiosynthesis of [<sup>18</sup>F]fluorinated cyclo(RGDfMeV) (2)**

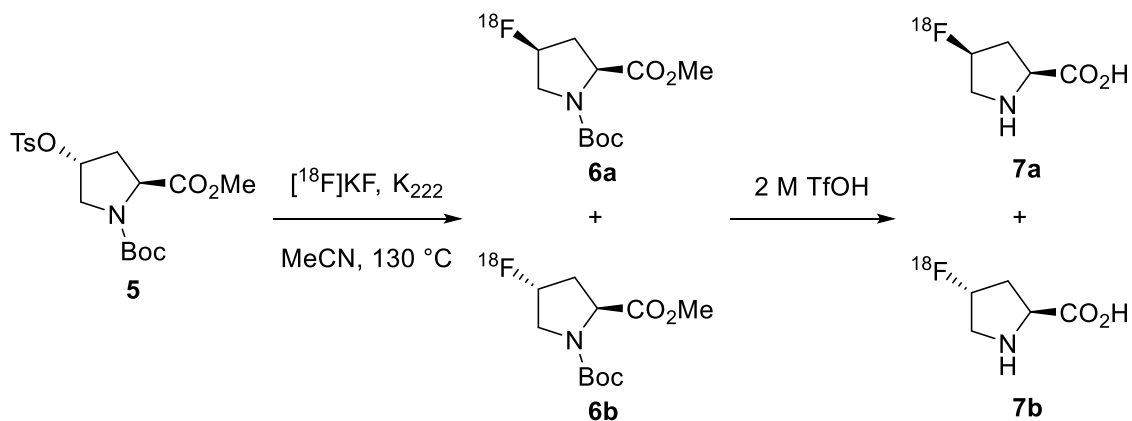
Electrophilic fluorination is also performed through the demetalation of organometallic compounds.<sup>34</sup> Organotin precursors are commonly used for this transformation and this

method has improved regioselectivity due to the presence of a functional handle attached to the molecule. The tin-carbon bond is strong enough to withstand many reaction conditions and can be incorporated early in the synthesis.<sup>35</sup> Furthermore, the toxicity of tin has not been an issue in translation of fluorine-18 radiopharmaceuticals to the clinic, with organotin precursor **3** for [<sup>18</sup>F]fluoro-L-DOPA (**4**) a good example (Scheme 3).<sup>36,37</sup> However, recent work by Makaravage *et al.* has shown that arylstannanes can be radiofluorinated with [<sup>18</sup>F]fluoride in the presence of a copper catalyst.<sup>38</sup> This study used the radiotracer [<sup>18</sup>F]fluoro-L-DOPA (**4**) as an example substrate. Avoiding the use of an electrophilic source of fluorine-18 in the synthesis of electron-rich aryl systems has become more popular, as better specific activity and radiochemical yield can be achieved from [<sup>18</sup>F]fluoride.



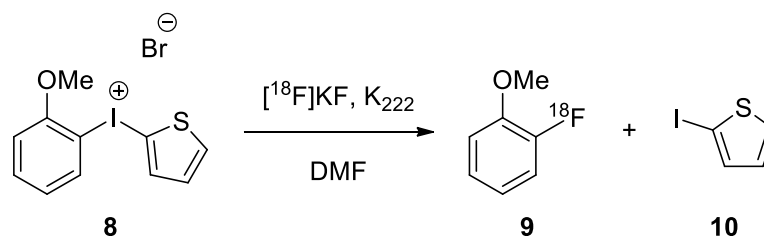
**Scheme 3: Radiosynthesis of [<sup>18</sup>F]fluoro-L-DOPA (**4**) from organotin precursor **3****

Aliphatic nucleophilic substitution reactions with [<sup>18</sup>F]fluoride are amongst the most straightforward and proceed *via* an S<sub>N</sub>2 reaction.<sup>34</sup> [<sup>18</sup>F]Fluoride from the cyclotron is highly solvated, so addition of a phase transfer catalyst (such as Kryptofix 222<sup>®</sup> or tetrabutylammonium hydrogencarbonate) followed by removal of water leaves an exposed fluoride, which is highly nucleophilic.<sup>39</sup> A precursor with a good leaving group is required for these reactions and is often in the form of a tosylate or triflate. This method was used in the production of *cis*-4-[<sup>18</sup>F]fluoro-L-proline (**7a**), a radiotracer for imaging increased collagen synthesis (Scheme 4). Direct nucleophilic [<sup>18</sup>F]fluorination of a tosylate precursor to form **6a** is followed by deprotection in triflic acid.<sup>40</sup> Further study of this fluorination reaction revealed that high temperature during the radiofluorination step caused a competing S<sub>N</sub>1 mechanism which resulted in a mixture of *cis*- and *trans*-isomers.<sup>41</sup>



**Scheme 4: Radiosynthesis of *cis*-4-[ $^{18}\text{F}$ ]fluoro-L-proline (**7a**) and competing  $\text{S}_{\text{N}}1$  reaction at high temperature to form *trans*-4-[ $^{18}\text{F}$ ]fluoro-L-proline (**7b**)**

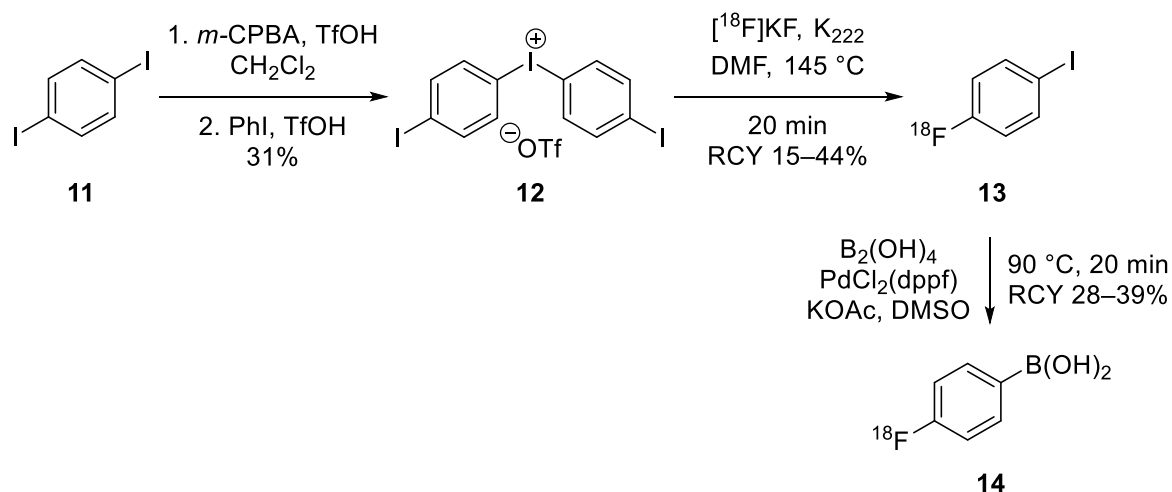
Nucleophilic aromatic substitution ( $\text{S}_{\text{N}}\text{Ar}$ ) reaction with [ $^{18}\text{F}$ ]fluoride plays an important role in the radiofluorination of arenes. However, for the success of this reaction it is important to have a highly electron-withdrawing group, such as a nitro or cyano in the *ortho*- or *para*-position to the leaving group. Effective leaving groups for  $\text{S}_{\text{N}}\text{Ar}$  include the nitro and trimethylammonium groups.<sup>42</sup> Halogens can also be used as leaving groups for  $\text{S}_{\text{N}}\text{Ar}$  reactions. *para*-Nitrophenyl halides show reactivity for radiofluorination with  $\text{Cl} > \text{Br}$  and the nitro group remaining intact.<sup>43</sup> These reactions are limited by the need for very electron-deficient aryl systems, however, radiofluorination of more electron-rich arenes can be performed using diaryliodonium salts. These reactions are believed to proceed *via* an  $\text{S}_{\text{N}}\text{Ar}$  mechanism and the radiofluorination occurs preferentially at the electron-deficient arene.<sup>44</sup> Further studies showed that regioselectivity could also be controlled by the steric bulk of the *ortho*-substituent.<sup>45</sup> The use of a 2-thienyl group has been shown as a method for incorporation of fluorine-18 in more electron-rich systems, such as anisole (Scheme 5).<sup>46</sup>



**Scheme 5: Radiosynthesis of *ortho*-[ $^{18}\text{F}$ ]fluoroanisole (**9**) using heteroaromatic iodonium salt **8****

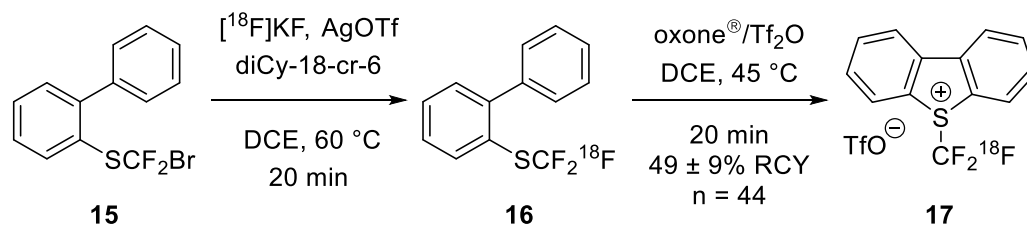
Diaryliodonium salts are also used in the synthesis of prosthetic groups for the indirect radiofluorination of larger molecules. Gao *et al.* reported the synthesis of 4-

[ $^{18}\text{F}$ ]fluorophenylboronic acid (**14**) that could be used to  $^{18}\text{F}$ -label polypeptides *via* an aqueous Suzuki-Miyaura coupling (Scheme 6).<sup>47</sup> Radiofluorination of a symmetrical diaryliodonium species **12** allowed for the synthesis of  $^{18}\text{F}$ -labelled iodobenzene **13**. Subsequent Miyaura borylation gave boronic acid **14** in 5–10% overall RCY. Many other methods exist that use prosthetic group approaches, with some of the most prevalent being ‘click chemistry’ reactions between alkynes and azides.<sup>48</sup>



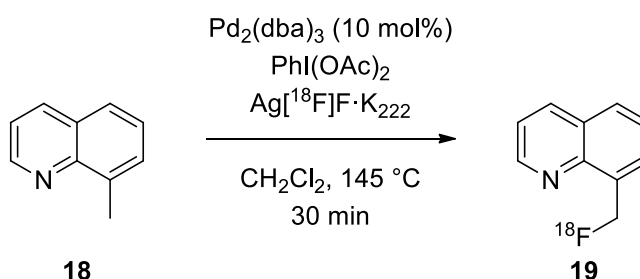
**Scheme 6: Synthesis of 4-[ $^{18}\text{F}$ ]fluorophenylboronic acid (**14**)**

Transition metal-free methodology for the selective radiofluorination of unmodified peptides was reported by Verhoog *et al.* (Scheme 7).<sup>49</sup> Halogen exchange of compound **15** with [ $^{18}\text{F}$ ]fluoride in the presence of  $\text{AgOTf}$  afforded  $^{18}\text{F}$ -labelled compound **16**. Subsequent cyclisation with oxone<sup>®</sup> and  $\text{Tf}_2\text{O}$  provided  $^{18}\text{F}$ -labelled Umemoto reagent **17** in 5% activity yield, calculated from [ $^{18}\text{F}$ ]fluoride. The authors showed that it was possible to radiofluorinate cysteine residues of unmodified peptides with the [ $^{18}\text{F}$ ]trifluoromethyl group. It was proposed that the soft nature of the sulfonium leaving group and of the thiol nucleophile guided the selectivity of the reaction.



**Scheme 7: Radiosynthesis of  $^{18}\text{F}$ -labelled Umemoto reagent **17****

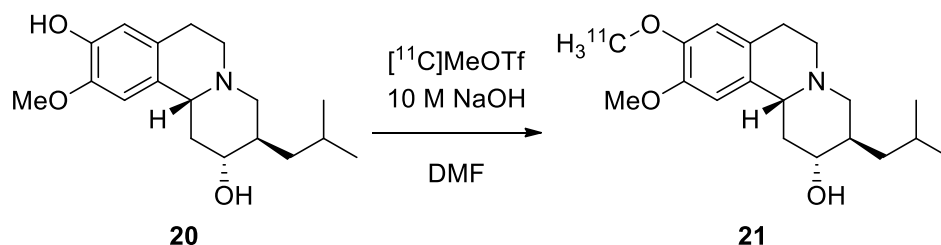
With the rise in interest of C–H functionalisation in organic chemistry, this methodology is becoming increasingly more common in the field of radiochemistry.<sup>50–52</sup> In 2019, Lee *et al.* reported a Pd-mediated C–H radiofluorination of 8-methylquinoline derivatives using Ag[<sup>18</sup>F]F, based on earlier work using fluorine-19 (Scheme 8).<sup>53,54</sup> The authors found that it was possible to automate this synthesis using a GE TRACERlab FX<sub>FN</sub> module, providing <sup>18</sup>F-analogue **19** in 4% RCY with a specific activity of 39 GBq mmol<sup>-1</sup>. This is demonstrated as a proof-of-concept, with the manual synthesis returning **19** in 21% RCY. Recently, Chen *et al.* reported the direct [<sup>18</sup>F]fluorination of C–H arenes *via* organic photoredox catalysis. This reaction required the use of an acridinium-based photooxidant and a 450 nm laser under an atmosphere of oxygen. The methodology was shown to be effective for electron rich arenes featuring a strong directing group such as anisole.<sup>55</sup>



**Scheme 8: Radiofluorination of 8-methylquinoline (**18**)**

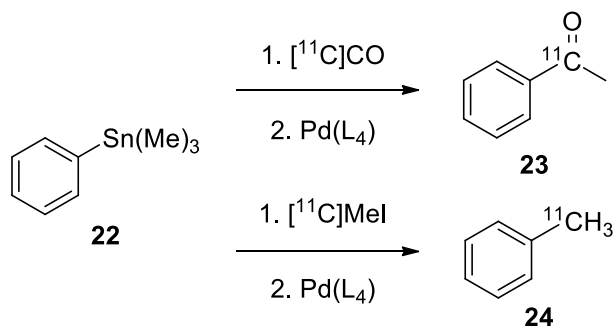
#### 1.2.5.4 Common labelling methods for carbon-11

The most popular method for incorporation of carbon-11 is the *N*-, *O*- and *S*-methylation of organic compounds. Since these motifs are found in abundance in drug-like molecules, often, very little modification of a known compound needs to take place to allow for a successful radiomethylation. The most commonly used reagent for this transformation is [<sup>11</sup>C]MeI; however, [<sup>11</sup>C]MeOTf is finding increased use due to its high reactivity and volatility.<sup>56</sup> This reagent is used in the routine production of [<sup>11</sup>C]DTBZ (**21**), a radiotracer for imaging the vesicular monoamine transporter 2 (VMAT2) in neurodegenerative disease (Scheme 9).<sup>57</sup> Due to the short half-life of carbon-11, radiosyntheses that have two or more reactive sites and require protecting group removal are commonly disfavoured. As a general rule, the time taken for a radiosynthesis should not exceed three half-lives of the radioisotope used.<sup>6</sup>



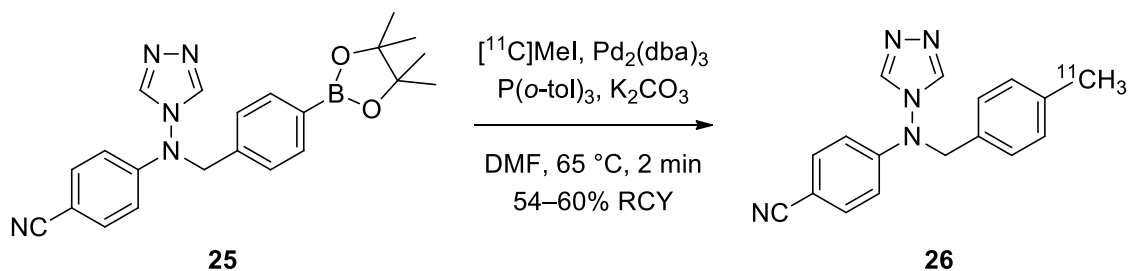
**Scheme 9: Production of the radiotracer [<sup>11</sup>C]DTBZ (21)**

The use of transition metal catalysis has also been translated to <sup>11</sup>C-labelling applications. Since the quantities of the transition metal catalyst are in high stoichiometric quantities with respect to the source of carbon-11, these reactions are often referred to as ‘transition metal-mediated’.<sup>58</sup> One of the most widely used is the palladium-mediated Stille coupling with [<sup>11</sup>C]MeI. This allows for <sup>11</sup>C-methylation of aryl and vinyl organotin species; however, it is susceptible to isotopic dilution if a trimethylstannane is used as a leaving group.<sup>58</sup> Ketones can be obtained from the Stille coupling if carbon monoxide is present in the reaction. Therefore, the use of either [<sup>11</sup>C]MeI or [<sup>11</sup>C]CO allows the synthesis of different products from the same precursor (Scheme 10).<sup>59,60</sup>



**Scheme 10: Radiosynthesis of <sup>11</sup>C-labelled products 23 and 24 from organotin precursor 22**

Since organotin precursors are known to be toxic, the Suzuki-Miyaura reaction from aryl or alkyl boronates is often utilised.<sup>61</sup> Given the versatility of the Suzuki-Miyaura reaction, its application is widespread in the production of radiotracers. Indeed, this method is used in the production of [<sup>11</sup>C]cetrozole (**26**), a PET imaging probe for aromatase imaging in the brain.<sup>62</sup>



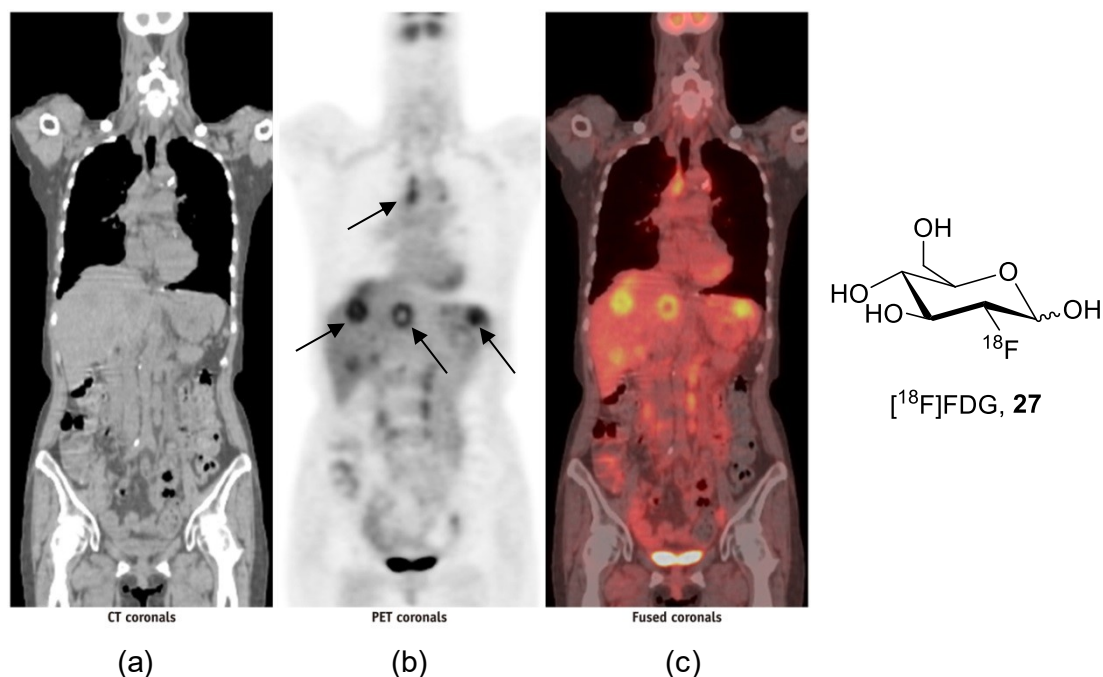
**Scheme 11: Suzuki-Miyaura reaction of boronic ester precursor **25** to form  $[^{11}\text{C}]\text{Cetozole}$  (**26**)**

The use of  $[^{11}\text{C}]\text{CO}_2$  as the reactive form of carbon-11 is an attractive option, as this bypasses the need to transform the reagent extensively after production from the cyclotron and can provide high yielding reactions. The radiosynthesis of  $[^{11}\text{C}]\text{acetate}$ , a tracer used in the diagnosis of prostate cancer, is produced from passing  $[^{11}\text{C}]\text{CO}_2$  through a loop coated with the Grignard reagent  $\text{MeMgBr}$ .<sup>63</sup> A RCY of 65% can be achieved in a total reaction time of 5 min using this process.<sup>64</sup> The problems associated with using the Grignard reaction are contamination with atmospheric  $\text{CO}_2$  and hydrolysis of the air sensitive organometallic reagent, which can unfavourably affect the specific activity.

## 1.2.6 Clinical Applications of Radiotracers

### 1.2.6.1 Applications of $^{18}\text{F}$ -labelled tracers

The most commonly used PET radiotracer is  $[^{18}\text{F}]\text{fluoro-2-deoxyglucose}$  (FDG) (**27**).<sup>65</sup>  $[^{18}\text{F}]\text{FDG}$  enters cells *via* plasma membrane transporters and becomes irreversibly trapped in most tissues. Since tumour cells have a higher rate of metabolic activity, the  $[^{18}\text{F}]\text{FDG}$  accumulates in tumour cells rather than normal tissue, in a similar manner to glucose. As such,  $[^{18}\text{F}]\text{FDG}$  has found widespread use in oncology as a tool for the diagnosis of cancer.<sup>66</sup> Rather uniquely for a radiotracer,  $[^{18}\text{F}]\text{FDG}$  works by a metabolic trapping mechanism:  $[^{18}\text{F}]\text{FDG}$  metabolism is inhibited due to a lack of 2-hydroxyl group and accumulates. When the fluorine-18 nuclide decays by positron emission, it transforms to the oxygen-18 nuclide and can then be metabolised and excreted.  $[^{18}\text{F}]\text{FDG}$  is limited as a diagnostic tool due to high uptake in brain and bladder tissues, making it impractical for the imaging of brain and prostate cancers. Shown below is a PET/CT scan of a patient post-hysterectomy after presenting with a neuroendocrine cervical carcinoma (Figure 4).<sup>67</sup> The CT image shows the anatomical data (Figure 4a), while the PET image shows the location of increased metabolic activity (Figure 4b). The fused image shows the location of metastases in the mediastinum, liver and abdominal lymphatic chain (Figure 4c).



**Figure 4:**  $[^{18}\text{F}]\text{FDG}$  PET/CT scan: (a) CT image; (b) PET image; (c) fused images

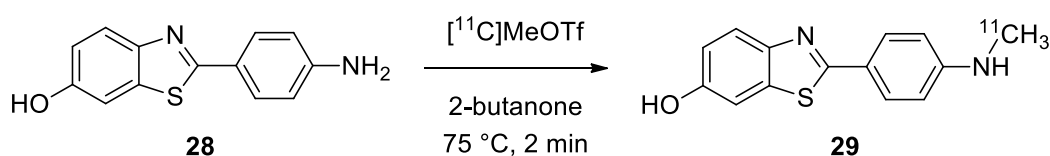
(Reprinted with permission from *Korean J. Radiol.*, 2012, **13**, 760–770. Copyright 2012 The Korean Society of Radiology)<sup>67</sup>

Another routinely used  $^{18}\text{F}$ -tracer in the clinic is the bone-seeking agent  $[^{18}\text{F}]\text{NaF}$ .<sup>68</sup> Most  $[^{18}\text{F}]\text{NaF}$  is taken up in bone after only a single pass of the blood and uptake is 10 times higher in areas of regenerating bone, compared with healthy bone tissue.<sup>69</sup> As such,  $[^{18}\text{F}]\text{NaF}$  has found use in the metabolic evaluation of benign bone and joint diseases (e.g. the detection of bone remodelling in the early stages of osteoarthritis) and in diagnosis of malignant diseases.<sup>70</sup> As  $[^{18}\text{F}]\text{fluoride}$  can be generated in high specific activity from the cyclotron, the reformulation to  $[^{18}\text{F}]\text{NaF}$  is simple and high yielding.

Despite  $[^{18}\text{F}]\text{FDG}$  and  $[^{18}\text{F}]\text{NaF}$  being amongst the most commonly used  $^{18}\text{F}$ -labelled radiotracers in a clinical setting, many others also exist. The previously mentioned  $[^{18}\text{F}]\text{fluoro-L-DOPA}$  (see section 1.2.5.3) is a radiofluorinated analogue of L-DOPA, a precursor in the biosynthesis of dopamine.  $[^{18}\text{F}]\text{Fluoro-L-DOPA}$  can cross the blood-brain barrier (BBB), unlike dopamine, and can then be transformed to  $[^{18}\text{F}]\text{fluoro-dopamine}$ .<sup>71</sup> Since disturbances in dopamine metabolism are characteristic of neurodegenerative diseases such as Parkinson's, tracing the dopaminergic pathway can provide early diagnosis and aid with monitoring disease progression. Other tracers that are seeing increased use are the previously described *cis*-4- $[^{18}\text{F}]\text{fluoro-L-proline}$  (**7a**) and *trans*-4- $[^{18}\text{F}]\text{fluoro-L-proline}$  (**7b**). However, it is the former that shows greater incorporation into proteins and is used to better understand the synthesis of collagen in connective tissues.<sup>72</sup>

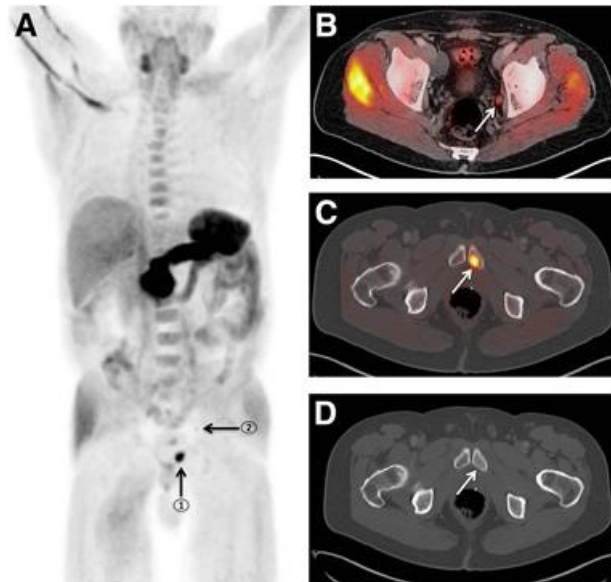
### 1.2.6.2 Applications of $^{11}\text{C}$ -labelled tracers

A common carbon-11 PET radiotracer is Pittsburgh compound B (PiB) which is used to image beta-amyloid plaques in neuronal tissue.<sup>73</sup> These plaques are found in the brains of patients with Alzheimer's disease (AD) and so [ $^{11}\text{C}$ ]PiB (**29**) can be used for differential diagnosis of AD and other dementias. The first radiosynthesis of [ $^{11}\text{C}$ ]PiB involved a MOM-protected phenol precursor and used [ $^{11}\text{C}$ ]MeI as the source of carbon-11.<sup>74</sup> This synthesis required forcing conditions for the methylation and subsequent deprotection of the phenyl alcohol, so only low radiochemical yields were achieved. A new radiosynthesis is now used that utilises [ $^{11}\text{C}$ ]MeOTf and requires no base, allowing for direct *N*-methylation from an unprotected precursor **28** (Scheme 12).



**Scheme 12: Radiosynthesis of [ $^{11}\text{C}$ ]PiB (**29**)**

The previously mentioned [ $^{11}\text{C}$ ]acetate is another radiotracer that is used in the detection of cancer.<sup>75</sup> It is used in studies of prostate, bladder and brain cancers, amongst others.<sup>76</sup> These are areas where [ $^{18}\text{F}$ ]FDG is not able to differentiate tumour cells due to being part of the excretion pathway or having increased uptake. [ $^{11}\text{C}$ ]Acetate is readily metabolised into acetyl-CoA, an important molecule in the Krebs cycle. This is taken up into cells that over-express fatty acid synthetase (FAS), such as tumour cells.<sup>75</sup> The figure below shows a PET/CT scan of a prostate cancer patient with increased uptake of [ $^{11}\text{C}$ ]acetate near the pubic symphysis (Figure 5).<sup>77</sup>



**Figure 5: PET scan of a cancer patient. (A) Coronal whole-body PET image; (B–D) Axial  $[^{11}\text{C}]$ acetate PET/CT images**

(This research was originally published in *J. Nucl. Med.*, 2016, **57**, 30S–37S. Copyright 2019 SNMMI)<sup>77</sup>

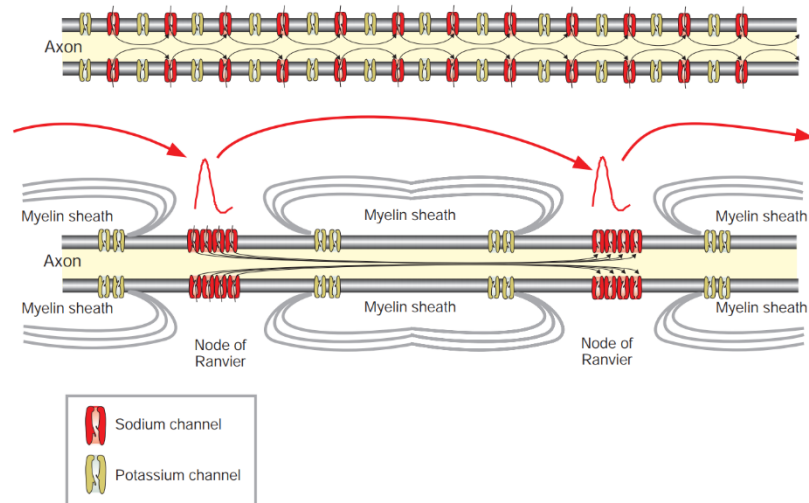
Another important radiotracer is the  $^{11}\text{C}$ -labelled amino acid  $[^{11}\text{C}]$ methionine. Since methionine is a vital amino acid in protein synthesis, it can be used to study cancerous tissue.<sup>78</sup> Most studies using  $[^{11}\text{C}]$ methionine focus on brain tumours, as unlike  $[^{18}\text{F}]$ FDG this does not accumulate in healthy brain tissue. A commonly used tracer in the assessment of prostate cancer is  $^{11}\text{C}$ -labelled choline. Since there is not much bladder uptake,  $[^{11}\text{C}]$ choline can assess tumours in the prostate.<sup>79</sup>  $[^{11}\text{C}]$ Choline is also the precursor in the biosynthesis of the neurotransmitter acetylcholine, which is impaired in many neurodegenerative diseases; however, as with  $[^{11}\text{C}]$ methionine,  $[^{11}\text{C}]$ choline is also a biomarker of brain tumours and is not taken up in the healthy brain tissue.<sup>80</sup>

## 1.3 Sphingosine-1-Phosphate 5 Receptor (S1P<sub>5</sub>)

### 1.3.1 Multiple Sclerosis

Multiple Sclerosis (MS) is an immune mediated disorder that affects over 2 million people worldwide.<sup>81</sup> In the UK alone, approximately 120,000 people have MS, with over 6000 new cases diagnosed per year.<sup>82</sup> A recent study showed a high prevalence of MS in the Orkney and Shetland islands with a marked increase in prevalence in Orkney over the last 30 years.<sup>83</sup> Work by Mokry *et al.* has identified a lowered vitamin D level with increased susceptibility to MS, suggesting that low levels of UV-B sunlight in these northerly areas may explain this prevalence.<sup>84</sup> However, these studies are yet to address whether vitamin D sufficiency can indeed delay MS onset. Over 70% of cases of MS are with females, indicating a sex difference in prevalence.<sup>82</sup> Although, the exact cause of MS is currently unknown.

Multiple sclerosis affects the central nervous system (CNS) and is thought to result from demyelination by autoreactive T-cells.<sup>85</sup> Some of the main characteristics of MS are the formation of plaques in the CNS and the destruction of myelin sheaths of neurons. A loss of myelin disrupts the communication between cells and causes a wide range of symptoms, such as: extreme tiredness, blurring of vision and problems with balance amongst many others. In MS, these symptoms are unpredictable and can develop and increase over time, or come and go periodically. A healthy myelin sheath will increase the speed of impulses by increasing the resistance and decreasing the capacitance. The signals propagate by saltatory conduction where the action potential jumps from one unmyelinated node of Ranvier to the next (Figure 6).<sup>86</sup> Voltage-gated ion channels are found more abundantly at these nodes of Ranvier so action potentials are not generated along the areas covered by the myelin sheath. Along an unmyelinated axon, the electrical impulse would move as a continuous wave, but the action potential propagation would decay as the current leaks across the membrane.



**Figure 6: Myelin sheath saltatory conduction**

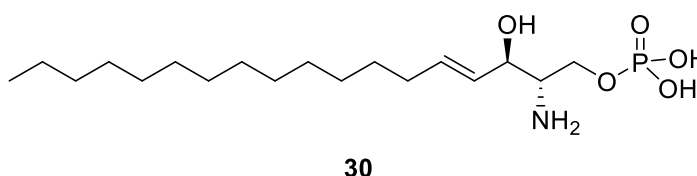
(Reprinted with permission from *Glial Physiology and Pathophysiology*, John Wiley & Sons, Ltd, Chichester, 2013, p. 245–319. Copyright 2013 John Wiley and Sons)<sup>86</sup>

A distinctive feature of multiple sclerosis is the formation of the sclerotic plaque that forms in the CNS.<sup>87</sup> This most commonly affects the white matter (so named due to the high lipid content of myelin) in the optic nerve, brain stem and spinal cord. This feature is a result of inflammation, demyelination and remyelination followed by oligodendrocyte depletion and neuronal and axon deterioration. However, the exact cause and underlying mechanism of action have yet to be elucidated.<sup>88</sup> Oligodendrocytes are a type of neuroglia: i.e. they are non-neuronal cells that maintain homeostasis; they are specialised to form the myelin sheaths surrounding neurons.<sup>86</sup> As demyelination occurs, the oligodendrocytes repair the myelin sheath of axons, however, remyelinated neurons have a thinner sheath and repeated demyelination leads to the formation of sclerotic plaque. This results in a loss of speed of conduction between neurons and, hence, a loss of communication between cells.

Diagnosis of multiple sclerosis is complicated, as currently there is no single test that can confirm or deny the presence of the disease. The diagnosis follows a set of guidelines known as the McDonald criteria and these are updated regularly, with the last update occurring in 2017.<sup>89</sup> Neurological examination, blood tests and examination of spinal fluid are commonly used methods, but now MRI is increasingly used in MS diagnosis as it is capable of showing lesions of sclerotic plaque.<sup>90</sup> However, by the time these plaques are visible by MRI, the damage is often very severe. Thus, a tool is needed that can represent the pathology in patients before the detection of lesions is visible.

## 1.3.2 Sphingosine-1-Phosphate Receptors

Sphingosine-1-phosphate (S1P) (Figure 7) is a lysophospholipid derived from the cell membrane that acts as an extracellular signal. S1P plays a fundamental role in cell growth and apoptosis in the CNS and the immune and cardiovascular systems. It acts by engaging with high-affinity S1P receptors.<sup>91</sup> There are currently five known different S1P receptors (S1P<sub>1</sub>–S1P<sub>5</sub>) that specifically bind S1P with low nanomolar affinities. S1P<sub>1</sub>–S1P<sub>3</sub> are predominantly expressed in immune cells and the cardiovascular system, where S1P<sub>1</sub> is highly expressed on T-cells and B-cells.<sup>92</sup> S1P<sub>4</sub> is expressed in the hematopoietic system and S1P<sub>5</sub> is expressed in the neural and glial cells, including astrocytes and oligodendrocytes.<sup>93</sup>



**Figure 7: Sphingosine-1-phosphate (S1P)**

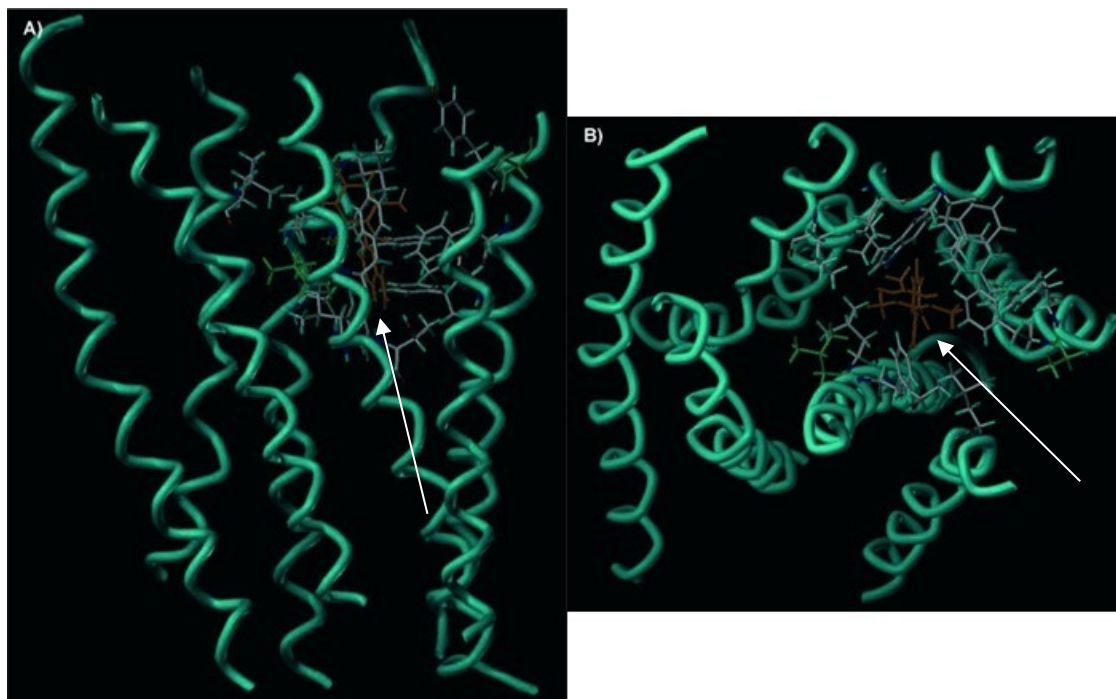
The distribution of S1P<sub>5</sub> suggests that it may play an important role in regulating the myelination process.<sup>94</sup> Indeed, S1P activation of S1P<sub>5</sub> has been shown to promote the survival of myelin-forming mature oligodendrocytes.<sup>94</sup> On that basis, the development of new selective agonists of the S1P<sub>5</sub> receptor may be beneficial for the treatment of neurodegenerative diseases such as MS. If so, minimal S1P<sub>1</sub> interaction would be favourable since this will decrease the risk of immune suppression and cardiovascular effects.<sup>91</sup>

## 1.3.3 S1P Receptor Agonists

### 1.3.3.1 Agonists for S1P<sub>5</sub> receptors

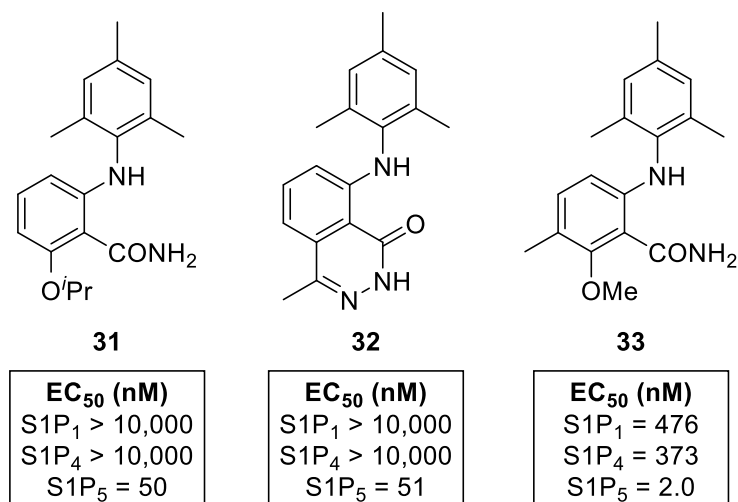
In 2010, a group from Novartis published a paper reporting the synthesis of various benzamide compounds that proved to be potent and selective S1P<sub>5</sub> receptor agonists.<sup>95</sup> These compounds were discovered by using high-throughput screening techniques to assess their *in vitro* potency towards S1P<sub>1</sub>, S1P<sub>4</sub> and S1P<sub>5</sub> receptors. To guide the optimisation process of these compounds, docking experiments of the benzamide compounds into homology models of the S1P receptors were carried out (Figure 8). Crucially, they found that the 2,6-dimethyl substituted aniline substituent causes twisting in the molecule, leading to effective binding within the proposed pockets. In the S1P<sub>5</sub>

receptor complex, the amide forms a hydrogen bond with threonine and the benzamide phenyl ring lies in a large hydrophobic pocket surrounded by phenylalanine, leucine and tryptophan. The aniline ring forms a T-shaped interaction with a phenylalanine residue and hydrophobic interactions with leucine. The *ortho*-methyl substituents fill a small pocket formed by tyrosine, valine and leucine residues. After the synthesis of various analogues of these benzamide compounds was complete, they were assayed for S1P<sub>5</sub>, S1P<sub>1</sub> and S1P<sub>4</sub> activation. Some of the more promising structures (**31–33**) are shown below (Figure 9).



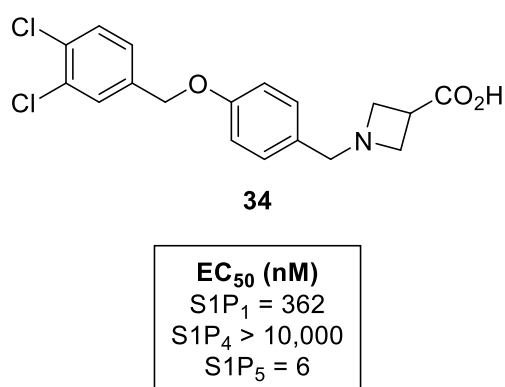
**Figure 8: A) Longitudinal and B) transverse views of the S1P<sub>5</sub> homology model with the benzamide compound docked.**

(Reprinted with permission from *ChemMedChem*, 2010, **5**, 1693–1696. Copyright 2010 John Wiley and Sons)<sup>95</sup>



**Figure 9: Potent benzamide agonists of S1P<sub>5</sub>**

A paper in 2015 reported the discovery of an orally bioavailable selective S1P<sub>5</sub> receptor agonist, **34** (Figure 10).<sup>96</sup> This compound was discovered through the application of a parallel synthesis, based on previous structures from the literature, followed by high throughput screening to identify compounds for structure activity relationship (SAR) experiments. Although it shows high potency for the S1P<sub>5</sub> receptor, it is not as selective as the benzamide compounds reported by Mattes *et al.* However, significant work determined the drug-like properties of the compound, supporting its suitability for *in vivo* studies of the biology of S1P<sub>5</sub>.<sup>96</sup>

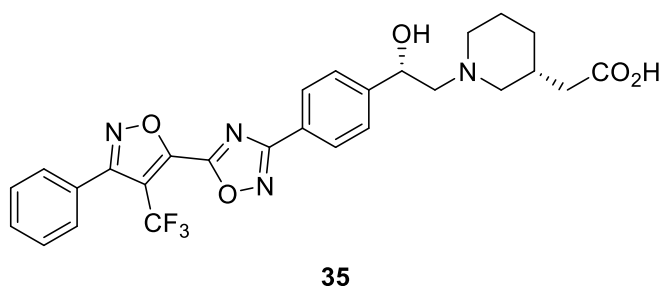


**Figure 10: S1P<sub>5</sub> receptor agonist 34**

### 1.3.3.2 Agonists for S1P<sub>1</sub>–S1P<sub>4</sub> receptors

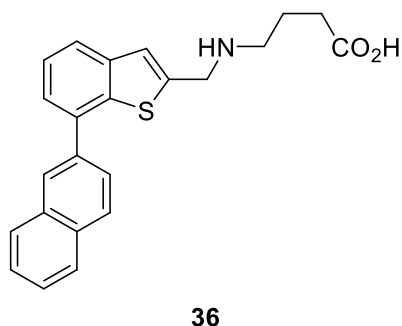
In 2016, Gilmore *et al.* reported the discovery of a series of ethanolamine-based agonists of S1P<sub>1</sub> (Figure 11).<sup>97</sup> They discovered a novel polar headgroup consisting of an ethanolamine scaffold with a terminal carboxylic acid, mimicked the structure of S1P.

Through SAR studies, they synthesised compound **35**, which had desirable pharmacokinetic and pharmacodynamic properties and has progressed to advanced studies for consideration as a clinical development candidate.



**Figure 11: 5-Substituted trifluoromethyloxazole ethanolamine 35**

Also in 2016, Hur *et al.*, reported the synthesis of a benzo[*b*]thiophene-based selective S1P<sub>4</sub> receptor agonist, **36** (Figure 12).<sup>98</sup> S1P<sub>4</sub> is expressed primarily in lymphoid tissues and suppresses T-cell proliferation, but is believed to possess additional functions.<sup>85</sup> Compound **36** has an EC<sub>50</sub> of 200 nM for S1P<sub>4</sub> and exhibits no activity for S1P<sub>1-3,5</sub>. Interestingly, many of the selective S1P<sub>4</sub> agonists reported in the literature have an overall “L-shaped” structure, suggesting that this backbone is specific for S1P<sub>4</sub> activation.

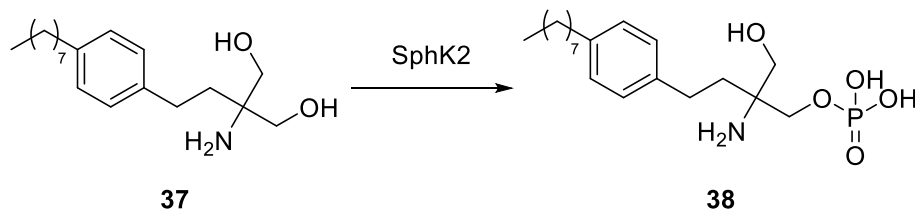


**Figure 12: Benzo[*b*]thiophene-based selective S1P<sub>4</sub> receptor agonist 36**

### 1.3.4 S1P Receptor Imaging Using PET

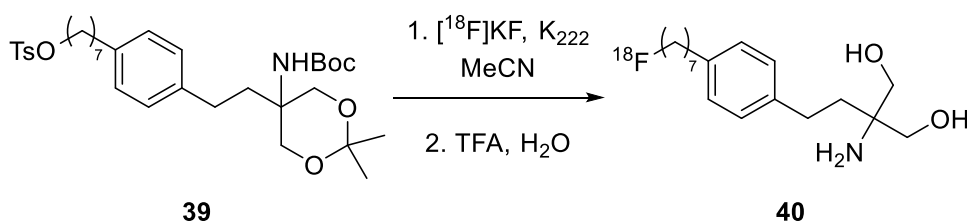
The drug fingolimod (**37**) (FTY720, trade name gilenya) is a compound that was approved by the European Medicines Agency in 2011 for the treatment of relapsing MS.<sup>99</sup> The compound is structurally very similar to S1P and was developed from SAR studies of the antibiotic myriocin. Fingolimod (**37**) is phosphorylated in the cell by sphingosine kinases to the active form (**38**) (Scheme 13).<sup>91</sup> Fingolimod-phosphate acts as an agonist for the S1P<sub>2</sub> and S1P<sub>5</sub> receptors, however, it is also a functional antagonist of S1P<sub>1</sub> and leads to the

sequestering of lymphocytes in lymph nodes preventing them from moving to sites of autoimmunity, transplanted organs and the CNS – averting a relapse in MS.<sup>99</sup>



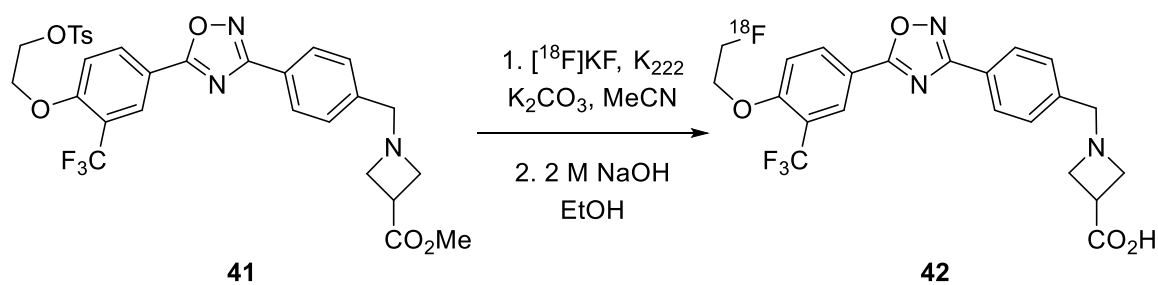
**Scheme 13: Phosphorylation of fingolimod (37) with sphingosine kinases**

Recent work by Shaikh *et al.* has generated various fluorinated structural analogues of fingolimod in an effort to develop a radiotracer (Scheme 14).<sup>91</sup> This was to study the organ distribution and pharmacokinetics of fingolimod and the S1P receptor biodistribution using PET. After testing the *in vitro* and *in vivo* biological activity of the radiotracer, *in vivo* biodistribution/PET imaging took place. PET revealed fast uptake and elimination of the tracer by the liver and the kidneys. An increased uptake was observed in S1P relevant tissues: the lungs and myocardium, as well as in the spleen.



**Scheme 14: Radiofluorination of fingolimod analogue precursor 39**

Rosenberg *et al.*, reported the synthesis and *in vitro* and *in vivo* evaluation of a S1P<sub>1</sub> PET tracer (Scheme 15).<sup>100</sup> After their screening process, they found a compound with a 2.63 nM potency for S1P<sub>1</sub> and selectivity >100-fold for S1P<sub>1</sub> over S1P<sub>2/3</sub>. This was successfully <sup>18</sup>F-labelled from the tosyl precursor **41** in both high yield and specific activity. The data collected suggests that uptake of this tracer reflects the expression of S1P<sub>1</sub> and has potential for use in quantifying S1P<sub>1</sub> expression in response to inflammation.



**Scheme 15: Radiosynthesis of S1P<sub>1</sub> PET tracer 42**

## 1.4 The Translocator Protein (TSPO)

### 1.4.1 Function and Distribution of TSPO

Since its discovery in 1977 by Braestrup and Squires, the translocator protein 18 kDa (TSPO) has been a major focus of research.<sup>101</sup> TSPO is expressed in a variety of different tissues and is involved in a number of cellular processes, including cholesterol transport, inflammation, tumour progression and, Parkinson's and Alzheimer's diseases.<sup>102</sup> In particular, TSPO is expressed at high levels in tissues that synthesise and distribute steroids, but in the CNS, TSPO expression is restricted mostly to glial cells.<sup>103</sup> At the subcellular level, TSPO localisation is mainly in the outer mitochondrial membrane.<sup>104</sup> This protein used to be known as the peripheral benzodiazepine receptor (PBR), however, it was renamed to TSPO to better describe its nature and function.<sup>103</sup>

Microglia are a type of glial cell located in the brain and spinal cord and act as brain-resident macrophages, maintaining local neurons and circuits.<sup>105</sup> These immune cells exist in their inactive form, but undergo change to an activated state in response to CNS inflammation that stimulates them to function as phagocytes.<sup>106</sup> Activation of microglia has been associated with a range of different neurodegenerative disorders such as MS, Parkinson's and Alzheimer's diseases amongst others. The receptor density of TSPO located in microglia cells in a healthy state is negligible, however, in response to CNS insults, expression of TSPO dramatically increases.<sup>106</sup> *In vivo* imaging of TSPO could therefore be an excellent target for understanding and treating diseases associated with neuro-inflammation.

The levels of TSPO expression are highest in steroid producing cells of the adrenal glands, testes and ovaries.<sup>102</sup> The expression in these tissues has led to the discovery that TSPO is responsible for the transport of cholesterol across the outer mitochondrial membrane, where it can be converted to pregnenolone before it is metabolised into specific steroids in a process called *de novo* steroidogenesis.<sup>107</sup> Indeed, studies have

shown that modulation of TSPO with the TSPO-specific ligand PK11195 (**41**), induced steroid hormone production in adrenocortical cell lines.<sup>108</sup> There is controversy in this area, as a report has shown that TSPO gene deletion in testicular Leydig cells had no effect on the production of testosterone.<sup>109</sup> However, studies to the contrary have been published (including embryonic lethality associated with TSPO gene deletion). As such, more research is required in this area.<sup>110,111</sup> TSPO is over-expressed in prostate cancer tissue and tumour cells have been shown to induce *de novo* steroidogenesis to evade the immune response.<sup>112</sup> The tumour-induced androgen synthesis results in resistance to androgen deprivation therapy and leads to the development of lethal metastatic castration resistant prostate cancer (mCRPC).<sup>113</sup> Thus, PET imaging of TSPO could give insight into the development of mCRPC and provide better tools for early detection.

### 1.4.2 Imaging agents for TSPO

The most widely used ligand for PET imaging of TSPO is the isoquinoline carboxamide [<sup>11</sup>C]PK11195 (**41**) (Figure 13).<sup>114</sup> Its widespread use notwithstanding, [<sup>11</sup>C]PK11195 (**41**) suffers from poor brain uptake and displays weak signal to noise ratio, complicating its quantification.<sup>115</sup> Additionally, the use of a <sup>11</sup>C-label limits the use of this tracer to facilities with an on-site cyclotron. Furthermore, labelling of this compound can be challenging due to its short half-life. Other attempts have been made to develop more effective imaging agents, however, except for PK11195 (**41**), the *in vitro* binding of these second-generation compounds (e.g. **42** and **43**) to human brain tissue is variable between different individuals due to TSPO single nucleotide polymorphism (rs6971).<sup>116,117</sup> These compounds can be categorised as high-affinity (HAB), low-affinity (LAB) or mixed-affinity binders (MAB).<sup>118</sup>

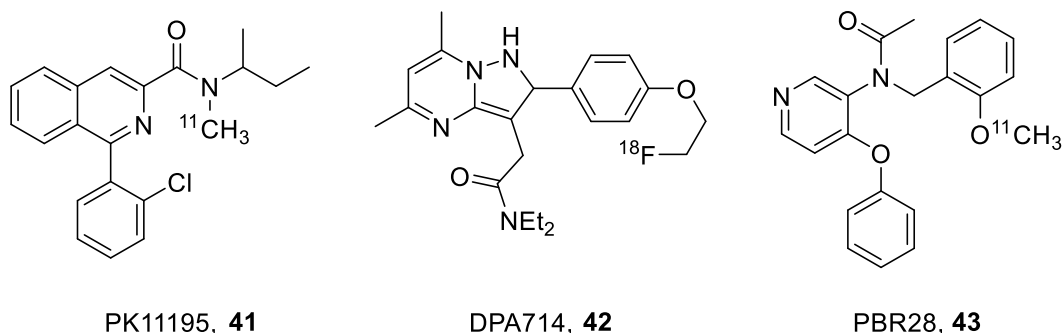
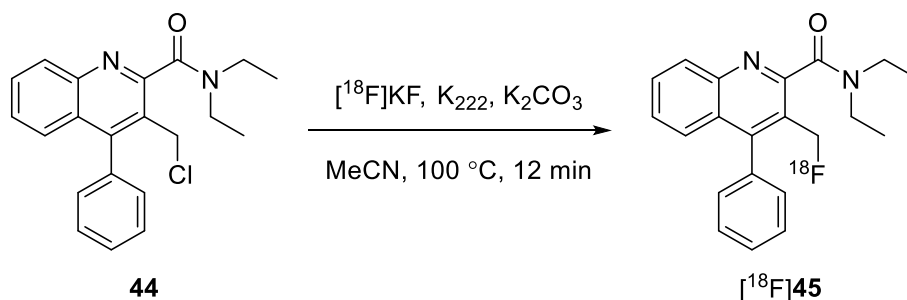


Figure 13: PK11195 (**41**) and second generation TSPO radiotracers

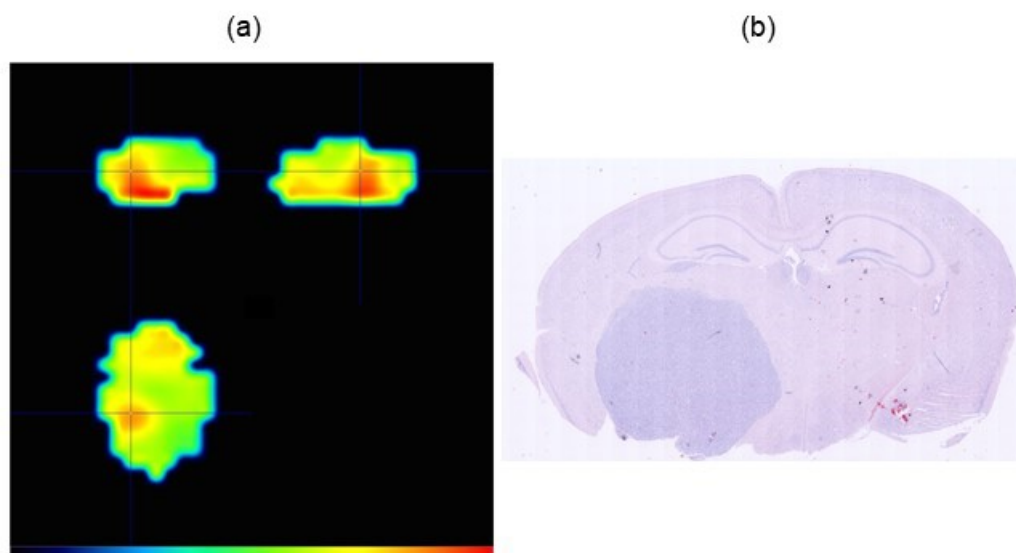
Considering this, Blair *et al.*, in 2015, reported the synthesis, biological evaluation and physicochemical properties of a novel 3-fluoromethylquinoline-2-carboxamide, AB5186 (**45**), for PET imaging of TSPO (Scheme 16).<sup>119</sup> Studies conducted previously in the

Sutherland group had revealed the rigidity and steric factors caused by the bulky amide and benzene moiety allowed for efficient binding to TSPO.<sup>120</sup> Competition binding assays measuring the displacement of PK11195 (**41**) revealed that AB5186 (**45**) has low nanomolar affinity for TSPO ( $K_i = 2.8$  nM). The key physicochemical parameters of AB5186 (**45**) ( $P_m$ ,  $K_m$  and %PPB) were also found to be optimal for use as an imaging agent.<sup>119</sup> A radiofluorination method was developed, involving a halogen exchange reaction from the chloride precursor **44**. This was treated with [<sup>18</sup>F]fluoride and Kryptofix<sup>®</sup> 222 at 100 °C for 12 min to afford [<sup>18</sup>F]AB5186 (**45**) in a RCY of  $38 \pm 19\%$  ( $n = 7$ ).<sup>119</sup>



**Scheme 16: Radiosynthesis of [<sup>18</sup>F]AB5186 (**45**)**

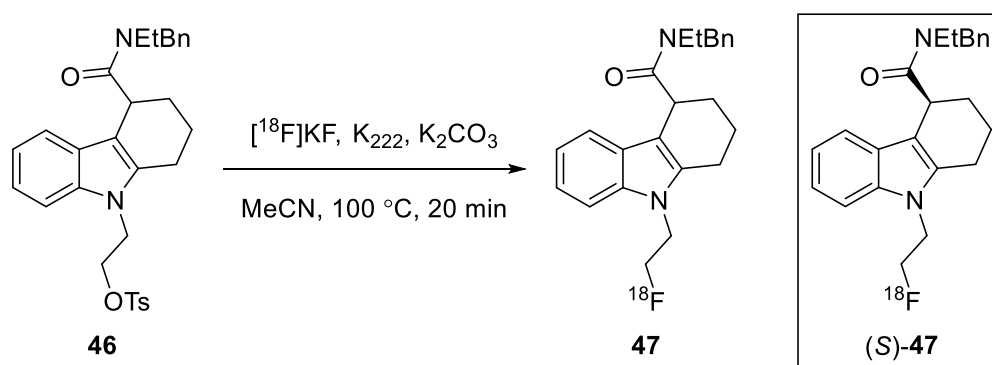
To investigate the behaviour of [<sup>18</sup>F]AB5186 (**45**) *in vivo*, *ex vivo* autoradiography was performed using glioma bearing mice and showed specific binding of [<sup>18</sup>F]AB5186 (**45**) to TSPO in tumour tissue.<sup>119</sup> [<sup>18</sup>F]AB5186 (**45**) could image TSPO in an intracranial glioma bearing mouse (Figure 14) and a PET scan was also successfully performed on a healthy baboon to show that [<sup>18</sup>F]AB5186 (**45**) was indeed capable of penetrating the blood-brain barrier (BBB) of a non-human primate.



**Figure 14: (a) PET image of a glioma bearing mouse following [ $^{18}\text{F}$ ]AB5186 (**45**) injection; (b) H&E staining of the tumour which stains dark blue**

(This research was originally published in *Chem. Sci.*, 2015, 6, 4772–4777. Published by The Royal Society of Chemistry)

In 2019, Qiao *et al.* reported the radiosynthesis of a TSPO radiotracer (*R,S*)-[ $^{18}\text{F}$ ]GE387 (**47**) (Scheme 17).<sup>121</sup> In order to test the affinity of this compound, a separation of the two enantiomers from the racemic material was desired. The use of a chiral derivatisation group to separate the diastereomers proved unsuccessful and the authors resorted to supercritical fluid chromatography to obtain the enantiopure compounds. The authors reported that the (*S*)-enantiomer showed low binding sensitivity to the polymorphism present in TSPO, using assays based on human embryonic cell lines. Their studies show that (*S*)-**47** binds with similar affinity to PK11195 and a LAB:HAB ratio of 1.3. Radiofluorination of the precursor **46** occurred after 20 min at 100 °C and the radiolabelled product was isolated in  $20.8 \pm 4.5\%$  RCY and with a molar activity of  $93.2 \pm 50.6$  GBq  $\mu\text{mol}^{-1}$  ( $n = 9$ ). Further biological evaluation of this radiotracer is ongoing.



**Scheme 17: Radiosynthesis of (*R,S*)-[ $^{18}\text{F}$ ]GE387 (**47**)**

## 2 Results and Discussion

### 2.1 New Selective PET Imaging Agents for the Sphingosine-1-Phosphate 5 Receptor

#### 2.1.1 Project Aims

The focus of this work was to develop tools to allow an understanding of the interdependence of S1P<sub>5</sub> receptors in demyelination, in particular, to focus on the design of PET imaging agents that act as S1P<sub>5</sub> agonists in the human brain. The first main objective was to synthesise a small library of compounds that specifically target the S1P<sub>5</sub> receptor. Using the benzamide compounds previously described by Mattes *et al.* as the basis for potential imaging agents (Figure 15), a synthetic route towards fluoride analogues of these compounds would be developed.<sup>95</sup> Crystal structure docking experiments carried out on the literature benzamide compounds showed that the methyl group at the top of the molecule was furthest from the binding pocket. As such, it was proposed that an ideal radiotracer would have the fluorine atom in this position. The libraries of compounds would be based on three of the most promising compounds from the literature: benzamide **31**, phthalazinone **32** and 3-methyl benzamide **33** (Figure 15). The most promising compounds would be assessed by physicochemical analysis using HPLC methodology and then tested for their affinity and selectivity for S1P<sub>5</sub>.<sup>122</sup> A precursor would be synthesised that would allow for <sup>11</sup>C-labelling of the most potent compound in the literature study, 3-methyl benzamide **33**, as this would provide insight into the behaviour of these compounds as PET radiotracers.

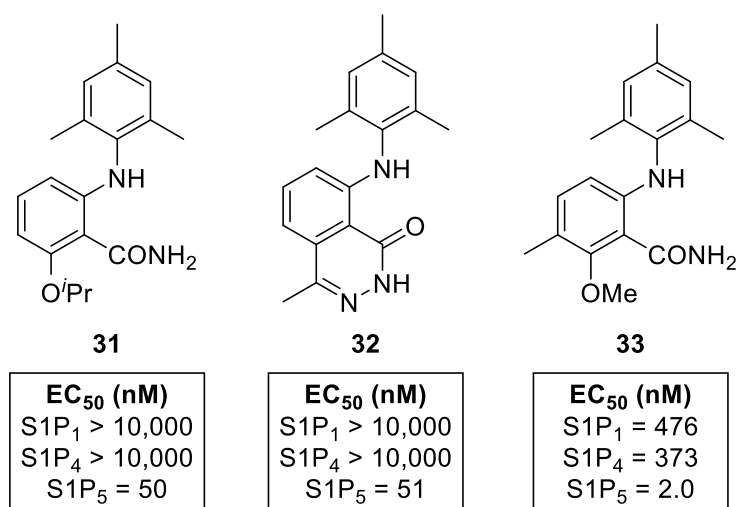
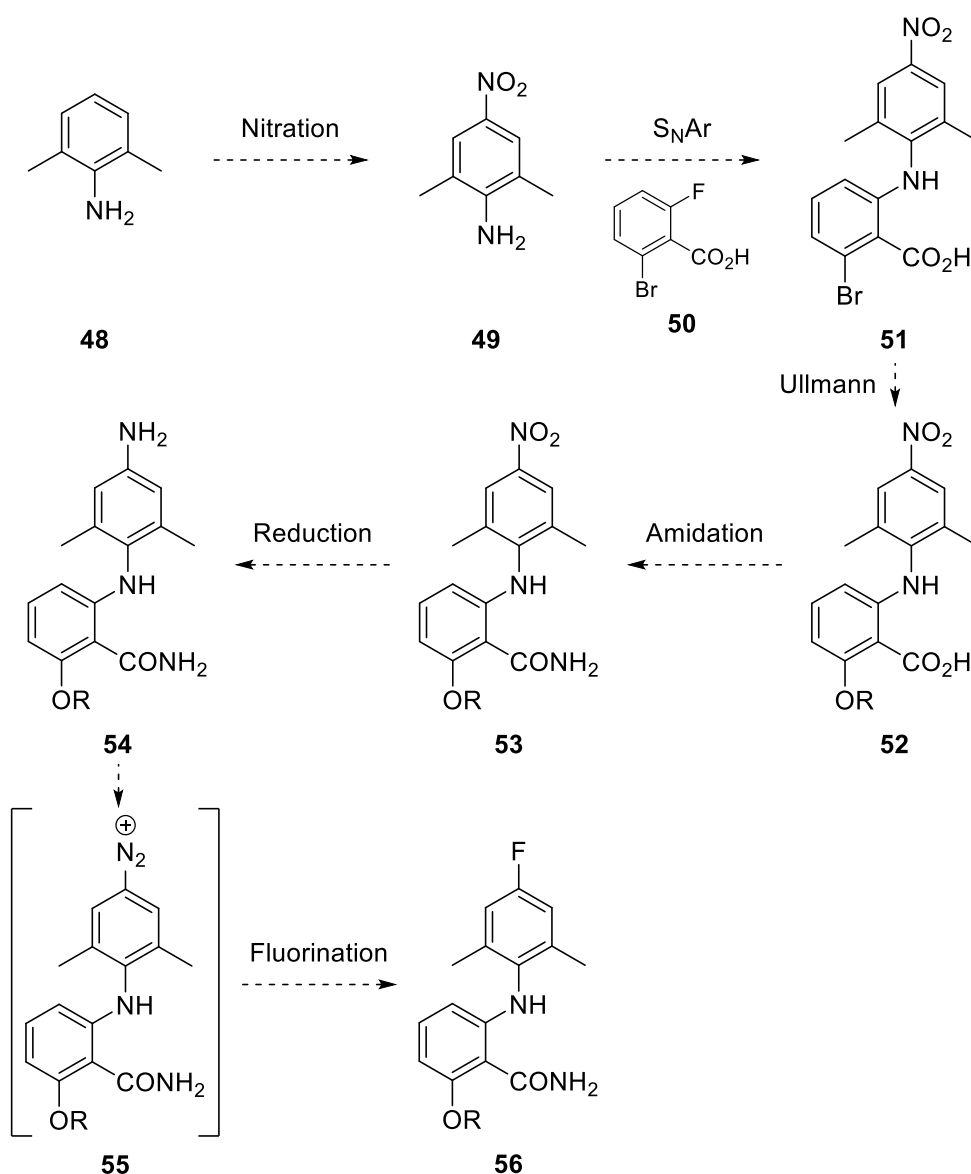


Figure 15: S1P<sub>5</sub> selective benzamide analogues

## 2.1.2 Synthesis of Fluoro-Benzamide Library

### 2.1.2.1 Proposed route

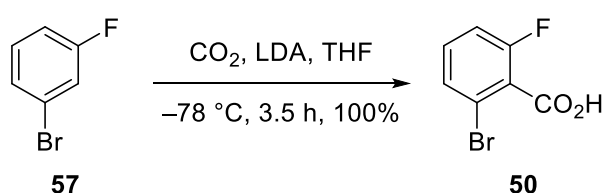
To incorporate a functional handle that could be used for late-stage fluorination of these compounds, a route was proposed that would allow access to fluorinated analogues of **31**. This began with the *para*-nitration of 2,6-dimethylaniline (**48**) to give aniline **49** and subsequent S<sub>N</sub>Ar reaction with benzoic acid **50** to give compound **51** (Scheme 18). Ullmann condensation reactions with various alcohols could be used to incorporate the ether substituent and amidation of the carboxylic acid group would provide the nitrated analogues **53**. The nitro group would then be reduced to an amine and the compound **54** could be fluorinated *via* diazonium salt **55** according to literature precedent.<sup>123</sup>



Scheme 18: Proposed route for functionalised derivatives

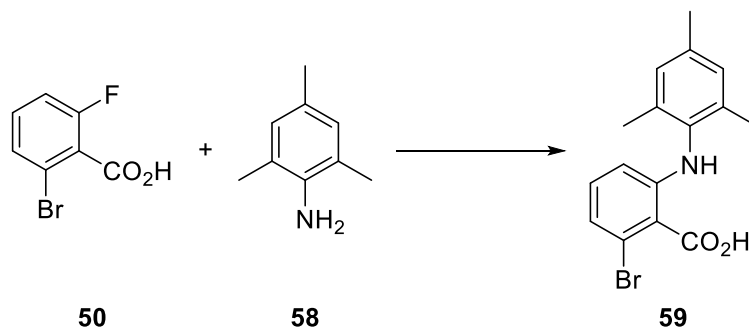
### 2.1.2.2 Optimisation of the synthetic route

Prior to nitration of aniline **48**, synthesis of benzamide **31** began in order to optimise the literature route. Multi-gram quantities of the required benzoic acid **50** were synthesised from the corresponding dihalobenzene **57** using a literature procedure (Scheme 19).<sup>124</sup> The carboxylation of the 1,3-dihalobenzene proceeded *via* directed *ortho*-metalation (DoM). Initially, LDA regioselectively deprotonated the halobenzene between the two halogens: both the fluorine and the bromine act as directing groups and enhance the acidity of the mutually *ortho*-hydrogen atom. Subsequent addition of CO<sub>2</sub> as the electrophile followed by acidic work-up afforded the desired benzoic acid **50** in a quantitative yield.



**Scheme 19: DoM of dihalobenzene **57** and subsequent carboxylation to form **50****

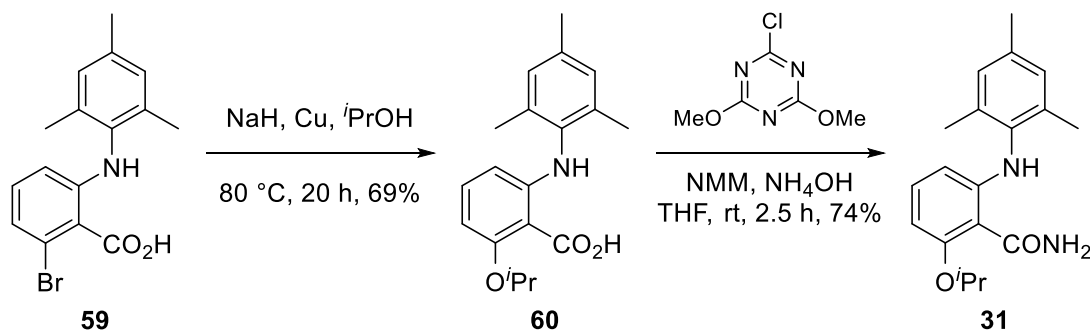
The next step involved the synthesis of the core structure **59** *via* an S<sub>N</sub>Ar reaction between benzoic acid **50** and 2,4,6-trimethylaniline (**58**) (Table 3). The first attempt employed conditions described in the Novartis paper, using LDA to deprotonate aniline **58** and allowing the reaction to warm to room temperature to perform the S<sub>N</sub>Ar reaction with **50** (entry 1).<sup>95</sup> After 20 h, only a 28% conversion to the product was observed by <sup>1</sup>H NMR spectroscopy. Substitution of LDA for LiHMDS, according to a similar literature reaction, allowed for a 100% conversion to the product after 72 h (entry 2).<sup>125</sup> However, this method only returned the desired product in 13% yield. It was proposed that the slow conversion in this reaction was due to the desired site of nucleophilic attack of **50** being *ortho*- to the deprotonated carboxylic acid, combined with the nucleophile being *ortho,ortho*-disubstituted. Consequently, it was found that heating the reaction to 40 °C allowed for a faster conversion and the desired S<sub>N</sub>Ar product **59** was isolated in 94% yield (entry 3).

Table 3: S<sub>N</sub>Ar reaction to form core structure **59**

Entry	Reagents	Temperature	Time	Yield
1	LDA, THF	-78 °C to rt	20 h	28% conversion
2	LiHMDS, THF	-78 °C to rt	72 h	13%
3	LiHMDS, THF	-78 to 40 °C	16 h	94%

To incorporate the ether substituent, the bromide of **59** was used in an Ullmann condensation reaction with isopropanol (Scheme 20). Ullmann condensations between an aryl halide and alcohol or amine nucleophile have been shown to work well with a variety of different copper catalysts, including sources of Cu(0), Cu(I) and Cu(II).<sup>126</sup> The mechanism of this reaction is widely disputed, however, the reactivity for the aryl halide is in the order I > Br > Cl, which implies the copper catalyst is somehow involved in its activation.<sup>127</sup> Aryl bromides have been shown to be more reactive when they possess an electron-withdrawing group in the *ortho*-position, making aryl bromide **59** an ideal substrate.<sup>128</sup> In this reaction, initial deprotonation of isopropanol with NaH was performed before addition of aryl bromide **59** and copper powder. After 20 h, the reaction was complete and ether-bearing product **60** was isolated in 69% yield.

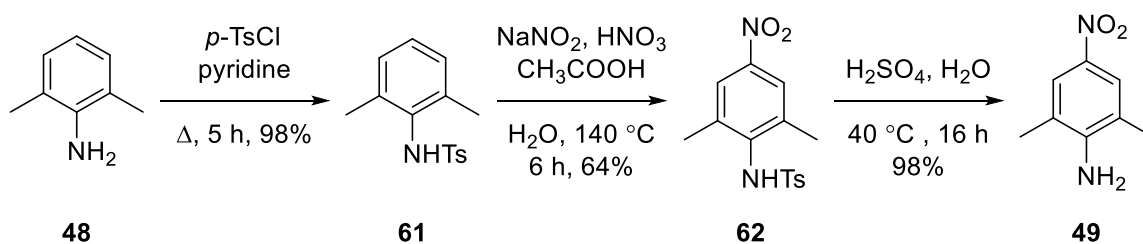
Following the Ullmann condensation reaction, the carboxylic acid of **60** was converted to an amide to give benzamide **31** (Scheme 20). This reaction utilised the coupling reagent CDMT (2-chloro-4,6-dimethoxy-1,3,5-triazine), which in the presence of NMM, formed the reactive intermediate 4-(4,6-dimethoxy-1,3,5-triazin-2-yl)-4-methylmorpholinium chloride (DMTMM) *in situ*.<sup>129</sup> Reaction of carboxylic acid **60** with DMTMM *via* an S<sub>N</sub>Ar mechanism yielded the activated ester, which upon addition of NH<sub>4</sub>OH, formed the benzamide product **31** in 74% yield.



**Scheme 20: Ullmann condensation and subsequent amidation to form benzamide 31**

### 2.1.2.3 Synthesis using nitrated analogue

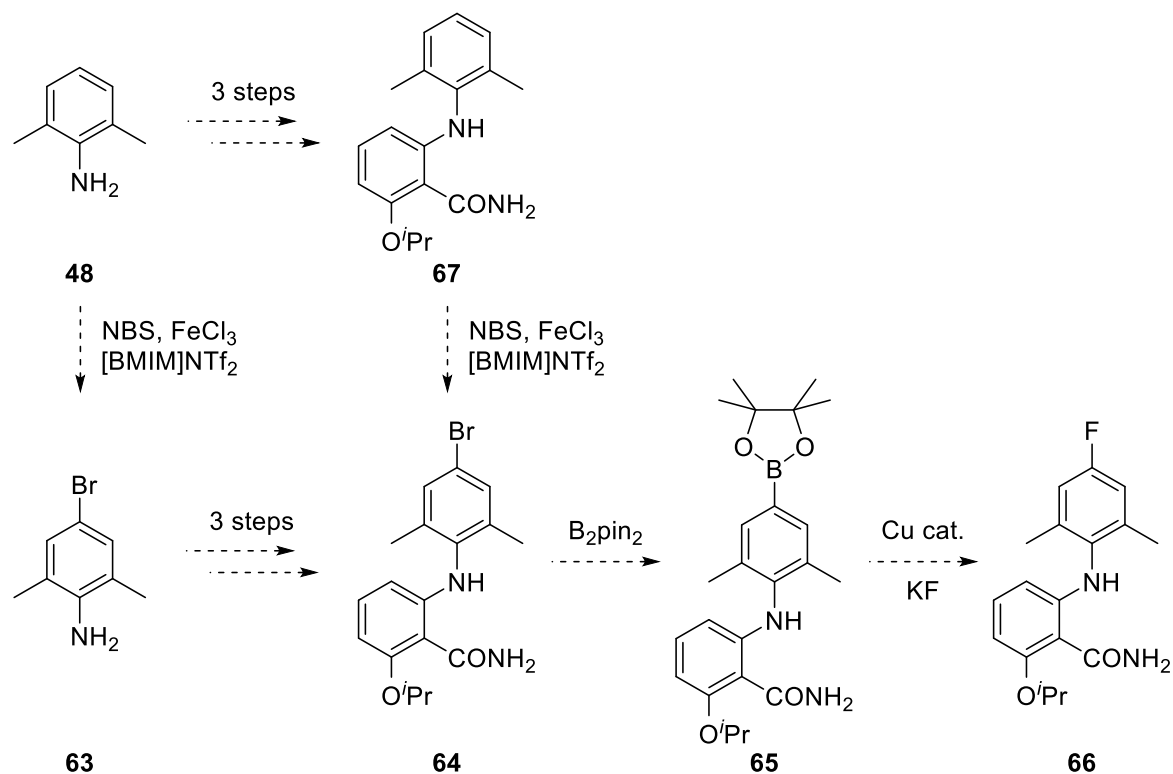
The first step in this synthesis involved the *para*-nitration of 2,6-dimethylaniline (**48**) to form **49**. This could not be achieved using a traditional one-step approach with nitric and sulfuric acids, as the aniline becomes protonated in acidic conditions. This anilinium cation acts as a *meta* director, forming both *meta*- and *para*-nitrated products. Instead, a three-step process was utilised. Following a literature procedure, the amine was first protected with a tosyl group, using *p*-toluenesulfonyl chloride in pyridine to afford product **61** in 98% yield (Scheme 21).<sup>130</sup> Regioselective electrophilic aromatic substitution at the *para* position was performed using sodium nitrite under acidic conditions and afforded a single nitrated product **62** in 64% yield. The tosyl group was removed using sulfuric acid to afford 2,6-dimethyl-4-nitroaniline (**49**) in 98% yield.



**Scheme 21: *para*-Nitration of aniline 48**

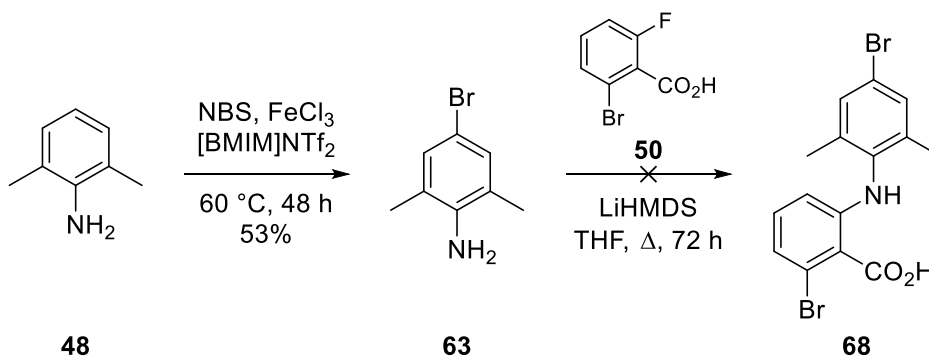
The reaction of nitrated aniline **49** with benzoic acid **50** was first attempted at 40 °C (Scheme 22). When no conversion to product was observed after 16 h, the reaction was heated under reflux. After a further 12 h, still no conversion could be observed. It was assumed that the explanation for no reaction was due to **49** being a very poor nucleophile: the presence of a *para*-nitro group made the aromatic ring very electron-deficient; furthermore, the aniline was poorly soluble in THF. The reaction was attempted again by





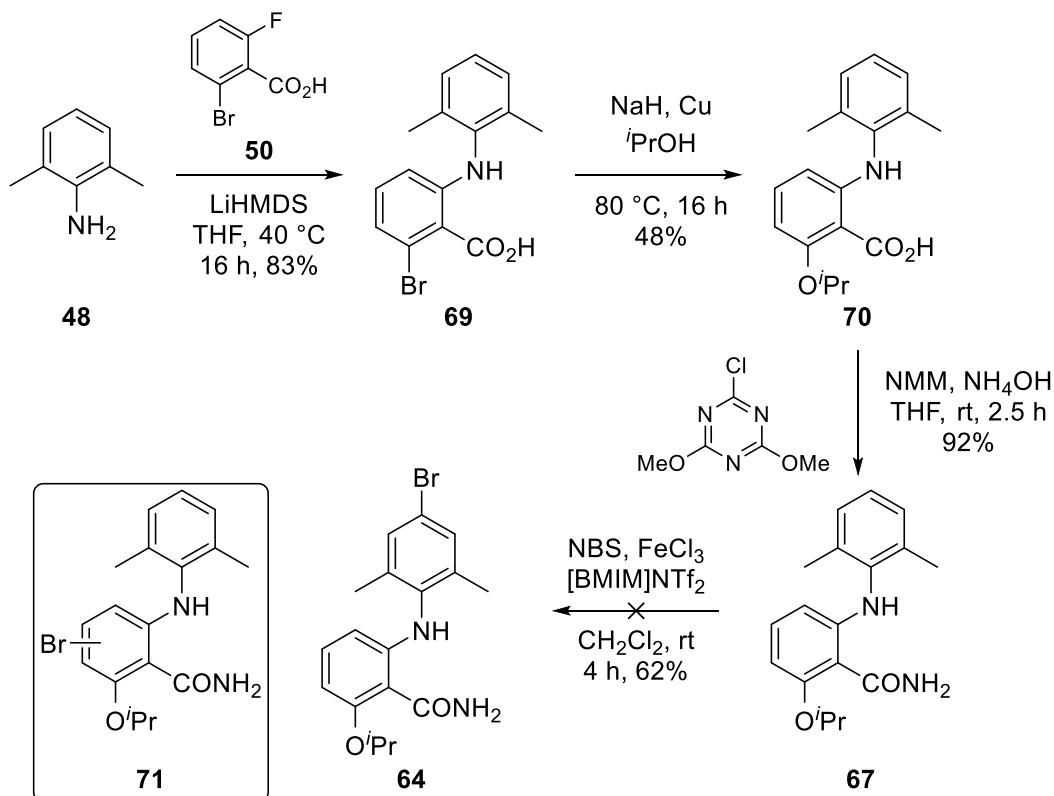
**Scheme 23: Alternative routes to target 64**

Bromination of **48** was first attempted at room temperature using conditions described in the literature (Scheme 24).<sup>131</sup> After 16 h of reaction time, there was no evidence of any product being formed. Therefore, the reaction was heated to 60 °C and full conversion to the desired product was observed after 48 h, giving aniline **63** in 53% yield. The  $\text{S}_{\text{N}}\text{Ar}$  reaction between benzoic acid **50** and aniline **63** was unsuccessful using the previously optimised conditions and yielded no product. When the reaction was heated under reflux and allowed to react over a longer period of 72 h, still no conversion was observed. It was assumed that the bromine atom had a similar deactivating effect on aniline **63** as the nitro group had on the previously described reaction. Thus, synthesis of brominated analogue **64** was attempted *via* the alternative route.



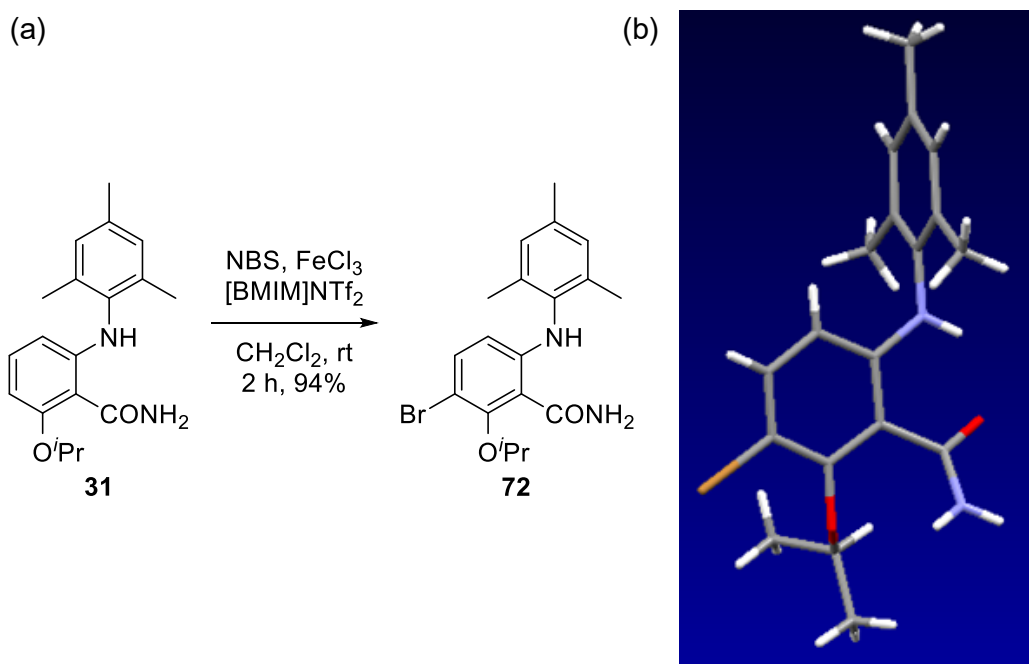
**Scheme 24: Bromination of aniline 48 and attempted  $S_NAr$  reaction with 63**

Reaction of aniline **48** with benzoic acid **50** occurred as expected using the previously optimised conditions and afforded **69** in 83% yield (Scheme 25). The subsequent Ullmann condensation with isopropanol and the following amidation reaction occurred in 48% and 92% yields, respectively. To perform the bromination reaction, it was necessary to dilute the reaction mixture in dichloromethane, as benzamide **67** was poorly soluble in the ionic liquid. Bromination of **67** yielded an inseparable mixture of mono- and di-brominated products. Further inspection of the  $^1\text{H}$  NMR spectrum of the mixture showed that the 3H multiplet corresponding to the three aryl protons of the upper ring was still present. Therefore, the mixture of products contained bromine in the C-3 and C-5 positions of the lower ring. It was not possible to determine which position was the initial site of bromination, so further analysis of this reaction was performed.



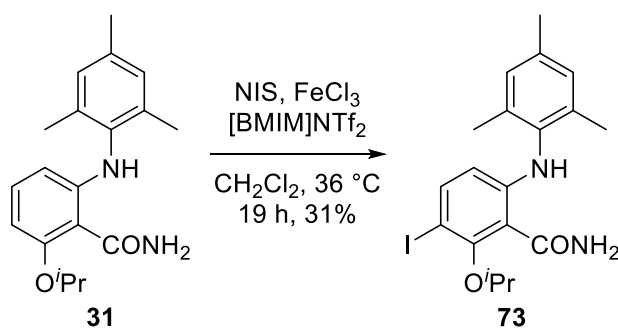
**Scheme 25: Bromination of 67 to form target 64**

The previously synthesised benzamide **31** was subjected to the bromination reaction conditions (Scheme 26a). Using 0.8 equivalents of NBS, it was possible to control the rate of bromination to synthesise a single mono-brominated product **72** in 77% yield. It was initially believed that examination of the structure of **31**, using NOE NMR experiments would provide insight into the site of bromination. However, the NOE difference spectra from irradiation of the signals of the isopropanol protons and of the *ortho*-methyl groups of the upper ring were inconclusive. Consequently, brominated product **72** was recrystallised from a mixture of  $\text{CH}_2\text{Cl}_2$  and hexane and a small molecule crystal structure was obtained (Scheme 26b). This clearly showed only bromination of the C-3 position and also demonstrated the significant twisting of the two aryl rings across the bridging nitrogen atom.



**Scheme 26: (a) Bromination reaction and (b) crystal structure of brominated product 72**

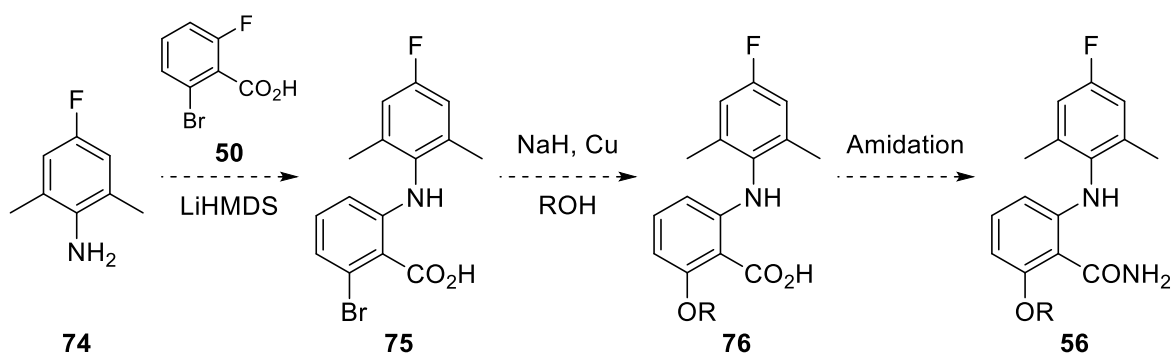
Given the successful incorporation of bromine into the structure, it was proposed that an iodine atom could be introduced using the same method and NIS (Scheme 27). This was proposed as a target, as this could be used as a SPECT radiotracer if labelled with [ $^{123}\text{I}$ ]iodide. An iodinated compound may also have more favourable pharmacokinetics, due to the added lipophilicity of the iodine atom. Under the same conditions used for the bromination only low conversion to product was observed after 16 h. By heating to 40 °C and adding 1 equivalent of NIS at the start of the reaction, before further addition of 0.4 equivalents after 16 h, it was possible to achieve full conversion to the product. Although NIS is a better electrophile than NBS due to the weaker nitrogen-iodine bond, the increased size of the iodine may have hindered this reaction. Hence, the reaction time was increased compared with the bromination conditions and iodinated analogue **73** was isolated in 31% yield.



**Scheme 27: Synthesis of iodinated analogue 73**

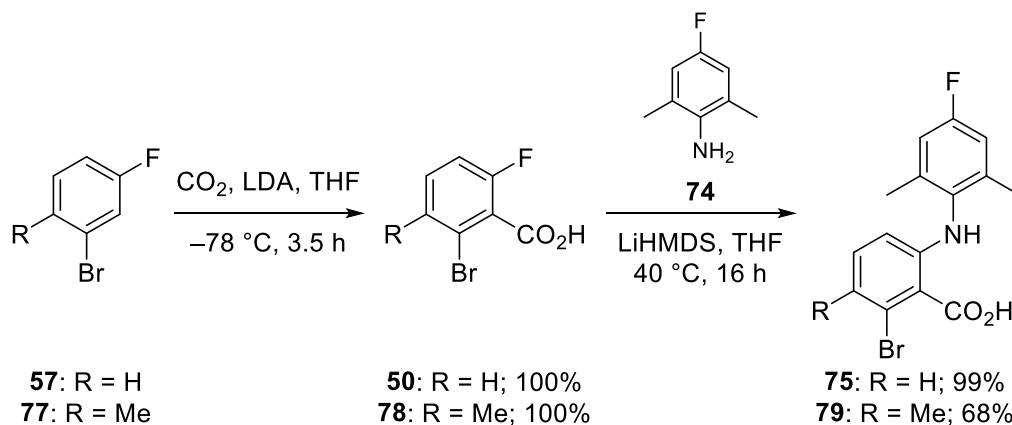
### 2.1.2.5 Incorporation of fluorine at an earlier stage of the synthesis

Since it was not possible to synthesise brominated analogue **64** due to the lower ring being more electron rich, a new route was proposed (Scheme 28). This involved the direct incorporation of fluorine *via* an  $S_NAr$  reaction between commercially available fluoroaniline **74** and benzoic acid **50**, with the rest of the synthesis proceeding as previously described. The obvious drawback to using this method was that fluorine was not incorporated in the final step and therefore the route would not be applicable to a radiosynthesis. Notwithstanding, it was deemed more crucial to synthesise derivatives that could be tested for their affinity and selectivity for  $S1P_5$  receptors. If there were any promising compounds after biological screening, time could then be spent on synthesising an appropriate precursor for radiofluorination.



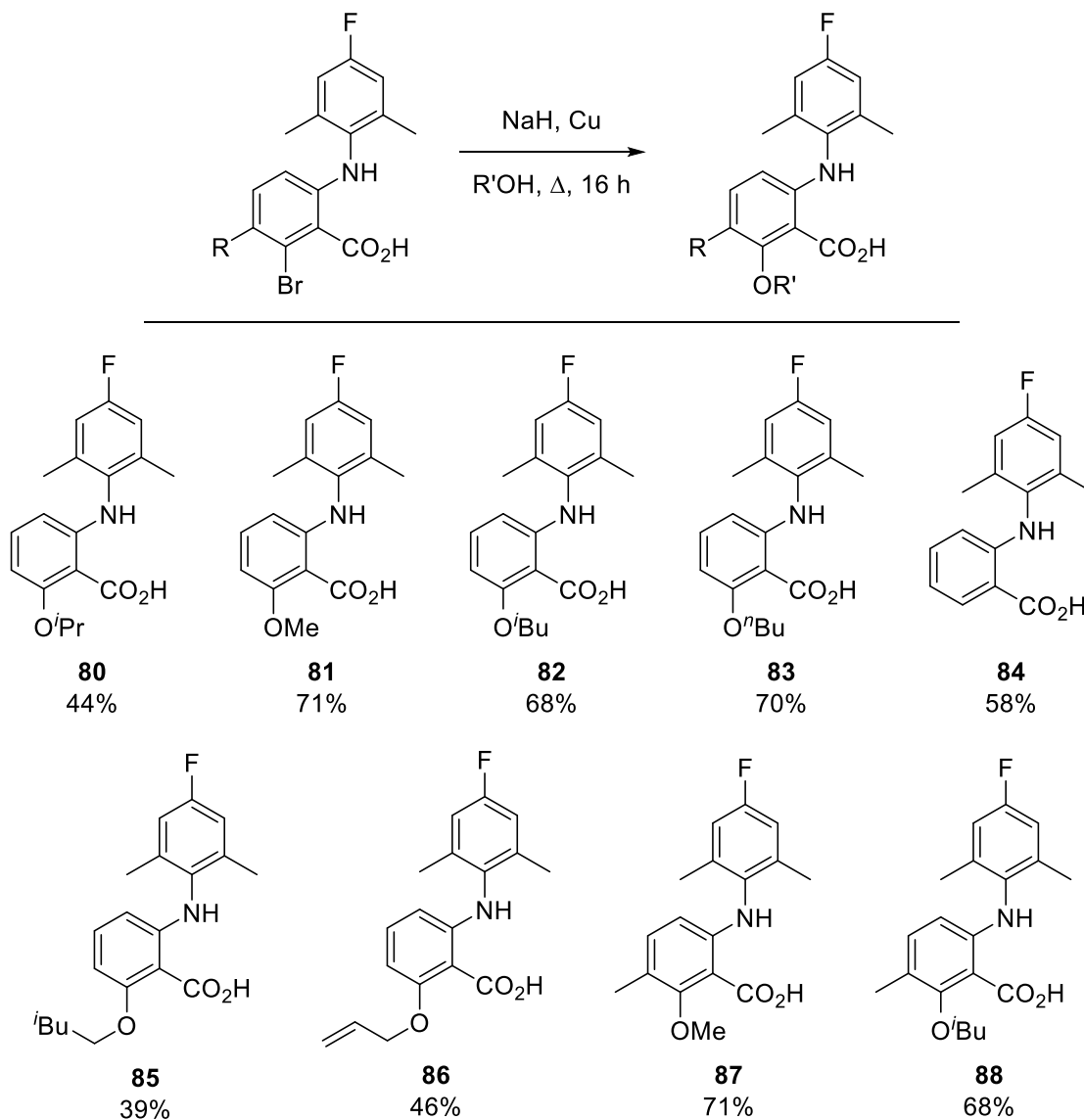
**Scheme 28: Proposed route towards fluorinated analogues**

One of the more promising benzamide compounds synthesised by Novartis featured a methyl group in the C-3 position of the benzamide ring (**33**). To provide a fluorinated analogue of this compound, benzoic acid **78** would need to be synthesised from the corresponding dihalobenzene **77** (Scheme 29). The reaction proceeded as previously described for **50** and benzoic acid **78** was isolated in a quantitative yield. The following  $S_NAr$  reaction with fluoroaniline **74** proceeded in an excellent yield to afford the des-methyl derivative **75**. However, the yield was reduced somewhat for the 3-methyl derivative, yielding product **79** in 68% yield.



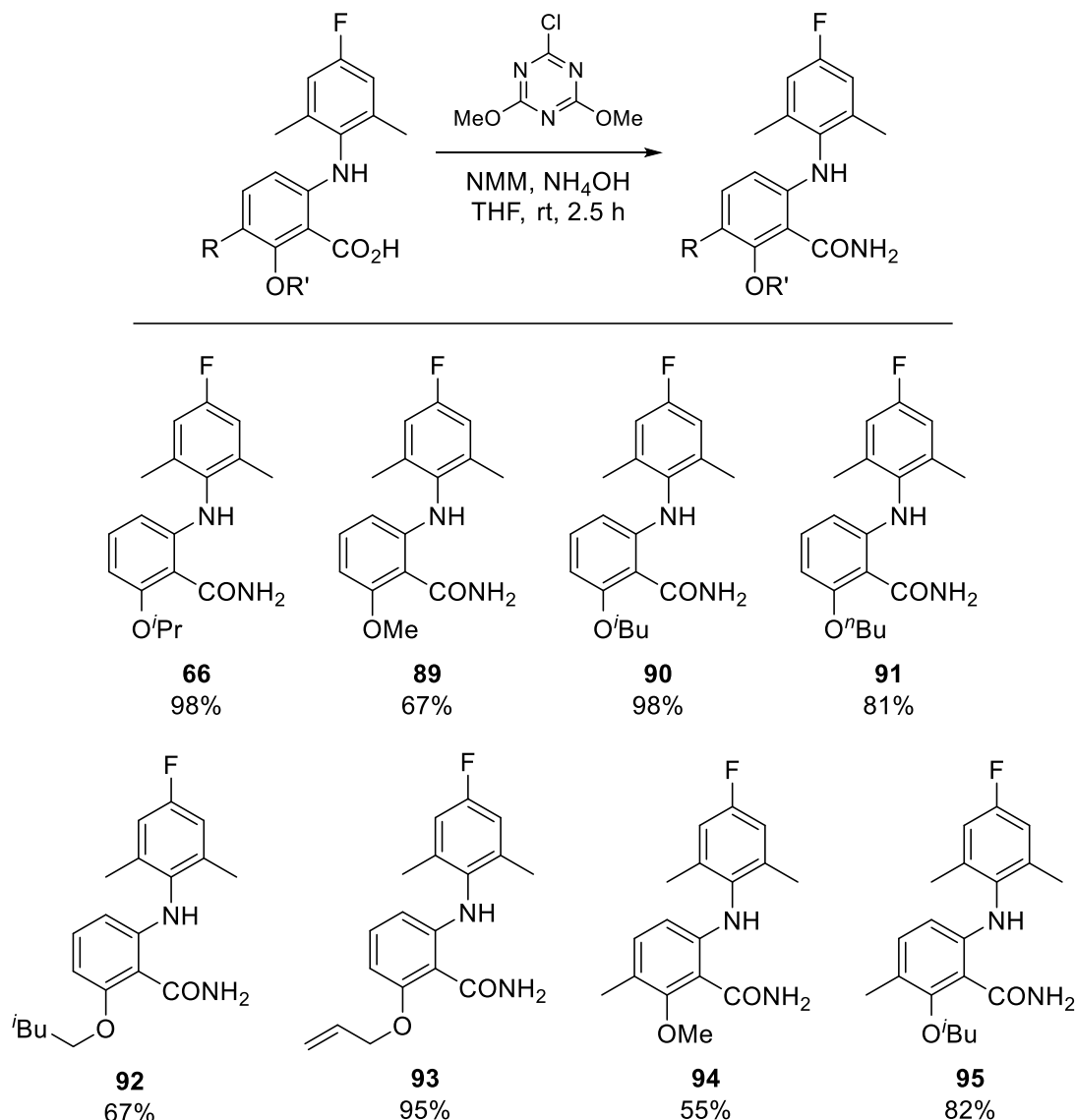
**Scheme 29: Carboxylation and S<sub>N</sub>Ar reaction of 3-H and 3-Me analogues**

To produce a small library of fluorobenzamide derivatives, the ether was varied by performing an Ullmann condensation reaction with various alcohols (Scheme 30). The isopropoxy (**80**) and methoxy (**81**) derivatives were synthesised in 44% and 71%, respectively, to provide fluorinated analogues of compounds previously synthesised in the Novartis paper.<sup>95</sup> However, to better explore the structure activity relationship of these compounds, other novel structures were synthesised. Isobutyl and *n*-butyl ethers were synthesised successfully in 68% and 70% yields, respectively, but reaction with *tert*-butanol afforded the debrominated product **84** in 58% yield. This was due to the poor nucleophilicity of the *tert*-butanol anion and so the reaction followed a proto-decupration mechanism instead. A similar result was observed when using isopropylamine as the coupling partner. Coupling of aryl bromide **75** with 3-fluoropropan-1-ol took place in THF rather than neat reaction conditions and provided terminal alkene product **86**, which was isolated in 46% yield. It was proposed that the desired product had been synthesised, but under the conditions of the reaction the alkene formed *via* an E1<sub>cb</sub> mechanism. Reaction of 3-methyl derivative **79** with methanol and also with isobutanol provided the products **87** and **88** in 71% and 68% yields, respectively. However, reaction with isopropanol or more sterically hindered alcohols was not successful and yielded debrominated analogue **84**. It was proposed that the *ortho,ortho*-disubstitution of this aryl bromide made this position less accessible.



**Scheme 30: Ullmann condensation reaction with various alcohols**

The amidation reaction to form the final fluorobenzamide products was straightforward and high yielding, affording the products in good to excellent yields (Scheme 31). The yield of the reaction was independent of the size of the ether substituent installed, but as sufficient quantities of the compounds had been synthesised for biological screening, no further optimisation of the reaction was considered.



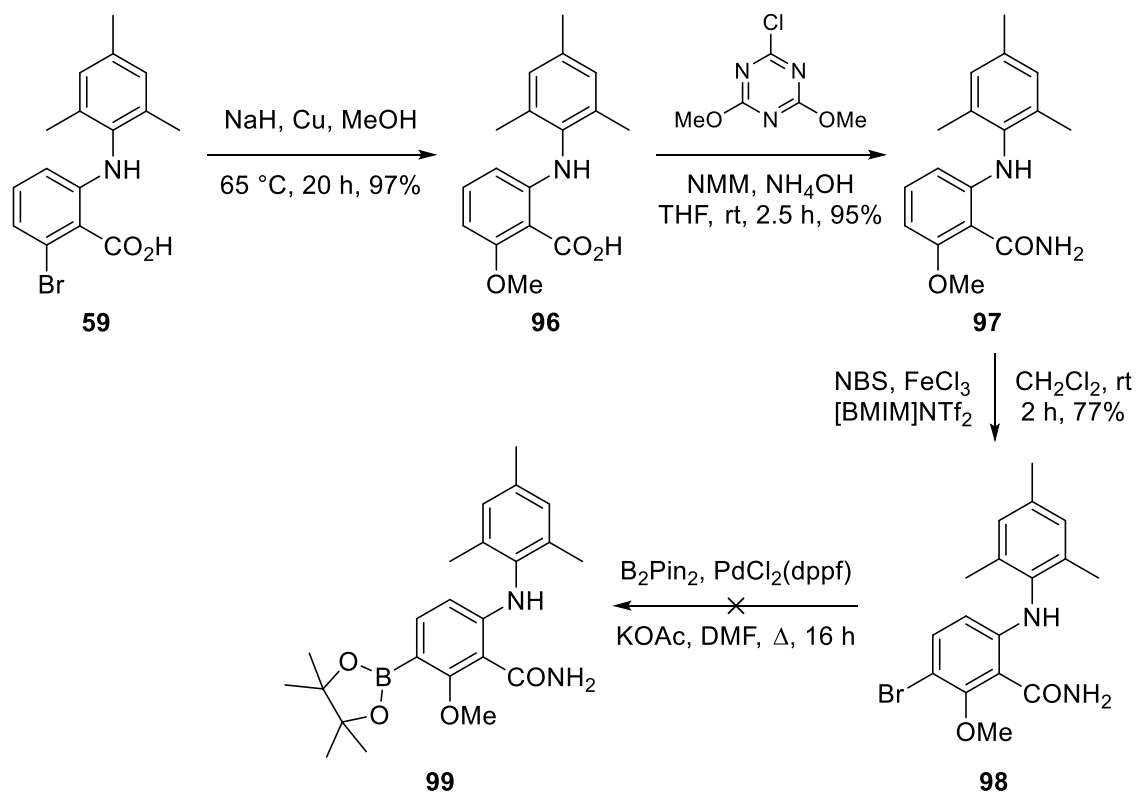
**Scheme 31: Amidation reaction to form final products**

## 2.1.3 Synthesis of 3-Substituted Benzamide Library

### 2.1.3.1 Synthesis of aryl bromide 98

The unexpected site of bromination observed in the reaction to form **72** (see section 2.1.2.4) inspired a new class of compounds. Since the bromination occurred in the C-3 position of the benzamide ring, this reaction could be used to provide aryl derivatives of potent compound **33**, described in the literature by Mattes *et al.*<sup>95</sup> The previously synthesised aryl bromide **59** was subjected to the Ullmann condensation reaction using methanol to give methoxy derivative **96** in 97% yield (Scheme 32). This was then successfully converted to benzamide **97** in 95% yield and then bromination using NBS gave brominated analogue **98** in 77% yield. Several attempts were made to incorporate a boronic ester in the structure *via* a Miyaura borylation reaction, which could then be used

as a precursor for fluorination. However, the reaction returned only the debrominated product **97** *via* a proto-depalladation mechanism.



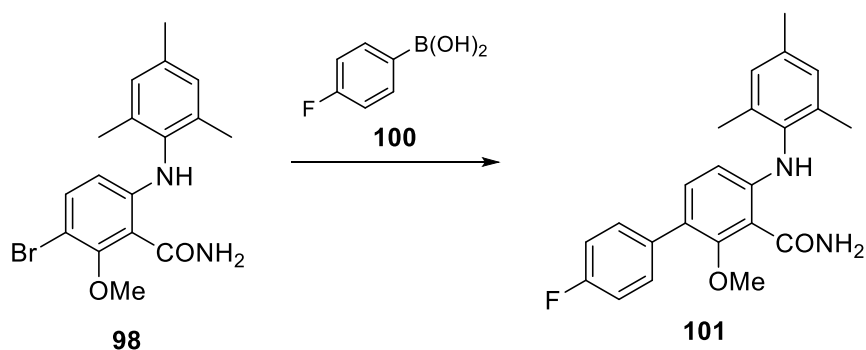
**Scheme 32: Synthesis of aryl bromide 98 and attempted Miyaura borylation**

### 2.1.3.2 Suzuki-Miyaura reaction

It was proposed that a Suzuki-Miyaura reaction would be a robust method for incorporating a range of aryl groups, containing either fluoride or methoxy substituents.<sup>135</sup> These compounds would have an advantage on those from the previous library, as the fluorine-18 or carbon-11 nuclide could be incorporated in the final step.<sup>47,136</sup> Consequently, a screening of reaction conditions took place using 4-fluorophenylboronic acid (**100**) as a coupling partner (Table 4). The initial reaction took place using  $\text{Pd}(\text{PPh}_3)_4$  as the catalyst, with  $\text{KH}_2\text{PO}_4$  as the base in DMF (entry 1). After 16 h, it was clear that none of the desired product had formed and analysis of the  $^1\text{H}$  NMR spectrum of the crude material showed only starting material and evidence of decomposition. It was proposed that decomposition may have been due to the high temperature, so the reaction was attempted again at  $80\text{ }^\circ\text{C}$  and the base was substituted for  $\text{K}_3\text{PO}_4$  (entry 2). Although there was not the same evidence of decomposition, after 48 h there was only the presence of starting material in the reaction. Changing the base to  $\text{K}_2\text{CO}_3$  and using similar conditions yielded the same result (entry 3). The catalyst was changed to  $\text{PdCl}_2(\text{dppf})$ , due to its reported air and moisture sensitivity and enhanced reactivity compared to other palladium catalysts.<sup>137</sup>

When  $\text{Cs}_2\text{CO}_3$  was used as a base in dioxane, full conversion of starting material was achieved in 16 h (entry 4). This provided a 3:1 mixture of coupled product **101** and debrominated analogue **97** in 92% yield. Since proto-depalladation had taken place, it implied that there was ineffective transmetalation in the reaction and it was believed this may have been due to poor solubility of the base in dioxane. Since Suzuki-Miyaura reactions can take place in aqueous media, a small quantity of water was added to the reaction mixture to improve the solubility of  $\text{Cs}_2\text{CO}_3$  and the desired product was isolated as a single product in 71% yield (entry 5).<sup>138</sup>

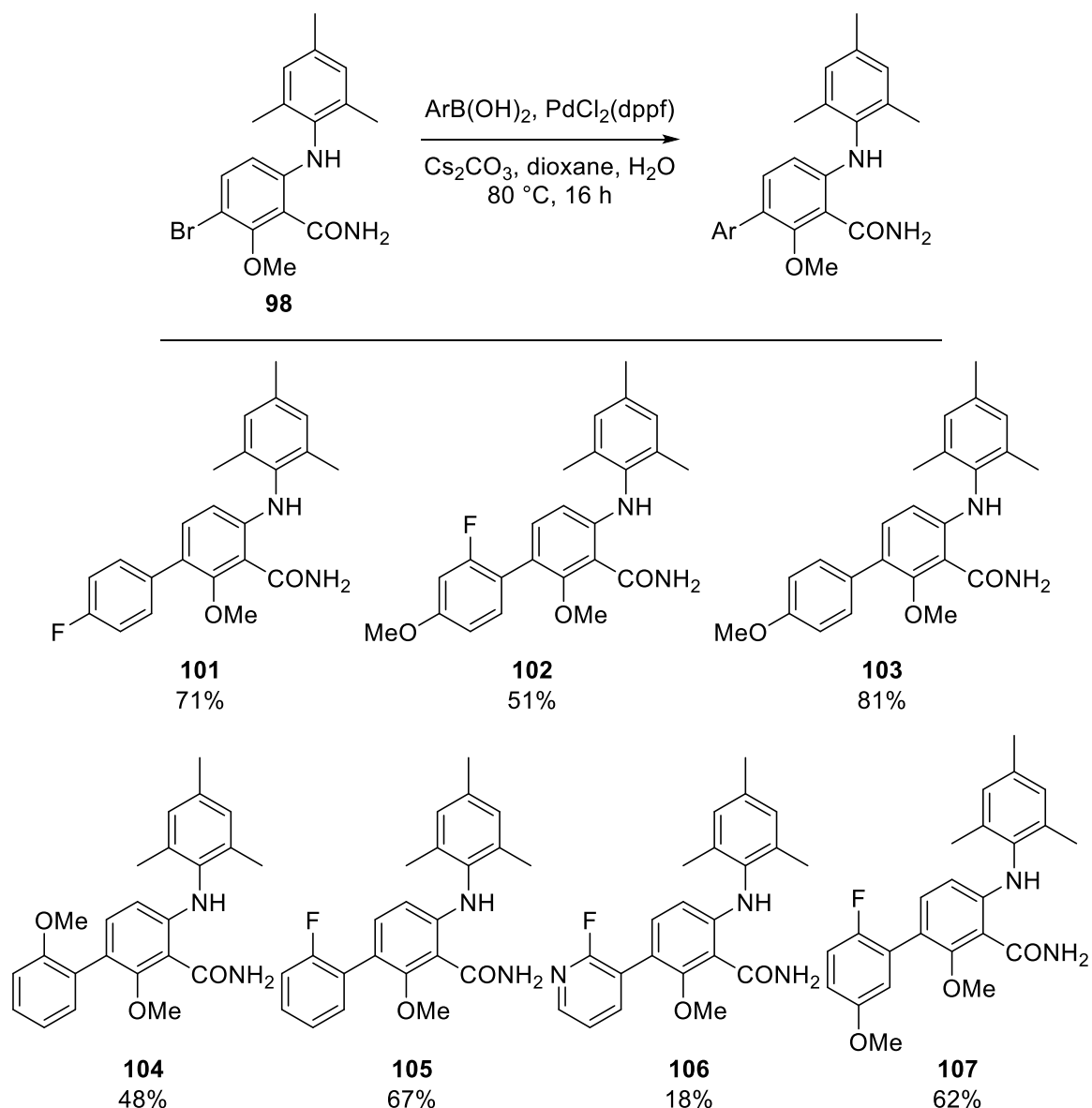
**Table 4: Optimisation of Suzuki-Miyaura reaction**



Entry	Catalyst	Base	Solvent	Temperature/Time	Yield
1	$\text{Pd}(\text{PPh}_3)_4$	$\text{KH}_2\text{PO}_4$	DMF	$\Delta$ , 16 h	n/a
2	$\text{Pd}(\text{PPh}_3)_4$	$\text{K}_3\text{PO}_4$	DMF	80 °C, 48 h	n/a
3	$\text{Pd}(\text{PPh}_3)_4$	$\text{K}_2\text{CO}_3$	DMF	80 °C, 48 h	n/a
4	$\text{PdCl}_2(\text{dppf})$	$\text{Cs}_2\text{CO}_3$	dioxane	80 °C, 16 h	92%*
5	$\text{PdCl}_2(\text{dppf})$	$\text{Cs}_2\text{CO}_3$	dioxane/ $\text{H}_2\text{O}$	80 °C, 16 h	71%

\*A mixture of **101** and **97**

With the optimised conditions now in hand, a library of 3-substituted products were synthesised (Scheme 33). Boronic acids featuring fluoride and methoxy substituents were used for the coupling to provide non-radioactive forms of the fluorine-18 and carbon-11 radiotracers, respectively. Most of the products were obtained in good yields, however compound **106** bearing a fluoropyridine motif was isolated in 18% yield. Nevertheless, there was sufficient quantity of material to use for biological screening.

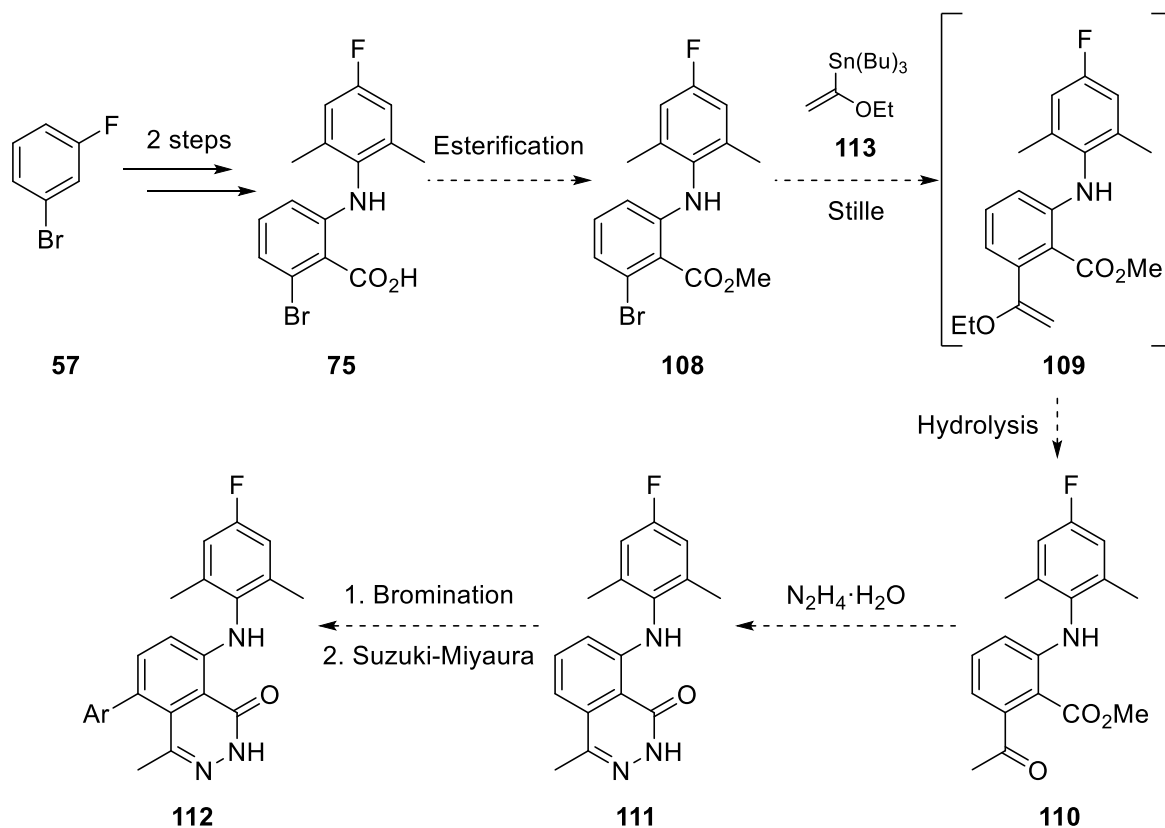


**Scheme 33: Library of 3-substituted benzamides**

## 2.1.4 Synthesis of Fluorophthalazinone Library

### 2.1.4.1 Proposed route

A third library of compounds was synthesised based on the selective phthalazinone agonist described by Mattes *et al.*<sup>95</sup> This series of compounds would be constructed from the previously synthesised fluoro-intermediate **75** (Scheme 34). An esterification followed by a Stille coupling reaction would afford the enol ether product **109**, which would then be hydrolysed *in situ* to form the keto ester **110**. Reaction with hydrazine would form the phthalazinone core structure and then further derivatives could be made by performing a regioselective bromination and following Suzuki-Miyaura reaction, as described for the previous library of compounds.

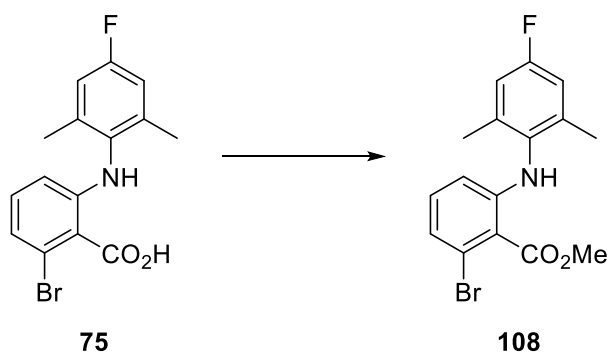


**Scheme 34: Proposed route towards fluorophthalazinone derivatives**

#### 2.1.4.2 Esterification reaction

The first step towards the synthesis of the phthalazinone core was esterification of **75** (Table 5). Initially, reaction with thionyl chloride and MeOH was attempted (entry 1).<sup>139</sup> After 18 h, a 50% conversion to product was observed by <sup>1</sup>H NMR spectroscopy, but after the addition of further equivalents of thionyl chloride, decarboxylation had occurred. Esterification was then attempted using oxalyl chloride, catalytic DMF and MeOH in a two-step process (entry 2).<sup>120</sup> As these conditions were milder, it was proposed that this procedure would prevent decarboxylation through the *in situ* formation of the Vilsmeier reagent, providing a stable intermediate for the formation of the acid chloride. On a small scale, **108** was formed in 61% yield, however, upon scale-up significant decarboxylation was observed. Eventually a method for the synthesis of **108** that was scalable was achieved using TMS-diazomethane in THF over 16 h (entry 3).<sup>95</sup> No decarboxylation was observed and the product was isolated in 88% yield.

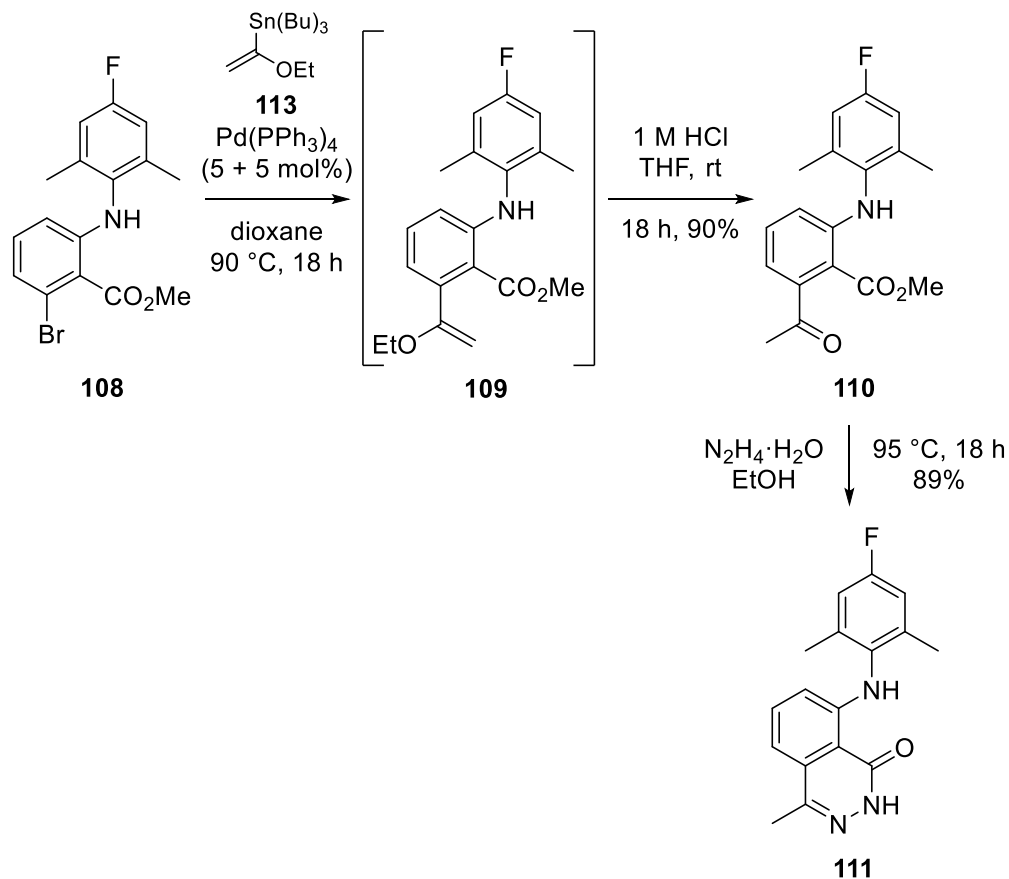
Table 5: Methyl ester synthesis conditions



Entry	Reagents	Temperature	Time	Yield
1	SOCl <sub>2</sub> , MeOH	0 °C to rt	48 h	n/a
2	1. (COCl) <sub>2</sub> , DMF (cat.) CH <sub>2</sub> Cl <sub>2</sub> 2. MeOH, CH <sub>2</sub> Cl <sub>2</sub>	0 °C to Δ	24 h	n/a
3	TMS-diazomethane THF	0 °C to rt	16 h	88%

#### 2.1.4.3 Construction of the phthalazinone core

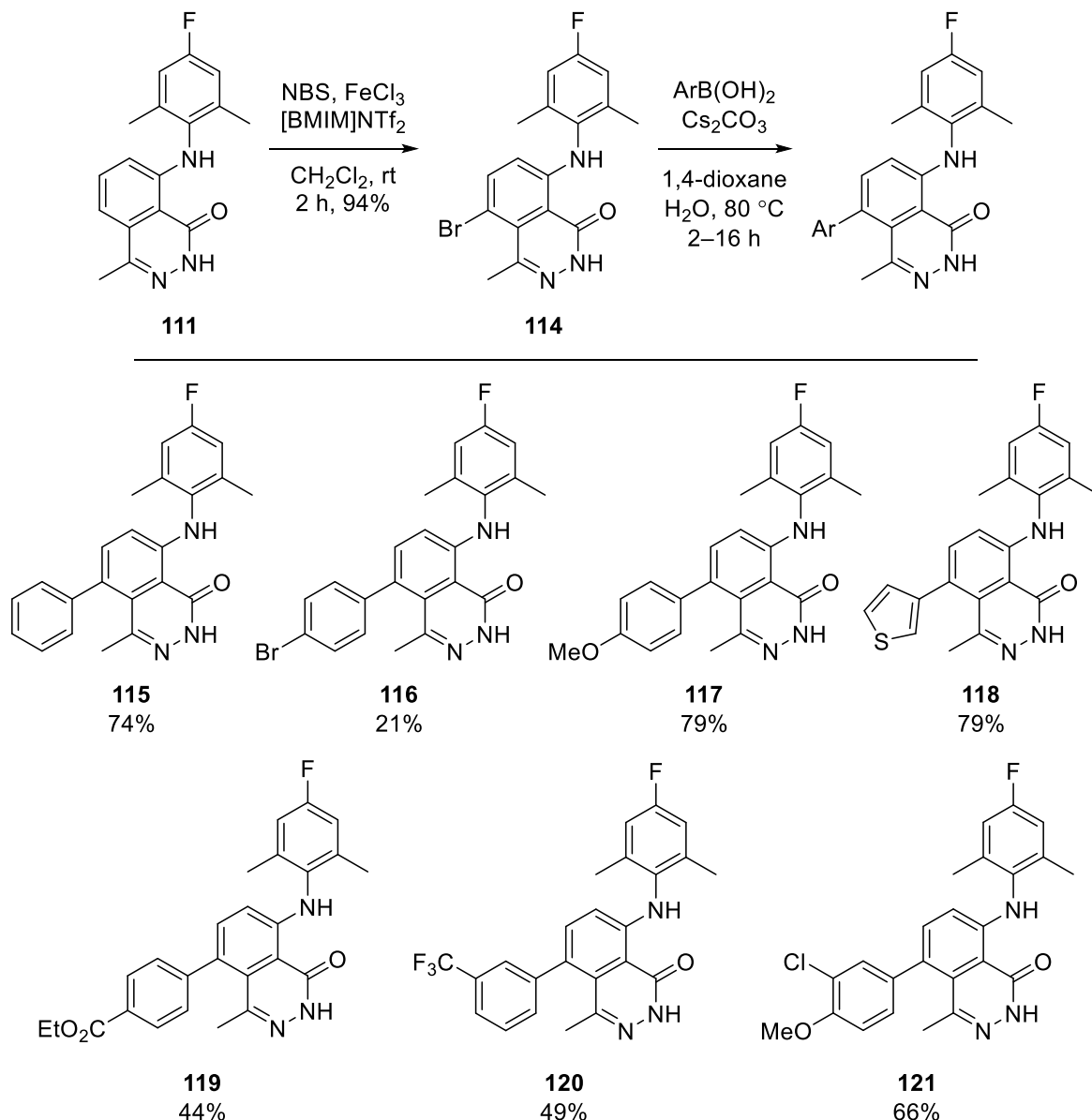
Next the phthalazinone core was assembled. This began with a Stille coupling using alkyl tin **113** and Pd(PPh<sub>3</sub>)<sub>4</sub> (Scheme 35). Initial reaction using 10 mol% of catalyst stalled after 24 h of reaction time, giving only 64% conversion to **109**. A second attempt using 5 mol% of catalyst followed by a further 5 mol% after 5 h allowed for complete conversion to enol ether product **109** and hydrolysis immediately followed using 1 M HCl. After initial purification, there was still evidence of alkyl tin impurities in the product. Washing with aqueous KF solution was not successful in removing the impurities. However, *via* a second column with 10% K<sub>2</sub>CO<sub>3</sub> (w/w) in silica as the stationary phase, it was possible to remove all traces of the tin byproducts. Keto ester product **110** was isolated in 90% yield over the two steps. The final step in forming the phthalazinone was the reaction of **110** with hydrazine, which afforded product **111** in 89% yield upon first attempt.



**Scheme 35: Synthesis of the fluorophthalazinone derivative 111**

#### 2.1.4.4 Synthesis of final compounds

The bromination of phthalazinone **111** used the same conditions as the attempt in the previous library of compounds and returned brominated analogue **114** in 94% yield (Scheme 36). As this series of compounds already had a fluorine atom incorporated as the potential site for radiolabelling, the choice of boronic acid coupling partners could be more varied. A library of seven compounds were synthesised in good yields, however, the coupling of 4-bromophenylboronic acid to form **116** occurred in a lower yield of 21%. Since this reagent was also an aryl bromide, there was a competing reaction between two of the boronic acids, forming byproducts. The synthesis of an iodinated analogue of the fluorophthalazinone may have resolved this issue, due to the greater order of reactivity for the aryl iodine. However, the iodination reaction was shown to be not as efficient on the benzamide **67** and the quantity of phthalazinone product obtained was sufficient for further studies.



**Scheme 36: Bromination and Suzuki-Miyaura reaction to form final fluorophthalazinones**

### 2.1.5 Investigation of Physicochemical Properties

The key physicochemical properties of the three libraries of potential radiotracers were assessed in order to rank the compounds for biological screening and to give insight into which structures may have more favourable pharmacokinetics. These compounds were intended to target receptors that lie within the central nervous system, so ability to penetrate the blood-brain barrier (BBB) would be crucial. Established methodology by Tavares *et al.* to determine radiotracer properties using HPLC was employed.<sup>122</sup> This allowed for rapid testing of the compounds, as the process was automated and multiple compounds could be assessed during a single run. The properties examined were the partition coefficient ( $\log P$ ), permeability ( $P_m$ ), membrane partition coefficient ( $K_m$ ) and plasma protein binding (%PPB).

### 2.1.5.1 Partition coefficient

The partition coefficient ( $\log P$ ) is defined as the ratio of concentration of a substance in two immiscible phases at equilibrium and therefore is a good measure of lipophilicity.<sup>140</sup> It is determined experimentally and traditionally measured using the “shake flask” method: calculated from the ratio of concentration of compound in octanol and water (Figure 16). One of the disadvantages of this method is that it is quite time-consuming, which made using the HPLC methodology desirable. Values for  $\log P$  were obtained by comparison of the retention times of the unknown compounds with those of known standards on a  $C_{18}$  column. Compounds require a good balance of lipophilicity to have good probability of penetrating the BBB, thus the value for  $\log P$  is an important selection criterion for radiotracer development.<sup>141,142</sup>

$$\log P = \log \left( \frac{[\text{Concentration}]_{\text{Octanol}}}{[\text{Concentration}]_{\text{Water}}} \right)$$

**Figure 16: Equation for the calculation of  $\log P$**

### 2.1.5.2 Permeability and membrane partition coefficient

Another important factor in penetration of the BBB is the ability of a compound to cross brain capillary endothelial cells. This factor can be greatly affected by solute-membrane interactions and is known as the membrane partition coefficient ( $K_m$ ). This provides information about the solute’s free energy of interaction ( $\Delta G_m$ ) with the fluid membrane according to the below equation (Figure 17).<sup>143</sup> This property can be measured using immobilised artificial membrane (IAM) chromatography, as this can model the solute-membrane interactions. IAM columns consist of monolayers of phospholipids covalently bonded to the surface of silica.<sup>144</sup> Permeability ( $P_m$ ) of drug *via* passive diffusion is directly proportional to  $K_m$  and depends upon the size of the molecule.

$$\Delta G_m = -RT \ln(K_m)$$

**Figure 17: Equation to show the relationship between  $\Delta G_m$  and  $K_m$**

### 2.1.5.3 Plasma protein binding

When a compound enters the bloodstream it interacts with plasma proteins, with two of the most common being human serum albumin (HSA) and  $\alpha_1$ -acid glycoprotein (AGP). A radiotracer with high percentage plasma protein binding (%PPB) means less compound is

available to cross the BBB and results in higher nuclear image noise from deposition of the tracer in the peripheral organs and build-up in the blood. The %PPB can be determined by measuring the retention time of compounds using HPLC and a column coated with HSA.<sup>145</sup>

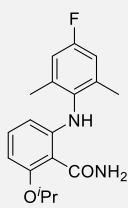
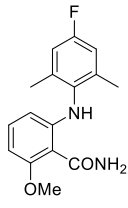
#### 2.1.5.4 Physicochemical properties of S1P<sub>5</sub> compounds

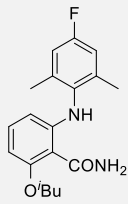
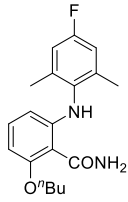
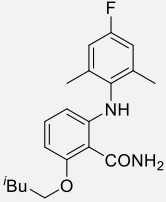
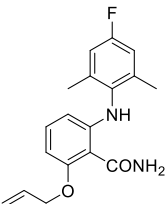
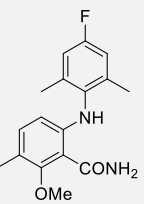
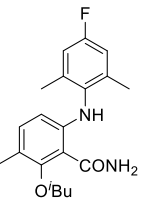
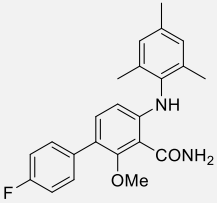
The HPLC methodology developed by Tavares *et al.* established a range of ideal values based on analysis of ten known radiotracers (Table 6).<sup>122</sup> Ideally the compounds tested would fall below these values; however, the purpose of this screening process was to rapidly assess and rank the libraries of compounds. All three libraries of compounds were submitted to this methodology, including iodinated analogue **73** (Table 7).

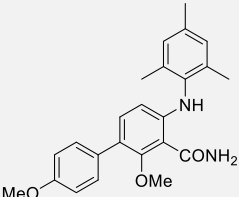
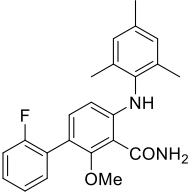
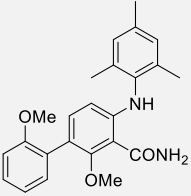
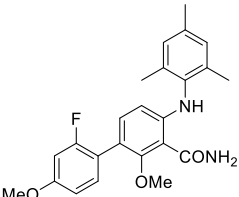
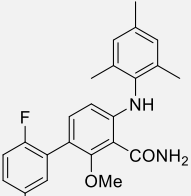
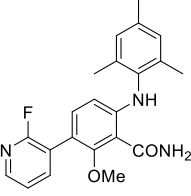
**Table 6: Ideal values for physicochemical properties**

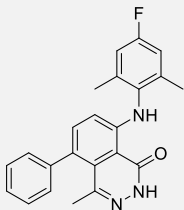
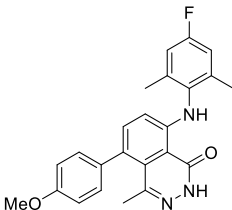
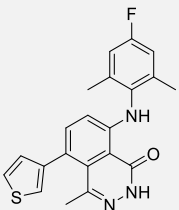
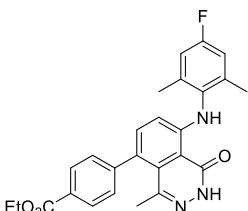
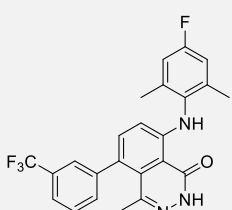
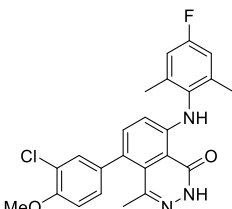
Physicochemical Property	Ideal Value
$\log P$	< 4.0
$P_m$	< 0.5
$K_m$	< 250
%PPB	< 95%

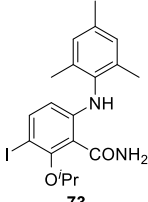
**Table 7: Physicochemical analysis of S1P<sub>5</sub> compounds**

Compound	$\log P$	$P_m$	$K_m$	%PPB
 <b>66</b>	5.35	0.319	101	99%
 <b>89</b>	4.56	0.223	64.4	99%

Compound	log <i>P</i>	<i>P</i> <sub>m</sub>	<i>K</i> <sub>m</sub>	%PPB
 90	5.74	0.487	101	100%
 92	5.89	0.509	168	100%
 92	6.14	0.646	223	100%
 93	5.22	0.285	89.6	100%
 94	5.01	0.233	70.5	99%
 95	6.21	0.518	178	100%
 101	6.16	0.650	246	100%

Compound	log <i>P</i>	<i>P<sub>m</sub></i>	<i>K<sub>m</sub></i>	%PPB
 <p><b>103</b></p>	5.97	0.539	210	100%
 <p><b>105</b></p>	6.08	0.514	195	100%
 <p><b>104</b></p>	5.79	0.378	148	100%
 <p><b>102</b></p>	5.95	0.465	190	100%
 <p><b>107</b></p>	5.88	0.446	182	100%
 <p><b>106</b></p>	5.03	0.211	79.9	99%

Compound	log <i>P</i>	<i>P</i> <sub>m</sub>	<i>K</i> <sub>m</sub>	%PPB
 115	5.69	0.562	210	100%
 117	5.53	0.477	193	100%
 118	5.49	0.499	189	100%
 119	5.82	0.561	250	100%
 120	6.03	0.618	273	100%
 121	5.76	0.611	268	100%

Compound	log <i>P</i>	<i>P<sub>m</sub></i>	<i>K<sub>m</sub></i>	%PPB
 <b>116</b>	6.20	0.786	355	100%
 <b>73</b>	6.39	0.578	253	100%

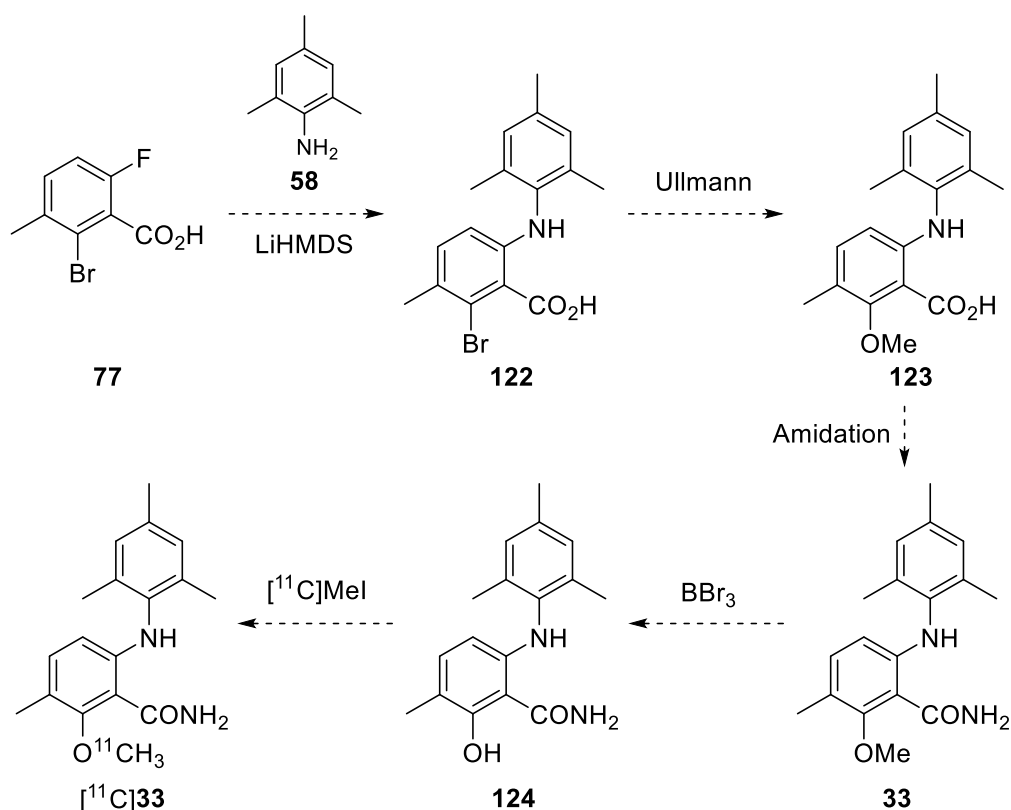
### 2.1.5.5 Analysis of physicochemical properties of S1P<sub>5</sub> compounds

Following the testing of the three libraries of compounds, the values were assessed and compared. The log *P* value obtained for many of the compounds was above the ideal limit of 4.0, with the exception of compound **89**. The compounds from fluorobenzamide library that did not feature longer alkyl chains had more ideal properties. Unsurprisingly, the further extension of the aromatic system present in the other two libraries of compounds was shown to increase the lipophilicity of the compounds. The benzamide analogue **73**, featuring an iodine atom, also had a much increased log *P* value due to the presence of an aromatic iodine substituent.<sup>146</sup> The membrane partition coefficient and permeability values obtained were mainly good across the libraries, with the fluorophthalazinone library having slightly increased values. The most promising compounds from this screening process were fluorobenzamides **89** and **93**. Analysis of the plasma protein binding showed that all of the compounds possessed values of 99% or 100%. This seemed unlikely, indeed study of a different class of compound described in a later chapter (see section 2.2.3.2) using the same methodology showed that the experimentally determined value for plasma protein binding was too high when compared to other methods. Consequently, it was believed that the HPLC column used to obtain these results was now unreliable and these values were not used to assess or rank the compounds.

## 2.1.6 Synthesis of a Carbon-11 Precursor

### 2.1.6.1 Proposed route

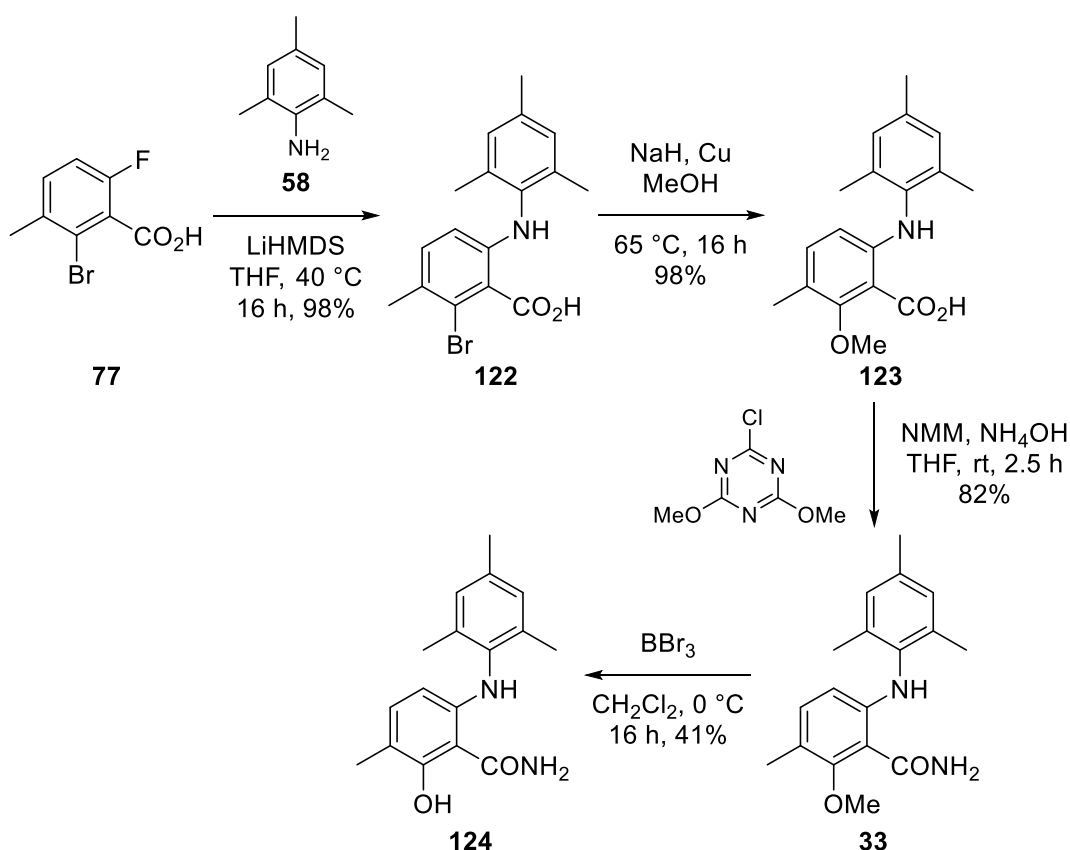
Whilst the three libraries of novel S1P<sub>5</sub> agonists were screened for their biological properties, a carbon-11 precursor based on an existing benzamide agonist from the literature was proposed (Scheme 37). The compound chosen was the 3-methyl derivative **33** that was shown to have particularly high affinity and selectivity for S1P<sub>5</sub>. This tracer would allow for initial investigation of the ability of this class of compounds to act as radiotracers to image S1P<sub>5</sub>. Biological data already existed for this compound, so a successful radiosynthesis would allow for evaluation of *in vivo* distribution. The phenol precursor **124** was proposed as a desirable target, as methylation of phenols using [<sup>11</sup>C]MeI or [<sup>11</sup>C]MeOTf is a robust, commonly used radiosynthesis. Indeed, this is the method of radiolabelling the PET radioligand [<sup>11</sup>C]DTBZ and allows for a fully automated synthesis.<sup>57,147</sup> To access precursor **124**, benzamide **33** would be synthesised from benzoic acid **77** using the previously described chemistry. Demethylation of the methoxy group using BBr<sub>3</sub> would provide the phenol for precursor **124**.



Scheme 37: Proposed route towards carbon-11 precursor **124**

### 2.1.6.2 Precursor synthesis via demethylation of 33

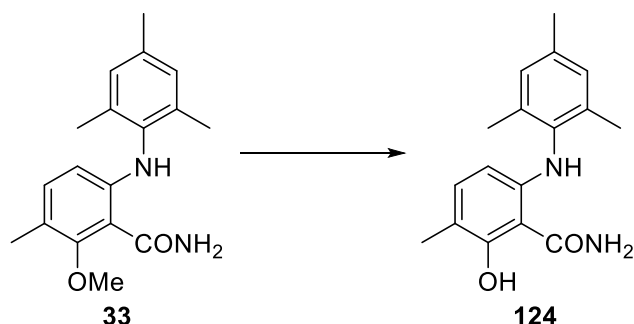
Synthesis of benzamide **33** was a high yielding process and gram-scale preparation was easily possible. Since this was the non-radioactive form of the proposed carbon-11 radiotracer and would be necessary for early preclinical work, rapid synthesis was advantageous. Initial reaction of **33** with the demethylating reagent  $\text{BBr}_3$  returned the phenol product **124** in 41% yield; however, the product contained some inseparable impurities and the yield was not reproducible on a larger scale. With this in mind, optimisation of the demethylation step took place.



**Scheme 38: Synthesis of demethylated precursor 124**

Conditions were altered in order to optimise the demethylation reaction (Table 8). To remove impurities and increase the rate of demethylation using  $\text{BBr}_3$ , the reaction was heated under reflux (entry 1). After 4 h, there was no evidence of product present and the starting material had begun to decompose under the reaction conditions. An attempt to prevent decomposition, where the reaction was cooled to  $-78^\circ\text{C}$  before warming room temperature was also unsuccessful (entry 2). Several other literature procedures for the demethylation of **33** were attempted, but these either resulted in no reaction or partial decomposition of the starting material.<sup>148–150</sup> A different approach was considered to avoid the use of a demethylation reaction.

Table 8: Optimisation of demethylation reaction

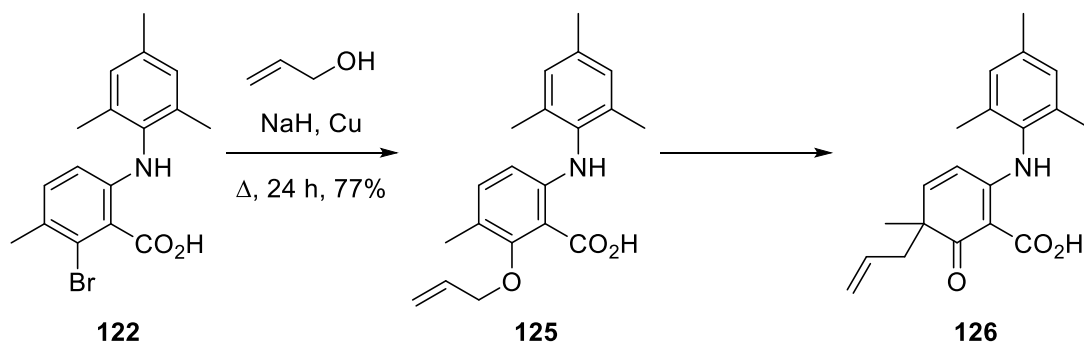


Entry	Reagents	Temperature	Time	Yield
1	BBr <sub>3</sub> , CH <sub>2</sub> Cl <sub>2</sub>	0 °C to Δ	4 h	n/a
2	BBr <sub>3</sub> , CH <sub>2</sub> Cl <sub>2</sub>	-78 °C to rt	24 h	n/a
3	AlCl <sub>3</sub> , CH <sub>2</sub> Cl <sub>2</sub>	0 °C to rt	16 h	n/a
4	BF <sub>3</sub> ·OEt <sub>2</sub> , CH <sub>2</sub> Cl <sub>2</sub>	0 °C to rt	16 h	n/a
5	LiCl, DMF	100 °C	24 h	n/a
6	NaSEt, DMF	100 °C	16 h	n/a

### 2.1.6.3 Use of an allyl protecting group

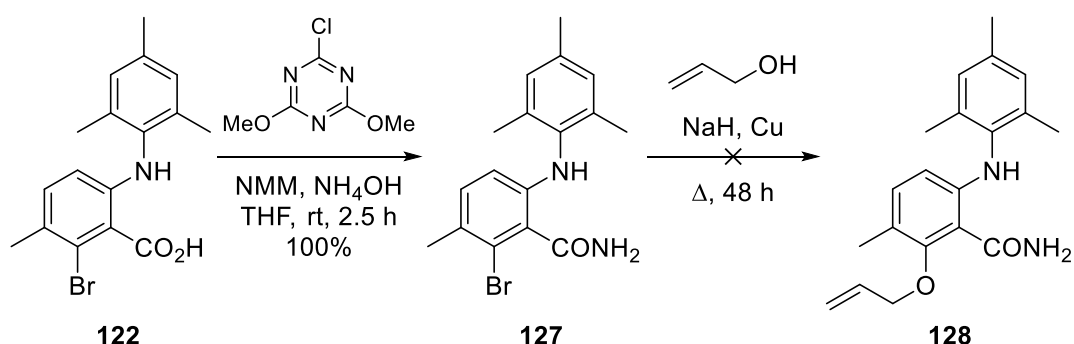
Rather than use a methyl group as protection for the alcohol, an allyl group was considered, as this could be removed using milder conditions to provide phenol precursor **124**. This moiety could be introduced through an Ullmann condensation reaction with allyl alcohol (Scheme 39). Initial reaction of aryl bromide **122** with allyl alcohol showed total conversion of starting material after 24 h, with a small amount of impurity also present in the reaction mixture. Formation of the desired product **125** was confirmed by <sup>1</sup>H NMR spectroscopy and isolated in 77% yield. However, rearrangement to a new compound took place after 1 h in a chloroform solution, prior to full characterisation. Further analysis of this solution confirmed the presence of rearranged product **126**, supported by the appearance of individual signals for the two diastereotopic sp<sup>3</sup> hydrogen atoms on the allyl group at 2.27 and 2.73 ppm in the <sup>1</sup>H NMR spectrum. Analysis of the <sup>13</sup>C NMR spectrum of **126** also confirmed the presence of a ketone carbonyl group. It was proposed that this compound had formed *via* an aromatic Claisen rearrangement, but no tautomerisation to the phenol product had taken place due the *ortho*-methyl group. In *ortho,ortho*-disubstituted allyl phenols a *para*-substituted allyl product forms *via* a tandem Claisen and Cope rearrangement.<sup>151</sup> However, the additional steric congestion at the C-5 position of the benzamide ring was proposed to make this transformation unfavourable. The synthesis was performed again and the product used immediately in the following

amidation step, but only conversion to the rearranged product **126** was evident and no amidation had taken place. Examination of the neat product immediately post-synthesis showed that the rearrangement was slowly taking place at room temperature and accelerated when in solution in chloroform. After 1 h of standing neat at room temperature, a 10% conversion to rearranged product **126** was observed using  $^1\text{H}$  NMR spectroscopy and after 24 h, the neat sample had formed a 1:1 ratio of **125** and **126**. The rearranged product **126** was formed quantitatively from **125** upon standing in a solution in chloroform after 2 h.



**Scheme 39: Attempted synthesis of allyl ether 125**

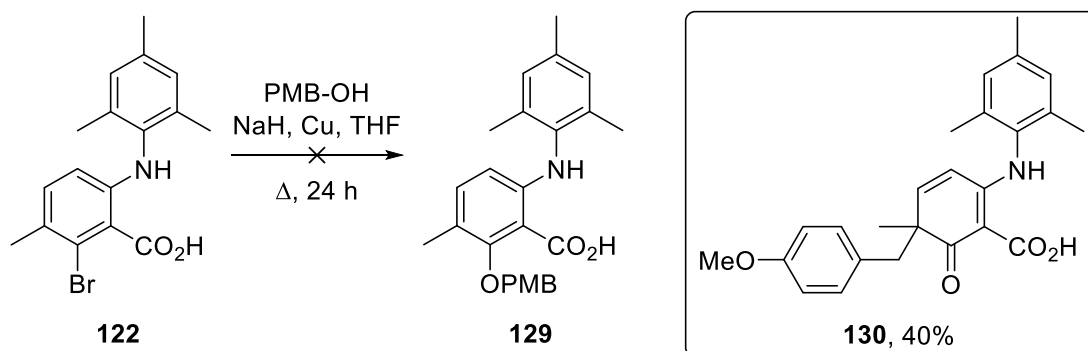
An alternative approach to allyl ether **128** was considered by initially conducting amidation, followed by the Ullmann reaction (Scheme 40). Amidation of **122** occurred as expected in a quantitative yield; however, when subjected to the Ullmann condensation conditions, no conversion to any product was observed. This may be due to the amide group not being as electron-withdrawing or inhibiting oxidative addition of the copper catalyst.<sup>127</sup>



**Scheme 40: Amidation of 122 prior to Ullmann condensation reaction**

#### 2.1.6.4 Use of a PMB protecting group

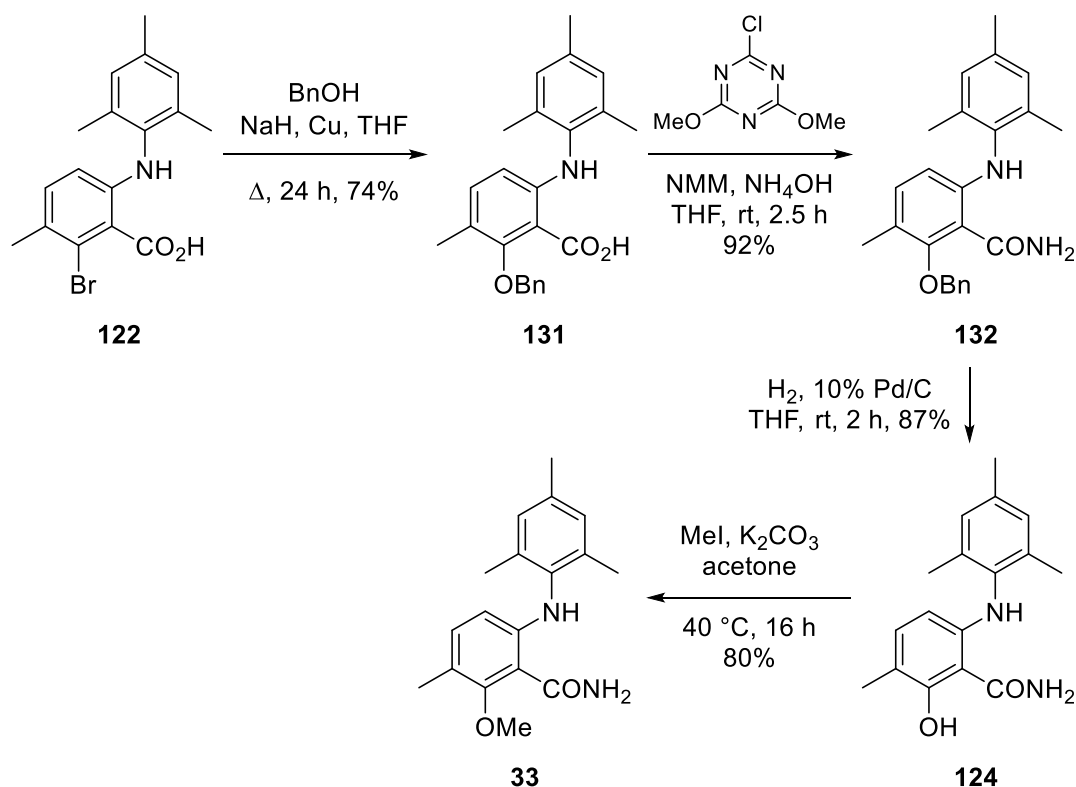
A new protecting group approach was considered for the synthesis of phenol precursor **124**. Next, a *para*-methoxybenzyl (PMB) group was used (Scheme 41). Ullmann condensation reaction with PMB alcohol took place in THF instead of neat alcohol for improved solubility and reduction in cost of materials. This reaction showed full conversion of starting material after 24 h, although none of the desired compound was formed and instead rearranged product **130** was isolated in 40% yield. The structure of **130** was confirmed by the presence of individual signals for the two diastereotopic hydrogen atoms in the benzyl position at 2.72 and 3.35 ppm in the  $^1\text{H}$  NMR spectrum. Additionally, as for the rearranged compound **126**, analysis of the  $^{13}\text{C}$  NMR spectrum of **130** also confirmed the presence of a ketone carbonyl group.



**Scheme 41: Ullmann condensation reaction with PMB-OH**

#### 2.1.6.5 Use of a benzyl protecting group

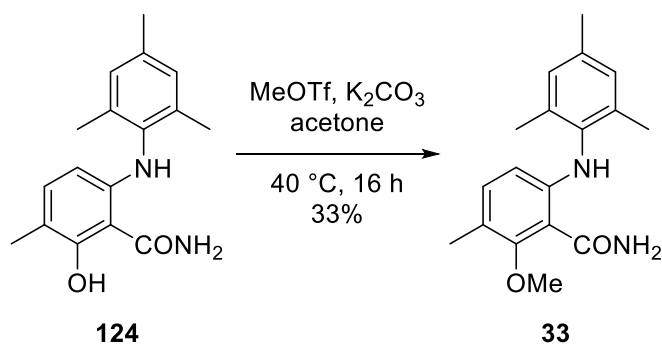
To investigate the role the electronics of the benzyl group plays in the rearrangement reaction, the Ullmann condensation reaction was attempted with benzyl alcohol (Scheme 42). After 24 h, full conversion to the desired product had taken place and benzyl ether **131** was isolated in 74% yield. No rearrangement of this product was observed by  $^1\text{H}$  NMR spectroscopy and the isolated product was still >95% pure after >72 h in chloroform at room temperature. It was proposed that benzyl group was not as efficient at stabilising a partial positive charge in the benzylic position compared to the PMB group, due to the absence of an electron-donating group. Subsequent amidation of **131** gave benzamide **132**, which was isolated in 92% yield. Deprotection of the benzyl group *via* hydrogenation was successful and the phenol precursor **124** was isolated in 87% yield. To show that this precursor was capable to undergo radiosynthesis with  $[^{11}\text{C}]\text{MeI}$ , standard methylation conditions were used to access non-radioactive benzamide **33** in 80% yield. Importantly, no impurities were observed to be formed in the methylation reaction, indicating precedent for a clean radiosynthesis.



**Scheme 42: Ullmann condensation reaction with BnOH and synthesis of precursor 124**

#### 2.1.6.6 Methylation of precursor 124

Another potential source of carbon-11 is the methylating reagent  $[^{11}\text{C}]\text{MeOTf}$ . This is a more powerful methylating reagent than  $[^{11}\text{C}]\text{MeI}$  and it is possible to perform methylations on weakly nucleophilic functional groups. As such, methylations using MeOTf tend to be much faster: an important factor to consider with the short half-life of the carbon-11 radionuclide.<sup>56</sup> Trial of this reagent prior to radiosynthesis would advise of its suitability for methylation of precursor **124**. Reaction of precursor **124** with MeOTf, using conditions similar to that of the MeI reaction, returned benzamide **33** in 33% yield (Scheme 43). Despite the lower yield obtained, this reaction produced no side products and so MeOTf could still be considered as a reagent for radiomethylation.

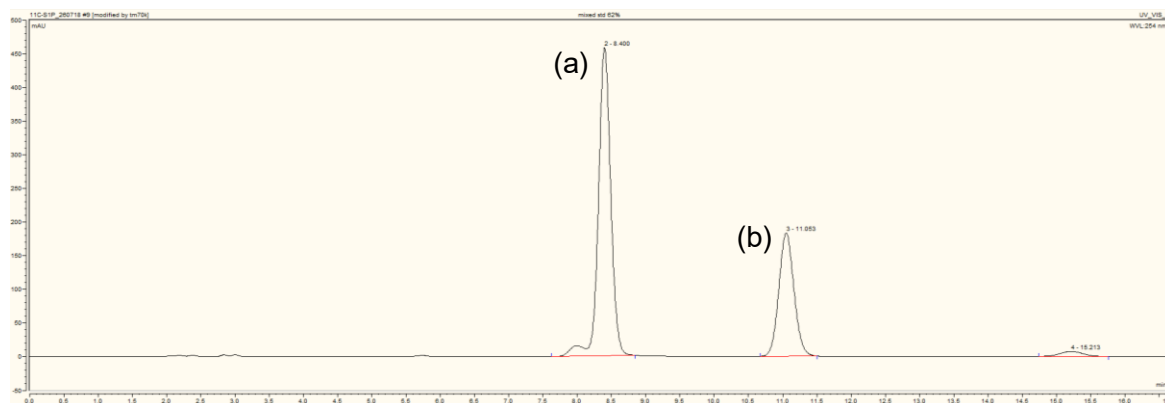


**Scheme 43: Methylation of precursor 124 using MeOTf**

## 2.1.7 Radiochemistry

### 2.1.7.1 Establishing an HPLC method

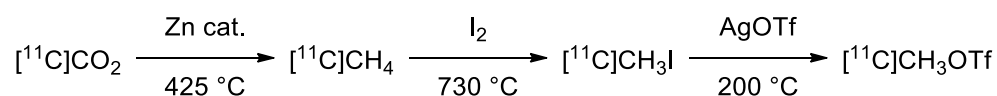
The limiting reagent of a radiomethylation reaction is the source of carbon-11; therefore, separation of the remaining precursor from the methylated product would need to take place. Many radiomethylations with carbon-11 avoid the use of semi-preparative HPLC for the purification of the radiotracer, instead adopting for a solid-phase extraction (SPE) method.<sup>147,152–154</sup> HPLC purification and reformulation from the eluent can be a lengthy process and due to the much shorter half-life of the carbon-11 radionuclide, this can significantly affect the specific activity of the product. On the other hand, SPE purification allows for quick trapping and elution from a small cartridge and can decrease the time required for purification. This also allows easy automation and reproducibility of the reaction – an important factor when taking a radiopharmaceutical through to clinical use. Nevertheless, a good separation of both precursor **124** and product **33** would need to be achieved in order to properly analyse the reaction and advise on the method of separation used in the synthesis. A sample was prepared containing a 1:1 mix of standard/precursor and examined by reverse phase HPLC (Figure 18). It was found that a mixture of 62% acetonitrile in water provided a good separation, but the product was only eluted from the column after 11 min due to its lipophilicity.



**Figure 18: HPLC chromatogram of (a) precursor 124 and (b) benzamide 33, using a C<sub>18</sub> column and 62% acetonitrile in water as the eluent**

### 2.1.7.2 Synthesis of [<sup>11</sup>C]MeI and [<sup>11</sup>C]MeOTf

The radioactive synthesis was carried out using a Synthra Wolpertinger synthesiser; the graphics overlay for this synthesiser is shown in Appendix I. The [<sup>11</sup>C]MeI required for the reaction was synthesised through a gas phase synthesis and its production was optimised prior to attempts of the radiomethylation reaction (Scheme 44). [<sup>11</sup>C]CO<sub>2</sub> was produced *via* the <sup>14</sup>N(p,α)<sup>11</sup>C nuclear reaction by cyclotron irradiation of a target containing [<sup>14</sup>N]N<sub>2</sub>.<sup>58</sup> The gas phase synthesis required little optimisation and an irradiation of the cyclotron target to produce approximately 10 GBq of [<sup>11</sup>C]CO<sub>2</sub> was sufficient for the synthesis of 5 GBq of [<sup>11</sup>C]MeI after 15 min. Production of [<sup>11</sup>C]MeOTf was not as successful, as initial attempts at its synthesis led to the activity being trapped inside the triflate oven. Further investigation found that the type of activated carbon used in the column was not allowing de-adsorption of [<sup>11</sup>C]MeOTf. Switching to a less active form of carbon for the column allowed de-adsorption to take place, providing 3–4 GBq of [<sup>11</sup>C]MeOTf.



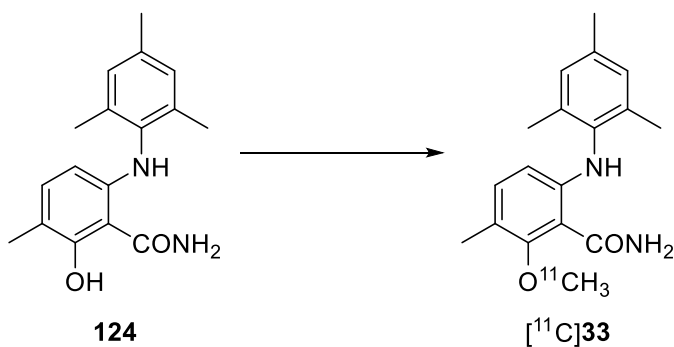
**Scheme 44: Gas phase synthesis of [<sup>11</sup>C]MeI and [<sup>11</sup>C]MeOTf**

### 2.1.7.3 Radiolabelling of precursor 124

To optimise the reaction conditions, HPLC and reformulation was bypassed and the reaction vessel was connected directly to a dispensing vial. The reaction mixture was then analysed with HPLC on a C<sub>18</sub> column, using both UV and gamma detectors. Any unreacted [<sup>11</sup>C]MeI or [<sup>11</sup>C]MeOTf quickly reacts with water in the eluent, forming [<sup>11</sup>C]MeOH. This was easily visible on the gamma trace of the HPLC and provided

quantitative conversion analysis of the reaction. For the first reactions, [ $^{11}\text{C}$ ]MeOTf was used as the source of carbon-11, with no base added due the enhanced reactivity compared to [ $^{11}\text{C}$ ]MeI (Table 9).<sup>155</sup> Cooling of the reaction mixture should increase the trapping of [ $^{11}\text{C}$ ]MeOTf, but after 5 min of reaction time at room temperature, no conversion to product was observed in the HPLC trace (entry 1). Heating the reaction to 100 °C for 10 min showed no improvement (entry 2). Adding TBAOH as a base at 40 °C for 5 min showed no conversion to product and increasing the reaction time and temperature was also unsuccessful (entries 3 and 4). The source of carbon-11 was changed to [ $^{11}\text{C}$ ]MeI and NaOH was used as a base in THF. The GM counter in the reaction vial showed that trapping was efficient at 40 °C and 60 °C, but still no conversion was observed (entries 5 and 6). Using conditions similar to the non-radioactive reaction was difficult, as  $\text{K}_2\text{CO}_3$  was not soluble in the reaction solvent and solid would cause blockages in the automated synthesiser. However,  $\text{K}_2\text{CO}_3$  was mixed with precursor **124** prior to injecting into the reaction vial to try and emulate these conditions. After 10 min, there was no product (entry 7). Addition of a 1 M TBAOH solution in THF showed a promising 2% conversion and heating the reaction to 80 °C, enabled 38% conversion after 10 min (entries 8 and 9). Literature procedures have shown that the use of TBAF enhances the efficiency of *N*- and *O*-methylations, as it is highly soluble in organic solvents compared to many other bases.<sup>156,157</sup> Using TBAF in THF at 80 °C gave 72% conversion of [ $^{11}\text{C}$ ]MeI after 5 min (entry 10). Changing the solvent to cyclohexanone and heating the reaction to 120 °C gave 83% conversion (entry 11). To further optimise this process, the reaction time was reduced to 0 min, i.e. transferring the reaction immediately after trapping of [ $^{11}\text{C}$ ]MeI (entry 12). This gave 94% conversion, which was more than sufficient to begin purification.

Table 9: Optimisation of reaction conditions



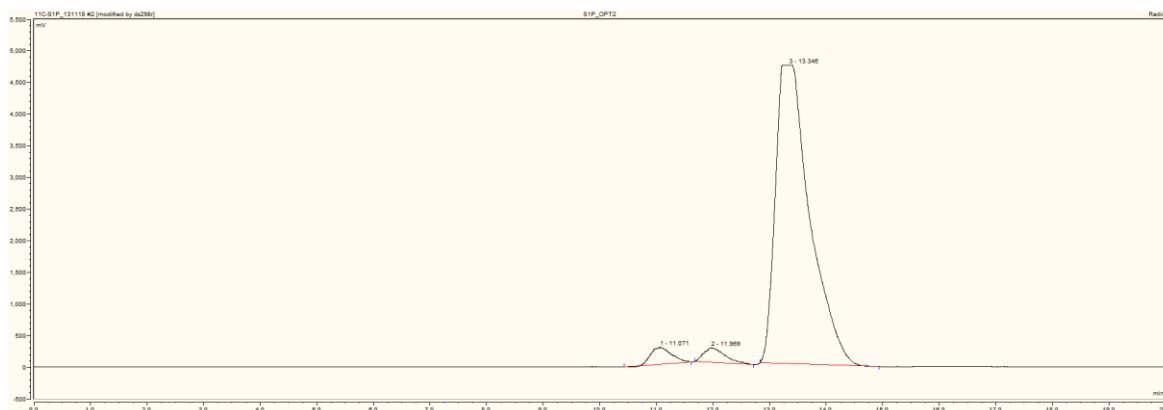
Entry	Carbon-11 Source	Base	Solvent	Temperature	Time*	Conversion
1	[ <sup>11</sup> C]MeOTf	None	Cyclohexanone	-20 °C–rt	5 min	0%
2	[ <sup>11</sup> C]MeOTf	None	Cyclohexanone	-20–100 °C	10 min	0%
3	[ <sup>11</sup> C]MeOTf	TBAOH	Cyclohexanone	40 °C	5 min	0%
4	[ <sup>11</sup> C]MeOTf	TBAOH	Cyclohexanone	60 °C	10 min	0%
5	[ <sup>11</sup> C]MeI	NaOH	THF	40 °C	5 min	0%
6	[ <sup>11</sup> C]MeI	NaOH	THF	80 °C	10 min	0%
7	[ <sup>11</sup> C]MeI	K <sub>2</sub> CO <sub>3</sub>	THF	40 °C	10 min	0%
8	[ <sup>11</sup> C]MeI	TBAOH	THF	40 °C	5 min	2%
9	[ <sup>11</sup> C]MeI	TBAOH	THF	0–80 °C	10 min	38%
10	[ <sup>11</sup> C]MeI	TBAF	THF	80 °C	5 min	72%
11	[ <sup>11</sup> C]MeI	TBAF	Cyclohexanone	120 °C	5 min	83%
12	[ <sup>11</sup> C]MeI	TBAF	Cyclohexanone	120 °C	0 min	94%

\* Time for reaction after 3 min of trapping [<sup>11</sup>C]MeI

#### 2.1.7.4 Purification and reformulation of product

The optimised conditions showed 94% conversion to desired product [<sup>11</sup>C]33. There was no residual [<sup>11</sup>C]MeI observed from the analysis, however, the remaining 6% impurities had similar retention times to the product (Figure 19). Consequently, SPE purification of the labelled product would be difficult, despite the absence of other radioimpurities. Purification using a C<sub>18</sub> cartridge was unsuccessful at removing both the radioimpurities and unreacted precursor. Use of an HLB cartridge allowed separation of the precursor

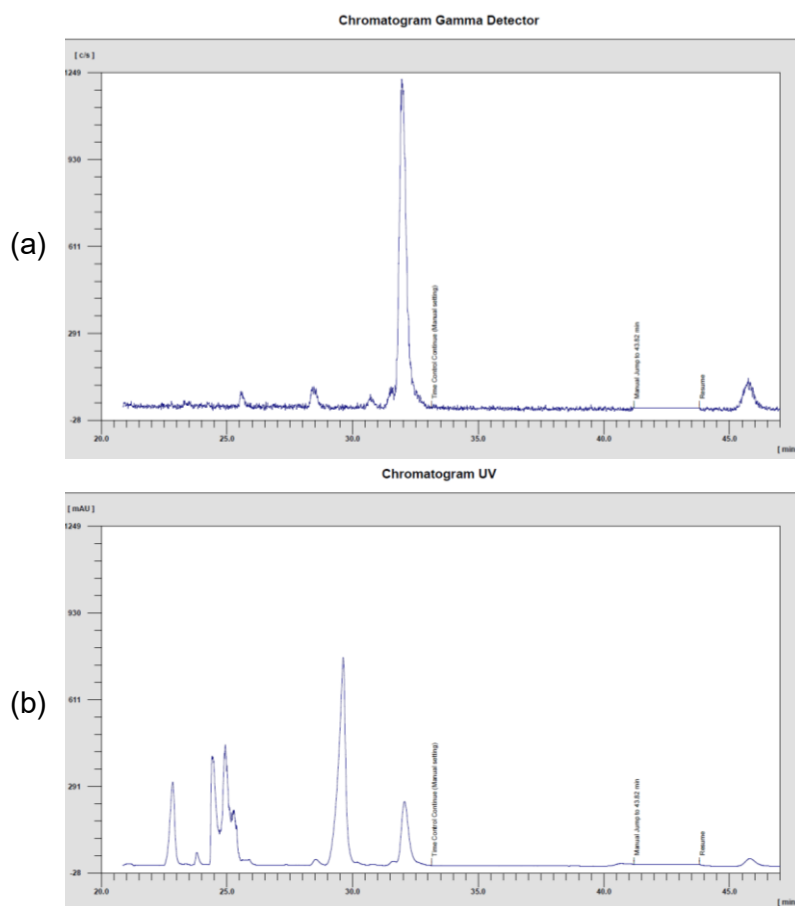
from the product, but not removal of the radioimpurities and so purification using HPLC was considered.



**Figure 19: HPLC gamma trace of the reaction mixture using the optimised conditions, using a C<sub>18</sub> column and 62% acetonitrile in water as the eluent. [<sup>11</sup>C]33 can be seen at a retention time of 13.3 min**

The preclinical analysis of the S1P<sub>5</sub> carbon-11 radiotracer will be carried out by collaborators at the University of Edinburgh. Consequently, a radiosynthesis was to be developed that could be transcribed to the radiochemistry unit at Edinburgh, since transport of carbon-11 tracers is currently impractical given its short half-life. The synthesiser used in Edinburgh is a TRACERlab FX<sub>C</sub> PRO; the graphics overlay is shown in Appendix II. This differs slightly from the Synthra Wolpertinger in its method of [<sup>11</sup>C]MeI synthesis, but also in the method of purification and reformulation. Reformulation on the Synthra takes place by evaporation of the HPLC fraction and then addition of the desired formulation, whereas the FX<sub>C</sub> PRO passes the HPLC fraction to an SPE cartridge for formulation. With this in mind, the purification and reformulation on the Synthra was adjusted to mimic that of the FX<sub>C</sub> PRO.

Semi-preparative HPLC was applied to the reaction and product [<sup>11</sup>C]33 successfully separated from its impurities (Figure 20). As the product was very lipophilic, this took over 30 min to elute from the column and needed to be diluted with 26 mL of water to prevent breakthrough on the SPE cartridge. Since this was not the intended purpose of this part of the synthesiser, it took over 20 min to transfer the mixture on the SPE for formulation. The compound was successfully reformulated and 80 MBq of clean product was isolated from a starting activity of approximately 5 GBq of [<sup>11</sup>C]MeI. This reaction took over 60 min to complete and so such a small amount of activity isolated was expected. However, this provided precedent for the reaction to take place on the FX<sub>C</sub> PRO where the transfer from HPLC to SPE would be much faster.

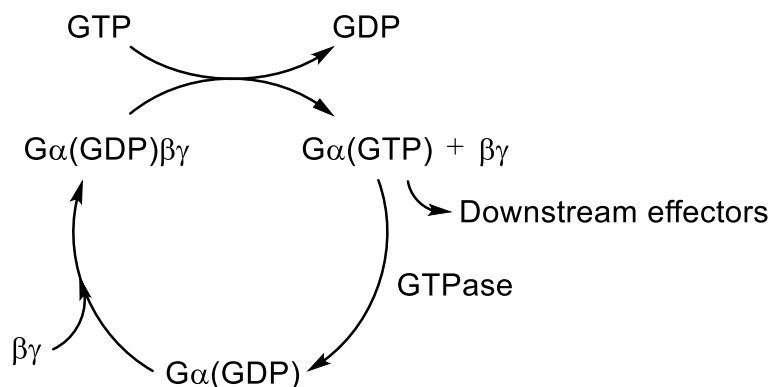


**Figure 20: Semi-preparative (a) radio and (b) UV HPLC chromatograms of the reaction mixture, using a C<sub>18</sub> column and 62% acetonitrile in water as the eluent. [<sup>11</sup>C]33 can be seen at a retention time of 32 min**

## 2.1.8 Biological Evaluation

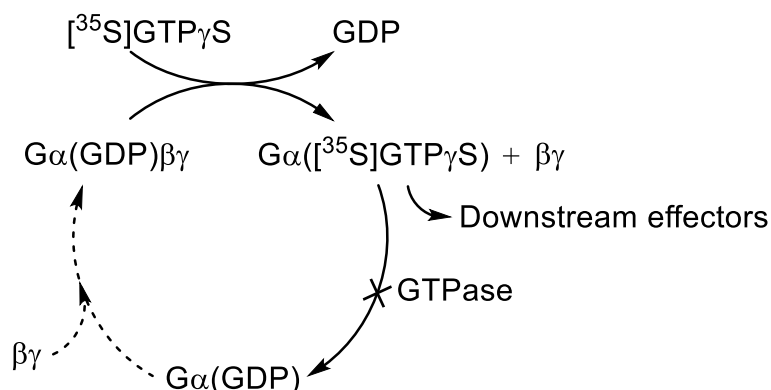
### 2.1.8.1 The [<sup>35</sup>S]GTPγS binding assay

The [<sup>35</sup>S]GTPγS assay is an *in vitro* assay used to determine binding to G protein coupled receptors (GPCRs). This assay measures the level of G protein activation following agonist activation of GPCRs.<sup>158</sup> The mechanism of GPCRs involves initial formation of a Gαβγ heterotrimer with GDP bound to the Gα subunit (Figure 21). A major function of βγ is inhibition of the Gα subunit. Activation of this receptor by an agonist leads to the dissociation of GDP and binding of GTP to the Gα subunit. Dissociation of the βγ takes place allowing activation of Gα, which is then able to interact with effector systems.<sup>158</sup> The G protein heterotrimer is reformed by the enzyme GTPase by hydrolysis of GTP to GDP and recombination of the βγ subunit.



**Figure 21: Mechanism of GPCR activation and GDP/GTP exchange**

In the [ $^{35}\text{S}$ ]GTP $\gamma$ S binding assay, GTP is substituted for  $^{35}\text{S}$  labelled GTP (Figure 22). Then GTPase enzyme is not able to hydrolyse this [ $^{35}\text{S}$ ]GTP $\gamma$ S to GDP and, therefore, accumulation of bound Gα([ $^{35}\text{S}$ ]GTP $\gamma$ S) take place. The assay measures the level of G-protein activation following binding of an agonist, thus, binding affinity of an agonist can be measured from the quantity of sulphur-35. To perform this assay, the sample is filtered and scintillation fluid is used to measure the level of radioactivity present on the filter.



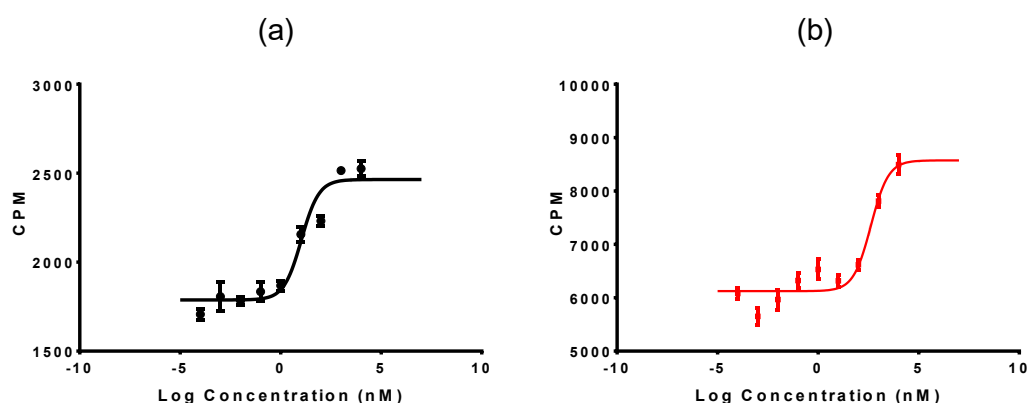
**Figure 22: Principle of the [ $^{35}\text{S}$ ]GTP $\gamma$ S binding assay**

### 2.1.8.2 Optimisation of the assay protocol

Before screening of the compounds could take place, optimisation of the assay protocol was carried out using the endogenous compound S1P and fluorobenzamide **66**. Preliminary data was collected using a protocol described in the literature by DeLapp *et al.* and the assay was carried out by filtration using a cell harvester.<sup>159</sup> The S1P $_5$  protein obtained was a solution of cell membranes and this was diluted as required. To determine the level of agonist stimulation on the protein, comparison of the total and basal binding was determined. A 10  $\mu\text{M}$  solution of S1P was used for the total binding and no compound

was added for the basal. After incubation and filtration there was no significant difference in the two values and the quantity of radiation was unexpectedly low. It was proposed that the [ $^{35}\text{S}$ ]GTP $\gamma$ S may not have bound to the protein, so saponin was added to the solution of protein to permeabilise the membranes and release more free protein. This increased the radiation counts slightly, but there was still little difference between the total and basal binding. Analysis of the documentation of the S1P $_5$  protein membranes showed that they were incapable of surviving one freeze-thaw cycle: i.e. the frozen sample of protein would need using straight after thawing and it was impossible to aliquot and refreeze without denaturing the protein. Further analysis showed that a much higher quantity of protein would be needed for the assay and this may have also explained the low counts of radiation. New assay conditions using a higher concentration of protein were developed.

Using S1P and fluorobenzamide **66**, the new conditions were attempted. To better visualise the affinity binding curves, nine different concentrations of each sample were used in the assay and the experiments were carried out in non-binding 96 well plates. Affinity binding curves were fitted for the data and significant difference between total and basal binding was observed (Figure 23).



**Figure 23: Non-linear fit of S1P $_5$  affinity data for (a) S1P and (b) fluorobenzamide **66****

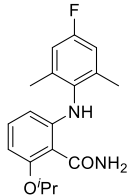
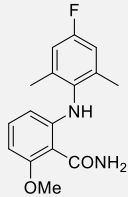
### 2.1.8.3 Evaluation of S1P agonist libraries

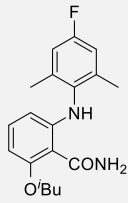
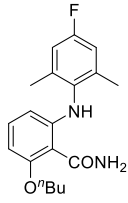
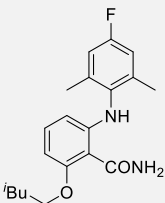
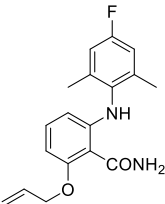
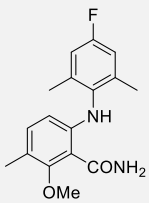
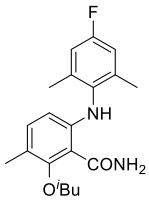
With the optimal conditions for the assay now in hand, the three libraries of compounds could be tested for their affinity for S1P $_5$ . The limiting factor in screening all of the compounds was the S1P receptor membranes. There was a sufficient quantity of S1P $_5$  cell membranes to test all of the compounds, but the most potent compounds would be tested for their affinity for the S1P $_{1-3}$  receptors. Another screening factor was the relative potency of a particular concentration for each compound versus that of the endogenous compound S1P. An ideal radiotracer would have the same potency (100%) as S1P, so

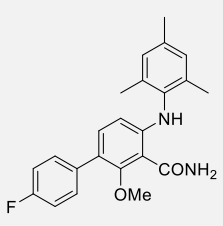
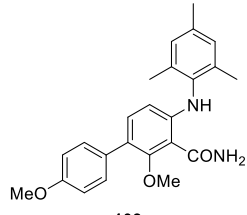
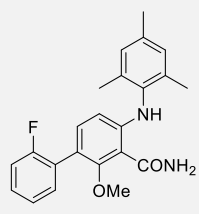
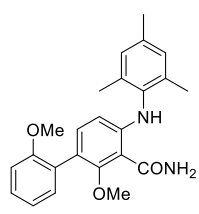
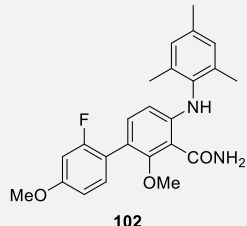
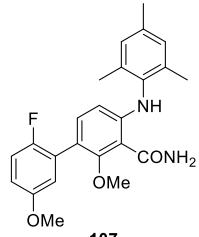
this would competitively bind for the S1P<sub>5</sub> receptors. If this value was too low, little or no binding of the tracer to S1P<sub>5</sub> would take place, given the abundance of the endogenous compound. Likewise, a value that was too high would mean that this tracer could not be displaced by S1P and poor imaging of the distribution would occur, as no competitive binding for the receptor would take place.

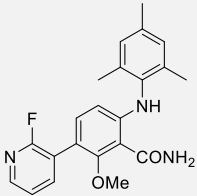
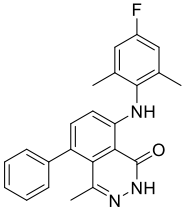
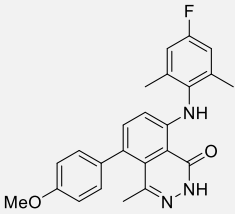
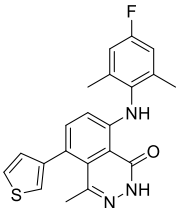
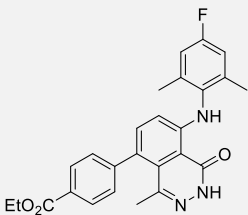
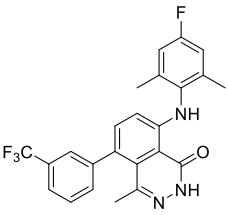
After the first set of assays, any compound with an EC<sub>50</sub> value above 35 nM was excluded from further screening (Table 10). This left six compounds: three from the fluorobenzamide library, two from the library of 3-aryl substituted compounds and one compound featuring a phthalazinone core. Since there was sufficient quantity of cell membranes to test the selectivity of these six compounds, the values for potency relative to S1P was disregarded in this screening process. To measure their selectivity, the compounds were tested for their affinity towards the S1P<sub>1-3</sub> receptors. The most potent compound for S1P<sub>5</sub>, allyl derivative **93**, showed high affinity for S1P<sub>1</sub> and S1P<sub>3</sub> in the 20–30 nM range. This selectivity for S1P<sub>5</sub> was too poor to consider this as a desirable target. The compound from the fluorophthalazinone library and the 3-substituted compounds **102** and **106** also showed high affinity for S1P<sub>1</sub>. The two most promising candidates from this screening process were the fluorobenzamides **89** and **94**, with the former exhibiting better %potency for S1P<sub>5</sub> and better selectivity; the latter showing higher affinity for S1P<sub>5</sub>. With the biological evaluation of these compounds completed, work began examining potential routes towards radiofluorination.

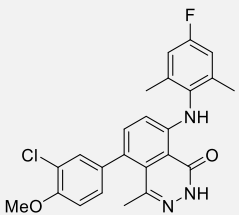
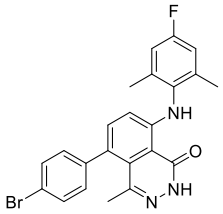
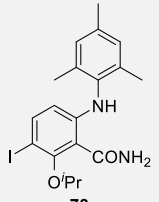
**Table 10: Biological evaluation of S1P agonist libraries with most promising compounds highlighted in red**

Compound	EC <sub>50</sub> (nM) S1P <sub>5</sub>	%Potency	EC <sub>50</sub> (nM) S1P <sub>1</sub>	EC <sub>50</sub> (nM) S1P <sub>2</sub>	EC <sub>50</sub> (nM) S1P <sub>3</sub>
<b>S1P</b>	10.7	100%	n/a	n/a	42.6
 <b>66</b>	419	105%	n/a	n/a	n/a
 <b>89</b>	<b>39.8</b>	<b>108%</b>	<b>&gt;10000</b>	<b>&gt;10000</b>	<b>&gt;10000</b>

Compound	EC <sub>50</sub> (nM) S1P <sub>5</sub>	%Potency	EC <sub>50</sub> (nM) S1P <sub>1</sub>	EC <sub>50</sub> (nM) S1P <sub>2</sub>	EC <sub>50</sub> (nM) S1P <sub>3</sub>
 90	180	137%	n/a	n/a	n/a
 92	234	140%	n/a	n/a	n/a
 92	49	102%	n/a	n/a	n/a
 93	6.66	164%	25.6	>10000	27.6
 94	<b>22.3</b>	<b>183%</b>	<b>104</b>	<b>&gt;10000</b>	<b>2030</b>
 95	2240	154%	n/a	n/a	n/a

Compound	EC <sub>50</sub> (nM) S1P <sub>5</sub>	%Potency	EC <sub>50</sub> (nM) S1P <sub>1</sub>	EC <sub>50</sub> (nM) S1P <sub>2</sub>	EC <sub>50</sub> (nM) S1P <sub>3</sub>
 101	72.3	129%	n/a	n/a	n/a
 103	77.8	154%	n/a	n/a	n/a
 105	954	136%	n/a	n/a	n/a
 104	4880	102%	n/a	n/a	n/a
 102	29.8	120%	76.0	>10000	>10000
 107	612	142%	n/a	n/a	n/a

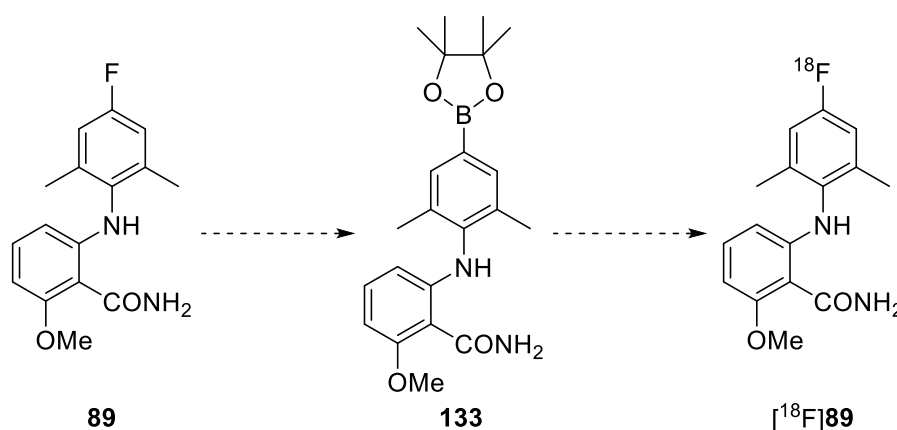
Compound	EC <sub>50</sub> (nM) S1P <sub>5</sub>	%Potency	EC <sub>50</sub> (nM) S1P <sub>1</sub>	EC <sub>50</sub> (nM) S1P <sub>2</sub>	EC <sub>50</sub> (nM) S1P <sub>3</sub>
 106	23.4	175%	0.336	>10000	172
 115	31.4	92%	5.221	>10000	197
 117	3260	62%	n/a	n/a	n/a
 118	3834	134%	n/a	n/a	n/a
 119	>10000	90%	n/a	n/a	n/a
 120	8490	101%	n/a	n/a	n/a

Compound	EC <sub>50</sub> (nM) S1P <sub>5</sub>	%Potency	EC <sub>50</sub> (nM) S1P <sub>1</sub>	EC <sub>50</sub> (nM) S1P <sub>2</sub>	EC <sub>50</sub> (nM) S1P <sub>3</sub>
 121	7350	53%	n/a	n/a	n/a
 116	>10000	27%	n/a	n/a	n/a
 73	49.2	45%	n/a	n/a	n/a

## 2.1.9 Lead Compound Fluorination

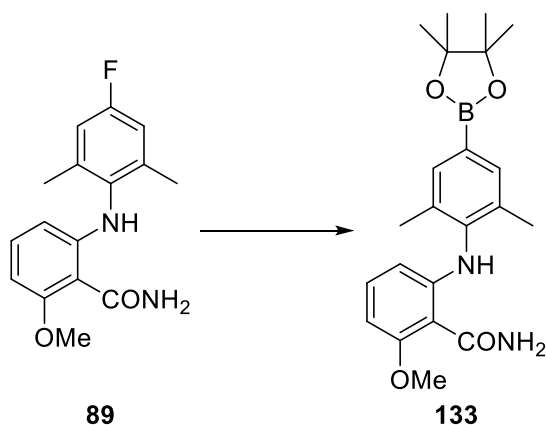
### 2.1.9.1 Synthesis of a precursor for fluorobenzamide **89**

The most promising analogue in terms of potency and selectivity for S1P<sub>5</sub> was fluorobenzamide **89**. As the synthesis of this library of compounds required incorporation of fluorine in an early step, a new route to access a precursor was considered. It was proposed that using *ipso*-defluoroborylation from aryl fluoride **89**, it would be possible to synthesise boronic ester **133**. This could then be radiofluorinated using established methodology.<sup>133</sup>



**Scheme 45: Proposed route to precursor 133 for radiofluorination**

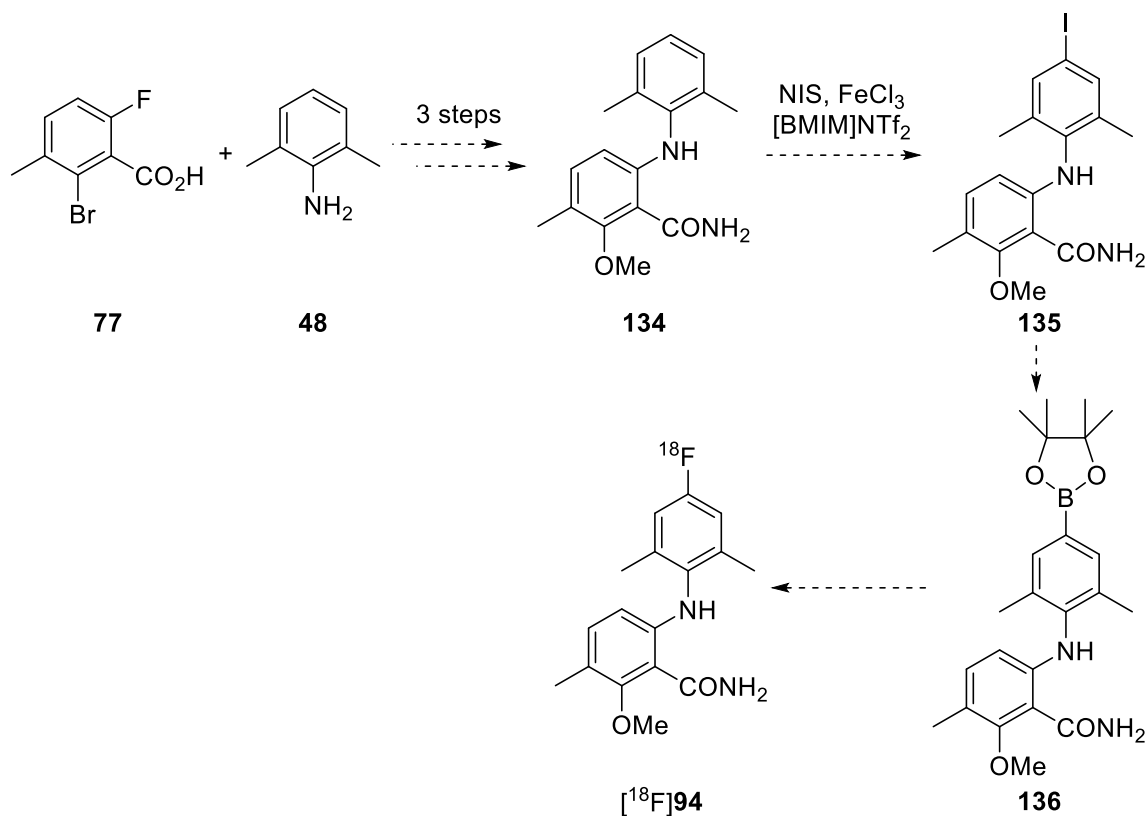
Firstly, a literature method by Zhao *et al.* that used a palladium catalyst and B<sub>2</sub>Pin<sub>2</sub> was attempted that did not require glovebox conditions (Table 11).<sup>160</sup> The mechanism of this reaction involved activation of B<sub>2</sub>Pin<sub>2</sub> and oxidative addition of the palladium into the C–F bond. Transmetalation takes place followed by reductive elimination to afford the boronic ester. Reaction of aryl fluoride **89** under these reaction conditions showed no conversion to any product after 16 h (entry 1). Instead, analysis of the <sup>1</sup>H NMR spectrum of the crude material showed only decomposition of the starting material. This reaction was attempted once more at a lower temperature, but a similar result was observed (entry 2). The authors report that this reaction does not work well with compounds bearing ester and amide functional groups, so this may explain the lack of reactivity. A different literature method using a copper catalyst and PCy<sub>3</sub> ligand was attempted (entry 3).<sup>161</sup> This reaction did not form any product and instead only returned starting material. Heating the reaction under reflux resulted in decomposition (entry 4). The proposed mechanism for this reaction involves electron donation from a copper species into the aryl fluoride.<sup>161</sup> This may explain why electron-rich aryl fluoride **89** did not undergo the reaction and indeed the authors do not report reaction with electron-rich aryl systems.

Table 11: Defluoroborylation reaction of aryl fluoride **89**

Entry	Reagents	Temperature	Yield
1	B <sub>2</sub> Pin <sub>2</sub> , Pd <sub>2</sub> (dba) <sub>3</sub> , LiHMDS, toluene	80 °C	n/a
2	B <sub>2</sub> Pin <sub>2</sub> , Pd <sub>2</sub> (dba) <sub>3</sub> , LiHMDS, toluene	40 °C	n/a
3	B <sub>2</sub> Pin <sub>2</sub> , CuCl, PCy <sub>3</sub> , CsF, toluene	50 °C	n/a
4	B <sub>2</sub> Pin <sub>2</sub> , CuCl, PCy <sub>3</sub> , CsF, toluene	Δ	n/a

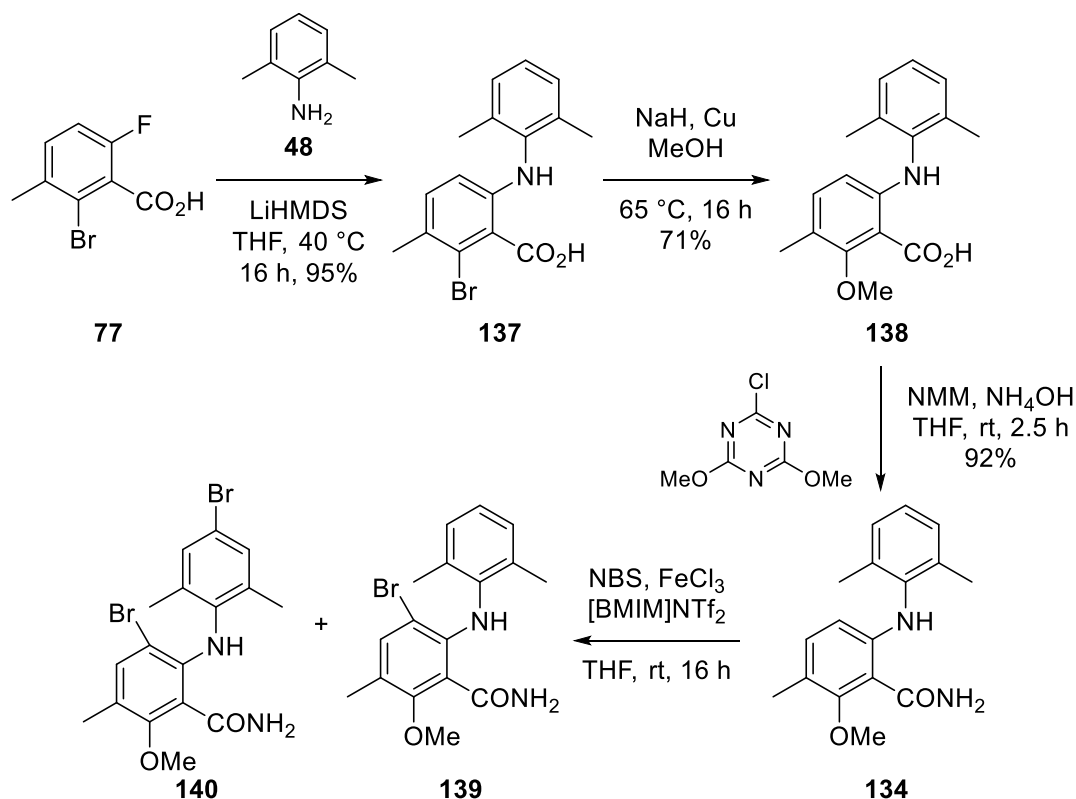
### 2.1.9.2 Synthesis of a precursor for fluorobenzamide **94**

The *ipso*-defluoroborylation to form a precursor for fluorobenzamide **89** was unsuccessful and so a new method to access a precursor for the other biologically active fluorobenzamide, **94** was proposed (Scheme 46). This required the synthesis of 3-methyl analogue **134** using the three established steps towards the benzamide core. It was proposed that the iron(III)-catalysed iodination of **134** would result in iodide **135** and this could be converted to the boronic ester *via* a Miyaura borylation reaction to provide a precursor for radiofluorination.



**Scheme 46: Synthesis of boronate precursor 136 by iodination of 134**

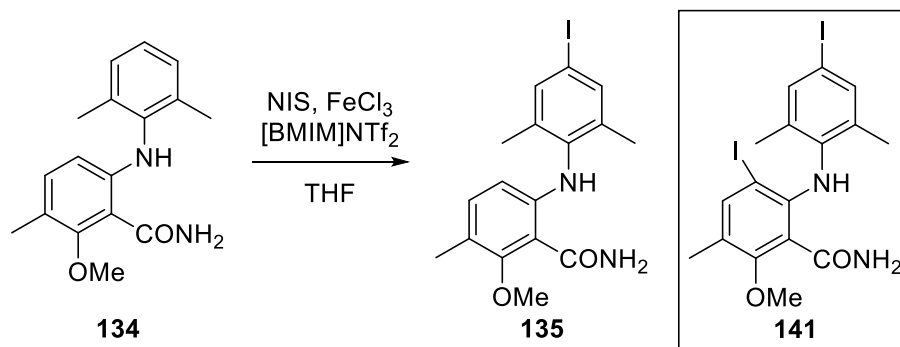
Synthesis of 3-methyl analogue **134** was straightforward using the previously described methodology (Scheme 47). The  $\text{S}_{\text{N}}\text{Ar}$  reaction between benzoic acid **77** and aniline **48** returned aryl bromide **137** in 95% yield; subsequent Ullmann condensation and amidation occurred in 71% and 92% yields, respectively. It was believed that NIS would be a more selective reagent for the upper aryl ring than NBS due to the larger atomic radius of the iodine atom. Nevertheless, the earlier reactions with NIS were not as efficient as those with NBS and so the bromination of **134** was attempted. After 16 h, conversion to mono- and di-brominated products **139** and **140** were observed. These products were isolated as an inseparable mixture in a 1:1 ratio. The mono-brominated product was identified as **139**, due to the presence of a 3H multiplet in the  $^1\text{H}$  NMR spectrum that corresponded to the three hydrogen atoms of the upper ring and disappearance of the two doublets corresponding to C-3 and C-5 of the benzamide ring. This confirmed the theory that, due to being more electron rich, this lower ring would be halogenated first.



**Scheme 47: Synthesis of benzamide 134 and attempted bromination**

For the initial reaction of **138** with NIS, THF was chosen as the solvent as this dissolved the reagents well and was capable of being heated to a higher temperature than dichloromethane (Table 12). The first attempts at the reaction used 1.0 equivalents of NIS and, after 16 h, showed no conversion to product at room temperature or under reflux (entries 1 and 2). Addition of 2.0 equivalents of NIS followed by heating under reflux for 20 h showed a 50% conversion of starting material to mono- and di-iodinated products (entry 3). The di-iodinated product **141** also showed iodination of the C-5 position in the benzamide ring. An attempt was made to separate the mono-iodinated compound, but only the di-iodinated product could be separated leaving a mixture of desired product **135** and starting material **134**. To push this reaction to completion and avoid as little di-iodination as possible, 2.0 equivalents of NIS were added followed by a further equivalent after 16 h (entry 4). After 20 h, full conversion of starting material was observed and iodinated product **135** was isolated in 5% yield; however, insufficient material was obtained for the subsequent Miyaura borylation of **135** to compound **136**.

Table 12: Optimisation of iodination reaction



Entry	NIS equivalents	Temperature	Time	Yield
1	1.0	rt	16 h	n/a
2	1.0	$\Delta$	16 h	n/a
3	2.0	$\Delta$	20 h	n/a
4	3.0	$\Delta$	20 h	5%

### 2.1.10 Conclusions

In summary, several routes towards fluoride analogues of the S1P<sub>5</sub> agonists described by Mattes *et al.* were investigated. A library of compounds was synthesised bearing an aryl fluoride moiety, through incorporation of the fluorine atom in an early step. An Ullmann condensation reaction was used to vary the ether side-chain and two compounds were synthesised that contained a methyl group in the C-3 position of the benzamide ring. A second library of compounds were synthesised, inspired by a serendipitous discovery made when attempting to prepare a precursor from the previous library. This bromination occurred in the C-3 position of the benzamide ring and so by utilising the Suzuki-Miyaura reaction to install fluorine and methoxy-bearing aryl rings, analogues of the most potent compound described in the literature could be synthesised. This library of compounds contained potential sites for fluorine-18 or carbon-11 radionuclides. A final library of compounds were synthesised based on a phthalazinone structure reported in the literature. These compounds also incorporated fluorine early in the synthesis and were further functionalised by the same bromination and subsequent Suzuki-Miyaura reaction as the previous library of compounds.

All three libraries of compounds were tested to obtain their physicochemical properties prior to biological screening. A [<sup>35</sup>S]GTPγS binding assay was used to determine the affinity and selectivity of these libraries for S1P<sub>5</sub> receptors. The two fluorobenzamide compounds **89** and **94** were identified as being the most favourable in terms of their

affinity and selectivity for S1P<sub>5</sub>, having relatively good physicochemical properties. A route towards a potential precursor for fluorobenzamide **89** was proposed that used an *ipso*-defluoroborylation to form boronic ester **133**, however, the reaction conditions were too harsh and not ideal for electron-rich aryl fluorides. A proposed route towards a potential precursor for fluorobenzamide **94** was proposed that began with iodination of benzamide **134** to form an aryl iodide that could be transformed into boronic ester **136**. Competing di-iodination made this reaction hard to control; however, it was possible to isolate aryl iodide **135** in 5% yield.

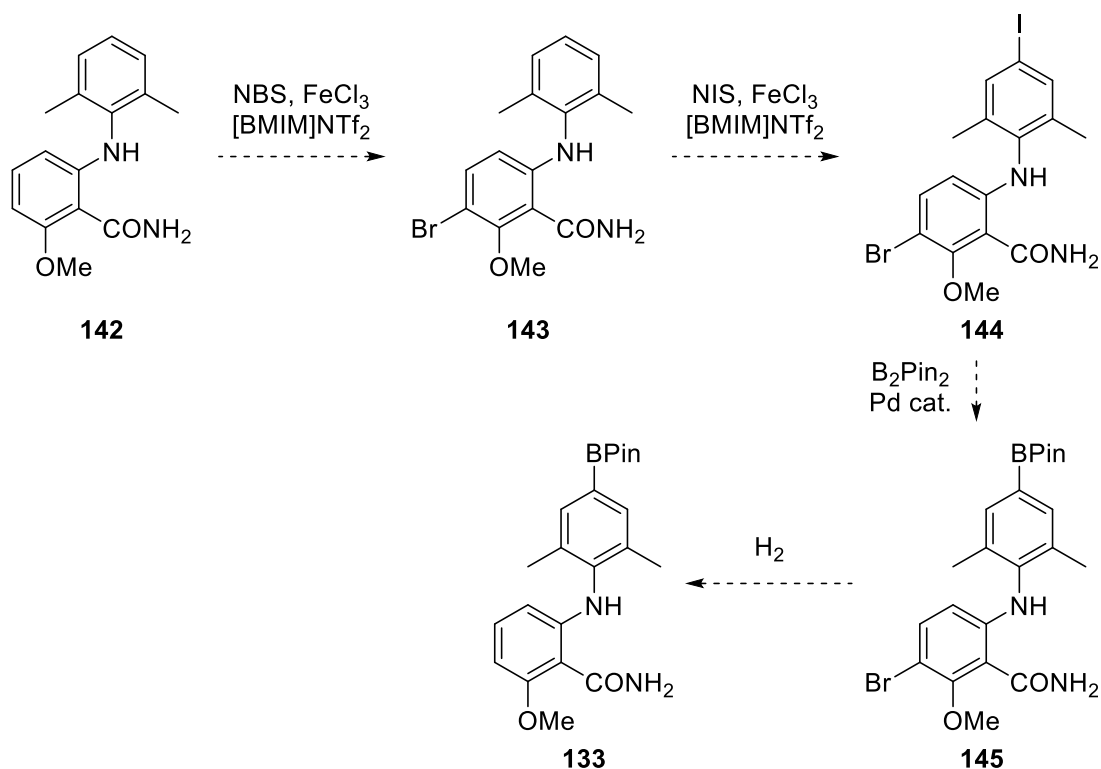
Attempts to synthesise a potential precursor for carbon-11 radiotracer [<sup>11</sup>C]**33** led to several unexpected rearrangement reactions. However, the use of a benzyl protecting group allowed for the synthesis of phenol **124** which could easily be methylated with MeI or MeOTf to give the non-radioactive compound **33**. Radiosynthesis of carbon-11 radiotracer [<sup>11</sup>C]**33** would allow our collaborators to image S1P<sub>5</sub> at the University of Edinburgh and the reaction was optimised on a Synthra Wolpertinger module. A 94% conversion to product was observed by radio-HPLC. This reaction was then purified using a method that could be used by the FX<sub>C</sub> PRO module in Edinburgh. This successfully provided a route towards radiochemically pure benzamide [<sup>11</sup>C]**33**, but would require adjustment to suit a different synthesiser and provide a superior radiochemical yield.

### 2.1.11 Future Work

Future work carried out at the University of Edinburgh will involve the synthesis of carbon-11 radiotracer [<sup>11</sup>C]**33** using an FX<sub>C</sub> PRO module. Since this reaction has already been optimised, this work will involve tailoring the purification to fit the synthesiser. Once a radiosynthesis has been established, preclinical work investigating the distribution and metabolism of this radiotracer *in vivo* will begin. A carbon-11 radiotracer that specifically targets S1P<sub>5</sub> can then begin to study the role this receptor plays in repair of neurons.

Optimisation of the iodination reaction to form mono-iodinated analogue **135** would allow for a larger quantity to be synthesised and the subsequent borylation and fluorination can be attempted. Attempting the iodination using different solvents may prove more effective, including the use of ionic liquid as the solvent. Other methods could be employed that use silver triflimide as a catalyst. This has been shown to be an effective catalyst for the iodination of arenes using NIS.<sup>125</sup> The larger size of the silver atom improves regioselectivity of the iodination reaction and may prevent unwanted iodination in the sterically congested benzamide ring.

To synthesise a potential precursor for fluorobenzamide **89**, selective bromination of **142** could provide brominated analogue **143** (Scheme 48). With this C-3 position blocked and the lower ring more electron-deficient, iodination of the upper ring may be more efficient. With the enhanced reactivity of the aryl iodide over the bromide, Miyaura borylation should provide boronic ester **145** selectively. The bromine could then be removed *via* hydrogenation to give boronic ester precursor **133**.



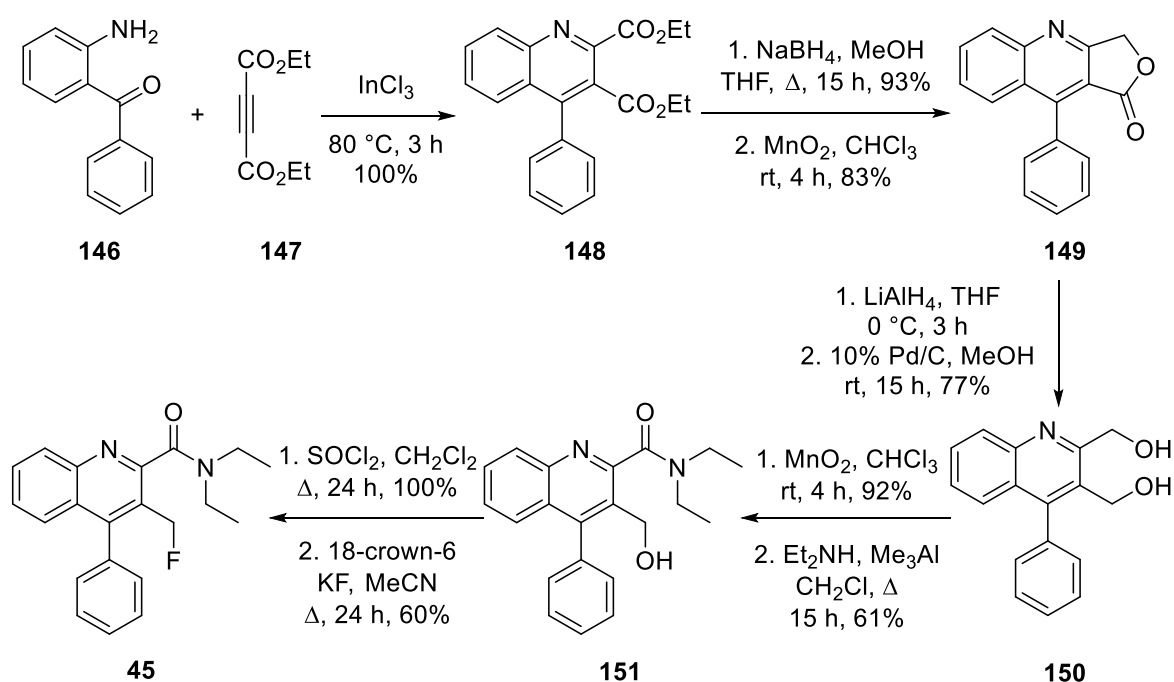
**Scheme 48: Proposed synthesis of a precursor for radiofluorination**

## 2.2 Synthesis of LW223: A PET Imaging Agent for TSPO

### 2.2.1 Project Aims

Following the initial success of AB5186 (**45**) through the early stages of preclinical testing (see section 1.4.2), larger quantities were required for human clinical trials. This required the synthesis of both AB5186 (**45**) and the chloride precursor **44** on a multi-gram scale. Therefore, work was carried out on improving the overall nine-step synthesis. Although the radiosynthesis was efficient, there was concern that when applied to an automated system, there may be difficulty in separating the radioactive product from the unreacted precursor compound. Thus, another objective was to investigate other potential precursors to improve automation of the radiofluorination step.

The first goal was to use the same nine-step procedure used by Blair *et al.*, (Scheme 49) and synthesise both AB5186 (**45**) and the chloride precursor **44** to assess further, the binding profile in human tissue.<sup>119</sup> Work began by assessment and optimisation of the route and synthesis of **44** on a large enough scale to investigate the incorporation of a different leaving group for the final radiofluorination step.

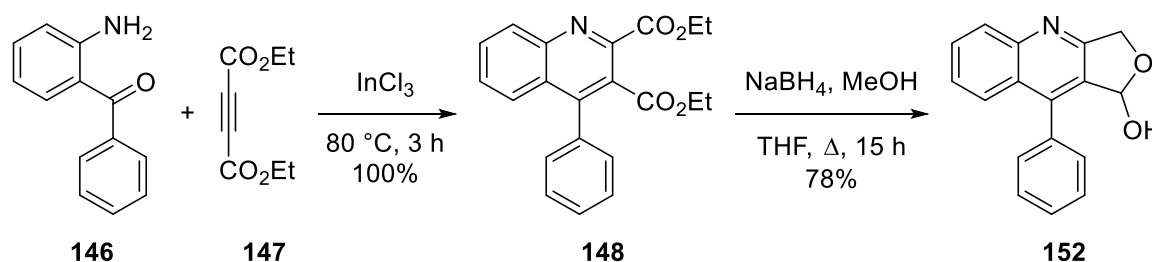


Scheme 49: Published synthesis of AB5186 (**45**)<sup>119</sup>

## 2.2.2 Synthesis and Evaluation of AB5186

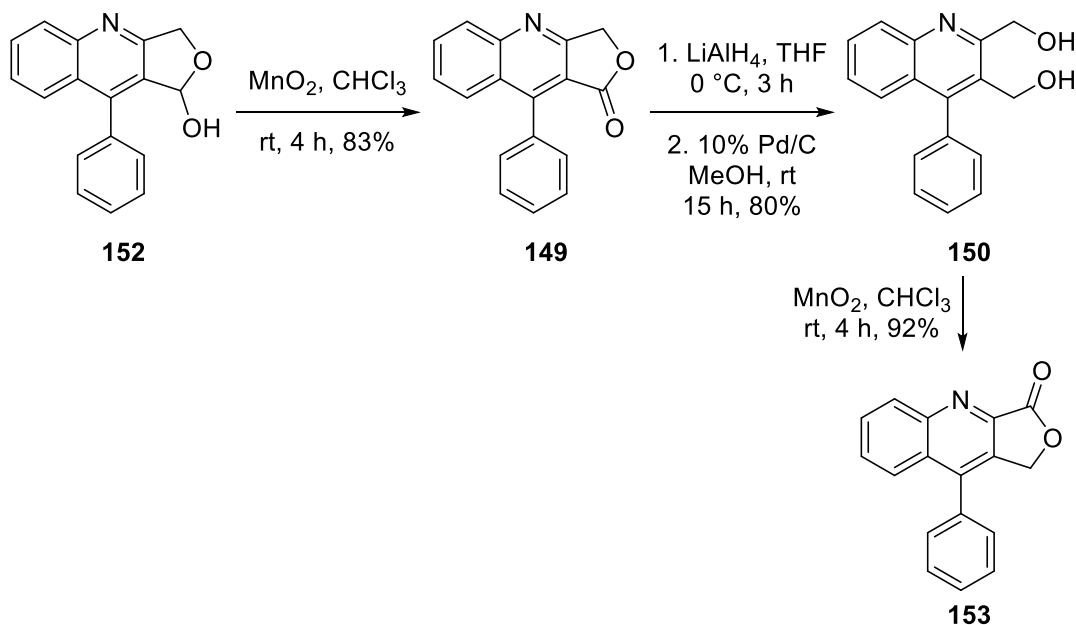
### 2.2.2.1 Initial synthesis

The first stage of this project involved using the same route as Blair *et al.*, to synthesise AB5186 (**45**).<sup>119</sup> This began with a one-pot two component reaction between 2-aminobenzophenone (**146**) and diethyl acetylenedicarboxylate (**147**) using indium(III) chloride as a catalyst to form quinoline **148** in a quantitative yield (Scheme 50).<sup>162</sup> This reaction was performed neat and used indium(III) chloride as a Lewis acid to activate the carbonyl of **147**. The next step involved a sodium borohydride reduction in methanol to reduce **148** to lactol **152** in 78% yield. The order of addition was important for this reaction, as initial attempts involving addition of starting material **148** to a solution of NaBH<sub>4</sub> in methanol and THF were very low yielding. It was believed this was due to decomposition of material through the slow addition of small quantities of **148** into a solution containing large quantities of NaBH<sub>4</sub>. A reversal of the order of addition, adding NaBH<sub>4</sub> to **148**, resulted in a much better yield.



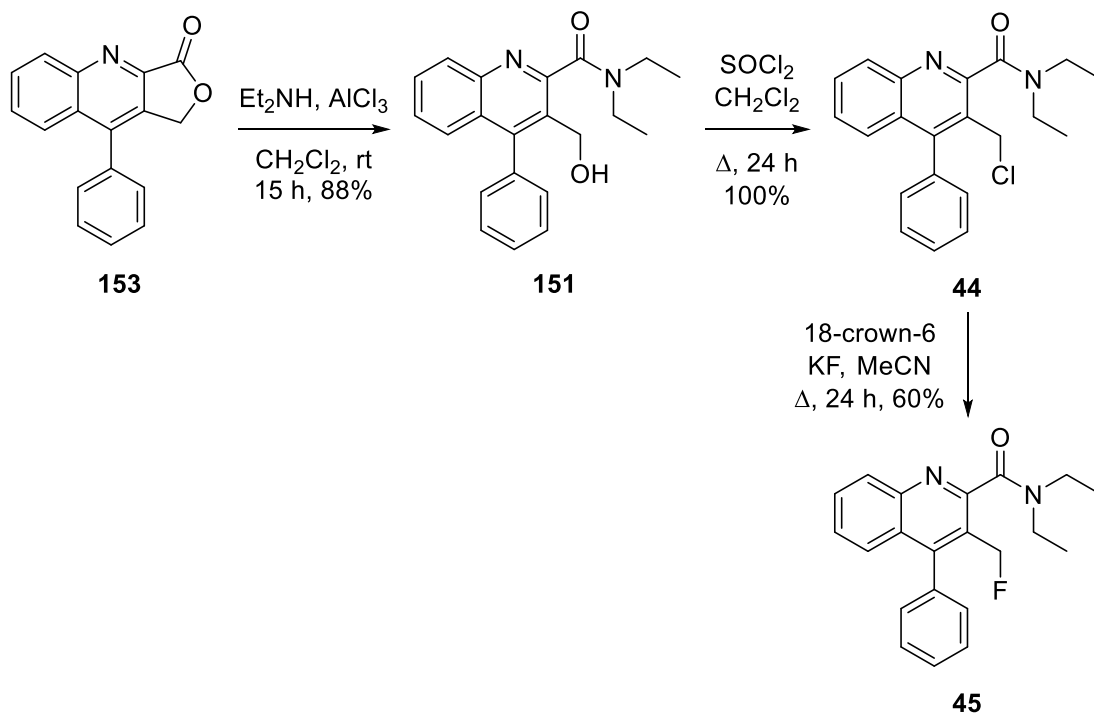
**Scheme 50: Initial coupling and reduction**

Lactol **152** was then oxidised to lactone **149** using manganese(IV) oxide in 83% yield over 4 h (Scheme 51). To switch the lactone from the C-3 to the C-2 position (**153**), lactone **149** was subjected to lithium aluminium hydride (LAH) reduction. The work-up for this reaction reported in the literature involved addition of 1 M aqueous hydrochloric acid followed by extraction with ethyl acetate. Work-up methods with LAH can often form aluminium emulsions that cause separation difficulties, further complicated in this case by the presence of the over-reduced quinoline. Instead of using an acidic work up, the Fieser method was employed (quenched with water, basified and filtered).<sup>163</sup> After subsequent re-oxidation of the nitrogen-carbon bond using 10% palladium on carbon in methanol, **150** was achieved in 80% yield. This was then treated with the same manganese(IV) dioxide conditions and through chelation control of the manganese with the nitrogen of the quinoline, gave desired lactone **153** in 92% yield.



**Scheme 51: Changing to an alternate lactone isomer**

The next step of the route was the trimethylaluminium-mediated incorporation of diethylamine and concurrent formation of the 3-hydroxymethyl group under reflux to form **151** in 61% yield. Trimethylaluminium is a powerful, highly pyrophoric reagent. Thus, before this reaction was attempted, a similar reaction using the more stable and milder Lewis acid aluminium(III) chloride was attempted (Scheme 52). This reaction reached completion after 15 h under these milder conditions, at room temperature and formed **151** in an improved yield of 88%. The final steps were chlorination using thionyl chloride and halogen-exchange using potassium fluoride and 18-crown-6. The 18-crown-6 was used to coordinate the potassium counter-ion, resulting in a more reactive fluoride nucleophile. This 18-crown-6 also acted as a phase transfer catalyst, allowing transport of the fluoride anions into the organic phase where the reaction took place. Given the hygroscopic nature of this crown ether, it was important to perform this fluorination under anhydrous conditions. These steps proceeded according to the literature in a quantitative yield and 60% yield, respectively.<sup>119</sup>

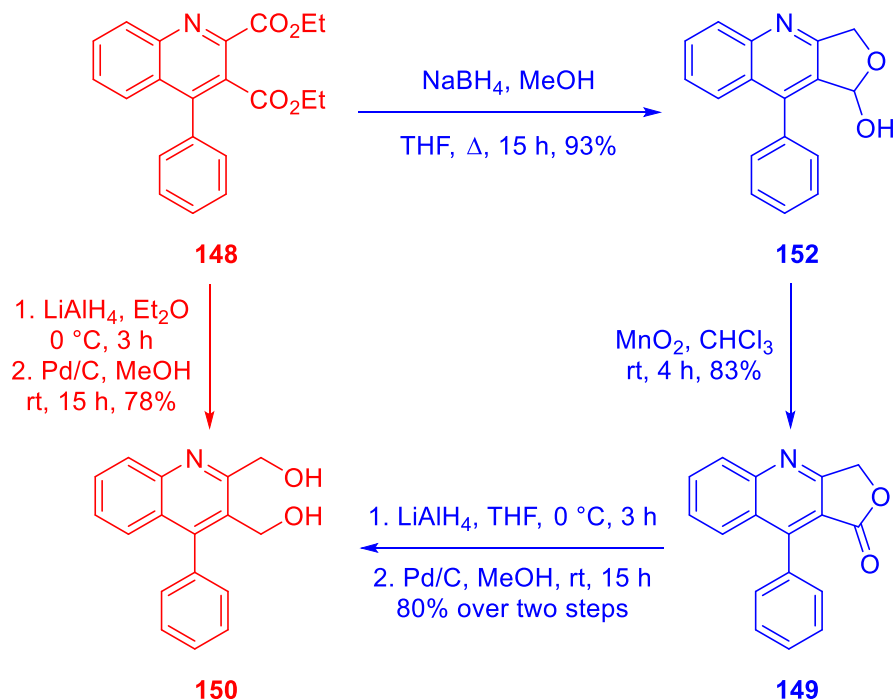


**Scheme 52: Synthesis of chloride precursor and successive fluorination**

### 2.2.2.2 Optimisation of the route

Following the successful substitution of aluminium(III) chloride for trimethylaluminium and the subsequent synthesis of AB5186 (**45**), further optimisation of the route was investigated. Initial analysis identified the switching of the lactone orientation, from diester **148** to lactone **149** (Scheme 51), as inefficient and an area that could be significantly improved. It was hypothesised that a direct reduction of the diester to the diol **150** would be possible using LAH as the reducing agent.

This reduction was attempted using LAH and the same conditions for the following Pd/C oxidation (Scheme 53). As previously mentioned, LAH reaction work-up procedures can be problematic due to the formation of complex aluminium emulsions. Therefore, the Fieser work-up was used to yield **150** in 78% yield over two steps. This improvement, along with the use of aluminium(III) chloride, meant that the multi-gram synthesis of AB5186 (**45**) was possible, requiring three fewer steps and with a higher overall yield (38% over five steps).

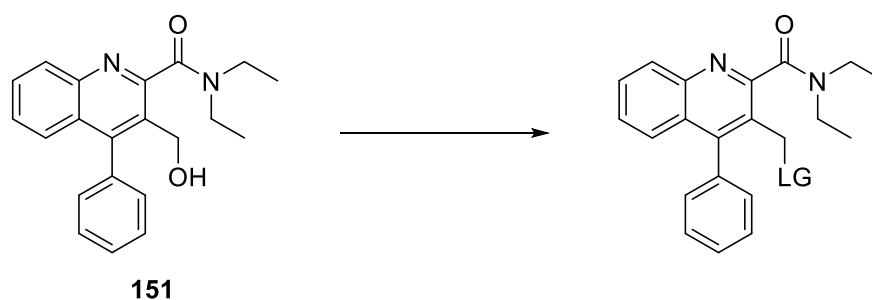


**Scheme 53: Direct reduction of 148 to 150 (shown in red) and previous route *via* lactone 149 (shown in blue)**

### 2.2.2.3 New leaving groups for fluorination

Now that it was possible to quickly generate a large quantity of alcohol **151**, work began to investigate different leaving groups for the fluorination. The first leaving group investigated was a tosylate (Table 13), however, when tosylation at both room temperature and under reflux was attempted, no conversion was observed (entries 2 and 3). This was most likely due to the size of the tosyl group and the steric bulk around the *ortho,ortho*-disubstituted benzyl alcohol. With this in mind, mesylation was attempted using the relatively smaller mesyl chloride (entry 4). Analysis of the reaction mixture showed no starting material and the formation of a new product. Instead of forming the mesylate, the chloride was isolated in 86% yield. In this case, it was assumed that the mesylate had formed, but been displaced by the chloride ion present. The reaction to form the mesylate was attempted again at room temperature, in the presence of 4-dimethylaminopyridine (DMAP). It was proposed that the milder conditions would leave the mesylate intact (entry 5). Unfortunately, the same result was observed and the chloride compound was isolated. Considering these results, the formation of a triflate was attempted using triflic anhydride, a reagent that has no chloride counter ion (entry 6). No conversion to product was observed and the alcohol **151** decomposed under the reaction conditions. Acetic anhydride was then used to form an acetate (entry 7). This successfully formed **154** in 83% yield. However, when **154** was subjected to typical fluorination conditions, no product was formed.

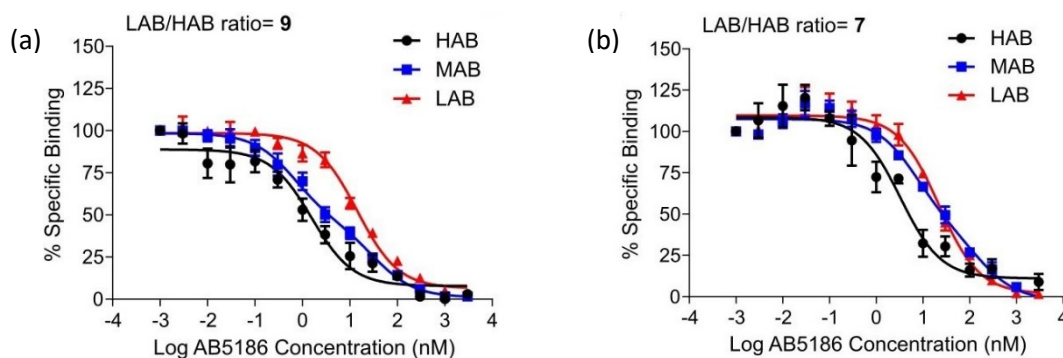
Table 13: Attempted synthesis of a new precursor



Entry	Leaving Group	Conditions	Temperature	Yield	Fluorination Yield
1	Cl	SOCl <sub>2</sub> , CH <sub>2</sub> Cl <sub>2</sub>	Δ	100%, <b>44</b>	60%
2	OTs	TsCl, NEt <sub>3</sub> , CH <sub>2</sub> Cl <sub>2</sub>	rt	0%	n/a
3	OTs	TsCl, NEt <sub>3</sub> , CH <sub>2</sub> Cl <sub>2</sub>	Δ	0%	n/a
4	OMs	MsCl, NEt <sub>3</sub> , CH <sub>2</sub> Cl <sub>2</sub>	Δ	86% <b>44</b>	n/a
5	OMs	MsCl, NEt <sub>3</sub> , DMAP, CH <sub>2</sub> Cl <sub>2</sub>	rt	74%, <b>44</b>	n/a
6	OTf	Tf <sub>2</sub> O, DIPEA, CH <sub>2</sub> Cl <sub>2</sub>	-78 °C to rt	0%	n/a
7	OAc	Ac <sub>2</sub> O, NEt <sub>3</sub> , DMAP, CH <sub>2</sub> Cl <sub>2</sub>	rt	83%, <b>154</b>	0%

#### 2.2.2.4 Biological Assessment of AB5186

Access to multi-gram quantities of AB5186 (**45**) allowed biological assessment to be carried out. Specifically, the evaluation of the specific binding in human brain and heart tissue samples to assess sensitivity to the single nucleotide polymorphism (rs6971). By using samples that were known to be high-affinity binders (HAB), low-affinity binders (LAB) and mixed (MAB), it was possible to quantify the level of sensitivity. Following testing by our colleagues at the University of Edinburgh, it was shown that AB5186 (**45**) was indeed sensitive to the polymorphs of TSPO (Figure 24), albeit to a lesser extent than some of the other second generation TSPO ligands (see section 1.4.2): the LAB/HAB ratio of PBR28 in human brain and heart tissue was 48 when compared in the same assay. It was clear that a new molecular target was necessary and a re-evaluation of the structure was therefore considered.

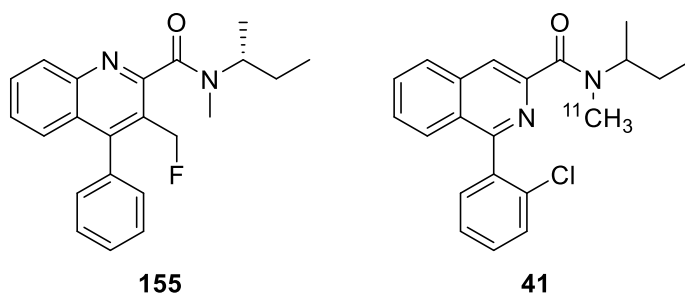


**Figure 24: Mean AB5186 (45) binding affinity curves in (a) human brain and (b) human heart, showing high (black), low (red) and mixed (blue) affinity binding**

## 2.2.3 Synthesis and Evaluation of LW223

### 2.2.3.1 Initial synthesis

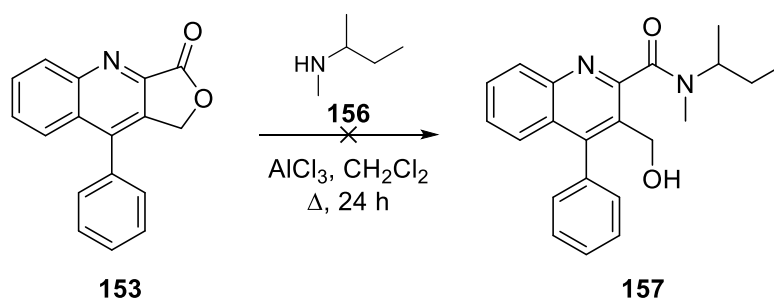
After reconsidering the structure of AB5186 (**45**), a new compound, LW223 (**155**) was proposed, featuring a *sec*-butyl chain in the amide part of the molecule (Figure 25). This particular functionality is observed in PK11195 (**41**) as a racemic mixture, but studies by Shah *et al.* showed that the (*R*)-enantiomer of PK11195 (**41**) shows 2-fold greater affinity than the (*S*)-enantiomer for the known binding sites *in vitro*.<sup>164</sup> Thus, the (*R*)-enantiomer of **155** was proposed as the desired target.



**Figure 25: New proposed structure (155) and PK11195 (41)**

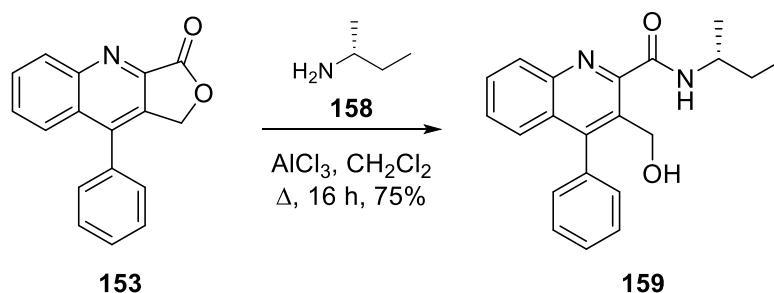
It was envisioned that the synthesis of LW223 (**155**) could be performed with only a small alteration to that of AB5186 (**45**): changing the amine from diethylamine to (*R*)-*N*-methyl-*sec*-butylamine (**156**) for the ring opening of the lactone **153**. Initial optimisation work was carried out with the racemic amine, as this was cheaper and more readily available. Attempts to open lactone **153** using amine **156** using the same conditions were unsuccessful. The reaction showed no conversion of starting material; increasing the time and the temperature of the reaction also had no effect. It was believed that amine **156** was

too sterically hindered to react with the lactone. Subsequently, it was proposed that using a less sterically hindered primary amine may be more successful.



**Scheme 54: Attempted ring opening reaction**

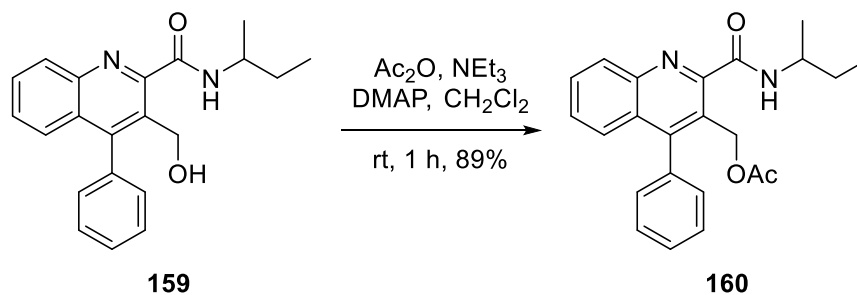
Ring opening of the lactone using (*R*)-*sec*-butylamine (**158**) was more successful, with the reaction reaching completion after 16 h under reflux. However, despite full conversion of starting material **153**, only a low yield of 30% was achieved for this process. It was believed that some of the product was being lost in the acidic work-up, which was used to remove the excess amine. Subsequently, this aqueous step of the work-up was removed and instead the reaction was filtered to remove solid impurities. The amine was then evaporated *in vacuo*. This adapted procedure afforded **159** in 75% yield for both the racemic and enantiomeric reactions (Scheme 55).



**Scheme 55: Lactone ring opening using amine 158**

With the ring-opened product **159** now in hand, attempts were made to complete the rest of the synthesis. The nitrogen of the amide would need to be methylated prior to the chlorination of the compound to form the precursor. This was not without challenge: any *N*-methylation procedures may also involve a competing *O*-methylation reaction. Consequently, it was proposed to first protect the alcohol of **159**. Prior investigation into an optimal leaving group for AB5186 (**45**) (Table 13) provided insight into which protecting groups could be installed, in particular, the synthesis of acetate **154**. The same conditions

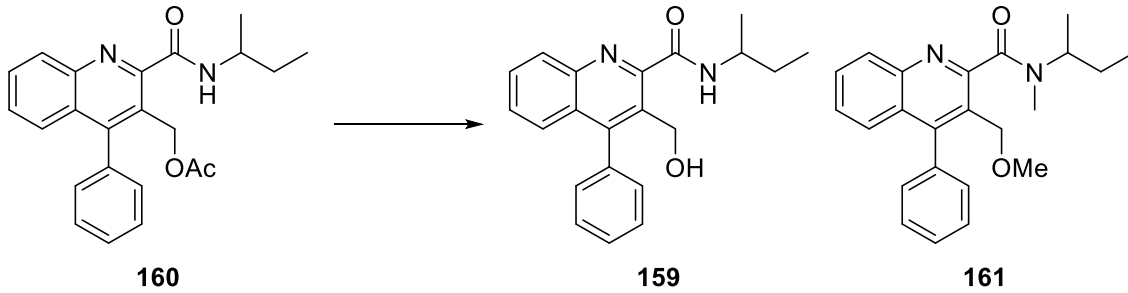
used for the AB5186 (**45**) route were effective in synthesising acetate **160** from alcohol **159** in 89% yield (Scheme 56).



**Scheme 56: Synthesis of acetate 160**

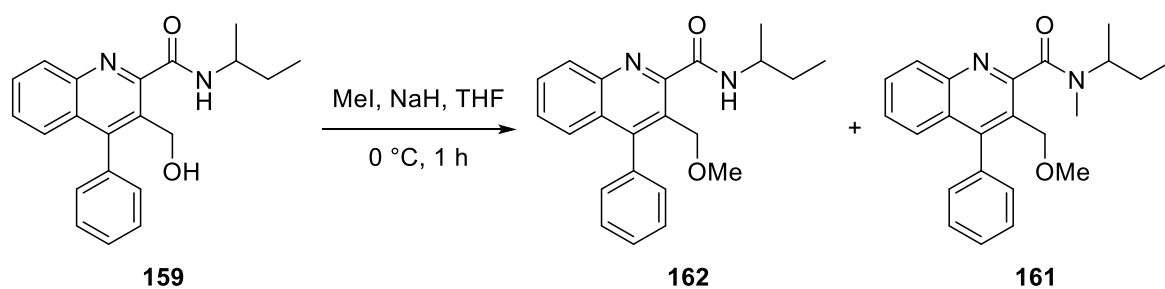
Acetate **160** was subjected to standard methylation conditions (Table 14), using iodomethane (1 equivalent) and sodium hydride in DMF (entry 1). At room temperature, no conversion of starting material was observed, but when the reaction was heated to 60 °C, there was full conversion of the starting material to the deprotected alcohol **159** (entry 2). Since these conditions resulted in removal of the acetate, but no methylation, silver oxide was added to the reaction in an attempt to remove any HI generated and allow the reaction to be carried out at a lower temperature (entry 3). This did improve the methylation, however, it still resulted in deprotection of the alcohol and the di-methylated product **161** was obtained in 41% yield (Table 14). Literature procedures using  $n\text{BuLi}$  and MeI to methylate amides in the presence of esters have been reported.<sup>165–167</sup> With this in mind, these conditions were applied to acetate **160** (entry 4). After 1 h of reaction at –78 °C, only the deprotected alcohol **159** was returned in 75% yield. Another method reported by Monteiro *et al.* describes the use of trimethyloxonium tetrafluoroborate as a methylating agent in the presence of esters.<sup>168</sup> When this method was applied (entry 5), the di-methylated product **161** was produced in 36% yield.

Table 14: Attempted methylation reaction



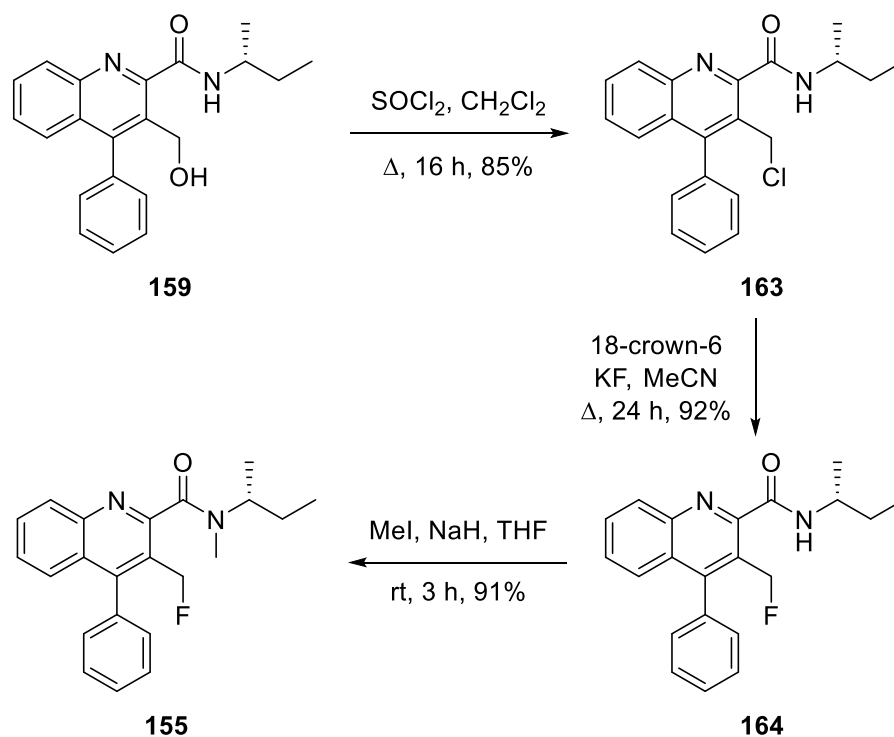
Entry	Reagents	Solvent	Temperature	Product	Yield
1	MeI, NaH	DMF	rt	n/a	n/a
2	MeI, NaH	DMF	60 °C	<b>159</b>	35%
3	MeI, NaH, Ag <sub>2</sub> O	DMF	rt	<b>161</b>	41%
4	<sup>t</sup> BuLi, MeI	THF	-78 °C	<b>159</b>	75%
5	<sup>t</sup> BuOK, Me <sub>3</sub> OBF <sub>4</sub>	CH <sub>2</sub> Cl <sub>2</sub>	rt	<b>161</b>	36%

The N-H hydrogen atom was believed to be of a very similar  $pK_a$  to that of the O-H. Nevertheless, careful control of the quantity of reagents could result in mono-methylation of one of the groups. Using the alcohol **159** and maintaining the quantity of MeI and NaH to 0.9 equivalents, the reaction was carried out at 0 °C in THF to improve the solubility of the reagents (Scheme 57). After 1 h, there was evidence of three products from the reaction, including a mono-methylated compound in 32% yield. This was confirmed as the O-methylated compound **162** by the absence of the broad triplet in the <sup>1</sup>H NMR spectrum. The di-methylated compound **161** and alcohol **159** were also obtained from this reaction in 27% and 19% yield, respectively.



Scheme 57: Methylation with 0.9 equivalents of MeI and NaH

With methylation of the amide being complicated by the presence of the alcohol, the route was redesigned so that the methylation was performed as a final step. Chlorination of **159** occurred as expected in 85% yield after 16 h (Scheme 58) and subsequent fluorination, using previously described conditions, gave **164** in 92% yield. The final methylation step, using standard conditions returned LW223 (**155**) in 91% yield after 3 h. Methylation also resulted in the appearance of rotamers in the  $^1\text{H}$  and  $^{13}\text{C}$  NMR spectra. This was observed most dramatically for the hydrogen atom of the chiral centre of the *sec*-butyl chain splitting into two peaks. This appeared as two separate signals at 3.60 ppm and 4.88 ppm (Figure 26). It was believed that the appearance of rotamers was due to restricted rotation of the amide bond as a result of a more sterically hindered side chain. It was not possible to coalesce the rotamer peaks in the  $^1\text{H}$  NMR spectrum, despite heating the sample to 100  $^\circ\text{C}$  in  $\text{DMSO-}d_6$ . However, the ratio of the rotamers did change from a 3:1 mixture to 1:1.



**Scheme 58: Initial synthesis of LW223 (155)**

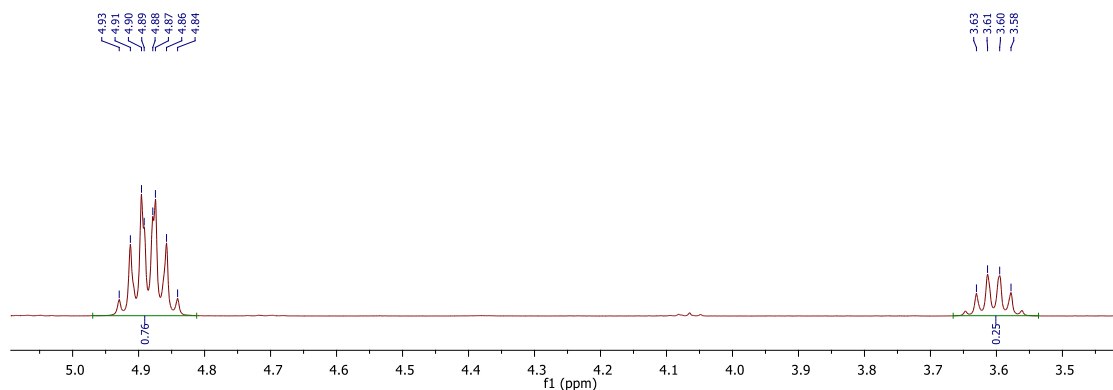


Figure 26: Expansion of the  $^1\text{H}$  NMR spectrum of LW223 (**155**) in  $\text{CDCl}_3$

Although this route was successful in producing the desired compound for testing, due to the fluorination being the penultimate step, another approach would be required for radiofluorination. Although many  $^{18}\text{F}$ -labelled tracers are produced in a two-step method (e.g.  $[^{18}\text{F}]\text{FDG}$  or  $[^{18}\text{F}]\text{FMISO}$ ), the steps that follow radiofluorination tend to be removal of protecting groups and are very fast. Consequently, this route would require re-examination depending on the success of human tissue affinity testing.

### 2.2.3.2 Biological assessment of LW223

LW223 (**155**) was next tested by our collaborators in human tissue samples for sensitivity to the genetic polymorphism (rs6971) in TSPO. In human brain and heart tissue, the affinity of LW223 (**155**) for TSPO demonstrated no significant difference between the HAB and LAB, giving a ratio of 1 (Figure 27). Furthermore, the mean binding affinity ( $K_i$ ) of LW223 (**155**) in human brain tissue was shown to be 0.6 nM, twice the potency of PK11195 (**41**) (1.2 nM). In human heart tissue, the  $K_i$  value of 1.7 nM for LW223 (**155**) was found to be the same as PK11195 (**41**).

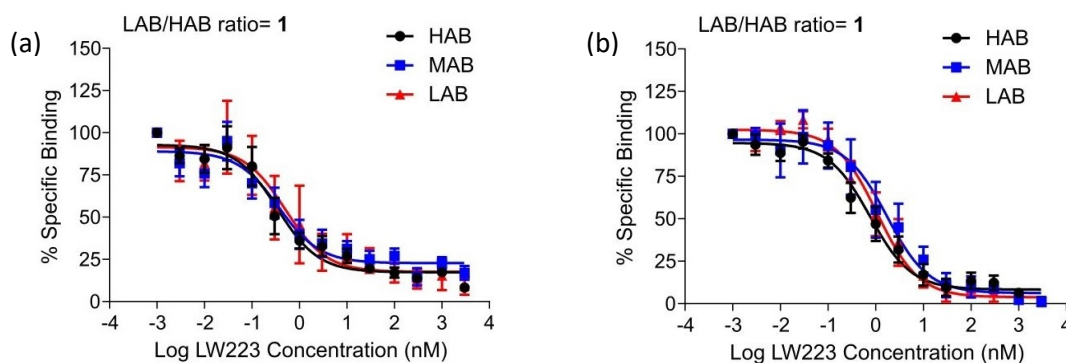


Figure 27: Mean LW223 (**155**) binding affinity curves in (a) human brain and (b) human heart showing high (black), low (red) and mixed (blue) affinity binding

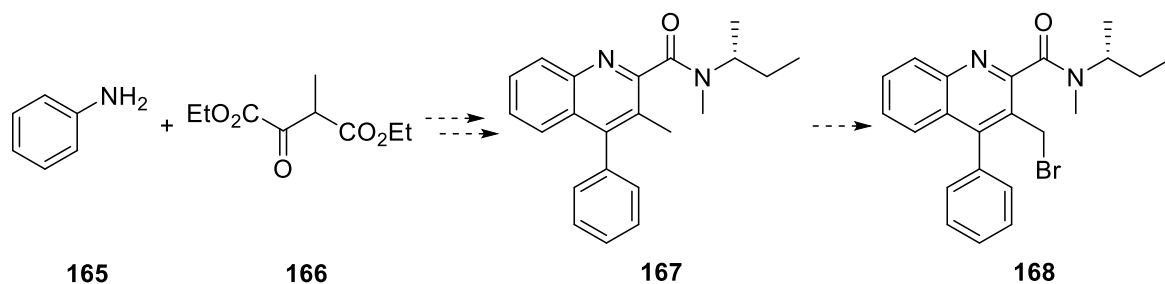
Given the promising affinity results, the physicochemical properties of LW223 (**155**) were assessed using the previously described HPLC methodology (see section 2.1.5).<sup>122</sup> These values were determined alongside those of PK11195 (**41**) and AB5186 (**45**) (Table 15). As expected, the physicochemical properties of LW223 (**155**) were not as ideal as those of AB5186 (**45**), since adding the *sec*-butyl chain resulted in a more lipophilic compound. However, the  $\log P$ ,  $K_m$  and  $P_m$  were within the predicted ideal properties of a radiotracer (see section 2.1.5.4).<sup>122</sup> The %PPB was very high for LW223 (**155**), however, the values obtained for PK11195 (**41**) and AB5186 (**45**) were also higher when compared with previously calculated values (92% and 90%, respectively).<sup>119,169</sup> Correcting this value, using PK11195 (**41**) and AB5186 (**45**) as standards to conform with previous studies, returns a %PPB of 92%.

**Table 15: Physicochemical properties of LW223**

Compound	$\log P$	%PPB	$K_m$	$P_m$
PK11195 ( <b>41</b> )	3.98	97%	184	0.52
AB5186 ( <b>45</b> )	3.74	96%	124	0.35
LW223 ( <b>155</b> )	4.17	98%	195	0.56

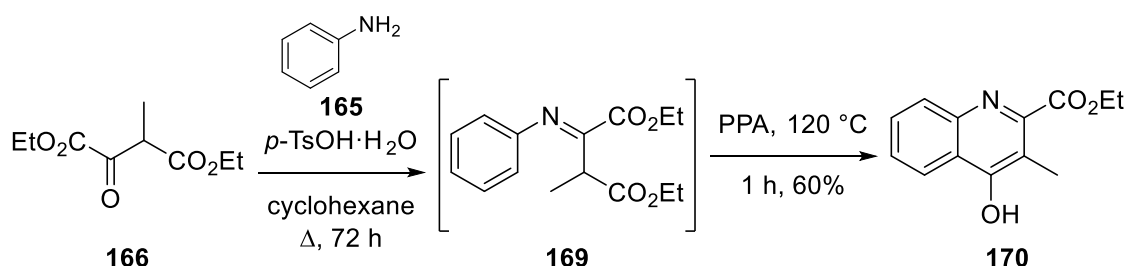
### 2.2.3.3 Synthesis of a precursor for LW223 (**155**)

As the majority of properties for LW223 (**155**) were found to be positive, work began on adapting the synthesis so as to allow for late stage radiofluorination. Previous work carried out within the Sutherland group investigated iodinated quinoline derived compounds for SPECT imaging.<sup>170,171</sup> Amongst the compounds reported were some featuring *N*-methylated amides with *sec*-butyl chains. This *N*-methylation was performed in the absence of any other groups that could potentially react. Thus an adaptation of this synthesis was attempted in order to develop an appropriate precursor. Utilisation of this literature route would allow access to 3-methyl quinolone **167** (Scheme 59). A radical bromination could provide the potential precursor **168**, which then could either be converted to the chloro-compound or used directly for a final step fluorination.



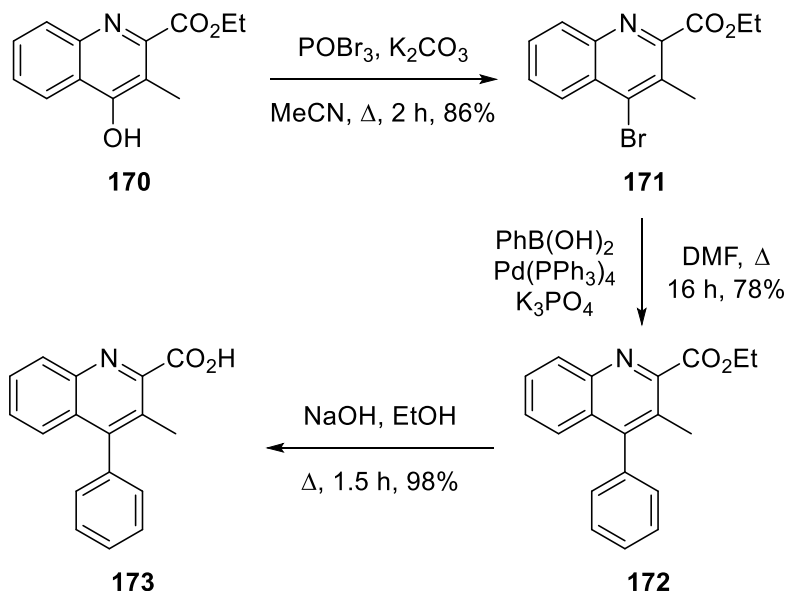
**Scheme 59: Proposed synthesis of a precursor (168) to perform a late stage fluorination**

The first step was the construction of the quinoline ring *via* a Combes quinoline synthesis using conditions developed by Bradbury *et al.* (Scheme 60).<sup>172,173</sup> This two part reaction consisted of condensation of aniline with diethyl oxalpropionate (**166**) to form imine **169** using catalytic tosic acid. The reaction took place under Dean-Stark conditions in order to remove water that was generated. Imine **169** was not isolated, but instead immediately subjected to acid-mediated cyclisation using polyphosphoric acid at 120 °C, forming quinoline **170** in 60% yield over the two steps.



**Scheme 60: Synthesis of quinoline 170**

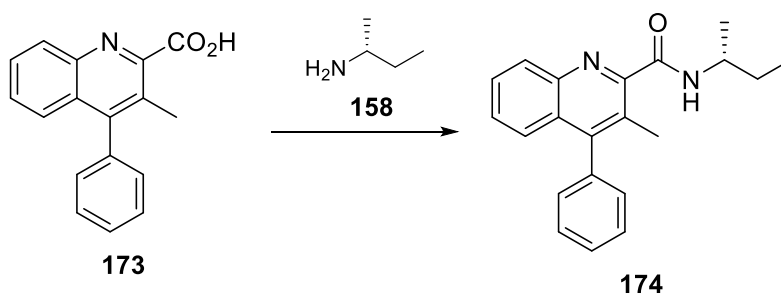
The next step was the incorporation of the phenyl ring onto the quinoline. To perform this, a bromination reaction was first employed, using phosphorus oxybromide (POBr<sub>3</sub>) in the presence of potassium carbonate (Scheme 61). This reaction was completed in 2 h and gave **171** in 86% yield. The incorporation of a bromine atom now allowed the use of a Suzuki-Miyaura reaction with benzeneboronic acid.<sup>135</sup> In the literature, this reaction took 48 h to go to completion and required an additional portion of boronic acid and base. It was believed that this slow conversion was due to oxidation of the palladium catalyst by dissolved oxygen in the solvent of the reaction. Consequently, the reaction mixture was degassed under argon before addition of Pd(PPh<sub>3</sub>)<sub>4</sub> (3 mol%) and full conversion of the reaction was confirmed after 16 h, giving **172** in 78% yield. To prepare the compound for an amide coupling, the ester was then converted to the acid in a hydrolysis reaction, using standard conditions, to give **173** in 98% yield.



**Scheme 61: Synthesis of acid 173**

Acid **173** was submitted to an amide coupling with *sec*-butylamine to form amide **174**, with conditions described in an earlier chapter (see section 2.1.4.2). This involved formation of the acid chloride intermediate with oxalyl chloride, followed by reaction with amine **158** (Table 16). The literature synthesis used 15 equivalents of the racemic amine and produced **174** in 70% yield (entry 1).<sup>170</sup> Since the compound of interest was a single enantiomer, a more conservative approach was required. Initially, the same reaction conditions were used, however, the equivalents of the amine were reduced to 1.5. The reaction did go to completion, but the yield was affected, giving **174** in 40% yield (entry 2). A different literature method by Cappelli *et al.* used 1.1 equivalents of amine alongside 20 equivalents of triethylamine to convert the acid chloride to the product.<sup>174</sup> When these conditions were applied, there was only a small amount of conversion to the desired product, with the reaction returning mostly starting material (entry 3). Considering all of these attempts required two-steps – conversion to the acid chloride followed by addition of the amine – a new method employing the coupling reagent HBTU in a single step was investigated (entry 4). After only 4.5 h of reaction time, full conversion to the desired product was observed and amide coupled product **174** was isolated in 91% yield. These optimised conditions only required 1.1 equivalents of chiral amine and had the advantage of taking less time and being a more operationally simple method.

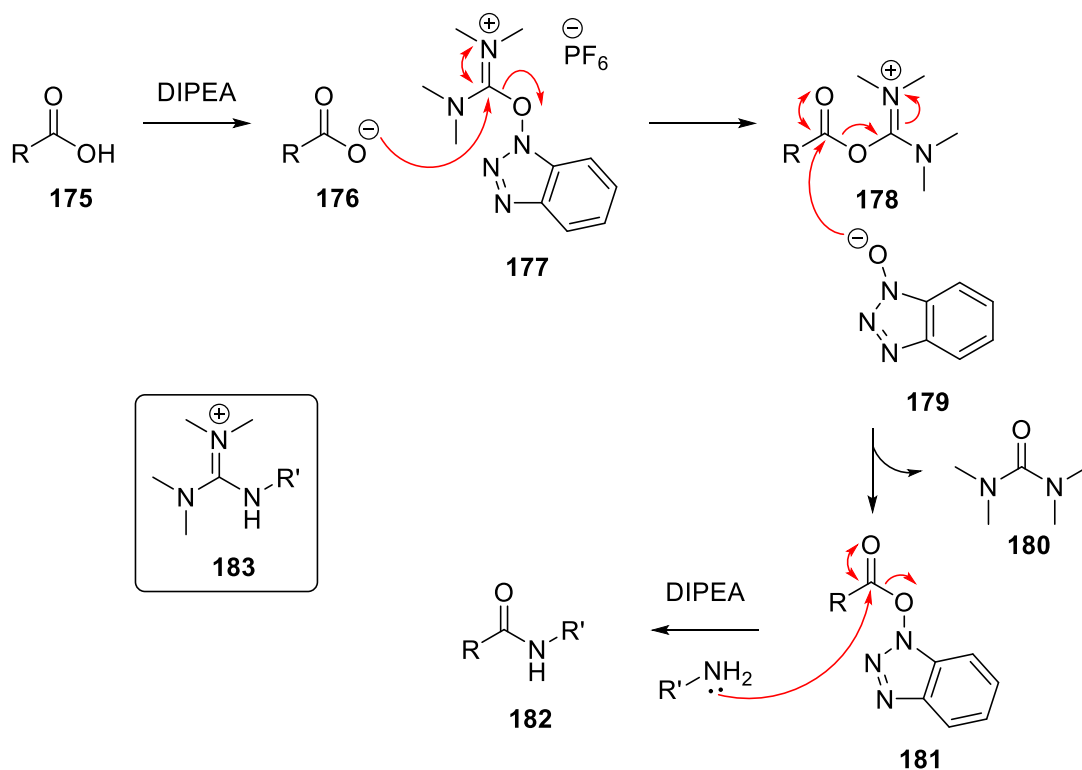
Table 16: Amide coupling reaction



Entry	Conditions	Equivalents of Amine	Yield
1*	1. (COCl) <sub>2</sub> , cat. DMF CH <sub>2</sub> Cl <sub>2</sub> , 0–50 °C, 2 h 2. amine, CH <sub>2</sub> Cl <sub>2</sub> 0–50 °C, 16 h	15	70%
2	1. (COCl) <sub>2</sub> , cat. DMF CH <sub>2</sub> Cl <sub>2</sub> , 0–50 °C, 2 h 2. amine, CH <sub>2</sub> Cl <sub>2</sub> 0–50 °C, 16 h	1.5	40%
3	1. (COCl) <sub>2</sub> , cat. DMF CH <sub>2</sub> Cl <sub>2</sub> , 0–50 °C, 2 h 2. NEt <sub>3</sub> , amine, CH <sub>2</sub> Cl <sub>2</sub> 0–50 °C, 16 h	1.1	30% conversion
4	HBTU, amine, DIPEA DMF, 50 °C, 4.5 h	1.1	91%

\*Racemic amine used

The proposed mechanism for the HBTU coupling is shown below (Scheme 62).<sup>175</sup> Deprotonation of the carboxylic acid gives carboxylate **176**, which can in turn perform nucleophilic attack of the uronium moiety of HBTU (**177**). Intermediate **178** then undergoes further reaction with benzotriazole **179**, producing the OBt activated ester **181** and tetramethylurea (**180**) as a by-product. Subsequent reaction of **181** with the amine gives amide coupled product **182**. The order of reagent addition for this reaction was important: if the amine is added too early, a side-reaction can take place between the amine and HBTU to form guanidinium by-product **183**. It was found that the addition of amine after 0.5 h of reaction time was sufficient to avoid formation of this unwanted by-product.

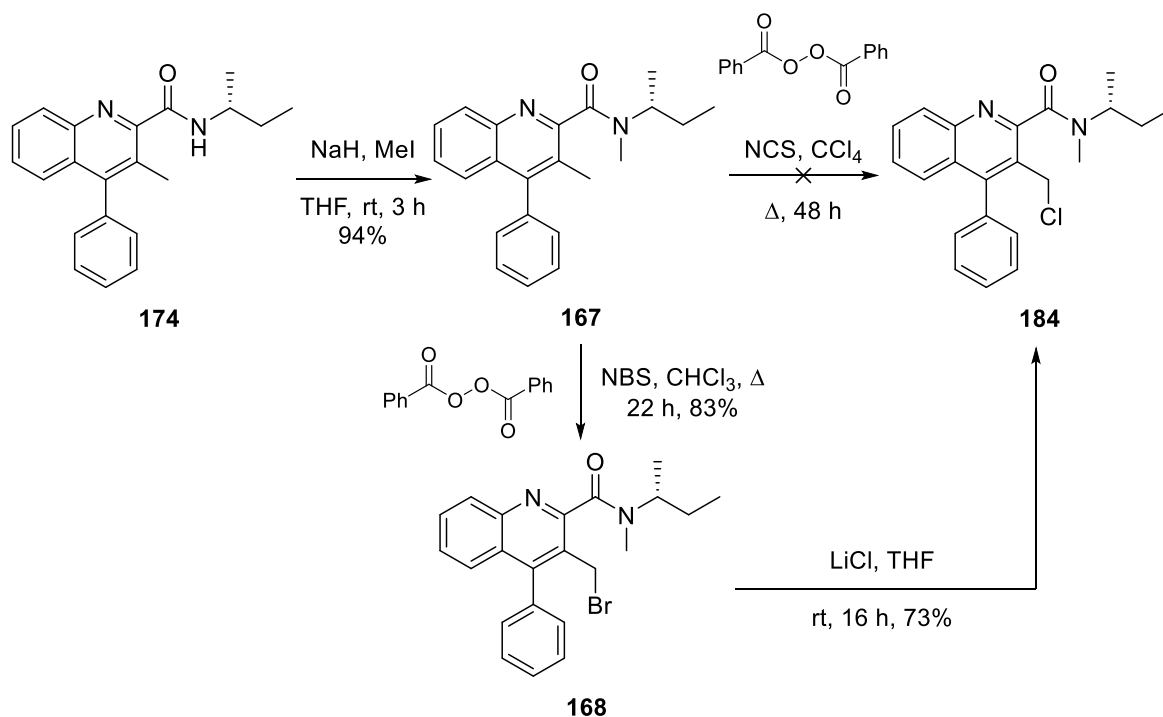


**Scheme 62: Mechanism of the HBTU coupling**

With the amide coupled product now in hand, the methylation of the amide could now take place. Using a standard procedure with iodomethane and sodium hydride, the methylation was complete within 3 h and gave **167** in 94% yield (Scheme 63). As with the initial synthesis of LW223 (**155**), after the methylation of **174**, the appearance of rotamers was observed in the  $^1\text{H}$  and  $^{13}\text{C}$  NMR spectra.

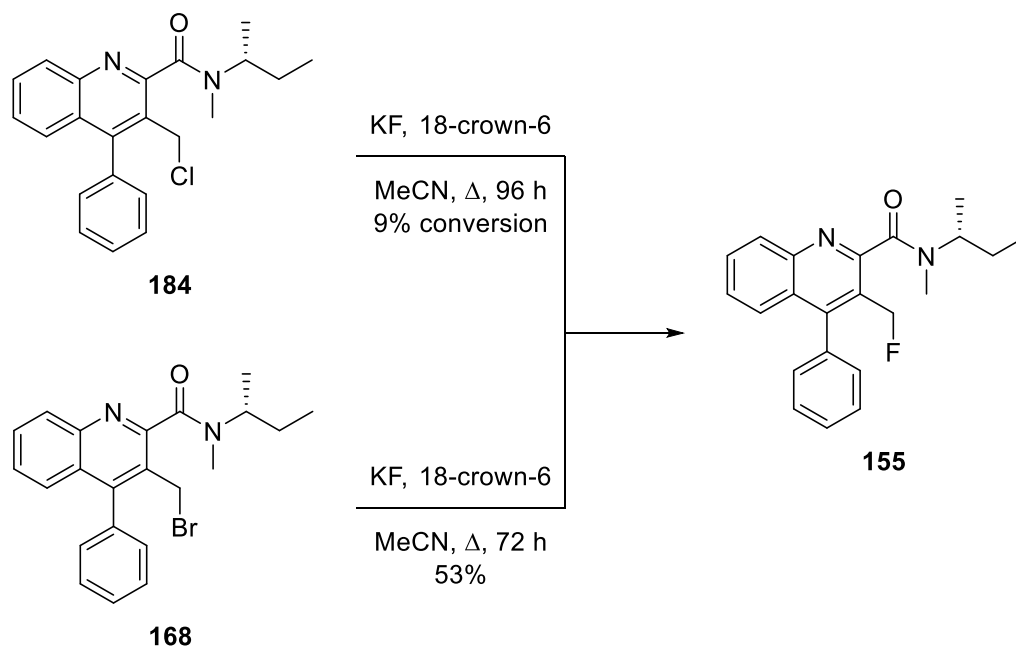
A chloride precursor proved to be an effective substrate for the radiofluorination and synthesis of [ $^{18}\text{F}$ ]AB5186 (**45**). For these reasons, it was believed that a chloro-derivative of LW223 (**155**) would also be an effective precursor. Therefore, a method for chlorination of the 3-methyl moiety was next studied. Examples in the literature used Wohl-Ziegler bromination conditions, substituting NBS for NCS.<sup>176,177</sup> An initial attempt using dibenzoyl peroxide and NCS in  $\text{CCl}_4$  only returned starting material **167** (Scheme 63). Variation of the radical initiator to either AIBN or the cyclohexane derivative, AHCN was ineffective and it was believed that the stronger N-Cl bond of NCS was preventing reaction. By utilising NBS, with the comparatively weaker N-Br bond (due to its larger size and poorer overlap of bonding orbitals), it was proposed that a radical-initiated bromination followed by a  $\text{S}_{\text{N}}2$  reaction using LiCl would yield the chlorinated precursor. Bromination proceeded very well, using Wohl-Ziegler conditions and gave **168** in 67% yield. Due to limited availability and toxicity issues, the solvent  $\text{CCl}_4$  was substituted with  $\text{CHCl}_3$ , which

provided **168** in an increased yield of 83%. The subsequent chlorination of **168** took place using LiCl anhydrous conditions and gave the chloro-precursor in 73% yield.



**Scheme 63: Synthesis of chloro-precursor 184**

Following synthesis of chloride **184**, fluorination with potassium fluoride was next investigated. Chloro-precursor **184** was subjected to the same conditions as previously used for the fluorination of AB5186 (**45**) (Scheme 64). After reflux for 96 h, only 9% conversion to product was observed by <sup>1</sup>H NMR spectroscopy. Although a good leaving group for the fluorination of AB5186 (**45**), the additional steric-bulk of the *sec*-butyl chain obviously makes this an inefficient process. Consequently, the fluorination reaction was attempted using bromo-precursor **168**. After reflux for 72 h, total conversion to the product was observed and LW223 (**155**) was isolated in 53% yield. In this case, the weaker carbon-halogen bond partially compensates for the steric hindrance associated with this reaction, allowing formation of the product in moderate yield.



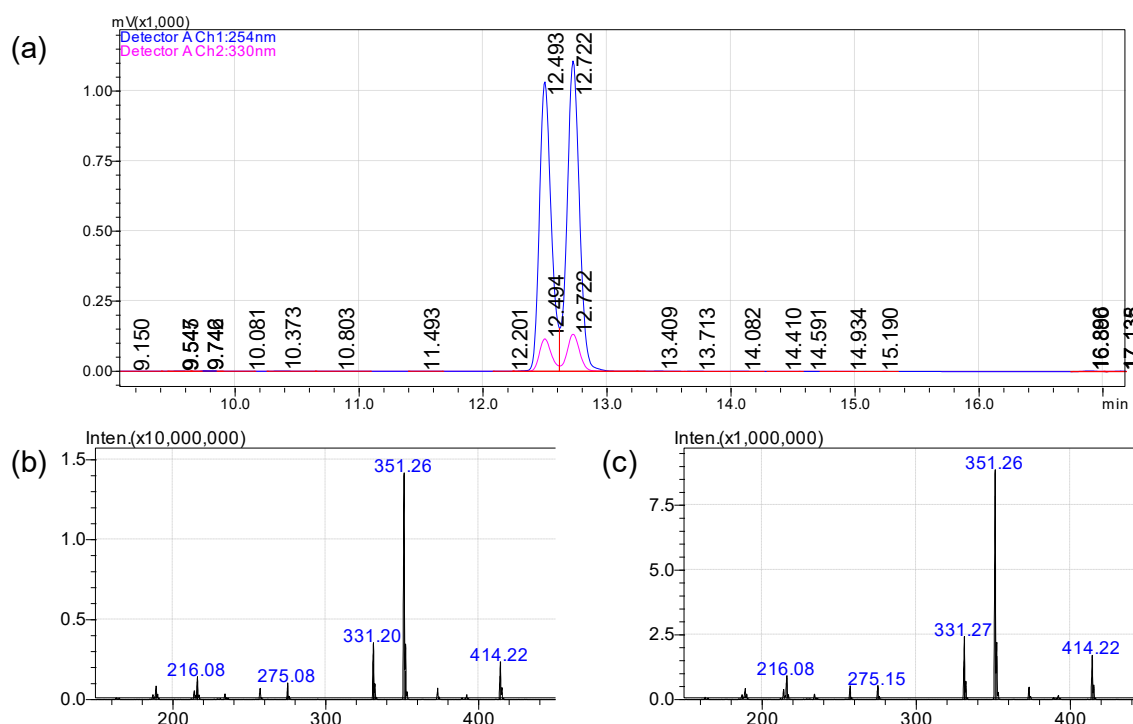
**Scheme 64: Non-radioactive fluorination of precursors**

Whilst the non-radioactive reaction to form LW223 (**155**) from the chloro-precursor was unsuccessful, this did not mean that it would be unsuitable for radiosynthesis. These reactions are pseudo-first-order with respect to the [ $^{18}\text{F}$ ]fluoride (see section 1.2.5.2) and, therefore, act differently to the non-radioactive process. Consequently, both the chloro- and bromo-precursors were considered for radiosynthesis.

#### 2.2.3.4 Conformational isomerism of LW223

The appearance of rotamers in the NMR spectra of LW223 (**155**) was not too surprising given the combined steric hindrance associated with the quinolone substituents and the bulky *sec*-butyl chain of the amide. However, what was initially unexpected was the appearance of two peaks in the HPLC chromatogram. These two peaks were initially in a 3:1 ratio, but upon standing in solution in an acetonitrile and water mixture, re-equilibrated to an approximate 1:1 ratio. This re-equilibration of the peaks, combined with the data collected from other standard analytical methods, suggested that the two peaks were as a result of conformational isomerism of LW223 (**155**), rather than that of an impurity. Indeed this phenomenon has been previously reported in the literature, including by Geffe *et al.*, who describe a formamide that produced double bands in TLC, as well as two peaks by HPLC.<sup>178</sup> As with LW223 (**155**), their compounds also showed no coalescence of  $^1\text{H}$  NMR signals when heated to 150 °C. This phenomenon was proposed to be due to the hindered rotation around the amide bond, similar to that of DMF where the two sets of methyl group hydrogen atoms show two distinct peaks in the  $^1\text{H}$  NMR spectrum. However, unlike DMF, heating the NMR sample did not overcome the energy barrier to rotation, due

to the amide nitrogen possessing a larger group, causing steric congestion. To confirm this theory, an LCMS of LW223 (**155**) was performed (Figure 28). This displayed good separation of the two peaks and mass analysis showed that their masses were identical.



**Figure 28:** (a) LCMS chromatogram of LW223 (**155**), using 10–90% MeCN/0.1% formic acid(aq) on a C<sub>18</sub> HPLC column at 1.2 mL min<sup>-1</sup>; (b) mass spectrum of peak at 12.49 min; (c) mass spectrum of peak at 12.72 min

It was not expected that the two peaks of LW223 (**155**) were as a result of racemisation of the stereocentre given that the compound only possesses one stereogenic centre and separation of enantiomers is not possible using standard analytical HPLC. Nevertheless, analytical chiral HPLC analysis of LW223 (**155**) was considered to confirm the enantiopurity and corroborate the amide rotamer hypothesis. To perform the chiral HPLC, racemic LW223 derivative **185** was synthesised as described before using racemic amine **158** (Figure 29a). This was then analysed by chiral HPLC using an AD-H column and 2.5% isopropanol in hexane. The double peaks made analysis of the two enantiomers challenging, however, using a 1 mL min<sup>-1</sup> flow rate gave four peaks, eluting over 15 min (Figure 29a). The same conditions were then applied to the analysis of the (*R*)-enantiomer (Figure 29b). This chromatogram showed that the two outer peaks (retention times 27.1 and 38.4 min) corresponded to the (*S*)-enantiomer and the inner peaks were the (*R*)-enantiomer. Indeed, small quantities of the (*S*)-enantiomer were present in the chiral sample, however, the enantiomeric excess of (*R*)-LW223 (**155**) was calculated as 99%.

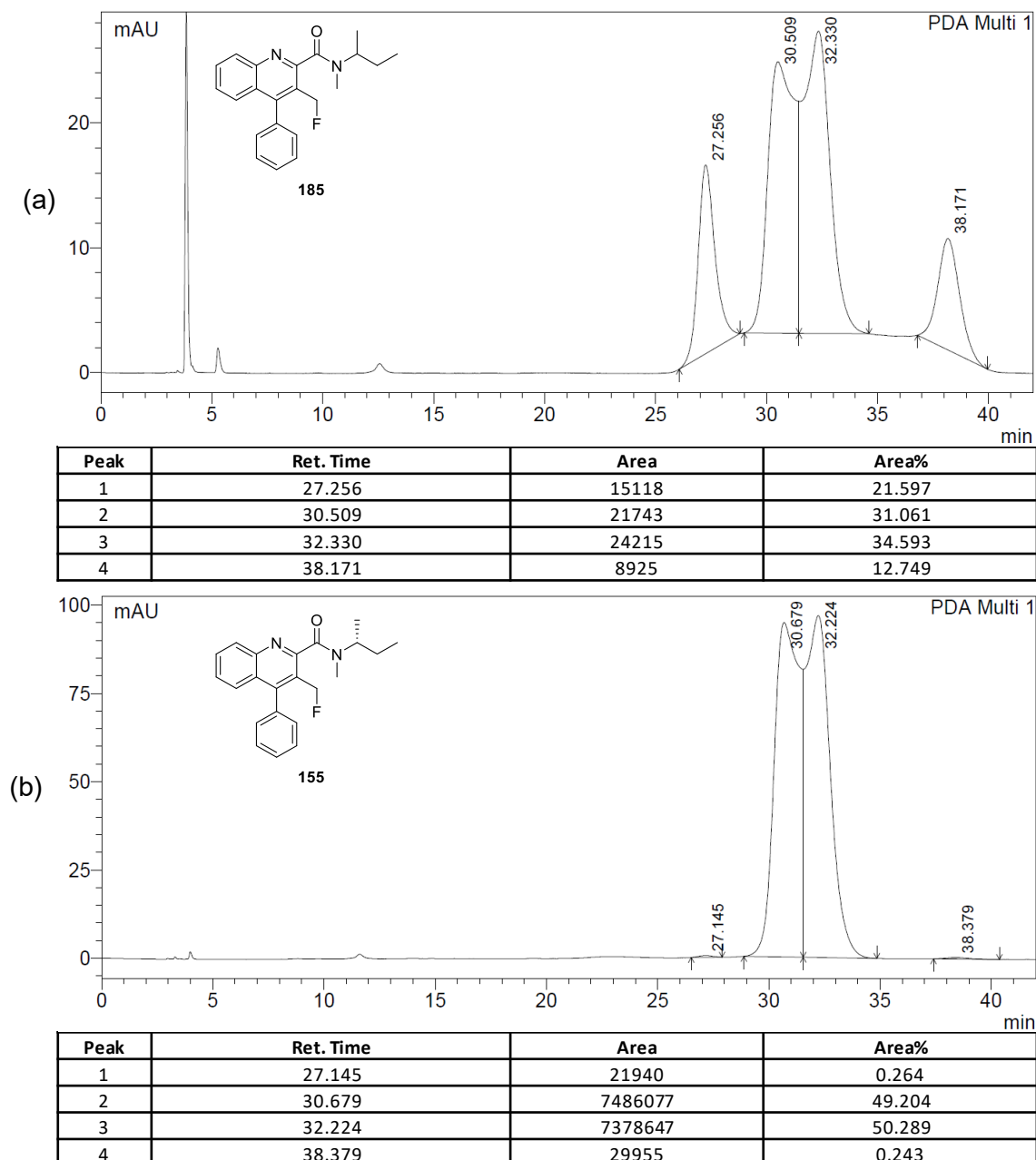


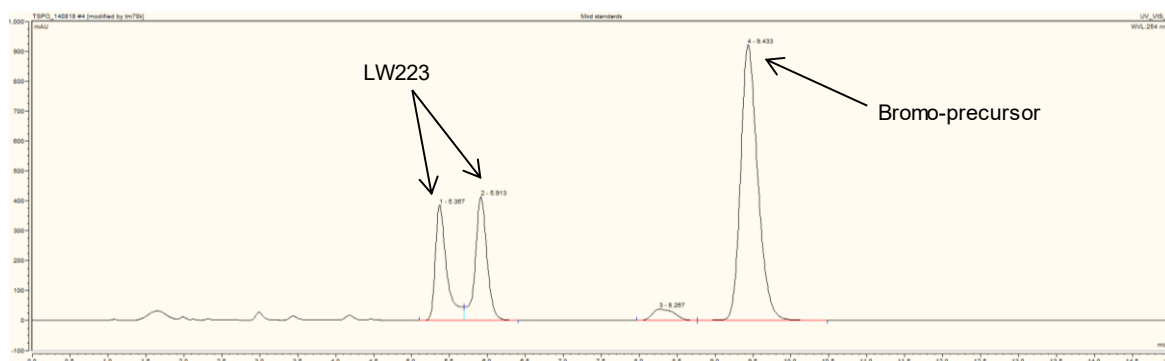
Figure 29: Chiral HPLC chromatograms of (a) racemic LW223 (**185**) and (b) (*R*)-LW223 (**155**), using 2.5% isopropanol in hexane on an AD-H column at 1.0 mL min<sup>-1</sup>

## 2.2.4 Radiosynthesis of [<sup>18</sup>F]LW223

### 2.2.4.1 Establishing an HPLC method

As the limiting reagent in the radioactive synthesis would be [<sup>18</sup>F]fluoride, the remaining precursor would need to be separated from the product post-synthesis, usually with semi-preparative HPLC. The synthesiser used for the reaction and purification would only allow an isocratic flow, therefore an isocratic HPLC method was established. With its superior reactivity, bromo-precursor **168** was chosen for this initial work. A sample was prepared

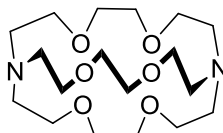
containing a 1:1 mix of LW223/precursor and examined by HPLC. The aim of this experiment was to find conditions for effective separation of the fluorinated product. Extra time spent separating the product during the radiosynthesis would result in less activity, due to the short half-life of the  $^{18}\text{F}$  nuclide, but also a wider peak would mean the product would be collected in a greater volume of solvent, which would make reformulating the product more difficult. Therefore optimal conditions for the elution of LW223 (**155**) were crucial. It was found that a mixture of 70% acetonitrile in water provided good separation of the two compounds.



**Figure 30: HPLC chromatogram of LW223 (**155**) and bromo-precursor **168**, using a  $\text{C}_{18}$  column and 70% acetonitrile in water as the eluent**

#### 2.2.4.2 Drying of [ $^{18}\text{F}$ ]fluoride

The radioactive synthesis was carried out using a TRACERlab  $\text{FX}_{\text{FN}}$  synthesiser (GE Healthcare); the graphics overlay for this synthesiser is shown in Appendix III. The [ $^{18}\text{F}$ ]fluoride was produced *via* the  $^{18}\text{O}(\text{p},\text{n})^{18}\text{F}$  nuclear reaction by cyclotron irradiation of a target containing [ $^{18}\text{O}$ ]H<sub>2</sub>O. This was then separated from the water by trapping on an ion exchange resin. The radioactivity trapped on the separation cartridge could then be measured using a Geiger-Muller (GM) counter. To elute the [ $^{18}\text{F}$ ]fluoride, a solution of  $\text{K}_2\text{CO}_3$  and Kryptofix 222<sup>®</sup> (Figure 31) was passed over the resin and transferred to the reaction vessel. The Kryptofix 222<sup>®</sup> fulfils a similar role to the 18-crown-6 used in the non-radioactive synthesis (see section 2.2.2.1), however, the cryptand is more strongly complexing, possessing a very slow de-complexation rate that results in a high binding strength.<sup>179</sup> This more superior complexing reagent was used for the radiosynthesis, as efficiency of binding potassium cations was crucial to allow for rapid radiolabelling.



**Figure 31: Kryptofix 222<sup>®</sup>**

After transfer of [<sup>18</sup>F]fluoride to the reaction vessel, it was then required to evaporate the solution and dry quantitatively to remove any remaining water. If the reaction was not dry, hydroxide ions are formed and compete with the nucleophilic fluorination, reducing the radiochemical yield. Drying was implemented by azeotropic distillation with acetonitrile, applying vacuum and a flow of anhydrous nitrogen gas. It was then possible to measure the radioactivity trapped in the reaction vial using another GM counter. Acetonitrile was chosen as the solvent for the reaction, as this was aprotic and dissolved both bromo-precursor **168** and LW223 (**155**). Since the reaction would take place under reflux in a sealed vial resistant to pressure changes, it was possible to heat the reaction above the boiling point of the solvent and so a higher boiling point solvent would only be needed for more extreme conditions.

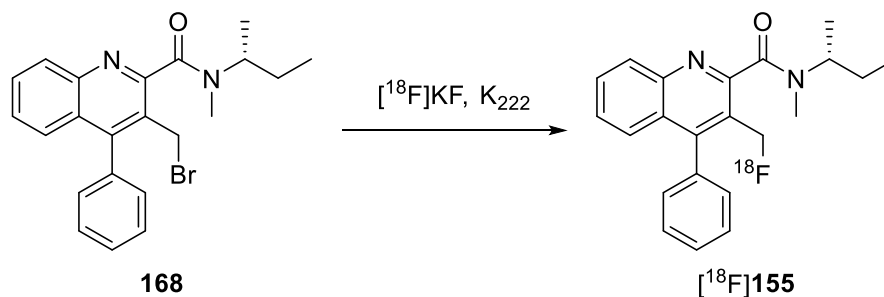
#### 2.2.4.3 Labelling

Initially, HPLC was omitted from the synthesis to allow for optimisation of the radiolabelling process. The reaction mixture was then sent directly into a dispensing vial so the radioactivity could be measured and the sample could be analysed with HPLC on a C<sub>18</sub> column, using both UV and gamma detectors. Since unreacted [<sup>18</sup>F]fluoride would be retained on the C<sub>18</sub> column and therefore not show on the gamma detector, analysis of the samples using radio-TLC was also considered. For these test reactions, only a small amount of radioactivity was required, thus, an [<sup>16</sup>O]H<sub>2</sub>O rinse of the cyclotron target, used for an earlier production of medical tracers was sufficient to deliver between 0.5–1.0 GBq of [<sup>18</sup>F]fluoride. The smaller quantity of radiation would allow for two reactions to take place in a single day. The first reaction was carried out using similar conditions to the non-radioactive synthesis (Table 17). After 10 min of reaction at 80 °C, a sample of the mixture was injected into an analytical HPLC. This showed no evidence of the product on the gamma trace (entry 1). An increase in reaction time and temperature showed a small improvement, but when the solvent was switched to DMSO there was no longer any product formed (entries 2–3).

Further examination of the bromo-precursor showed that small quantities of hydrolysed compound had formed during storage at –20 °C after some months. Although this impurity was small, this may explain the poor conversion to the product observed in the reaction.

Following re-purification of bromide **168** by silica chromatography, the reaction was attempted again using acetonitrile at 110 °C for 10 min (entry 4). This showed promising conversion and was unaffected by the reduction in reaction time to 5 min (entry 5). Overall, the optimised procedure allowed an 88% conversion after a reaction time of 5 min.

**Table 17: Optimisation of reaction conditions**



Entry	Solvent	Temperature	Time	Conversion
1	MeCN	80 °C	10 min	0%
2	MeCN	100 °C	15 min	40%
3	DMSO	120 °C	15 min	0%
4	MeCN	110 °C	10 min	91%
5	MeCN	110 °C	5 min	88%

#### 2.2.4.4 Purification and reformulation

After optimisation of the reaction conditions, HPLC was incorporated into the method. Following the reaction, the mixture was passed through an Al<sub>2</sub>O<sub>3</sub> cartridge to absorb any remaining fluoride prior to injection into the HPLC. Only trace quantities of the product were observed on the gamma trace of the HPLC, despite having high radioactivity in the reaction vial. It was believed that [<sup>18</sup>F]LW223 (**155**) may have also been retained on the Al<sub>2</sub>O<sub>3</sub> cartridge, a theory which was confirmed by passing non-radioactive LW223 (**155**) through a cartridge using the same conditions. Ultimately it was decided to remove the Al<sub>2</sub>O<sub>3</sub> cartridge from the method, as the conversion from [<sup>18</sup>F]fluoride had already been shown to be efficient.

The purpose of this radiotracer would be to image TSPO *in vivo*, therefore, the acetonitrile/water mixture of the HPLC fraction collected would be reformulated into saline with a minimum amount of ethanol prior to injection. To perform this reformulation, the HPLC fraction was collected in a round-bottomed flask containing 20 mL of water with stirring. This diluted the acetonitrile in the solution from 70% to around 10–15%. This

solution was then pushed through a C<sub>18</sub> solid phase extraction (SPE) cartridge, retarding the product on the cartridge and passing the water and acetonitrile to waste. This was washed once more with water to remove any remaining acetonitrile, before eluting the product with ethanol and diluting with saline. Initially, [<sup>18</sup>F]LW223 (**155**) was reformulated with 10% ethanol in saline, however, it was found this could be reduced to 5% with no loss in radioactivity.

#### 2.2.4.5 Productions of [<sup>18</sup>F]LW223

After optimisation of the radiosynthesis and formulation, three productions of [<sup>18</sup>F]LW223 (**155**) were performed using bromo-precursor **168**. An irradiation of the target for 1 min at 65  $\mu$ A was used to produce the [<sup>18</sup>F]fluoride for these syntheses. Consistent radiochemical yields (non-decay corrected) were obtained for each production, with an average of 49% (Table 18). As per the new nomenclature rules for radiopharmaceuticals, these radiochemical yields were decay corrected according to the formula:  $A_t = A_0 \times e^{-\lambda t}$ , where  $A_t$  is the activity at time  $t$  and  $\lambda$  is the decay constant, calculated for fluorine-18 as  $1.05 \times 10^{-4} \text{ s}^{-1}$ .<sup>30</sup> This gave an average radiochemical yield of 60% and radiochemical purity was shown to be greater than 99%, based on the gamma trace of the analytical HPLC. Molar activity ( $A_m$ ) was calculated by running known concentrations of non-radioactive LW223 (**155**) on the same HPLC system, giving activity per  $\mu$ mol. Accordingly, specific activity ( $A_s$ ) was calculated from this value to give activity per mg.

**Table 18: Productions of [<sup>18</sup>F]LW223 (**155**) from bromo-precursor **168****

Production	Starting Activity (GBq)	End Activity (GBq)	Non-Decay Corrected RCY	Decay Corrected RCY	$A_m$ (GBq $\mu$ mol <sup>-1</sup> )	$A_s$ (GBq mg <sup>-1</sup> )
1	2.89	1.52	53%	65%	4.57	13.1
2	2.89	1.43	50%	61%	10.5	29.9
3	2.89	1.28	44%	54%	7.90	22.6
Average	-	-	49% $\pm$ 3%	60% $\pm$ 3%	7.65 $\pm$ 1.71	21.9 $\pm$ 4.86

It was expected that bromo-precursor **168** would be more effective than the chloride analogue **184**, however, it was deemed prudent to check the efficiency of the radiosynthesis from this precursor using the same method. Using exactly the same conditions, chloro-precursor **184** returned a decay corrected radiochemical yield of 59%, very similar to that of bromo-precursor **168** (Table 19). Moreover, the  $A_s$  calculated for this

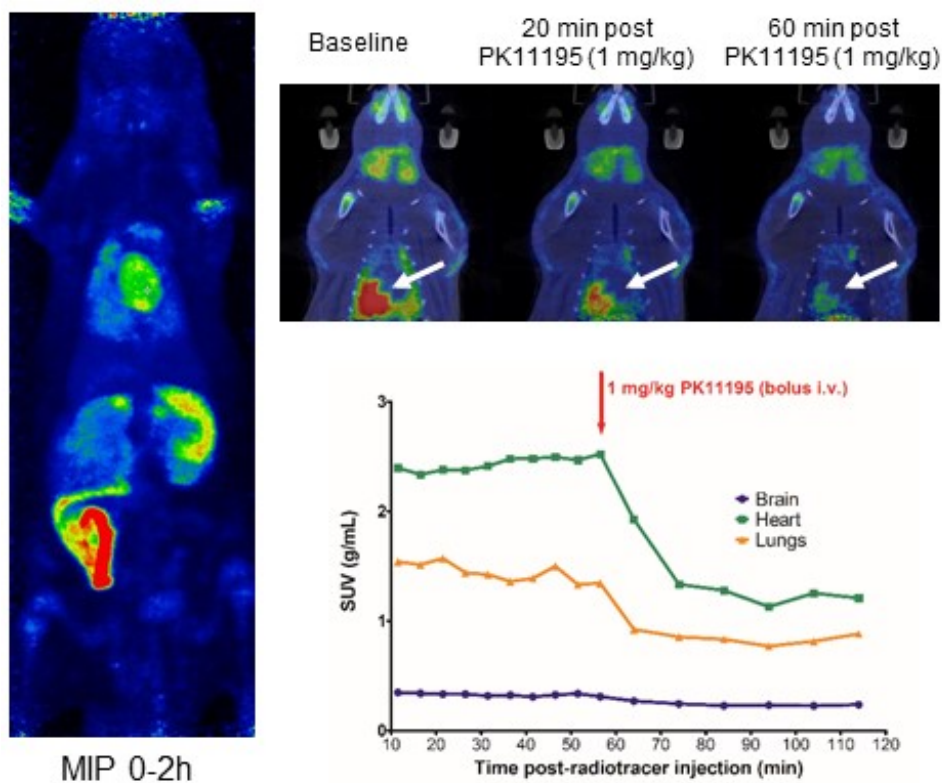
synthesis was 48.1 GBq mg<sup>-1</sup>, twice that of the previous syntheses. The reactivity of the chloride versus that of the bromide did not impede the reaction. Based on these results and its enhanced stability, the chloride was chosen as the precursor for the preclinical trials of [<sup>18</sup>F]LW223 (**155**). Further productions of [<sup>18</sup>F]LW223 (**155**) from chloro-precursor **184** were of a much higher starting activity (irradiation for 10 min at 65 μA), so the radiochemical yields are not directly comparable to previous productions. However, these still gave good and consistent yields for [<sup>18</sup>F]LW223 (**155**) with improved A<sub>s</sub>.

**Table 19: Productions of [<sup>18</sup>F]LW223 (**155**) from chloro-precursor 184**

<b>Production</b>	<b>Starting Activity (GBq)</b>	<b>End Activity (GBq)</b>	<b>Non-Decay Corrected RCY</b>	<b>Decay Corrected RCY</b>	<b>A<sub>m</sub> (GBq μmol<sup>-1</sup>)</b>	<b>A<sub>s</sub> (GBq mg<sup>-1</sup>)</b>
1	2.89	1.39	48%	59%	16.9	48.1
2	27.0	7.68	28%	35%	58.2	165.9
3	27.0	7.75	29%	35%	52.2	149.1
4	27.0	5.14	19%	23%	29.7	84.8
5	27.0	7.54	28%	34%	61.3	175.0

## 2.2.5 Preclinical Studies

With radiofluorination optimised, preclinical evaluation of the radiotracer began. This work was carried out by collaborators at the University of Edinburgh. Small animals injected with [<sup>18</sup>F]LW223 (**155**) were scanned in a microPET system and images were produced that showed uptake in tissues associated with high levels of TSPO (Figure 32). Uptake in the heart and lungs was high, but since levels of TSPO are low in healthy brain tissue, only a small amount of uptake was observed in the brain. Elimination of the tracer was shown to be *via* the intestines. To show that [<sup>18</sup>F]LW223 (**155**) was reversibly binding to TSPO and to also assess the specific binding, displacement studies were carried out using non-radioactive PK11195 (**41**). After 60 min post-injection of PK11195 (**41**), the signal had reduced considerably from the heart and lungs, with uptake in the surrounding tissue low. This demonstrated that [<sup>18</sup>F]LW223 (**155**) was indeed reversibly binding to TSPO and that non-specific binding was low.



**Figure 32: Displacement study of [ $^{18}\text{F}$ ]LW223 (**155**) using PK11195 (**41**). Bound [ $^{18}\text{F}$ ]LW223 (**155**) can be shown to be reversibly binding to the target after injection of PK11195 (**41**) 60 min post injection**

## 2.2.6 Conclusions

An optimised synthesis towards the potential TSPO radiotracer AB5186 (**45**) was designed, which allowed for multi-gram quantities of the precursor and non-radioactive compound to be produced. Following biological evaluation, it was found that AB5186 (**45**) was sensitive to the single nucleotide polymorphism that afflicts many second generation TSPO radiotracers. As such, a new structure was proposed and the compound LW223 (**155**) was synthesised, albeit using a method that would not allow late-stage radiosynthesis. After biological evaluation showed that LW223 (**155**) was not sensitive to the single nucleotide polymorphism, a new synthesis was designed that allowed for the synthesis of two potential precursors. A radiofluorination method was designed and optimised from bromo-precursor **168** to produce [ $^{18}\text{F}$ ]LW223 (**155**) in  $60\% \pm 6\%$  decay corrected radiochemical yield and a radiochemical purity of greater than 99% ( $n = 3$ ). Comparison of the radiosynthesis from both precursors showed that there was very little difference in efficiency and therefore, chloro-precursor **184** was chosen for the preclinical work of [ $^{18}\text{F}$ ]LW223 (**155**) due to its superior stability. Preclinical studies have shown that [ $^{18}\text{F}$ ]LW223 (**155**) images TSPO *in vivo*, consistent with the known expression of the receptor; clearance studies using non-radioactive PK11195 (**41**), show that this binding to

TSPO is reversible. Future work has been proposed that includes preclinical imaging of TSPO in myocardial infarction and also investigating the role of TSPO in prostate cancer using [ $^{18}\text{F}$ ]LW223 (**155**).

### 2.2.7 Future Work

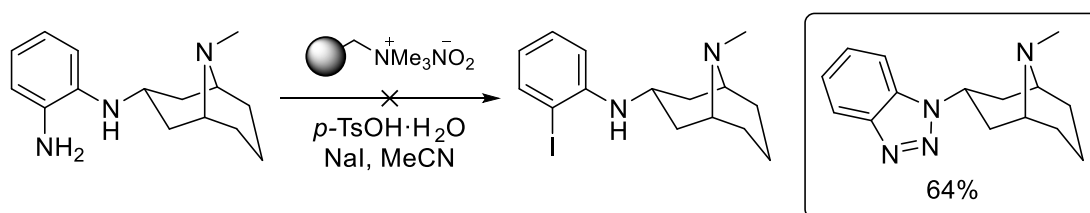
Following the preclinical evaluation of [ $^{18}\text{F}$ ]LW223 (**155**), future work will involve the preparation of this tracer for phase I clinical trials. The safety and dosimetry properties of the tracer will be established. Toxicology for a radiotracer often falls into a lower category for pharmaceuticals due to the small dose of compound administered. For example, only 1.5  $\mu\text{g}$  of a tracer is injected in a 250 MBq dose, if the tracer has a molecular weight of 300  $\text{g mol}^{-1}$  and  $A_m$  of 50  $\text{GBq } \mu\text{mol}^{-1}$ .<sup>31</sup> The major difference for radiotracers, compared to other pharmaceuticals, is that an estimate of the radiation dosimetry is required. Following the success of these studies, phase II clinical trials can begin.

Further preclinical work, carried out by collaborators at The Beatson Institute for Cancer Research, will look at using [ $^{18}\text{F}$ ]LW223 (**155**) to image TSPO and investigate the role that this protein plays in *de novo* androgen biosynthesis in prostate cancer cells. These studies will provide insight into the *in vivo* mechanism of the development of lethal metastatic castration-resistant prostate cancer and allow for early detection in patients.<sup>113,180</sup>

## 2.3 Novel Benzotriazole Derived $\alpha$ -Amino Acids

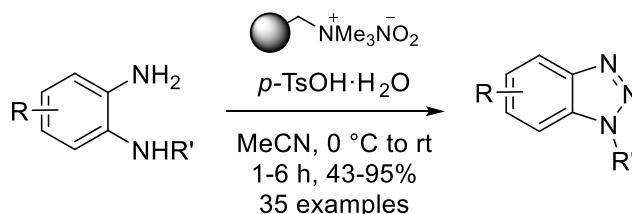
### 2.3.1 Project Aims

In 2008, Filimonov *et al.* developed the synthesis of stable aryl diazonium tosylate salts by using a polymer-supported nitrite reagent under mild acidic conditions.<sup>181</sup> These diazonium salts could be used for a variety of transformations and previous work by Sloan *et al.* has shown that, by utilising this reagent, it was possible to incorporate radioactive [<sup>125</sup>I]iodine into aryl amines *via* these stable diazonium salts in a one-pot process.<sup>182</sup> Within the Sutherland group, further application of this reaction for the synthesis of more complex molecular imaging agents was explored.<sup>183</sup> Amongst many other targets, this led to the attempted synthesis of AT-1012: a selective antagonist for the  $\alpha 3\beta 4$  nicotinic acetylcholine receptor (nAChR).<sup>184</sup> However, instead of the expected outcome, a diazotisation-cyclisation product was observed in the form of a benzotriazole (Scheme 65).<sup>183</sup>



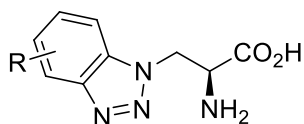
**Scheme 65: Attempted iodination of AT-1012**

Traditionally the synthesis of benzotriazoles has involved the mono-diazotisation of 1,2-aryldiamines, using sodium nitrite and acidic conditions, followed by intramolecular cyclisation.<sup>185</sup> More recently, *N*-substituted benzotriazoles have been synthesised *via* “click” chemistry: a [3+2] cycloaddition of azides with benzyne, using mild conditions.<sup>186</sup> Other methods include: 1,7-palladium migration *via* C-H activation, followed by intramolecular cyclisation, allowing the regioselective synthesis of benzotriazoles, and also the use of alkyl nitrites under catalyst-free and mild conditions.<sup>187</sup> However, many of these approaches are limited by the need for high temperatures, the use of acidic conditions, nitrite reagents that can decay to toxic nitrogen oxides, or the need to have highly functionalised starting materials. To overcome some of the drawbacks of these other approaches and encouraged by the success of this earlier incidental reaction, Faggyas *et al.* developed methodology towards the preparation of *N*-substituted benzotriazoles from 1,2-aryldiamines *via* diazotisation and intramolecular cyclisation, using the polymer-supported nitrite reagent and *p*-tosic acid (Scheme 66).<sup>188</sup>



**Scheme 66: Synthesis of *N*-substituted benzotriazoles from 1,2-aryldiamines**

Previously within the Sutherland group, various fluorescent  $\alpha$ -amino acid derivatives have been developed, however, one of the drawbacks of these compounds is the rather lengthy synthesis required.<sup>189–191</sup> Inspired by the use of the polymer-supported nitrite reagent approach for the synthesis of benzotriazoles, it was envisaged that this methodology would allow easy and quick access to a range of benzotriazole derived  $\alpha$ -amino acids (Figure 33). Access to these compounds in relatively few steps would allow for greater diversification of the structure and for the investigation of the fluorescent properties of this class of compound.

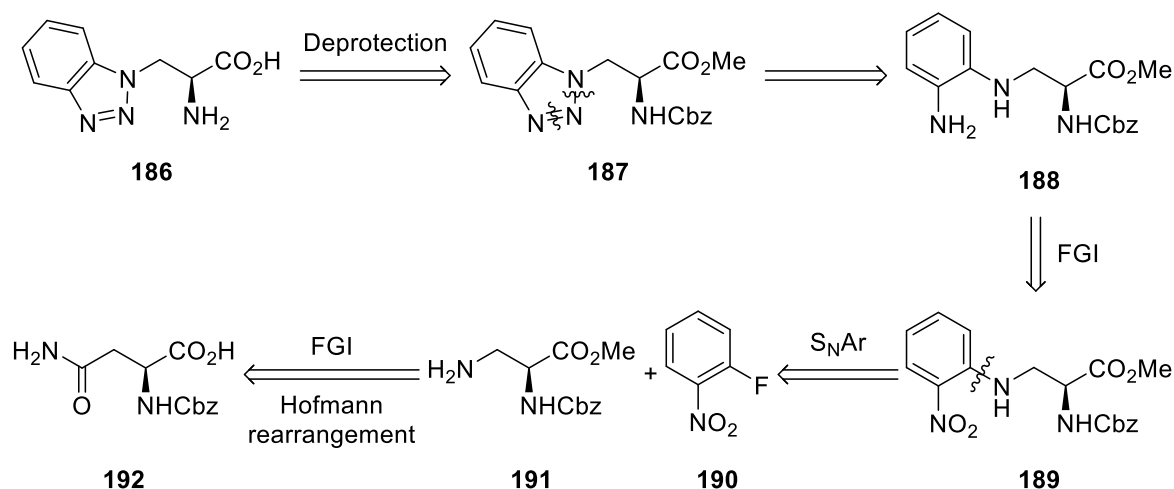


**Figure 33: Proposed benzotriazole substituted  $\alpha$ -amino acids**

## 2.3.2 Synthesis of Benzotriazole Derived $\alpha$ -Amino Acids

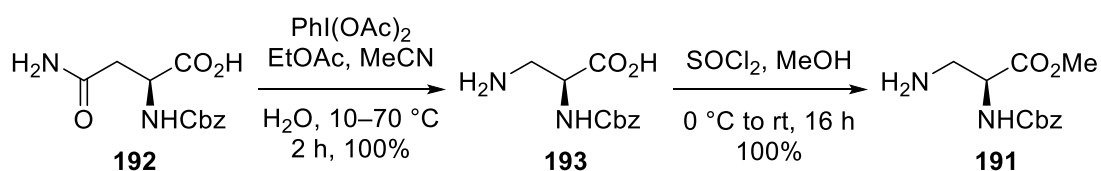
### 2.3.2.1 Synthesis of the unsubstituted benzotriazole derived $\alpha$ -amino acid

The first goal was the preparation of the unsubstituted benzotriazole derived  $\alpha$ -amino acid (**186**). Beginning from the naturally occurring L-amino acid would allow introduction of the correct stereochemistry from the beginning of the synthesis, thus avoiding the need for asymmetric synthesis later in the route. It was proposed that starting from the cheap and readily available Cbz-L-asparagine (**192**), a Hofmann rearrangement could be performed followed by an esterification to yield the amine **191** (Scheme 67). This could be coupled with *ortho*-fluoronitrobenzene (**190**) in a  $S_NAr$  reaction and then be reduced to the aryl amine **188**. Next would come the key step: diazotisation and intramolecular cyclisation to form the protected benzotriazole substituted  $\alpha$ -amino acid **187**, followed by deprotection of the amine and acid groups to give **186**.



**Scheme 67: Proposed retrosynthesis of the benzotriazole derived  $\alpha$ -amino acid**

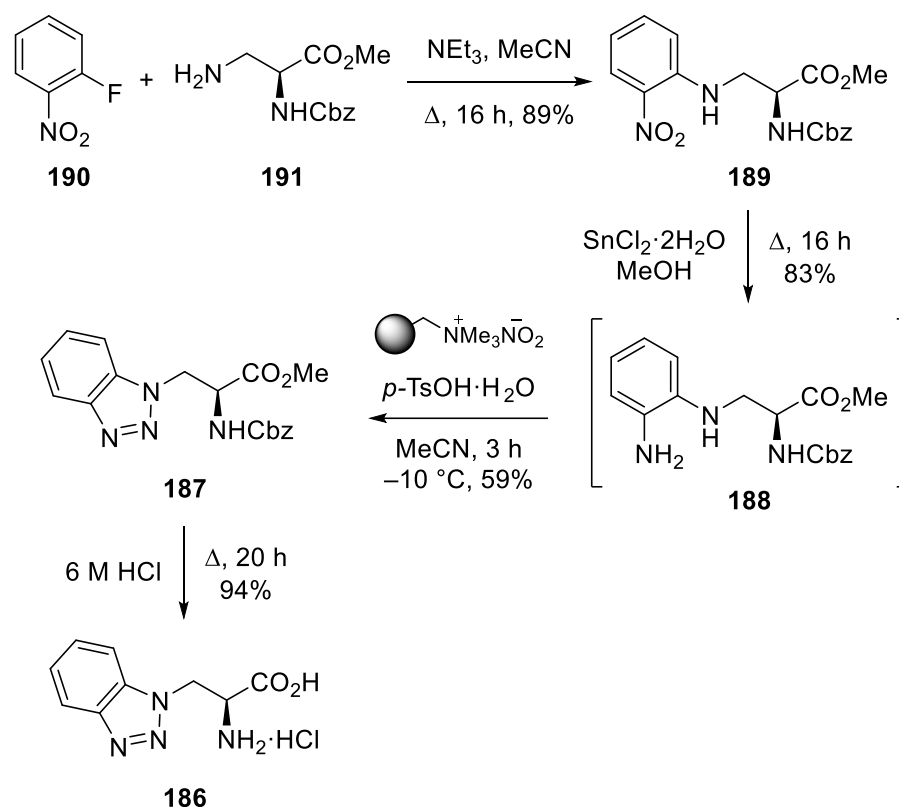
With this proposed route in mind, the synthesis of **191** began from Cbz-L-asparagine (**192**). Previous work within the Sutherland group involved optimisation of this transformation.<sup>192</sup> Initially, (bis(trifluoroacetoxy)iodo)benzene was used in various solvent systems, but the best results were achieved by using the hypervalent iodine reagent (diacetoxyiodo)benzene in a mixed solvent system. It was then possible to perform a Hofmann rearrangement of **192** to **193** in a quantitative yield (Scheme 68).<sup>193</sup> This was followed by an esterification using thionyl chloride and methanol to yield **191**, again quantitatively.<sup>194</sup>



**Scheme 68: Hofmann rearrangement and esterification**<sup>193,194</sup>

Amine **191** was used in a nucleophilic aromatic substitution reaction, with *ortho*-fluoronitrobenzene (**190**) and triethylamine (Scheme 69), and gave nitrobenzene product **189** in 89% yield according to literature conditions.<sup>195</sup> Nitrobenzene **189** was reduced using tin(II) chloride to form aryl amine **188**, using literature conditions developed by Bellamy.<sup>196</sup> Methanol was used as the solvent instead of ethanol to avoid unwanted transesterification. Completion of the reaction was evident from thin-layer chromatography (TLC), as product **188** stained brightly with ninhydrin. Due to the reactivity and instability of **188**, this was used immediately in the next step without extensive characterisation. The key step in this synthesis was the transformation of **188** to benzotriazole **187**. The

polymer-supported nitrite reagent was prepared beforehand by ion exchange of Amberlyst A26 resin with sodium nitrite. Treatment of **188** with the polymer-supported nitrite reagent and *p*-tosic acid gave benzotriazole **187** in 59% yield. The final step in the synthesis was the deprotection of the  $\alpha$ -amino acid portion of **187**. To remove the benzyl carbonate protecting group and hydrolyse the methyl ester, **187** was heated in 6 M aqueous hydrochloric acid for 20 h. Recrystallisation from methanol and diethyl ether gave **186** as the hydrochloric acid salt in 94% yield.

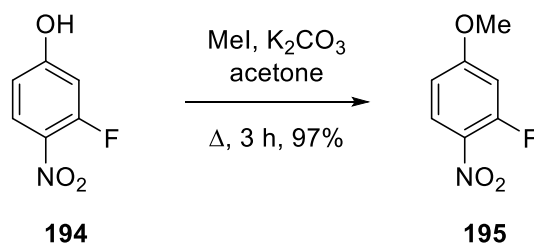


**Scheme 69: Synthesis of the unsubstituted benzotriazole  $\alpha$ -amino acid**

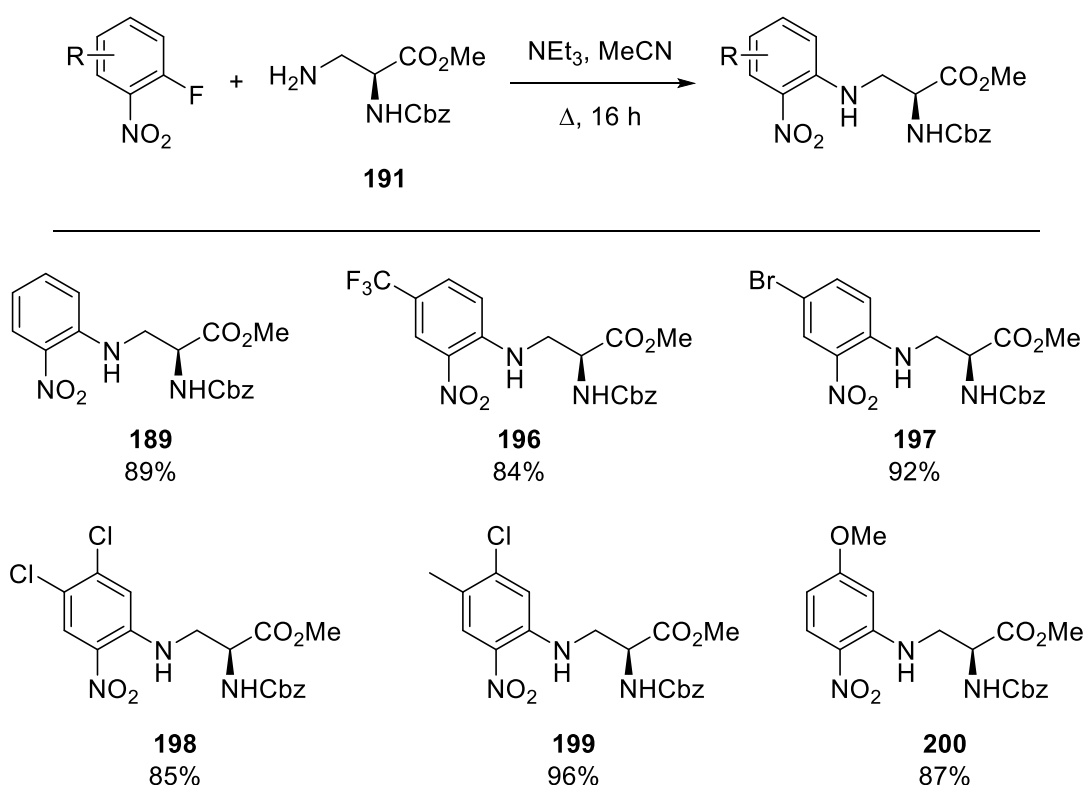
### 2.3.2.2 Synthesis of substituted benzotriazole derived $\alpha$ -amino acids

Given the success of the synthesis of amino acid **186**, work then began on the synthesis of analogues, using other *ortho*-fluoronitrobenzenes for the  $\text{S}_{\text{N}}\text{Ar}$  reaction with **191**. The *ortho*-fluorobenzene featuring a methoxy substituent was prepared beforehand *via* an *O*-methylation using potassium carbonate and iodomethane at room temperature for 16 h.<sup>197</sup> However, this literature procedure was improved by heating the reaction to reflux, allowing completion in 3 h (Scheme 70). The  $\text{S}_{\text{N}}\text{Ar}$  reaction consistently gave excellent yields with a range of *ortho*-fluoronitrobenzenes bearing either electron-withdrawing or electron-donating groups (Scheme 71). One of the advantages of this reaction is how well *ortho*-fluoronitrobenzenes work as electrophiles: having a leaving group *ortho* to the electron

withdrawing nitro group greatly activates the ring towards nucleophilic attack, with the fluorine atom being a particularly good leaving group for  $S_NAr$  reactions.



**Scheme 70: Methylation reaction to form 195**

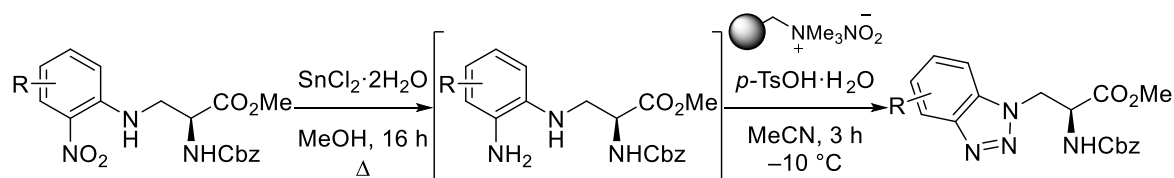


**Scheme 71:  $S_NAr$  reaction of derivatives**

Each analogue was reduced with tin(II) chloride and gave good yields for most of the derivatives. However, a more modest yield was observed for the methoxy analogue (Table 20). Since the other derivatives contained electron-withdrawing groups, it is presumed that the electron-donating effect of the methoxy group contributed to a more electron-rich aromatic ring, which in turn was not able to receive electrons from the tin(II) chloride. Nevertheless, the reaction gave enough product to proceed with the subsequent step. The anilines were then subjected to the one-pot diazotisation and cyclisation by reaction with the polymer-supported nitrite reagent and *p*-tosic acid. This gave

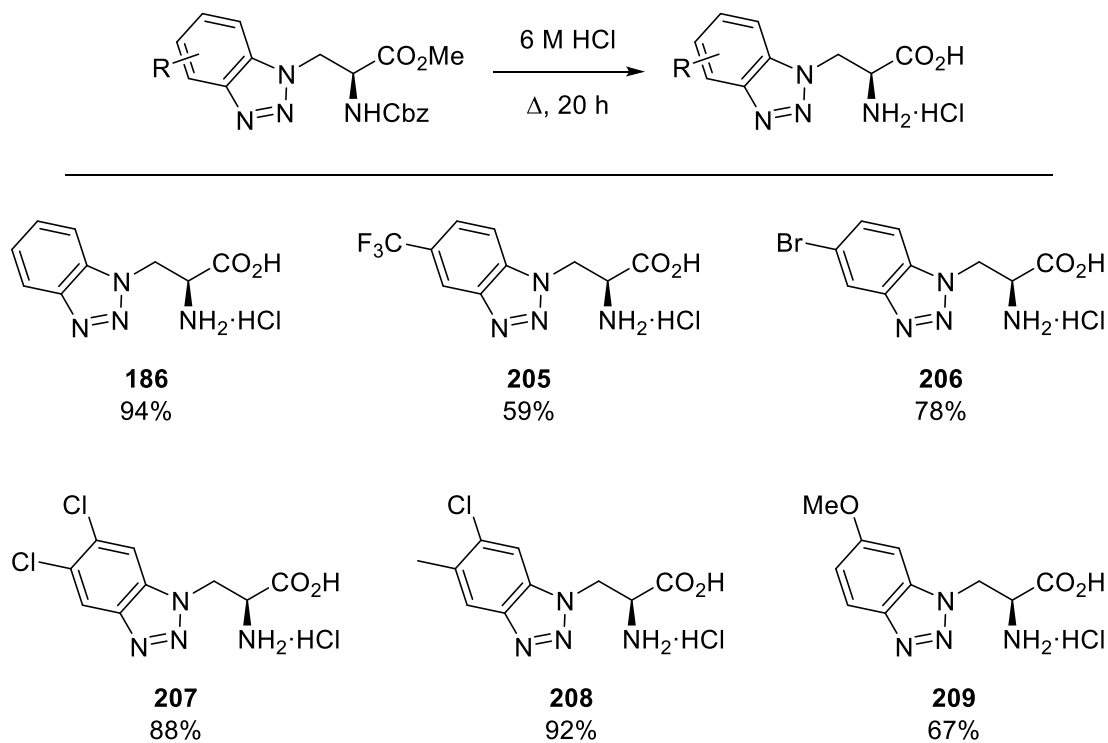
benzotriazoles **187–204** in modest to good yields. Again, the electron-donating methoxy derivative **201** was produced in 39% yield, despite full conversion of the starting material. Various conditions were trialled for this reaction, using fewer equivalents of reagents and varying reaction time. However, the best yield was achieved using the initial method.

**Table 20: Reduction and cyclisation of derivatives**



Entry	R	Yield for 1 <sup>st</sup> Step	Yield for 2 <sup>nd</sup> Step
1	H, <b>187</b>	83%	59%
2	5-CF <sub>3</sub> , <b>200</b>	85%	57%
3	6-MeO, <b>201</b>	59%	39%
4	5,6-Dichloro, <b>202</b>	89%	80%
5	5-Me-6-Cl, <b>203</b>	65%	78%
6	5-Br, <b>204</b>	76%	66%

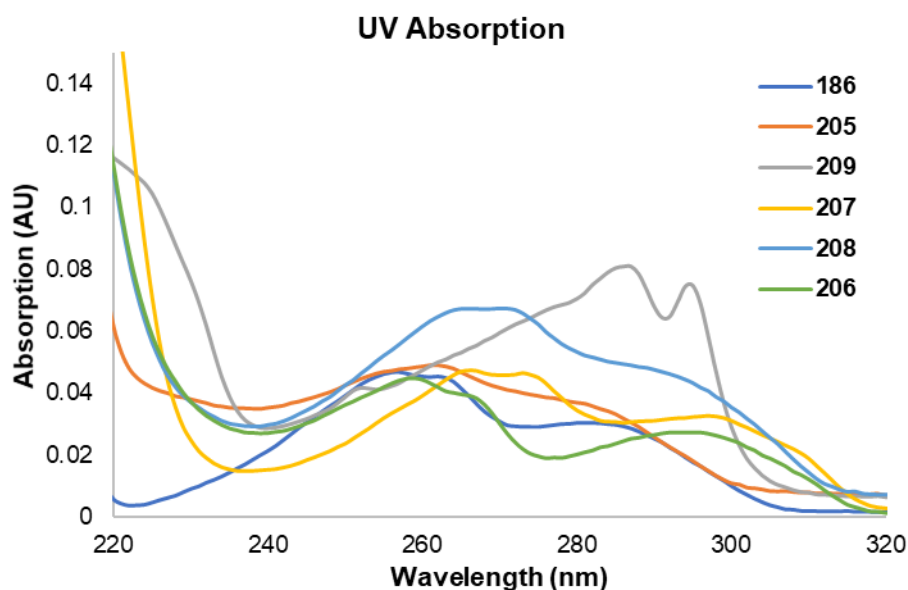
The final step in the synthesis involved the acid mediated deprotection and gave all the target compounds in good yields. The two slightly lower yields for  $\alpha$ -amino acids **205** and **209** were most probably due to the difficulty in purification of these by recrystallisation.



**Scheme 72: Deprotection of benzotriazole  $\alpha$ -amino acids**

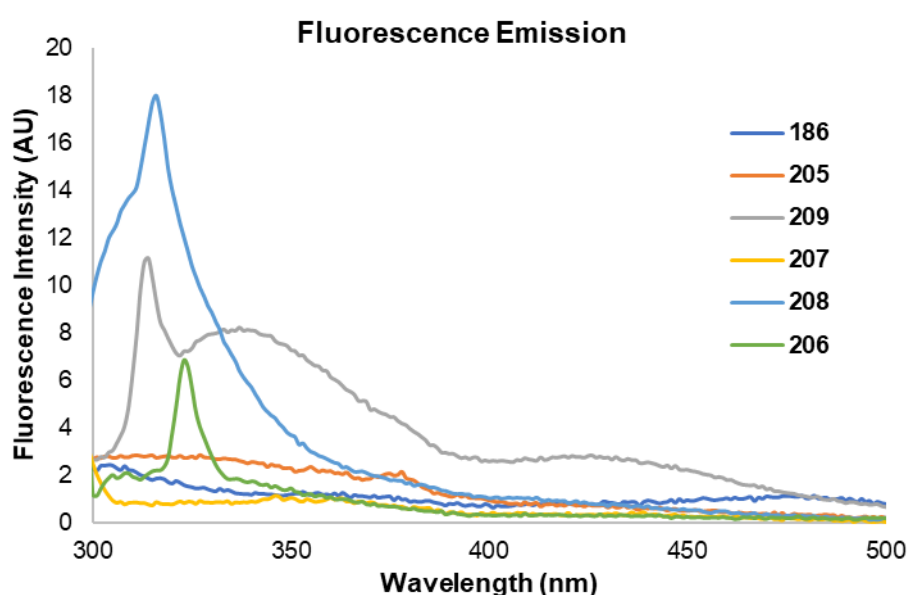
### 2.3.2.3 Analysis of fluorescent properties

With the deprotected benzotriazoles now in hand, the optical properties of these compounds were assessed. The UV-visible absorption were recorded for each compound (Figure 34), using 5  $\mu$ M and 10  $\mu$ M solutions in methanol. This revealed the absorption maximum for each amino acid which was used for excitation.



**Figure 34: Graph showing UV absorption data for substituted benzotriazole  $\alpha$ -amino acids**

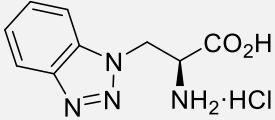
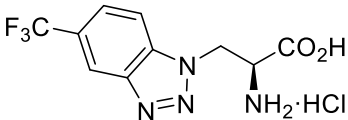
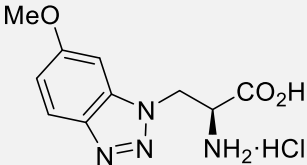
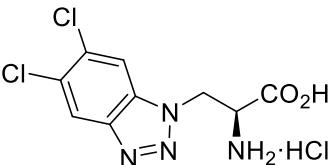
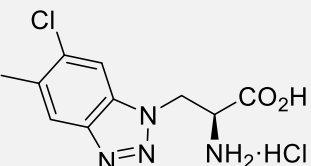
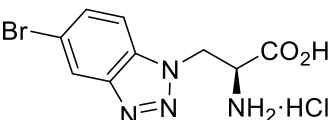
It was immediately clear from the emission spectra that none of these compounds were fluorescent (Figure 35). This was expected due to the limited size of the conjugated system and indeed the main purpose of the synthesis of this library of compounds was to showcase the versatility of the synthetic route. The fluorescence emission does however provide preliminary data on which of these compounds should be further investigated. Analysis provided values for the Stokes shift: an important factor in fluorescence imaging, as this shows the difficulty with which the excitation light can be separated from the probe emission.<sup>198</sup> Another useful factor is the molar extinction coefficient ( $\epsilon$ ), determined from the absorption spectrum using the Beer-Lambert Law. This value is defined as how well a substance absorbs light at a particular wavelength and contributes to the measure of brightness for potential fluorophores.



**Figure 35: Graph showing fluorescence emission for substituted benzotriazole  $\alpha$ -amino acids**

Of the compounds tested, 6-methoxy derivative **209** had the highest molar extinction coefficient of  $8320 \text{ cm}^{-1} \text{ M}^{-1}$  and a Stokes shift of 52 nm (Table 21). Compound **207** showed a Stokes shift of 70 nm; however, showed very weak fluorescence.

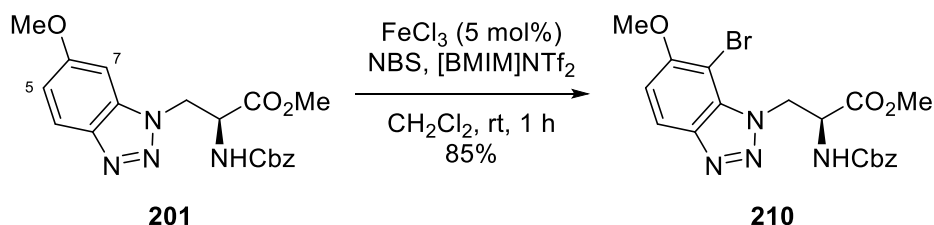
Table 21: Optical properties for library of benzotriazole  $\alpha$ -amino acids

Compound	Absorption maximum (nm)	Molar Extinction Coefficient ( $\epsilon$ ) ( $\text{cm}^{-1} \text{M}^{-1}$ )	Emission maximum (nm)	Stokes shift (nm)
 186	255	4857	312	57
 205	262	5750	315	53
 209	286	8320	338	52
 207	273	5000	343	70
 208	288	4720	316	28
 206	265	5601	318	53

## 2.3.3 Further Functionalisation and Analysis

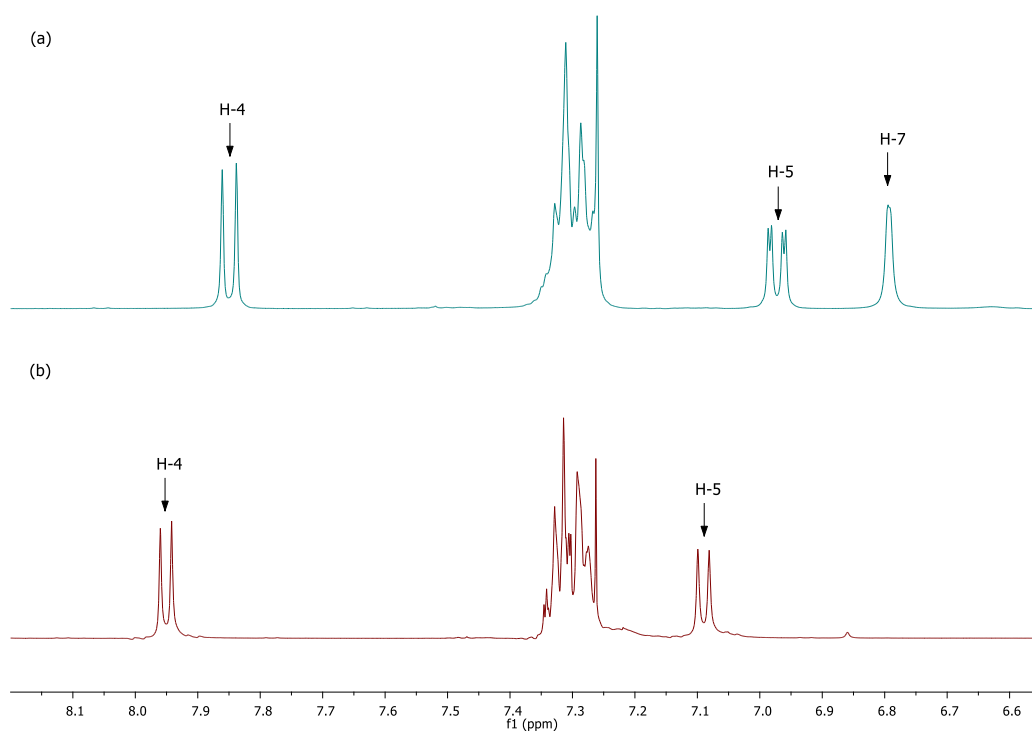
### 2.3.3.1 Functionalisation of the 6-methoxy analogue

With 6-methoxy analogue **209** showing more promising fluorescence emission properties and having a strong directing group for electrophilic aromatic substitution in the form of the methoxy group, work then began on the further functionalisation of this compound. By utilising the aforementioned bromination reaction, using iron(III) chloride and the ionic liquid [BMIM]NTf<sub>2</sub> to generate Fe(NTf<sub>2</sub>)<sub>3</sub> *in situ*, it was proposed that with the more active *para*-position blocked, bromination would occur in one of the two *ortho*-positions to the methoxy group.<sup>131,199</sup> It was expected that, of the two positions, bromination would be more likely at the C-5 position of the benzotriazole given that it is the least hindered. Reaction of **201** with NBS in the presence of FeCl<sub>3</sub> (5 mol%) and [BMIM]NTf<sub>2</sub> gave **210** in 85% yield as the only product (Scheme 73).



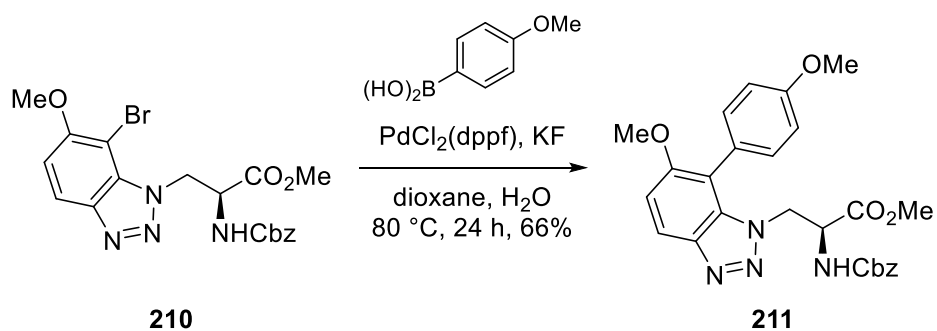
**Scheme 73: Bromination of 201**

Confirmation of the outcome of this reaction was obtained from <sup>1</sup>H NMR spectroscopy (Figure 36). The <sup>1</sup>H NMR spectrum of **210** clearly showed two doublets in the aromatic region with *ortho*-coupling constants (Figure 36a) and disappearance of the broad singlet observed in starting material **201** (Figure 36b). This regiochemistry can be explained by possible coordination of the NBS-iron catalyst with the amino acid moiety of **201**, directing bromination to the C-7 position.



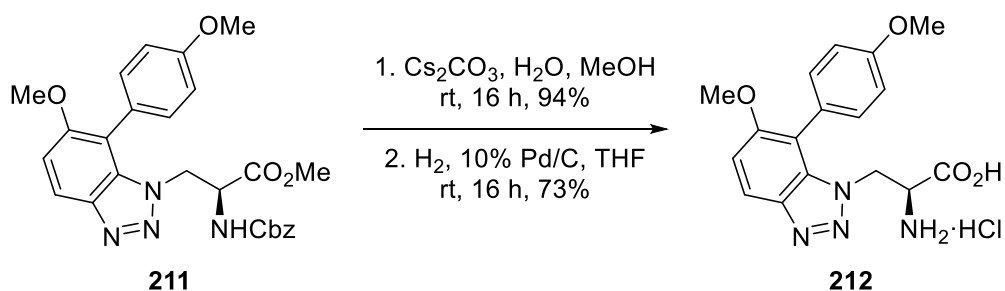
**Figure 36: Expansion of the aromatic region of the  $^1\text{H}$  NMR spectrum of (a) **201** and (b) **210****

Although unexpected, this product was still an ideal substrate for further functionalisation by palladium cross-coupling reactions. A Suzuki-Miyaura reaction was proposed, as this uses fairly mild conditions and could be used to introduce an aromatic ring and extend the conjugation of the amino acid side chain.<sup>135,200</sup> With this in mind, **210** was subjected to a Suzuki-Miyaura reaction with 4-methoxyphenylboronic acid using similar conditions to previously described reactions (see section 2.1.3.2). In this reaction, potassium fluoride was used as the base, since caesium carbonate would likely cause hydrolysis of the ester (Scheme 74). The reaction was complete after 24 h and successfully produced **211** in 66% yield.



**Scheme 74: Suzuki-Miyaura reaction to form **211****

The final step in this synthesis was the deprotection of **211** to form parent amino acid **212**. Initially, it was proposed that using the same deprotection as the previous analogues may not be appropriate, given the harsh acidic conditions may result in some demethylation of the aryl methoxy groups of **211**. Instead a milder two-step approach was proposed, using caesium carbonate to hydrolyse the ester followed by a short reaction with 6 M hydrochloric acid to remove the benzyl carbamate.<sup>201</sup> The hydrolysis was successful, proceeding in 94% yield (Scheme 75), however, despite the milder conditions, amino group deprotection with 6 M HCl resulted in small quantities of demethylation giving a mix of products that were inseparable. It was then proposed that hydrogenation of the amino group may be a better method for deprotection of the benzyl carbamate. Standard conditions of 10% palladium on carbon under a hydrogen atmosphere were applied, initially using ethyl acetate as the solvent. After 24 h none of the desired product was observed. However, when the solvent was changed to tetrahydrofuran, full conversion to the desired product was observed, giving **212** in 73% yield.



**Scheme 75: Deprotection of 211**

### 2.3.3.2 Analysis of fluorescent properties

The photophysical properties of  $\alpha$ -amino acid **212** were recorded at 10  $\mu$ M concentration in methanol (Figure 37). The absorption spectrum showed a maximum of 283 nm, while the emission spectrum revealed strong fluorescence, with the major band at 432 nm. This data showed that **212** possessed a MegaStokes shift of 148 nm. The quantum yield ( $\Phi_F$ ) describes the efficiency of the fluorescence and is defined as the ratio of the number of photons emitted to the number of photons absorbed. This was calculated for **212** as 0.09, using anthracene and L-tryptophan as standards. By finding the product of the quantum yield and the molar extinction coefficient ( $\epsilon$ ), the brightness of **212** was calculated as 856  $\text{cm}^{-1} \text{M}^{-1}$  (Figure 38).

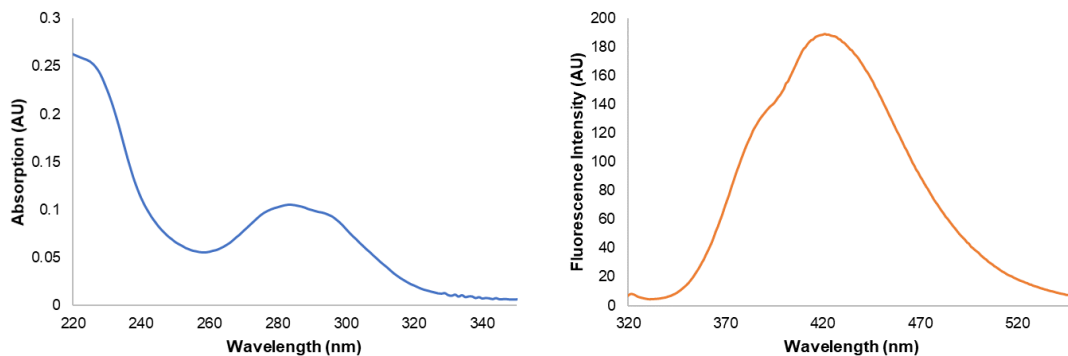
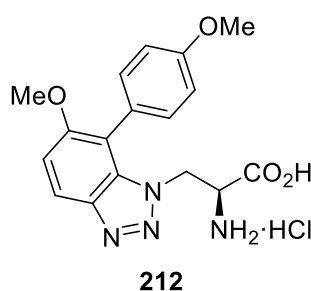


Figure 37: **212** absorption and emission spectra



$$\lambda_{\text{abs.}} = 283 \text{ nm}$$

$$\lambda_{\text{emi.}} = 432 \text{ nm}$$

$$\epsilon = 9516 \text{ cm}^{-1} \text{ M}^{-1}$$

$$\Phi_{\text{F}} = 0.09$$

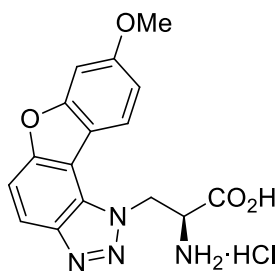
$$\text{Brightness} = 856 \text{ cm}^{-1} \text{ M}^{-1}$$

Figure 38: Optical properties of **212**

## 2.3.4 Synthesis of More Conjugated Benzotriazole $\alpha$ -Amino Acids

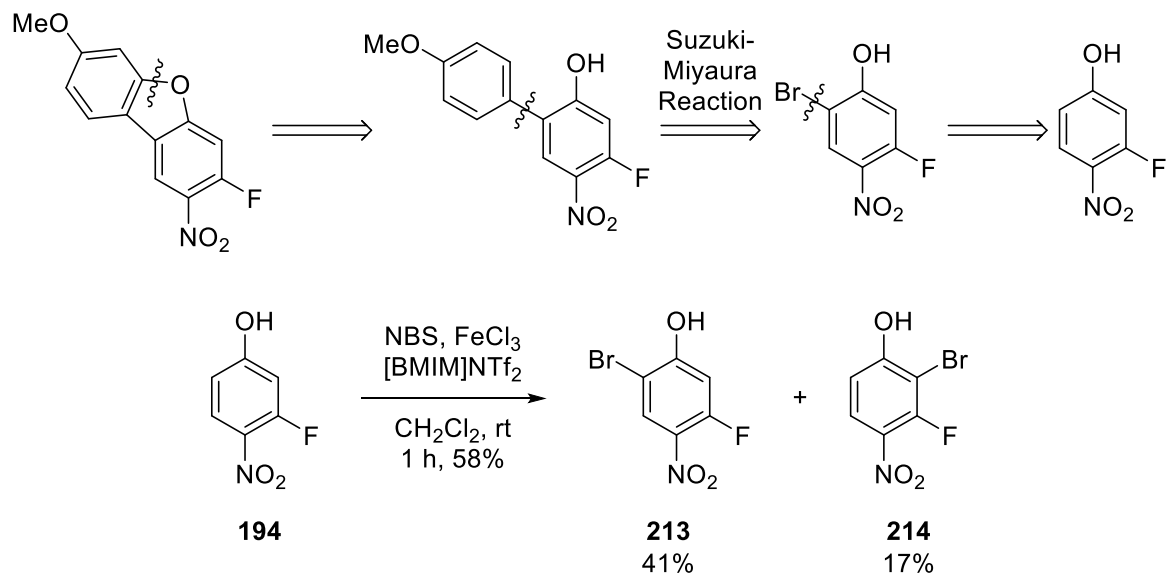
### 2.3.4.1 Dibenzofuran analogue of **212**

Given the difference in fluorescent properties that were observed with the addition of an aromatic ring to form **212**, work began on modifying the structure further. Indeed, one of the potential drawbacks of **212** may be the twisting of the molecule due to the di-*ortho*-substituted biaryl system: ideally these two rings would adopt a planar confirmation, allowing charge transfer across the aryl system and thus enhancing the fluorescence further.<sup>200</sup> It was proposed that conformational restriction of the aryl system to form a dibenzofuran (Figure 39) would produce an  $\alpha$ -amino acid with enhanced photophysical properties.



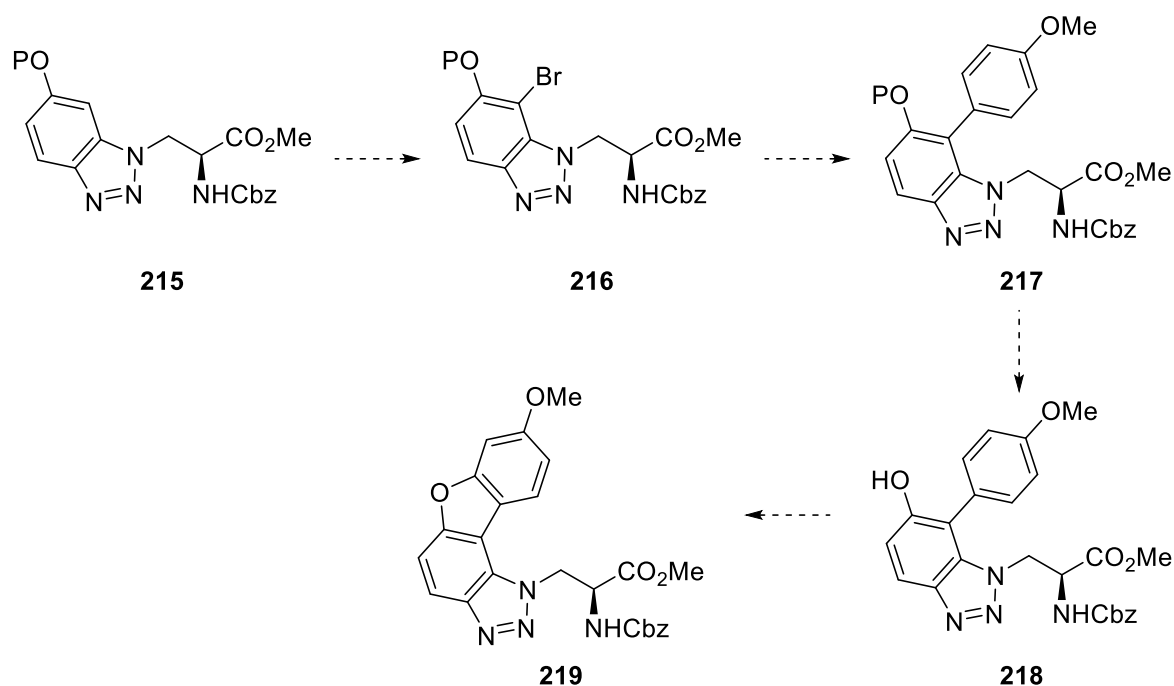
**Figure 39: Dibenzofuran benzotriazole  $\alpha$ -amino acid target**

Forming a dibenzofuran after synthesis of the benzotriazole looked to be a challenging reaction, however, conditions developed by Zhao *et al.* (Scheme 76) show that *ortho*-arylphenols with electron withdrawing groups in the *para*-position are good substrates for C-H cycloetherification.<sup>202</sup> With this in mind, a synthesis was proposed towards a dibenzofuran featuring an *ortho*-fluoronitro moiety for use in the  $S_NAr$  reaction. Bromination of phenol **194**, using NBS and the iron(III) triflimide method proved to be unselective and gave mono-brominated compounds **213** and **214** in a 2.5:1 ratio. Although the regiochemistry was not important, these two regioisomers were inseparable. Attempts at the same reaction at a lower temperature (0 °C) gave the same ratio of compounds and iodination (switching NBS for NIS) produced only a small amount of di-iodinated product. This lack of selectivity is likely due to the similar steric hindrance of both *ortho*-positions (i.e. the similar size of H versus F). With this in mind, a final iodination attempt was made using NIS and silver triflimide (AgNTf<sub>2</sub>) instead of the ionic liquid, [BMIM]NTf<sub>2</sub>. This method was developed by Racys *et al.*, who showed that the larger size of the silver atom aided the regioselectivity by tuning down the reactivity.<sup>125</sup> The reaction, however, showed no sign of any product and so the proposed route was re-examined.



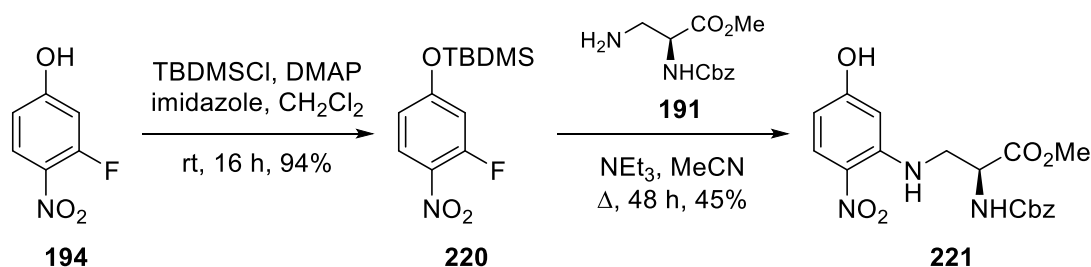
**Scheme 76: Proposed synthesis of a dibenzofuran and attempted bromination**

Since the attempted bromination of **201** to form **210** was selective, a new approach was considered in which the dibenzofuran would be prepared after the benzotriazole unit (Scheme 77). This would involve bromination of a protected phenol **215**, followed by a Suzuki-Miyaura coupling and selective deprotection of the alcohol, before attempting the C-H cycloetherification to form a dibenzofuran **219**. The choice of protecting group for the alcohol would be important, as this would need to be orthogonal to both the methyl ester and the benzyl carbamate and would also need to remain intact throughout the route.



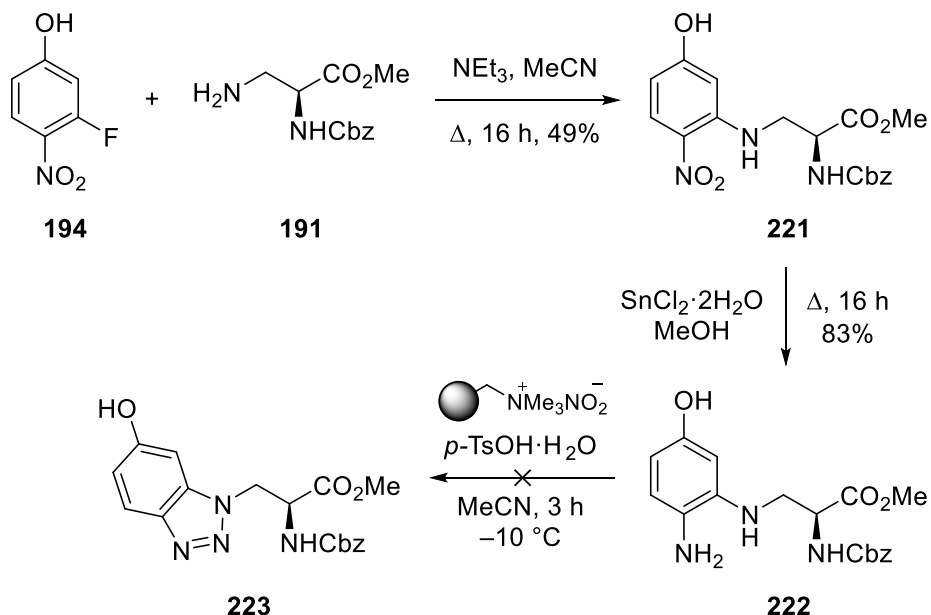
**Scheme 77: New route towards dibenzofuran analogue (P = protecting group)**

The silyl protecting group, TBDMS was first considered, as this could be easily deprotected using TBAF at a later stage. The initial attempt at TBDMS protection of **194** used TBDMS-Cl and imidazole in dichloromethane, stirring at room temperature for 24 h and gave **220** in 70% yield. In order to improve upon this result, the second attempt also used 10 mol% of DMAP. Having an amine in the *para*-position pushing electrons into the aromatic system makes DMAP a more effective nucleophile than just pyridine itself. It can be used to activate the TBDMSCl, facilitating nucleophilic attack of the phenolic alcohol of **194**. These conditions gave **220** in 94% yield after 16 h (Scheme 78). Compound **220** was then submitted to the S<sub>N</sub>Ar reaction conditions with 3-aminoalanine **191**. Conversion of the starting material was slow, and the reaction took 48 h. However, instead of the desired product, the only compound isolated was deprotected coupled amino acid, **221** in 45% yield. This deprotection may have been caused by the presence of fluoride generated from the S<sub>N</sub>Ar reaction. Therefore a different approach was considered.



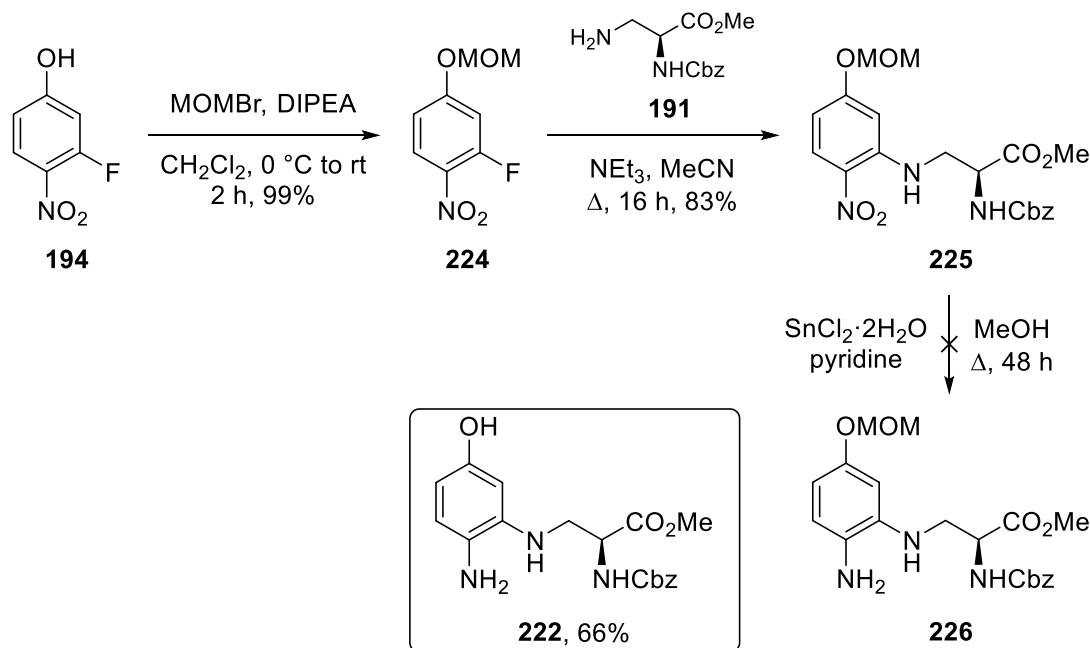
**Scheme 78: Synthesis of 221 and attempted coupling with 191**

Given that the attempted S<sub>N</sub>Ar reaction of **220** gave **221** in a moderate yield, this suggested that a protecting group may not be necessary for the route. Reaction of phenol **194** with **191** gave the desired S<sub>N</sub>Ar product in 49% yield (Scheme 79) and reduction of the nitro group with tin(II) chloride to form **222** proceeded as expected, in 83% yield. Attempted diazotisation and cyclisation of **222** with the polymer-supported nitrite reagent and *p*-tosic acid was unsuccessful. After 3 h, there was no starting material visible in the <sup>1</sup>H NMR spectrum of the crude material, nor was there any evidence of the desired product, **223**. Attempts to cool down the reaction and add fewer equivalents of reagents led to no improvement, as it seemed that the starting material was decomposing during the reaction. This was possibly due to the hydroxyl group interference with the diazotisation step.



**Scheme 79: Attempted synthesis of benzotriazole amino acid 223**

Since protection of the alcohol seemed necessary, a MOM group was next considered. Although MOM groups can be removed using acid, it was expected that the reduction could be performed using non-acidic conditions and the mild conditions of the cyclisation should leave the group unaltered. Initial protection of phenol **194** to give MOM-protected **224** was performed using MOMBr and DIPEA in dichloromethane (Scheme 80). This successfully gave **224** in 99% yield. The subsequent  $\text{S}_{\text{N}}\text{Ar}$  reaction of **224** with 3-aminoalanine **191** occurred well to give **225** in 83% yield, using the same conditions as previous reactions. To perform the reduction of the nitro group, tin(II) chloride in the presence of pyridine was used. This procedure has been used previously with compounds containing acid-labile moieties, such as Boc-protecting groups.<sup>203</sup> Unfortunately the reduction of **225** was very slow, taking 48 h to go to completion. None of the desired product was observed. Instead, deprotected product **222** was formed in 66% yield.



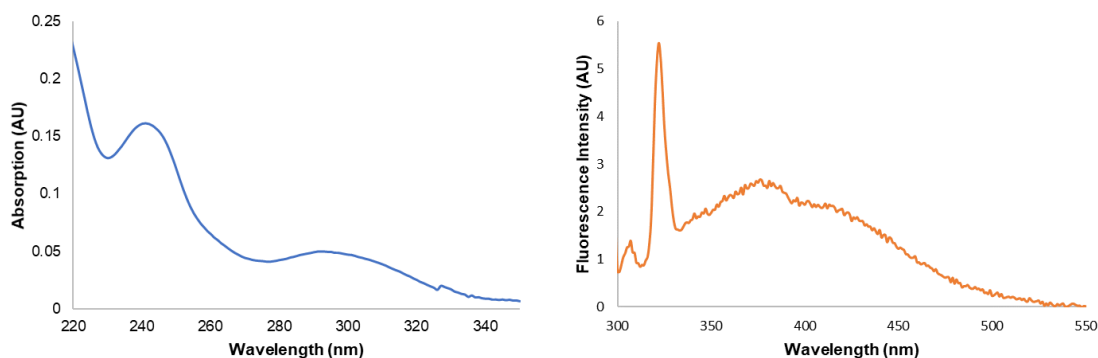
**Scheme 80: Use of MOM-protected phenol 224 for the attempted synthesis of 226**

The final attempt at using a protecting group involved the incorporation of a PMB group. The initial synthesis of **227** was performed using PMBCl and potassium carbonate in DMF at 80 °C. This provided **227** in 65% yield after 2 h. This yield was improved by changing the solvent to acetone, reducing the temperature and the addition of catalytic tetrabutylammonium iodide. Since PMBCl is not as reactive on its own due to the chloride leaving group, this additive allows for the *in situ* generation of the iodide which is more reactive and allows the reaction to be carried out faster at a lower temperature. The yield of **227** improved to 93% after 2 h (Scheme 81). Conversion of **227** into **228** via the  $S_NAr$  coupling occurred successfully in 86% yield. The use of tin(II) chloride to reduce the nitro group was very slow and after 72 h, only a small conversion to the desired product was observed. Other methods of reduction that would not affect the other functionality of **228** were investigated. A reaction with sodium dithionite and potassium carbonate in 95% aqueous ethanol at room temperature was attempted, however, none of the desired product was formed after 16 h. Only hydrolysis of the starting material was observed. A reaction with sodium sulphide in a 3:1 ethanol:water mixture was also attempted, however, a similar result to the previous reaction was observed.





shift of **231** was found to be 80 nm and the molar extinction coefficient was calculated at  $5670 \text{ cm}^{-1} \text{ M}^{-1}$ .



**Figure 40: 231 absorption and emission spectra**

### 2.3.5 Conclusions

In summary, a small library of substituted  $\alpha$ -amino acid benzotriazoles were synthesised *via* diazotisation and intramolecular cyclisation of diarylamines, using a polymer-supported nitrite reagent and *p*-tosic acid as the key step. This reaction was most efficient for compounds featuring an electron-withdrawing group on the aryl ring. Analysis of the optical properties for these compounds showed that they were not fluorescent, possibly due to the absence of an extended conjugated system, and so methods to further functionalise these compounds were investigated. The 6-methoxy analogue, **201**, proved a good substrate for performing electrophilic aromatic substitution reactions, as it contained a strong directing group. This was successfully brominated to form a single regioisomer. Suzuki-Miyaura reaction with 4-methoxyphenylboronic acid followed by a mild, two-step deprotection method, gave amino acid **212**. This  $\alpha$ -amino acid benzotriazole showed very promising optical properties: a Stokes shift of 139 nm and strong fluorescence in the visible region (432 nm). Attempts to optimise these properties further involved avoiding twisting of the biaryl system in **212** by forming a dibenzofuran. Several approaches were implemented, however, none resulted in the desired product. Synthesis of compound **229** enabled attempts at C-H cycloetherification, but the various reaction conditions proved too harsh for the substrate. Notwithstanding, the compound was deprotected to form parent amino acid **231** so that the optical properties could be assessed. Future work has been proposed that describes several potential new approaches towards a dibenzofuran analogue, but also a variation on the structure of **212** that could be used to further assess how the electronics of the aromatic system affect the optical properties of these  $\alpha$ -amino acids.

## 2.3.6 Future work

### 2.3.6.1 Variation of the electronics of **212**

Given the promising fluorescent properties of **212**, future work will investigate the incorporation of alternative aryl groups through the late-stage Suzuki-Miyaura reaction. Amino acid **212** with a *p*-methoxy substituent was prepared as it was thought that the electron-rich substituent would suitably complement the electron-withdrawing triazole moiety and provide the molecule with strong push-pull properties. Such is the case with many promising fluorophores.<sup>206,207</sup> However, taking into account the methoxy group already present on the benzotriazole aryl ring, it would be desirable to install an electron-withdrawing group to enhance the push-pull dynamic in this structure (Figure 41).

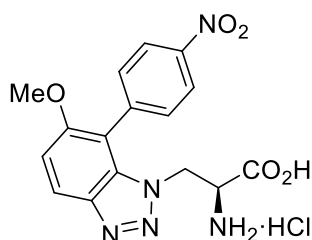
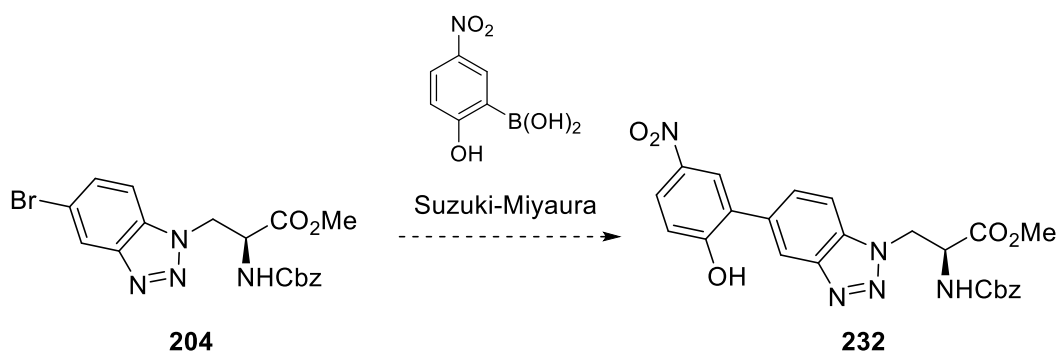


Figure 41: Proposed future target

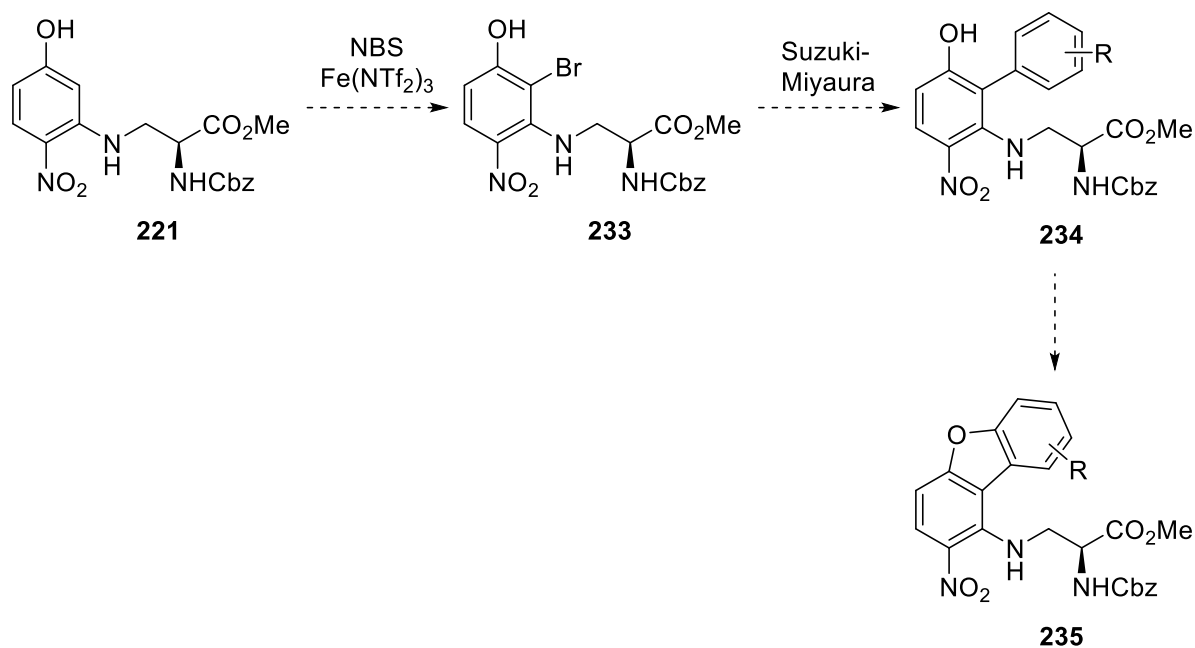
### 2.3.6.2 Potential synthetic routes towards a dibenzofuran analogue

The conditions used for the cycloetherification to form a dibenzofuran proved too harsh for the Suzuki-Miyaura product, **229** (see section 2.3.4.2). However, the cyclisation reaction may have failed due to the absence of an electron-withdrawing group *para* to the hydroxyl group. To test this theory, the Suzuki-Miyaura reaction between **204** and a boronic acid featuring a nitro group should be investigated (Scheme 85). Compound **232** could then be used in a cycloetherification reaction.



Scheme 85: Proposed synthesis of a cycloetherification substrate

Likewise, earlier in this chapter, the synthesis of compound **221** was described (see section 2.3.4.1). Although at the time the focus was on the synthesis of the benzotriazole, coupled product **234** could instead be used for a cycloetherification. Bromination of **221** *via* an electrophilic aromatic bromination would potentially be more difficult due to the electron-withdrawing effect of the nitro group, however the alcohol is strongly electron-donating and moreover, this reduction in reactivity may result in better regiochemical control (Scheme 86). A Suzuki-Miyaura reaction using either the 4-methoxy or other boronic acids would give compound **234**, which could be subjected to the cycloetherification conditions. The advantage of this method is that, so long as the second aryl ring was symmetrical, only a single product would be formed.



Scheme 86: New approach to cycloetherification

## 3 Experimental

### 3.1 General

All reagents and starting materials were obtained from commercial sources and used as received. All reactions were performed under an atmosphere of air unless otherwise stated. All dry solvents were purified using a PureSolv 500 MD solvent purification system. Brine is defined as a saturated solution of aqueous sodium chloride. Flash column chromatography was carried out using Merck Geduran Si 60 (40–63  $\mu\text{m}$ ). Merck aluminium-backed plates pre-coated with silica gel 60 (UV<sub>254</sub>) were used for thin layer chromatography and were visualised under ultraviolet light and by staining with  $\text{KMnO}_4$ , ninhydrin or vanillin.  $^1\text{H}$  NMR and  $^{13}\text{C}$  NMR spectra were recorded on a Bruker DPX 400 spectrometer or Bruker 500 spectrometer with chemical shift values in ppm relative to tetramethylsilane ( $\delta_{\text{H}}$  0.00 and  $\delta_{\text{C}}$  0.0) or residual chloroform ( $\delta_{\text{H}}$  7.26 and  $\delta_{\text{C}}$  77.2) as the standard. Assignment of  $^1\text{H}$  and  $^{13}\text{C}$  NMR signals are based on 2-dimensional COSY, HSQC and DEPT experiments. Infrared spectra were recorded using a Shimadzu FTIR-84005 spectrometer and mass spectra were obtained using a JEOL JMS-700 spectrometer or a Bruker MicroTOFq high resolution mass spectrometer. Melting points were determined on a Gallenkamp melting point apparatus. Optical rotations were determined as solutions irradiating with the sodium D line ( $\lambda = 589 \text{ nm}$ ) using an Autopol V polarimeter.  $[\alpha]_{\text{D}}$  values are given in units  $10^{-1} \text{ deg cm}^2 \text{ g}^{-1}$ . UV-Vis spectra were recorded on a Perkin Elmer Lambda 25 instrument. Fluorescence spectra were recorded on a Shimadzu RF-5301PC spectrofluorophotometer and emission data were measured using an excitation slit width of 3 nm and emission slit width of 3 nm. Quantum yield data were measured using anthracene and L-tryptophan as standard references.

### 3.2 S1P<sub>5</sub> Experimental

#### General Procedure A: Carboxylation of Dihalobenzenes<sup>124</sup>

To a solution of freshly distilled diisopropylamine (1.7 equiv.) in tetrahydrofuran (2.0 mL/mmol) in an oven dried flask under argon at  $-10 \text{ }^\circ\text{C}$  was added *n*-butyllithium (1.6 equiv.; 2.5 M in hexanes). The mixture was stirred for 0.5 h, before cooling to  $-78 \text{ }^\circ\text{C}$ . The dihalobenzene (1.0 equiv.) was then added dropwise. After 1 h of stirring,  $\text{CO}_2$  was bubbled into the reaction via syringe (a pellet of dry ice was added to a 10 mL syringe). The addition was continued for 0.3 h and then the reaction mixture was allowed to reach room temperature over 2 h. The mixture was diluted with water (2.0 mL/mmol) and extracted with a 1 M aqueous sodium hydroxide solution ( $3 \times 2.0 \text{ mL/mmol}$ ). The aqueous layers were then back-extracted with ethyl acetate (4.0 mL/mmol) and the organic layer

discarded. The aqueous layers were acidified to pH 1 using a 6 M aqueous hydrochloric acid solution and subsequently extracted with ethyl acetate (6.0 mL/mmol). The organic layer was then washed with brine (6.0 mL/mmol), dried (MgSO<sub>4</sub>), filtered and concentrated *in vacuo* to afford the product.

#### **General Procedure B: Nucleophilic Aromatic Substitution of 2-Fluorobenzoic Acids**

The benzoic acid (1.0 equiv.) was dissolved in tetrahydrofuran (4.5 mL/mmol) under an atmosphere of argon. The aniline (2.0 equiv.) was added and the mixture cooled to -78 °C. Lithium bis(trimethylsilyl)amide (3.0 equiv.; 1.0 M in tetrahydrofuran) was then slowly added over 0.1 h. The reaction mixture was then allowed to reach room temperature before heating to 40 °C and stirring for 16 h. The reaction was quenched with water (2.5 mL/mmol) and acidified to pH 2 with 10% aqueous hydrochloric acid. The mixture was then extracted with ethyl acetate (3 × 5.0 mL), dried (MgSO<sub>4</sub>), filtered and concentrated *in vacuo*. The resulting residue was then purified by flash column chromatography, eluting with 20–40% ethyl acetate in petroleum ether (40–60) to afford the benzoic acid derivative.

#### **General Procedure C: Ullmann Condensation of 2-Bromobenzoic Acids<sup>95</sup>**

Sodium hydride (3.0 equiv.; 60% in mineral oil) was added to a dry flask under argon. The sodium hydride was then washed with hexane (2 × 3.3 mL/mmol) to remove the oil and the flask cooled to 0 °C. The required dry alcohol (3.3 mL/mmol) was added to the reaction vessel carefully over 0.1 h and then stirred for 0.5 h. The benzoic acid derivative (1.0 equiv.) was added followed by the addition of copper powder (0.4 equiv.) and the reaction mixture heated to 80 °C for 18 h. The reaction mixture was cooled to room temperature and filtered through a pad of Celite<sup>®</sup>. The filtrate was concentrated *in vacuo* and taken up in water (3.3 mL/mmol). The mixture was acidified to pH 2 using 10% aqueous hydrochloric acid and extracted with dichloromethane (3 × 5.0 mL/mmol). The organic layer was dried (MgSO<sub>4</sub>), filtered and concentrated *in vacuo*. The resulting residue was then purified by flash column chromatography, eluting with 20% ethyl acetate in petroleum ether (40–60) to afford the ether product.

#### **General Procedure D: Amidation of Benzoic Acid Ether Derivatives<sup>95</sup>**

The benzoic acid ether derivative (1.0 equiv.) was dissolved in tetrahydrofuran (3.0 mL/mmol) and 2-chloro-4,6-dimethoxy-1,3,5-triazine (1.2 equiv.) and *N*-methylmorpholine (3.0 equiv.) were added. The mixture was then stirred for 2 h at room temperature. The precipitate was filtered and ammonium hydroxide (9.0 mL/mmol) was added to the filtrate. The reaction mixture was stirred for 0.5 h at room temperature and then filtered. 2 M

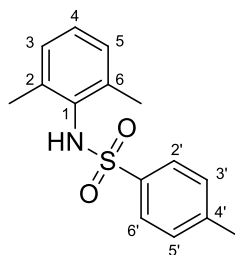
Sodium hydroxide (9.0 mL/mmol) was added to the filtrate and the crude product was extracted with ethyl acetate (3 × 9.0 mL/mmol). The organic layer was dried (MgSO<sub>4</sub>), filtered and concentrated *in vacuo*. The resulting residue was then purified by flash column chromatography, eluting with 10% ethyl acetate in petroleum ether (40–60) to afford the benzamide product.

#### **General Procedure E: Bromination of Benzamide and Phthalazinone Derivatives<sup>131</sup>**

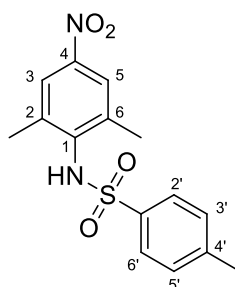
To a dry flask under argon was added iron(III) chloride (5 mol%) and [BMIM]NTf<sub>2</sub> (2.0 equiv.) and the mixture stirred for 0.5 h. The derivative (1.0 equiv.) was then added as a solution in dichloromethane (2.5 mL/mmol) and *N*-bromosuccinimide (0.8 equiv.) was added slowly to the mixture. After 1 h of stirring at room temperature, *N*-bromosuccinimide (0.25 equiv.) was added and the reaction stirred for a further 1 h. The mixture was diluted with ethyl acetate (5.0 mL/mmol) and filtered through a short pad of silica. The filtrate was then washed with 1 M sodium thiosulfate (2 × 10 mL/mmol) and brine (10 mL/mmol). It was dried (MgSO<sub>4</sub>), filtered and concentrated *in vacuo*. The resulting residue was then purified by flash column chromatography, eluting with 20% ethyl acetate in petroleum ether (40–60) to afford the brominated product.

#### **General Procedure F: Suzuki-Miyaura Reaction of Benzamide and Phthalazinone Bromides**

To a reaction vessel containing the aryl bromide (1.0 equiv) in 1,4-dioxane (15 mL/mmol) and water (1.1 mL/mmol) was added [1,1'-bis(diphenylphosphino)ferrocene]dichloropalladium(II) (1:1) (5 mol%), the boronic acid (1.6 equiv.) and caesium carbonate (3.0 equiv). The reaction mixture was then sealed and degassed under argon for 0.2 h, before heating to 80 °C for 2–16 h. The reaction mixture was cooled and filtered through Celite<sup>®</sup>, washed with ethyl acetate (50 mL/mmol). The filtrate was washed with water (3 × 50 mL/mmol) and brine (50 mL/mmol) and the organic layer dried (MgSO<sub>4</sub>), filtered and concentrated *in vacuo*. The resulting residue was then purified by flash column chromatography to afford the coupled product.

***N*-Tosyl-2,6-dimethylaniline (61)**<sup>130</sup>

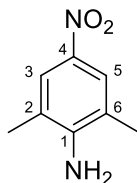
2,6-Dimethylaniline (6.10 mL, 49.5 mmol) and *p*-toluenesulfonyl chloride (11.3 g, 59.4 mmol) were suspended in pyridine (120 mL) and heated under reflux for 5 h. The reaction was quenched with 2 M aqueous hydrochloric acid (250 mL) and extracted with diethyl ether (3 × 100 mL). The organic layer was then dried (MgSO<sub>4</sub>), filtered and concentrated *in vacuo*. Toluene (50 mL) was added to the residue and the resulting suspension concentrated *in vacuo* to afford *N*-tosyl-2,6-dimethylaniline (**61**) as a white solid (13.4 g, 98%). Mp 123–125 °C, lit.<sup>130</sup> 124–126 °C; δ<sub>H</sub> (400 MHz, CDCl<sub>3</sub>) 2.04 (6H, s, 2-CH<sub>3</sub> and 6-CH<sub>3</sub>), 2.42 (3H, s, 4'-CH<sub>3</sub>), 6.08 (1H, br s, NH), 7.00 (2H, d, *J* 7.5 Hz, 3-H and 5-H), 7.05–7.12 (1H, m, 4-H), 7.24 (2H, d, *J* 8.2 Hz, 3'-H and 5'-H), 7.60 (2H, d, *J* 8.2 Hz, 2'-H and 6'-H); δ<sub>C</sub> (101 MHz, CDCl<sub>3</sub>) 18.7 (2 × CH<sub>3</sub>), 21.6 (CH<sub>3</sub>), 127.2 (2 × CH), 127.8 (CH), 128.8 (2 × CH), 129.6 (2 × CH), 132.6 (C), 137.7 (2 × C), 137.8 (C) 143.7 (C); *m/z* (ESI) 298 (MNa<sup>+</sup>, 100%).

***N*-Tosyl-2,6-dimethyl-4-nitroaniline (62)**<sup>130</sup>

*N*-Tosyl-2,6-dimethylaniline (**61**) (5.00 g, 18.1 mmol) was suspended in glacial acetic acid (100 mL), water (100 mL) and concentrated nitric acid (21 mL). Sodium nitrite (2.50 g, 36.3 mmol) was added and the reaction mixture was heated at 140 °C for 6 h. The reaction mixture was cooled to room temperature and then stored in a refrigerator overnight. The resulting colourless crystals were filtered and washed repeatedly with water until the washings were neutral to afford *N*-tosyl-2,6-dimethyl-4-nitroaniline (**62**) as colourless crystals (3.69 g, 64%). Mp 163–165 °C, lit.<sup>130</sup> 165–167 °C; δ<sub>H</sub> (400 MHz, CDCl<sub>3</sub>) 2.16 (6H, s, 2-CH<sub>3</sub> and 6-CH<sub>3</sub>), 2.45 (3H, s, 4'-CH<sub>3</sub>), 6.13 (1H, br s, NH), 7.29 (2H, d, *J* 8.2 Hz, 3'-H and 5'-H), 7.60 (2H, d, *J* 8.2 Hz, 2'-H and 6'-H), 7.89 (2H, s, 3-H and 5-

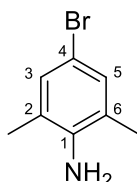
H);  $\delta_{\text{C}}$  (126 MHz,  $\text{CDCl}_3$ ) 19.1 (2  $\times$   $\text{CH}_3$ ), 21.6 ( $\text{CH}_3$ ), 123.6 (2  $\times$  CH), 127.1 (2  $\times$  CH), 130.0 (2  $\times$  CH), 137.2 (2  $\times$  C), 138.7 (C), 139.2 (C), 144.5 (C), 146.3 (C);  $m/z$  (ESI) 343 ( $\text{MNa}^+$ , 100%).

#### 2,6-Dimethyl-4-nitroaniline (**49**)<sup>130</sup>

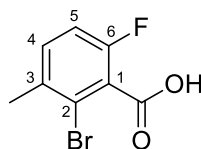


*N*-Tosyl-2,6-dimethyl-4-nitroaniline (**62**) (3.00 g, 9.40 mmol) was dissolved in sulfuric acid (15 mL) and water (1 mL) and heated at 40 °C for 16 h. The reaction mixture was poured slowly into an ice/water/sodium hydroxide mixture (300 mL). This was then extracted with ethyl acetate (3  $\times$  100 mL), dried ( $\text{MgSO}_4$ ), filtered and concentrated *in vacuo* to afford 2,6-dimethyl-4-nitroaniline (**49**) as yellow crystals (1.52 g, 98%). Mp 167–169 °C, lit.<sup>130</sup> 165–167 °C;  $\delta_{\text{H}}$  (400 MHz,  $\text{CDCl}_3$ ) 2.22 (6H, s, 2  $\times$   $\text{CH}_3$ ), 4.29 (2H, br s,  $\text{NH}_2$ ), 7.90 (2H, s, 3-H and 5-H);  $\delta_{\text{C}}$  (126 MHz,  $\text{CDCl}_3$ ) 17.5 (2  $\times$   $\text{CH}_3$ ), 120.5 (2  $\times$  C), 124.6 (2  $\times$  CH), 138.3 (C), 149.3 (C);  $m/z$  (ESI) 189 ( $\text{MNa}^+$ , 100%).

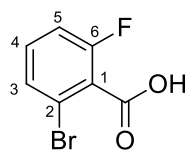
#### 4-Bromo-2,6-dimethylaniline (**63**)<sup>208</sup>



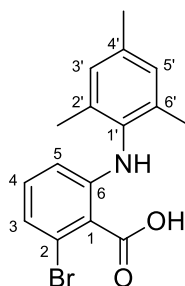
To a small dry vial fitted with a magnetic stirrer was added iron(III) chloride (0.0040 g, 0.025 mmol) and  $[\text{BMIM}]\text{NTf}_2$  (0.30 mL, 1.0 mmol). The mixture was stirred at room temperature for 0.5 h, before adding 2,6-dimethylaniline (0.061 mL, 0.50 mmol). *N*-Bromosuccinimide (0.098 g, 0.55 mmol) was then added in three portions over 1 h and the reaction mixture was heated to 60 °C for 48 h. The reaction mixture was cooled to room temperature and taken up in 5% ethyl acetate in hexane and sonicated for 0.1 h. The resulting solution was washed with 1 M aqueous sodium thiosulfate (50 mL) and brine (50 mL), dried ( $\text{MgSO}_4$ ), filtered and then concentrated *in vacuo*. The crude material was purified by flash column chromatography, eluting with 5–15% diethyl ether in petroleum ether (40–60) to afford 4-bromo-2,6-dimethylaniline (**63**) as an orange solid (0.053 g, 53%). Mp 46–49 °C, lit.<sup>208</sup> 44–48 °C;  $\delta_{\text{H}}$  (500 MHz,  $\text{CDCl}_3$ ) 2.15 (6H, s, 2- $\text{CH}_3$  and 6- $\text{CH}_3$ ), 3.57 (2H, br s,  $\text{NH}_2$ ), 7.06 (2H, s, 3-H and 5-H);  $\delta_{\text{C}}$  (126 MHz,  $\text{CDCl}_3$ ) 17.4 (2  $\times$   $\text{CH}_3$ ), 109.4 (C), 123.6 (2  $\times$  C), 130.5 (2  $\times$  CH), 141.8 (C);  $m/z$  (ESI) 200 ( $\text{MH}^+$ , 100%).

**2-Bromo-6-fluoro-3-methylbenzoic acid (78)**<sup>124</sup>

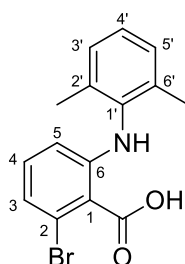
The reaction was carried out according to general procedure A using diisopropylamine (3.75 mL, 27.0 mmol) *n*-butyllithium (10.2 mL, 25.5 mmol, 2.5 M in hexanes) and 2-bromo-4-fluorotoluene (1.95 mL, 15.9 mmol) in tetrahydrofuran (30 mL). This afforded 2-bromo-6-fluoro-3-methylbenzoic acid (**78**) as a white solid (3.70 g, 100%). The spectroscopic data were consistent with the literature.<sup>124</sup> Mp 104–106 °C;  $\delta_{\text{H}}$  (500 MHz, CDCl<sub>3</sub>) 2.42 (3H, s, 3-CH<sub>3</sub>), 7.05 (1H, t, *J* 8.6 Hz, 5-H), 7.31 (1H, dd, *J* 8.6, 5.9 Hz, 4-H), 11.39 (1H, br s, OH);  $\delta_{\text{C}}$  (101 MHz, CDCl<sub>3</sub>) 22.7 (CH<sub>3</sub>), 114.7 (CH, d, <sup>2</sup>*J*<sub>CF</sub> 20.8 Hz), 121.7 (C, d, <sup>3</sup>*J*<sub>CF</sub> 4.0 Hz), 123.7 (C, d, <sup>2</sup>*J*<sub>CF</sub> 19.4 Hz), 132.8 (CH, d, <sup>3</sup>*J*<sub>CF</sub> 8.3 Hz), 134.9 (C, d, <sup>4</sup>*J*<sub>CF</sub> 3.7 Hz), 157.6 (C, d, <sup>1</sup>*J*<sub>CF</sub> 252.6 Hz), 169.8 (C); *m/z* (EI) 232 (M<sup>+</sup>, 100%), 215 (55), 153 (38), 107 (38), 84 (34).

**2-Bromo-6-fluorobenzoic acid (50)**<sup>209</sup>

The reaction was carried out according to general procedure A using diisopropylamine (2.70 mL, 19.4 mmol) *n*-butyllithium (7.48 mL, 18.7 mmol, 2.5 M in hexanes) and 1-bromo-3-fluorobenzene (1.28 mL, 11.4 mmol) in tetrahydrofuran (20 mL). This afforded 2-bromo-6-fluorobenzoic acid (**50**) as a white solid (2.49 g, 100%). Mp 148–150 °C, lit.<sup>209</sup> 152–154 °C;  $\delta_{\text{H}}$  (400 MHz, CDCl<sub>3</sub>) 7.14 (1H, ddd, *J* 9.3, 8.5, 1.0 Hz, 5-H), 7.33 (1H, td, *J* 8.5, 5.8 Hz, 4-H), 7.45 (1H, dt, *J* 8.1, 0.9 Hz, 3-H);  $\delta_{\text{C}}$  (126 MHz, CDCl<sub>3</sub>) 115.2 (CH, d, <sup>2</sup>*J*<sub>CF</sub> 21.5 Hz), 120.5 (C, d, <sup>3</sup>*J*<sub>CF</sub> 3.6 Hz), 123.2 (C, d, <sup>2</sup>*J*<sub>CF</sub> 19.0 Hz), 129.0 (CH, d, <sup>4</sup>*J*<sub>CF</sub> 3.5 Hz), 132.6 (CH, d, <sup>3</sup>*J*<sub>CF</sub> 9.1 Hz), 159.9 (C, d, <sup>1</sup>*J*<sub>CF</sub> 256.3 Hz), 168.5 (C); *m/z* (EI) 218 (M<sup>+</sup>, 100%), 201 (98), 94 (58), 83 (30), 75 (24).

**2-Bromo-6-(mesitylamino)benzoic acid (59)<sup>95</sup>**

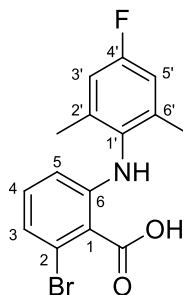
The reaction was carried out according to general procedure B using 2-bromo-6-fluorobenzoic acid (**50**) (1.00 g, 4.57 mmol) and 2,4,6-dimethylaniline (1.36 mL, 9.13 mmol) in tetrahydrofuran (20 mL), followed by treatment with lithium bis(trimethylsilyl)amide (13.7 mL, 13.7 mmol, 1.0 M in tetrahydrofuran). The crude material was purified by flash column chromatography, eluting with 20% ethyl acetate in petroleum ether (40–60) to afford 2-bromo-6-(mesitylamino)benzoic acid (**59**) as a brown solid (1.44 g, 94%). The spectroscopic data were consistent with the literature.<sup>95</sup> Mp 169–171 °C;  $\delta_{\text{H}}$  (400 MHz,  $\text{CDCl}_3$ ) 2.15 (6H, s, 2'- $\text{CH}_3$  and 6'- $\text{CH}_3$ ), 2.31 (3H, s, 4'- $\text{CH}_3$ ), 6.18 (1H, dd,  $J$  7.8, 1.8 Hz, 5-H), 6.89–7.00 (4H, m, 3-H, 4-H, 3'-H and 5'-H);  $\delta_{\text{C}}$  (101 MHz,  $\text{CDCl}_3$ ) 18.1 (2  $\times$   $\text{CH}_3$ ), 21.0 ( $\text{CH}_3$ ), 112.2 (CH), 113.1 (C), 122.8 (CH), 123.4 (C), 129.3 (2  $\times$  CH), 133.5 (CH), 134.0 (C), 136.2 (2  $\times$  C), 136.5 (C), 150.3 (C), 172.5 (C);  $m/z$  (EI) 333 ( $\text{M}^+$ , 100%), 315 (55), 300 (64), 208 (25), 135 (21).

**2-Bromo-6-[(2',6'-dimethylphenyl)amino]benzoic acid (69)**

The reaction was carried out according to general procedure B using 2-bromo-6-fluorobenzoic acid (**50**) (0.300 g, 1.37 mmol) and 2,6-dimethylaniline (0.337 mL, 2.74 mmol) in tetrahydrofuran (8 mL), followed by treatment with lithium bis(trimethylsilyl)amide (4.11 mL, 4.11 mmol, 1.0 M in tetrahydrofuran). The crude material was purified by flash column chromatography, eluting with 20% ethyl acetate in petroleum ether (40–60) to afford 2-bromo-6-[(2,6-dimethylphenyl)amino]benzoic acid (**69**) as a brown solid (0.367 g, 83%). Mp 176–178 °C;  $\nu_{\text{max}}/\text{cm}^{-1}$  (neat) 3356 (NH/OH), 2921 (CH), 1644 (CO), 1556 (C=C), 1484, 1429, 1239, 772;  $\delta_{\text{H}}$  (500 MHz,  $\text{CDCl}_3$ ) 2.19 (6H, s, 2'- $\text{CH}_3$  and 6'- $\text{CH}_3$ ), 6.18 (1H, dd,  $J$  8.0, 1.3 Hz, 5-H), 6.96 (1H, t,  $J$  8.0 Hz, 4-H), 6.99 (1H, dd,  $J$  8.0, 1.3 Hz, 3-H),

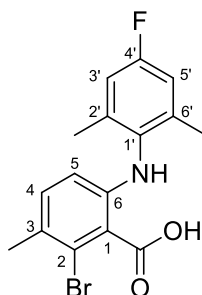
7.07–7.16 (3H, m, 3'-H, 4'-H and 5'-H);  $\delta_{\text{C}}$  (126 MHz,  $\text{CDCl}_3$ ) 18.2 ( $2 \times \text{CH}_3$ ), 112.2 (CH), 113.4 (C), 123.0 (CH), 123.4 (C), 126.8 (CH), 128.7 ( $2 \times \text{CH}$ ), 133.5 (CH), 136.4 ( $2 \times \text{C}$ ), 136.7 (C), 149.8 (C), 172.0 (C);  $m/z$  (ESI) 318.0128 ( $[\text{M}-\text{H}]^-$ .  $\text{C}_{15}\text{H}_{13}^{79}\text{BrNO}_2$  requires 318.0135).

### 2-Bromo-6-[(4'-fluoro-2',6'-dimethylphenyl)amino]benzoic acid (**75**)



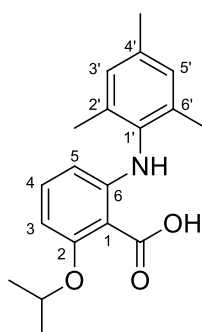
The reaction was carried out according to general procedure B using 2-bromo-6-fluorobenzoic acid (**50**) (1.00 g, 4.56 mmol) and 4-fluoro-2,6-dimethylaniline (1.17 mL, 9.13 mmol) in tetrahydrofuran (20 mL), followed by treatment with lithium bis(trimethylsilyl)amide (13.7 mL, 13.7 mmol, 1.0 M in tetrahydrofuran). The crude material was purified by flash column chromatography, eluting with 20% ethyl acetate in petroleum ether (40–60) to afford 2-bromo-6-[(4'-fluoro-2',6'-dimethylphenyl)amino]benzoic acid (**75**) as a brown solid (1.53 g, 99%). Mp 148–150 °C;  $\nu_{\text{max}}/\text{cm}^{-1}$  (neat) 2953 (NH/OH), 2920 (CH), 1672 (CO), 1595 (C=C), 1560, 1481, 1451, 1242, 858, 767;  $\delta_{\text{H}}$  (500 MHz,  $\text{CDCl}_3$ ) 2.18 (6H, s, 2'- $\text{CH}_3$  and 6'- $\text{CH}_3$ ), 6.15 (1H, dd,  $J$  7.8, 1.4 Hz, 5-H), 6.85 (2H, d,  $J$  9.0 Hz, 3'-H and 5'-H), 6.97 (1H, t,  $J$  7.8 Hz, 4-H), 7.00 (1H, dd,  $J$  7.8, 1.4 Hz, 3-H);  $\delta_{\text{C}}$  (126 MHz,  $\text{CDCl}_3$ ) 18.4 ( $2 \times \text{CH}_3$ ), 111.9 (CH), 113.2 (C), 115.1 ( $2 \times \text{CH}$ , d,  $^2J_{\text{CF}}$  21.9 Hz), 123.2 (C), 123.5 (CH), 132.5 (C, d,  $^4J_{\text{CF}}$  2.8 Hz), 133.7 (CH), 138.9 ( $2 \times \text{C}$ , d,  $^3J_{\text{CF}}$  8.9 Hz), 150.1 (C), 161.0 (C, d,  $^1J_{\text{CF}}$  245.3 Hz), 172.1 (C);  $m/z$  (EI) 337.0122 ( $\text{M}^+$ .  $\text{C}_{15}\text{H}_{13}^{79}\text{BrFNO}_2$  requires 337.0114), 319 (72%), 293 (58), 212 (100).

## 2-Bromo-6-[(4'-fluoro-2',6'-dimethylphenyl)amino]-3-methylbenzoic acid (**79**)



The reaction was carried out according to general procedure B using 2-bromo-6-fluoro-3-methylbenzoic acid (**78**) (0.500 g, 2.15 mmol) and 4-fluoro-2,6-dimethylaniline (0.553 mL, 4.30 mmol) in tetrahydrofuran (10 mL), followed by treatment with lithium bis(trimethylsilyl)amide (6.45 mL, 6.45 mmol, 1.0 M in tetrahydrofuran). The crude material was purified by flash column chromatography, eluting with 20% ethyl acetate in petroleum ether (40–60) to afford 2-bromo-6-[(4'-fluoro-2',6'-dimethylphenyl)amino]benzoic acid (**79**) as a brown solid (0.103 g, 68%). Mp 130–132 °C;  $\nu_{\max}/\text{cm}^{-1}$  (neat) 2955 (NH/OH), 2924 (CH), 1696 (CO), 1606 (C=C), 1565, 1491, 1215, 1129, 1019, 862, 757;  $\delta_{\text{H}}$  (400 MHz,  $\text{CDCl}_3$ ) 2.17 (6H, s, 2'- $\text{CH}_3$  and 6'- $\text{CH}_3$ ), 2.32 (3H, s, 3- $\text{CH}_3$ ), 6.08 (1H, d,  $J$  8.5 Hz, 5-H), 6.82 (2H, d,  $J$  9.0 Hz, 3'-H and 5'-H), 7.01 (1H, d,  $J$  8.5 Hz, 4-H);  $\delta_{\text{C}}$  (101 MHz,  $\text{CDCl}_3$ ) 18.4 (2  $\times$   $\text{CH}_3$ ), 23.0 ( $\text{CH}_3$ ), 112.0 (CH), 115.0 (2  $\times$  CH, d,  $^2J_{\text{CF}}$  21.8), 116.8 (C), 124.2 (C), 128.1 (C), 133.0 (C, d,  $^4J_{\text{CF}}$  2.8 Hz), 134.1 (CH), 138.6 (2  $\times$  C, d,  $^3J_{\text{CF}}$  8.6 Hz), 146.2 (C), 160.7 (C, d,  $^1J_{\text{CF}}$  245.0 Hz), 173.2 (C);  $m/z$  (ESI) 350.0197 ( $[\text{M}-\text{H}]^-$ .  $\text{C}_{16}\text{H}_{14}^{79}\text{BrFNO}_2$  requires 350.0197).

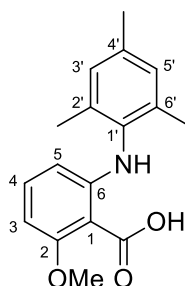
## 2-Isopropoxy-6-(mesitylamino)benzoic acid (**60**)<sup>95</sup>



The reaction was carried out according to general procedure C using sodium hydride (0.0792 g, 1.98 mmol, 60% in mineral oil), isopropanol (2.4 mL), 2-bromo-6-(mesitylamino)benzoic acid (**59**) (0.220 g, 0.660 mmol) and copper powder (0.0168 g, 0.264 mmol). The crude material was purified by flash column chromatography, eluting with 20% ethyl acetate in petroleum ether (40–60) to afford 2-isopropoxy-6-

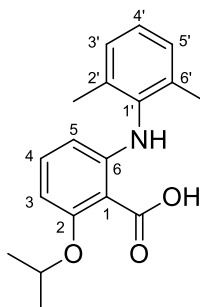
(mesitylamino)benzoic acid (**60**) as an orange solid (0.142 g, 69%). The spectroscopic data were consistent with the literature.<sup>95</sup> Mp 148–150 °C;  $\delta_{\text{H}}$  (400 MHz,  $\text{CDCl}_3$ ) 1.50 (6H, d,  $J$  6.1 Hz,  $\text{OCH}(\text{CH}_3)_2$ ), 2.13 (6H, s, 2'- $\text{CH}_3$  and 6'- $\text{CH}_3$ ), 2.31 (3H, s, 4'- $\text{CH}_3$ ), 4.82 (1H, sept,  $J$  6.1 Hz,  $\text{OCH}(\text{CH}_3)_2$ ), 5.91 (1H, dd,  $J$  8.3, 0.8 Hz, 5-H), 6.20 (1H, br d,  $J$  8.3 Hz, 3-H), 6.94 (2H, s, 3'-H and 5'-H), 7.07 (1H, t,  $J$  8.3 Hz, 4-H), 9.91 (1H, br s, NH), 12.03 (1H, br s, OH);  $\delta_{\text{C}}$  (101 MHz,  $\text{CDCl}_3$ ) 18.1 (2  $\times$   $\text{CH}_3$ ), 21.0 ( $\text{CH}_3$ ), 22.1 (2  $\times$   $\text{CH}_3$ ), 74.2 (CH), 99.8 (C), 100.0 (CH), 107.1 (CH), 129.1 (2  $\times$  CH), 134.1 (CH), 134.5 (C), 136.3 (C), 136.6 (2  $\times$  C), 152.9 (C), 158.2 (C), 169.3 (C);  $m/z$  (EI) 313 ( $\text{M}^+$ , 91%), 253 (100), 252 (22), 238 (54).

### 6-(Mesitylamino)-2-methoxybenzoic acid (**96**)<sup>95</sup>



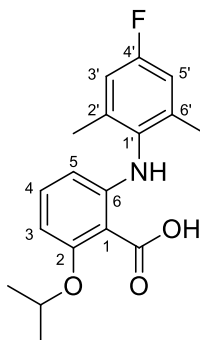
The reaction was carried out according to general procedure C using sodium hydride (0.720 g, 18.0 mmol, 60% in mineral oil), methanol (20 mL), 2-bromo-6-(mesitylamino)benzoic acid (**59**) (2.00 g, 5.98 mmol) and copper powder (0.152 g, 2.39 mmol). The crude material was purified by flash column chromatography, eluting with 20% ethyl acetate in petroleum ether (40–60) to afford 6-(mesitylamino)-2-methoxybenzoic acid (**96**) as an orange solid (1.62 g, 95%). The spectroscopic data were consistent with the literature.<sup>95</sup> Mp 83–85 °C;  $\delta_{\text{H}}$  (500 MHz,  $\text{CDCl}_3$ ) 2.14 (6H, s, 2'- $\text{CH}_3$  and 6'- $\text{CH}_3$ ), 2.31 (3H, s, 4'- $\text{CH}_3$ ), 4.04 (3H, s,  $\text{OCH}_3$ ), 5.96 (1H, d,  $J$  8.3 Hz, 5-H), 6.22 (1H, d,  $J$  8.3 Hz, 3-H), 6.95 (2H, s, 3'-H and 5'-H), 7.10 (1H, t,  $J$  8.3 Hz, 4-H), 9.93 (1H, s, NH), 11.50 (1H, br s, OH);  $\delta_{\text{C}}$  (126 MHz,  $\text{CDCl}_3$ ) 18.1 (2  $\times$   $\text{CH}_3$ ), 21.0 ( $\text{CH}_3$ ), 56.8 ( $\text{CH}_3$ ), 97.7 (CH), 98.6 (C), 107.4 (CH), 129.2 (2  $\times$  CH), 134.3 (CH), 134.4 (C), 136.4 (C), 136.5 (2  $\times$  C), 152.8 (C), 159.9 (C), 169.1 (C);  $m/z$  (ESI) 308 ( $\text{MNa}^+$ , 100%).

**6-[(2',6'-Dimethylphenyl)amino]-2-isopropoxybenzoic acid (70)**



The reaction was carried out according to general procedure C using sodium hydride (0.0564 g, 1.41 mmol, 60% in mineral oil), isopropanol (1.6 mL), 2-bromo-6-[(2,6-dimethylphenyl)amino]benzoic acid (**69**) (0.150 g, 0.468 mmol) and copper powder (0.0119 g, 0.187 mmol). The crude material was purified by flash column chromatography, eluting with 20% ethyl acetate in petroleum ether (40–60) to afford 6-[(2',6'-dimethylphenyl)amino]-2-isopropoxybenzoic acid (**70**) as an orange solid (0.067 g, 48%). Mp 84–86 °C;  $\nu_{\max}/\text{cm}^{-1}$  (neat) 3230 (NH/OH), 2980 (CH), 1695 (CO), 1576 (C=C), 1458, 1248;  $\delta_{\text{H}}$  (500 MHz,  $\text{CDCl}_3$ ) 1.50 (6H, d,  $J$  6.1 Hz,  $\text{OCH}(\text{CH}_3)_2$ ), 2.18 (6H, s, 2'- $\text{CH}_3$  and 6'- $\text{CH}_3$ ), 4.82 (1H, sept,  $J$  6.1 Hz,  $\text{OCH}(\text{CH}_3)_2$ ), 5.90 (1H, dd,  $J$  8.4, 0.6 Hz, 5-H), 6.22 (1H, br d,  $J$  8.4 Hz, 3-H), 7.08 (1H, t,  $J$  8.4 Hz, 4-H), 7.10–7.16 (3H, m, 3'-H, 4'-H and 5'-H), 9.99 (1H, br s, NH), 12.03 (1H, br s, OH);  $\delta_{\text{C}}$  (126 MHz,  $\text{CDCl}_3$ ) 18.2 (2  $\times$   $\text{CH}_3$ ), 22.1 (2  $\times$   $\text{CH}_3$ ), 74.2 (CH), 99.8 (C), 100.3 (CH), 107.1 (CH), 126.7 (CH), 128.4 (2  $\times$  CH), 134.1 (CH), 136.9 (2  $\times$  C), 137.2 (C), 152.5 (C), 158.2 (C), 169.3 (C);  $m/z$  (ESI) 322.1402 ( $\text{MNa}^+$ .  $\text{C}_{18}\text{H}_{21}\text{NNaO}_3$  requires 322.1414).

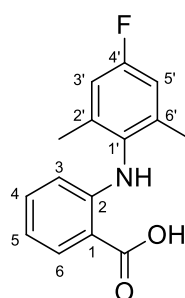
**6-[(4'-Fluoro-2',6'-dimethylphenyl)amino]-2-isopropoxybenzoic acid (80)**



The reaction was carried out according to general procedure C using sodium hydride (0.0532 g, 1.33 mmol, 60% in mineral oil), isopropanol (1.6 mL), 2-bromo-6-[(4'-fluoro-2',6'-dimethylphenyl)amino]benzoic acid (**75**) (0.150 g, 0.444 mmol) and copper powder (0.0112 g, 0.177 mmol). The crude material was purified by flash column chromatography, eluting with 20% ethyl acetate in petroleum ether (40–60) to afford 6-[(4'-fluoro-2',6'-

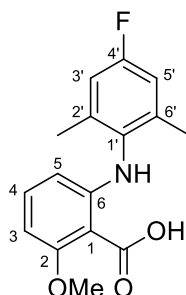
dimethylphenyl)amino]-2-isopropoxybenzoic acid (**80**) as an orange solid (0.062 g, 44%). Mp 99–101 °C;  $\nu_{\max}/\text{cm}^{-1}$  (neat) 3250 (NH/OH), 2982 (CH), 1697 (CO), 1578 (C=C), 1458, 1252;  $\delta_{\text{H}}$  (400 MHz,  $\text{CDCl}_3$ ) 1.50 (6H, d,  $J$  6.1 Hz,  $\text{OCH}(\text{CH}_3)_2$ ), 2.16 (6H, s, 2'- $\text{CH}_3$  and 6'- $\text{CH}_3$ ), 4.83 (1H, sept,  $J$  6.1 Hz,  $\text{OCH}(\text{CH}_3)_2$ ), 5.87 (1H, dd,  $J$  8.4, 0.8 Hz, 5-H), 6.24 (1H, br d,  $J$  8.4 Hz, 3-H), 6.83 (2H, d,  $J$  9.0 Hz, 3'-H and 5'-H), 7.10 (1H, t,  $J$  8.4 Hz, 4-H), 9.89 (1H, br s, NH), 12.04 (1H, br s, OH);  $\delta_{\text{C}}$  (101 MHz,  $\text{CDCl}_3$ ) 18.4 (2  $\times$   $\text{CH}_3$ ), 22.1 (2  $\times$   $\text{CH}_3$ ), 74.3 (CH), 100.0 (C), 100.5 (CH), 106.8 (CH), 114.8 (2  $\times$  CH, d  $^2J_{\text{CF}}$  21.7 Hz), 133.0 (C, d,  $^4J_{\text{CF}}$  2.8 Hz), 134.2 (CH), 139.2 (2  $\times$  C, d,  $^3J_{\text{CF}}$  8.7 Hz), 152.7 (C), 158.3 (C), 160.9 (C, d,  $^1J_{\text{CF}}$  244.9 Hz), 169.3 (C);  $m/z$  (ESI) 340.1306 ( $\text{MNa}^+$ ).  $\text{C}_{18}\text{H}_{20}\text{FNNO}_3$  requires 340.1319).

## 2-[(4'-Fluoro-2',6'-dimethylphenyl)amino]benzoic acid (**84**)



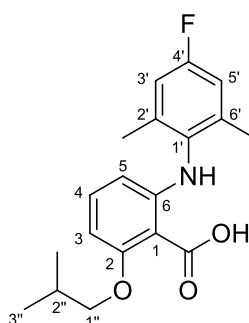
The reaction was carried out according to general procedure C using sodium hydride (0.018 g, 0.44 mmol, 60% in mineral oil), *tert*-butanol (0.8 mL), 2-bromo-6-[(4'-fluoro-2',6'-dimethylphenyl)amino]benzoic acid (**75**) (0.050 g, 0.15 mmol) and copper powder (0.0040 g, 0.060 mmol). The crude material was purified by flash column chromatography, eluting with 20% ethyl acetate in petroleum ether (40–60) to afford 2-[(4'-fluoro-2',6'-dimethylphenyl)amino]benzoic acid (**84**) as a brown solid (0.022 g, 58%). Mp 225–228 °C;  $\nu_{\max}/\text{cm}^{-1}$  (neat) 3325 (NH/OH), 2857 (CH), 1651 (CO), 1578 (C=C), 1506, 1443, 1265, 750;  $\delta_{\text{H}}$  (400 MHz,  $\text{CDCl}_3$ ) 2.19 (6H, s, 2'- $\text{CH}_3$  and 6'- $\text{CH}_3$ ), 6.19 (1H, dd,  $J$  7.8, 0.7 Hz, 3-H), 6.67 (1H, td,  $J$  7.8, 0.7 Hz, 5-H), 6.86 (2H, d,  $J$  9.0, 3'-H and 5'-H), 7.26 (1H, td,  $J$  7.8, 1.6 Hz, 4-H), 8.03 (1H, dd,  $J$  7.8, 1.6 Hz, 6-H), 8.78 (1H, br s, NH), 11.4 (1H, br s, OH);  $\delta_{\text{C}}$  (126 MHz,  $\text{CDCl}_3$ ) 18.4 (2  $\times$   $\text{CH}_3$ ), 108.7 (C), 112.5 (CH), 114.9 (2  $\times$  CH, d,  $^2J_{\text{CF}}$  21.9 Hz), 115.9 (CH), 132.5 (CH), 132.7 (C, d,  $^4J_{\text{CF}}$  3.1 Hz), 135.7 (CH), 139.3 (2  $\times$  C, d,  $^3J_{\text{CF}}$  8.4 Hz), 150.7 (C), 161.0 (C, d,  $^1J_{\text{CF}}$  245.1 Hz), 173.5 (C);  $m/z$  (EI) 259.1011 ( $\text{M}^+$ ).  $\text{C}_{15}\text{H}_{14}\text{FNO}_2$  requires 259.1009), 241 (74%), 226 (80), 212 (42), 198 (26), 106 (10), 77 (18), 51 (12).

**6-[(4'-Fluoro-2',6'-dimethylphenyl)amino]-2-methoxybenzoic acid (81)**



The reaction was carried out according to general procedure C using sodium hydride (0.018 g, 0.44 mmol, 60% in mineral oil), methanol (0.8 mL), 2-bromo-6-[(4'-fluoro-2',6'-dimethylphenyl)amino]benzoic acid (**75**) (0.050 g, 0.15 mmol) and copper powder (0.0040 g, 0.060 mmol). The crude material was purified by flash column chromatography, eluting with 20% ethyl acetate in petroleum ether (40–60) to afford 6-[(4'-fluoro-2',6'-dimethylphenyl)amino]-2-methoxybenzoic acid (**81**) as a brown solid (0.031 g, 71%). Mp 100–101 °C;  $\nu_{\max}/\text{cm}^{-1}$  (neat) 3246 (NH/OH), 2953 (CH), 1694 (CO), 1576 (C=C), 1464, 1442, 1255, 1084, 806;  $\delta_{\text{H}}$  (500 MHz,  $\text{CDCl}_3$ ) 2.15 (6H, s, 2'- $\text{CH}_3$  and 6'- $\text{CH}_3$ ), 4.05 (3H, s,  $\text{OCH}_3$ ), 5.91 (1H, dd,  $J$  8.4, 0.9 Hz, 5-H), 6.25 (1H, dd,  $J$  8.4, 0.9 Hz, 3-H), 6.83 (2H, d,  $J$  9.0 Hz, 3'-H and 5'-H), 7.13 (1H, t,  $J$  8.4, 4-H), 9.90 (1H, br s, NH), 11.50 (1H, br s, OH);  $\delta_{\text{C}}$  (126 MHz,  $\text{CDCl}_3$ ) 18.4 (2  $\times$   $\text{CH}_3$ ), 56.9 ( $\text{CH}_3$ ), 98.0 (CH), 98.8 (C), 107.2 (CH), 114.8 (2  $\times$  CH, d,  $^2J_{\text{CF}}$  21.9 Hz), 132.9 (C, d,  $^4J_{\text{CF}}$  2.7 Hz), 134.4 (CH), 139.2 (2  $\times$  C, d,  $^3J_{\text{CF}}$  8.9 Hz), 152.7 (C), 159.9 (C), 160.9 (C, d,  $^1J_{\text{CF}}$  245.0 Hz), 169.0 (C);  $m/z$  (ESI) 312.0994 ( $\text{MNa}^+$ .  $\text{C}_{16}\text{H}_{16}\text{FNNaO}_3$  requires 312.1006).

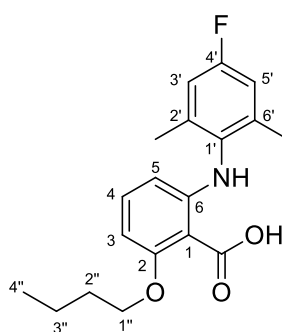
**6-[(4'-Fluoro-2',6'-dimethylphenyl)amino]-2-isobutoxybenzoic acid (82)**



The reaction was carried out according to general procedure C using sodium hydride (0.018 g, 0.44 mmol, 60% in mineral oil), isobutanol (0.8 mL), 2-bromo-6-[(4'-fluoro-2',6'-dimethylphenyl)amino]benzoic acid (**75**) (0.050 g, 0.15 mmol) and copper powder (0.0040 g, 0.060 mmol). The crude material was purified by flash column chromatography, eluting with 20% ethyl acetate in petroleum ether (40–60) to afford 6-[(4'-fluoro-2',6'-dimethylphenyl)amino]-2-isobutoxybenzoic acid (**82**) as an orange solid (0.033 g, 68%).

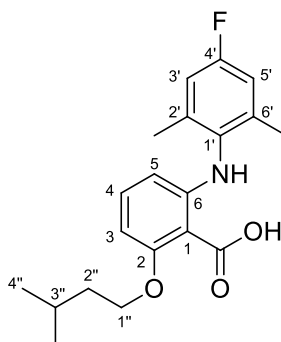
Mp 74–76 °C;  $\nu_{\max}/\text{cm}^{-1}$  (neat) 3255 (NH/OH), 2966 (CH), 1695 (CO), 1577 (C=C), 1456, 1407, 1252, 1057, 756;  $\delta_{\text{H}}$  (500 MHz,  $\text{CDCl}_3$ ) 1.11 (6H, d,  $J$  6.4 Hz, 2''-CH<sub>3</sub> and 3''-H<sub>3</sub>), 2.16 (6H, s, 2'-CH<sub>3</sub> and 6'-CH<sub>3</sub>), 2.19–2.29 (1H, m, 2''-H), 3.99 (2H, d,  $J$  6.4 Hz, 1''-H<sub>2</sub>), 5.89 (1H, d,  $J$  8.3 Hz, 5-H), 6.22 (1H, d,  $J$  8.3 Hz, 3-H), 6.83 (2H, d,  $J$  9.1 Hz, 3'-H and 5'-H), 7.10 (1H, t,  $J$  8.3 Hz, 4-H), 9.90 (1H, br s, NH), 11.77 (1H, br s, OH);  $\delta_{\text{C}}$  (126 MHz,  $\text{CDCl}_3$ ) 18.4 (2 × CH<sub>3</sub>), 19.2 (2 × CH<sub>3</sub>), 28.1 (CH), 76.7 (CH<sub>2</sub>), 98.9 (C), 98.9 (CH), 106.9 (CH), 114.8 (2 × CH, d,  $^2J_{\text{CF}}$  21.6 Hz), 132.9 (C, d,  $^4J_{\text{CF}}$  2.8 Hz), 134.4 (CH), 139.2 (2 × C, d,  $^3J_{\text{CF}}$  8.7 Hz), 152.6 (C), 159.5 (C), 160.9 (C, d,  $^1J_{\text{CF}}$  244.6 Hz), 169.1 (C);  $m/z$  (ESI) 354.1465 (MNa<sup>+</sup>. C<sub>19</sub>H<sub>22</sub>FNNaO<sub>3</sub> requires 354.1476).

### 2-*n*-Butoxy-6-[(4'-fluoro-2',6'-dimethylphenyl)amino]benzoic acid (**83**)



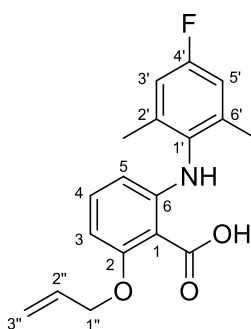
The reaction was carried out according to general procedure C using sodium hydride (0.018 g, 0.44 mmol, 60% in mineral oil), *n*-butanol (0.8 mL), 2-bromo-6-[(4'-fluoro-2',6'-dimethylphenyl)amino]benzoic acid (**75**) (0.050 g, 0.15 mmol) and copper powder (0.0040 g, 0.060 mmol). The crude material was purified by flash column chromatography, eluting with 20% ethyl acetate in petroleum ether (40–60) to afford 2-*n*-butoxy-6-[(4'-fluoro-2',6'-dimethylphenyl)amino]benzoic acid (**83**) as a brown solid (0.033 g, 70%). Mp 77–79 °C;  $\nu_{\max}/\text{cm}^{-1}$  (neat) 3246 (NH/OH), 2963 (CH), 1694 (CO), 1578 (C=C), 1456, 1408, 1252, 1219, 754;  $\delta_{\text{H}}$  (500 MHz,  $\text{CDCl}_3$ ) 1.02 (3H, t,  $J$  7.4 Hz, 4''-H<sub>3</sub>), 1.49–1.60 (2H, m, 3''-H<sub>2</sub>), 1.87–1.95 (2H, m, 2''-H<sub>2</sub>), 2.16 (6H, s, 2'-CH<sub>3</sub> and 6'-CH<sub>3</sub>), 4.22 (2H, t,  $J$  6.5 Hz, 1''-H<sub>2</sub>), 5.89 (1H, dd,  $J$  8.3, 0.8 Hz, 5-H), 6.23 (1H, dd,  $J$  8.3, 0.8 Hz, 3-H), 6.83 (2H, d,  $J$  9.2 Hz, 3'-H and 5'-H), 7.10 (1H, t,  $J$  8.3 Hz, 4-H), 9.90 (1H, br s, NH), 11.78 (1H, br s, OH);  $\delta_{\text{C}}$  (126 MHz,  $\text{CDCl}_3$ ) 13.7 (CH<sub>3</sub>), 18.4 (2 × CH<sub>3</sub>), 19.2 (CH<sub>2</sub>), 30.9 (CH<sub>2</sub>), 70.2 (CH<sub>2</sub>), 99.0 (CH), 106.9 (CH), 114.8 (2 × CH, d,  $^2J_{\text{CF}}$  21.9 Hz), 126.4 (C), 132.9 (C, d,  $^4J_{\text{CF}}$  2.7 Hz), 134.4 (CH), 139.2 (2 × C, d,  $^3J_{\text{CF}}$  8.9 Hz), 152.6 (C), 159.4 (C), 160.9 (C, d,  $^1J_{\text{CF}}$  244.6 Hz), 169.1 (C);  $m/z$  (ESI) 354.1466 (MNa<sup>+</sup>. C<sub>19</sub>H<sub>22</sub>FNNaO<sub>3</sub> requires 354.1476).

**6-[(4'-Fluoro-2',6'-dimethylphenyl)amino]-2-(3''-methyl-*n*-butoxy)benzoic acid (85)**



The reaction was carried out according to general procedure C using sodium hydride (0.018 g, 0.44 mmol, 60% in mineral oil), 3-methyl-*n*-butanol (0.8 mL), 2-bromo-6-[(4'-fluoro-2',6'-dimethylphenyl)amino]benzoic acid (**75**) (0.050 g, 0.15 mmol) and copper powder (0.0040 g, 0.060 mmol). The crude material was purified by flash column chromatography, eluting with 20% ethyl acetate in petroleum ether (40–60) to afford 6-[(4'-fluoro-2',6'-dimethylphenyl)amino]-2-(3''-methyl-*n*-butoxy)benzoic acid (**85**) as a brown viscous oil (0.020 g, 39%).  $\nu_{\max}/\text{cm}^{-1}$  (neat) 3244 (NH/OH), 2959 (CH), 1694 (CO), 1578 (C=C), 1458, 1408, 1252, 1217, 1076, 754;  $\delta_{\text{H}}$  (400 MHz,  $\text{CDCl}_3$ ) 1.01 (6H, d,  $J$  6.4 Hz, 3''-CH<sub>3</sub> and 4''-H<sub>3</sub>), 1.77–1.91 (3H, m, 2''-H<sub>2</sub> and 3''-H), 2.16 (6H, s, 2'-CH<sub>3</sub> and 6'-CH<sub>3</sub>), 4.24 (2H, t,  $J$  6.5 Hz, 1''-H<sub>2</sub>), 5.89 (1H, dd,  $J$  8.3, 0.8 Hz, 5-H), 6.24 (1H, br d,  $J$  8.3 Hz, 3-H), 6.83 (2H, d,  $J$  9.0 Hz, 3'-H and 5'-H), 7.11 (1H, t,  $J$  8.3 Hz, 4-H), 9.90 (1H, br s, NH), 11.69 (1H, br s, OH);  $\delta_{\text{C}}$  (126 MHz,  $\text{CDCl}_3$ ) 18.4 (2 × CH<sub>3</sub>), 22.5 (2 × CH<sub>3</sub>), 25.1 (CH), 37.7 (CH<sub>2</sub>), 69.0 (CH<sub>2</sub>), 99.0 (CH), 99.0 (C), 107.0 (CH), 114.8 (2 × CH, d,  $^2J_{\text{CF}}$  21.9 Hz), 133.0 (C, d,  $^4J_{\text{CF}}$  2.7 Hz), 134.3 (CH), 139.2 (2 × C, d,  $^3J_{\text{CF}}$  8.4 Hz), 152.6 (C), 159.4 (C), 160.9 (C, d,  $^1J_{\text{CF}}$  244.8 Hz), 169.1 (C);  $m/z$  (ESI) 368.1620 (MNa<sup>+</sup>. C<sub>20</sub>H<sub>24</sub>FNNaO<sub>3</sub> requires 368.1632).

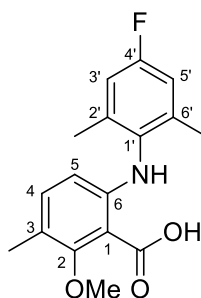
**2-(Allyloxy)-6-[(4'-fluoro-2',6'-dimethylphenyl)amino]benzoic acid (86)**



The reaction was carried out according to general procedure C using sodium hydride (0.0532 g, 1.33 mmol, 60% in mineral oil), 3-fluoropropan-1-ol (0.134 mL, 11.8 mmol), 2-bromo-6-[(4'-fluoro-2',6'-dimethylphenyl)amino]benzoic acid (**75**) (0.150 g, 0.444 mmol),

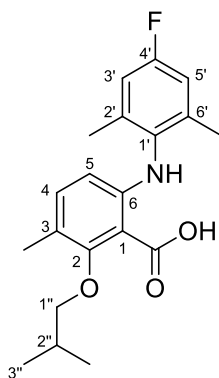
tetrahydrofuran (1.6 mL) and copper powder (0.0113 g, 0.178 mmol). The crude material was purified by flash column chromatography, eluting with 20% ethyl acetate in petroleum ether (40–60) to afford 2-(allyloxy)-6-[(4'-fluoro-2',6'-dimethylphenyl)amino]benzoic acid (**86**) as a brown viscous oil (0.0643 g, 46%).  $\nu_{\max}/\text{cm}^{-1}$  (neat) 3258 (NH/OH), 2920 (CH), 1694 (CO), 1576 (C=C), 1456, 1252, 1051, 806;  $\delta_{\text{H}}$  (500 MHz,  $\text{CDCl}_3$ ) 2.15 (6H, s, 2'- $\text{CH}_3$  and 6'- $\text{CH}_3$ ), 4.76 (2H, d,  $J$  5.8 Hz, 1''- $\text{H}_2$ ), 5.45 (1H, dd,  $J$  10.5, 0.8 Hz, 3''- $\text{HH}$ ), 5.51 (1H, dd,  $J$  17.0, 0.8 Hz, 3''- $\text{HH}$ ), 5.91 (1H, d,  $J$  8.2 Hz, 5-H), 6.12 (1H, ddt,  $J$  17.0, 10.5, 5.8 Hz, 2''-H), 6.23 (1H, d,  $J$  8.2 Hz, 3-H), 6.84 (2H, d,  $J$  9.1 Hz, 3'-H and 5'-H), 7.10 (1H, t,  $J$  8.2 Hz, 4-H), 9.89 (1H, br s, NH), 11.60 (1H, br s, OH);  $\delta_{\text{C}}$  (126 MHz,  $\text{CDCl}_3$ ) 18.3 (2  $\times$   $\text{CH}_3$ ), 71.2 ( $\text{CH}_2$ ), 99.2 (C), 99.4 (CH), 107.3 (CH), 114.8 (2  $\times$  CH,  $^2J_{\text{CF}}$  21.8 Hz), 120.7 ( $\text{CH}_2$ ), 131.0 (CH), 132.9 (C, d,  $^4J_{\text{CF}}$  2.7 Hz), 134.3 (CH), 139.1 (2  $\times$  C, d,  $^3J_{\text{CF}}$  8.3 Hz), 152.7 (C), 159.0 (C), 160.9 (C, d,  $^1J_{\text{CF}}$  245.0 Hz), 168.9 (C);  $m/z$  (ESI) 338.1151 ( $\text{MNa}^+$ .  $\text{C}_{18}\text{H}_{18}\text{FNNaO}_3$  requires 338.1163).

### 6-[(4'-Fluoro-2',6'-dimethylphenyl)amino]-2-methoxy-3-methylbenzoic acid (**87**)



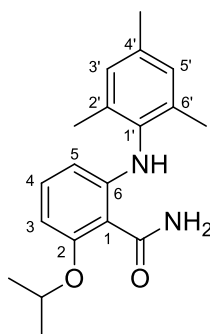
The reaction was carried out according to general procedure C using sodium hydride (0.017 g, 0.43 mmol, 60% in mineral oil), methanol (0.8 mL), 2-bromo-6-[(4'-fluoro-2',6'-dimethylphenyl)amino]-3-methylbenzoic acid (**79**) (0.050 g, 0.14 mmol) and copper powder (0.0040 g, 0.057 mmol). The crude material was purified by flash column chromatography, eluting with 20% ethyl acetate in petroleum ether (40–60) to afford 6-[(4'-fluoro-2',6'-dimethylphenyl)amino]-2-methoxy-3-methylbenzoic acid (**87**) as an orange viscous oil (0.0307 g, 71%).  $\nu_{\max}/\text{cm}^{-1}$  (neat) 3308 (NH/OH), 2926 (CH), 1700 (CO), 1574 (C=C), 1504, 1216, 757;  $\delta_{\text{H}}$  (500 MHz,  $\text{CDCl}_3$ ) 2.15 (6H, s, 2'- $\text{CH}_3$  and 6'- $\text{CH}_3$ ), 2.20 (3H, s, 3- $\text{CH}_3$ ), 3.93 (3H, s,  $\text{OCH}_3$ ), 5.98 (1H, d,  $J$  8.7 Hz, 5-H), 6.83 (2H, d,  $J$  9.1 Hz, 3'-H and 5'-H), 7.02 (1H, d,  $J$  8.7 Hz, 4-H), 9.45 (1H, br s, NH), 11.94 (1H, br s, OH);  $\delta_{\text{C}}$  (126 MHz,  $\text{CDCl}_3$ ) 15.1 ( $\text{CH}_3$ ), 18.3 (2  $\times$   $\text{CH}_3$ ), 62.2 ( $\text{CH}_3$ ), 102.2 (C), 109.8 (CH), 114.8 (2  $\times$  CH, d,  $^2J_{\text{CF}}$  21.7 Hz), 116.5 (C), 133.0 (C, d,  $^4J_{\text{CF}}$  2.7 Hz), 137.2 (CH), 139.2 (2  $\times$  C, d,  $^3J_{\text{CF}}$  8.9 Hz), 150.3 (C), 158.2 (C), 160.9 (C, d,  $^1J_{\text{CF}}$  244.6 Hz), 168.7 (C);  $m/z$  (ESI) 326.1148 ( $\text{MNa}^+$ .  $\text{C}_{17}\text{H}_{16}\text{FNNaO}_3$  requires 326.1163).

**6-[(4'-Fluoro-2',6'-dimethylphenyl)amino]-2-isobutoxy-3-methylbenzoic acid (88)**



The reaction was carried out according to general procedure C using sodium hydride (0.034 g, 0.85 mmol, 60% in mineral oil), isobutanol (1.2 mL), 2-bromo-6-[(4'-fluoro-2',6'-dimethylphenyl)amino]-3-methylbenzoic acid (**79**) (0.10 g, 0.28 mmol) and copper powder (0.0070 g, 0.11 mmol). The crude material was purified by flash column chromatography, eluting with 20% ethyl acetate in petroleum ether (40–60) to afford 6-[(4'-fluoro-2',6'-dimethylphenyl)amino]-2-isobutoxy-3-methylbenzoic acid (**88**) as an orange solid (0.073 g, 74%). Mp 130–132 °C;  $\nu_{\max}/\text{cm}^{-1}$  (neat) 3294 (NH), 3125 (OH), 2963 (CH), 1705 (CO), 1573 (C=C), 1504, 1404, 1227, 1034, 818;  $\delta_{\text{H}}$  (400 MHz,  $\text{CDCl}_3$ ) 1.11 (6H, d,  $J$  6.7 Hz, 2''- $\text{CH}_3$  and 3''- $\text{H}_3$ ), 2.15 (6H, s, 2'- $\text{CH}_3$  and 6'- $\text{CH}_3$ ), 2.18 (3H, s, 3- $\text{CH}_3$ ), 2.18–2.28 (1H, m, 2''-H), 3.76 (2H, d,  $J$  6.7 Hz, 1''- $\text{H}_2$ ), 5.97 (1H, d,  $J$  8.7 Hz, 5-H), 6.83 (2H, d,  $J$  9.1 Hz, 3'-H and 5'-H), 7.02 (1H, d,  $J$  8.7 Hz, 4-H), 9.44 (1H, br s, NH), 12.25 (1H, br s, OH);  $\delta_{\text{C}}$  (101 MHz,  $\text{CDCl}_3$ ) 15.2 ( $\text{CH}_3$ ), 18.4 ( $2 \times \text{CH}_3$ ), 19.0 ( $2 \times \text{CH}_3$ ), 29.1 (CH), 82.1 ( $\text{CH}_2$ ), 102.6 (C), 109.6 (CH), 114.9 ( $2 \times \text{CH}$ , d,  $^2J_{\text{CF}}$  21.9 Hz), 116.8 (C), 133.0 (C, d,  $^4J_{\text{CF}}$  2.7 Hz), 137.1 (CH), 139.2 ( $2 \times \text{C}$ , d,  $^3J_{\text{CF}}$  8.5 Hz), 150.3 (C), 157.2 (C), 160.9 (C, d,  $^1J_{\text{CF}}$  244.8 Hz), 168.7 (C);  $m/z$  (ESI) 368.1619 ( $\text{MNa}^+$ ).  $\text{C}_{20}\text{H}_{24}\text{FNNaO}_3$  requires 368.1632).

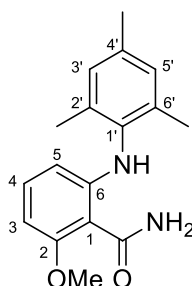
**2-Isopropoxy-6-(mesitylamino)benzamide (31)<sup>95</sup>**



The reaction was carried out according to general procedure D using 2-isopropoxy-6-(mesitylamino)benzoic acid (**60**) (0.100 g, 0.319 mmol), 2-chloro-4,6-dimethoxy-1,3,5-triazine (0.0673 g, 0.383 mmol) and *N*-methylmorpholine (0.105 mL, 0.957 mmol) in

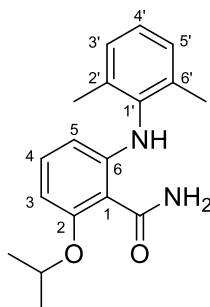
tetrahydrofuran (1.0 mL). The crude material was purified by flash column chromatography, eluting with 10% ethyl acetate in petroleum ether (40–60) to afford 2-isopropoxy-6-(mesitylamino)benzamide (**31**) as a pale yellow solid (0.074 g, 74%). The spectroscopic data were consistent with the literature.<sup>95</sup> Mp 215–217 °C;  $\delta_{\text{H}}$  (500 MHz,  $\text{CDCl}_3$ ) 1.43 (6H, d,  $J$  6.1 Hz,  $\text{OCH}(\text{CH}_3)_2$ ), 2.15 (6H, s, 2'- $\text{CH}_3$  and 6'- $\text{CH}_3$ ), 2.30 (3H, s, 4'- $\text{CH}_3$ ), 4.69 (1H, sept,  $J$  6.1 Hz,  $\text{OCH}(\text{CH}_3)_2$ ), 5.60 (1H, br s, NH), 5.84 (1H, dd,  $J$  8.3, 0.9 Hz, 5-H), 6.17 (1H, br d,  $J$  8.3 Hz, 3-H), 6.93 (2H, s, 3'-H and 5'-H), 6.99 (1H, t,  $J$  8.3 Hz, 4-H), 8.14 (1H, br s, NH), 10.13 (1H, br s, NH);  $\delta_{\text{C}}$  (101 MHz,  $\text{CDCl}_3$ ) 18.2 (2  $\times$   $\text{CH}_3$ ), 20.9 ( $\text{CH}_3$ ), 22.3 (2  $\times$   $\text{CH}_3$ ), 72.0 (CH), 100.5 (CH), 103.1 (C), 106.2 (CH), 129.0 (2  $\times$  CH), 132.5 (CH), 135.5 (C), 135.6 (C), 136.6 (2  $\times$  C), 152.2 (C), 158.2 (C), 171.6 (C);  $m/z$  (EI) 312 ( $\text{M}^+$ , 95%) 295 (25), 253 (100), 252 (55), 238 (68).

### 6-(Mesitylamino)-2-methoxybenzamide (**97**)<sup>95</sup>



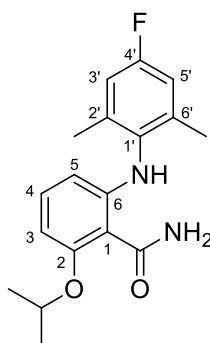
The reaction was carried out according to general procedure D using 6-(mesitylamino)-2-methoxybenzoic acid (**96**) (1.62 g, 5.68 mmol), 2-chloro-4,6-dimethoxy-1,3,5-triazine (1.20 g, 6.81 mmol) and *N*-methylmorpholine (1.87 mL, 17.0 mmol) in tetrahydrofuran (20 mL). The crude material was purified by flash column chromatography, eluting with 20% ethyl acetate in petroleum ether (40–60) to afford 6-(mesitylamino)-2-methoxybenzamide (**97**) as a white solid (1.56 g, 97%). The spectroscopic data were consistent with the literature.<sup>95</sup> Mp 180–182 °C;  $\delta_{\text{H}}$  (500 MHz,  $\text{CDCl}_3$ ) 2.15 (6H, s, 2'- $\text{CH}_3$  and 6'- $\text{CH}_3$ ), 2.29 (3H, s, 4'- $\text{CH}_3$ ), 3.89 (3H, s,  $\text{OCH}_3$ ), 5.88 (1H, dd,  $J$  8.3, 0.9 Hz, 5-H), 6.09 (1H, br s, NH), 6.17 (1H, dd,  $J$  8.3, 0.9 Hz, 3-H), 6.92 (2H, s, 3'-H and 5'-H), 7.01 (1H, t,  $J$  8.3 Hz, 4-H), 7.90 (1H, br s, NH), 10.18 (1H, br s, NH);  $\delta_{\text{C}}$  (126 MHz,  $\text{CDCl}_3$ ) 18.2 (2  $\times$   $\text{CH}_3$ ), 20.9 ( $\text{CH}_3$ ), 55.9 ( $\text{CH}_3$ ), 98.0 (CH), 102.0 (C), 106.6 (CH), 129.0 (2  $\times$  CH), 132.6 (CH), 135.4 (C), 135.6 (C), 136.5 (2  $\times$  C), 152.1 (C), 159.9 (C), 171.5 (C);  $m/z$  (ESI) 307 ( $\text{MNa}^+$ , 100%).

**6-[(2',6'-Dimethylphenyl)amino]-2-isopropoxybenzamide (67)**



The reaction was carried out according to general procedure D using 6-[(2',6'-dimethylphenyl)amino]-2-isopropoxybenzoic acid (**70**) (0.0670 g, 0.224 mmol), 2-chloro-4,6-dimethoxy-1,3,5-triazine (0.0472 g, 0.269 mmol) and *N*-methylmorpholine (0.0739 mL, 0.672 mmol) in tetrahydrofuran (1.0 mL). The crude material was purified by flash column chromatography, eluting with 10% ethyl acetate in petroleum ether (40–60) to afford 6-[(2',6'-dimethylphenyl)amino]-2-isopropoxybenzamide (**67**) as a pale yellow solid (0.0613 g, 92%). Mp 180–182 °C;  $\nu_{\max}/\text{cm}^{-1}$  (neat) 3433 (NH), 2980 (CH), 1643 (CO), 1584 (C=C), 1456, 1248, 1111;  $\delta_{\text{H}}$  (400 MHz,  $\text{CDCl}_3$ ) 1.43 (6H, d,  $J$  6.1 Hz,  $\text{OCH}(\text{CH}_3)_2$ ), 2.20 (6H, s, 2'- $\text{CH}_3$  and 6'- $\text{CH}_3$ ), 4.69 (1H, sept,  $J$  6.1 Hz,  $\text{OCH}(\text{CH}_3)_2$ ), 5.76 (1H, br s, NH), 5.83 (1H, dd,  $J$  8.3, 0.9 Hz, 5-H), 6.19 (1H, br d,  $J$  8.3 Hz, 3-H), 7.00 (1H, t,  $J$  8.3 Hz, 4-H), 7.05–7.16 (3H, m, 3'-H, 4'-H and 5'-H), 8.15 (1H, br s, NH), 10.20 (1H, br s, NH);  $\delta_{\text{C}}$  (101 MHz,  $\text{CDCl}_3$ ) 18.3 (2  $\times$   $\text{CH}_3$ ), 22.3 (2  $\times$   $\text{CH}_3$ ), 72.0 (CH), 100.7 (CH), 103.1 (C), 106.2 (CH), 126.1 (CH), 128.3 (2  $\times$  CH), 132.5 (CH), 136.8 (2  $\times$  C), 138.2 (C), 151.9 (C), 158.2 (C), 171.6 (C);  $m/z$  (ESI) 321.1565 ( $\text{MNa}^+$ .  $\text{C}_{18}\text{H}_{22}\text{N}_2\text{NaO}_2$  requires 321.1573).

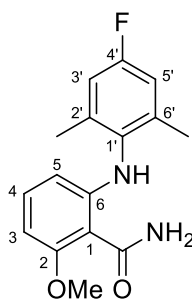
**6-[(4'-Fluoro-2',6'-dimethylphenyl)amino]-2-isopropoxybenzamide (66)**



The reaction was carried out according to general procedure D using 6-[(4'-fluoro-2',6'-dimethylphenyl)amino]-2-isopropoxybenzoic acid (**80**) (0.0400 g, 0.126 mmol), 2-chloro-4,6-dimethoxy-1,3,5-triazine (0.0265 g, 0.151 mmol) and *N*-methylmorpholine (0.0416 mL, 0.378 mmol) in tetrahydrofuran (0.5 mL). The crude material was purified by flash column chromatography, eluting with 10% ethyl acetate in petroleum ether (40–60) to afford 6-[(4'-

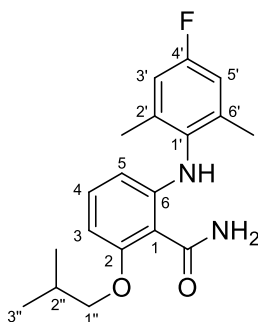
fluoro-2',6'-dimethylphenyl)amino]-2-isopropoxybenzamide (**66**) as a pale yellow solid (0.0392 g, 98%). Mp 204–206 °C;  $\nu_{\max}/\text{cm}^{-1}$  (neat) 3444 (NH), 3188 (NH), 2982 (CH), 1638 (CO), 1584 (C=C), 1456, 1250, 1111, 1044;  $\delta_{\text{H}}$  (400 MHz,  $\text{CDCl}_3$ ) 1.43 (6H, d,  $J$  6.1 Hz,  $\text{OCH}(\text{CH}_3)_2$ ), 2.18 (6H, s, 2'- $\text{CH}_3$  and 6'- $\text{CH}_3$ ), 4.70 (1H, sept,  $J$  6.1 Hz,  $\text{OCH}(\text{CH}_3)_2$ ), 5.65 (1H, br s, NH), 5.80 (1H, dd,  $J$  8.3, 0.9 Hz, 5-H), 6.20 (1H, br d,  $J$  8.3 Hz, 3-H), 6.82 (2H, d,  $J$  9.2 Hz, 3'-H and 5'-H), 7.01 (1H, t,  $J$  8.3 Hz, 4-H), 8.16 (1H, br s, NH), 10.14 (1H, br s, NH);  $\delta_{\text{C}}$  (126 MHz,  $\text{CDCl}_3$ ) 18.5 (2  $\times$   $\text{CH}_3$ ), 22.3 (2  $\times$   $\text{CH}_3$ ), 72.0 (CH), 100.9 (CH), 103.2 (C), 105.9 (CH), 114.6 (2  $\times$  CH, d  $^2J_{\text{CF}}$  21.8 Hz), 132.6 (CH), 134.0 (C, d,  $^4J_{\text{CF}}$  2.7 Hz), 139.1 (2  $\times$  C, d,  $^3J_{\text{CF}}$  8.2 Hz), 152.1 (C), 158.3 (C), 160.6 (C, d,  $^1J_{\text{CF}}$  244.0 Hz), 171.5 (C);  $m/z$  (ESI) 339.1465 ( $\text{MNa}^+$ .  $\text{C}_{18}\text{H}_{21}\text{FN}_2\text{NaO}_2$  requires 339.1479).

### 6-[(4'-Fluoro-2',6'-dimethylphenyl)amino]-2-methoxybenzamide (**89**)



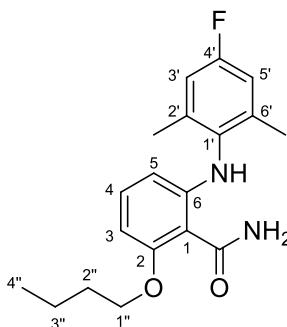
The reaction was carried out according to general procedure D using 6-[(4'-fluoro-2',6'-dimethylphenyl)amino]-2-methoxybenzoic acid (**81**) (0.0300 g, 0.104 mmol), 2-chloro-4,6-dimethoxy-1,3,5-triazine (0.0219 g, 0.125 mmol) and *N*-methylmorpholine (0.0412 mL, 0.375 mmol) in tetrahydrofuran (0.5 mL). The crude material was purified by flash column chromatography, eluting with 20% ethyl acetate in petroleum ether (40–60) to afford 6-[(4'-fluoro-2',6'-dimethylphenyl)amino]-2-methoxybenzamide (**89**) as a pale yellow solid (0.0201 g, 67%). Mp 171–173 °C;  $\nu_{\max}/\text{cm}^{-1}$  (neat) 3462 (NH), 3186 (NH), 2924 (CH), 1638 (CO), 1580 (C=C), 1458, 1250, 1128, 752;  $\delta_{\text{H}}$  (400 MHz,  $\text{CDCl}_3$ ) 2.17 (6H, s, 2'- $\text{CH}_3$  and 6'- $\text{CH}_3$ ), 3.92 (3H, s,  $\text{OCH}_3$ ), 5.77 (1H, br s, NH), 5.84 (1H, dd,  $J$  8.4, 0.9 Hz, 5-H), 6.22 (1H, dd,  $J$  8.4, 0.9 Hz, 3-H), 6.82 (2H, d,  $J$  9.0 Hz, 3'-H and 5'-H), 7.05 (1H, t,  $J$  8.4 Hz, 4-H), 7.94 (1H, br s, NH), 10.17 (1H, br s, NH);  $\delta_{\text{C}}$  (101 MHz,  $\text{CDCl}_3$ ) 18.4 ( $\text{CH}_3$ ), 18.5 ( $\text{CH}_3$ ), 56.0 ( $\text{CH}_3$ ), 98.4 (CH), 102.1 (C), 106.4 (CH), 114.6 (2  $\times$  CH, d,  $^2J_{\text{CF}}$  21.8 Hz), 132.8 (CH), 133.9 (C, d,  $^4J_{\text{CF}}$  2.6 Hz), 139.1 (2  $\times$  C, d,  $^3J_{\text{CF}}$  8.7 Hz), 152.0 (C), 160.0 (C), 160.6 (C, d,  $^1J_{\text{CF}}$  245.0 Hz), 171.3 (C);  $m/z$  (ESI) 311.1158 ( $\text{MNa}^+$ .  $\text{C}_{16}\text{H}_{17}\text{FN}_2\text{NaO}_2$  requires 311.1166).

**6-[(4'-Fluoro-2',6'-dimethylphenyl)amino]-2-isobutoxybenzamide (90)**



The reaction was carried out according to general procedure D using 6-[(4'-fluoro-2',6'-dimethylphenyl)amino]-2-isobutoxybenzoic acid (**82**) (0.0300 g, 0.0905 mmol), 2-chloro-4,6-dimethoxy-1,3,5-triazine (0.0191 g, 0.109 mmol) and *N*-methylmorpholine (0.0300 mL, 0.273 mmol) in tetrahydrofuran (0.5 mL). The crude material was purified by flash column chromatography, eluting with 10% ethyl acetate in petroleum ether (40–60) to afford 6-[(4'-fluoro-2',6'-dimethylphenyl)amino]-2-isobutoxybenzamide (**90**) as an orange solid (0.0294 g, 98%). Mp 152–154 °C;  $\nu_{\max}/\text{cm}^{-1}$  (neat) 3455 (NH), 3181 (NH), 2922 (CH), 1636 (CO), 1582 (C=C), 1493, 1449, 1398, 1246, 1060, 864, 754;  $\delta_{\text{H}}$  (500 MHz,  $\text{CDCl}_3$ ) 1.08 (6H, d,  $J$  6.7 Hz, 2''-CH<sub>3</sub> and 3''-H<sub>3</sub>), 2.13–2.21 (1H, m, 2''-H), 2.17 (6H, s, 2'-CH<sub>3</sub> and 6'-CH<sub>3</sub>), 3.86 (2H, d,  $J$  6.4 Hz, 1''-H<sub>2</sub>), 5.73 (1H, br s, NH), 5.82 (1H, dd,  $J$  8.5, 0.8 Hz, 5-H), 6.19 (1H, br d,  $J$  8.5 Hz, 3-H), 6.82 (2H, d,  $J$  9.1 Hz, 3'-H and 5'-H), 7.02 (1H, t,  $J$  8.5 Hz, 4-H), 8.06 (1H, br s, NH), 10.14 (1H, br s, NH);  $\delta_{\text{C}}$  (126 MHz,  $\text{CDCl}_3$ ) 18.5 (CH<sub>3</sub>), 18.5 (CH<sub>3</sub>), 19.5 (2 × CH<sub>3</sub>), 28.3 (CH), 75.7 (CH<sub>2</sub>), 99.3 (CH), 102.1 (C), 106.1 (CH), 114.6 (2 × CH, d,  $^2J_{\text{CF}}$  21.4 Hz), 132.8 (CH), 133.9 (C, d,  $^4J_{\text{CF}}$  2.7 Hz), 139.1 (2 × C, d,  $^3J_{\text{CF}}$  8.4 Hz), 152.0 (C), 159.5 (C), 160.6 (C, d,  $^1J_{\text{CF}}$  243.6 Hz), 171.4 (C);  $m/z$  (ESI) 353.1623 (MNa<sup>+</sup>. C<sub>19</sub>H<sub>23</sub>FN<sub>2</sub>NaO<sub>2</sub> requires 353.1636).

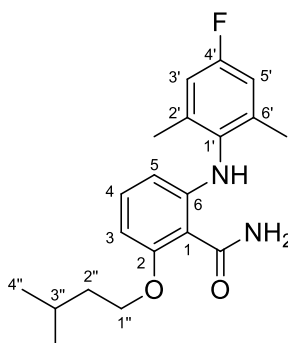
**2-*n*-Butoxy-6-[(4'-fluoro-2',6'-dimethylphenyl)amino]benzamide (91)**



The reaction was carried out according to general procedure D using 2-butoxy-6-[(4'-fluoro-2',6'-dimethylphenyl)amino]benzoic acid (**83**) (0.0300 g, 0.0905 mmol), 2-chloro-4,6-dimethoxy-1,3,5-triazine (0.0191 g, 0.109 mmol) and *N*-methylmorpholine (0.0300 mL,

0.273 mmol) in tetrahydrofuran (0.5 mL). The crude material was purified by flash column chromatography, eluting with 10% ethyl acetate in petroleum ether (40–60) to afford 2-*n*-butoxy-6-[(4'-fluoro-2',6'-dimethylphenyl)amino] benzamide (**91**) as a pale orange solid (0.0244 g, 81%). Mp 156–158 °C;  $\nu_{\max}/\text{cm}^{-1}$  (neat) 3460 (NH), 3181 (NH), 2932 (CH), 1645 (CO), 1570 (C=C), 1491, 1445, 1248, 752;  $\delta_{\text{H}}$  (500 MHz,  $\text{CDCl}_3$ ) 1.00 (3H, t,  $J$  7.5 Hz, 4''-H<sub>3</sub>), 1.47–1.57 (2H, m, 3''-H<sub>2</sub>), 1.81–1.90 (2H, m, 2''-H<sub>2</sub>), 2.17 (6H, s, 2'-CH<sub>3</sub> and 6'-CH<sub>3</sub>), 4.09 (2H, t,  $J$  6.5 Hz, 1''-H<sub>2</sub>), 5.70 (1H, br s, NH), 5.82 (1H, dd,  $J$  8.5, 0.8 Hz, 5-H), 6.20 (1H, dd,  $J$  8.5, 0.8 Hz, 3-H), 6.81 (2H, d,  $J$  9.1 Hz, 3'-H and 5'-H), 7.01 (1H, t,  $J$  8.5 Hz, 4-H), 8.06 (1H, br s, NH), 10.16 (1H, br s, NH);  $\delta_{\text{C}}$  (126 MHz,  $\text{CDCl}_3$ ) 13.8 (CH<sub>3</sub>), 18.4 (2 × CH<sub>3</sub>), 19.4 (CH<sub>2</sub>), 31.3 (CH<sub>2</sub>), 69.0 (CH<sub>2</sub>), 99.3 (CH), 102.1 (C), 106.1 (CH), 114.6 (2 × CH, d,  $^2J_{\text{CF}}$  21.7 Hz), 132.8 (CH), 134.0 (C, d,  $^4J_{\text{CF}}$  2.8 Hz), 139.1 (C, d,  $^3J_{\text{CF}}$  8.4 Hz), 152.0 (C), 159.5 (C), 160.6 (C, d,  $^1J_{\text{CF}}$  243.9 Hz), 171.4 (C);  $m/z$  (ESI) 353.1623 (MNa<sup>+</sup>. C<sub>19</sub>H<sub>23</sub>FN<sub>2</sub>NaO<sub>2</sub> requires 353.1636).

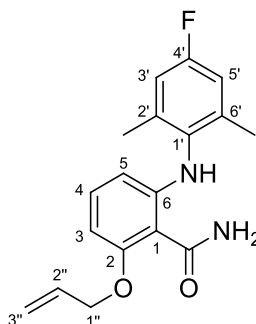
### 6-[(4'-Fluoro-2',6'-dimethylphenyl)amino]-2-(3''-methyl-*n*-butoxy)benzamide (**92**)



The reaction was carried out according to general procedure D using 6-[(4'-fluoro-2',6'-dimethylphenyl)amino]-2-(3''-methyl-*n*-butoxy)benzoic acid (**85**) (0.020 g, 0.058 mmol), 2-chloro-4,6-dimethoxy-1,3,5-triazine (0.012 g, 0.070 mmol) and *N*-methylmorpholine (0.019 mL, 0.17 mmol) in tetrahydrofuran (0.5 mL). The crude material was purified by flash column chromatography, eluting with 10% ethyl acetate in petroleum ether (40–60) to afford 6-[(4'-fluoro-2',6'-dimethylphenyl)amino]-2-(3''-methyl-*n*-butoxy)benzamide (**92**) as a pale yellow solid (0.014 g, 67%). Mp 143–145 °C;  $\nu_{\max}/\text{cm}^{-1}$  (neat) 3467 (NH), 3200 (NH), 2960 (CH), 1641 (CO), 1580 (C=C), 1451, 1245, 1216, 754;  $\delta_{\text{H}}$  (500 MHz,  $\text{CDCl}_3$ ) 0.99 (6H, d,  $J$  6.4 Hz, 3''-CH<sub>3</sub> and 4''-H<sub>3</sub>), 1.73–1.87 (3H, m, 2''-H<sub>2</sub> and 3''-H), 2.17 (6H, s, 2'-CH<sub>3</sub> and 6'-CH<sub>3</sub>), 4.11 (2H, t,  $J$  6.6 Hz, 1''-H<sub>2</sub>), 5.65 (1H, br s, NH), 5.82 (1H, dd,  $J$  8.5, 0.8 Hz, 5-H), 6.21 (1H, br d,  $J$  8.5 Hz, 3-H), 6.81 (2H, d,  $J$  9.1 Hz, 3'-H and 5'-H), 7.02 (1H, t,  $J$  8.5 Hz, 4-H), 8.05 (1H, br s, NH), 10.16 (1H, br s, NH);  $\delta_{\text{C}}$  (126 MHz,  $\text{CDCl}_3$ ) 18.5 (CH<sub>3</sub>), 18.5 (CH<sub>3</sub>), 22.6 (2 × CH<sub>3</sub>), 25.3 (CH), 38.1 (CH<sub>2</sub>), 67.8 (CH<sub>2</sub>), 99.3 (CH), 102.2 (C), 106.2 (CH), 114.6 (2 × CH, d,  $^2J_{\text{CF}}$  21.4 Hz), 132.8 (CH), 133.9 (C, d,  $^4J_{\text{CF}}$  2.7 Hz), 139.1 (2 × C,

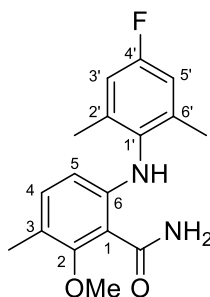
d,  $^3J_{CF}$  8.8 Hz), 152.1 (C), 159.5 (C), 160.6 (C, d,  $^1J_{CF}$  243.7 Hz), 171.4 (C);  $m/z$  (ESI) 367.1771 (MNa<sup>+</sup>. C<sub>20</sub>H<sub>25</sub>FN<sub>2</sub>NaO<sub>2</sub> requires 367.1792).

### 2-(Allyloxy)-6-[(4'-fluoro-2',6'-dimethylphenyl)amino]benzamide (93)



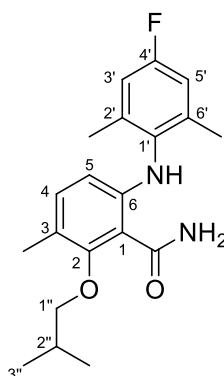
The reaction was carried out according to general procedure D using 2-(allyloxy)-6-[(4'-fluoro-2',6'-dimethylphenyl)amino]benzoic acid (**86**) (0.0500 g, 0.149 mmol), 2-chloro-4,6-dimethoxy-1,3,5-triazine (0.0314 g, 0.179 mmol) and *N*-methylmorpholine (0.0491 mL, 0.447 mmol) in tetrahydrofuran (0.5 mL). The crude material was purified by flash column chromatography, eluting with 10% ethyl acetate in petroleum ether (40–60) to afford 2-(allyloxy)-6-[(4'-fluoro-2',6'-dimethylphenyl)amino]benzamide (**93**) as a pale yellow solid (0.0445 g, 95%). Mp 176–178 °C;  $\nu_{\max}/\text{cm}^{-1}$  (neat) 3443 (NH), 3181 (NH), 2920 (CH), 1647 (CO), 1605 (C=C), 1582 (C=C), 1451, 1238, 1053, 810;  $\delta_{\text{H}}$  (500 MHz, CDCl<sub>3</sub>) 2.17 (6H, s, 2'-CH<sub>3</sub> and 6'-CH<sub>3</sub>), 4.63 (2H, d,  $J$  5.6 Hz, 1''-H<sub>2</sub>), 5.36 (1H, dd,  $J$  10.5, 1.2 Hz, 3''-HH), 5.46 (1H, dd,  $J$  17.2, 1.2 Hz, 3''-HH), 5.75 (1H, br s, NH), 5.84 (1H, dd,  $J$  8.2, 0.8 Hz, 5-H), 6.11 (1H, ddt,  $J$  17.2, 10.5, 5.6 Hz, 2''-H), 6.20 (1H, br d,  $J$  8.2 Hz, 3-H), 6.82 (2H, d,  $J$  9.1 Hz, 3'-H and 5'-H), 7.02 (1H, t,  $J$  8.2 Hz, 4-H), 7.99 (1H, br s, NH), 10.12 (1H, br s, NH);  $\delta_{\text{C}}$  (126 MHz, CDCl<sub>3</sub>) 18.4 (CH<sub>3</sub>), 18.5 (CH<sub>3</sub>), 70.1 (CH<sub>2</sub>), 99.7 (CH), 102.5 (C), 106.5 (CH), 114.6 (2 × CH,  $^2J_{CF}$  21.4 Hz), 119.2 (CH<sub>2</sub>), 132.4 (CH), 132.7 (CH), 133.9 (C, d,  $^4J_{CF}$  2.7 Hz), 139.1 (2 × C, d,  $^3J_{CF}$  8.4 Hz), 152.0 (C), 159.0 (C), 160.6 (C, d,  $^1J_{CF}$  244.1 Hz), 171.3 (C);  $m/z$  (ESI) 337.1313 (MNa<sup>+</sup>. C<sub>18</sub>H<sub>19</sub>FN<sub>2</sub>NaO<sub>2</sub> requires 337.1323).

**6-[(4'-Fluoro-2',6'-dimethylphenyl)amino]-2-methoxy-3-methylbenzamide (94)**



The reaction was carried out according to general procedure D using 6-[(4'-fluoro-2',6'-dimethylphenyl)amino]-2-methoxy-3-methylbenzoic acid (**87**) (0.030 g, 0.099 mmol), 2-chloro-4,6-dimethoxy-1,3,5-triazine (0.021 g, 0.12 mmol) and *N*-methylmorpholine (0.033 mL, 0.30 mmol) in tetrahydrofuran (0.5 mL). The crude material was purified by flash column chromatography, eluting with 10% ethyl acetate in petroleum ether (40–60) to afford 6-[(4'-fluoro-2',6'-dimethylphenyl)amino]-2-methoxy-3-methylbenzamide (**94**) as a pale yellow solid (0.016 g, 55%). Mp 136–138 °C;  $\nu_{\max}/\text{cm}^{-1}$  (neat) 3464 (NH), 3226 (NH), 2923 (CH), 1623 (CO), 1569 (C=C), 1496, 1404, 1368, 1257, 1130, 1046, 1020, 865, 702;  $\delta_{\text{H}}$  (500 MHz,  $\text{CDCl}_3$ ) 2.17 (3H, s, 3- $\text{CH}_3$ ), 2.17 (6H, s, 2'- $\text{CH}_3$  and 6'- $\text{CH}_3$ ), 3.78 (3H, s,  $\text{OCH}_3$ ), 5.74 (1H, br s, NH), 5.91 (1H, d,  $J$  8.6 Hz, 5-H), 6.81 (2H, d,  $J$  9.1 Hz, 3'-H and 5'-H), 6.94 (1H, d,  $J$  8.6 Hz, 4-H), 7.95 (1H, br s, NH), 9.36 (1H, br s, NH);  $\delta_{\text{C}}$  (126 MHz,  $\text{CDCl}_3$ ) 15.2 ( $\text{CH}_3$ ), 18.5 (2  $\times$   $\text{CH}_3$ ), 61.2 ( $\text{CH}_3$ ), 106.9 (C), 109.0 (CH), 114.6 (2  $\times$  CH, d,  $^2J_{\text{CF}}$  21.8 Hz), 117.7 (C), 134.0 (C, d,  $^4J_{\text{CF}}$  2.7 Hz), 135.1 (CH), 139.0 (2  $\times$  C, d,  $^3J_{\text{CF}}$  8.5 Hz), 149.2 (C), 158.2 (C), 160.5 (C, d,  $^1J_{\text{CF}}$  243.7 Hz), 170.8 (C);  $m/z$  (ESI) 325.1315 ( $\text{MNa}^+$ .  $\text{C}_{17}\text{H}_{16}\text{FNNaO}_3$  requires 325.1323).

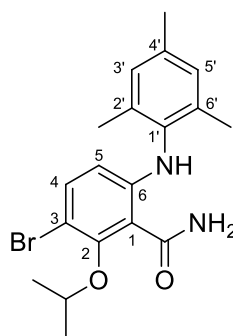
**6-[(4'-Fluoro-2',6'-dimethylphenyl)amino]-2-isobutoxy-3-methylbenzamide (95)**



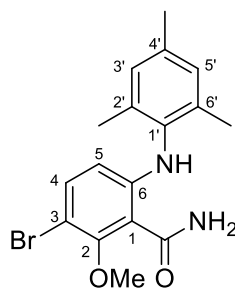
The reaction was carried out according to general procedure D using 6-[(4'-fluoro-2',6'-dimethylphenyl)amino]-2-isobutoxy-3-methylbenzoic acid (**88**) (0.0720 g, 0.208 mmol), 2-chloro-4,6-dimethoxy-1,3,5-triazine (0.0438 g, 0.250 mmol) and *N*-methylmorpholine

(0.0687 mL, 0.625 mmol) in tetrahydrofuran (0.5 mL). The crude material was purified by flash column chromatography, eluting with 10% ethyl acetate in petroleum ether (40–60) to afford 6-[(4'-fluoro-2',6'-dimethylphenyl)amino]-2-isobutoxy-3-methylbenzamide (**95**) as a white solid (0.059 g, 82%). Mp 125–127 °C;  $\nu_{\max}/\text{cm}^{-1}$  (neat) 3449 (NH), 3233 (NH), 2963 (CH), 1651 (CO), 1574 (C=C), 1497, 1258, 1042;  $\delta_{\text{H}}$  (400 MHz,  $\text{CDCl}_3$ ) 1.06 (6H, d,  $J$  6.7 Hz, 2''-CH<sub>3</sub> and 3''-H<sub>3</sub>), 2.06–2.22 (1H, m, 2''-H), 2.15 (3H, s, 3-CH<sub>3</sub>), 2.17 (6H, s, 2'-CH<sub>3</sub> and 6'-CH<sub>3</sub>), 3.62 (2H, d,  $J$  6.7 Hz, 1''-H<sub>2</sub>), 5.90 (1H, d,  $J$  8.6 Hz, 5-H), 5.92 (1H, br s, NH), 6.81 (2H, d,  $J$  9.1 Hz, 3'-H and 5'-H), 6.93 (1H, d,  $J$  8.6 Hz, 4-H), 7.93 (1H, br s, NH), 9.23 (1H, br s, NH);  $\delta_{\text{C}}$  (101 MHz,  $\text{CDCl}_3$ ) 15.4 (CH<sub>3</sub>), 18.5 (CH<sub>3</sub>), 18.5 (CH<sub>3</sub>), 19.3 (2 × CH<sub>3</sub>), 29.3 (CH), 80.7 (CH<sub>2</sub>), 107.7 (C), 108.8 (CH), 114.6 (2 × CH, d,  $^2J_{\text{CF}}$  21.7 Hz), 118.0 (C), 134.0 (C, d,  $^4J_{\text{CF}}$  2.8 Hz), 135.0 (CH), 139.0 (2 × C, d,  $^3J_{\text{CF}}$  8.6 Hz), 148.9 (C), 157.1 (C), 160.5 (C, d,  $^1J_{\text{CF}}$  243.7 Hz), 171.0 (C);  $m/z$  (ESI) 367.1781 ( $\text{MNa}^+$ .  $\text{C}_{20}\text{H}_{25}\text{FN}_2\text{NaO}_2$  requires 367.1792).

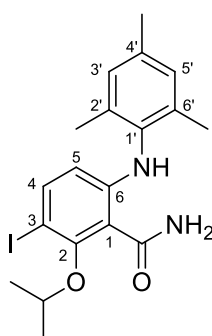
### 3-Bromo-2-isopropoxy-6-(mesitylamino)benzamide (**72**)



The reaction was carried out according to general procedure E using iron(III) chloride (0.0016 g, 0.010 mmol), [BMIM]NTf<sub>2</sub> (0.12 mL, 0.40 mmol), 2-isopropoxy-6-(mesitylamino)benzamide (**67**) (0.060 g, 0.20 mmol) and *N*-bromosuccinimide (0.098 g, 0.55 mmol) in dichloromethane (0.5 mL). The crude material was purified by flash column chromatography, eluting with 10% diethyl ether in petroleum ether (40–60) to afford 3-bromo-2-isopropoxy-6-(mesitylamino)benzamide (**72**) as a white solid (0.073 g, 94%). Mp 205–207 °C;  $\nu_{\max}/\text{cm}^{-1}$  (neat) 3435 (NH), 3185 (NH), 2976 (CH), 1647 (CO), 1564 (C=C), 1487, 1406, 1258, 1098;  $\delta_{\text{H}}$  (500 MHz,  $\text{CDCl}_3$ ) 1.39 (6H, d,  $J$  6.2 Hz,  $\text{OCH}(\text{CH}_3)_2$ ), 2.14 (6H, s, 2'-CH<sub>3</sub> and 6'-CH<sub>3</sub>), 2.30 (3H, s, 4'-CH<sub>3</sub>), 4.56 (1H, sept,  $J$  6.2 Hz,  $\text{OCH}(\text{CH}_3)_2$ ), 5.73 (1H, br s, NH), 5.90 (1H, d,  $J$  9.0 Hz, 5-H), 6.93 (2H, s, 3'-H and 5'-H), 7.20 (1H, d,  $J$  9.0 Hz, 4-H), 7.57 (1H, br s, NH), 9.18 (1H, br s, NH);  $\delta_{\text{C}}$  (126 MHz,  $\text{CDCl}_3$ ) 18.2 (2 × CH<sub>3</sub>), 20.9 (CH<sub>3</sub>), 21.9 (2 × CH<sub>3</sub>), 78.2 (CH), 102.9 (C), 110.3 (CH), 110.8 (C), 129.1 (2 × CH), 134.7 (C), 136.0 (C), 136.1 (CH), 136.4 (2 × C), 149.6 (C), 154.0 (C), 170.2 (C);  $m/z$  (ESI) 413.0824 ( $\text{MNa}^+$ .  $\text{C}_{19}\text{H}_{23}^{79}\text{BrN}_2\text{NaO}_2$  requires 413.0835).

**3-Bromo-6-(mesitylamino)-2-methoxybenzamide (98)**

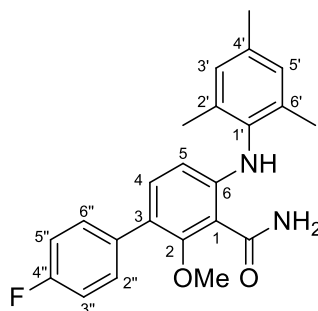
The reaction was carried out according to general procedure E using iron(III) chloride (0.0446 g, 0.275 mmol), [BMIM]NTf<sub>2</sub> (2.30 mL, 11.0 mmol), 2-methoxy-6-(mesitylamino)benzamide (**97**) (1.56 g, 5.49 mmol) and *N*-bromosuccinimide (0.980 g, 5.49 mmol) in dichloromethane (14 mL). The crude material was purified by flash column chromatography, eluting with 20% ethyl acetate in petroleum ether (40–60) to afford 3-bromo-6-(mesitylamino)-2-methoxybenzamide (**98**) as a white solid (1.54 g, 77%). Mp 184–186 °C;  $\nu_{\max}/\text{cm}^{-1}$  (neat) 3456 (NH), 3256 (NH), 2924 (CH), 1651 (CO), 1566 (C=C), 1489, 1404, 1258, 1042, 818;  $\delta_{\text{H}}$  (400 MHz, CDCl<sub>3</sub>) 2.14 (2'-CH<sub>3</sub> and 6'-CH<sub>3</sub>), 2.30 (3H, s, 4'-CH<sub>3</sub>), 3.89 (3H, s, OCH<sub>3</sub>), 5.90 (1H, br s, NH), 5.94 (1H, d, *J* 9.1, Hz, 5-H), 6.93 (2H, s, 3'-H and 5'-H), 7.22 (1H, d, *J* 9.1 Hz, 4-H), 7.82 (1H, br s, NH), 9.55 (1H, br s, NH);  $\delta_{\text{C}}$  (126 MHz, CDCl<sub>3</sub>) 18.1 (2 × CH<sub>3</sub>), 20.9 (CH<sub>3</sub>), 61.8 (CH<sub>3</sub>), 101.9 (C), 108.1 (C), 110.9 (CH), 129.2 (2 × CH), 134.6 (C), 136.1 (C), 136.3 (2 × C), 136.3 (CH), 150.6 (C), 156.6 (C), 169.9 (C); *m/z* (ESI) 385.0512 (MNa<sup>+</sup>. C<sub>17</sub>H<sub>19</sub><sup>79</sup>BrN<sub>2</sub>NaO<sub>2</sub> requires 385.0522).

**3-Iodo-2-isopropoxy-6-(mesitylamino)benzamide (73)**

To a dry flask under argon was added iron(III) chloride (0.0016 g, 0.010 mmol) and [BMIM]NTf<sub>2</sub> (0.12 mL, 0.40 mmol) and the mixture stirred for 0.5 h. 2-Isopropoxy-6-(mesitylamino)benzamide (**67**) (0.060 g, 0.20 mmol) was then added as a solution in dichloromethane (0.5 mL) and *N*-iodosuccinimide (0.045 g, 0.20 mmol) was added slowly to the mixture. After 16 h of stirring at 36 °C, *N*-iodosuccinimide (0.018 g, 0.080 mmol) was added and the reaction mixture stirred for a further 3 h. The mixture was diluted with ethyl acetate (10 mL) and filtered through a short pad of silica. The filtrate was then

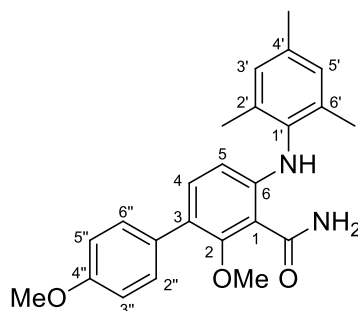
washed with 1 M sodium thiosulfate (10 mL) and brine (10 mL). The solution was dried ( $\text{MgSO}_4$ ), filtered and concentrated *in vacuo*. The resulting residue was then purified by flash column chromatography, eluting with 15% diethyl ether in petroleum ether (40–60) to afford 3-iodo-2-isopropoxy-6-(mesitylamino)benzamide (**73**) as a white solid (0.028 g, 31%). Mp 215–217 °C;  $\nu_{\text{max}}/\text{cm}^{-1}$  (neat) 3447 (NH), 3198 (NH), 2972 (CH), 1643 (CO), 1560 (C=C), 1485, 1256, 758;  $\delta_{\text{H}}$  (400 MHz,  $\text{CDCl}_3$ ) 1.40 (6H, d,  $J$  6.2 Hz,  $\text{OCH}(\text{CH}_3)_2$ ), 2.14 (2'- $\text{CH}_3$  and 6'- $\text{CH}_3$ ), 2.30 (3H, s, 4'- $\text{CH}_3$ ), 4.53 (1H, sept,  $J$  6.2 Hz,  $\text{OCH}(\text{CH}_3)_2$ ), 5.81 (1H, d,  $J$  9.0 Hz, 5-H), 5.83 (1H, br s, NH), 6.92 (2H, s, 3'-H and 5'-H), 7.40 (1H, d,  $J$  9.0 Hz, 4-H), 7.47 (1H, br s, NH), 9.11 (1H, br s, NH);  $\delta_{\text{C}}$  (101 MHz,  $\text{CDCl}_3$ ) 18.1 (2  $\times$   $\text{CH}_3$ ), 20.9 ( $\text{CH}_3$ ), 22.0 (2  $\times$   $\text{CH}_3$ ), 75.0 (C), 78.4 (CH), 110.9 (C), 111.3 (CH), 129.2 (2  $\times$  CH), 134.7 (C), 136.0 (C), 136.3 (2  $\times$  C), 141.9 (CH), 150.3 (C), 156.4 (C), 170.2 (C);  $m/z$  (ESI) 461.0689 ( $\text{MNa}^+$ .  $\text{C}_{19}\text{H}_{23}\text{IN}_2\text{NaO}_2$  requires 461.0696).

### 3-(4''-Fluorophenyl)-6-(mesitylamino)-2-methoxybenzamide (**101**)



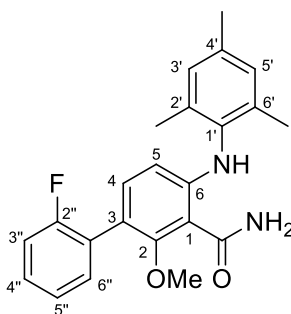
The reaction was carried out according to general procedure F using 3-bromo-6-(mesitylamino)-2-methoxybenzamide (**98**) (0.100 g, 0.275 mmol), 4-fluorophenylboronic acid (0.0616 g, 0.440 mmol), [1,1'-bis(diphenylphosphino)ferrocene]dichloropalladium(II) (1:1) (0.0113 g, 0.0138 mmol) and caesium carbonate (0.270 g, 0.825 mmol) in 1,4-dioxane (4.0 mL) and water (0.30 mL). The crude material was purified by flash column chromatography, eluting with 20% ethyl acetate in petroleum ether (40–60) to afford 3-(4''-fluorophenyl)-6-(mesitylamino)-2-methoxybenzamide (**101**) as a white solid (0.0738 g, 71%). Mp 209–211 °C;  $\nu_{\text{max}}/\text{cm}^{-1}$  (neat) 3449 (NH), 3225 (NH), 2924 (CH), 1651 (CO), 1489, 1250, 1227, 1042, 818, 756;  $\delta_{\text{H}}$  (400 MHz,  $\text{CDCl}_3$ ) 2.18 (6H, s, 2'- $\text{CH}_3$  and 6'- $\text{CH}_3$ ), 2.31 (3H, s, 4'- $\text{CH}_3$ ), 3.45 (3H, s,  $\text{OCH}_3$ ), 5.82 (1H, br s, NH), 6.08 (1H, d,  $J$  8.8 Hz, 5-H), 6.95 (2H, s, 3'-H and 5'-H), 7.05 (1H, d,  $J$  8.8 Hz, 4-H), 7.07 (2H, t,  $J$  8.7 Hz, 3''-H and 5''-H), 7.45 (2H, dd,  $J$  8.7, 5.5 Hz, 2''-H and 6''-H), 8.07 (1H, br s, NH), 9.72 (1H, br s, NH);  $\delta_{\text{C}}$  (101 MHz,  $\text{CDCl}_3$ ) 18.3 (2  $\times$   $\text{CH}_3$ ), 21.0 ( $\text{CH}_3$ ), 61.3 ( $\text{CH}_3$ ), 106.6 (C), 109.6 (CH), 115.1 (2  $\times$  CH, d,  $^2J_{\text{CF}}$  21.2 Hz), 121.2 (C), 129.1 (2  $\times$  CH), 130.6 (2  $\times$  CH, d,  $^3J_{\text{CF}}$  7.8 Hz), 134.4 (C, d,  $^4J_{\text{CF}}$  3.4 Hz), 134.6 (CH), 135.0 (C) 135.9 (C), 136.4 (2  $\times$  C), 150.8 (C), 157.6 (C), 161.7 (C, d,  $^1J_{\text{CF}}$  245.6 Hz), 170.9 (C);  $m/z$  (ESI) 401.1623 ( $\text{MNa}^+$ .  $\text{C}_{23}\text{H}_{23}\text{FN}_2\text{NaO}_2$  requires 401.1636).

### 3-(4''-Methoxyphenyl)-6-(mesitylamino)-2-methoxybenzamide (103)



The reaction was carried out according to general procedure F using 3-bromo-6-(mesitylamino)-2-methoxybenzamide (**98**) (0.100 g, 0.275 mmol), 4-methoxyphenylboronic acid (0.0669 g, 0.440 mmol), [1,1'-bis(diphenylphosphino)ferrocene]dichloropalladium(II) (1:1) (0.0113 g, 0.0138 mmol) and caesium carbonate (0.270 g, 0.825 mmol) in 1,4-dioxane (4.0 mL) and water (0.30 mL). The crude material was purified by flash column chromatography, eluting with 20% ethyl acetate in petroleum ether (40–60) to afford 3-(4''-methoxyphenyl)-6-(mesitylamino)-2-methoxybenzamide (**103**) as a white solid (0.0873 g, 81%). Mp 184–185 °C;  $\nu_{\max}/\text{cm}^{-1}$  (neat) 3449 (NH), 3194 (NH), 2932 (CH), 1643 (CO), 1489, 1242, 1042, 756;  $\delta_{\text{H}}$  (400 MHz,  $\text{CDCl}_3$ ) 2.19 (6H, s, 2'- $\text{CH}_3$  and 6'- $\text{CH}_3$ ), 2.31 (3H, s, 4'- $\text{CH}_3$ ), 3.45 (3H, s, 2-O $\text{CH}_3$ ), 3.83 (3H, s, 4''-O $\text{CH}_3$ ), 5.81 (1H, br s, NH), 6.07 (1H, d,  $J$  8.7 Hz, 5-H), 6.93 (2H, d,  $J$  8.3 Hz, 3''-H and 5''-H), 6.94 (2H, s, 3'-H and 5'-H), 7.07 (1H, d,  $J$  8.7 Hz, 4-H), 7.41 (2H, d,  $J$  8.3 Hz, 2''-H and 6''-H), 8.11 (1H, br s, NH), 9.70 (1H, br s, NH);  $\delta_{\text{C}}$  (101 MHz,  $\text{CDCl}_3$ ) 18.3 (2  $\times$   $\text{CH}_3$ ), 21.0 ( $\text{CH}_3$ ), 55.3 ( $\text{CH}_3$ ), 61.1 ( $\text{CH}_3$ ), 106.6 (C), 109.5 (CH), 113.7 (2  $\times$  CH), 121.9 (C), 129.1 (2  $\times$  CH), 130.1 (2  $\times$  CH), 130.9 (C), 134.7 (CH), 135.2 (C), 135.8 (C), 136.4 (2  $\times$  C), 150.4 (C), 157.6 (C), 158.4 (C), 171.1 (C);  $m/z$  (ESI) 413.1819 ( $\text{MNa}^+$ .  $\text{C}_{24}\text{H}_{26}\text{N}_2\text{NaO}_3$  requires 413.1836).

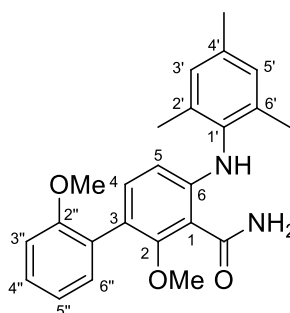
### 3-(2''-Fluorophenyl)-6-(mesitylamino)-2-methoxybenzamide (105)



The reaction was carried out according to general procedure F using 3-bromo-6-(mesitylamino)-2-methoxybenzamide (**98**) (0.100 g, 0.275 mmol), 2-fluorophenylboronic

acid (0.0616 g, 0.440 mmol), [1,1'-bis(diphenylphosphino)ferrocene]dichloropalladium(II) (1:1) (0.0113 g, 0.0138 mmol) and caesium carbonate (0.270 g, 0.825 mmol) in 1,4-dioxane (4.0 mL) and water (0.30 mL). The crude material was purified by flash column chromatography, eluting with 20% ethyl acetate in petroleum ether (40–60) to afford 3-(2''-fluorophenyl)-6-(mesitylamino)-2-methoxybenzamide (**105**) as a white solid (0.0698 g, 67%). Mp 219–221 °C;  $\nu_{\max}/\text{cm}^{-1}$  (neat) 3464 (NH), 3264 (NH), 2916 (CH), 1620 (CO), 1481, 1396, 1373, 1242, 1034, 748;  $\delta_{\text{H}}$  (400 MHz,  $\text{CDCl}_3$ ) 2.20 (6H, s, 2'- $\text{CH}_3$  and 6'- $\text{CH}_3$ ), 2.30 (3H, s, 4'- $\text{CH}_3$ ), 3.47 (3H, s,  $\text{OCH}_3$ ), 5.88 (1H, br s, NH), 6.08 (1H, d,  $J$  8.7 Hz, 5-H), 6.94 (2H, s, 3'-H and 5'-H), 7.04 (1H, d,  $J$  8.7 Hz, 4-H), 7.07–7.20 (2H, m, ArH), 7.24–7.34 (1H, m, ArH), 7.37 (1H, t,  $J$  7.5 Hz, ArH), 8.11 (1H, br s, NH), 9.70 (1H, br s, NH);  $\delta_{\text{C}}$  (101 MHz,  $\text{CDCl}_3$ ) 18.3 (2  $\times$   $\text{CH}_3$ ), 20.9 ( $\text{CH}_3$ ), 61.6 ( $\text{CH}_3$ ), 106.4 (C), 109.3 (CH), 115.7 (CH, d,  $^2J_{\text{CF}}$  22.8 Hz), 116.2 (C), 123.9 (CH, d,  $^3J_{\text{CF}}$  3.6 Hz), 126.0 (C, d,  $^2J_{\text{CF}}$  15.7 Hz), 128.7 (CH, d,  $^3J_{\text{CF}}$  8.1 Hz), 129.1 (2  $\times$  CH), 132.1 (CH, d,  $^4J_{\text{CF}}$  3.1 Hz), 135.0 (C), 135.1 (CH), 135.9 (C), 136.4 (2  $\times$  C), 151.2 (C), 158.3 (C), 160.0 (C, d,  $^1J_{\text{CF}}$  246.4 Hz), 170.9 (C);  $m/z$  (ESI) 401.1621 ( $\text{MNa}^+$ .  $\text{C}_{23}\text{H}_{23}\text{FN}_2\text{NaO}_2$  requires 401.1636).

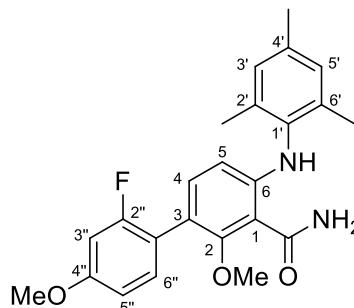
### 3-(2''-Methoxyphenyl)-6-(mesitylamino)-2-methoxybenzamide (**104**)



The reaction was carried out according to general procedure F using 3-bromo-6-(mesitylamino)-2-methoxybenzamide (**98**) (0.100 g, 0.275 mmol), 2-methoxyphenylboronic acid (0.0669 g, 0.440 mmol), [1,1'-bis(diphenylphosphino)ferrocene]dichloropalladium(II) (1:1) (0.0113 g, 0.0138 mmol) and caesium carbonate (0.270 g, 0.825 mmol) in 1,4-dioxane (4.0 mL) and water (0.30 mL). The crude material was purified by flash column chromatography, eluting with 20% ethyl acetate in petroleum ether (40–60) to afford 3-(2''-methoxyphenyl)-6-(mesitylamino)-2-methoxybenzamide (**104**) as a white solid (0.0518 g, 48%). Mp 240–241 °C;  $\nu_{\max}/\text{cm}^{-1}$  (neat) 3456 (NH), 3217 (NH), 2916 (CH), 1620 (CO), 1481, 1242, 1034, 748;  $\delta_{\text{H}}$  (400 MHz,  $\text{CDCl}_3$ ) 2.20 (6H, s, 2'- $\text{CH}_3$  and 6'- $\text{CH}_3$ ), 2.30 (3H, s, 4'- $\text{CH}_3$ ), 3.44 (3H, s, 2- $\text{OCH}_3$ ), 3.77 (3H, s, 2''- $\text{OCH}_3$ ), 5.64 (1H, br s, NH), 6.05 (1H, d,  $J$  8.7 Hz, 5-H), 6.94 (2H, s, 3'-H and 5'-H), 6.95–7.00 (2H, m, 3''-H and 5''-H), 7.02 (1H, d,  $J$  8.7 Hz, 4-H), 7.26–7.34 (2H, m, 4''-H and 6''-H), 8.06 (1H, br s, NH), 9.74 (1H, br s, NH);  $\delta_{\text{C}}$  (101 MHz,  $\text{CDCl}_3$ ) 18.4 (2  $\times$   $\text{CH}_3$ ), 20.9 ( $\text{CH}_3$ ), 55.7 ( $\text{CH}_3$ ), 61.3 ( $\text{CH}_3$ ), 106.3 (C), 108.9 (CH), 111.2 (CH), 118.8 (C), 120.4 (CH), 127.4 (C),

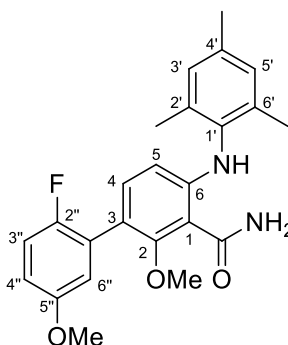
128.4 (CH), 129.0 (2 × CH), 131.9 (CH), 135.3 (C), 135.6 (C), 135.7 (CH), 136.5 (2 × C), 150.7 (C), 157.1 (C), 158.1 (C), 171.1 (C);  $m/z$  (ESI) 413.1819 ( $MNa^+$ .  $C_{24}H_{26}FN_2NaO_3$  requires 413.1836).

### 3-(2''-Fluoro-4''-methoxyphenyl)-6-(mesitylamino)-2-methoxybenzamide (102)



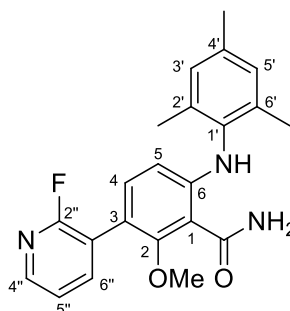
The reaction was carried out according to general procedure (General Procedure F) using 3-bromo-6-(mesitylamino)-2-methoxybenzamide (**98**) (0.100 g, 0.275 mmol), 2-fluoro-4-methoxyphenylboronic acid (0.0748 g, 0.440 mmol), [1,1'-bis(diphenylphosphino)ferrocene]dichloropalladium(II) (1:1) (0.0113 g, 0.0138 mmol) and caesium carbonate (0.270 g, 0.825 mmol) in 1,4-dioxane (4.0 mL) and water (0.30 mL). The crude material was purified by flash column chromatography, eluting with 20% ethyl acetate in petroleum ether (40–60) and then triturated with 10% ethyl acetate in petroleum ether (40–60) to afford 3-(2''-fluoro-4''-methoxyphenyl)-6-(mesitylamino)-2-methoxybenzamide (**102**) as a white solid (0.0573 g, 51%). Mp 206–210 °C;  $\nu_{max}/cm^{-1}$  (neat) 3466 (NH), 2913 (CH), 1624 (CO), 1557 (C=C), 1489, 1373, 1257, 1040, 951, 823;  $\delta_H$  (400 MHz,  $CDCl_3$ ) 2.19 (6H, s, 2'-CH<sub>3</sub> and 6'-CH<sub>3</sub>), 2.30 (3H, s, 4'-CH<sub>3</sub>), 3.47 (3H, s, 2-OCH<sub>3</sub>), 3.83 (3H, s, 4''-OCH<sub>3</sub>), 5.79 (1H, br s, NH), 6.07 (1H, d,  $J$  8.6 Hz, 5-H), 6.65–6.77 (2H, m, 5''-H and 6''-H), 6.94 (2H, s, 3'-H and 5'-H), 7.02 (1H, d,  $J$  8.6 Hz, 4-H), 7.19–7.36 (1H, m, 3''-H), 8.04 (1H, br s, NH), 9.75 (1H, br s, NH);  $\delta_C$  (101 MHz,  $CDCl_3$ ) 18.3 (2 × CH<sub>3</sub>), 20.9 (CH<sub>3</sub>), 55.6 (CH<sub>3</sub>), 61.5 (CH<sub>3</sub>), 101.7 (CH, d,  $^2J_{CF}$  26.6 Hz), 106.4 (C), 109.2 (CH), 109.8 (CH, d,  $^4J_{CF}$  3.0 Hz), 116.1 (C), 118.1 (C, d,  $^2J_{CF}$  16.2 Hz), 129.1 (2 × CH), 132.3 (CH, d,  $^3J_{CF}$  5.2 Hz), 135.1 (C), 135.3 (CH), 135.8 (C), 136.4 (2 × C), 151.0 (C), 158.3 (C), 160.0 (C, d,  $^3J_{CF}$  10.8 Hz), 160.5 (C, d,  $^1J_{CF}$  246.2 Hz), 170.9 (C);  $m/z$  (ESI) 431.1721 ( $MNa^+$ .  $C_{24}H_{25}FN_2NaO_3$  requires 431.1741).

**3-(2''-Fluoro-5''-methoxyphenyl)-6-(mesitylamino)-2-methoxybenzamide (107)**



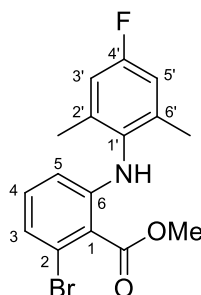
The reaction was carried out according to general procedure F using 3-bromo-6-(mesitylamino)-2-methoxybenzamide (**98**) (0.100 g, 0.275 mmol), 2-fluoro-5-methoxyphenylboronic acid (0.0748 g, 0.440 mmol), [1,1'-bis(diphenylphosphino)ferrocene]dichloropalladium(II) (1:1) (0.0113 g, 0.0138 mmol) and caesium carbonate (0.270 g, 0.825 mmol) in 1,4-dioxane (4.0 mL) and water (0.30 mL). The crude material was purified by flash column chromatography, eluting with 20% ethyl acetate in petroleum ether (40–60) and then triturated with 10% ethyl acetate in petroleum ether (40–60) to afford 3-(2''-fluoro-5''-methoxyphenyl)-6-(mesitylamino)-2-methoxybenzamide (**107**) as a white solid (0.0694 g, 62%). Mp 196–198 °C;  $\nu_{\max}/\text{cm}^{-1}$  (neat) 3456 (NH), 2934 (CH), 1647 (CO), 1564 (C=C), 1489, 1404, 1245, 1206, 1038, 752;  $\delta_{\text{H}}$  (400 MHz,  $\text{CDCl}_3$ ) 2.19 (6H, s, 2'- $\text{CH}_3$  and 6'- $\text{CH}_3$ ), 2.31 (3H, s, 4'- $\text{CH}_3$ ), 3.51 (3H, s, 2-O $\text{CH}_3$ ), 3.80 (3H, s, 5''-O $\text{CH}_3$ ), 5.68 (1H, br s, NH), 6.08 (1H, d,  $J$  8.8 Hz, 5-H), 6.81 (1H, dt,  $J$  8.8, 3.5 Hz, 4''-H), 6.90 (1H, dd,  $J$  6.0, 3.5 Hz, 6''-H), 6.94 (2H, s, 3'-H and 5'-H), 7.00–7.07 (1H, m, 3''-H), 7.02 (1H, d,  $J$  8.8 Hz, 4-H), 8.03 (1H, br s, NH), 9.78 (1H, br s, NH);  $\delta_{\text{C}}$  (101 MHz,  $\text{CDCl}_3$ ) 18.3 (2  $\times$   $\text{CH}_3$ ), 21.0 ( $\text{CH}_3$ ), 55.8 ( $\text{CH}_3$ ), 61.7 ( $\text{CH}_3$ ), 106.4 (C), 109.2 (CH), 113.7 (CH, d,  $^3J_{\text{CF}}$  8.0 Hz), 116.1 (CH, d,  $^2J_{\text{CF}}$  28.7 Hz), 116.2 (C), 116.7 (CH, d,  $^3J_{\text{CF}}$  3.1 Hz), 126.6 (C, d,  $^2J_{\text{CF}}$  17.5 Hz), 129.1 (2  $\times$  CH), 135.0 (C), 135.1 (CH), 135.9 (C), 136.4 (2  $\times$  C), 151.3 (C), 154.5 (C, d,  $^1J_{\text{CF}}$  238.9 Hz), 155.4 (C, d,  $^4J_{\text{CF}}$  2.0 Hz), 158.2 (C), 170.8 (C);  $m/z$  (ESI) 431.1723 ( $\text{MNa}^+$ .  $\text{C}_{24}\text{H}_{25}\text{FN}_2\text{NaO}_3$  requires 431.1741).

**3-(2''-Fluoropyridin-3''-yl)-6-(mesitylamino)-2-methoxybenzamide (106)**

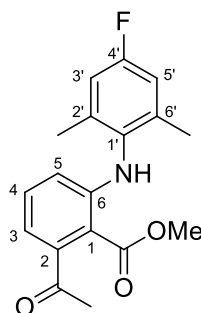


The reaction was carried out according to general procedure F using 3-bromo-6-(mesitylamino)-2-methoxybenzamide (**98**) (0.100 g, 0.275 mmol), 2-fluoropyridin-3-ylboronic acid (0.0620 g, 0.440 mmol), [1,1'-bis(diphenylphosphino)ferrocene]dichloropalladium(II) (1:1) (0.0113 g, 0.0138 mmol) and caesium carbonate (0.270 g, 0.825 mmol) in 1,4-dioxane (4.0 mL) and water (0.30 mL). The crude material was purified by flash column chromatography, eluting with 30% ethyl acetate in petroleum ether (40–60) followed by recrystallisation from diethyl ether to afford 3-(2''-fluoropyridin-3''-yl)-6-(mesitylamino)-2-methoxybenzamide (**106**) as a white solid (0.0190 g, 18%). Mp 214–216 °C;  $\nu_{\max}/\text{cm}^{-1}$  (neat) 3441 (NH), 3233 (NH), 3163 (CH), 1667 (CO), 1566 (C=C), 1427, 1258, 1034, 825, 756;  $\delta_{\text{H}}$  (400 MHz,  $\text{CDCl}_3$ ) 2.18 (6H, s, 2'-CH<sub>3</sub> and 6'-CH<sub>3</sub>), 2.31 (3H, s, 4'-CH<sub>3</sub>), 3.49 (3H, s, OCH<sub>3</sub>), 5.76 (1H, br s, NH), 6.10 (1H, br d, *J* 8.8 Hz, 5-H), 6.95 (2H, s, 3'-H and 5'-H), 7.06 (1H, dd, *J* 8.8, 1.3 Hz, 4-H), 7.23 (1H, ddd, *J* 7.3, 4.8, 1.7 Hz, 5''-H), 7.85 (1H, ddd, *J* 9.5, 7.3, 1.9 Hz, 6''-H), 7.93 (1H, br s, NH), 8.18 (1H, ddd, *J* 4.8, 1.9, 1.1 Hz, 4''-H), 9.77 (1H, br s, NH);  $\delta_{\text{C}}$  (101 MHz,  $\text{CDCl}_3$ ) 18.2 (2 × CH<sub>3</sub>), 21.0 (CH<sub>3</sub>), 61.9 (CH<sub>3</sub>), 106.5 (C), 109.5 (CH), 114.3 (C, d,  $^3J_{\text{CF}}$  4.5 Hz), 120.8 (C, d,  $^2J_{\text{CF}}$  30.4 Hz), 121.3 (CH, d,  $^4J_{\text{CF}}$  4.3 Hz), 129.2 (2 × CH), 134.7 (C), 134.7 (CH,  $^4J_{\text{CF}}$  2.1 Hz), 136.1 (C), 136.4 (2 × C), 142.3 (CH, d,  $^3J_{\text{CF}}$  4.4 Hz), 146.1 (CH, d,  $^3J_{\text{CF}}$  14.5 Hz), 151.7 (C), 158.3 (C), 160.9 (C, d,  $^1J_{\text{CF}}$  239.5 Hz), 170.5 (C); *m/z* (ESI) 402.1578 (MNa<sup>+</sup>. C<sub>22</sub>H<sub>22</sub>FN<sub>3</sub>NaO<sub>2</sub> requires 402.1588).

**Methyl 2-bromo-6-[(4'-fluoro-2',6'-dimethylphenyl)amino]benzoate (108)**

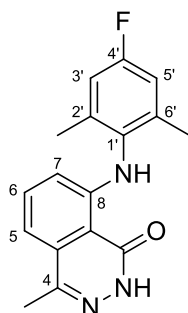


Trimethylsilyldiazomethane (0.0740 mL, 0.148 mmol, 2.0 M in diethyl ether) was added dropwise at 0 °C to a solution of 2-bromo-6-[(4'-fluoro-2',6'-dimethylphenyl)amino]benzoic acid (**75**) (1.52 g, 4.50 mmol) in methanol (20 mL) and tetrahydrofuran (60 mL) in an oven dried flask under argon. The reaction mixture was allowed to warm to room temperature and stirred for 24 h. Acetic acid (6.0 mL) was added and the reaction mixture stirred for 0.1 h. The mixture was diluted with ethyl acetate (20 mL) and the organic layer washed with water (20 mL), brine (20 mL) and saturated aqueous sodium bicarbonate (20 mL). The organic layer was dried (MgSO<sub>4</sub>) and concentrated *in vacuo* to afford a brown residue. The crude material was purified by flash column chromatography eluting with 2.5% ethyl acetate in petroleum ether (40–60) to afford methyl 2-bromo-6-[(4'-fluoro-2',6'-dimethylphenyl)amino]benzoate (**108**) as a brown solid (1.03 g, 65%). Mp 84–88 °C;  $\nu_{\max}/\text{cm}^{-1}$  (neat) 3379 (NH), 2955 (CH), 1697 (CO), 1566 (C=C), 1489, 1443, 1296, 1230, 1103, 895, 772;  $\delta_{\text{H}}$  (400 MHz, CDCl<sub>3</sub>) 2.16 (6H, s, 2'-CH<sub>3</sub> and 6'-CH<sub>3</sub>), 3.98 (3H, s, OCH<sub>3</sub>), 6.10 (1H, dd, *J* 7.4, 1.4 Hz, 5-H), 6.83 (2H, d, *J* 9.0 Hz, 3'-H and 5'-H), 6.90–6.98 (2H, m, 3-H and 4-H), 7.10 (1H, br s, NH);  $\delta_{\text{C}}$  (101 MHz, CDCl<sub>3</sub>) 18.3 (CH<sub>3</sub>), 18.4 (CH<sub>3</sub>), 52.1 (CH<sub>3</sub>), 111.5 (CH), 115.0 (2 × CH, d, <sup>2</sup>*J*<sub>CF</sub> 21.9 Hz), 116.8 (C), 122.3 (C), 122.7 (CH), 132.5 (CH), 132.8 (C, d, <sup>4</sup>*J*<sub>CF</sub> 2.8 Hz), 138.7 (2 × C, d, <sup>3</sup>*J*<sub>CF</sub> 8.7 Hz), 148.2 (C), 160.8 (C, d, <sup>1</sup>*J*<sub>CF</sub> 244.8 Hz), 168.3 (C); *m/z* (ESI) 374.0147 (MNa<sup>+</sup>. C<sub>16</sub>H<sub>15</sub><sup>79</sup>BrFNNaO<sub>2</sub> requires 374.0162).

**Methyl 2-acetyl-6-[(4'-fluoro-2',6'-dimethylphenyl)amino]benzoate (110)**


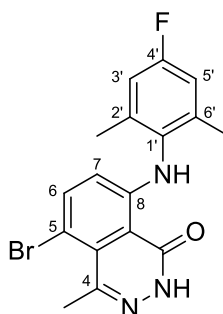
Methyl 2-bromo-6-[(4'-fluoro-2',6'-dimethylphenyl)amino]benzoate (**108**) (1.03 g, 2.92 mmol), tributyl(1-ethoxyvinyl)tin (1.48 mL, 4.39 mmol, 2.0 M in diethyl ether) and tetrakis(triphenylphosphine)palladium(0) (0.169 g, 0.146 mmol, 5 mol%) were added to 1,4-dioxane (14 mL) in an oven dried flask under argon. The reaction mixture was stirred at 90 °C for 5 h before further addition of tetrakis(triphenylphosphine)palladium(0) (0.169 g, 0.146 mmol, 5 mol%). The mixture was stirred for a further 18 h. The reaction mixture was filtered through Celite<sup>®</sup>, diluted with ethyl acetate (20 mL) and washed with water (20 mL), brine (20 mL) and saturated aqueous sodium bicarbonate (20 mL). The organic layer was dried (MgSO<sub>4</sub>) and concentrated *in vacuo* to afford a yellow residue. The residue was dissolved in tetrahydrofuran (14 mL) and a 1.0 M aqueous solution of hydrochloric acid (7.0 mL) was added. The mixture was stirred at room temperature for 18 h before being concentrated *in vacuo*. The crude material was purified by flash column chromatography eluting with 10% ethyl acetate in petroleum ether (40–60) to afford a yellow oil. The product was further purified by flash column chromatography using 10% potassium carbonate (w/w) in silica, eluting with 10% ethyl acetate in petroleum ether (40–60) to afford methyl 2-acetyl-6-[(4'-fluoro-2',6'-dimethylphenyl)amino]benzoate (**110**) as a yellow solid (0.830 g, 90%). Mp 222–226 °C;  $\nu_{\max}/\text{cm}^{-1}$  (neat) 3338 (NH), 2952 (CH), 1689 (CO), 1606 (C=C), 1496, 1464, 1436, 1304, 1259, 1238, 1180, 1138, 1019, 807;  $\delta_{\text{H}}$  (400 MHz, CDCl<sub>3</sub>) 2.16 (6H, s, 2'-CH<sub>3</sub> and 6'-CH<sub>3</sub>), 2.49 (3H, s, COCH<sub>3</sub>), 3.87 (3H, s, OCH<sub>3</sub>), 6.23 (1H, dd, *J* 8.5, 1.0 Hz, 5-H), 6.58 (1H, dd, *J* 7.3, 1.0 Hz, 3-H), 6.84 (2H, d, *J* 9.0 Hz, 3'-H and 5'-H), 7.19 (1H, ddd, *J* 8.5, 7.3, 0.5 Hz, 4-H), 8.43 (1H, br s, NH);  $\delta_{\text{C}}$  (101 MHz, CDCl<sub>3</sub>) 18.4 (CH<sub>3</sub>), 18.4 (CH<sub>3</sub>), 30.3 (CH<sub>3</sub>), 51.9 (CH<sub>3</sub>), 107.9 (C), 114.0 (CH), 114.1 (CH), 115.0 (2 × CH, d, <sup>2</sup>*J*<sub>CF</sub> 21.9 Hz), 132.6 (C, d, <sup>4</sup>*J*<sub>CF</sub> 2.8 Hz), 133.4 (CH), 139.0 (2 × C, d, <sup>3</sup>*J*<sub>CF</sub> 8.7 Hz), 145.8 (C), 149.2 (C), 160.9 (C, d, <sup>1</sup>*J*<sub>CF</sub> 245.1 Hz), 168.4 (C), 203.7 (C); *m/z* (ESI) 338.1151 (MNa<sup>+</sup>. C<sub>18</sub>H<sub>18</sub>FNNaO<sub>3</sub> requires 338.1163).

**8-[(4'-Fluoro-2',6'-dimethylphenyl)amino]-4-methyl-1(2*H*)-phthalazinone (111)**



To a solution of methyl 2-acetyl-6-[(4'-fluoro-2',6'-dimethylphenyl)amino]benzoate (**110**) (0.830 g, 2.63 mmol) in ethanol (15 mL) was added hydrazine monohydrate (0.260 mL, 5.26 mmol). The reaction mixture was stirred at 95 °C for 16 h and then cooled to room temperature. The reaction mixture was concentrated *in vacuo* to afford 8-[(4'-fluoro-2',6'-dimethylphenyl)amino]-4-methyl-1(2*H*)-phthalazinone (**111**) as a yellow solid (0.696 g, 89%). Mp 120–124 °C;  $\nu_{\max}/\text{cm}^{-1}$  (neat) 3257 (NH), 3052 (CH), 1640 (CO), 1606 (C=C), 1588, 1563, 1500, 1473, 1299, 1273, 810;  $\delta_{\text{H}}$  (400 MHz,  $\text{CDCl}_3$ ) 2.21 (6H, s, 2'- $\text{CH}_3$  and 6'- $\text{CH}_3$ ), 2.50 (3H, s, 4- $\text{CH}_3$ ), 6.30 (1H, dd,  $J$  8.4, 0.9 Hz, 7-H), 6.86 (2H, d,  $J$  9.0 Hz, 3'-H and 5'-H), 6.90 (1H, dd,  $J$  7.8, 0.9 Hz, 5-H), 7.44 (1H, dd,  $J$  8.4, 7.8 Hz, 6-H), 10.09 (1H, br s, NH), 10.16 (1H, br s, NH);  $\delta_{\text{C}}$  (101 MHz,  $\text{CDCl}_3$ ) 18.4 ( $\text{CH}_3$ ), 18.5 ( $\text{CH}_3$ ), 19.3 ( $\text{CH}_3$ ), 110.3 (C), 111.5 (CH), 112.1 (CH), 114.9 (2  $\times$  CH, d,  $^2J_{\text{CF}}$  21.8 Hz), 132.2 (C), 132.7 (C, d,  $^4J_{\text{CF}}$  2.8 Hz), 134.9 (CH), 139.1 (2  $\times$  C, d,  $^3J_{\text{CF}}$  8.7 Hz), 145.7 (C), 149.7 (C), 161.0 (C, d,  $^1J_{\text{CF}}$  244.9 Hz), 163.6 (C);  $m/z$  (ESI) 320.1161 ( $\text{MNa}^+$ .  $\text{C}_{17}\text{H}_{16}\text{FN}_3\text{NaO}$  requires 320.1170).

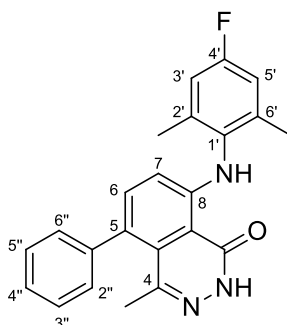
**5-Bromo-8-[(4'-fluoro-2',6'-dimethylphenyl)amino]-4-methyl-1(2*H*)-phthalazinone (114)**



The reaction was carried out according to general procedure E using iron(III) chloride (0.0190 g, 0.117 mmol), [BMIM]NTf<sub>2</sub> (1.36 mL, 4.68 mmol), 8-[(4'-fluoro-2',6'-dimethylphenyl)amino]-4-methyl-1(2*H*)-phthalazinone (**111**) (0.695 g, 2.34 mmol) and *N*-bromosuccinimide (0.980 g, 5.49 mmol) in dichloromethane (6.0 mL). The crude material was purified by flash column chromatography, eluting with 5% ethyl acetate in dichloromethane to afford 5-bromo-8-[(4'-fluoro-2',6'-dimethylphenyl)amino]-4-methyl-

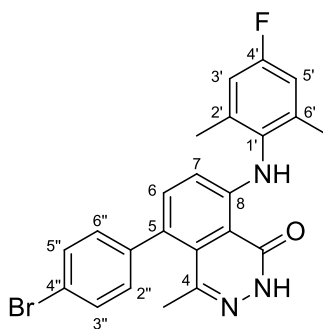
1(2*H*)-phthalazinone (**114**) as a white solid (0.695 g, 94%). Mp 200–204 °C;  $\nu_{\max}/\text{cm}^{-1}$  (neat) 3242 (NH), 3012 (CH), 1636 (CO), 1484, 1314, 1274, 1216, 1128, 1020, 819, 753;  $\delta_{\text{H}}$  (400 MHz,  $\text{CDCl}_3$ ) 2.19 (6H, s, 2'- $\text{CH}_3$  and 6'- $\text{CH}_3$ ), 2.89 (3H, s, 4- $\text{CH}_3$ ), 6.15 (1H, d,  $J$  9.1 Hz, 7-H), 6.86 (2H, d,  $J$  9.0 Hz, 3'-H and 5'-H), 7.64 (1H, d,  $J$  9.1 Hz, 6-H), 10.59 (1H, br s, NH), 10.99 (1H, br s, NH);  $\delta_{\text{C}}$  (101 MHz,  $\text{CDCl}_3$ ) 18.4 ( $\text{CH}_3$ ), 18.4 ( $\text{CH}_3$ ), 26.1 ( $\text{CH}_3$ ), 103.1 (C), 112.3 (C), 113.4 (CH), 115.1 (2  $\times$  CH, d,  $^2J_{\text{CF}}$  21.9 Hz), 130.8 (C), 132.3 (C, d,  $^4J_{\text{CF}}$  2.9 Hz), 139.0 (2  $\times$  C, d,  $^3J_{\text{CF}}$  8.7 Hz), 142.0 (CH), 144.9 (C), 149.8 (C), 161.1 (C, d,  $^1J_{\text{CF}}$  245.4 Hz), 163.3 (C);  $m/z$  (ESI) 398.0269 ( $\text{MNa}^+$ .  $\text{C}_{17}\text{H}_{15}^{79}\text{BrFN}_3\text{NaO}$  requires 398.0275).

### 5-Phenyl-8-[(4'-fluoro-2',6'-dimethylphenyl)amino]-4-methyl-1(2*H*)-phthalazinone (**115**)



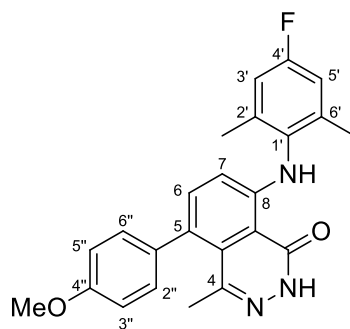
The reaction was carried out according to general procedure F using 5-bromo-8-[(4'-fluoro-2',6'-dimethylphenyl)amino]-4-methyl-1(2*H*)-phthalazinone (**114**) (0.100 g, 0.266 mmol), benzenboronic acid (0.0518 g, 0.425 mmol), [1,1'-bis(diphenylphosphino)ferrocene]dichloropalladium(II) (1:1) (0.0109 g, 0.0133 mmol) and caesium carbonate (0.260 g, 0.798 mmol) in 1,4-dioxane (4.0 mL) and water (0.30 mL). The crude material was purified by flash column chromatography, eluting with 20% ethyl acetate in petroleum ether (40–60) to afford 5-phenyl-8-[(4'-fluoro-2',6'-dimethylphenyl)amino]-4-methyl-1(2*H*)-phthalazinone (**115**) as a white solid (0.073 g, 74%). Mp 280–284 °C;  $\nu_{\max}/\text{cm}^{-1}$  (neat) 3246 (NH), 3021 (CH), 1639 (CO), 1485, 1256, 1128, 1018, 758, 702;  $\delta_{\text{H}}$  (400 MHz,  $\text{CDCl}_3$ ) 1.84 (3H, s, 4- $\text{CH}_3$ ), 2.24 (6H, s, 2'- $\text{CH}_3$  and 6'- $\text{CH}_3$ ), 6.30 (1H, d,  $J$  8.6 Hz, 7-H), 6.88 (2H, d,  $J$  9.1 Hz, 3'-H and 5'-H), 7.09–7.31 (3H, m, 6-H, 3''-H and 5''-H), 7.35–7.61 (3H, m, 2''-H, 4''-H and 6''-H), 10.21 (1H, br s, NH), 10.47 (1H, br s, NH);  $\delta_{\text{C}}$  (101 MHz,  $\text{CDCl}_3$ ) 18.5 ( $\text{CH}_3$ ), 18.5 ( $\text{CH}_3$ ), 24.8 ( $\text{CH}_3$ ), 110.5 (C), 111.3 (CH), 115.0 (2  $\times$  CH, d,  $^2J_{\text{CF}}$  21.8 Hz), 127.3 (CH), 127.4 (C), 127.9 (2  $\times$  CH), 130.0 (2  $\times$  CH), 129.8 (C), 132.8 (C, d,  $^4J_{\text{CF}}$  2.8 Hz), 138.5 (CH), 139.1 (2  $\times$  C, d,  $^3J_{\text{CF}}$  8.7 Hz), 142.7 (C), 145.9 (C), 149.4 (C), 160.9 (C, d,  $^1J_{\text{CF}}$  244.9 Hz), 163.6 (C);  $m/z$  (ESI) 396.1471 ( $\text{MNa}^+$ .  $\text{C}_{23}\text{H}_{20}\text{FN}_3\text{NaO}$  requires 396.1483).

**5-(4''-Bromophenyl)-8-[(4'-fluoro-2',6'-dimethylphenyl)amino]-4-methyl-1(2H)-phthalazinone (116)**



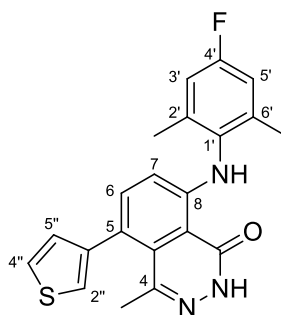
The reaction was carried out according to general procedure F using 5-bromo-8-[(4'-fluoro-2',6'-dimethylphenyl)amino]-4-methyl-1(2H)-phthalazinone (**114**) (0.043 g, 0.16 mmol), 4-bromophenylboronic acid (0.050 g, 0.25 mmol), [1,1'-bis(diphenylphosphino)ferrocene]dichloropalladium(II) (1:1) (0.0064 g, 0.0078 mmol) and caesium carbonate (0.15 g, 0.47 mmol) in 1,4-dioxane (2.0 mL) and water (0.2 mL). The crude material was purified by flash column chromatography, eluting with 10–15% ethyl acetate in petroleum ether (40–60) to afford 5-(4''-bromophenyl)-8-[(4'-fluoro-2',6'-dimethylphenyl)amino]-4-methyl-1(2H)-phthalazinone (**116**) as a yellow viscous oil (0.015 g, 21%).  $\nu_{\max}/\text{cm}^{-1}$  (neat) 3256 (NH), 3013 (CH), 1643 (CO), 1483, 1252, 1128, 1011, 819, 754;  $\delta_{\text{H}}$  (400 MHz,  $\text{CDCl}_3$ ) 1.87 (3H, s, 4- $\text{CH}_3$ ), 2.23 (6H, s, 2'- $\text{CH}_3$  and 6'- $\text{CH}_3$ ), 6.29 (1H, d,  $J$  8.6 Hz, 7-H), 6.87 (2H, d,  $J$  9.0 Hz, 3'-H and 5'-H), 7.14 (2H, d,  $J$  7.6 Hz, 2''-H and 6''-H), 7.21 (1H, d,  $J$  8.6 Hz, 6-H), 7.51 (2H, d,  $J$  7.6 Hz, 3''-H and 5''-H), 10.28 (1H, br s, NH), 10.49 (1H, br s, NH);  $\delta_{\text{C}}$  (101 MHz,  $\text{CDCl}_3$ ) 18.5 ( $\text{CH}_3$ ), 18.5 ( $\text{CH}_3$ ), 25.1 ( $\text{CH}_3$ ), 110.6 (C), 111.4 (CH), 115.0 (2  $\times$  CH, d,  $^2J_{\text{CF}}$  21.8 Hz), 121.6 (C), 125.8 (C), 129.8 (C), 131.1 (2  $\times$  CH), 131.6 (2  $\times$  CH), 132.6 (C, d,  $^4J_{\text{CF}}$  2.9 Hz), 138.4 (CH), 139.1 (2  $\times$  C, d,  $^3J_{\text{CF}}$  8.7 Hz), 141.6 (C), 145.5 (C), 149.7 (C), 161.0 (C, d,  $^1J_{\text{CF}}$  245.0 Hz), 163.5 (C);  $m/z$  (ESI) 474.0568 ( $\text{MNa}^+$ .  $\text{C}_{23}\text{H}_{19}^{79}\text{BrFN}_3\text{NaO}$  requires 474.0588).

**5-(4''-Methoxyphenyl)-8-[(4'-fluoro-2',6'-dimethylphenyl)amino]-4-methyl-1(2H)-phthalazinone (117)**



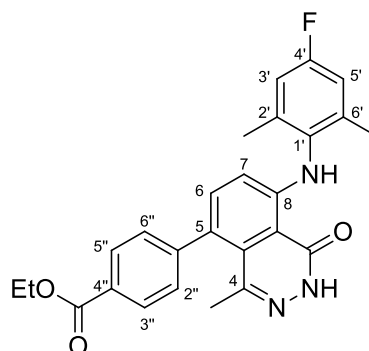
The reaction was carried out according to general procedure F using 5-bromo-8-[(4'-fluoro-2',6'-dimethylphenyl)amino]-4-methyl-1(2H)-phthalazinone (**114**) (0.100 g, 0.266 mmol), 4-methoxyphenylboronic acid (0.0646 g, 0.425 mmol), [1,1'-bis(diphenylphosphino)ferrocene]dichloropalladium(II) (1:1) (0.0119 g, 0.0133 mmol) and caesium carbonate (0.260 g, 0.798 mmol) in 1,4-dioxane (4.0 mL) and water (0.3 mL). The crude material was purified by flash column chromatography, eluting with 20% ethyl acetate in petroleum ether (40–60) to afford 5-(4''-methoxyphenyl)-8-[(4'-fluoro-2',6'-dimethylphenyl)amino]-4-methyl-1(2H)-phthalazinone (**117**) as a pale yellow solid (0.127 g, 79%). Mp 222–226 °C;  $\nu_{\max}/\text{cm}^{-1}$  (neat) 3163 (NH), 2995 (CH), 1637 (CO), 1494 (C=C), 1292, 1250, 1030, 862, 760;  $\delta_{\text{H}}$  (400 MHz,  $\text{CDCl}_3$ ) 1.86 (3H, s, 4- $\text{CH}_3$ ), 2.24 (6H, s, 2'- $\text{CH}_3$  and 6'- $\text{CH}_3$ ), 3.86 (3H, s,  $\text{OCH}_3$ ), 6.28 (1H, d,  $J$  8.6 Hz, 7-H), 6.87 (2H, d,  $J$  9.0 Hz, 3'-H and 5'-H), 6.91 (2H, d,  $J$  7.4 Hz, 3''-H and 5''-H), 7.16 (2H, d,  $J$  7.4 Hz, 2''-H and 6''-H), 7.25 (1H, d,  $J$  8.6 Hz, 6-H), 10.07 (1H, br s, NH), 10.45 (1H, br s, NH);  $\delta_{\text{C}}$  (101 MHz,  $\text{CDCl}_3$ ) 18.5 ( $\text{CH}_3$ ), 18.5 ( $\text{CH}_3$ ), 24.8 ( $\text{CH}_3$ ), 55.3 ( $\text{CH}_3$ ), 110.5 (C), 111.4 (CH), 113.4 (2  $\times$  CH), 115.0 (2  $\times$  CH, d,  $^2J_{\text{CF}}$  21.8 Hz), 127.1 (C), 130.0 (C), 131.0 (2  $\times$  CH), 132.8 (C, d,  $^4J_{\text{CF}}$  2.8 Hz), 134.9 (C), 138.8 (CH), 139.1 (2  $\times$  C, d,  $^3J_{\text{CF}}$  8.7 Hz), 146.1 (C), 149.3 (C), 159.0 (C), 160.9 (C, d,  $^1J_{\text{CF}}$  244.8 Hz), 163.6 (C);  $m/z$  (ESI) 426.1575 ( $\text{MNa}^+$ .  $\text{C}_{24}\text{H}_{22}\text{FN}_3\text{NaO}_2$  requires 426.1588).

**5-(Thiophen-3''-yl)-8-[(4'-fluoro-2',6'-dimethylphenyl)amino]-4-methyl-1(2H)-phthalazinone (118)**



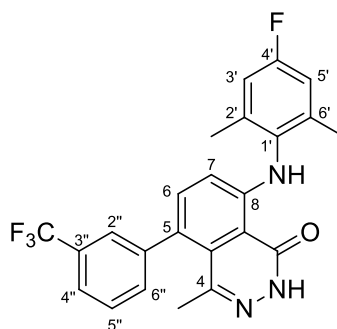
The reaction was carried out according to general procedure F using 5-bromo-8-[(4'-fluoro-2',6'-dimethylphenyl)amino]-4-methyl-1(2H)-phthalazinone (**114**) (0.100 g, 0.266 mmol), 3-thienylboronic acid (0.0544 g, 0.425 mmol), [1,1'-bis(diphenylphosphino)ferrocene]dichloropalladium(II) (1:1) (0.0119 g, 0.0133 mmol) and caesium carbonate (0.260 g, 0.798 mmol) in 1,4-dioxane (4.0 mL) and water (0.3 mL). The crude material was purified by flash column chromatography, eluting with 5% ethyl acetate in dichloromethane to afford 5-(thiophen-3''-yl)-8-[(4'-fluoro-2',6'-dimethylphenyl)amino]-4-methyl-1(2H)-phthalazinone (**118**) as a pale yellow solid (0.079 g, 79%). Mp 279–281 °C;  $\nu_{\max}/\text{cm}^{-1}$  (neat) 3158 (NH), 3019 (NH), 2920 (CH), 1638 (CO), 1499, 1261, 837, 770, 675;  $\delta_{\text{H}}$  (400 MHz,  $\text{CDCl}_3$ ) 1.94 (3H, s, 4- $\text{CH}_3$ ), 2.23 (6H, s, 2'- $\text{CH}_3$  and 6'- $\text{CH}_3$ ), 6.28 (1H, d,  $J$  8.6 Hz, 7-H), 6.87 (2H, d,  $J$  9.0 Hz, 3'-H and 5'-H), 7.02 (1H, dd,  $J$  4.9, 1.3 Hz, 4''-H), 7.11 (1H, dd,  $J$  3.0, 1.3 Hz, 2''-H), 7.28 (1H, d,  $J$  8.6 Hz, 6-H), 7.34 (1H, dd,  $J$  4.9, 3.0 Hz, 5''-H), 10.02 (1H, br s, NH), 10.48 (1H, br s, NH);  $\delta_{\text{C}}$  (101 MHz,  $\text{CDCl}_3$ ) 18.5 ( $\text{CH}_3$ ), 18.5 ( $\text{CH}_3$ ), 23.6 ( $\text{CH}_3$ ), 110.6 (C), 111.3 (CH), 115.0 (CH, d,  $^2J_{\text{CF}}$  21.8 Hz), 121.6 (C), 123.5 (CH), 125.0 (CH), 130.2 (CH), 130.5 (C), 132.7 (C, d,  $^4J_{\text{CF}}$  2.8 Hz), 138.7 (CH), 139.1 (C, d,  $^3J_{\text{CF}}$  8.7 Hz), 142.3 (C), 145.9 (C), 149.6 (C), 161.0 (C, d,  $^1J_{\text{CF}}$  244.9 Hz), 163.5 (C);  $m/z$  (EI) 379.1151 ( $\text{M}^+$ .  $\text{C}_{21}\text{H}_{18}\text{FN}_3\text{OS}$  requires 379.1155) 364 (7%), 226 (5).

**5-(4''-Ethoxycarbonylphenyl)-8-[(4'-fluoro-2',6'-dimethylphenyl)amino]-4-methyl-1(2*H*)-phthalazinone (119)**



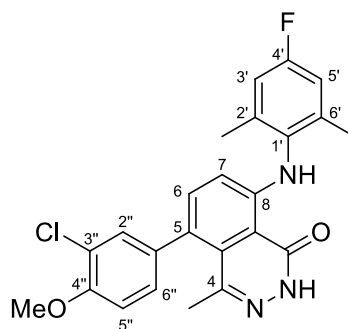
The reaction was carried out according to general procedure F using 5-bromo-8-[(4'-fluoro-2',6'-dimethylphenyl)amino]-4-methyl-1(2*H*)-phthalazinone (**114**) (0.065 g, 0.17 mmol), 4-ethoxycarbonylphenylboronic acid (0.054 g, 0.28 mmol), [1,1'-bis(diphenylphosphino)ferrocene]dichloropalladium(II) (1:1) (0.0074 g, 0.0090 mmol) and caesium carbonate (0.17 g, 0.52 mmol) in 1,4-dioxane (3.0 mL) and water (0.2 mL). The crude material was purified by flash column chromatography, eluting with 5% ethyl acetate in dichloromethane to afford 5-(4''-ethoxycarbonylphenyl)-8-[(4'-fluoro-2',6'-dimethylphenyl)amino]-4-methyl-1(2*H*)-phthalazinone (**119**) as a pale yellow solid (0.034 g, 44%). Mp 206–208 °C;  $\nu_{\max}/\text{cm}^{-1}$  (neat) 3198 (NH), 2924 (CH), 1717 (CO), 1639 (CO), 1495, 1271, 1101, 1020, 775;  $\delta_{\text{H}}$  (400 MHz,  $\text{CDCl}_3$ ) 1.42 (3H, t,  $J$  7.1 Hz,  $\text{OCH}_2\text{CH}_3$ ), 1.85 (3H, s, 4- $\text{CH}_3$ ), 2.24 (6H, s, 2'- $\text{CH}_3$  and 6'- $\text{CH}_3$ ), 4.41 (2H, q,  $J$  7.1 Hz,  $\text{OCH}_2\text{CH}_3$ ), 6.31 (1H, d,  $J$  8.6 Hz, 7-H), 6.88 (2H, d,  $J$  9.0 Hz, 3'-H and 5'-H), 7.24 (1H, d,  $J$  8.6 Hz, 6-H), 7.36 (2H, d,  $J$  8.0 Hz, 2''-H and 6''-H), 8.07 (2H, d,  $J$  8.0 Hz, 3''-H and 5''-H), 10.53 (1H, br s, NH), 10.60 (1H, br s, NH);  $\delta_{\text{C}}$  (101 MHz,  $\text{CDCl}_3$ ) 14.4 ( $\text{CH}_3$ ), 18.5 ( $\text{CH}_3$ ), 18.5 ( $\text{CH}_3$ ), 25.0 ( $\text{CH}_3$ ), 61.1 ( $\text{CH}_2$ ), 110.6 (C), 111.3 (CH), 115.0 (2  $\times$  CH, d,  $^2J_{\text{CF}}$  21.8 Hz), 126.0 (C), 129.2 (2  $\times$  CH), 129.5 (C), 129.8 (C), 130.0 (2  $\times$  CH), 132.6 (C, d,  $^4J_{\text{CF}}$  2.8 Hz), 138.2 (CH), 139.1 (2  $\times$  C, d,  $^3J_{\text{CF}}$  8.7 Hz), 145.5 (C), 147.4 (C), 149.8 (C), 161.0 (C, d,  $^1J_{\text{CF}}$  245.1 Hz), 163.6 (C), 166.4 (C);  $m/z$  (ESI) 468.1673 ( $\text{MNa}^+$ .  $\text{C}_{26}\text{H}_{24}\text{FN}_3\text{NaO}_3$  requires 468.1694).

**5-[3''-(Trifluoromethyl)phenyl]-8-[(4'-fluoro-2',6'-dimethylphenyl)amino]-4-methyl-1(2*H*)-phthalazinone (**120**)**



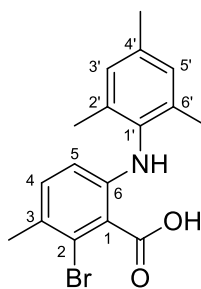
The reaction was carried out according to general procedure F using 5-bromo-8-[(4'-fluoro-2',6'-dimethylphenyl)amino]-4-methyl-1(2*H*)-phthalazinone (**114**) (0.060 g, 0.16 mmol), 3-(trifluoromethyl)phenylboronic acid (0.048 g, 0.26 mmol), [1,1'-bis(diphenylphosphino)ferrocene]dichloropalladium(II) (1:1) (0.0065 g, 0.0080 mmol) and caesium carbonate (0.16 g, 0.48 mmol) in 1,4-dioxane (2.0 mL) and water (0.2 mL). The crude material was purified by flash column chromatography, eluting with 20% ethyl acetate in petroleum ether (40–60) to afford 5-[3''-(trifluoromethyl)phenyl]-8-[(4'-fluoro-2',6'-dimethylphenyl)amino]-4-methyl-1(2*H*)-phthalazinone (**120**) as a pale yellow solid (0.034 g, 49%). Mp 104–106 °C;  $\nu_{\max}/\text{cm}^{-1}$  (neat) 3190 (NH), 2924 (CH), 1639 (CO), 1485, 1329, 1167, 1128, 714;  $\delta_{\text{H}}$  (400 MHz,  $\text{CDCl}_3$ ) 1.81 (3H, s, 4- $\text{CH}_3$ ), 2.25 (6H, s, 2'- $\text{CH}_3$  and 6'- $\text{CH}_3$ ), 6.31 (1H, d,  $J$  8.6 Hz, 7-H), 6.88 (2H, d,  $J$  9.0 Hz, 3'-H and 5'-H), 7.24 (1H, d,  $J$  8.6 Hz, 6-H), 7.45–7.54 (2H, m, 5''-H and 6''-H), 7.55 (1H, s, 2''-H), 7.64 (1H, d,  $J$  7.4 Hz, 4''-H), 10.69 (1H, br s, NH), 10.55 (1H, br s, NH);  $\delta_{\text{C}}$  (101 MHz,  $\text{CDCl}_3$ ) 18.5 (2  $\times$   $\text{CH}_3$ ), 25.2 ( $\text{CH}_3$ ), 110.6 (C), 111.3 (CH), 115.0 (CH, d,  $^2J_{\text{CF}}$  21.9 Hz), 115.1 (CH, d,  $^2J_{\text{CF}}$  21.9 Hz), 124.0 (C, q,  $^1J_{\text{CF}}$  272.5 Hz), 124.1 (CH, q,  $^3J_{\text{CF}}$  3.8 Hz), 125.3 (C), 126.8 (CH, q,  $^3J_{\text{CF}}$  3.8 Hz), 128.5 (CH), 129.9 (C), 130.4 (C, q,  $^2J_{\text{CF}}$  32.5 Hz), 132.5 (C, d,  $^4J_{\text{CF}}$  2.8 Hz), 133.2 (CH), 138.4 (CH), 139.0 (C, d,  $^3J_{\text{CF}}$  8.7 Hz), 139.1 (C, d,  $^3J_{\text{CF}}$  8.7 Hz), 143.4 (C), 145.2 (C), 149.9 (C), 161.0 (C, d,  $^1J_{\text{CF}}$  245.1 Hz), 163.7 (C);  $m/z$  (ESI) 464.1341 ( $\text{MNa}^+$ .  $\text{C}_{24}\text{H}_{19}\text{F}_4\text{N}_3\text{NaO}$  requires 464.1356).

**5-(3''-Chloro-4''-methoxyphenyl)-8-[(4'-fluoro-2',6'-dimethylphenyl)amino]-4-methyl-1(2H)-phthalazinone (121)**



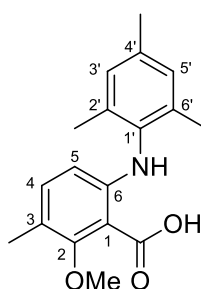
The reaction was carried out according to general procedure F using 5-bromo-8-[(4'-fluoro-2',6'-dimethylphenyl)amino]-4-methyl-1(2H)-phthalazinone (**114**) (0.055 g, 0.15 mmol), 3-chloro-4-methoxyphenylboronic acid (0.044 g, 0.23 mmol), [1,1'-bis(diphenylphosphino)ferrocene]dichloropalladium(II) (1:1) (0.0060 g, 0.0073 mmol) and caesium carbonate (0.14 g, 0.44 mmol) in 1,4-dioxane (2.0 mL) and water (0.2 mL). The crude material was purified by flash column chromatography, eluting with 20% ethyl acetate in petroleum ether (40–60) to afford 5-(3''-chloro-4''-methoxyphenyl)-8-[(4'-fluoro-2',6'-dimethylphenyl)amino]-4-methyl-1(2H)-phthalazinone (**121**) as a pale yellow solid (0.043 g, 66%). Mp 217–219 °C;  $\nu_{\max}/\text{cm}^{-1}$  (neat) 3183 (NH), 3009 (NH), 2926 (CH), 1638 (CO), 1487, 1285, 1250, 1064, 756;  $\delta_{\text{H}}$  (400 MHz,  $\text{CDCl}_3$ ) 1.90 (3H, s, 4- $\text{CH}_3$ ), 2.24 (6H, s, 2'- $\text{CH}_3$  and 6'- $\text{CH}_3$ ), 3.95 (3H, s,  $\text{OCH}_3$ ), 6.28 (1H, d,  $J$  8.6 Hz, 7-H), 6.87 (2H, d,  $J$  9.0 Hz, 3'-H and 5'-H), 6.94 (1H, d,  $J$  8.4 Hz, 5''-H), 7.11 (1H, dd,  $J$  8.4, 2.2 Hz, 6''-H), 7.23 (1H, d,  $J$  8.6 Hz, 6-H), 7.29 (1H, d,  $J$  2.2 Hz, 2''-H), 10.50 (1H, br s, NH), 10.60 (1H, br s, NH);  $\delta_{\text{C}}$  (101 MHz,  $\text{CDCl}_3$ ) 18.5 ( $\text{CH}_3$ ), 18.5 ( $\text{CH}_3$ ), 25.1 ( $\text{CH}_3$ ), 56.2 ( $\text{CH}_3$ ), 110.5 (C), 111.3 (CH), 111.4 (CH), 115.0 (CH, d,  $^2J_{\text{CF}}$  21.8 Hz), 115.0 (CH, d,  $^2J_{\text{CF}}$  21.8 Hz), 121.9 (C), 125.4 (C), 129.2 (CH), 130.0 (C), 131.6 (CH), 132.7 (C, d,  $^4J_{\text{CF}}$  2.8 Hz), 135.8 (C), 138.7 (CH), 139.0 (C, d,  $^3J_{\text{CF}}$  8.5 Hz), 139.1 (C, d,  $^3J_{\text{CF}}$  8.5 Hz), 145.6 (C), 149.6 (C), 154.4 (C), 161.0 (C, d,  $^1J_{\text{CF}}$  245.0 Hz), 163.7 (C);  $m/z$  (ESI) 460.1185 ( $\text{MNa}^+$ ).  $\text{C}_{24}\text{H}_{21}^{35}\text{ClFN}_3\text{NaO}_2$  requires 460.1199).

### 2-Bromo-6-(mesitylamino)-3-methylbenzoic acid (**122**)<sup>95</sup>



The reaction was carried out according to general procedure B using 2-bromo-6-fluoro-3-methylbenzoic acid (**77**) (2.00 g, 8.58 mmol) and 2,4,6-trimethylaniline (2.60 mL, 17.2 mmol) in tetrahydrofuran (50 mL), followed by treatment with lithium bis(trimethylsilyl)amide (25.7 mL, 25.7 mmol, 1.0 M in tetrahydrofuran). The crude material was purified by flash column chromatography, eluting with 20–40% ethyl acetate in petroleum ether (40–60) to afford 2-bromo-6-(mesitylamino)-3-methylbenzoic acid (**122**) as a brown solid (2.93 g, 98%). The spectroscopic data were consistent with the literature.<sup>95</sup> Mp 142–144 °C;  $\delta_{\text{H}}$  (400 MHz,  $\text{CDCl}_3$ ) 2.17 (6H, s, 2'- $\text{CH}_3$  and 6'- $\text{CH}_3$ ), 2.33 (6H, br s, 3- $\text{CH}_3$  and 4'- $\text{CH}_3$ ), 6.14 (1H, d,  $J$  8.5 Hz, 5-H), 6.96 (2H, s, 3'-H and 5'-H), 7.00 (1H, d,  $J$  8.5 Hz, 4-H), 9.26 (1H, br s, OH);  $\delta_{\text{C}}$  (101 MHz,  $\text{CDCl}_3$ ) 18.1 (2  $\times$   $\text{CH}_3$ ), 20.9 ( $\text{CH}_3$ ), 22.9 ( $\text{CH}_3$ ), 112.2 (CH), 117.3 (C), 123.9 (C), 127.5 (C), 129.3 (2  $\times$  CH), 133.7 (CH), 134.5 (C), 135.9 (2  $\times$  C), 135.9 (C), 146.1 (C), 173.4 (C);  $m/z$  (ESI) 370 ( $\text{MNa}^+$ , 100%).

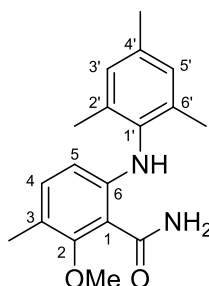
### 6-(Mesitylamino)-2-methoxy-3-methylbenzoic acid (**123**)<sup>95</sup>



The reaction was carried out according to general procedure C using sodium hydride (0.474 g, 11.8 mmol, 60% in mineral oil), methanol (10 mL), 2-bromo-6-(mesitylamino)-3-methylbenzoic acid (**122**) (0.820 g, 2.37 mmol) and copper powder (0.0602 g, 0.947 mmol). The crude material was purified by flash column chromatography, eluting with 20% ethyl acetate in petroleum ether (40–60) to afford 6-(mesitylamino)-2-methoxy-3-methylbenzoic acid (**123**) as an orange solid (0.695 g, 98%). The spectroscopic data were consistent with the literature.<sup>95</sup> Mp 97–99 °C;  $\delta_{\text{H}}$  (400 MHz,  $\text{CDCl}_3$ ) 2.12 (6H, s, 2'- $\text{CH}_3$  and

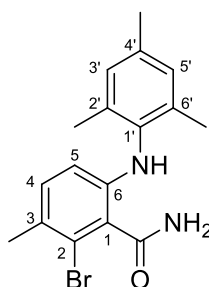
6'-CH<sub>3</sub>), 2.19 (3H, s, 3-CH<sub>3</sub>), 2.30 (3H, s, 4'-CH<sub>3</sub>), 3.92 (3H, s, OCH<sub>3</sub>), 6.02 (1H, d, *J* 8.8 Hz, 5-H), 6.94 (2H, s, 3'-H and 5'-H), 6.99 (1H, d, *J* 8.8 Hz, 4-H), 9.48 (1H, br s, NH), 12.06 (1H, br s, OH);  $\delta_{\text{C}}$  (101 MHz, CDCl<sub>3</sub>) 15.1 (CH<sub>3</sub>), 18.1 (2 × CH<sub>3</sub>), 21.0 (CH<sub>3</sub>), 62.2 (CH<sub>3</sub>), 102.0 (C), 110.1 (CH), 116.0 (C), 129.2 (2 × CH), 134.5 (C), 136.3 (C), 136.6 (2 × C), 137.1 (CH), 150.6 (C), 158.2 (C), 168.6 (C); *m/z* (ESI) 322 (MNa<sup>+</sup>, 100%).

### 6-(Mesitylamino)-2-methoxy-3-methylbenzamide (**33**)<sup>95</sup>



The reaction was carried out according to general procedure D using 6-(mesitylamino)-2-methoxy-3-methylbenzoic acid (**123**) (0.690 g, 2.30 mmol), 2-chloro-4,6-dimethoxy-1,3,5-triazine (0.485 g, 2.76 mmol) and *N*-methylmorpholine (0.759 mL, 6.90 mmol) in tetrahydrofuran (11 mL). The crude material was purified by flash column chromatography, eluting with 10% ethyl acetate in petroleum ether (40–60) to afford 6-(mesitylamino)-2-methoxy-3-methylbenzamide (**33**) as a white solid (0.565 g, 82%). The spectroscopic data were consistent with the literature.<sup>95</sup> Mp 131–133 °C;  $\delta_{\text{H}}$  (400 MHz, CDCl<sub>3</sub>) 2.16 (6H, s, 2'-CH<sub>3</sub> and 6'-CH<sub>3</sub>), 2.17 (3H, s, 3-CH<sub>3</sub>), 2.31 (3H, s, 4'-CH<sub>3</sub>), 3.78 (3H, s, OCH<sub>3</sub>), 5.90 (1H, br s, NH), 5.97 (1H, d, *J* 8.6 Hz, 5-H), 6.89–6.97 (2H, m, 4-H, 3'-H and 5'-H), 7.93 (1H, br s, NH), 9.38 (1H, br s, OH);  $\delta_{\text{C}}$  (101 MHz, CDCl<sub>3</sub>) 15.2 (CH<sub>3</sub>), 18.2 (2 × CH<sub>3</sub>), 20.9 (CH<sub>3</sub>), 61.1 (CH<sub>3</sub>), 106.8 (C), 109.3 (CH), 117.3 (C), 129.0 (2 × CH), 134.9 (CH), 135.4 (C), 135.5 (C), 136.4 (2 × C), 149.3 (C), 158.1 (C), 170.9 (C); *m/z* (ESI) 321 (MNa<sup>+</sup>, 100%).

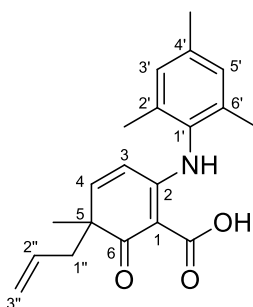
### 2-Bromo-6-(mesitylamino)-3-methylbenzamide (**127**)



The reaction was carried out according to general procedure D using 2-bromo-6-(mesitylamino)-3-methylbenzoic acid (**122**) (0.0500 g, 0.144 mmol), 2-chloro-4,6-

dimethoxy-1,3,5-triazine (0.0302 g, 0.172 mmol) and *N*-methylmorpholine (0.0474 mL, 0.431 mmol) in tetrahydrofuran (1.0 mL). The crude material was purified by flash column chromatography, eluting with 10% ethyl acetate in petroleum ether (40–60) to afford 2-bromo-6-(mesitylamino)-3-methylbenzamide (**127**) as a white solid (0.0499 g, 100%). Mp 138–140 °C;  $\nu_{\max}/\text{cm}^{-1}$  (neat) 3364 (NH), 2916 (CH), 1658 (CO), 1604 (C=C), 1489, 1257, 756;  $\delta_{\text{H}}$  (400 MHz,  $\text{CDCl}_3$ ) 2.13 (6H, s, 2'-CH<sub>3</sub> and 6'-CH<sub>3</sub>), 2.28 (6H, br s, 3-CH<sub>3</sub> and 4'-CH<sub>3</sub>), 6.07 (1H, d, *J* 8.4 Hz, 5-H), 6.10 (1H, br s, NH), 6.33 (1H, br s, NH), 6.49 (1H, br s, NH), 6.90 (2H, s, 3'-H and 5'-H), 6.92 (1H, d, *J* 8.4 Hz, 4-H);  $\delta_{\text{C}}$  (101 MHz,  $\text{CDCl}_3$ ) 18.1 (2 × CH<sub>3</sub>), 20.9 (CH<sub>3</sub>), 22.6 (CH<sub>3</sub>), 111.8 (CH), 121.6 (C), 122.7 (C), 126.7 (C), 129.2 (2 × CH), 132.0 (CH), 134.8 (C), 135.6 (C), 135.7 (2 × C), 144.1 (C), 170.5 (C); *m/z* (EI) 346.0688 (M<sup>+</sup>. C<sub>17</sub>H<sub>19</sub><sup>79</sup>BrN<sub>2</sub>O requires 346.0681), 329 (93%), 314 (52), 250 (69).

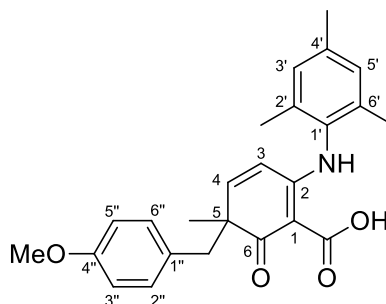
### 5-Allyl-2-(mesitylamino)-5-methyl-6-oxocyclohexa-1,3-dienecarboxylic acid (**126**)



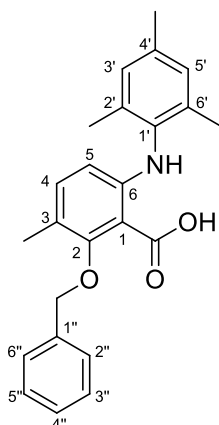
Sodium hydride (0.028 g, 0.72 mmol, 60% in mineral oil) was added to a dry flask under argon and cooled to 0 °C. Allyl alcohol (1.0 mL) was added to the reaction vessel dropwise over 0.1 h and then stirred for 0.5 h. 2-Bromo-6-(mesitylamino)-3-methylbenzamide (**122**) (0.050 g, 0.14 mmol) and copper powder (0.0040 g, 0.058 mmol) were then added and the reaction mixture stirred at 80 °C for 24 h. The reaction mixture was cooled to room temperature and filtered through a pad of Celite®. The filtrate was concentrated *in vacuo* and taken up in water (2 mL). The mixture was acidified to pH 2 using 10% aqueous hydrochloric acid and extracted with dichloromethane (3 × 10 mL). The organic layer was dried (MgSO<sub>4</sub>), filtered and concentrated *in vacuo*. The crude material was purified by flash column chromatography, eluting with 20% ethyl acetate in petroleum ether (40–60) to afford 5-allyl-2-(mesitylamino)-5-methyl-6-oxocyclohexa-1,3-dienecarboxylic acid (**126**) as a pale orange solid (0.036 g, 77%). Mp 99–100 °C;  $\nu_{\max}/\text{cm}^{-1}$  (neat) 3460 (OH), 2972 (CH), 2920 (NH), 1670 (CO), 1551 (C=C), 1441, 1414, 1381, 1209, 922, 827;  $\delta_{\text{H}}$  (400 MHz,  $\text{CDCl}_3$ ) 1.33 (3H, s, 5-CH<sub>3</sub>), 2.12 (3H, s, 2'-CH<sub>3</sub>), 2.15 (3H, s, 6'-CH<sub>3</sub>), 2.27 (1H, dd, *J* 13.4, 7.4 Hz, 1''-HH), 2.32 (3H, s, 4'-CH<sub>3</sub>), 2.73 (1H, dd, *J* 13.4, 7.4 Hz, 1''-HH), 4.99 (1H, br d, *J* 9.8 Hz, 3''-HH), 5.00 (1H, br d, *J* 17.2 Hz, 3''-HH), 5.50 (1H, ddt, *J* 17.2, 9.8, 7.4 Hz, 2''-H), 6.00 (1H, d, *J* 10.2 Hz, 3-H), 6.49 (1H, dd, *J* 10.2 Hz, 4-H), 6.96 (2H, s, 3'-H and 5'-H), 12.42 (1H, br s, NH), 15.79 (1H, s, OH);  $\delta_{\text{C}}$  (101

MHz, CDCl<sub>3</sub>) 18.2 (CH<sub>3</sub>), 18.2 (CH<sub>3</sub>), 21.0 (CH<sub>3</sub>), 24.9 (CH<sub>3</sub>), 44.7 (CH<sub>2</sub>), 48.5 (C), 95.3 (C), 115.9 (CH), 118.8 (CH<sub>2</sub>), 129.3 (CH), 129.4 (CH), 131.2 (C), 132.2 (CH), 134.9 (C), 135.0 (C), 138.6 (C), 153.4 (CH), 163.9 (C), 172.3 (C), 200.5 (C); *m/z* (EI) 325.1681 (M<sup>+</sup>. C<sub>20</sub>H<sub>23</sub>NO<sub>3</sub> requires 325.1678), 307 (72%), 281 (100), 266 (87), 238 (50), 91 (50).

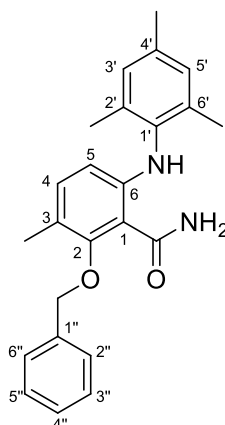
**2-(Mesitylamino)-5-(4''-methoxybenzyl)-5-methyl-6-oxocyclohexa-1,3-dienecarboxylic acid (130)**



To a suspension of sodium hydride (0.017 g, 0.43 mmol, 60% in mineral oil) in tetrahydrofuran (1.0 mL) at 0 °C under argon was added dropwise 4-methoxybenzyl alcohol (0.054 mL, 0.43 mmol) and the resulting solution stirred for 0.5 h. 2-Bromo-6-(mesitylamino)-3-methylbenzamide (**122**) (0.050 g, 0.14 mmol) and copper powder (0.0040 g, 0.058 mmol) were then added and the reaction mixture stirred at 80 °C for 24 h. The reaction mixture was cooled to room temperature and filtered through a pad of Celite®. The filtrate was concentrated *in vacuo* and water (2 mL) was added. The mixture was acidified to pH 2 using 10% aqueous hydrochloric acid and extracted with dichloromethane (3 × 10 mL). The organic layer was dried (MgSO<sub>4</sub>), filtered and concentrated *in vacuo*. The crude material was purified by flash column chromatography, eluting with 10% ethyl acetate in petroleum ether (40–60) to afford 2-(mesitylamino)-5-(4''-methoxybenzyl)-5-methyl-6-oxocyclohexa-1,3-dienecarboxylic acid (**130**) as a white solid (0.023 g, 40%). Mp 105–107 °C;  $\nu_{\max}/\text{cm}^{-1}$  (neat) 2926 (CH), 1667 (CO), 1557 (C=C), 1510, 1477, 1435, 1383, 1246, 1034, 827, 733;  $\delta_{\text{H}}$  (400 MHz, CDCl<sub>3</sub>) 1.41 (3H, s, 5-CH<sub>3</sub>), 1.66 (3H, s, 2'-CH<sub>3</sub>), 2.10 (3H, s, 6'-CH<sub>3</sub>), 2.29 (3H, s, 4'-CH<sub>3</sub>), 2.72 (1H, d, *J* 13.2 Hz, CHHAr), 3.35 (1H, d, *J* 13.2 Hz, CHHAr), 3.73 (3H, s, OCH<sub>3</sub>), 5.82 (1H, br d, *J* 10.1 Hz, 3-H), 6.52 (1H, dd, *J* 10.1 Hz, 4-H), 6.68 (2H, d, *J* 8.8 Hz, 3''-H and 5''-H), 6.85–6.93 (4H, m, 3'-H, 5'-H, 2''-H and 6''-H), 12.22 (1H, br s, NH), 15.93 (1H, s, OH);  $\delta_{\text{C}}$  (101 MHz, CDCl<sub>3</sub>) 17.6 (CH<sub>3</sub>), 18.1 (CH<sub>3</sub>), 21.0 (CH<sub>3</sub>), 25.0 (CH<sub>3</sub>), 46.5 (CH<sub>2</sub>), 50.0 (C), 55.2 (CH<sub>3</sub>), 96.0 (C), 113.3 (2 × CH), 116.1 (CH), 128.1 (C), 129.2 (CH), 129.2 (CH), 130.5 (2 × CH), 131.1 (C), 134.8 (C), 135.1 (C), 138.4 (C), 153.3 (CH), 158.5 (C), 163.8 (C), 172.2 (C), 200.5 (C); *m/z* (ESI) 428.1816 (MNa<sup>+</sup>. C<sub>25</sub>H<sub>27</sub>NNaO<sub>4</sub> requires 428.1832).

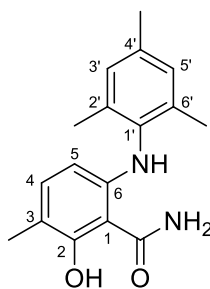
**2-(Benzyloxy)-6-(mesitylamino)-3-methylbenzoic acid (131)**

To a suspension of sodium hydride (1.15 g, 28.7 mmol) in tetrahydrofuran (16 mL) at 0 °C under argon was added dropwise benzyl alcohol (2.96 mL, 28.7 mmol) and the resulting solution stirred for 0.5 h. 2-Bromo-6-(mesitylamino)-3-methylbenzamide (**122**) (2.00 g, 5.74 mmol) and copper powder (0.146 g, 2.30 mmol) were then added and the reaction mixture stirred at 80 °C for 24 h. The reaction mixture was cooled to room temperature and filtered through a pad of Celite®. The filtrate was concentrated *in vacuo* and taken up in water (20 mL). The mixture was acidified to pH 2 using 10% aqueous hydrochloric acid and extracted with dichloromethane (3 × 30 mL). The organic layer was dried (MgSO<sub>4</sub>), filtered and concentrated *in vacuo*. The crude material was purified by flash column chromatography, eluting with 10% ethyl acetate in petroleum ether (40–60) to afford 2-(benzyloxy)-6-(mesitylamino)-3-methylbenzoic acid (**131**) as a brown solid (1.60 g, 74%). Mp 89–91 °C;  $\nu_{\max}/\text{cm}^{-1}$  (neat) 3294 (NH), 3032 (OH), 2916 (CH), 1697 (CO), 1501 (C=C), 1396, 1381, 1223, 814, 698;  $\delta_{\text{H}}$  (400 MHz, CDCl<sub>3</sub>) 2.13 (6H, s, 2'-CH<sub>3</sub> and 6'-CH<sub>3</sub>), 2.28 (3H, s, CH<sub>3</sub>), 2.31 (3H, s, CH<sub>3</sub>), 4.97 (2H, s, CH<sub>2</sub>Ph), 6.05 (1H, d, *J* 8.8 Hz, 5-H), 6.94 (2H, s, 3'-H and 5'-H), 7.03 (1H, d, *J* 8.8 Hz, 4-H), 7.36–7.58 (5H, m, Ph), 9.47 (1H, br s, NH), 12.09 (1H, br s, OH);  $\delta_{\text{C}}$  (101 MHz, CDCl<sub>3</sub>) 15.4 (CH<sub>3</sub>), 18.1 (2 × CH<sub>3</sub>), 21.0 (CH<sub>3</sub>), 77.6 (CH<sub>2</sub>), 102.7 (C), 110.2 (CH), 116.4 (C), 129.0 (2 × CH), 129.0 (2 × CH), 129.2 (2 × CH), 129.3 (CH), 134.4 (C), 134.4 (C), 136.3 (C), 136.6 (2 × C), 137.0 (CH), 150.6 (C), 156.6 (C), 168.6 (C); *m/z* (ESI) 398.1712 (MNa<sup>+</sup>. C<sub>24</sub>H<sub>25</sub>NNaO<sub>3</sub> requires 398.1727).

**2-(Benzyloxy)-6-(mesitylamino)-3-methylbenzamide (132)**

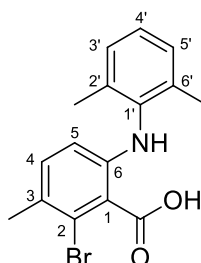
The reaction was carried out according to general procedure D using 2-(benzyloxy)-6-(mesitylamino)-3-methylbenzoic acid (**131**) (1.60 g, 4.26 mmol), 2-chloro-4,6-dimethoxy-1,3,5-triazine (0.897 g, 5.11 mmol) and *N*-methylmorpholine (1.41 mL, 12.8 mmol) in tetrahydrofuran (20 mL). The crude material was purified by flash column chromatography, eluting with 10% ethyl acetate in petroleum ether (40–60) to afford 2-(benzyloxy)-6-(mesitylamino)-3-methylbenzamide (**132**) as a white solid (1.37 g, 92%). Mp 122–124 °C;  $\nu_{\max}/\text{cm}^{-1}$  (neat) 3451 (NH), 3260 (NH), 2916 (CH), 1651 (CO), 1574 (C=C), 1495, 1366, 1261, 1040, 912, 743;  $\delta_{\text{H}}$  (400 MHz,  $\text{CDCl}_3$ ) 2.17 (6H, s, 2'- $\text{CH}_3$  and 6'- $\text{CH}_3$ ), 2.22 (3H, s,  $\text{CH}_3$ ), 2.30 (3H, s,  $\text{CH}_3$ ), 4.87 (2H, s,  $\text{CH}_2\text{Ph}$ ), 5.65 (1H, br s, NH), 5.99 (1H, d,  $J$  8.6 Hz, 5-H), 6.93 (2H, s, 3'-H and 5'-H), 6.95 (1H, d,  $J$  8.6 Hz, 4-H), 7.33–7.54 (5H, m, Ph), 7.86 (1H, br s, NH), 9.32 (1H, br s, NH);  $\delta_{\text{C}}$  (101 MHz,  $\text{CDCl}_3$ ) 15.5 ( $\text{CH}_3$ ), 18.2 (2 ×  $\text{CH}_3$ ), 20.9 ( $\text{CH}_3$ ), 76.1 ( $\text{CH}_2$ ), 107.3 (C), 109.5 (CH), 117.6 (C), 128.1 (2 × CH), 128.5 (CH), 128.7 (2 × CH), 129.0 (2 × CH), 134.9 (CH), 135.4 (C), 135.6 (C), 136.4 (2 × C), 136.5 (C), 149.3 (C), 156.6 (C), 170.8 (C);  $m/z$  (ESI) 397.1871 ( $\text{MNa}^+$ ,  $\text{C}_{24}\text{H}_{26}\text{N}_2\text{NaO}_2$  requires 397.1886).

### 2-Hydroxy-6-(mesitylamino)-3-methylbenzamide (124)



To a solution of 2-(benzyloxy)-6-(mesitylamino)-3-methylbenzamide (**132**) (1.36 g, 3.63 mmol) in tetrahydrofuran (100 mL) was added 10% palladium on carbon (0.770 g) and the reaction mixture purged under hydrogen gas for 1 h, before stirring at room temperature under a hydrogen atmosphere for a further 1 h. The reaction mixture was then filtered through Celite®, washed with ethyl acetate (50 mL) and the filtrate was concentrated *in vacuo*. The crude material was purified by flash column chromatography, eluting with 10–20% ethyl acetate in petroleum ether (40–60) to afford 2-hydroxy-6-(mesitylamino)-3-methylbenzamide (**124**) as a white solid (0.900 g, 87%). Mp 145–147 °C;  $\nu_{\max}/\text{cm}^{-1}$  (neat) 3298 (OH), 3177 (NH), 2914 (CH), 1645 (CO), 1612, 1587 (C=C), 1483, 1377, 1244, 1225, 1040, 912, 802, 741;  $\delta_{\text{H}}$  (400 MHz,  $\text{CDCl}_3$ ) 2.13 (6H, s, 2'-CH<sub>3</sub> and 6'-CH<sub>3</sub>), 2.15 (3H, s, 3-CH<sub>3</sub>), 2.30 (3H, s, 4'-CH<sub>3</sub>), 5.24 (1H, br s, NH), 5.87 (1H, d, *J* 8.1 Hz, 5-H), 6.92 (2H, s, 3'-H and 5'-H), 6.94 (1H, d, *J* 8.1 Hz, 4-H), 7.49 (2H, br s, NH), 12.72 (1H, s, OH);  $\delta_{\text{C}}$  (101 MHz,  $\text{CDCl}_3$ ) 15.5 (CH<sub>3</sub>), 18.1 (2 × CH<sub>3</sub>), 20.8 (CH<sub>3</sub>), 105.2 (C), 108.1 (CH), 119.9 (C), 129.6 (2 × CH), 132.7 (2 × C), 134.6 (CH), 134.7 (C), 136.2 (C), 144.1 (C), 161.2 (C), 173.5 (C); *m/z* (ESI) 307.1409 (MNa<sup>+</sup>. C<sub>17</sub>H<sub>20</sub>N<sub>2</sub>NaO<sub>2</sub> requires 307.1417).

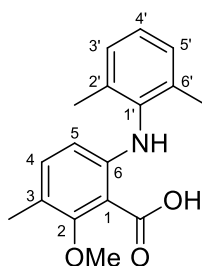
### 2-Bromo-6-[(2',6'-dimethylphenyl)amino]-3-methylbenzoic acid (137)



The reaction was carried out according to general procedure B using 2-bromo-6-fluoro-3-methylbenzoic acid (**77**) (2.00 g, 8.58 mmol) and 2,4,6-trimethylaniline (2.10 mL, 17.2 mmol) in tetrahydrofuran (50 mL), followed by treatment with lithium bis(trimethylsilyl)amide (25.7 mL, 25.7 mmol, 1.0 M in tetrahydrofuran). The crude

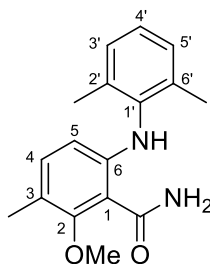
material was purified by flash column chromatography, eluting with 20–40% ethyl acetate in petroleum ether (40–60) to afford 2-bromo-6-[(2',6'-dimethylphenyl)amino]-3-methylbenzoic acid (**137**) as a brown solid (2.74 g, 95%). Mp 126–128 °C;  $\nu_{\max}/\text{cm}^{-1}$  (neat) 3389 (NH), 2918 (OH/CH), 1690 (CO), 1661, 1489, 1234, 773;  $\delta_{\text{H}}$  (500 MHz,  $\text{CDCl}_3$ ) 2.20 (6H, s, 2'- $\text{CH}_3$  and 6'- $\text{CH}_3$ ), 2.34 (3H, s, 3- $\text{CH}_3$ ), 6.14 (1H, d,  $J$  8.5 Hz, 5-H), 7.02 (1H, d,  $J$  8.5 Hz, 4-H), 7.07–7.17 (3H, m, 3'-H, 4'-H and 5'-H), 10.29 (1H, br s, OH);  $\delta_{\text{C}}$  (126 MHz,  $\text{CDCl}_3$ ) 18.2 (2  $\times$   $\text{CH}_3$ ), 23.0 ( $\text{CH}_3$ ), 112.5 (CH), 116.9 (C), 124.0 (C), 126.4 (CH), 128.0 (C), 128.6 (2  $\times$  CH), 134.0 (CH), 136.0 (2  $\times$  C), 137.1 (C), 146.0 (C), 173.4 (C);  $m/z$  (ESI) 356.0250 ( $\text{MNa}^+$ .  $\text{C}_{16}\text{H}_{16}^{79}\text{BrNNaO}_2$  requires 356.0257).

### 6-[(2',6'-Dimethylphenyl)amino]-2-methoxy-3-methylbenzoic acid (**138**)



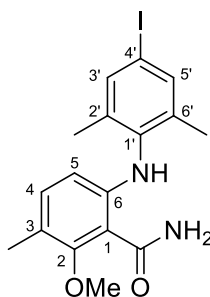
The reaction was carried out according to general procedure C using sodium hydride (0.896 g, 22.4 mmol, 60% in mineral oil), methanol (27 mL), 2-bromo-6-[(2',6'-dimethylphenyl)amino]-3-methylbenzoic acid (**137**) (2.50 g, 7.48 mmol) and copper powder (0.190 g, 2.99 mmol). The crude material was purified by flash column chromatography, eluting with 20% ethyl acetate in petroleum ether (40–60) to afford 6-[(2',6'-dimethylphenyl)amino]-2-methoxy-3-methylbenzoic acid (**138**) as a brown solid (1.51 g, 71%). Mp 92–94 °C;  $\nu_{\max}/\text{cm}^{-1}$  (neat) 3289 (NH), 3094 (OH), 2945 (CH), 1699 (CO), 1570 (C=C), 1501, 1414, 1385, 1223, 1040, 818, 770;  $\delta_{\text{H}}$  (500 MHz,  $\text{CDCl}_3$ ) 2.18 (6H, s, 2'- $\text{CH}_3$  and 6'- $\text{CH}_3$ ), 2.20 (3H, s, 3- $\text{CH}_3$ ), 3.93 (3H, s,  $\text{OCH}_3$ ), 6.03 (1H, d,  $J$  8.7 Hz, 5-H), 7.01 (1H, d,  $J$  8.7 Hz, 4-H), 7.06–7.18 (3H, m, 3'-H, 4'-H and 5'-H), 9.59 (1H, br s, NH), 12.15 (1H, br s, OH);  $\delta_{\text{C}}$  (126 MHz,  $\text{CDCl}_3$ ) 15.1 ( $\text{CH}_3$ ), 18.2 (2  $\times$   $\text{CH}_3$ ), 62.2 ( $\text{CH}_3$ ), 102.1 (C), 110.0 (CH), 116.3 (C), 126.7 (CH), 128.5 (2  $\times$  CH), 136.7 (2  $\times$  C), 137.1 (C), 137.1 (CH), 150.2 (C), 158.2 (C), 168.7 (C);  $m/z$  (ESI) 308.1248 ( $\text{MNa}^+$ .  $\text{C}_{17}\text{H}_{19}\text{NNaO}_3$  requires 308.1257).

### 6-[(2',6'-Dimethylphenyl)amino]-2-methoxy-3-methylbenzamide (**134**)



The reaction was carried out according to general procedure D using 6-[(2',6'-dimethylphenyl)amino]-2-methoxy-3-methylbenzoic acid (**138**) (1.40 g, 4.91 mmol), 2-chloro-4,6-dimethoxy-1,3,5-triazine (1.03 g, 5.89 mmol) and *N*-methylmorpholine (1.62 mL, 14.7 mmol) in tetrahydrofuran (28 mL). The crude material was purified by flash column chromatography, eluting with 20% ethyl acetate in petroleum ether (40–60) to afford 6-[(2',6'-dimethylphenyl)amino]-2-methoxy-3-methylbenzamide (**134**) as a white solid (1.29 g, 92%). Mp 116–118 °C;  $\nu_{\max}/\text{cm}^{-1}$  (neat) 3443 (NH), 3184 (NH), 2936 (CH), 1645 (CO), 1570 (C=C), 1497, 1366, 1261, 1047, 816, 731;  $\delta_{\text{H}}$  (400 MHz,  $\text{CDCl}_3$ ) 2.18 (3H, s, 3-CH<sub>3</sub>), 2.21 (6H, s, 2'-CH<sub>3</sub> and 6'-CH<sub>3</sub>), 3.79 (3H, s, OCH<sub>3</sub>), 5.96 (1H, d, *J* 8.6 Hz, 5-H), 6.04 (1H, br s, NH), 6.94 (1H, d, *J* 8.6 Hz, 4-H), 7.03–7.19 (3H, m, 3'-H, 4'-H and 5'-H), 7.93 (1H, br s, NH), 9.47 (1H, br s, NH);  $\delta_{\text{C}}$  (101 MHz,  $\text{CDCl}_3$ ) 15.2 (CH<sub>3</sub>), 18.4 (2 × CH<sub>3</sub>), 61.1 (CH<sub>3</sub>), 107.0 (C), 109.3 (CH), 117.5 (C), 126.0 (CH), 128.3 (2 × CH), 134.9 (CH), 136.6 (2 × C), 138.1 (C), 148.9 (C), 158.1 (C), 170.9 (C); *m/z* (ESI) 307.1409 ( $\text{MNa}^+$ .  $\text{C}_{17}\text{H}_{20}\text{N}_2\text{NaO}_2$  requires 307.1417).

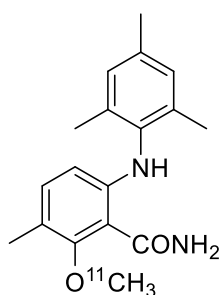
### 6-[(4'-Iodo-2',6'-dimethylphenyl)amino]-2-methoxy-3-methylbenzamide (**135**)



To a dry flask under argon was added iron(III) chloride (0.0029 g, 0.018 mmol) and [BMIM]NTf<sub>2</sub> (0.21 mL, 0.70 mmol) and the mixture stirred for 0.5 h. 6-[(2',6'-Dimethylphenyl)amino]-2-methoxy-3-methylbenzamide (**134**) (0.10 g, 0.35 mmol) was then added as a solution in tetrahydrofuran (1.5 mL) and *N*-iodosuccinimide (0.16 g, 0.70 mmol) was added slowly to the mixture. After 16 h of stirring at 70 °C, *N*-iodosuccinimide (0.080 g, 0.35 mmol) was added and the reaction mixture stirred for a further 4 h. After cooling to ambient temperature, the reaction mixture was filtered through a short pad of Celite<sup>®</sup>,

washed with ethyl acetate (5 mL) and the filtrate was concentrated *in vacuo*. The crude material was purified by flash column chromatography, eluting with 10% ethyl acetate in petroleum ether (40–60) to afford 6-[(4'-iodo-2',6'-dimethylphenyl)amino]-2-methoxy-3-methylbenzamide (**135**) as a white solid (0.0073 g, 5%). Mp 143–144 °C;  $\nu_{\max}/\text{cm}^{-1}$  (neat) 3333 (NH), 3181 (NH), 2938 (CH), 1655 (CO), 1591 (C=C), 1458, 1418, 1231, 1213, 1167, 970, 756, 732, 611;  $\delta_{\text{H}}$  (400 MHz,  $\text{CDCl}_3$ ) 2.16 (6H, s, 2'- $\text{CH}_3$  and 6'- $\text{CH}_3$ ), 2.17 (3H, s, 3- $\text{CH}_3$ ), 3.78 (3H, s,  $\text{OCH}_3$ ), 5.65 (1H, br s, NH), 5.92 (1H, d,  $J$  8.6 Hz, 5-H), 6.95 (1H, d,  $J$  8.6 Hz, 4-H), 7.10 (2H, s, 3'-H and 5'-H), 7.93 (1H, br s, NH), 9.40 (1H, br s, NH);  $\delta_{\text{C}}$  (101 MHz,  $\text{CDCl}_3$ ) 15.2 ( $\text{CH}_3$ ), 18.3 (2  $\times$   $\text{CH}_3$ ), 61.2 ( $\text{CH}_3$ ), 90.8 (C), 107.2 (C), 109.2 (CH), 118.0 (C), 128.1 (2  $\times$  CH), 131.0 (C), 135.0 (CH), 138.5 (2  $\times$  C), 148.6 (C), 158.2 (C), 170.7 (C);  $m/z$  (ESI) 433.0379 ( $\text{MNa}^+$ .  $\text{C}_{17}\text{H}_{19}\text{N}_2\text{NaO}_2$  requires 433.0383).

### Radiosynthesis of 6-(mesitylamino)-2-[ $^{11}\text{C}$ ]methoxy-3-methylbenzamide ([ $^{11}\text{C}$ ]33)



Radiochemistry was carried out on a Synthra Wolpertinger synthesiser and [ $^{11}\text{C}$ ]CO<sub>2</sub> was produced *via* the  $^{14}\text{N}(\text{p},\alpha)^{11}\text{C}$  nuclear reaction by cyclotron irradiation of a target containing [ $^{14}\text{N}$ ]N<sub>2</sub>. The [ $^{11}\text{C}$ ]CO<sub>2</sub> was trapped in a stainless steel loop at  $-180$  °C and rinsed with He gas. Conversion to [ $^{11}\text{C}$ ]CH<sub>4</sub> took place at  $425$  °C in an oven coated with an activated Zn catalyst and was then passed through an Ascarite® trap. The [ $^{11}\text{C}$ ]CH<sub>4</sub> was trapped on activated carbon at  $-120$  °C and rinsed with He to remove residual H<sub>2</sub> gas. The conversion to [ $^{11}\text{C}$ ]MeI took place by passing the [ $^{11}\text{C}$ ]CH<sub>4</sub> through an iodine oven heated to  $95$  °C, then passing through a high temperature oven at  $730$  °C. The [ $^{11}\text{C}$ ]MeI was separated by trapping on a Porapak Q column and any residual [ $^{11}\text{C}$ ]CH<sub>4</sub> was circulated in a loop, repeating this process. The [ $^{11}\text{C}$ ]MeI was de-adsorbed and bubbled into a mixture of 2-hydroxy-6-(mesitylamino)-3-methylbenzamide (**124**) (5.0 mg, 0.017 mmol) and tetra-*n*-butylammonium fluoride (20  $\mu\text{L}$ , 0.020 mmol; 1 M solution in tetrahydrofuran) in cyclohexanone (0.5 mL) at  $120$  °C for 3 min at a flow rate of  $2$  mL  $\text{min}^{-1}$ . The reaction mixture was then diluted with acetonitrile (0.62 mL) and water (0.38 mL) and loaded onto a C<sub>18</sub> Synergi Hydro-RP 80 Å,  $150 \times 10$  mm,  $4$   $\mu\text{m}$  column (Phenomenex, UK). A 62% solution of acetonitrile in water was used as the mobile phase at a flow rate of  $5.5$  mL  $\text{min}^{-1}$ . The radiolabelled product was detected by the HPLC gamma-detector and eluted at approximately 32 min. The collected fraction was diluted with water (26 mL) and then

transferred onto a Sep-Pak® Plus Light HLB cartridge. This was rinsed with water (10 mL) and the product eluted with ethanol (0.5 mL) then saline (12 mL). This provided a 4% ethanol/saline formulation of the product in a total synthesis time of 63 min. The radiolabelled product was isolated with a radiochemical yield of 13% and a radiochemical purity of >99%.

### 3.3 HPLC Methods for Physicochemical Analysis<sup>122</sup>

All physicochemical analyses were performed using a Dionex Ultimate 3000 series and data acquisition and processing performed using Chromeleon 6.8 Chromatography software. Standard and test compounds were dissolved in 1:1 organic/aqueous phases and prepared to a concentration of 0.25 mg/mL. The HPLC system was set to 25 °C and UV detection achieved using a diode array detector (190–800 nm). Analysis was performed using 5 µL sample injections.

#### **C<sub>18</sub> chromatography for determination of lipophilicity (log *P*)<sup>122</sup>**

Log *P* values were determined using a Phenomenex Luna<sup>®</sup> 5 µm C<sub>18</sub> 100 Å (50 × 3 mm) column. The retention time for each compound was measured using filtered acetonitrile and 0.01 mM phosphate buffered saline (PBS) as the mobile phase at pH 4.0, pH 7.4 and pH 10.0. The pH was adjusted by the addition of concentrated hydrochloric acid or 0.05 M aqueous sodium hydroxide solution, respectively. The mobile phase flow rate was set at 1.0 mL min<sup>-1</sup>. Chromatographic hydrophobicity index (CHI) values for all compounds were determined by measuring the compound retention time (*t<sub>r</sub>*) under the following conditions: 0–10.5 min, 0–100% acetonitrile; 10.5–11.5 min, 100% acetonitrile; 11.5–12.0 min, 100–0% acetonitrile; 12.0–15.0 min, 0% acetonitrile. System calibration was achieved using the following compounds and plotting their mean CHI values against the measured *t<sub>r</sub>* under all three pH conditions: theophylline (CHI = 15.76), phenyltetrazole (CHI = 20.18), benzimidazole (CHI = 30.71), colchicine (CHI = 41.37), acetophenone (CHI = 64.90), indole (CHI = 69.15), butyrophenone (CHI = 88.49) and valerophenone (CHI = 97.67). Using the calibration curves obtained and the following equations from a validated study, the log *P* of the compounds was calculated using Excel 2016 software.

$$\text{CHI log } D = 0.054\text{CHI} - 1.467$$

Where CHI log *D* is the CHI value projected to the logarithmic scale.

$$\log P = 0.047\text{CHIN} + 0.036\text{HBC} - 1.10$$

Where CHIN is the gradient chromatographic hydrophobicity index of the non-ionised compound and HBC is the hydrogen bond donor count.

### Immobilised artificial membrane (IAM) chromatography for determination of membrane permeability ( $P_m$ ) and membrane partition coefficient ( $K_m$ )<sup>122</sup>

$P_m$  and  $K_m$  values were determined using previously developed methodology on a Registech IAM.PC.DD2 (150 × 4.6 mm) column. Acetonitrile and 0.01 mM PBS at pH 7.4 was used as the mobile phase, with a flow rate of 1.0 mL min<sup>-1</sup>. The  $t_r$  of each compound was measured under an isocratic mobile phase, with the percentage of acetonitrile ranging from 30–70%. The retention time of citric acid as an unretained compound, under an isocratic mobile phase of 100% PBS was used for system corrections. The following equations were used to calculate  $P_m$  and  $K_m$  of the compounds of interest using Excel 2016 software.

$$k_{IAM} = \frac{t_r - t_0}{t_0}$$

Where  $k_{IAM}$  = solute capacity factor on the column,  $t_r$  = retention time of compound and  $t_0$  =  $t_r$  of unretained compound.

$$k_{IAM} = \left( \frac{V_s}{V_m} \right) \times K_m$$

Where  $V_s$  = volume of the IAM interphase created by the immobilised phospholipids,  $V_m$  = total volume of the solvent within the IAM column and  $K_m$  = membrane partition coefficient.

$$V_m = \frac{W_{PhC}}{\delta_{PhC}} + \frac{W_{C10}}{\delta_{C10}} + \frac{W_{C3}}{\delta_{C3}}$$

Where the specific weight of PhC ( $\delta_{PhC}$ ) = 1.01779 g mL<sup>-1</sup> and  $C_{10}/C_3$  ( $\delta_{C10/C3}$ ) = 0.86 g mL<sup>-1</sup>;  $W_{PhC}$  = 133 mg,  $W_{C10}$  = 12.73 mg and  $W_{C3}$  = 2.28 mg.

$$V_m = f_r \times t_0$$

Where  $f_r$  = flow rate.

$$P_m = \frac{K_m}{MW}$$

Where  $P_m$  = permeability and MW = molecular weight.

**Human serum albumin (HSA) chromatography for determination of percentage of plasma protein binding (%PPB)<sup>122</sup>**

A ChromTech HSA 5  $\mu\text{m}$  (3.0  $\times$  50 mm) column was used for determination of %PPB, using previously developed methodology. Isopropanol and 0.01 mM PBS at pH 7.4 was used as the mobile phase, with a flow rate of 1.8 mL min<sup>-1</sup>. The retention time of each compound was measured under the following mobile phase conditions: 0–3 min, 0–30% isopropanol; 3–10 min, 30% isopropanol; 10.5–11.0 min, 30–0% isopropanol; 11.0–15.0 min, 0% isopropanol. System calibration was achieved using the following reference compounds: warfarin (%PPB = 98.0), nizatidine (%PPB = 35.0), bromazepam (%PPB = 60.0), carbamazepine (%PPB = 75.0), nicardipine (%PPB = 95.0), ketoprofen (%PPB = 98.7), indomethacin (%PPB = 99.0) and diclofenac (%PPB = 99.8). The %PPB for the reference compounds were converted to the linear free energy related log k values, which when plotted against the  $t_r$  on the HSA column, afforded a line equation from which the log k values of the unknown compounds could be extracted. The log k values could then be converted to %PPB. Log k and subsequent %PPB calculations for the compounds of interest were performed using Excel 2016 software.

$$\log k = \log \left( \frac{\%PPB}{101 - \%PPB} \right)$$

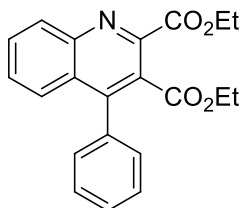
$$\%PPB = \left[ \frac{(101 - 10^{\log k})}{(1 + 10^{\log k})} \right]$$

### 3.4 Procedure for the [<sup>35</sup>S]GTPγS Binding Assay<sup>159</sup>

The assay buffer was prepared from HEPES (20 mM), NaCl (100 mM), MgCl<sub>2</sub> (10 mM) and fatty acid-free BSA (0.1%) at pH 7.4. ChemiScreen™ S1P<sub>1-3,5</sub> lysophospholipid receptor membrane preparations were obtained from Eurofins. The membrane preparation was diluted to 0.4 g mL<sup>-1</sup> with assay buffer and mixed 1:1 (v/v) with a 0.4 mg mL<sup>-1</sup> solution of saponin in assay buffer. Nine concentrations of the compounds to be tested were prepared (10 μM, 1 μM, 100 nM, 10 nM, 1 nM, 100 pM, 10 pM, 1 pM, 100 fM). Merck™ Multiscreen® HTS 96 well filter plates were pre-wet with 70% aqueous EtOH (50 μL/well) for 30 seconds and then washed twice with assay buffer (200 μL/well). To each well was added membrane preparation (25 μL), GDP in assay buffer (25 μL, 2 μM), [<sup>35</sup>S]GTPγS in assay buffer (25 μL, 1.2 nM) and test compound (25 μL). For total binding, S1P solution in assay buffer (25 μL, 10 μM) was added and for basal, assay buffer (25 μL) was added. The assay plate was incubated at 30 °C for 30 min before the addition of cold assay buffer (100 μL/well) to stop the reaction. The plate was filtered using a Millipore vacuum manifold, with a pressure between 600–800 mbar and then dried at 50 °C for 1–2 h. Betaplate Scint Scintillation Cocktail (30 μL/well) was added and the disintegrations per minute were determined using a Wallac 1450 Microbeta Trilux liquid scintillation and luminescence counter. EC<sub>50</sub> values were derived from non-linear regression analysis using GraphPad Prism Version 6 (GraphPad Software Inc).

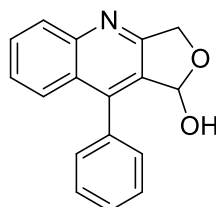
### 3.5 TSPO Experimental

#### Diethyl 4-phenylquinoline-2,3-dicarboxylate (**148**)<sup>162</sup>



Indium(III) chloride (0.680 g, 3.07 mmol) was added to 2-aminobenzophenone (5.00 g, 15.3 mmol) and diethyl acetylenedicarboxylate (2.95 mL, 18.4 mmol), and the neat mixture stirred at 80 °C for 3 h. On cooling to ambient temperature, water (50 mL) was added and the mixture extracted using ethyl acetate (3 × 50 mL). The organic layer was then washed with water (100 mL) and brine (100 mL), dried (MgSO<sub>4</sub>), filtered and concentrated *in vacuo*. The crude material was purified by flash column chromatography, eluting with 15% ethyl acetate in petroleum ether (40–60) to afford diethyl 4-phenylquinoline-2,3-dicarboxylate (**148**) as a yellow solid (5.36 g, 100%). Mp 89–91 °C, lit.<sup>162</sup> 95–96 °C;  $\delta_{\text{H}}$  (400 MHz, CDCl<sub>3</sub>) 0.99 (3H, t, *J* 7.2 Hz, OCH<sub>2</sub>CH<sub>3</sub>), 1.47 (3H, t, *J* 7.2 Hz, OCH<sub>2</sub>CH<sub>3</sub>), 4.09 (2H, q, *J* 7.2 Hz, OCH<sub>2</sub>CH<sub>3</sub>), 4.54 (2H, q, *J* 7.2 Hz, OCH<sub>2</sub>CH<sub>3</sub>), 7.34–7.40 (2H, m, 2 × ArH), 7.47–7.53 (3H, m, 3 × ArH), 7.57 (1H, ddd, *J* 8.4, 6.4, 1.6 Hz, ArH), 7.63 (1H, ddd, *J* 8.4, 1.6, 0.6 Hz, ArH), 7.81 (1H, ddd, *J* 8.4, 6.4, 1.6 Hz, ArH), 8.38 (1H, ddd, *J* 8.4, 1.6, 0.6 Hz, ArH);  $\delta_{\text{C}}$  (101 MHz, CDCl<sub>3</sub>) 13.6 (CH<sub>3</sub>), 14.2 (CH<sub>3</sub>), 61.6 (CH<sub>2</sub>), 62.6 (CH<sub>2</sub>), 126.6 (CH), 127.1 (C), 127.5 (C), 128.2 (2 × CH), 128.7 (CH), 129.0 (CH), 129.4 (2 × CH), 130.7 (CH), 130.9 (CH), 134.8 (C), 145.9 (C), 147.1 (C), 148.0 (C), 165.3 (C), 167.2 (C); *m/z* (EI) 349 (M<sup>+</sup>, 100%), 305 (20), 276 (55), 205 (100), 204 (82), 165 (12), 84 (5).

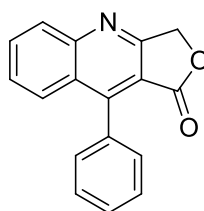
#### 9-Phenyl-1*H*,3*H*-furo[3,4-*b*]quinolin-1-ol (**152**)<sup>119</sup>



A solution of diethyl 4-phenylquinoline-2,3-dicarboxylate (**148**) (4.72 g, 13.5 mmol) in tetrahydrofuran (50 mL) under argon was heated under reflux with vigorous stirring. Sodium borohydride (5.11 g, 135 mmol) was added slowly followed by methanol (50 mL), and the reaction mixture stirred under reflux for 15 h. After cooling to ambient temperature, the reaction was quenched by the dropwise addition of a saturated aqueous

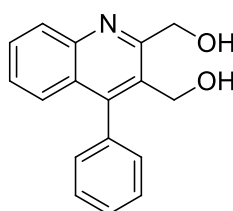
solution of ammonium chloride (50 mL). The crude reaction mixture was extracted using dichloromethane (3 × 50 mL) and washed with water (2 × 50 mL), dried (MgSO<sub>4</sub>), filtered and concentrated *in vacuo*. Trituration with diethyl ether afforded 9-phenyl-1*H*,3*H*-furo[3,4-*b*]quinolin-1-ol (**152**) as a pale yellow solid (2.77 g, 78%). Mp 208–210 °C, lit.<sup>119</sup> 208–210 °C;  $\delta_{\text{H}}$  (400 MHz, DMSO-*d*<sub>6</sub>) 4.87 (1H, dd, *J* 15.7, 0.8 Hz, CHHO), 4.98 (1H, br d, *J* 15.7 Hz, CHHO), 5.02 (1H, br s, CHOH), 6.87–6.94 (2H, m, 2 × ArH), 7.04 (1H, d, *J* 6.8 Hz, ArH), 7.10–7.17 (2H, m, 2 × ArH), 7.18–7.28 (4H, m, 4 × ArH), 10.0 (1H, br s, CHOH);  $\delta_{\text{C}}$  (101 MHz, DMSO-*d*<sub>6</sub>) 65.0 (CH<sub>2</sub>), 95.2 (CH), 116.2 (CH), 123.1 (CH), 124.3 (C), 126.2 (CH), 127.5 (CH), 127.6 (2 × CH), 128.3 (2 × CH), 128.7 (C), 130.8 (CH), 136.1 (C), 146.8 (C), 158.5 (C), 172.0 (C); *m/z* (ESI) 286 (MNa<sup>+</sup>, 100%).

### 9-Phenylfuro[3,4-*b*]quinolin-1(3*H*)-one (**149**)<sup>210</sup>



To a solution of 9-phenyl-1*H*,3*H*-furo[3,4-*b*]quinolin-1-ol (**152**) (3.29 g, 12.5 mmol) in chloroform (150 mL) was added activated manganese(IV) oxide (32.6 g, 374 mmol) in one portion. The reaction mixture was stirred vigorously at room temperature for 4 h and then filtered through Celite®. After washing with chloroform (200 mL), the solvent was removed *in vacuo* to afford 9-phenylfuro[3,4-*b*]quinolin-1(3*H*)-one (**149**) as a white solid (2.72 g, 83%). This was used without further purification. Mp 201–203 °C, lit.<sup>210</sup> 203–204 °C;  $\delta_{\text{H}}$  (500 MHz, CDCl<sub>3</sub>) 5.45 (2H, s, OCH<sub>2</sub>), 7.43–7.49 (2H, m, 2 × ArH), 7.57–7.61 (4H, m, 4 × ArH), 7.89–7.93 (2H, m, 2 × ArH), 8.19–8.22 (1H, m, ArH);  $\delta_{\text{C}}$  (126 MHz, CDCl<sub>3</sub>) 69.6 (CH<sub>2</sub>), 113.5 (C), 127.1 (C), 127.4 (CH), 128.1 (CH), 128.3 (2 × CH), 129.4 (CH), 129.5 (CH), 129.8 (2 × CH), 131.6 (C), 132.6 (CH), 151.3 (C), 51.5 (C), 163.6 (C), 167.9 (C); *m/z* (EI) 261 (M<sup>+</sup>, 100%), 232 (56), 204 (42), 203 (32), 176 (21), 151 (9), 131 (8), 91 (10).

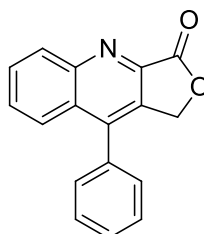
### 2,3-Bis(hydroxymethyl)-4-phenylquinoline (**150**)<sup>210</sup>



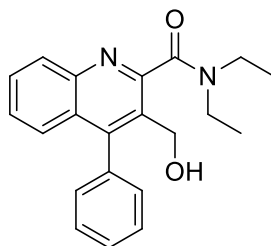
A suspension of lithium aluminium hydride (3.90 g, 103 mmol) in diethyl ether (90 mL) under argon was cooled to 0 °C, and to this was added dropwise a solution of diethyl 4-

phenylquinoline-2,3-dicarboxylate (**148**) (9.00 g, 26.0 mmol) in diethyl ether (90 mL). The temperature of the reaction mixture was maintained at 0 °C and stirred vigorously for 3 h. Water (4.0 mL) was added, followed by 15% aqueous sodium hydroxide (4.0 mL) and allowed to stir at 0 °C for 0.2 h. Water (12 mL) was then added and the reaction mixture allowed to reach room temperature followed by stirring with MgSO<sub>4</sub> for 0.5 h. The reaction mixture was then filtered and concentrated *in vacuo* to afford a colourless residue which was dissolved in methanol (250 mL). 10% Palladium on carbon (0.90 g) was added to the reaction flask and the reaction mixture stirred at room temperature for 15 h. The suspension was then filtered through a pad of Celite<sup>®</sup>, washed with methanol and concentrated *in vacuo*. Trituration with diethyl ether afforded 2,3-bis(hydroxymethyl)-4-phenylquinoline (**150**) as a white solid (4.50 g, 65%). Mp 171–173 °C, lit.<sup>210</sup> 175–177 °C;  $\delta_{\text{H}}$  (400 MHz, CD<sub>3</sub>OD) 4.59 (2H, s, CH<sub>2</sub>OH), 5.11 (2H, s, CH<sub>2</sub>OH), 7.34–7.38 (2H, m, 2 × ArH), 7.41 (1H, dd, *J* 8.4, 1.2 Hz, ArH), 7.44–7.50 (1H, m, ArH), 7.51–7.60 (3H, m, 3 × ArH), 7.73 (1H, ddd, *J* 8.4, 6.4, 1.2 Hz, ArH), 8.11 (1H, d, *J* 8.4 Hz, ArH);  $\delta_{\text{C}}$  (101 MHz, CD<sub>3</sub>OD) 59.1 (CH<sub>2</sub>), 64.6 (CH<sub>2</sub>), 127.8 (CH), 127.9 (CH), 128.6 (C), 129.4 (CH), 129.5 (CH), 129.5 (2 × CH), 130.0 (C), 130.8 (CH), 130.8 (2 × CH), 137.2 (C), 147.4 (C), 150.4 (C), 160.9 (C); *m/z* (CI) 266 (MH<sup>+</sup>, 100%), 264 (50), 248 (42), 218 (21), 206 (4), 151 (3).

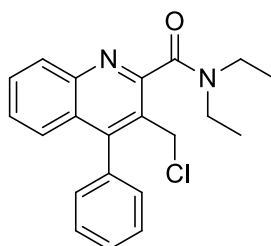
#### 9-Phenylfuro[3,4-*b*]quinolin-3(1*H*)-one (**153**)<sup>210</sup>



To a solution of 2,3-bis(hydroxymethyl)-4-phenylquinoline (**150**) (0.780 g, 2.93 mmol) in chloroform (50 mL) was added activated manganese(IV) oxide (7.64 g, 87.9 mmol) in one portion. The reaction mixture was stirred vigorously at room temperature for 4 h and then filtered through Celite<sup>®</sup>. After washing with chloroform (100 mL), the solvent was removed *in vacuo* to afford 9-phenylfuro[3,4-*b*]quinolin-3(1*H*)-one (**153**) as a white solid (0.70 g, 92%), which was used without further purification. Mp 188–190 °C, lit.<sup>210</sup> 190–192 °C;  $\delta_{\text{H}}$  (400 MHz, CDCl<sub>3</sub>) 5.41 (2H, s, OCH<sub>2</sub>), 7.45 (2H, dd, *J* 8.0, 2.0 Hz, 2 × ArH), 7.57–7.70 (4H, m, 4 × ArH), 7.84–7.90 (1H, m, ArH), 7.92 (1H, d, *J* 8.4 Hz, ArH), 8.46 (1H, d, *J* 8.4 Hz, ArH);  $\delta_{\text{C}}$  (101 MHz, CDCl<sub>3</sub>) 67.8 (CH<sub>2</sub>), 125.7 (CH), 127.9 (C), 128.9 (2 × CH), 129.3 (2 × CH), 129.4 (CH), 129.6 (CH), 130.7 (CH), 131.5 (CH), 132.3 (C), 133.6 (C), 143.9 (C), 144.4 (C), 150.7 (C), 168.7 (C); *m/z* (ESI) 284. (MNa<sup>+</sup>, 100%).

**3-(Hydroxymethyl)-4-phenylquinoline-2-*N*-diethylcarboxamide (151)**<sup>119</sup>


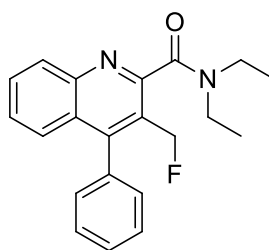
To a solution of diethylamine (1.06 mL, 10.2 mmol) in dichloromethane (70 mL) under argon was added aluminium(III) chloride (1.36 g, 10.2 mmol), and the mixture stirred at room temperature for 0.3 h. A solution of 9-phenylfuro[3,4-*b*]quinolin-3(1*H*)-one (**153**) (0.890 g, 3.41 mmol) in dichloromethane (20 mL) was then added dropwise and the reaction mixture stirred at room temperature for 15 h. The reaction was quenched by the careful addition of a 1 M aqueous hydrochloric acid solution (25 mL) and the crude mixture extracted using dichloromethane (2 × 40 mL). The organic layer was dried (MgSO<sub>4</sub>), filtered and concentrated *in vacuo*. The crude material was purified by flash column chromatography, eluting with 20% ethyl acetate in petroleum ether (40–60) to afford 3-(hydroxymethyl)-4-phenylquinoline-2-*N*-diethylcarboxamide (**151**) as a pale yellow solid (1.00 g, 88%). Mp 117–119 °C, lit.<sup>119</sup> 117–119 °C;  $\delta_{\text{H}}$  (400 MHz, CDCl<sub>3</sub>) 1.27 (3H, t, *J* 7.2 Hz, NCH<sub>2</sub>CH<sub>3</sub>), 1.36 (3H, t, *J* 7.2 Hz, NCH<sub>2</sub>CH<sub>3</sub>), 3.42 (2H, q, *J* 7.2 Hz, NCH<sub>2</sub>CH<sub>3</sub>), 3.68 (2H, q, *J* 7.2 Hz, NCH<sub>2</sub>CH<sub>3</sub>), 4.12 (1H, t, *J* 6.4 Hz, CH<sub>2</sub>OH), 4.39 (2H, d, *J* 6.4 Hz, CH<sub>2</sub>OH), 7.41–7.58 (7H, m, 7 × ArH), 7.72 (1H, ddd, *J* 8.4, 6.8, 1.6 Hz, ArH), 8.12 (1H, ddd, *J* 8.4, 1.2, 0.8 Hz, ArH);  $\delta_{\text{C}}$  (101 MHz, CDCl<sub>3</sub>) 12.9 (CH<sub>3</sub>), 14.2 (CH<sub>3</sub>), 40.3 (CH<sub>2</sub>), 43.7 (CH<sub>2</sub>), 59.7 (CH<sub>2</sub>), 127.0 (CH), 127.4 (CH), 127.6 (C), 128.4 (3 × CH), 129.4 (C), 129.6 (CH), 129.7 (CH), 129.9 (2 × CH), 135.2 (C), 146.1 (C), 149.3 (C), 155.1 (C), 169.8 (C); *m/z* (ESI) 357 (MNa<sup>+</sup>, 100%).

**3-(Chloromethyl)-4-phenylquinoline-2-*N*-diethylcarboxamide (44)**<sup>119</sup>


To a solution of 3-(hydroxymethyl)-4-phenylquinoline-2-*N*-diethylcarboxamide (**151**) (0.450 g, 1.35 mmol) in dichloromethane (45 mL) under argon was added thionyl chloride (2.94 mL, 40.5 mmol) and the reaction mixture stirred under reflux for 24 h. On cooling to ambient temperature, the mixture was concentrated *in vacuo* and azeotroped with toluene

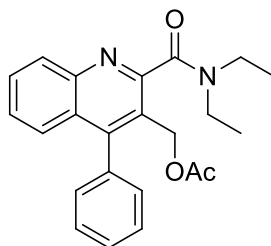
(3 × 30 mL). The crude material was purified by flash column chromatography, eluting with 50% diethyl ether in petroleum ether (40–60) to afford 3-(chloromethyl)-4-phenylquinoline-2-*N*-diethylcarboxamide (**44**) as a colourless oil (0.423 g, 89%). The spectroscopic data were consistent with the literature.<sup>119</sup>  $\delta_{\text{H}}$  (500 MHz,  $\text{CDCl}_3$ ) 1.30 (3H, t,  $J$  7.0 Hz,  $\text{NCH}_2\text{CH}_3$ ), 1.35 (3H, t,  $J$  7.5 Hz,  $\text{NCH}_2\text{CH}_3$ ), 3.28 (2H, q,  $J$  7.0 Hz,  $\text{NCH}_2\text{CH}_3$ ), 3.68 (2H, q,  $J$  7.5 Hz,  $\text{NCH}_2\text{CH}_3$ ), 4.70 (2H, s,  $\text{CH}_2\text{Cl}$ ), 7.36–7.40 (2H, m, 2 × ArH), 7.41–7.59 (5H, m, 5 × ArH), 7.73 (1H, ddd,  $J$  8.5, 6.5, 1.5 Hz, ArH), 8.13 (1H, d,  $J$  8.5 Hz, ArH);  $\delta_{\text{C}}$  (126 MHz,  $\text{CDCl}_3$ ) 12.3 ( $\text{CH}_3$ ), 13.5 ( $\text{CH}_3$ ), 39.2 ( $\text{CH}_2$ ), 40.3 ( $\text{CH}_2$ ), 43.6 ( $\text{CH}_2$ ), 125.9 (C), 126.9 (CH), 127.3 (C), 127.4 (CH), 128.6 (2 × CH), 128.7 (CH), 129.4 (2 × CH), 129.6 (CH), 130.2 (CH), 134.9 (C), 146.4 (C), 149.4 (C), 155.6 (C), 168.1 (C);  $m/z$  (ESI) 375 ( $\text{MNa}^+$ , 100%).

### 3-(Fluoromethyl)-4-phenylquinoline-2-*N*-diethylcarboxamide (**45**)<sup>119</sup>



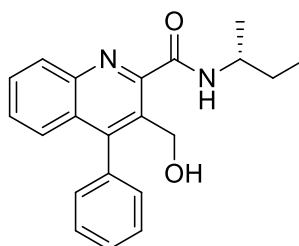
To a solution of 18-crown-6 (0.038 g, 0.140 mmol) in acetonitrile (2.5 mL) under argon was added potassium fluoride (0.041 g, 0.710 mmol) and the suspension stirred at room temperature for 0.5 h. A solution of 3-(chloromethyl)-4-phenylquinoline-2-*N*-diethylcarboxamide (**44**) (0.050 g, 0.140 mmol) in acetonitrile (2.5 mL) was then added dropwise and the reaction mixture stirred under reflux for 24 h. On cooling to ambient temperature, water (10 mL) was added to the mixture and the product extracted using dichloromethane (3 × 15 mL). The combined organic layers were dried ( $\text{MgSO}_4$ ), filtered and concentrated *in vacuo*. The crude material was purified by flash column chromatography, eluting with 50% diethyl ether in petroleum ether (40–60) to afford 3-(fluoromethyl)-4-phenylquinoline-2-*N*-diethylcarboxamide (**45**) as a white solid (0.030 g, 60%). The spectroscopic data were consistent with the literature.<sup>119</sup> Mp 126–128 °C;  $\delta_{\text{H}}$  (400 MHz,  $\text{CDCl}_3$ ) 1.22 (3H, t,  $J$  7.2 Hz,  $\text{NCH}_2\text{CH}_3$ ), 1.34 (3H, t,  $J$  7.2 Hz,  $\text{NCH}_2\text{CH}_3$ ), 3.28 (2H, q,  $J$  7.2 Hz,  $\text{NCH}_2\text{CH}_3$ ), 3.67 (2H, q,  $J$  7.2 Hz,  $\text{NCH}_2\text{CH}_3$ ), 5.38 (2H, d,  $J$  47.8 Hz,  $\text{CH}_2\text{F}$ ), 7.32–7.38 (2H, m, 2 × ArH), 7.46–7.57 (5H, m, 5 × ArH), 7.73–7.78 (1H, m, ArH), 8.16 (1H, d,  $J$  8.4 Hz, ArH);  $\delta_{\text{C}}$  (101 MHz,  $\text{CDCl}_3$ ) 12.6 ( $\text{CH}_3$ ), 13.7 ( $\text{CH}_3$ ), 39.4 ( $\text{CH}_2$ ), 43.2 ( $\text{CH}_2$ ), 79.2 ( $\text{CH}_2$ , d,  $^1J_{\text{CF}}$  162.2 Hz), 123.4 (C, d,  $^2J_{\text{CF}}$  15.1 Hz), 127.0 (CH), 127.1 (C, d,  $^4J_{\text{CF}}$  1.8 Hz), 127.4 (CH), 128.5 (2 × CH), 128.7 (CH), 129.6 (CH), 129.7 (2 × CH), 130.5 (CH, d,  $^5J_{\text{CF}}$  1.5 Hz), 134.8 (C), 147.1 (C, d,  $^3J_{\text{CF}}$  2.9 Hz), 150.7 (C, d,  $^3J_{\text{CF}}$  4.9 Hz), 155.9 (C, d,  $^4J_{\text{CF}}$  1.7 Hz), 168.2 (C);  $m/z$  (ESI) 359 ( $\text{MNa}^+$ , 100%).

### 3-(Acetoxymethyl)-4-phenylquinoline-2-*N*-diethylcarboxamide (**154**)



To a solution of 3-(hydroxymethyl)-4-phenylquinoline-2-*N*-diethylcarboxamide (**151**) (0.050 g, 0.150 mmol) in dichloromethane (2.0 mL) was added triethylamine (0.031 mL, 0.225 mmol), acetic anhydride (0.028 mL, 0.300 mmol) and 4-dimethylaminopyridine (0.002 g, 0.015 mmol) and the reaction mixture stirred under argon at room temperature for 16 h. The reaction mixture was dissolved in ethyl acetate (10 mL) and washed with saturated aqueous sodium bicarbonate (10 mL), water (10 mL) and brine (10 mL). The organic layer was then dried (MgSO<sub>4</sub>), filtered and concentrated *in vacuo*. The crude material was purified by flash column chromatography, eluting with 40% ethyl acetate in petroleum ether (40–60) to afford 3-(acetoxymethyl)-4-phenylquinoline-2-*N*-diethylcarboxamide (**154**) as a colourless oil (0.047 g, 83%).  $\nu_{\max}/\text{cm}^{-1}$  (neat) 2978 (CH), 1736 (CO), 1636 (CO), 1558 (C=C), 1481, 1227, 1072, 1026, 772;  $\delta_{\text{H}}$  (400 MHz, CDCl<sub>3</sub>) 1.26 (3H, t, *J* 7.1 Hz, NCH<sub>2</sub>CH<sub>3</sub>), 1.31 (3H, t, *J* 7.1 Hz, NCH<sub>2</sub>CH<sub>3</sub>), 1.96 (3H, s, OCOCH<sub>3</sub>), 3.30 (2H, q, *J* 7.1 Hz, NCH<sub>2</sub>CH<sub>3</sub>), 3.65 (2H, q, *J* 7.1 Hz, NCH<sub>2</sub>CH<sub>3</sub>), 5.10 (2H, s, CH<sub>2</sub>OAc), 7.30–7.35 (2H, m, 2 × ArH), 7.43–7.57 (5H, m, 5 × ArH), 7.69–7.78 (1H, m, ArH), 8.15 (1H, d, *J* 8.4 Hz, ArH);  $\delta_{\text{C}}$  (101 MHz, CDCl<sub>3</sub>) 12.7 (CH<sub>3</sub>), 13.8 (CH<sub>3</sub>), 20.7 (CH<sub>3</sub>), 39.4 (CH<sub>2</sub>), 43.1 (CH<sub>2</sub>), 61.3 (CH<sub>2</sub>), 123.0 (C), 126.7 (CH), 127.3 (C), 127.3 (CH), 128.5 (2 × CH), 128.6 (CH), 129.4 (2 × CH), 129.6 (CH), 130.1 (CH), 135.1 (C), 146.7 (C), 150.4 (C), 155.6 (C), 168.2 (C), 169.9 (C); *m/z* (ESI) 399.1672 (MNa<sup>+</sup>. C<sub>23</sub>H<sub>24</sub>N<sub>2</sub>NaO<sub>3</sub> requires 399.1679).

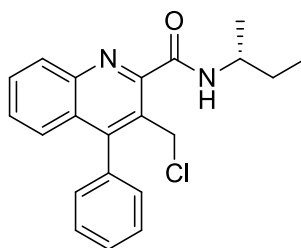
### (*R*)-(N-*sec*-Butyl)-3-(hydroxymethyl)-4-phenylquinoline-2-carboxamide (**159**)



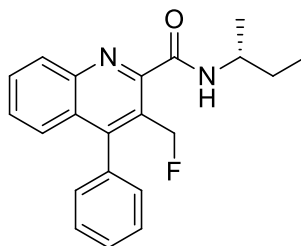
To a stirred suspension of aluminium(III) chloride (0.770 g, 5.74 mmol) in dichloromethane (18 mL) under argon was added (*R*)-*sec*-butylamine (0.580 mL, 5.74 mmol) dropwise and the mixture stirred for 0.5 h at room temperature. A solution of 9-phenylfuro[3,4-*b*]quinolin-3(1*H*)-one (**153**) (0.500 g, 1.91 mmol) in dichloromethane (18 mL) was added and the

reaction mixture was stirred at 40 °C for 16 h. The mixture was then filtered through a short pad of Celite<sup>®</sup>, washed with ethyl acetate (50 mL) and the filtrate was concentrated *in vacuo*. The crude material was purified by flash column chromatography, eluting with 20% ethyl acetate in petroleum ether (40–60) to afford (*R*)-(*N*-*sec*-butyl)-3-(hydroxymethyl)-4-phenylquinoline-2-carboxamide (**159**) as a white solid (0.482 g, 75%). Mp 133–134 °C;  $\nu_{\max}/\text{cm}^{-1}$  (neat) 3387 (OH), 2961 (NH), 1651 (CO), 1518, 1402, 1161, 1015;  $[\alpha]_{\text{D}}^{30}$  –24.8 (*c* 1.0, CHCl<sub>3</sub>);  $\delta_{\text{H}}$  (400 MHz, CDCl<sub>3</sub>) 1.04 (3H, t, *J* 7.5 Hz, CH<sub>2</sub>CH<sub>3</sub>), 1.35 (3H, d, *J* 6.6 Hz, CHCH<sub>3</sub>), 1.65–1.76 (2H, m, CH<sub>2</sub>CH<sub>3</sub>), 4.10–4.23 (1H, m, CHCH<sub>3</sub>), 4.67 (2H, d, *J* 7.6 Hz, 3-CH<sub>2</sub>), 5.39 (1H, t, *J* 7.6 Hz, OH), 7.34–7.38 (2H, m, ArH), 7.47–7.56 (5H, m, ArH), 7.68–7.77 (1H, m, ArH), 8.13 (1H, dt, *J* 8.4, 0.9 Hz, ArH), 8.28 (1H, d, *J* 8.4 Hz, NH);  $\delta_{\text{C}}$  (101 MHz, CDCl<sub>3</sub>) 10.7 (CH<sub>3</sub>), 20.5 (CH<sub>3</sub>), 29.9 (CH<sub>2</sub>), 47.3 (CH), 59.9 (CH<sub>2</sub>), 127.2 (CH), 128.2 (CH), 128.4 (CH), 128.6 (CH), 128.6 (CH), 128.7 (C), 129.7 (CH), 129.9 (CH), 130.0 (CH), 130.0 (CH), 131.5 (C), 136.0 (C), 145.5 (C), 149.8 (C), 150.1 (C), 166.4 (C); *m/z* (ESI) 357.1563 (MNa<sup>+</sup>. C<sub>21</sub>H<sub>22</sub>N<sub>2</sub>NaO<sub>2</sub> requires 357.1573).

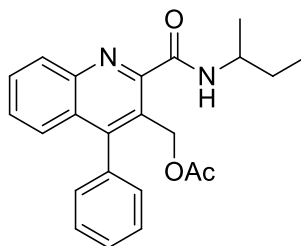
**(*R*)-(*N*-*sec*-Butyl)-3-(chloromethyl)-4-phenylquinoline-2-carboxamide (163)**



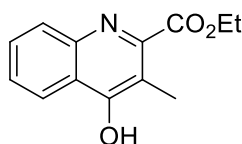
To a solution of (*R*)-*N*-(*sec*-butyl)-3-(hydroxymethyl)-4-phenylquinoline-2-carboxamide (**159**) (0.223 g, 0.667 mmol) in dichloromethane (20 mL) under argon was added thionyl chloride (1.45 mL, 20.0 mmol). The resultant solution was stirred at room temperature for 16 h. The reaction mixture was concentrated *in vacuo* and subsequently azeotroped with toluene to yield an off-white solid. The crude material was purified by trituration (Et<sub>2</sub>O) to afford (*R*)-(*N*-*sec*-butyl)-3-(chloromethyl)-4-phenylquinoline-2-carboxamide (**163**) as a white solid (0.200 g, 85%). Mp 218–219 °C;  $\nu_{\max}/\text{cm}^{-1}$  (neat) 3277 (CH), 2965 (NH), 1651 (CO), 1637, 1541, 1277, 1163;  $[\alpha]_{\text{D}}^{30}$  –28.3 (*c* 1.0, CHCl<sub>3</sub>);  $\delta_{\text{H}}$  (400 MHz, CDCl<sub>3</sub>) 1.04 (3H, t, *J* 7.4 Hz, CH<sub>2</sub>CH<sub>3</sub>), 1.35 (3H, d, *J* 6.6 Hz, CHCH<sub>3</sub>), 1.62–1.77 (2H, m, CH<sub>2</sub>CH<sub>3</sub>), 4.12–4.25 (1H, m, CHCH<sub>3</sub>), 5.18 (1H, d, *J* 10.4 Hz, 3-CHH), 5.24 (1H, d, *J* 10.4 Hz, 3-CHH), 7.33–7.41 (3H, m, ArH), 7.46–7.52 (1H, m, ArH), 7.53–7.60 (3H, m, ArH), 7.73 (1H, t, *J* 8.1 Hz, ArH), 7.88 (1H, d, *J* 8.1 Hz, NH), 8.17 (1H, d, *J* 8.4 Hz, ArH);  $\delta_{\text{C}}$  (101 MHz, CDCl<sub>3</sub>); 10.7 (CH<sub>3</sub>), 20.5 (CH<sub>3</sub>), 29.9 (CH<sub>2</sub>), 40.6 (CH<sub>2</sub>), 47.2 (CH), 127.1 (CH), 128.3 (CH), 128.5 (C), 128.6 (C), 128.7 (2 × CH), 128.8 (CH), 129.5 (CH), 129.5 (CH), 129.6 (CH), 130.5 (CH), 135.2 (C), 145.5 (C), 149.2 (C), 151.3 (C), 165.1 (C); *m/z* (ESI) 375.1220 (MNa<sup>+</sup>. C<sub>21</sub>H<sub>21</sub><sup>35</sup>ClN<sub>2</sub>NaO requires 375.1235).

**(R)-(N-sec-Butyl)-3-(fluoromethyl)-4-phenylquinoline-2-carboxamide (164)**

To a solution of 18-crown-6 (0.180 g, 0.680 mmol) in acetonitrile (13 mL) under argon was added potassium fluoride (0.200 g, 3.40 mmol) and the suspension stirred at room temperature for 0.5 h. A solution of (*R*)-(*N*-sec-butyl)-3-(chloromethyl)-4-phenylquinoline-2-carboxamide (**163**) (0.240 g, 0.680 mmol) in acetonitrile (13 mL) and dichloromethane (6.5 mL) was then added dropwise and the reaction mixture stirred under reflux for 24 h. On cooling to ambient temperature, water (20 mL) was added to the mixture and the product extracted using dichloromethane (3 × 20 mL). The combined organic extracts were dried (MgSO<sub>4</sub>), filtered and concentrated *in vacuo*. The crude material was purified by flash column chromatography, eluting with 30% ethyl acetate in petroleum ether (40–60) to afford (*R*)-(*N*-sec-butyl)-3-(fluoromethyl)-4-phenylquinoline-2-carboxamide (**164**) as a white solid (0.214 g, 92%). Mp 176–177 °C;  $\nu_{\max}/\text{cm}^{-1}$  (neat) 3283 (CH), 2965 (NH), 1640 (CO), 1539, 1452, 1402, 1207, 1157, 980;  $[\alpha]_{\text{D}}^{30}$  –25.5 (*c* 0.5, CHCl<sub>3</sub>);  $\delta_{\text{H}}$  (400 MHz, CDCl<sub>3</sub>) 1.03 (3H, t, *J* 7.4 Hz, CH<sub>2</sub>CH<sub>3</sub>), 1.34 (3H, d, *J* 6.6 Hz, CHCH<sub>3</sub>), 1.62–1.76 (2H, m, CH<sub>2</sub>CH<sub>3</sub>), 4.12–4.23 (1H, m, CHCH<sub>3</sub>), 5.80 (1H, dd, *J* 11.4, 9.8 Hz, 3-CHH), 5.90, (1H, dd, *J* 11.4, 9.8 Hz, 3-CHH), 7.29–7.36 (2H, m, ArH), 7.45–7.57 (5H, m, ArH), 7.74–7.79 (1H, m, ArH), 7.90 (1H, d, *J* 8.1 Hz, NH), 8.16 (1H, d, *J* 8.5 Hz, ArH);  $\delta_{\text{C}}$  (101 MHz, CDCl<sub>3</sub>) 10.5 (CH<sub>3</sub>), 20.4 (CH<sub>3</sub>), 29.8 (CH<sub>2</sub>), 46.9 (CH), 78.5 (CH<sub>2</sub>, d,  $^1J_{\text{CF}}$  162.9 Hz), 125.5 (C, d,  $^2J_{\text{CF}}$  15.4 Hz), 127.1 (CH), 128.1 (CH), 128.3 (C, d,  $^4J_{\text{CF}}$  1.9 Hz), 128.4 (2 × CH), 128.6 (CH), 129.7 (CH), 129.7 (2 × CH), 130.5 (CH, d,  $^5J_{\text{CF}}$  0.9 Hz), 135.2 (C), 146.2 (C, d,  $^3J_{\text{CF}}$  2.4 Hz), 150.0 (C), 152.5 (C, d,  $^3J_{\text{CF}}$  4.9 Hz), 165.1 (C); *m/z* (ESI) 359.1514 (MNa<sup>+</sup>. C<sub>21</sub>H<sub>21</sub>FN<sub>2</sub>NaO requires 359.1530).

**(±)-3-(Acetoxymethyl)-(N-sec-butyl)-4-phenylquinoline-2-carboxamide (160)**

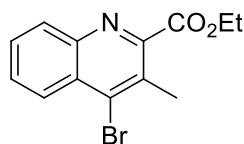
To a solution of (±)-(*N*-sec-butyl)-3-(hydroxymethyl)-4-phenylquinoline-2-carboxamide (**159**) (0.10 g, 0.30 mmol) in dichloromethane (4.0 mL) was added triethylamine (0.062 mL, 0.45 mmol), acetic anhydride (0.057 mL, 0.60 mmol) and 4-dimethylaminopyridine (0.0040 g, 0.030 mmol) and the reaction mixture was stirred under argon at room temperature for 1 h. The reaction mixture was dissolved in ethyl acetate (20 mL) and washed with saturated aqueous sodium bicarbonate (20 mL), water (20 mL) and brine (20 mL). The organic layer was then dried ( $\text{MgSO}_4$ ), filtered and concentrated *in vacuo*. The crude material was purified by flash column chromatography, eluting with 20% ethyl acetate in petroleum ether (40–60) to afford (±)-3-(acetoxymethyl)-(*N*-sec-butyl)-4-phenylquinoline-2-carboxamide (**160**) as a white solid (0.10 g, 89%). Mp 138–140 °C;  $\nu_{\text{max}}/\text{cm}^{-1}$  (neat) 3337 (NH), 2967 (CH), 1740 (CO), 1667 (CO), 1514 (C=C), 1487, 1236, 1028, 768;  $\delta_{\text{H}}$  (400 MHz,  $\text{CDCl}_3$ ) 1.03 (3H, t,  $J$  7.4 Hz,  $\text{CH}_2\text{CH}_3$ ), 1.32 (3H, d,  $J$  6.7 Hz,  $\text{CHCH}_2$ ), 1.59–1.76 (2H, m,  $\text{CH}_2\text{CH}_3$ ), 1.97 (3H, s,  $\text{OCOCH}_3$ ), 4.10–4.20 (1H, m,  $\text{CHCH}_3$ ), 5.48 (1H, d,  $J$  15.8 Hz, 3- $\text{CHH}$ ), 5.50 (1H, d,  $J$  15.8 Hz, 3- $\text{CHH}$ ), 7.24–7.32 (2H, m, ArH), 7.39–7.56 (5H, m, ArH), 7.74 (1H, ddd,  $J$  7.0, 6.7, 1.5 Hz, ArH), 7.84 (1H, d,  $J$  8.6 Hz, NH), 8.15 (1H, d,  $J$  8.5 Hz, ArH);  $\delta_{\text{C}}$  (101 MHz,  $\text{CDCl}_3$ ) 10.5 ( $\text{CH}_3$ ), 20.5 ( $\text{CH}_3$ ), 20.8 ( $\text{CH}_3$ ), 29.8 ( $\text{CH}_2$ ), 46.8 (CH), 61.2 ( $\text{CH}_2$ ), 125.7 (C), 126.8 (CH), 128.0 (CH), 128.3 (C), 128.4 (2 × CH), 128.5 (CH), 129.42 (CH), 129.44 (CH), 129.6 (CH), 130.2 (CH), 135.4 (C), 145.9 (C), 150.2 (C), 151.9 (C), 165.2 (C), 170.2 (C);  $m/z$  (ESI) 399.1666 ( $\text{MNa}^+$ .  $\text{C}_{23}\text{H}_{24}\text{N}_2\text{NaO}_3$  requires 399.1679).

**Ethyl 4-hydroxy-3-methylquinoline-2-carboxylate (170)<sup>170</sup>**

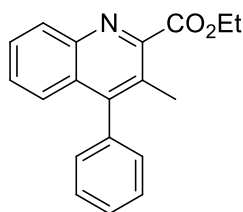
To a solution of aniline (2.25 mL, 24.7 mmol) and diethyl oxalpropionate (4.67 mL, 24.7 mmol) in cyclohexane (200 mL) under argon was added *p*-toluenesulfonic acid (0.0300 g, 0.170 mmol) and the reaction mixture heated under reflux at 120 °C using a Dean-Stark condenser for 72 h. After cooling to ambient temperature, the reaction mixture was

filtered, washed with hexane (100 mL) and the filtrate concentrated *in vacuo*. To this crude product was added polyphosphoric acid (20.0 g) and the mixture stirred at 120 °C for 1 h. After cooling to ambient temperature, a 2.4 M aqueous sodium carbonate solution (100 mL) was added slowly and the resulting yellow precipitate filtered. The crude material was purified by flash column chromatography, eluting with 50% ethyl acetate in petroleum ether (40–60) to afford ethyl 4-hydroxy-3-methylquinoline-2-carboxylate (**170**) as a pale yellow solid (3.41 g, 60%). Mp 176–178 °C, lit.<sup>170</sup> 176–178 °C;  $\delta_{\text{H}}$  (400 MHz,  $\text{CDCl}_3$ ) 1.48 (3H, t,  $J$  7.2 Hz,  $\text{OCH}_2\text{CH}_3$ ), 2.49 (3H, s, 3- $\text{CH}_3$ ), 4.52 (2H, q,  $J$  7.2 Hz,  $\text{OCH}_2\text{CH}_3$ ), 7.31–7.37 (2H, m, ArH), 7.62 (1H, ddd,  $J$  8.4, 5.5, 1.5 Hz, ArH), 8.35 (1H,  $J$  8.4 Hz, ArH), 9.04 (1H, s, OH);  $\delta_{\text{C}}$  (101 MHz,  $\text{CDCl}_3$ ) 11.7 ( $\text{CH}_3$ ), 14.2 ( $\text{CH}_3$ ), 63.3 ( $\text{CH}_2$ ), 117.5 (CH), 122.8 (C), 123.7 (C), 123.8 (CH), 126.6 (CH), 132.7 (CH), 132.8 (C), 138.3 (C), 164.4 (C), 179.7 (C);  $m/z$  (EI) 231 ( $\text{M}^+$ , 100%), 202 (100), 157 (98), 129 (46), 84 (41).

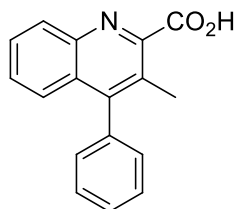
#### Ethyl 4-bromo-3-methylquinoline-2-carboxylate (**171**)<sup>170</sup>



To a solution of ethyl 4-hydroxy-3-methylquinoline-2-carboxylate (**170**) (3.40 g, 14.7 mmol) in acetonitrile (187 mL) under argon was added phosphorous oxybromide (12.6 g, 44.1 mmol) and potassium carbonate (6.10 g, 44.1 mmol) and the reaction mixture heated under reflux for 2 h. After cooling to ambient temperature, the reaction mixture was concentrated *in vacuo*. Water (100 mL) was added to the residue and the product was extracted with ethyl acetate (3 × 100 mL), dried ( $\text{MgSO}_4$ ), filtered and concentrated *in vacuo* to afford ethyl 4-bromo-3-methylquinoline-2-carboxylate (**171**) as a brown solid (3.71 g, 86%). Mp 48–50 °C, lit.<sup>170</sup> 48–50 °C;  $\delta_{\text{H}}$  (400 MHz,  $\text{CDCl}_3$ ) 1.48 (3H, t,  $J$  7.1 Hz,  $\text{OCH}_2\text{CH}_3$ ), 2.72 (3H, s, 3- $\text{CH}_3$ ), 4.55 (2H, q,  $J$  7.1 Hz,  $\text{OCH}_2\text{CH}_3$ ), 7.68 (1H, ddd,  $J$  8.3, 6.9, 1.4 Hz, ArH), 7.75 (1H, ddd,  $J$  8.3, 6.9, 1.4 Hz, ArH), 8.18 (1H, br d,  $J$  8.3 Hz, ArH), 8.25 (1H, br d,  $J$  8.3 Hz, ArH);  $\delta_{\text{C}}$  (101 MHz,  $\text{CDCl}_3$ ) 14.2 ( $\text{CH}_3$ ), 19.8 ( $\text{CH}_3$ ), 62.3 ( $\text{CH}_2$ ), 126.8 (CH), 128.5 (C), 129.2 (CH), 129.4 (C), 129.9 (CH), 130.2 (CH), 137.3 (C), 146.0 (C), 151.1 (C), 166.5 (C);  $m/z$  (EI) 293 ( $\text{M}^+$ , 100%), 264 (39), 221 (73), 140 (100), 114 (21), 84 (81).

**Ethyl 3-methyl-4-phenylquinoline-2-carboxylate (172)**<sup>210</sup>

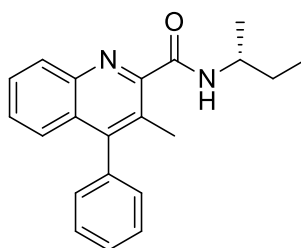
To a solution of ethyl 4-bromo-3-methylquinoline-2-carboxylate (**171**) (3.70 g, 12.6 mmol) in *N,N*-dimethylformamide (200 mL) was added benzeneboronic acid (2.00 g, 16.4 mmol) and potassium phosphate tribasic (3.48 g, 16.4 mmol) and the reaction mixture degassed under argon for 0.2 h. To this solution was added tetrakis(triphenylphosphine)palladium(0) (0.440 g, 0.378 mmol) and the reaction stirred under reflux for 16 h. After cooling to ambient temperature, the reaction mixture was filtered through a short pad of Celite<sup>®</sup>, washing with ethyl acetate (500 mL) and the filtrate washed with water (3 × 500 mL) and brine (500 mL). The organic layer was dried (MgSO<sub>4</sub>), filtered and concentrated *in vacuo*. The crude material was purified by flash column chromatography, eluting with 20% ethyl acetate in petroleum ether (40–60) and recrystallised from hexane to afford ethyl 3-methyl-4-phenylquinoline-2-carboxylate (**172**) as white crystals (2.88 g, 78%). Mp 110–112 °C, lit.<sup>210</sup> 114–115 °C;  $\delta_{\text{H}}$  (400 MHz, CDCl<sub>3</sub>) 1.48 (3H, t, *J* 7.2 Hz, OCH<sub>2</sub>CH<sub>3</sub>), 2.32 (3H, s, 3-CH<sub>3</sub>), 4.55 (2H, q, *J* 7.2 Hz, OCH<sub>2</sub>CH<sub>3</sub>), 7.23–7.27 (2H, m, ArH), 7.37–7.56 (5H, m, ArH), 7.67 (1H, ddd, *J* 8.3, 6.7, 1.4 Hz, ArH), 8.19 (1H, br d, *J* 8.3 Hz, ArH);  $\delta_{\text{C}}$  (101 MHz, CDCl<sub>3</sub>) 14.3 (CH<sub>3</sub>), 16.8 (CH<sub>3</sub>), 62.1 (CH<sub>2</sub>), 126.0 (CH), 126.2 (C), 127.7 (CH), 128.1 (CH), 128.2 (C), 128.7 (2 × CH), 129.0 (CH), 129.2 (2 × CH), 129.8 (CH), 136.7 (C), 145.6 (C), 148.7 (C), 151.5 (C), 167.4 (C); *m/z* (CI) 292 (MH<sup>+</sup>, 100%), 220 (48), 137 (3), 113 (9), 85 (19).

**3-Methyl-4-phenylquinoline-2-carboxylic acid (173)**<sup>210</sup>

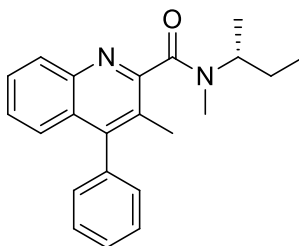
To a solution of ethyl 3-methyl-4-phenylquinoline-2-carboxylate (**172**) (2.88 g, 9.88 mmol) in 50% aqueous ethanol (200 mL) was added sodium hydroxide (1.58 g, 39.5 mmol) and the reaction mixture heated at 80 °C for 1.5 h. After cooling to ambient temperature, the ethanol was removed *in vacuo* and the reaction mixture acidified to pH 1 with a 1 M aqueous hydrochloric acid solution. The product was extracted into dichloromethane (3 ×

100 mL) and washed with water (100 mL) and brine (100 mL). The organic extracts were dried ( $\text{MgSO}_4$ ), filtered and concentrated *in vacuo* to afford 3-methyl-4-phenylquinoline-2-carboxylic acid (**173**) as a white solid (2.54 g, 98%). The spectroscopic data were consistent with the literature.<sup>210</sup> Mp 130–132 °C;  $\delta_{\text{H}}$  (400 MHz,  $\text{CDCl}_3$ ) 2.65 (3H, s, 3- $\text{CH}_3$ ), 7.23–7.25 (2H, m, ArH), 7.43 (1H, br d,  $J$  8.3 Hz, ArH), 7.50–7.60 (4H, m, ArH), 7.75 (1H, ddd,  $J$  8.3, 6.9, 1.2 Hz, ArH), 8.14 (1H, br d,  $J$  8.3 Hz, ArH);  $\delta_{\text{C}}$  (101 MHz,  $\text{CDCl}_3$ ) 17.4 ( $\text{CH}_3$ ), 126.5 (CH), 128.4 (CH), 128.8 (2  $\times$  CH), 129.0 (CH), 129.1 (CH), 129.2 (2  $\times$  CH), 129.7 (C), 129.8 (CH), 130.2 (C), 136.4 (C), 143.6 (C), 144.2 (C), 151.4 (C), 164.4 (C);  $m/z$  (CI) 264 ( $\text{MH}^+$ , 100%), 220 (19), 188 (3), 85 (27).

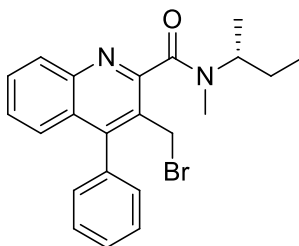
**(R)-(N-sec-Butyl)-3-methyl-4-phenylquinoline-2-carboxamide (174)**<sup>174</sup>



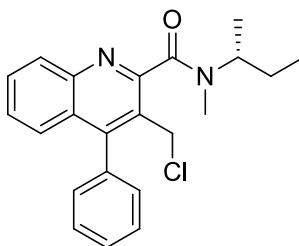
To a solution of 3-methyl-4-phenylquinoline-2-carboxylic acid (**173**) (2.54 g, 9.65 mmol) in anhydrous *N,N*-dimethylformamide (250 mL) was added *O*-(benzotriazol-1-yl)-*N,N,N,N*-tetramethyluronium hexafluorophosphate (5.49 g, 14.5 mmol) and *N,N*-diisopropylethylamine (3.40 mL, 19.3 mmol). The reaction mixture was stirred at room temperature for 0.5 h before the addition of (*R*)-(-)-*sec*-butylamine (1.10 mL, 10.6 mmol). The reaction mixture was then heated at 50 °C for 4 h. The reaction mixture was cooled to room temperature, diluted with ethyl acetate (300 mL) and washed with water (3  $\times$  200 mL) and brine (200 mL). The organic layer was dried ( $\text{MgSO}_4$ ), filtered and concentrated *in vacuo* to give a brown oil. The crude material was purified by flash column chromatography, eluting with 20% ethyl acetate in petroleum ether (40–60) to afford (*R*)-(*N-sec*-butyl)-3-methyl-4-phenylquinoline-2-carboxamide (**174**) as a white solid (2.81 g, 91%). Mp 152–154 °C, lit.<sup>174</sup> 157–158 °C;  $[\alpha]_{\text{D}}^{25}$  -26.7 ( $c$  1.0,  $\text{CHCl}_3$ );  $\delta_{\text{H}}$  (400 MHz,  $\text{CDCl}_3$ ) 1.03 (3H, t,  $J$  7.4 Hz,  $\text{CH}_2\text{CH}_3$ ), 1.33 (3H, d,  $J$  6.6 Hz,  $\text{CHCH}_3$ ), 1.61–1.75 (2H, m,  $\text{CH}_2\text{CH}_3$ ), 2.56 (3H, s, 3- $\text{CH}_3$ ), 4.07–4.21 (1H, m,  $\text{CHCH}_3$ ), 7.21–7.25 (2H, m, ArH), 7.35 (1H, br d,  $J$  8.3 Hz, ArH), 7.40–7.55 (4H, m, ArH), 7.65 (1H, ddd,  $J$  8.3, 6.8, 1.4 Hz, ArH), 7.90 (1H, d,  $J$  8.3 Hz, NH), 8.09 (1H, br d,  $J$  8.3 Hz, ArH);  $\delta_{\text{C}}$  (101 MHz,  $\text{CDCl}_3$ ) 10.6 ( $\text{CH}_3$ ), 17.6 ( $\text{CH}_3$ ), 20.5 ( $\text{CH}_3$ ), 29.9 ( $\text{CH}_2$ ), 46.8 (CH), 126.1 (CH), 127.5 (CH), 127.9 (CH), 128.6 (C), 128.6 (2  $\times$  CH), 128.7 (CH), 128.8 (C), 129.3 (2  $\times$  CH), 129.5 (CH), 137.3 (C), 144.7 (C), 149.5 (C), 150.1 (C), 166.2 (C);  $m/z$  (CI) 319 ( $\text{MH}^+$ , 100%), 220 (19), 202 (5), 148 (6), 113 (16), 85 (77).

**(R)-(N-sec-Butyl)-N-methyl-3-methyl-4-phenylquinoline-2-carboxamide (167)**<sup>174</sup>

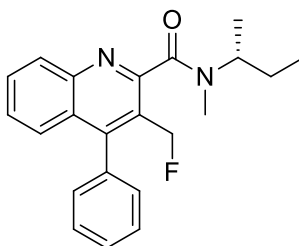
To a solution of (*R*)-(*N*-sec-butyl)-3-methyl-4-phenylquinoline-2-carboxamide (**174**) (2.81 g, 8.82 mmol) in tetrahydrofuran (176 mL) was added sodium hydride (0.710 g, 17.6 mmol, 60% dispersion in mineral oil) and the reaction mixture stirred under argon at room temperature for 0.5 h. Iodomethane (2.75 mL, 44.1 mmol) was then added and the reaction mixture stirred at room temperature for a further 3 h. The reaction was quenched by the addition of water (20 mL) and the tetrahydrofuran was removed *in vacuo*. The aqueous phase was extracted with diethyl ether (3 × 50 mL) and the combined organic layers were washed with a 1 M aqueous solution of sodium thiosulfate (100 mL), brine (100 mL), dried (MgSO<sub>4</sub>), filtered and concentrated *in vacuo*. The crude material was purified by flash column chromatography, eluting with 25% ethyl acetate in petroleum ether (40–60) to afford (*R*)-(*N*-sec-butyl)-*N*-methyl-3-methyl-4-phenylquinoline-2-carboxamide (**167**) as a white solid (2.75 g, 94%). Mp 114–117 °C, lit.<sup>174</sup> 117–118 °C; [α]<sub>D</sub><sup>23</sup> –6.3 (*c* 1.0, CHCl<sub>3</sub>); NMR spectra showed a 1:1 mixture of rotamers. Signals for both rotamers are recorded. δ<sub>H</sub> (400 MHz, CDCl<sub>3</sub>) 0.86 (3H, t, *J* 7.3 Hz, CH<sub>2</sub>CH<sub>3</sub>), 1.03 (3H, t, *J* 7.3 Hz, CH<sub>2</sub>CH<sub>3</sub>), 1.24 (3H, d, *J* 6.6 Hz, CHCH<sub>3</sub>), 1.28 (3H, d, *J* 6.6 Hz, CHCH<sub>3</sub>), 1.36–1.49 (2H, m, CH<sub>2</sub>CH<sub>3</sub>), 1.53–1.74 (2H, m, CH<sub>2</sub>CH<sub>3</sub>), 2.21 (3H, s, 3-CH<sub>3</sub>), 2.23 (3H, s, 3-CH<sub>3</sub>), 2.73 (3H, s, NCH<sub>3</sub>), 3.04 (3H, s, NCH<sub>3</sub>), 3.43–3.55 (1H, m, CHCH<sub>3</sub>), 4.83–4.95 (1H, m, CHCH<sub>3</sub>), 7.23–7.31 (4H, m, ArH), 7.38–7.44 (4H, m, ArH), 7.45–7.57 (6H, m, ArH), 7.60–7.67 (2H, m, ArH), 8.09 (1H, d, *J* 8.3 Hz, ArH), 8.12 (1H, d, *J* 8.3 Hz, ArH); δ<sub>C</sub> (101 MHz, CDCl<sub>3</sub>) 11.2 (CH<sub>3</sub>), 11.3 (CH<sub>3</sub>), 16.0 (CH<sub>3</sub>), 16.4 (CH<sub>3</sub>), 17.3 (CH<sub>3</sub>), 18.6 (CH<sub>3</sub>), 25.5 (CH<sub>3</sub>), 26.5 (CH<sub>2</sub>), 27.2 (CH<sub>2</sub>), 29.3 (CH<sub>3</sub>), 49.6 (CH), 55.8 (CH), 124.6 (C), 125.3 (C), 125.9 (CH), 126.0 (CH), 126.8 (CH), 126.8 (CH), 127.4 (C), 127.4 (C), 128.0 (2 × CH), 128.6 (CH), 128.6 (2 × CH), 128.7 (CH), 128.7 (CH), 129.2 (CH), 129.2 (4 × CH), 129.4 (CH), 129.4 (CH), 136.7 (C), 136.8 (C), 145.8 (C), 146.1 (C), 148.0 (C), 148.1 (C), 156.1 (C), 156.6 (C), 169.4 (C), 169.7 (C); *m/z* (CI) 333 (MH<sup>+</sup>, 100%), 291 (48), 250 (41), 220 (14), 86 (23).

**(R)-3-Bromomethyl-(N-sec-butyl)-N-methyl-4-phenylquinoline-2-carboxamide (168)**

A solution of (*R*)-(*N*-sec-butyl)-*N*-methyl-3-methyl-4-phenylquinoline-2-carboxamide (**167**) (2.70 g, 8.12 mmol) in chloroform (300 mL) was degassed under argon for 0.2 h. To this was added *N*-bromosuccinimide (2.17 g, 12.2 mmol) and dibenzoyl peroxide (0.200 g, 0.812 mmol) and the solution heated under reflux for 6 h. A further portion of *N*-bromosuccinimide (1.00 g, 5.62 mmol) was then added and the solution heated under reflux for a further 16 h. After cooling to ambient temperature, the reaction mixture was filtered, and the solvent removed *in vacuo*. The crude residue was then diluted with ethyl acetate (100 mL) and washed with water (3 × 100 mL). The organic layer was dried (MgSO<sub>4</sub>), filtered and concentrated *in vacuo*. The crude material was purified by flash column chromatography, eluting with 0–5% ethyl acetate in dichloromethane to afford (*R*)-3-bromomethyl-(*N*-sec-butyl)-*N*-methyl-4-phenylquinoline-2-carboxamide (**168**) as a pale yellow solid (2.76 g, 83%). Mp 160–164 °C;  $\nu_{\max}/\text{cm}^{-1}$  (KBr) 2970 (CH), 1631 (CO), 1484, 1397, 1046, 766;  $[\alpha]_{\text{D}}^{28}$  –9.0 (*c* 1.0, CHCl<sub>3</sub>); NMR spectra showed a 2:1 mixture of rotamers. Only signals for the major rotamer are recorded.  $\delta_{\text{H}}$  (400 MHz, CDCl<sub>3</sub>) 1.09 (3H, t, *J* 7.4 Hz, CH<sub>2</sub>CH<sub>3</sub>), 1.32 (3H, d, *J* 6.8 Hz, CHCH<sub>3</sub>), 1.51–1.80 (2H, m, CH<sub>2</sub>CH<sub>3</sub>), 2.86 (3H, s, NCH<sub>3</sub>), 4.60 (1H, d, *J* 10.2 Hz, 3-CHH), 4.67 (1H, d, *J* 10.2 Hz, 3-CHH), 4.81–4.94 (1H, m, CHCH<sub>3</sub>), 7.37–7.48 (4H, m, ArH), 7.51–7.59 (3H, m, ArH), 7.70 (1H, ddd, *J* 8.3, 6.7, 1.5 Hz, ArH), 8.12 (1H, d, *J* 8.8 Hz, ArH);  $\delta_{\text{C}}$  (101 MHz, CDCl<sub>3</sub>) 11.1 (CH<sub>3</sub>), 17.1 (CH<sub>3</sub>), 26.6 (CH<sub>2</sub>), 27.7 (CH<sub>2</sub>), 30.5 (CH<sub>3</sub>), 50.1 (CH), 126.3 (C), 126.7 (2 × CH), 127.3 (C), 127.4 (CH), 128.6 (2 × CH), 128.7 (CH), 129.1 (CH), 129.5 (CH), 130.1 (CH), 134.9 (C), 146.4 (C), 149.3 (C), 156.0 (C), 168.4 (C); *m/z* (EI) 410.0992 (M<sup>+</sup>. C<sub>22</sub>H<sub>23</sub><sup>79</sup>BrN<sub>2</sub>O requires 410.0994), 298 (15%), 296 (14), 217 (57), 189 (28), 151 (10), 86 (100).

**(R)-(N-sec-Butyl)-3-chloromethyl-N-methyl-4-phenylquinoline-2-carboxamide (184)**

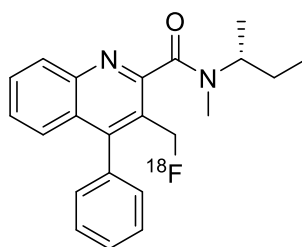
To a solution of (*R*)-3-bromomethyl-(*N*-sec-butyl)-*N*-methyl-4-phenylquinoline-2-carboxamide (**168**) (0.500 g, 1.22 mmol) in tetrahydrofuran (10 mL) under argon was added lithium chloride (0.160 g, 3.66 mmol) and the reaction mixture stirred at room temperature for 16 h. The reaction was quenched with water (30 mL) and the mixture was extracted into ethyl acetate (3 × 30 mL). The organic layers were combined and washed with brine (90 mL), dried (MgSO<sub>4</sub>), filtered and concentrated *in vacuo*. The crude material was purified by flash column chromatography, eluting with 5% ethyl acetate in dichloromethane to afford (*R*)-(*N*-sec-butyl)-3-chloromethyl-*N*-methyl-4-phenylquinoline-2-carboxamide (**184**) as a white solid (0.327 g, 73%). Mp 140–142 °C;  $\nu_{\max}/\text{cm}^{-1}$  (neat) 2970 (CH), 1620 (CO), 1481, 1404, 1219, 748;  $[\alpha]_{\text{D}}^{28}$  –11.6 (*c* 1.0, CHCl<sub>3</sub>); NMR spectra showed a 1.5:1 mixture of rotamers. Only signals for the major rotamer are recorded.  $\delta_{\text{H}}$  (400 MHz, CDCl<sub>3</sub>) 1.08 (3H, t, *J* 7.4 Hz, CH<sub>2</sub>CH<sub>3</sub>), 1.30 (3H, d, *J* 6.8 Hz, CHCH<sub>3</sub>), 1.49–1.79 (2H, m, CH<sub>2</sub>CH<sub>3</sub>), 2.84 (3H, s, NCH<sub>3</sub>), 4.67 (1H, d, *J* 10.6 Hz, 3-CHH), 4.72 (1H, d, *J* 10.6 Hz, 3-CHH), 4.81–4.93 (1H, m, CHCH<sub>3</sub>), 7.34–7.61 (7H, m, ArH), 7.69–7.75 (1H, m, ArH), 8.13 (1H, d, *J* 8.4 Hz, ArH);  $\delta_{\text{C}}$  (101 MHz, CDCl<sub>3</sub>) 11.1 (CH<sub>3</sub>), 17.1 (CH<sub>3</sub>), 26.6 (CH<sub>2</sub>), 30.4 (CH<sub>3</sub>), 40.4 (CH<sub>2</sub>), 50.1 (CH), 125.8 (C), 126.8 (CH), 127.2 (C), 127.4 (CH), 128.5 (2 × CH), 128.7 (CH), 129.4 (CH), 129.6 (2 × CH), 130.1 (CH), 134.9 (C), 146.6 (C), 149.5 (C), 156.1 (C), 168.5 (C); *m/z* (ESI) 389.1381 (MNa<sup>+</sup>. C<sub>22</sub>H<sub>23</sub><sup>35</sup>ClN<sub>2</sub>NaO requires 389.1391).

**(R)-(N-sec-Butyl)-3-(fluoromethyl)-N-methyl-4-phenylquinoline-2-carboxamide (155)**

To a solution of 18-crown-6 (0.032 g, 0.12 mmol) in acetonitrile (2.5 mL) under argon was added potassium fluoride (0.036 g, 0.61 mmol) and the suspension stirred at ambient temperature for 0.5 h. A solution of (*R*)-(*N*-sec-butyl)-3-bromomethyl-*N*-methyl-4-

phenylquinoline-2-carboxamide (**168**) (0.050 g, 0.122 mmol) in acetonitrile (6.0 mL) and dichloromethane (3.0 mL) was then added dropwise to the reaction mixture. The mixture was stirred under reflux for 72 h. On cooling to ambient temperature, water (20 mL) was added to the mixture and the product extracted using dichloromethane (3 × 20 mL). The combined organic layers were dried (MgSO<sub>4</sub>), filtered and concentrated *in vacuo*. The crude material was purified by flash column chromatography, eluting with 30% ethyl acetate in petroleum ether (40–60) to afford (*R*)-(*N*-sec-butyl)-3-(fluoromethyl)-*N*-methyl-4-phenylquinoline-2-carboxamide (**155**) as a white solid (0.023 g, 53%). Mp 146–148 °C;  $\nu_{\max}/\text{cm}^{-1}$  (neat) 2972 (CH), 1628 (CO), 1559, 1485, 1398, 1049, 970;  $[\alpha]_{\text{D}}^{30}$  –12.6 (*c* 0.5, CHCl<sub>3</sub>); NMR spectra showed a 3:1 mixture of rotamers. Only signals for the major rotamer are recorded.  $\delta_{\text{H}}$  (400 MHz, CDCl<sub>3</sub>) 1.05 (3H, t, *J* 7.4 Hz, CH<sub>2</sub>CH<sub>3</sub>), 1.29 (3H, d, *J* 6.8 Hz, CHCH<sub>3</sub>), 1.41–1.78 (2H, m, CH<sub>2</sub>CH<sub>3</sub>), 2.77 (3H, s, NCH<sub>3</sub>), 4.84–4.95 (1H, m, CHCH<sub>3</sub>), 5.35 (1H, dd, *J* 48.0, 10.5 Hz, 3-CHH), 5.40 (1H, dd, *J* 48.0, 10.5 Hz, 3-CHH), 7.31–7.40 (2H, m, ArH), 7.43–7.58 (5H, m, ArH), 7.74 (1H, t, *J* 7.6 Hz, ArH), 8.17 (1H, d, *J* 8.4 Hz, ArH);  $\delta_{\text{C}}$  (101 MHz, CDCl<sub>3</sub>) 10.9 (CH<sub>3</sub>), 17.4 (CH<sub>3</sub>), 26.5 (CH<sub>3</sub>), 29.9 (CH<sub>2</sub>), 50.0 (CH), 79.2 (CH<sub>2</sub>, <sup>1</sup>*J*<sub>CF</sub> 162.8 Hz), 123.0 (C, <sup>2</sup>*J*<sub>CF</sub> 15.1 Hz), 127.0 (CH), 127.1 (C, <sup>4</sup>*J*<sub>CF</sub> 2.3 Hz), 127.4 (CH, <sup>5</sup>*J*<sub>CF</sub> 1.2 Hz), 128.5 (2 × CH), 128.7 (CH), 129.6 (2 × CH), 129.7 (CH), 130.4 (CH), 134.8 (C, <sup>4</sup>*J*<sub>CF</sub> 1.5 Hz), 147.4 (C, <sup>3</sup>*J*<sub>CF</sub> 2.5 Hz), 150.8 (C, <sup>3</sup>*J*<sub>CF</sub> 4.7 Hz), 156.6 (C, <sup>5</sup>*J*<sub>CF</sub> 2.1 Hz), 168.8 (C); *m/z* (ESI) 373.1670 (MNa<sup>+</sup>. C<sub>22</sub>H<sub>23</sub>FN<sub>2</sub>NaO requires 373.1687); Enantiomeric excess was determined by HPLC analysis with a Chiralcel AD-H column (hexane:PrOH 97.5:2.5, flow rate 1.0 mL/min), *t*<sub>major</sub> = 30.68 and 32.22 min, *t*<sub>minor</sub> = 27.15 and 38.38 min; er = 99.5:0.5.

#### Radiosynthesis of (*R*)-(*N*-sec-Butyl)-3-([<sup>18</sup>F]fluoromethyl)-*N*-methyl-4-phenylquinoline-2-carboxamide ([<sup>18</sup>F]**155**)



Radiofluorination was carried out on a GE TRACERlab FX<sub>FN</sub> synthesiser. [<sup>18</sup>F]Fluoride was produced by cyclotron irradiation of a target containing [<sup>18</sup>O]water *via* the <sup>18</sup>O(p,n)<sup>18</sup>F nuclear reaction. After trapping on a Sep-Pak® Light QMA cartridge, the activity was eluted into the reaction vial using a solution of Kryptofix® 222 (16 mg) and potassium carbonate (2.9 mg) in acetonitrile (1.7 mL) and water (0.3 mL). Azeotropic drying took place using acetonitrile (1.0 mL), (*R*)-(*N*-sec-butyl)-3-chloromethyl-*N*-methyl-4-phenylquinoline-2-carboxamide (**184**) (5.0 mg) in acetonitrile (1.0 mL) was added and the

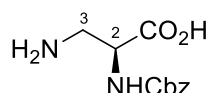
reaction heated to 110 °C for 5 min. The reaction mixture was then diluted with acetonitrile (0.5 mL) and water (2.5 mL) and loaded onto a C<sub>18</sub> Synergi Hydro-RP 80 Å, 150×10 mm, 4 µm column (Phenomenex, UK). A 70% solution of acetonitrile in water was used as the mobile phase at a flow rate of 3 mL min<sup>-1</sup>. The radiolabelled product was detected by the HPLC gamma-detector and eluted at approximately 10 min. The collected fraction was diluted with water (20 mL) and then transferred onto a Sep-Pak<sup>®</sup> Plus Light C<sub>18</sub> cartridge. This was rinsed with water (1 mL) and the product eluted with ethanol (0.25 mL) then saline (4.75 mL). This provided a 5% ethanol/saline formulation of the product in a total synthesis time of 32 min. The radiolabelled product was isolated with a radiochemical yield of 32% ± 2.9% and a specific activity of 144 ± 20 GBq mg<sup>-1</sup> (n = 4). The radiochemical purity was >99%.

### 3.6 Benzotriazoles Experimental

#### General procedure for the preparation of polymer-supported nitrite<sup>181</sup>

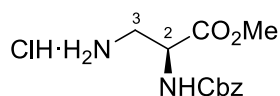
The polymer-supported nitrite reagent was prepared by the addition of Amberlyst® A26 hydroxide form resin (10.0 g, 40.0 mmol) to a solution of sodium nitrite (5.50 g, 80.0 mmol) in water (200 mL). The mixture was stirred at room temperature for 0.5 h. The polymer-supported nitrite was filtered and washed with water until the pH of the filtrate became neutral. The content of the polymer-supported nitrite was 3.5 mmol of NO<sub>2</sub><sup>-</sup> per g.<sup>181</sup>

#### (2S)-3-Amino-2-[(benzyloxycarbonyl)amino]propionic acid (**193**)<sup>193</sup>



To a suspension of *N*<sub>α</sub>-(benzyloxycarbonyl)-L-asparagine (10.0 g, 37.6 mmol) in acetonitrile (19.2 mL), ethyl acetate (19.2 mL) and water (9.6 mL) was added (diacetoxyiodo)benzene (14.6 g, 45.1 mmol) and the reaction mixture cooled to between 10–15 °C and stirred for 0.75 h at this temperature. The reaction mixture was then allowed to reach room temperature over 0.75 h and heated to 70 °C for 0.1 h before allowing to cool to ambient temperature. The reaction mixture was filtered and the resulting solid washed with diethyl ether (100 mL) to afford (2S)-3-amino-2-[(benzyloxycarbonyl)amino]propionic acid (**193**) as a white solid (8.96 g, 100%). Mp 208–210 °C; [α]<sub>D</sub><sup>23</sup> -7.9 (c 1.2, 1 M NaOH), lit.<sup>193</sup> [α]<sub>D</sub><sup>23</sup> -7.7 (c 0.4, 1 M NaOH); δ<sub>H</sub> (400 MHz, DMSO-*d*<sub>6</sub>/TFA) 2.99–3.06 (1H, m, 3-*HH*), 3.21–3.28 (1H, m, 3-*HH*), 4.30 (1H, dt, *J* 8.9, 4.6 Hz, 2-H), 5.07 (2H, s, OCH<sub>2</sub>Ph), 7.28–7.37 (5H, m, Ph), 7.70 (1H, d, *J* 8.9 Hz, NH), 7.91 (2H, s, NH<sub>2</sub>); δ<sub>C</sub> (101 MHz, DMSO-*d*<sub>6</sub>/TFA) 40.4 (CH<sub>2</sub>), 51.9 (CH), 66.0 (CH<sub>2</sub>), 127.95 (2 × CH), 128.0 (CH), 128.5 (2 × CH), 136.8 (C), 156.4 (C), 170.9 (C); *m/z* (ESI) 261 (MNa<sup>+</sup>, 100%).

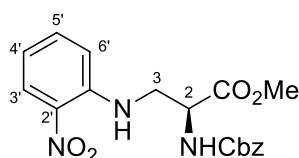
#### Methyl (2S)-3-amino-2-[(benzyloxycarbonyl)amino]propanoate hydrochloride (**191**)<sup>194</sup>



To a suspension of (2S)-3-amino-2-[(benzyloxycarbonyl)amino]propionic acid (**193**) (8.96 g, 37.6 mmol) in methanol (144 mL) at 0 °C under argon was added dropwise thionyl chloride (4.12 mL, 56.4 mmol). The reaction mixture was allowed to reach room

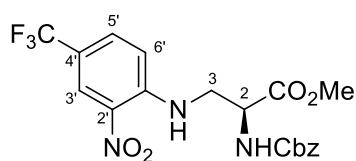
temperature and stirred for 16 h. The solution was then concentrated *in vacuo* and azeotroped with toluene (3 × 50 mL) to remove excess thionyl chloride. The resulting residue was triturated with diethyl ether to afford methyl (2*S*)-3-amino-2-[(benzyloxycarbonyl)amino]propanoate hydrochloride (**191**) as a white solid (9.48 g, 100%). Mp 165–168 °C, lit.<sup>211</sup> 165–167 °C;  $[\alpha]_D^{22}$  –41.4 (c 1.1, MeOH), lit.<sup>211</sup>  $[\alpha]_D^{20}$  –42.5 (c 1.0, MeOH);  $\delta_H$  (400 MHz, CD<sub>3</sub>OD) 3.23 (1H, dd, *J* 13.2, 8.8 Hz, 3-*HH*), 3.45 (1H, dd, *J* 13.2, 5.1 Hz, 3-*HH*), 3.78 (3H, s, OCH<sub>3</sub>), 4.51 (1H, dd, *J* 8.8, 5.1 Hz, 2-H), 5.14 (2H, s, OCH<sub>2</sub>Ph), 7.30–7.40 (5H, m, PhH);  $\delta_C$  (101 MHz, CD<sub>3</sub>OD) 41.3 (CH<sub>2</sub>), 53.1 (CH), 53.4 (CH<sub>3</sub>), 68.2 (CH<sub>2</sub>), 129.0 (2 × CH), 129.2 (CH), 129.5 (2 × CH), 137.8 (C), 158.7 (C), 170.9 (C); *m/z* (ESI) 275 (MNa<sup>+</sup>, 100%).

### Methyl (2*S*)-2-[(benzyloxycarbonyl)amino]-3-[(2'-nitrophenyl)amino]propanoate (**189**)



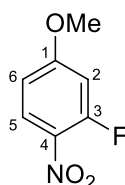
To a solution of methyl (2*S*)-3-amino-2-[(benzyloxycarbonyl)amino]propanoate hydrochloride (**191**) (0.250 g, 0.991 mmol) in acetonitrile (7.5 mL) under argon was added 2-fluoronitrobenzene (0.310 mL, 2.97 mmol) and triethylamine (0.410 mL, 2.97 mmol) and the reaction mixture stirred under reflux for 16 h. After cooling the reaction to ambient temperature, the solvent was removed *in vacuo*. The resulting residue was dissolved in ethyl acetate (50 mL), washed with water (3 × 50 mL) and brine (50 mL). The organic layer was dried (MgSO<sub>4</sub>), filtered and concentrated *in vacuo*. Crude material was purified by flash column chromatography, eluting with 0–20% ethyl acetate in dichloromethane to afford methyl (2*S*)-2-[(benzyloxycarbonyl)amino]-3-[(2'-nitrophenyl)amino]propanoate (**189**) as a yellow solid (0.330 g, 89%). Mp 82–84 °C;  $\nu_{\max}/\text{cm}^{-1}$  (neat) 3348 (NH), 2956 (CH), 1721 (CO), 1620, 1512 (C=C), 1265, 1234, 741;  $[\alpha]_D^{25}$  +50.8 (c 0.3, CHCl<sub>3</sub>);  $\delta_H$  (400 MHz, CDCl<sub>3</sub>) 3.64–3.74 (5H, m, 3-H<sub>2</sub> and OCH<sub>3</sub>), 4.57 (1H, dt, *J* 6.7, 5.7 Hz, 2-H), 5.04 (2H, s, OCH<sub>2</sub>Ph), 5.63 (1H, d, *J* 6.7 Hz, NH), 6.69 (1H, br t, *J* 8.6 Hz, 4'-H), 6.98 (1H, d, *J* 8.7 Hz, 6'-H), 7.27–7.51 (6H, m, Ph and 5'-H), 8.16 (1H, dd, *J* 8.6, 1.2 Hz, 3'-H), 8.22 (1H, t, *J* 5.6 Hz, NH);  $\delta_C$  (101 MHz, CDCl<sub>3</sub>) 44.6 (CH<sub>2</sub>), 53.1 (CH<sub>3</sub>), 53.6 (CH), 67.4 (CH<sub>2</sub>), 113.7 (CH), 116.3 (CH), 127.0 (CH), 128.3 (2 × CH), 128.4 (CH), 128.7 (2 × CH), 132.8 (C), 136.0 (C), 136.4 (CH), 144.9 (C), 155.9 (C), 170.8 (C); *m/z* (ESI) 396.1158 (MNa<sup>+</sup>, C<sub>18</sub>H<sub>19</sub>N<sub>3</sub>NaO<sub>6</sub> requires 396.1166).

**Methyl (2S)-2-(benzyloxycarbonyl)amino]-3-{{2'-nitro-4'-(trifluoromethyl)phenyl}amino}propanoate (196)**



Methyl (2S)-2-(benzyloxycarbonyl)amino]-3-{{2'-nitro-4'-(trifluoromethyl)phenyl}amino}propanoate (**196**) was synthesised as described for methyl (2S)-2-[(benzyloxycarbonyl)amino]-3-[(2'-nitrophenyl)amino]propanoate (**189**) using methyl (2S)-3-amino-2-[(benzyloxycarbonyl)amino]propanoate hydrochloride (**191**) (0.200 g, 0.793 mmol), 2-fluoro-5-(trifluoromethyl)-1-nitrobenzene (0.333 mL, 2.38 mmol) and triethylamine (0.332 mL, 2.38 mmol) in acetonitrile (6.0 mL). The crude material was purified by flash column chromatography, eluting with 0–20% ethyl acetate in dichloromethane to afford methyl (2S)-2-(benzyloxycarbonyl)amino]-3-{{2'-nitro-4'-(trifluoromethyl)phenyl}amino}propanoate (**196**) as a yellow solid (0.295 g, 84%). Mp 84–86 °C;  $\nu_{\max}/\text{cm}^{-1}$  (neat) 3356 (NH), 2955 (CH), 1713 (CO), 1636 (CO), 1535 (C=C), 1435, 1319, 1227, 1111, 756, 694;  $[\alpha]_{\text{D}}^{23}$  +25.9 (*c* 1.0, CHCl<sub>3</sub>);  $\delta_{\text{H}}$  (500 MHz, CDCl<sub>3</sub>) 3.75–3.82 (4H, m, 3-*HH* and OCH<sub>3</sub>), 3.85 (1H, ddd, *J* 13.8, 5.8, 5.4 Hz, 3-*HH*), 4.65 (1H, dt, *J* 6.9, 5.4 Hz, 2-H), 5.09 (1H, d, *J* 12.1 Hz, OCHHPh), 5.14 (1H, d, *J* 12.1 Hz, OCHHPh), 5.83 (1H, d, *J* 6.9 Hz, NH), 7.08 (1H, d, *J* 9.0 Hz, 6'-H), 7.27–7.43 (5H, m, Ph), 7.56 (1H, d, *J* 9.0 Hz, 5'-H), 8.42 (1H, s, 3'-H), 8.48 (1H, t, *J* 5.8 Hz, NH);  $\delta_{\text{C}}$  (126 MHz, CDCl<sub>3</sub>) 44.5 (CH<sub>2</sub>), 53.2 (CH<sub>3</sub>), 53.5 (CH), 67.4 (CH<sub>2</sub>), 114.5 (CH), 118.2 (C, q,  $^2J_{\text{CF}}$  34.4 Hz), 123.5 (C, q,  $^1J_{\text{CF}}$  271.0 Hz), 125.0 (CH, q,  $^3J_{\text{CF}}$  4.3 Hz), 128.3 (2 × CH), 128.5 (CH), 128.6 (2 × CH), 131.6 (C), 132.3 (CH, q,  $^3J_{\text{CF}}$  3.2 Hz), 135.9 (C), 146.6 (C), 156.0 (C), 170.4 (C); *m/z* (ESI) 464.1040 (MNa<sup>+</sup>. C<sub>19</sub>H<sub>18</sub>F<sub>3</sub>N<sub>3</sub>NaO<sub>6</sub> requires 464.1040).

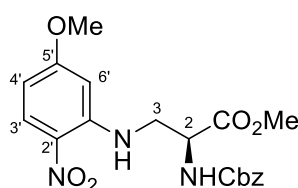
**3-Fluoro-4-nitroanisole (195)<sup>212</sup>**



To a solution of 3-fluoro-4-nitrophenol (1.00 g, 6.37 mmol) in acetone (14 mL) under argon was added potassium carbonate (1.76 g, 12.7 mmol) and iodomethane (0.790 mL, 12.7 mmol). The reaction was stirred at room temperature for 0.1 h before heating under reflux for 3 h. The reaction mixture was then filtered, washed with dichloromethane (20 mL) and the solvent removed *in vacuo*. Dichloromethane (40 mL) was added and the organic layer

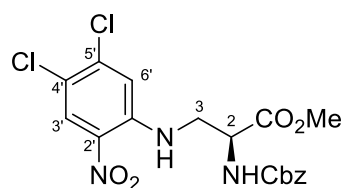
washed with water (3 × 40 mL) and brine (40 mL), dried (MgSO<sub>4</sub>), filtered and the solvent removed *in vacuo*. The resulting residue was purified by flash column chromatography, eluting with 20% ethyl acetate in petroleum ether (40–60) to afford 3-fluoro-4-nitroanisole (**195**) as a white solid (1.06 g, 97%). Mp 59–61 °C, lit.<sup>212</sup> 61 °C;  $\delta_{\text{H}}$  (400 MHz, CDCl<sub>3</sub>) 3.90 (3H, s, OCH<sub>3</sub>), 6.73 (1H, dd, *J* 12.8, 2.6 Hz, 2-H), 6.76 (1H, ddd, *J* 9.2, 2.6, 1.0 Hz, 6-H), 8.09 (1H, dd, *J* 9.2, 8.7 Hz, 5-H);  $\delta_{\text{C}}$  (101 MHz, CDCl<sub>3</sub>) 56.4 (CH<sub>3</sub>), 103.2 (CH, d, <sup>2</sup>*J*<sub>CF</sub> 24.2 Hz), 110.4 (CH, d, <sup>3</sup>*J*<sub>CF</sub> 3.1 Hz), 127.9 (CH, d, <sup>4</sup>*J*<sub>CF</sub> 1.6 Hz), 130.7 (C, d, <sup>2</sup>*J*<sub>CF</sub> 7.6 Hz), 157.5 (C, d, <sup>1</sup>*J*<sub>CF</sub> 265.0 Hz), 165.2 (C, d, <sup>3</sup>*J*<sub>CF</sub> 11.0 Hz); *m/z* (ESI) 194 (MNa<sup>+</sup>. 100%).

**Methyl (2S)-2-(benzyloxycarbonyl)amino]-3-[(5'-methoxy-2'-nitrophenyl)amino]propanoate (200)**



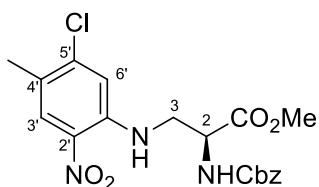
Methyl (2S)-2-(benzyloxycarbonyl)amino]-3-[(5'-methoxy-2'-nitrophenyl)amino]propanoate (**200**) was synthesised as described for methyl (2S)-2-[(benzyloxycarbonyl)amino]-3-[(2'-nitrophenyl)amino]propanoate (**189**) using methyl (2S)-3-amino-2-[(benzyloxycarbonyl)amino]propanoate hydrochloride (**200**) (0.200 g, 0.793 mmol), 3-fluoro-4-nitroanisole (**195**) (0.407 g, 2.38 mmol) and triethylamine (0.332 mL, 2.38 mmol) in acetonitrile (6.0 mL). The crude material was purified by flash column chromatography, eluting with 0–20% ethyl acetate in dichloromethane to afford methyl (2S)-2-(benzyloxycarbonyl)amino]-3-[(5'-methoxy-2'-nitrophenyl)amino]propanoate (**200**) as a yellow solid (0.277 g, 87%). Mp 82–84 °C;  $\nu_{\text{max}}/\text{cm}^{-1}$  (neat) 3356 (NH), 2955 (CH), 1713 (CO), 1620 (CO), 1582 (C=C), 1497, 1226, 1221, 748;  $[\alpha]_{\text{D}}^{23}$  +20.7 (*c* 1.0, CHCl<sub>3</sub>);  $\delta_{\text{H}}$  (400 MHz, CDCl<sub>3</sub>) 3.73 (1H, ddd, *J* 13.7, 6.2, 5.7 Hz, 3-*HH*), 3.77 (1H, ddd, *J* 13.7, 6.2, 5.7 Hz, 3-*HH*), 3.80 (3H, s, OCH<sub>3</sub>), 3.87 (3H, s, OCH<sub>3</sub>), 4.64 (1H, dt, *J* 6.9, 6.2 Hz, 2-H), 5.13 (2H, s, CH<sub>2</sub>Ph), 5.63 (1H, d, *J* 6.9 Hz, NH), 6.27 (1H, dd, *J* 9.5, 2.5 Hz, 4'-H), 6.43 (1H, d, *J* 2.5 Hz, 6'-H), 7.28–7.42 (5H, m, Ph), 8.14 (1H, d, *J* 9.5 Hz, 3'-H), 8.52 (1H, t, *J* 5.7 Hz, NH);  $\delta_{\text{C}}$  (101 MHz, CDCl<sub>3</sub>) 44.6 (CH<sub>2</sub>), 53.1 (CH<sub>3</sub>), 53.2 (CH), 55.9 (CH<sub>3</sub>), 67.3 (CH<sub>2</sub>), 95.4 (CH), 105.6 (CH), 127.0 (C), 128.2 (2 × CH), 128.4 (CH), 128.6 (2 × CH), 129.3 (CH), 135.9 (C), 147.3 (C), 155.7 (C), 166.2 (C), 170.7 (C); *m/z* (ESI) 426.1266 (MNa<sup>+</sup>. C<sub>19</sub>H<sub>21</sub>N<sub>3</sub>NaO<sub>7</sub> requires 426.1272).

**Methyl (2S)-2-(benzyloxycarbonyl)amino]-3-[(4',5'-dichloro-2'-nitrophenyl)amino]propanoate (198)**



Methyl (2S)-2-(benzyloxycarbonyl)amino]-3-[(4',5'-dichloro-2'-nitrophenyl)amino]propanoate (**198**) was synthesised as described for methyl (2S)-2-[(benzyloxycarbonyl)amino]-3-[(2'-nitrophenyl)amino]propanoate (**189**) using methyl (2S)-3-amino-2-[(benzyloxycarbonyl)amino]propanoate hydrochloride (**191**) (0.400 g, 1.59 mmol), 2-fluoro-4,5-dichloro-1-nitrobenzene (0.628 mL, 4.77 mmol) and triethylamine (0.665 mL, 4.77 mmol) in acetonitrile (12 mL). The crude material was purified by flash column chromatography, eluting with 0–20% ethyl acetate in dichloromethane to afford methyl (2S)-2-(benzyloxycarbonyl)amino]-3-[(4',5'-dichloro-2'-nitrophenyl)amino]propanoate (**198**) as a yellow solid (0.599 g, 85%). Mp 94–96 °C;  $\nu_{\max}/\text{cm}^{-1}$  (neat) 3358 (NH), 2953 (CH), 1716 (CO), 1612 (CO), 1521 (C=C), 1485, 1223, 759;  $[\alpha]_{\text{D}}^{23}$  +28.4 ( $c$  1.0,  $\text{CHCl}_3$ );  $\delta_{\text{H}}$  (400 MHz,  $\text{CDCl}_3$ ) 3.72 (1H, ddd,  $J$  13.6, 5.6, 5.0 Hz, 3- $HH$ ), 3.76 (1H, ddd,  $J$  13.6, 5.6, 5.0 Hz, 3- $HH$ ), 3.81 (3H, s,  $\text{OCH}_3$ ), 4.64 (1H, dt,  $J$  6.1, 5.6 Hz, 2-H), 5.13 (2H, s,  $\text{CH}_2\text{Ph}$ ), 5.71 (1H, d,  $J$  6.1 Hz, NH), 7.13 (1H, s, 6'-H), 7.27–7.44 (5H, m, Ph), 8.18 (1H, t,  $J$  5.0 Hz, NH), 8.26 (1H, s, 3'-H);  $\delta_{\text{C}}$  (101 MHz,  $\text{CDCl}_3$ ) 44.8 ( $\text{CH}_2$ ), 53.2 ( $\text{CH}_3$ ), 53.4 (CH), 67.6 ( $\text{CH}_2$ ), 115.1 (CH), 119.7 (C), 127.9 (CH), 128.2 (2  $\times$  CH), 128.4 (CH), 128.6 (2  $\times$  CH), 131.2 (C), 135.7 (C), 141.3 (C), 143.6 (C), 155.9 (C), 170.3 (C);  $m/z$  (ESI) 464.0373 ( $\text{MNa}^+$ .  $\text{C}_{18}\text{H}_{17}^{35}\text{Cl}_2\text{N}_3\text{NaO}_6$  requires 464.0387).

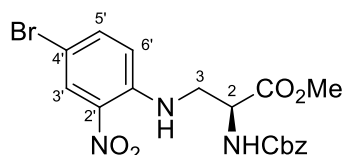
**Methyl (2S)-2-(benzyloxycarbonyl)amino]-3-[(5'-chloro-4'-methyl-2'-nitrophenyl)amino]propanoate (199)**



Methyl (2S)-2-(benzyloxycarbonyl)amino]-3-[(5'-chloro-4'-methyl-2'-nitrophenyl)amino]propanoate (**199**) was synthesised as described for methyl (2S)-2-[(benzyloxycarbonyl)amino]-3-[(2'-nitrophenyl)amino]propanoate (**189**) using methyl (2S)-3-amino-2-[(benzyloxycarbonyl)amino]propanoate hydrochloride (**191**) (0.400 g, 1.59 mmol), 1-chloro-5-fluoro-2-methyl-4-nitrobenzene (0.904 g, 4.77 mmol) and triethylamine (0.665 mL, 4.77 mmol) in acetonitrile (12 mL). The crude material was purified by flash

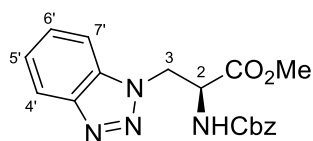
column chromatography, eluting with 0–20% ethyl acetate in dichloromethane to afford methyl (2*S*)-2-(benzyloxycarbonyl)amino]-3-[(5'-chloro-4'-methyl-2'-nitrophenyl)amino]propanoate (**199**) as a yellow oil (0.643 g, 96%).  $\nu_{\max}/\text{cm}^{-1}$  (neat) 3360 (NH), 2951 (CH), 1738 (CO), 1726 (CO), 1626, 1501 (C=C), 1228, 1217, 978;  $[\alpha]_{\text{D}}^{23} +23.5$  (*c* 1.0, CHCl<sub>3</sub>);  $\delta_{\text{H}}$  (400 MHz, CDCl<sub>3</sub>) 2.28 (3H, s, 4'-CH<sub>3</sub>), 3.71 (1H, ddd, *J* 13.6, 5.7, 5.3 Hz, 3-HH), 3.75 (1H, ddd, *J* 13.6, 5.7, 5.3 Hz, 3-HH), 3.80 (3H, s, OCH<sub>3</sub>), 4.65 (1H, dt, *J* 6.3, 5.3 Hz, 2-H), 5.13 (2H, s, CH<sub>2</sub>Ph), 5.70 (1H, d, *J* 6.3 Hz, NH), 7.00 (1H, s, 6'-H), 7.27–7.39 (5H, m, Ph), 8.03 (1H, s, 3'-H), 8.08 (1H, t, *J* 5.7 Hz, NH);  $\delta_{\text{C}}$  (101 MHz, CDCl<sub>3</sub>) 18.9 (CH<sub>3</sub>), 44.7 (CH<sub>2</sub>), 53.1 (CH<sub>3</sub>), 53.5 (CH), 67.4 (CH<sub>2</sub>), 113.8 (CH), 124.2 (C), 128.1 (CH), 128.2 (2 × CH), 128.3 (CH), 128.6 (2 × CH), 131.0 (C), 135.9 (C), 143.6 (C), 143.6 (C), 155.9 (C), 170.5 (C); *m/z* (ESI) 444.0916 (MNa<sup>+</sup>. C<sub>19</sub>H<sub>20</sub><sup>35</sup>ClN<sub>3</sub>NaO<sub>6</sub> requires 444.0933).

**Methyl (2*S*)-2-(benzyloxycarbonyl)amino]-3-[(4'-bromo-2'-nitrophenyl)amino]propanoate (197)**



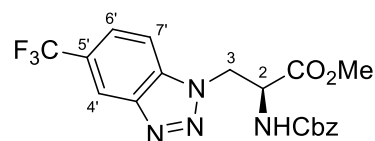
Methyl (2*S*)-2-(benzyloxycarbonyl)amino]-3-[(4'-bromo-2'-nitrophenyl)amino]propanoate (**197**) was synthesised as described for methyl (2*S*)-2-[(benzyloxycarbonyl)amino]-3-[(2'-nitrophenyl)amino]propanoate (**189**) using methyl (2*S*)-3-amino-2-[(benzyloxycarbonyl)amino]propanoate hydrochloride (**191**) (3.97 g, 13.8 mmol), 5-bromo-2-fluoro-1-nitrobenzene (5.10 mL, 41.3 mmol) and triethylamine (5.90 mL, 41.3 mmol) in acetonitrile (50 mL). The crude material was purified by flash column chromatography, eluting with 0–20% ethyl acetate in dichloromethane to afford methyl (2*S*)-2-(benzyloxycarbonyl)amino]-3-[(4'-bromo-2'-nitrophenyl)amino]propanoate (**197**) as a yellow solid (5.75 g, 92%). Mp 86–89 °C;  $\nu_{\max}/\text{cm}^{-1}$  (neat) 3364 (NH), 2955 (CH), 1721 (CO), 1612 (CO), 1504 (C=C), 1227, 1065;  $[\alpha]_{\text{D}}^{25} +14.3$  (*c* 1.1, CHCl<sub>3</sub>);  $\delta_{\text{H}}$  (400 MHz, CDCl<sub>3</sub>) 3.60–3.76 (5H, m, 3-H<sub>2</sub> and OCH<sub>3</sub>), 4.60 (1H, dt, *J* 6.9, 5.8 Hz, 2-H), 5.06 (1H, d, *J* 12.2 Hz, OCHHPh), 5.11 (1H, d, *J* 12.2 Hz, OCHHPh), 6.06 (1H, d, *J* 6.9 Hz, NH), 6.81 (1H, d, *J* 9.1 Hz, 6'-H), 7.20–7.30 (5H, m, Ph), 7.36 (1H, dd, *J* 9.1, 1.5 Hz, 5'-H), 8.16 (1H, d, *J* 1.5 Hz, 3'-H), 8.19 (1H, t, *J* 6.0 Hz, NH);  $\delta_{\text{C}}$  (101 MHz, CDCl<sub>3</sub>) 44.2 (CH<sub>2</sub>), 52.8 (CH<sub>3</sub>), 53.2 (CH), 67.0 (CH<sub>2</sub>), 107.0 (C), 115.3 (CH), 127.9 (2 × CH), 128.1 (CH), 128.3 (2 × CH), 128.6 (CH), 132.5 (C), 135.8 (C), 138.7 (CH), 143.6 (C), 155.9 (C), 170.4 (C); *m/z* (ESI) 474.0276 (MNa<sup>+</sup>. C<sub>18</sub>H<sub>18</sub><sup>79</sup>BrN<sub>3</sub>NaO<sub>6</sub> requires 474.0271).

**Methyl (2S)-2-[(benzyloxycarbonyl)amino]-3-(1H-benzo[d][1.2.3]triazol-1'-yl)propanoate (187)**



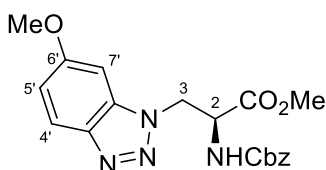
To a solution of (2S)-2-[(benzyloxycarbonyl)amino]-3-[(2'-nitrophenyl)amino]propanoate (**189**) (0.320 g, 0.857 mmol) in methanol (12 mL) was added tin(II) dichloride dihydrate (0.970 g, 4.29 mmol) and the reaction mixture stirred under reflux for 20 h. After cooling the reaction to ambient temperature, the solvent was removed *in vacuo* and the resulting residue dissolved in ethyl acetate (50 mL) and mixed with a saturated solution of aqueous sodium hydrogen carbonate (30 mL). The biphasic mixture was filtered through a pad of Celite® and the organic layer separated from the aqueous layer. The product was further extracted from the aqueous layer with ethyl acetate (2 × 30 mL) and the combined organic layers were washed with brine (50 mL), dried (MgSO<sub>4</sub>), filtered and concentrated *in vacuo*. The crude material was purified by flash column chromatography, eluting with 10% ethyl acetate in dichloromethane to afford methyl (2S)-2-[(benzyloxycarbonyl)amino]-3-[(2'-aminophenyl)amino]propanoate (**188**) as a white solid (0.244 g, 83%). This material was then used immediately in the following step. To a solution of methyl (2S)-2-[(benzyloxycarbonyl)amino]-3-[(2'-aminophenyl)amino]propanoate (**188**) (0.244 g, 0.711 mmol) in acetonitrile (12 mL) at -10 °C was added *p*-toluenesulfonic acid (0.405 g, 2.13 mmol) and polymer-supported nitrite (0.609 g, containing 2.13 mmol of NO<sub>2</sub><sup>-</sup>) and the reaction mixture stirred at this temperature for 3 h. The reaction mixture was filtered, and the resin washed with dichloromethane (50 mL). The organic layers were washed with a saturated solution of aqueous sodium hydrogen carbonate (50 mL) and brine (50 mL), dried (MgSO<sub>4</sub>), filtered and concentrated *in vacuo*. The crude material was purified by flash column chromatography, eluting with 10% ethyl acetate in dichloromethane to afford methyl (2S)-2-[(benzyloxycarbonyl)amino]-3-(1H-benzo[d][1.2.3]triazol-1'-yl)propanoate (**187**) as a white solid (0.148 g, 59%). Mp 82–85 °C;  $\nu_{\max}/\text{cm}^{-1}$  (neat) 3325 (NH), 2955 (CH), 1713 (CO), 1504 (C=C), 1211, 1057, 741;  $[\alpha]_{\text{D}}^{25} +37.0$  (*c* 0.4, CHCl<sub>3</sub>);  $\delta_{\text{H}}$  (400 MHz, CDCl<sub>3</sub>) 3.75 (3H, s, OCH<sub>3</sub>), 4.88 (1H, dt, *J* 7.0, 4.4 Hz, 2-H), 5.05–5.18 (4H, m, 3-H<sub>2</sub> and OCH<sub>2</sub>Ph), 5.66 (1H, d, *J* 7.0 Hz, NH), 7.29–7.45 (8H, m, Ph, 5'-H, 6'-H and 7'-H), 8.03 (1H, br d, *J* 8.0, 4'-H);  $\delta_{\text{C}}$  (101 MHz, CDCl<sub>3</sub>) 48.7 (CH<sub>2</sub>), 53.3 (CH<sub>3</sub>), 54.4 (CH), 67.4 (CH<sub>2</sub>), 109.2 (CH), 120.2 (CH), 124.2 (CH), 127.9 (CH), 128.3 (2 × CH), 128.5 (CH), 128.7 (2 × CH), 133.9 (C), 136.0 (C), 145.8 (C), 155.8 (C), 169.5 (C); *m/z* (ESI) 377.1223 (MNa<sup>+</sup>. C<sub>18</sub>H<sub>18</sub>N<sub>4</sub>NaO<sub>4</sub> requires 377.1220).

**Methyl (2S)-2-[(benzyloxycarbonyl)amino]-3-[5'-(trifluoromethyl)-1H-benzo[d][1.2.3]triazol-1'-yl]propanoate (200)**



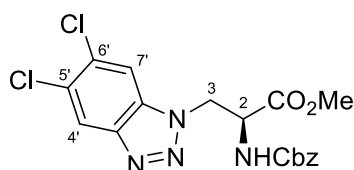
Methyl (2S)-2-[(benzyloxycarbonyl)amino]-3-[5'-(trifluoromethyl)-1H-benzo[d][1.2.3]triazol-1'-yl]propanoate (**200**) was synthesised as described for methyl (2S)-2-[(benzyloxycarbonyl)amino]-3-(1H-benzo[d][1.2.3]triazol-1'-yl)propanoate (**187**) using methyl (2S)-2-(benzyloxycarbonyl)amino]-3-[[2'-nitro-4'-(trifluoromethyl)phenyl]amino]propanoate (**196**) (0.290 g, 0.657 mmol), tin(II) dichloride dihydrate (0.742 g, 3.29 mmol) in methanol (9.0 mL). The crude material was purified by flash column chromatography, eluting with 0–20% ethyl acetate in dichloromethane to afford methyl (2S)-2-[(benzyloxycarbonyl)amino]-3-[[2'-amino-4'-(trifluoromethyl)phenyl]amino]propanoate as a white solid (0.229 g, 85%). The next step was carried out as described previously using methyl (2S)-2-(benzyloxycarbonyl)amino]-3-[[2'-amino-4'-(trifluoromethyl)phenyl]amino]propanoate (0.229 g, 5.57 mmol), *p*-toluenesulfonic acid (0.313 g, 1.67 mmol) and polymer-supported nitrite (0.477 g, containing 1.67 mmol of NO<sub>2</sub><sup>-</sup>) in acetonitrile (9.0 mL). The crude material was purified by flash column chromatography, eluting with 20–40% ethyl acetate in petroleum ether (40–60) to afford methyl (2S)-2-[(benzyloxycarbonyl)amino]-3-[5'-(trifluoromethyl)-1H-benzo[d][1.2.3]triazol-1'-yl]propanoate (**200**) as a white solid (0.129 g, 57%). Mp 130–132;  $\nu_{\max}/\text{cm}^{-1}$  (neat) 3333 (NH), 2957 (CH), 1742 (CO), 1717 (CO), 1526 (C=C), 1331, 1209, 1123;  $[\alpha]_{\text{D}}^{23} +12.7$  (c 1.0, CHCl<sub>3</sub>);  $\delta_{\text{H}}$  (500 MHz, CDCl<sub>3</sub>) 3.79 (3H, s, OCH<sub>3</sub>), 4.85 (1H, dt, *J* 6.4, 4.4 Hz, 2-H), 5.05 (1H, d, *J* 4.4 Hz, 3-HH), 5.16 (1H, d, *J* 4.4 Hz, 3-HH), 5.18 (2H, s, OCH<sub>2</sub>Ph), 5.65 (1H, d, *J* 6.4 Hz, NH), 7.27–7.43 (5H, m, Ph), 7.48 (1H, d, *J* 8.7 Hz, 7'-H), 7.52 (1H, d, *J* 8.7 Hz, 6'-H), 8.33 (1H, s, 4'-H);  $\delta_{\text{C}}$  (126 MHz, CDCl<sub>3</sub>) 48.6 (CH<sub>2</sub>), 53.4 (CH<sub>3</sub>), 54.3 (CH), 67.4 (CH<sub>2</sub>), 110.2 (CH), 118.4 (CH, q, <sup>3</sup>*J*<sub>CF</sub> 4.4 Hz), 124.0 (C, q, <sup>1</sup>*J*<sub>CF</sub> 272 Hz), 124.5 (CH, q, <sup>3</sup>*J*<sub>CF</sub> 3.0 Hz), 126.8 (C, q, <sup>2</sup>*J*<sub>CF</sub> 32.9 Hz), 128.4 (2 × CH), 128.5 (CH), 128.6 (2 × CH), 135.3 (C), 135.8 (C), 144.8 (C), 155.6 (C), 169.1 (C); *m/z* (ESI) 445.1095 (MNa<sup>+</sup>. C<sub>19</sub>H<sub>17</sub>F<sub>3</sub>N<sub>4</sub>NaO<sub>4</sub> requires 445.1094).

**Methyl (2S)-2-[(benzyloxycarbonyl)amino]-3-(6'-methoxy-1*H*-benzo[*d*][1.2.3]triazol-1'-yl)propanoate (201)**



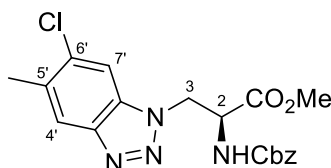
Methyl (2*S*)-2-[(benzyloxycarbonyl)amino]-3-(6'-methoxy-1*H*-benzo[*d*][1.2.3]triazol-1'-yl)propanoate (**201**) was synthesised as described for methyl (2*S*)-2-[(benzyloxycarbonyl)amino]-3-(1*H*-benzo[*d*][1.2.3]triazol-1'-yl)propanoate (**187**) using methyl (2*S*)-2-(benzyloxycarbonyl)amino]-3-[(5'-methoxy-2'-nitrophenyl)amino]propanoate (**200**) (0.270 g, 0.669 mmol), tin(II) dichloride dihydrate (0.756 g, 3.35 mmol) in methanol (9.0 mL). The crude material was purified by flash column chromatography, eluting with 0–20% ethyl acetate in dichloromethane to afford methyl (2*S*)-2-[(benzyloxycarbonyl)amino]-3-[(5'-methoxy-2'-aminophenyl)amino]propanoate as a brown solid (0.147 g, 59%). The next step was carried out as described previously using methyl (2*S*)-2-(benzyloxycarbonyl)amino]-3-[(5'-methoxy-2'-aminophenyl)amino]propanoate (0.147 g, 0.394 mmol), *p*-toluenesulfonic acid (0.224 g, 1.18 mmol) and polymer-supported nitrite (0.338 g, containing 1.18 mmol of NO<sub>2</sub><sup>-</sup>) in acetonitrile (6.0 mL). The crude material was purified by flash column chromatography, eluting with 0–20% ethyl acetate in dichloromethane to afford methyl (2*S*)-2-[(benzyloxycarbonyl)amino]-3-(6'-methoxy-1*H*-benzo[*d*][1.2.3]triazol-1'-yl)propanoate (**201**) as a brown oil (0.056 g, 39%).  $\nu_{\max}/\text{cm}^{-1}$  (neat) 3333 (NH), 2953 (CH), 1717 (CO), 1622 (CO), 1505 (C=C), 1233, 1020, 698;  $[\alpha]_{\text{D}}^{23} +17.7$  (*c* 1.0, CHCl<sub>3</sub>);  $\delta_{\text{H}}$  (400 MHz, CDCl<sub>3</sub>) 3.73 (3H, s, OCH<sub>3</sub>), 3.80 (3H, s, OCH<sub>3</sub>), 4.88 (1H, dt, *J* 7.6, 4.4 Hz, 2-H), 4.99 (1H, dd, *J* 14.5, 4.4 Hz, 3-*HH*), 5.08 (1H, dd, *J* 14.5, 4.4 Hz, 3-*HH*), 5.11 (2H, s, OCH<sub>2</sub>Ph), 5.79 (1H, d, *J* 7.6 Hz, NH), 6.80 (1H, d, *J* 2.2 Hz, 7'-H), 6.98 (1H, dd, *J* 9.0, 2.2 Hz, 5'-H), 7.22–7.40 (5H, m, Ph), 7.85 (1H, d, *J* 9.0 Hz, 4'-H);  $\delta_{\text{C}}$  (101 MHz, CDCl<sub>3</sub>) 48.4 (CH<sub>2</sub>), 53.2 (CH<sub>3</sub>), 54.1 (CH), 55.7 (CH<sub>3</sub>), 67.2 (CH<sub>2</sub>), 89.4 (CH), 116.6 (CH), 120.7 (CH), 128.0 (2 × CH), 128.3 (CH), 128.6 (2 × CH), 134.9 (C), 135.8 (C), 141.0 (C), 155.7 (C), 160.3 (C), 169.5 (C); *m/z* (ESI) 407.1324 (MNa<sup>+</sup>. C<sub>19</sub>H<sub>20</sub>N<sub>4</sub>NaO<sub>5</sub> requires 407.1326).

**Methyl (2S)-2-[(benzyloxycarbonyl)amino]-3-(5',6'-dichloro-1H-benzo[d][1.2.3]triazol-1'-yl)propanoate (202)**



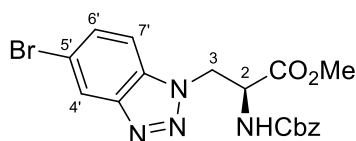
Methyl (2S)-2-[(benzyloxycarbonyl)amino]-3-(5',6'-dichloro-1H-benzo[d][1.2.3]triazol-1'-yl)propanoate (**202**) was synthesised as described for methyl (2S)-2-[(benzyloxycarbonyl)amino]-3-(1H-benzo[d][1.2.3]triazol-1'-yl)propanoate (**187**) using methyl (2S)-2-(benzyloxycarbonyl)amino]-3-[(4',5'-dichloro-2'-nitrophenyl)amino]propanoate (**198**) (0.440 g, 0.669 mmol), tin(II) dichloride dihydrate (1.10 g, 4.98 mmol) in methanol (14 mL). The crude material was purified by flash column chromatography, eluting with 0–20% ethyl acetate in dichloromethane to afford methyl (2S)-2-[(benzyloxycarbonyl)amino]-3-[(4',5'-dichloro-2'-aminophenyl)amino]propanoate as a brown oil (0.365 g, 89%). The next step was carried out as described previously using methyl (2S)-2-(benzyloxycarbonyl)amino]-3-[(5'-methoxy-2'-aminophenyl)amino]propanoate (0.365 g, 0.889 mmol), *p*-toluenesulfonic acid (0.508 g, 2.67 mmol) and polymer-supported nitrite (0.762 g, containing 2.67 mmol of NO<sub>2</sub><sup>-</sup>) in acetonitrile (14 mL). The crude material was purified by flash column chromatography, eluting with 0–20% ethyl acetate in dichloromethane to afford methyl (2S)-2-[(benzyloxycarbonyl)amino]-3-(5',6'-dichloro-1H-benzo[d][1.2.3]triazol-1'-yl)propanoate (**202**) as a white solid (0.297 g, 80%). Mp 98–100 °C;  $\nu_{\max}/\text{cm}^{-1}$  (neat) 3322 (NH), 2957 (CH), 1709 (CO), 1514 (C=C), 1434, 1208, 751;  $[\alpha]_{\text{D}}^{23} +11.2$  (*c* 1.0, CHCl<sub>3</sub>);  $\delta_{\text{H}}$  (400 MHz, CDCl<sub>3</sub>) 3.76 (3H, s, OCH<sub>3</sub>), 4.84 (1H, dt, *J* 7.0, 4.5 Hz, 2-H), 4.97–5.15 (4H, m, 3-H<sub>2</sub> and OCH<sub>2</sub>Ph), 6.00–6.13 (1H, m, NH), 7.21–7.36 (5H, m, Ph), 7.67 (1H, s, 7'-H), 8.01 (1H, s, 4'-H);  $\delta_{\text{C}}$  (101 MHz, CDCl<sub>3</sub>) 48.8 (CH<sub>2</sub>), 53.3 (CH<sub>3</sub>), 54.2 (CH), 67.5 (CH<sub>2</sub>), 110.7 (CH), 120.8 (CH), 128.0 (2 × CH), 128.3 (CH), 128.6 (2 × CH), 128.9 (C), 132.9 (2 × C), 135.7 (C), 144.3 (C), 155.8 (C), 169.2 (C); *m/z* (ESI) 445.0432 (MNa<sup>+</sup>. C<sub>18</sub>H<sub>16</sub><sup>35</sup>Cl<sub>2</sub>N<sub>4</sub>NaO<sub>4</sub> requires 445.0441).

**Methyl (2S)-2-[(benzyloxycarbonyl)amino]-3-(6'-chloro-5'-methyl-1*H*-benzo[*d*][1.2.3]triazol-1'-yl)propanoate (203)**



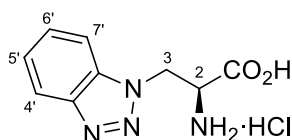
Methyl (2S)-2-[(benzyloxycarbonyl)amino]-3-(6'-chloro-5'-methyl-1*H*-benzo[*d*][1.2.3]triazol-1'-yl)propanoate (**203**) was synthesised as described for methyl (2S)-2-[(benzyloxycarbonyl)amino]-3-(1*H*-benzo[*d*][1.2.3]triazol-1'-yl)propanoate (**187**) using methyl (2S)-2-(benzyloxycarbonyl)amino]-3-[(5'-chloro-4'-methyl-2'-nitrophenyl)amino]propanoate (**199**) (0.520 g, 1.23 mmol), tin(II) dichloride dihydrate (1.40 g, 6.15 mmol) in methanol (17 mL). The crude material was purified by flash column chromatography, eluting with 0–20% ethyl acetate in dichloromethane to afford methyl (2S)-2-[(benzyloxycarbonyl)amino]-3-[(5'-chloro-4'-methyl-2'-aminophenyl)amino]propanoate as a brown oil (0.315 g, 65%). The next step was carried out as described previously using methyl (2S)-2-(benzyloxycarbonyl)amino]-3-[(5'-chloro-4'-methyl-2'-aminophenyl)amino]propanoate (0.315 g, 0.803 mmol), *p*-toluenesulfonic acid (0.458 g, 2.41 mmol) and polymer-supported nitrite (0.689 g, containing 2.41 mmol of NO<sub>2</sub><sup>−</sup>) in acetonitrile (13 mL). The crude material was purified by flash column chromatography, eluting with 0–20% ethyl acetate in dichloromethane to afford methyl (2S)-2-[(benzyloxycarbonyl)amino]-3-(6'-chloro-5'-methyl-1*H*-benzo[*d*][1.2.3]triazol-1'-yl)propanoate (**203**) as a white solid (0.247 g, 78%). Mp 86–88 °C;  $\nu_{\text{max}}/\text{cm}^{-1}$  (neat) 3310 (NH), 2955 (CH), 1747 (CO), 1713 (CO), 1516 (C=C), 1437, 1213, 754;  $[\alpha]_{\text{D}}^{23}$  +13.7 (*c* 1.0, CHCl<sub>3</sub>);  $\delta_{\text{H}}$  (500 MHz, CDCl<sub>3</sub>) 2.40 (3H, s, 5'-CH<sub>3</sub>), 3.74 (3H, s, OCH<sub>3</sub>), 4.84 (1H, dt, 7.4, 4.8 Hz, 2-H), 5.03 (2H, br d, *J* 4.8 Hz, 3-H<sub>2</sub>), 5.08 (2H, s, OCH<sub>2</sub>Ph), 6.08–6.23 (1H, m, NH), 7.18–7.38 (5H, m, Ph), 7.52 (1H, s, 4'-H), 7.70 (1H, s, 7'-H);  $\delta_{\text{C}}$  (101 MHz, CDCl<sub>3</sub>) 20.7 (CH<sub>3</sub>), 48.5 (CH<sub>2</sub>), 53.1 (CH<sub>3</sub>), 54.2 (CH), 67.3 (CH<sub>2</sub>), 109.2 (CH), 120.3 (CH), 128.1 (2 × CH), 128.3 (CH), 128.5 (2 × CH), 132.5 (C), 132.9 (C), 135.3 (C), 135.8 (C), 144.4 (C), 155.8 (C), 169.4 (C); *m/z* (ESI) 425.0975 (MNa<sup>+</sup>. C<sub>19</sub>H<sub>19</sub><sup>35</sup>ClN<sub>4</sub>NaO<sub>4</sub> requires 425.0987).

**Methyl (2S)-2-[(benzyloxycarbonyl)amino]-3-(5'-bromo-1*H*-benzo[*d*][1.2.3]triazol-1'-yl)propanoate (204)**



Methyl (2*S*)-2-[(benzyloxycarbonyl)amino]-3-(5'-bromo-1*H*-benzo[*d*][1.2.3]triazol-1'-yl)propanoate (**204**) was synthesised as described for methyl (2*S*)-2-[(benzyloxycarbonyl)amino]-3-(1*H*-benzo[*d*][1.2.3]triazol-1'-yl)propanoate (**187**) using methyl (2*S*)-2-(benzyloxycarbonyl)amino]-3-[(5'-bromo-2'-nitrophenyl)amino]propanoate (**197**) (9.00 g, 19.9 mmol), tin(II) dichloride dihydrate (22.0 g, 99.5 mmol) in methanol (100 mL). The crude material was purified by flash column chromatography, eluting with 0–20% ethyl acetate in dichloromethane to afford methyl (2*S*)-2-(benzyloxycarbonyl)amino]-3-[(5'-bromo-2'-aminophenyl)amino]propanoate as a brown oil (6.42 g, 76%). The next step was carried out as described previously using methyl (2*S*)-2-(benzyloxycarbonyl)amino]-3-[(5'-bromo-2'-aminophenyl)amino]propanoate (6.30 g, 14.9 mmol), *p*-toluenesulfonic acid (8.50 g, 44.7 mmol) and polymer-supported nitrite (12.8 g, containing 44.7 mmol of NO<sub>2</sub><sup>-</sup>) in acetonitrile (200 mL). The crude material was purified by flash column chromatography, eluting with 0–20% ethyl acetate in dichloromethane to afford methyl (2*S*)-2-[(benzyloxycarbonyl)amino]-3-(5'-bromo-1*H*-benzo[*d*][1.2.3]triazol-1'-yl)propanoate (**204**) as a white solid (4.25 g, 66%). Mp 110–114 °C;  $\nu_{\max}/\text{cm}^{-1}$  (neat) 3321 (NH), 2954 (CH), 1717 (CO), 1512 (C=C), 1211, 1057, 752;  $[\alpha]_{\text{D}}^{22}$  -22.2 (*c* 1.0, CHCl<sub>3</sub>);  $\delta_{\text{H}}$  (500 MHz, CDCl<sub>3</sub>) 3.77 (3H, s, OCH<sub>3</sub>), 4.84 (1H, dt, *J* 6.6, 4.5 Hz, 2-H), 5.00–5.20 (4H, m, 3-H<sub>2</sub> and OCH<sub>2</sub>Ph), 5.69 (1H, d, *J* 6.6 Hz, NH), 7.22–7.47 (7H, m, Ph, 6'-H and 7'-H), 8.15 (1H, d, *J* 1.0 Hz, 4'-H);  $\delta_{\text{C}}$  (126 MHz, CDCl<sub>3</sub>) 48.6 (CH<sub>2</sub>), 53.3 (CH<sub>3</sub>), 54.2 (CH), 67.3 (CH<sub>2</sub>), 110.4 (CH), 117.4 (C), 122.6 (CH), 128.3 (2 × CH), 128.4 (CH), 128.6 (2 × CH), 131.2 (CH), 132.8 (C), 135.8 (C), 146.7 (C), 155.6 (C), 169.1 (C); *m/z* (ESI) 455.0325 (MNa<sup>+</sup>. C<sub>18</sub>H<sub>17</sub><sup>79</sup>BrN<sub>4</sub>NaO<sub>4</sub> requires 455.0325).

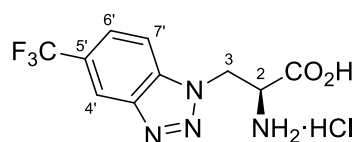
**(2S)-2-Amino-3-(1H-benzo[*d*][1.2.3]triazol-1'-yl)propanoic acid hydrochloride (186)**



A solution of methyl (2*S*)-2-[(benzyloxycarbonyl)amino]-3-(1*H*-benzo[*d*][1.2.3]triazol-1'-yl)propanoate (**187**) (0.0830 g, 0.236 mmol) in 6 M aqueous hydrochloric acid solution (10 mL) was heated under reflux for 20 h. After cooling to ambient temperature, the reaction

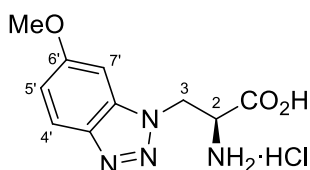
mixture was concentrated *in vacuo* and the resulting residue recrystallised from methanol and diethyl ether to afford (2*S*)-2-amino-3-(1*H*-benzo[*d*][1.2.3]triazol-1'-yl)propanoic acid hydrochloride (**186**) as a pale brown solid (0.054 g, 94%). Mp 190–192 °C;  $\nu_{\max}/\text{cm}^{-1}$  (neat) 2893 (NH/CH), 2739 (OH), 1728 (CO), 1234, 1165, 756;  $[\alpha]_{\text{D}}^{24} +11.9$  (*c* 0.7, MeOH);  $\delta_{\text{H}}$  (400 MHz, CD<sub>3</sub>OD) 4.79 (1H, dd, *J* 5.8, 4.1 Hz, 2-H), 5.26 (1H, dd, *J* 15.5, 4.1 Hz, 3-*HH*), 5.37 (1H, dd, *J* 15.5, 5.8 Hz, 3-*HH*), 7.49 (1H, ddd, *J* 8.4, 7.0, 0.9 Hz, 5'-H), 7.63 (1H, ddd, *J* 8.5, 7.0, 0.9 Hz, 6'-H), 7.84 (1H, dt, *J* 8.5, 0.9 Hz, 7'-H), 8.05 (1H, dt, *J* 8.4, 0.9 Hz, 4'-H);  $\delta_{\text{C}}$  (101 MHz, CD<sub>3</sub>OD) 48.0 (CH<sub>2</sub>), 53.5 (CH), 111.1 (CH), 120.3 (CH), 126.0 (CH), 129.5 (CH), 134.9 (C), 146.8 (C), 168.9 (C); *m/z* (ESI) 229.0706 (MNa<sup>+</sup>. C<sub>9</sub>H<sub>10</sub>N<sub>4</sub>NaO<sub>2</sub> requires 229.0696).

**(2*S*)-2-Amino-3-[5'-(trifluoromethyl)-1*H*-benzo[*d*][1.2.3]triazol-1'-yl]propanoic acid hydrochloride (205)**



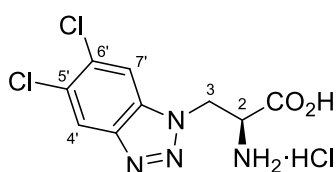
(2*S*)-2-Amino-3-[5'-(trifluoromethyl)-1*H*-benzo[*d*][1.2.3]triazol-1'-yl]propanoic acid hydrochloride (**205**) was synthesised as described for (2*S*)-2-amino-3-(1*H*-benzo[*d*][1.2.3]triazol-1'-yl)propanoic acid hydrochloride (**186**) using methyl (2*S*)-2-[(benzyloxycarbonyl)amino]-3-[5'-(trifluoromethyl)-1*H*-benzo[*d*][1.2.3]triazol-1'-yl]propanoate (**200**) (0.120 g, 0.284 mmol) in 6 M aqueous hydrochloric acid solution (20 mL). The crude material was purified by recrystallisation from methanol and diethyl ether to afford (2*S*)-2-amino-3-[5'-(trifluoromethyl)-1*H*-benzo[*d*][1.2.3]triazol-1'-yl]propanoic acid hydrochloride (**205**) as a pale brown solid (0.046 g, 59%). Mp 185–187 °C (dec);  $\nu_{\max}/\text{cm}^{-1}$  (neat) 3381 (NH), 2916 (OH/CH), 1743 (CO), 1331, 1215, 1125, 816;  $[\alpha]_{\text{D}}^{24} +2.0$  (*c* 1.0, MeOH);  $\delta_{\text{H}}$  (400 MHz, CD<sub>3</sub>OD) 4.83 (1H, br t, *J* 4.7 Hz, 2-H), 5.36 (1H, dd, *J* 15.5, 4.7 Hz, 3-*HH*), 5.45 (1H, dd, *J* 15.5, 4.7 Hz, 3-*HH*), 7.88 (1H, dd, *J* 8.8, 0.9 Hz, 6'-H), 8.09 (1H, d, *J* 8.8 Hz, 7'-H), 8.42 (1H, br s, 4'-H);  $\delta_{\text{C}}$  (101 MHz, CD<sub>3</sub>OD) 47.0 (CH<sub>2</sub>), 52.2 (CH), 111.6 (CH), 117.3 (CH, q, <sup>3</sup>*J*<sub>CF</sub> 4.5 Hz), 124.2 (C, q, <sup>1</sup>*J*<sub>CF</sub> 271 Hz), 124.3 (CH, q, <sup>3</sup>*J*<sub>CF</sub> 3.2 Hz), 126.8 (C, q, <sup>2</sup>*J*<sub>CF</sub> 32.7 Hz), 135.2 (C), 144.7 (C), 167.6 (C); *m/z* (ESI) 297.0574 (MNa<sup>+</sup>. C<sub>10</sub>H<sub>9</sub>F<sub>3</sub>N<sub>4</sub>NaO<sub>2</sub> requires 297.0570).

**(2S)-2-Amino-3-(6'-methoxy-1*H*-benzo[*d*][1.2.3]triazol-1'-yl)propanoic acid hydrochloride (209)**



(2S)-2-Amino-3-(6'-methoxy-1*H*-benzo[*d*][1.2.3]triazol-1'-yl)propanoic acid hydrochloride (**209**) was synthesised as described for (2S)-2-amino-3-(1*H*-benzo[*d*][1.2.3]triazol-1'-yl)propanoic acid hydrochloride (**186**) using methyl (2S)-2-[(benzyloxycarbonyl)amino]-3-(6'-methoxy-1*H*-benzo[*d*][1.2.3]triazol-1'-yl)propanoate (**201**) (0.056 g, 0.146 mmol) in 6 M aqueous hydrochloric acid solution (11 mL). The crude material was purified by recrystallisation from methanol and diethyl ether to afford (2S)-2-amino-3-(6'-methoxy-1*H*-benzo[*d*][1.2.3]triazol-1'-yl)propanoic acid hydrochloride (**209**) as a pale brown solid (0.023 g, 67%). Mp 179–180 °C (dec);  $\nu_{\max}/\text{cm}^{-1}$  (neat) 3403 (NH), 2895 (OH/CH), 1746 (CO), 1624 (C=C), 1506, 1236, 820;  $[\alpha]_{\text{D}}^{24} +7.3$  (*c* 1.0, MeOH);  $\delta_{\text{H}}$  (400 MHz, CD<sub>3</sub>OD) 4.77 (1H, dd, *J* 5.4, 4.2 Hz, 2-H), 5.21 (1H, dd, *J* 15.4, 4.2 Hz, 3-*HH*), 5.31 (1H, dd, *J* 15.4, 5.4 Hz, 3-*HH*), 7.08 (1H, dd, *J* 9.1, 2.2 Hz, 5'-H), 7.25 (1H, d, *J* 2.2 Hz, 7'-H), 7.86 (1H, d, *J* 9.1 Hz, 4'-H);  $\delta_{\text{C}}$  (101 MHz, CD<sub>3</sub>OD) 46.4 (CH<sub>2</sub>), 52.2 (CH), 55.2 (CH<sub>3</sub>), 89.9 (CH), 117.3 (CH), 119.5 (CH), 134.9 (C), 140.6 (C), 160.9 (C), 167.7 (C); *m/z* (ESI) 259.0808 (MNa<sup>+</sup>. C<sub>10</sub>H<sub>12</sub>N<sub>4</sub>NaO<sub>3</sub> requires 259.0802).

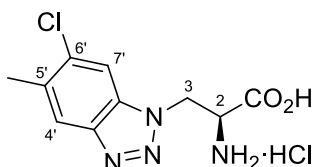
**(2S)-2-Amino-3-(5',6'-dichloro-1*H*-benzo[*d*][1.2.3]triazol-1'-yl)propanoic acid hydrochloride (207)**



(2S)-2-Amino-3-(5',6'-dichloro-1*H*-benzo[*d*][1.2.3]triazol-1'-yl)propanoic acid hydrochloride (**207**) was synthesised as described for (2S)-2-amino-3-(1*H*-benzo[*d*][1.2.3]triazol-1'-yl)propanoic acid hydrochloride (**186**) using methyl (2S)-2-[(benzyloxycarbonyl)amino]-3-(5',6'-dichloro-1*H*-benzo[*d*][1.2.3]triazol-1'-yl)propanoate (**202**) (0.290 g, 0.685 mmol) in 6 M aqueous hydrochloric acid solution (48 mL). The crude material was purified by recrystallisation from methanol and diethyl ether to afford (2S)-2-amino-3-(5',6'-dichloro-1*H*-benzo[*d*][1.2.3]triazol-1'-yl)propanoic acid hydrochloride (**207**) as a pale brown solid (0.167 g, 88%). Mp 180–182 °C (dec);  $\nu_{\max}/\text{cm}^{-1}$  (neat) 3381 (NH), 2875 (OH/CH), 1740 (CO), 1507, 1434, 1214, 822;  $[\alpha]_{\text{D}}^{23} +11.4$  (*c* 1.0, MeOH);  $\delta_{\text{H}}$  (400 MHz, CD<sub>3</sub>OD) 4.81 (1H, br t, *J* 4.8 Hz, 2-H), 5.29 (1H, dd, *J* 15.5, 4.8 Hz, 3-*HH*), 5.38 (1H, dd, *J* 15.5, 4.8 Hz, 3-

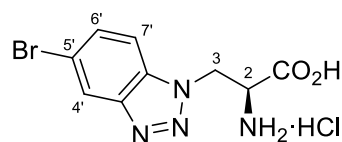
*HH*), 8.18 (1H, s, 7'-H), 8.24 (1H, s, 4'-H);  $\delta_c$  (101 MHz, CD<sub>3</sub>OD) 47.0 (CH<sub>2</sub>), 52.1 (CH), 111.8 (CH), 120.1 (CH), 128.9 (C), 132.6 (C), 132.7 (C), 144.4 (C), 167.5 (C); *m/z* (ESI) 296.9915 (MNa<sup>+</sup>. C<sub>9</sub>H<sub>8</sub><sup>35</sup>Cl<sub>2</sub>N<sub>4</sub>NaO<sub>2</sub> requires 296.9917).

**(2S)-2-Amino-3-(6'-chloro-5'-methyl-1*H*-benzo[*d*][1.2.3]triazol-1'-yl)propanoic acid hydrochloride (208)**



(2S)-2-Amino-3-(6'-chloro-5'-methyl-1*H*-benzo[*d*][1.2.3]triazol-1'-yl)propanoic acid hydrochloride (**208**) was synthesised as described for (2S)-2-amino-3-(1*H*-benzo[*d*][1.2.3]triazol-1'-yl)propanoic acid hydrochloride (**186**) using methyl (2S)-2-[(benzyloxycarbonyl)amino]-3-(6'-chloro-5'-methyl-1*H*-benzo[*d*][1.2.3]triazol-1'-yl)propanoate (**203**) (0.240 g, 0.596 mmol) in 6 M aqueous hydrochloric acid solution (42 mL). The crude material was purified by recrystallisation from methanol and diethyl ether to afford (2S)-2-amino-3-(6'-chloro-5'-methyl-1*H*-benzo[*d*][1.2.3]triazol-1'-yl)propanoic acid hydrochloride (**208**) as a pale brown solid (0.139 g, 92%). Mp 199–201 °C (dec);  $\nu_{\max}/\text{cm}^{-1}$  (neat) 3376 (NH), 2951 (OH/CH), 1744 (CO), 1454, 1228, 1001, 865;  $[\alpha]_D^{23} +11.1$  (c 1.0, MeOH);  $\delta_H$  (400 MHz, CD<sub>3</sub>OD) 2.53 (3H, s, 5'-CH<sub>3</sub>), 4.78 (1H, dd, *J* 5.5, 4.2 Hz, 2-H), 5.22 (1H, dd, *J* 15.5, 4.2 Hz, 3-*HH*), 5.32 (1H, dd, *J* 15.5, 5.5 Hz, 3-*HH*), 7.94 (1H, s, 7'-H), 7.95 (1H, s, 4'-H);  $\delta_c$  (101 MHz, CD<sub>3</sub>OD) 19.4 (CH<sub>3</sub>), 46.7 (CH<sub>2</sub>), 52.1 (CH), 110.0 (CH), 119.6 (CH), 132.7 (C), 133.3 (C), 135.5 (C), 144.5 (C), 167.5 (C); *m/z* (ESI) 255.0651 (MH<sup>+</sup>. C<sub>10</sub>H<sub>12</sub><sup>35</sup>ClN<sub>4</sub>O<sub>2</sub> requires 255.0643).

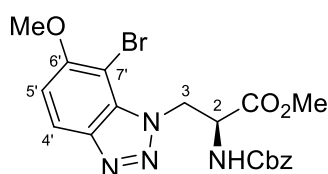
**(2S)-2-Amino-3-(5'-bromo-1*H*-benzo[*d*][1.2.3]triazol-1'-yl)propanoic acid hydrochloride (206)**



(2S)-2-Amino-3-(5'-bromo-1*H*-benzo[*d*][1.2.3]triazol-1'-yl)propanoic acid hydrochloride (**206**) was synthesised as described for (2S)-2-amino-3-(1*H*-benzo[*d*][1.2.3]triazol-1'-yl)propanoic acid hydrochloride (**186**) using methyl (2S)-2-[(benzyloxycarbonyl)amino]-3-(5'-bromo-1*H*-benzo[*d*][1.2.3]triazol-1'-yl)propanoate (**204**) (0.200 g, 0.462 mmol) in 6 M aqueous hydrochloric acid solution (20 mL). The crude material was purified by recrystallisation from methanol and diethyl ether to afford (2S)-2-amino-3-(5'-bromo-1*H*-

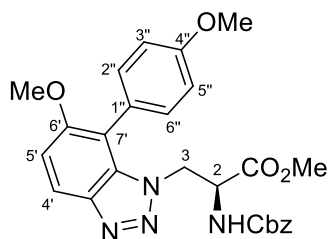
benzo[*d*][1.2.3]triazol-1'-yl)propanoic acid hydrochloride (**206**) as a pale brown solid (0.103 g, 78%). Mp 168–172 °C;  $\nu_{\max}/\text{cm}^{-1}$  (neat) 3387 (NH), 2847 (OH/CH), 1744 (CO), 1474, 1211, 802;  $[\alpha]_{\text{D}}^{22} +9.1$  (*c* 0.7, MeOH);  $\delta_{\text{H}}$  (500 MHz, CD<sub>3</sub>OD) 4.74 (1H, dd, *J* 5.9, 4.0 Hz, 2-H), 5.24 (1H, dd, *J* 15.5, 4.0 Hz, 3-*HH*), 5.34 (1H, dd, *J* 15.5, 5.9 Hz, 3-*HH*), 7.73 (1H, dd, *J* 8.8, 1.7 Hz, 6'-H), 7.78 (1H, dd, *J* 8.8, 0.5 Hz, 7'-H), 8.26 (1H, dd, *J* 1.7, 0.5 Hz, 4'-H);  $\delta_{\text{C}}$  (126 MHz, CD<sub>3</sub>OD) 48.3 (CH<sub>2</sub>), 53.6 (CH), 112.9 (CH), 119.0 (C), 123.1 (CH), 132.7 (CH), 134.0 (C), 148.1 (C), 169.0 (C); *m/z* (ESI) 284.9978 (MH<sup>+</sup>. C<sub>9</sub>H<sub>10</sub><sup>79</sup>BrN<sub>4</sub>O<sub>2</sub> requires 284.9982).

**Methyl (2*S*)-2-[(benzyloxycarbonyl)amino]-3-(7'-bromo-6'-methoxy-1*H*-benzo[*d*][1.2.3]triazol-1'-yl)propanoate (210)**



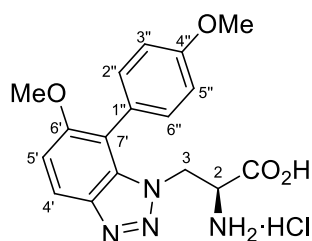
To a dry flask under argon was added iron(III) chloride (0.0030 g, 0.018 mmol) and [BMIM]NTf<sub>2</sub> (0.21 mL, 0.73 mmol) and the mixture stirred for 0.5 h. Methyl (2*S*)-2-[(benzyloxycarbonyl)amino]-3-(6'-methoxy-1*H*-benzo[*d*][1.2.3]triazol-1'-yl)propanoate (**201**) (0.14 g, 0.36 mmol) was then added as a solution in dichloromethane (5.0 mL), followed by *N*-bromosuccinimide (0.065 g, 0.36 mmol). After 1 h of stirring at room temperature, the mixture was diluted with ethyl acetate (20 mL) and filtered through a short pad of silica. The filtrate was washed with a 1 M aqueous solution of sodium thiosulfate (2 × 20 mL) and brine (20 mL), dried (MgSO<sub>4</sub>), filtered and concentrated *in vacuo*. The crude material was purified by flash column chromatography, eluting with 10% ethyl acetate in dichloromethane to afford methyl (2*S*)-2-[(benzyloxycarbonyl)amino]-3-(7'-bromo-6'-methoxy-1*H*-benzo[*d*][1.2.3]triazol-1'-yl)propanoate (**210**) as a white solid (0.14 g, 85%). Mp 122–124 °C;  $\nu_{\max}/\text{cm}^{-1}$  (neat) 3331 (NH), 2953 (CH), 1724 (CO), 1501 (C=C), 1261, 1065;  $[\alpha]_{\text{D}}^{23} -5.4$  (*c* 1.0, CHCl<sub>3</sub>);  $\delta_{\text{H}}$  (500 MHz, CDCl<sub>3</sub>) 3.76 (3H, s, OCH<sub>3</sub>), 4.00 (3H, s, OCH<sub>3</sub>), 4.96–5.12 (3H, m, 2-H and OCH<sub>2</sub>Ph), 5.28 (1H, dd, *J* 14.4, 6.9 Hz, 3-*HH*), 5.47 (1H, dd, *J* 14.4, 4.8 Hz, 3-*HH*), 5.68 (1H, d, *J* 8.1 Hz, NH), 7.09 (1H, d, *J* 9.0 Hz, 5'-H), 7.24–7.36 (5H, m, Ph), 7.95 (1H, d, *J* 9.0 Hz, 4'-H);  $\delta_{\text{C}}$  (126 MHz, CDCl<sub>3</sub>) 49.8 (CH<sub>2</sub>), 53.0 (CH<sub>3</sub>), 54.4 (CH), 57.5 (CH<sub>3</sub>), 67.2 (CH<sub>2</sub>), 90.1 (C), 111.2 (CH), 119.8 (CH), 128.1 (2 × CH), 128.2 (CH), 128.5 (2 × CH), 132.9 (C), 135.9 (C), 142.3 (C), 155.7 (C), 156.2 (C), 169.7 (C); *m/z* (ESI) 485.0430 (MNa<sup>+</sup>. C<sub>19</sub>H<sub>19</sub><sup>79</sup>BrN<sub>4</sub>NaO<sub>5</sub> requires 485.0430).

**Methyl (2S)-2-[(benzyloxycarbonyl)amino]-3-[6'-methoxy-7'-(4''-methoxyphenyl)-1H-benzo[d][1.2.3]triazol-1'-yl]propanoate (211)**

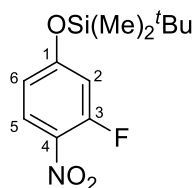


To a solution of methyl (2S)-2-[(benzyloxycarbonyl)amino]-3-(7'-bromo-6'-methoxy-1H-benzo[d][1.2.3]triazol-1'-yl)propanoate (**210**) (0.140 g, 0.302 mmol) in 1,4-dioxane (3.0 mL) and water (0.23 mL) was added 4-methoxyphenylboronic acid (0.0734 g, 0.483 mmol), potassium fluoride (0.0526 g, 0.906 mmol) and [1,1'-bis(diphenylphosphino)ferrocene]dichloropalladium(II) (1:1) (0.0186 g, 0.0227 mmol). The mixture was degassed under argon for 0.25 h before heating to 80 °C for 24 h. The reaction was then cooled to ambient temperature and filtered through a pad of Celite®, diluted with ethyl acetate (20 mL) and washed with water (3 × 20 mL) and brine (20 mL). The organic layer was dried (MgSO<sub>4</sub>), filtered and concentrated *in vacuo*. The crude material was purified by flash column chromatography, eluting with 10% ethyl acetate in dichloromethane to afford methyl (2S)-2-[(benzyloxycarbonyl)amino]-3-[6'-methoxy-7'-(4''-methoxyphenyl)-1H-benzo[d][1.2.3]triazol-1'-yl]propanoate (**211**) as a pale orange oil (0.0979 g, 66%).  $\nu_{\max}/\text{cm}^{-1}$  (neat) 3350 (NH), 2954 (CH), 1748 (CO), 1723 (CO), 1519 (C=C), 1497, 1288, 1065, 1028, 752;  $[\alpha]_{\text{D}}^{20}$  -26.7 (*c* 1.0, CHCl<sub>3</sub>);  $\delta_{\text{H}}$  (400 MHz, CDCl<sub>3</sub>) 3.62 (3H, s, OCH<sub>3</sub>), 3.83 (3H, s, OCH<sub>3</sub>), 3.88 (3H, s, OCH<sub>3</sub>), 4.31 (1H, dd, *J* 13.8, 3.6 Hz, 3-*HH*), 4.43–4.58 (2H, m, 2-H and 3-*HH*), 4.98 (2H, s, OCH<sub>2</sub>Ph), 5.57 (1H, d, *J* 8.6 Hz, NH), 6.97–7.07 (2H, m, 3''-H and 5''-H), 7.17 (1H, d, *J* 9.1 Hz, 5'-H), 7.21–7.38 (7H, m, Ph, 2''-H and 6''-H), 8.00 (1H, d, *J* 9.1 Hz, 4'-H);  $\delta_{\text{C}}$  (101 MHz, CDCl<sub>3</sub>) 49.9 (CH<sub>2</sub>), 52.7 (CH<sub>3</sub>), 53.6 (CH), 55.3 (CH<sub>3</sub>), 57.2 (CH<sub>3</sub>), 67.1 (CH<sub>2</sub>), 111.2 (CH), 111.8 (C), 114.0 (CH), 114.2 (CH), 119.7 (CH), 124.5 (C), 127.9 (2 × CH), 128.1 (CH), 128.5 (2 × CH), 131.7 (CH), 131.8 (CH), 133.0 (C), 136.0 (C), 141.7 (C), 155.6 (C), 156.7 (C), 159.6 (C), 169.6 (C); *m/z* (EI) 490.1831 (M<sup>+</sup>. C<sub>26</sub>H<sub>26</sub>N<sub>4</sub>O<sub>6</sub> requires 490.1852), 382 (90%), 240 (94), 227 (42), 212 (37), 108 (52), 91 (100), 79 (49).

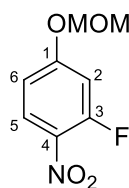
**(2S)-2-Amino-3-(6'-methoxy-7'-(4''-methoxyphenyl)-1H-benzo[d][1.2.3]triazol-1'-yl)propanoic acid hydrochloride (212)**



To a solution of methyl (2S)-2-[(benzyloxycarbonyl)amino]-3-[6'-methoxy-7'-(4''-methoxyphenyl)-1H-benzo[d][1.2.3]triazol-1'-yl]propanoate (**211**) (0.097 g, 0.198 mmol) in methanol (7.0 mL) and water (3.0 mL) was added caesium carbonate (0.084 g, 0.257 mmol) and the reaction stirred at room temperature for 16 h. The reaction mixture was concentrated *in vacuo* and dissolved in water (5.0 mL), before the addition of 1 M aqueous hydrochloric acid solution (10 mL). The product was extracted with dichloromethane (3 × 20 mL), dried (MgSO<sub>4</sub>), filtered and concentrated *in vacuo* to afford (2S)-2-[(benzyloxycarbonyl)amino]-3-[6'-methoxy-7'-(4''-methoxyphenyl)-1H-benzo[d][1.2.3]triazol-1'-yl]propanoic acid as a yellow foam (0.089 g, 94%). This material was then used immediately in the following step. To a solution of (2S)-2-[(benzyloxycarbonyl)amino]-3-[6'-methoxy-7'-(4''-methoxyphenyl)-1H-benzo[d][1.2.3]triazol-1'-yl]propanoic acid (0.044 g, 0.092 mmol) in tetrahydrofuran (5 mL) was added 10% palladium on carbon (0.019 g) and the reaction mixture purged under hydrogen gas for 1 h, before stirring at room temperature under a hydrogen atmosphere for 16 h. The reaction mixture was then treated with a 1 M aqueous solution of hydrochloric acid (0.50 mL), filtered through Celite<sup>®</sup>, washed with methanol (10 mL) and the filtrate was concentrated *in vacuo*. The resulting residue was recrystallised from methanol and diethyl ether to afford (2S)-2-amino-3-(6'-methoxy-7'-(4''-methoxyphenyl)-1H-benzo[d][1.2.3]triazol-1'-yl)propanoic acid hydrochloride (**212**) as a white solid (0.023 g, 73%). Mp 130–132 °C;  $\nu_{\max}/\text{cm}^{-1}$  (neat) 3698 (NH), 2931 (OH/CH), 1686 (CO), 1595 (C=C), 1354, 1252, 1169, 984;  $[\alpha]_{\text{D}}^{19}$  -6.2 (c 0.1, MeOH);  $\delta_{\text{H}}$  (400 MHz, CD<sub>3</sub>OD) 3.83 (3H, s, OCH<sub>3</sub>), 3.85–3.97 (4H, m, OCH<sub>3</sub> and 2-H), 4.43 (1H, dd, *J* 15.2, 9.6 Hz, 3-HH), 4.57 (1H, dd, *J* 15.2, 2.5 Hz, 3-HH), 7.00–7.12 (2H, m, 3''-H and 5''-H), 7.23–7.34 (2H, m, 2''-H and 6''-H), 7.37 (1H, d, *J* 9.1 Hz, 5'-H), 7.99 (1H, d, *J* 9.1 Hz, 4'-H);  $\delta_{\text{C}}$  (126 MHz, CD<sub>3</sub>OD) 50.8 (CH<sub>2</sub>), 55.1 (CH), 55.8 (CH<sub>3</sub>), 57.7 (CH<sub>3</sub>), 113.5 (CH), 113.9 (C), 115.2 (CH), 115.3 (CH), 120.0 (CH), 125.6 (C), 132.8 (CH), 133.2 (CH), 134.3 (C), 142.7 (C), 158.6 (C), 161.3 (C), 170.2 (C); *m/z* (ESI) 365.1210 (MNa<sup>+</sup>. C<sub>17</sub>H<sub>18</sub>N<sub>4</sub>NaO<sub>4</sub> requires 365.1220).

***tert*-Butyl-(3-fluoro-4-nitrophenoxy)dimethylsilane (220)**

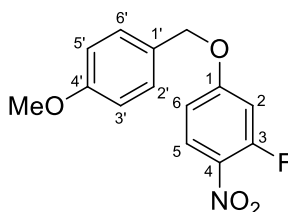
To a solution of 3-fluoro-4-nitrophenol (2.00 g, 12.7 mmol) in dichloromethane (50 mL) under argon was added *tert*-butyldimethylsilyl chloride (2.30 g, 15.3 mmol), imidazole (1.70 g, 25.4 mmol) and 4-dimethylaminopyridine (0.155 g, 1.27 mmol). The reaction mixture was stirred for 16 h at room temperature. The mixture was then diluted with dichloromethane (50 mL) and washed with water (3 × 50 mL) and brine (100 mL), dried (MgSO<sub>4</sub>), filtered and the solvent removed *in vacuo*. The crude material was purified by flash column chromatography, eluting with 5% ethyl acetate in petroleum ether (40–60) to afford *tert*-butyl-(3-fluoro-4-nitrophenoxy)dimethylsilane (**220**) as a yellow oil (3.24 g, 94%).  $\nu_{\max}/\text{cm}^{-1}$  (neat) 2931 (CH), 1597 (C=C), 1328, 1284, 1093, 982, 824, 783;  $\delta_{\text{H}}$  (400 MHz, CDCl<sub>3</sub>) 0.27 (6H, s, OSi(CH<sub>3</sub>)<sub>2</sub>), 0.98 (9H, s, C(CH<sub>3</sub>)<sub>3</sub>), 6.64–6.72 (2H, m, 2-H and 6-H), 8.03 (1H, dd,  $J$  9.5, 8.9 Hz, 5-H);  $\delta_{\text{C}}$  (101 MHz, CDCl<sub>3</sub>) -4.4 (2 × CH<sub>3</sub>), 18.2 (C), 25.4 (3 × CH<sub>3</sub>), 109.3 (CH, d,  $^2J_{\text{CF}}$  21.9 Hz), 116.0 (CH, d,  $^3J_{\text{CF}}$  3.1 Hz), 127.7 (CH, d,  $^4J_{\text{CF}}$  1.5 Hz), 131.4 (C, d,  $^2J_{\text{CF}}$  6.3 Hz), 157.2 (C, d,  $^1J_{\text{CF}}$  265.6 Hz), 162.3 (C, d,  $^3J_{\text{CF}}$  11.5 Hz);  $m/z$  (ESI) 294.0924 (MNa<sup>+</sup>. C<sub>12</sub>H<sub>18</sub>FNNaO<sub>3</sub>Si requires 294.0932).

**3-Fluoro-1-(methoxymethoxy)-4-nitrobenzene (224)**

To a solution of 3-fluoro-4-nitrophenol (1.00 g, 6.37 mmol) in dichloromethane (35 mL) at 0 °C under argon was added *N,N*-diisopropylethylamine (1.70 mL, 9.56 mmol) and stirred for 0.1 h. Bromomethyl methyl ether (0.570 mL, 7.01 mmol) was then added and the reaction mixture stirred for 0.5 h before heating under reflux for 2 h. The reaction was taken up in water (50 mL) and extracted with dichloromethane (15 mL) and then ethyl acetate (2 × 50 mL). The combined organic layers were dried (MgSO<sub>4</sub>), filtered and the solvent removed *in vacuo*. The crude material was purified by flash column chromatography, eluting with 10% ethyl acetate in petroleum ether (40–60) to afford 3-fluoro-1-(methoxymethoxy)-4-nitrobenzene (**224**) as a yellow oil (1.27 g, 99%).  $\nu_{\max}/\text{cm}^{-1}$  (neat) 2940 (CH), 1605 (C=C), 1520 (C=C), 1342, 1273, 1150, 1072, 988, 748, 733;  $\delta_{\text{H}}$

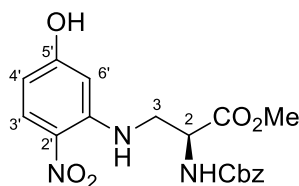
(400 MHz, CDCl<sub>3</sub>) 3.45 (3H, s, OCH<sub>3</sub>), 5.21 (2H, s, OCH<sub>2</sub>), 6.82–6.90 (2H, m, 2-H and 6-H), 8.01 (1H, br t, *J* 9.0 Hz, 5-H); δ<sub>C</sub> (101 MHz, CDCl<sub>3</sub>) 56.7 (CH<sub>3</sub>), 94.6 (CH<sub>2</sub>), 105.4 (CH, d, <sup>2</sup>*J*<sub>CF</sub> 24.3 Hz), 112.2 (CH, d, <sup>3</sup>*J*<sub>CF</sub> 3.2 Hz), 127.8 (CH, d, <sup>4</sup>*J*<sub>CF</sub> 1.7 Hz), 131.4 (C, d, <sup>2</sup>*J*<sub>CF</sub> 6.7 Hz), 157.3 (C, d, <sup>1</sup>*J*<sub>CF</sub> 264.6 Hz), 163.0 (C, d, <sup>3</sup>*J*<sub>CF</sub> 11.1 Hz); *m/z* (ESI) 224.0324 (MNa<sup>+</sup>. C<sub>8</sub>H<sub>8</sub>FNNaO<sub>4</sub> requires 224.0330).

### 3-Fluoro-1-(4'-methoxybenzyloxy)-4-nitrobenzene (**227**)



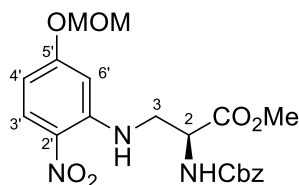
To a solution of 3-fluoro-4-nitrophenol (1.00 g, 6.37 mmol) in acetone (20 mL) under argon was added 4-methoxybenzyl chloride (0.950 mL, 7.01 mmol), potassium carbonate (1.80 g, 12.7 mmol) and tetrabutylammonium iodide (0.24 g, 0.637 mmol) and the reaction stirred under reflux for 2 h. The solvent was removed *in vacuo* and the residue dissolved in ethyl acetate (50 mL) and washed with water (3 × 50 mL). The combined organic layers were dried (MgSO<sub>4</sub>), filtered and the solvent removed *in vacuo*. The crude material was purified by flash column chromatography, eluting with dichloromethane and subsequently recrystallised from hexane to afford 3-fluoro-1-(4'-methoxybenzyloxy)-4-nitrobenzene (**227**) as white crystals (1.64 g, 93%). Mp 101–103 °C; *v*<sub>max</sub>/cm<sup>-1</sup> (neat) 2940 (CH), 1605 (C=C), 1512 (C=C), 1342, 1296, 1250, 1173, 1096, 833; δ<sub>H</sub> (400 MHz, CDCl<sub>3</sub>) 3.82 (3H, s, OCH<sub>3</sub>), 5.06 (2H, s, OCH<sub>2</sub>Ar), 6.79 (1H, dd, *J* 12.7, 2.7 Hz, 2-H), 6.82 (1H, ddd, *J* 9.0, 2.7, 0.9 Hz, 6-H), 6.94 (2H, d, *J* 8.6 Hz, 3'-H and 5'-H), 7.35 (2H, d, *J* 8.6 Hz, 2'-H and 6'-H), 8.07 (1H, dd, *J* 9.2, 9.0 Hz, 5-H); δ<sub>C</sub> (101 MHz, CDCl<sub>3</sub>) 55.4 (CH<sub>3</sub>), 71.0 (CH<sub>2</sub>), 104.1 (CH, d, <sup>2</sup>*J*<sub>CF</sub> 24.2 Hz), 111.1 (CH, d, <sup>3</sup>*J*<sub>CF</sub> 3.1 Hz), 114.3 (2 × CH), 126.9 (C), 127.9 (CH, d, <sup>4</sup>*J*<sub>CF</sub> 1.5 Hz), 129.5 (2 × CH), 130.8 (C, d, <sup>2</sup>*J*<sub>CF</sub> 6.8 Hz), 157.4 (C, d, <sup>1</sup>*J*<sub>CF</sub> 265.0 Hz), 160.0 (C), 164.5 (C, d, <sup>3</sup>*J*<sub>CF</sub> 11.0 Hz); *m/z* (ESI) 300.0633 (MNa<sup>+</sup>. C<sub>14</sub>H<sub>12</sub>FNNaO<sub>4</sub> requires 300.0643).

**Methyl (2S)-2-(benzyloxycarbonyl)amino]-3-[(5'-hydroxy-2'-nitrophenyl)amino]propanoate (221)**



Methyl (2S)-2-(benzyloxycarbonyl)amino]-3-[(5'-hydroxy-2'-nitrophenyl)amino]propanoate (**221**) was synthesised as described for methyl (2S)-2-[(benzyloxycarbonyl)amino]-3-[(2'-nitrophenyl)amino]propanoate (**189**) using methyl (2S)-3-amino-2-[(benzyloxycarbonyl)amino]propanoate hydrochloride (**191**) (0.050 g, 0.20 mmol), 3-fluoro-4-nitrophenol (0.093 g, 0.59 mmol) and triethylamine (0.083 mL, 0.59 mmol) in acetonitrile (3.0 mL). The crude material was purified by flash column chromatography, eluting with 5% ethyl acetate and 1% tetrahydrofuran in dichloromethane to afford methyl (2S)-2-(benzyloxycarbonyl)amino]-3-[(5'-hydroxy-2'-nitrophenyl)amino]propanoate (**221**) as a yellow solid (0.023 g, 49%). Mp 85–87 °C;  $\nu_{\max}/\text{cm}^{-1}$  (neat) 3348 (NH), 2924 (CH), 1701 (CO), 1620 (CO), 1516 (C=C), 1227, 1061;  $[\alpha]_{\text{D}}^{22} +18.8$  (c 1.0,  $\text{CHCl}_3$ );  $\delta_{\text{H}}$  (400 MHz,  $\text{CDCl}_3$ ) 3.69 (2H, br t,  $J$  6.5 Hz, 3-H<sub>2</sub>), 3.80 (3H, s, OCH<sub>3</sub>), 4.63 (1H, dt,  $J$  6.7, 6.1 Hz, 2-H), 5.14 (2H, s, CH<sub>2</sub>Ph), 5.71 (1H, d,  $J$  6.7 Hz, NH), 6.17 (1H, dd,  $J$  9.3, 2.3 Hz, 4'-H), 6.37 (1H, d,  $J$  2.3 Hz, 6'-H), 6.72 (1H, br s, OH), 7.29–7.41 (5H, m, Ph), 8.10 (1H, d,  $J$  9.3 Hz, 3'-H), 8.44 (1H, t,  $J$  6.5 Hz, NH);  $\delta_{\text{C}}$  (101 MHz,  $\text{CDCl}_3$ ) 44.6 (CH<sub>2</sub>), 53.1 (CH<sub>3</sub>), 53.1 (CH), 67.6 (CH<sub>2</sub>), 97.6 (CH), 106.3 (CH), 127.2 (C), 128.1 (2 × CH), 128.5 (CH), 128.7 (2 × CH), 129.9 (CH), 135.6 (C), 147.2 (C), 156.1 (C), 163.2 (C), 170.6 (C);  $m/z$  (ESI) 412.1111 (MNa<sup>+</sup>. C<sub>18</sub>H<sub>19</sub>N<sub>3</sub>NaO<sub>7</sub> requires 412.1115).

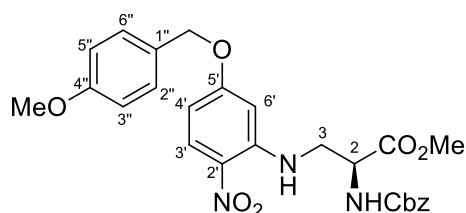
**Methyl (2S)-2-(benzyloxycarbonyl)amino]-3-[[5'-(methoxymethoxy)-2'-nitrophenyl]amino]propanoate (225)**



Methyl (2S)-2-(benzyloxycarbonyl)amino]-3-[[5'-(methoxymethoxy)-2'-nitrophenyl]amino]propanoate (**225**) was synthesised as described for methyl (2S)-2-[(benzyloxycarbonyl)amino]-3-[(2'-nitrophenyl)amino]propanoate (**189**) using methyl (2S)-3-amino-2-[(benzyloxycarbonyl)amino]propanoate hydrochloride (**191**) (0.400 g, 1.59 mmol), 3-fluoro-1-(methoxymethoxy)-4-nitrobenzene (0.960 g, 4.77 mmol) and triethylamine (0.665 mL, 4.77 mmol) in acetonitrile (12 mL). The crude material was

purified by flash column chromatography, eluting with 0–20% ethyl acetate in dichloromethane to afford methyl (2*S*)-2-(benzyloxycarbonyl)amino]-3-[[5'-(methoxymethoxy)-2'-nitrophenyl]amino]propanoate (**225**) as a yellow oil (0.572 g, 83%).  $\nu_{\max}/\text{cm}^{-1}$  (neat) 3356 (NH), 2955 (CH), 1721 (CO), 1620 (CO), 1497 (C=C), 1211, 748;  $[\alpha]_{\text{D}}^{23} +17.1$  (*c* 1.0,  $\text{CHCl}_3$ );  $\delta_{\text{H}}$  (400 MHz,  $\text{CDCl}_3$ ) 3.47 (3H, s,  $\text{OCH}_2\text{OCH}_3$ ), 3.72 (2H, br t,  $J$  5.9 Hz, 3- $\text{H}_2$ ), 3.79 (3H, s,  $\text{OCH}_3$ ), 4.65 (1H, dt,  $J$  6.9, 5.7 Hz, 2-H), 5.12 (2H, s,  $\text{CH}_2\text{Ph}$ ), 5.21 (1H, d,  $J$  6.8 Hz,  $\text{OCHH}_2\text{OCH}_3$ ), 5.24 (1H, d,  $J$  6.8 Hz,  $\text{OCHH}_2\text{OCH}_3$ ), 5.68 (1H, d,  $J$  6.9 Hz, NH), 6.37 (1H, dd,  $J$  9.5, 2.5 Hz, 4'-H), 6.53 (1H, d,  $J$  2.5 Hz, 6'-H), 7.28–7.42 (5H, m, Ph), 8.14 (1H, d,  $J$  9.5 Hz, 3'-H), 8.42 (1H, t,  $J$  5.9 Hz, NH);  $\delta_{\text{C}}$  (101 MHz,  $\text{CDCl}_3$ ) 44.7 ( $\text{CH}_2$ ), 53.0 ( $\text{CH}_3$ ), 53.3 (CH), 56.5 ( $\text{CH}_3$ ), 67.4 ( $\text{CH}_2$ ), 94.2 ( $\text{CH}_2$ ), 98.2 (CH), 106.2 (CH), 127.7 (C), 128.1 (2  $\times$  CH), 128.3 (CH), 128.6 (2  $\times$  CH), 129.3 (CH), 135.9 (C), 147.0 (C), 155.8 (C), 163.7 (C), 170.7 (C);  $m/z$  (ESI) 456.1365 ( $\text{MNa}^+$ .  $\text{C}_{20}\text{H}_{23}\text{N}_3\text{NaO}_8$  requires 456.1377).

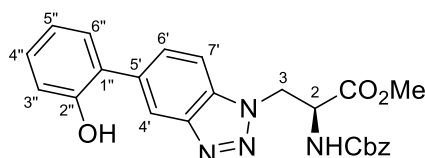
**Methyl (2*S*)-2-(benzyloxycarbonyl)amino]-3-[[5'-(4''-methoxybenzyloxy)-2'-nitrophenyl]amino]propanoate (228)**



Methyl (2*S*)-2-(benzyloxycarbonyl)amino]-3-[[5'-(4''-methoxybenzyloxy)-2'-nitrophenyl]amino]propanoate (**228**) was synthesised as described for methyl (2*S*)-2-[(benzyloxycarbonyl)amino]-3-[(2'-nitrophenyl)amino]propanoate (**189**) using methyl (2*S*)-3-amino-2-[(benzyloxycarbonyl)amino]propanoate hydrochloride (**191**) (0.400 g, 1.59 mmol), 3-fluoro-1-(4-methoxybenzyloxy)-4-nitrobenzene (1.32 g, 4.77 mmol) and triethylamine (0.665 mL, 4.77 mmol) in acetonitrile (12 mL). The crude material was purified by flash column chromatography, eluting with 0–20% ethyl acetate in dichloromethane to afford methyl (2*S*)-2-(benzyloxycarbonyl)amino]-3-[[5'-(4''-methoxybenzyloxy)-2'-nitrophenyl]amino]propanoate (**228**) as a yellow oil (0.694 g, 86%). Mp 79–81 °C;  $\nu_{\max}/\text{cm}^{-1}$  (neat) 3356 (NH), 2955 (CH), 1721 (CO), 1613 (CO), 1497 (C=C), 1219, 903, 725;  $[\alpha]_{\text{D}}^{22} +13.6$  (*c* 1.0,  $\text{CHCl}_3$ );  $\delta_{\text{H}}$  (400 MHz,  $\text{CDCl}_3$ ) 3.63–3.74 (2H, m, 3- $\text{H}_2$ ), 3.76 (3H, s,  $\text{OCH}_3$ ), 3.79 (3H, s,  $\text{OCH}_3$ ), 4.62 (1H, dt,  $J$  7.0, 6.1 Hz, 2-H), 5.04 (1H, d,  $J$  11.3 Hz,  $\text{CHHAr}$ ), 5.07 (1H, d,  $J$  11.3 Hz,  $\text{CHHAr}$ ), 5.08 (1H, d,  $J$  12.2 Hz,  $\text{CHHPh}$ ), 5.12 (1H, d,  $J$  12.2 Hz,  $\text{CHHPh}$ ), 5.77 (1H, d,  $J$  7.0 Hz, NH), 6.30 (1H, dd,  $J$  9.5, 2.5 Hz, 4'-H), 6.49 (1H, d,  $J$  2.5 Hz, 6'-H), 6.91 (2H, d,  $J$  8.7 Hz, 3''-H and 5''-H), 7.25–7.38 (5H, m, Ph), 7.33 (2H, d,  $J$  8.7 Hz, 2''-H and 6''-H), 8.10 (1H, d,  $J$  9.5 Hz, 3'-H), 8.49 (1H, t,  $J$  5.8 Hz, NH);  $\delta_{\text{C}}$  (101 MHz,  $\text{CDCl}_3$ ) 44.5 ( $\text{CH}_2$ ), 53.0 ( $\text{CH}_3$ ), 53.2 (CH), 55.3 ( $\text{CH}_3$ ), 67.3 ( $\text{CH}_2$ ), 70.3

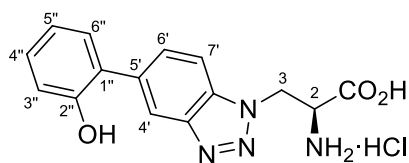
(CH<sub>2</sub>), 96.4 (CH), 106.1 (CH), 114.1 (2 × CH), 127.0 (C), 127.8 (C), 128.1 (2 × CH), 128.3 (CH), 128.5 (2 × CH), 129.2 (CH), 129.4 (2 × CH), 135.9 (C), 147.2 (C), 155.8 (C), 159.7 (C), 165.3 (C), 170.7 (C); *m/z* (ESI) 532.1677 (MNa<sup>+</sup>. C<sub>26</sub>H<sub>27</sub>N<sub>3</sub>NaO<sub>8</sub> requires 532.1690).

**Methyl (2S)-2-[(benzyloxycarbonyl)amino]-3-[5'-(2''-hydroxyphenyl)-1H-benzo[d][1.2.3]triazol-1'-yl]propanoate (229)**



Methyl (2S)-2-[(benzyloxycarbonyl)amino]-3-[5'-(2''-hydroxyphenyl)-1H-benzo[d][1.2.3]triazol-1'-yl]propanoate (**229**) was synthesised as described for methyl (2S)-2-[(benzyloxycarbonyl)amino]-3-[6'-methoxy-7'-(4''-methoxyphenyl)-1H-benzo[d][1.2.3]triazol-1'-yl]propanoate (**211**) using methyl (2S)-2-[(benzyloxycarbonyl)amino]-3-(5'-bromo-1H-benzo[d][1.2.3]triazol-1'-yl)propanoate (**204**) (0.400 g, 0.920 mmol), 2-hydroxyphenylboronic acid (0.200 g, 1.47 mmol), potassium fluoride (0.160 g, 2.76 mmol) and [1,1'-bis(diphenylphosphino)ferrocene]dichloropalladium(II) (1:1) (0.0566 g, 0.0690 mmol) in 1,4-dioxane (8.0 mL) and water (0.60 mL). The crude material was purified by flash column chromatography, eluting with 10% ethyl acetate in dichloromethane to afford methyl (2S)-2-[(benzyloxycarbonyl)amino]-3-[5'-(2''-hydroxyphenyl)-1H-benzo[d][1.2.3]triazol-1'-yl]propanoate (**229**) as a pale orange solid (0.380 g, 93%). Mp 55–56 °C;  $\nu_{\text{max}}/\text{cm}^{-1}$  (neat) 3337 (NH/OH), 2953 (CH), 1695 (CO), 1510 (C=C), 1454, 1211, 1057, 752;  $[\alpha]_{\text{D}}^{19}$  +15.4 (*c* 1.0, CHCl<sub>3</sub>);  $\delta_{\text{H}}$  (400 MHz, CDCl<sub>3</sub>) 4.69 (3H, s, OCH<sub>3</sub>), 4.82 (1H, dt, *J* 7.1, 4.4 Hz, 2-H), 4.95–5.15 (4H, m, 3-H<sub>2</sub> and OCH<sub>2</sub>Ph), 5.86 (1H, d, *J* 7.1 Hz, NH), 6.95 (1H, br t, *J* 7.9 Hz, 5''-H), 7.03 (1H, d, 7.8 Hz, 3''-H), 7.20 (1H, ddd, *J* 7.9, 7.8, 1.6 Hz, 4''-H), 7.22–7.32 (6H, m, Ph and 6''-H), 7.37 (1H, d, *J* 8.6 Hz, 7'-H), 7.55 (1H, s, OH), 7.56 (1H, dd, *J* 8.6, 1.3 Hz, 6'-H), 8.18 (1H, br s, 4'-H);  $\delta_{\text{C}}$  (101 MHz, CDCl<sub>3</sub>) 48.6 (CH<sub>2</sub>), 53.2 (CH<sub>3</sub>), 54.2 (CH), 67.3 (CH<sub>2</sub>), 109.0 (CH), 116.5 (CH), 119.9 (CH), 120.6 (CH), 127.4 (C), 128.2 (2 × CH), 128.3 (CH), 128.5 (2 × CH), 129.2 (CH), 130.1 (CH), 130.8 (CH), 132.9 (C), 134.8 (C), 135.8 (C), 145.6 (C), 153.4 (C), 155.8 (C), 169.3 (C); *m/z* (ESI) 469.1477 (MNa<sup>+</sup>. C<sub>24</sub>H<sub>22</sub>N<sub>4</sub>NaO<sub>5</sub> requires 469.1482).

**(2S)-2-Amino-3-(5'-(2''-hydroxyphenyl)-1H-benzo[d][1.2.3]triazol-1'-yl)propanoic acid hydrochloride (231)**



To a solution of methyl (2S)-2-[(benzyloxycarbonyl)amino]-3-[5'-(2''-hydroxyphenyl)-1H-benzo[d][1.2.3]triazol-1'-yl]propanoate (**229**) (0.100 g, 0.224 mmol) in 1,4-dioxane (1.0 mL) was added 6 M aqueous hydrochloric acid solution (5 mL). The reaction mixture was heated under reflux for 4 h. After cooling to ambient temperature, the reaction mixture was concentrated *in vacuo* and the resulting residue recrystallised from methanol and diethyl ether to afford (2S)-2-amino-3-(5'-(2''-hydroxyphenyl)-1H-benzo[d][1.2.3]triazol-1'-yl)propanoic acid hydrochloride (**231**) as a pale brown solid (0.065 g, 97%). Mp 198–200 °C;  $\nu_{\max}/\text{cm}^{-1}$  (neat) 3165 (NH), 2945 (OH/CH), 1746 (CO), 1603 (C=C), 1485, 1238, 754;  $[\alpha]_{\text{D}}^{19}$  +9.4 (*c* 1.0, MeOH);  $\delta_{\text{H}}$  (500 MHz, CD<sub>3</sub>OD) 4.81 (1H, dd, *J* 5.7, 4.1 Hz, 2-H), 5.29 (1H, dd, *J* 15.5, 4.1 Hz, 3-HH), 5.38 (1H, dd, *J* 15.5, 5.7 Hz, 3-HH), 6.90–6.98 (2H, m, 3''-H and 5''-H), 7.21 (1H, ddd, *J* 8.9, 7.5, 1.6 Hz, 4''-H), 7.33 (1H, dd, *J* 7.8, 1.6 Hz, 6''-H), 7.83 (1H, d, *J* 8.7 Hz, 7'-H), 7.87 (1H, dd, *J* 8.7, 1.3 Hz, 6'-H), 8.16 (1H, br s, 4'-H);  $\delta_{\text{C}}$  (126 MHz, CD<sub>3</sub>OD) 46.7 (CH<sub>2</sub>), 52.2 (CH), 108.8 (CH), 115.6 (CH), 118.7 (CH), 119.7 (CH), 127.3 (C), 128.7 (CH), 130.5 (CH), 130.6 (CH), 132.5 (C), 136.4 (C), 145.8 (C), 154.2 (C), 167.6 (C); *m/z* (ESI) 299.1135 (MH<sup>+</sup>). C<sub>15</sub>H<sub>15</sub>N<sub>4</sub>O<sub>3</sub> requires 299.1139).

## 4 References

1. U. Haberkorn and M. Eisenhut, *Eur. J. Nucl. Med. Mol. Imaging*, 2005, **32**, 1354–1359.
2. S. M. Ametamey, M. Honer and P. A. Schubiger, *Chem. Rev.*, 2008, **108**, 1501–1516.
3. S. Vallabhajosula, *Molecular Imaging: Radiopharmaceuticals for PET and SPECT*, Springer Berlin Heidelberg, Berlin, 2009.
4. S. L. Pimlott and A. Sutherland, *Chem. Soc. Rev.*, 2011, **40**, 149–162.
5. P. F. Sharp and A. Welch, in *Practical Nuclear Medicine*, eds. P. F. Sharp, H. G. Gemmell and A. D. Murray, Springer, London, 2005, p. 35–48.
6. P. W. Miller, N. J. Long, R. Vilar and A. D. Gee, *Angew. Chem. Int. Ed.*, 2008, **47**, 8998–9033.
7. W. W. Moses, *Nucl. Instrum. Methods Phys. Res.*, 2011, **648 Supplement 1**, S236–S240.
8. L. Martí-Bonmatí, R. Sopena, P. Bartumeus and P. Sopena, *Contrast Media Mol. Imaging*, 2010, **5**, 180–189.
9. P. E. Kinahan, D. W. Townsend, T. Beyer and D. Sashin, *Med. Phys.*, 1998, **25**, 2046–2053.
10. J. M. Martí-Clement, E. Prieto, V. Morán, L. Sancho, M. Rodríguez-Fraile, J. Arbizu, M. J. García-Velloso and J. A. Richter, *EJNMMI Res.*, 2017, **7**, 37.
11. S. Vandenberghe and P. K. Marsden, *Phys. Med. Biol.*, 2015, **60**, R115–R154.
12. S. Musafargani, K. K. Ghosh, S. Mishra, P. Mahalakshmi, P. Padmanabhan and B. Gulyás, *Eur. J. Hybrid Imaging*, 2018, **2**, 12.
13. A. F. Chatziaoannou, S. R. Cherry, Y. Shao, R. W. Silverman, K. Meadors, T. H. Farquhar, M. Pedarsani and M. E. Phelps, *J. Nucl. Med.*, 1999, **40**, 1164–1175.

14. R. D. Badawi, H. Shi, P. Hu, S. Chen, T. Xu, P. M. Price, Y. Ding, B. A. Spencer, L. Nardo, W. Liu, J. Bao, T. Jones, H. Li and S. R. Cherry, *J. Nucl. Med.*, 2019, **60**, 299.
15. S. R. Cherry, R. D. Badawi, J. S. Karp, W. W. Moses, P. Price and T. Jones, *Sci. Transl. Med.*, 2017, **9**, eaaf6169.
16. E. O. Lawrence and M. S. Livingston, *Phys. Rev.*, 1931, **38**, 834–834.
17. W. Scharf, *Biomedical Particle Accelerators*, American Institute of Physics Press, New York, 1994.
18. S. M. Qaim, J. C. Clark, C. Crouzel, M. Guillaume, H. J. Helmeke, B. Nebeling, V. W. Pike and G. Stöcklin, in *Radiopharmaceuticals for Positron Emission Tomography: Methodological Aspects*, eds. G. Stöcklin and V. W. Pike, Springer Netherlands, Dordrecht, 1993, p. 1–43.
19. E. Hess, G. Blessing, H. H. Coenen and S. M. Qaim, *Appl. Radiat. Isot.*, 2000, **52**, 1431–1440.
20. D. R. Christman, R. D. Finn, K. I. Karlstrom and A. P. Wolf, *Int. J. Appl. Radiat. Isot.*, 1975, **26**, 435–442.
21. G. Antoni, T. Kihlberg and B. Långström, in *Handbook of Nuclear Chemistry*, eds. A. Vértes, S. Nagy, Z. Klencsár, R. G. Lovas and F. Rösch, Springer US, Boston, MA, 2011, p. 1977–2019.
22. R. Bolton, *J. Label. Compd. Radiopharm.*, 2001, **44**, 701–736.
23. V. Gómez-Vallejo, V. Gaja, J. Kozirowski and J. Llop, in *Positron Emission Tomography – Current Clinical and Research Aspects*, ed. C.-H. Hsieh, InTech, Rijeka, 2012, pp. 183–210.
24. M.-R. Zhang and K. Suzuki, *Appl. Radiat. Isot.*, 2005, **62**, 447–450.
25. K. Tanaka and K. Fukase, *Org. Biomol. Chem.*, 2008, **6**, 815–828.
26. B. M. Zeglis and J. S. Lewis, *Dalton Trans.*, 2011, **40**, 6168–6195.

27. I. Velikyan, H. Maecke and B. Langstrom, *Bioconjugate Chem.*, 2008, **19**, 569–573.
28. W. J. McBride, R. M. Sharkey, H. Karacay, C. A. D'Souza, E. A. Rossi, P. Laverman, C.-H. Chang, O. C. Boerman and D. M. Goldenberg, *J. Nucl. Med.*, 2009, **50**, 991–998.
29. G. B. Saha, *Basics of PET Imaging: Physics, Chemistry and Regulations*, Springer, New York, 2005.
30. H. H. Coenen, A. D. Gee, M. Adam, G. Antoni, C. S. Cutler, Y. Fujibayashi, J. M. Jeong, R. H. Mach, T. L. Mindt, V. W. Pike and A. D. Windhorst, *Nucl. Med. Biol.*, 2017, **55**, v–xi.
31. I. Peñuelas and P. H. Elsinga, in *Radiopharmaceutical Chemistry*, eds. J. S. Lewis, A. D. Windhorst and B. M. Zeglis, Springer International Publishing, Cham, 2019, p. 607–618.
32. O. Jacobson, D. O. Kiesewetter and X. Chen, *Bioconjugate Chem.*, 2015, **26**, 1–18.
33. M. Ogawa, K. Hatano, S. Oishi, Y. Kawasumi, N. Fujii, M. Kawaguchi, R. Doi, M. Imamura, M. Yamamoto, K. Ajito, T. Mukai, H. Saji and K. Ito, *Nucl. Med. Biol.*, 2003, **30**, 1–9.
34. H. H. Coenen, in *PET Chemistry*, eds. P. A. Schubiger, L. Lehmann and M. Friebe, Springer Berlin Heidelberg, Berlin, Heidelberg, 2007, p. 15–50.
35. K. C. Molloy, in *Chemistry of Tin*, ed. P. J. Smith, Springer Netherlands, Dordrecht, 1998, DOI: 10.1007/978-94-011-4938-9\_5, p. 138–175.
36. C. T. Li, M. Palotti, J. E. Holden, J. Oh, O. Okonkwo, B. T. Christian, B. B. Bendlin, L. Buyan-Dent, S. J. Harding, C. K. Stone, O. T. DeJesus, R. J. Nickles and C. L. Gallagher, *Synapse*, 2014, **68**, 325–331.
37. M. Namavari, A. Bishop, N. Satyamurthy, G. Bida and J. R. Barrio, *Int. J. Radiat. Appl. Instrum. Part A*, 1992, **43**, 989–996.

38. K. J. Makaravage, A. F. Brooks, A. V. Mossine, M. S. Sanford and P. J. H. Scott, *Org. Lett.*, 2016, **18**, 5440–5443.
39. K. Hamacher and H. H. Coenen, *Appl. Radiat. Isot.*, 2002, **57**, 853–856.
40. K. Hamacher, *J. Label. Compd. Radiopharm.*, 1999, **42**, 1135–1144.
41. B. Behnam Azad, R. Ashique, N. R. Labiris and R. Chirakal, *J. Label. Compd. Radiopharm.*, 2012, **55**, 23–28.
42. K. Hamacher and W. Hamkens, *Appl. Radiat. Isot.*, 1995, **46**, 911–916.
43. M. Karramkam, F. Hinnen, Y. Bramoullé, S. Jubeau and F. Dollé, *J. Label. Compd. Radiopharm.*, 2002, **45**, 1103–1113.
44. A. Shah, V. W. Pike and D. A. Widdowson, *J. Chem. Soc., Perkin Trans. 1*, 1998, 2043–2046.
45. Y. Yorinobu and O. Makoto, *Bull. Chem. Soc. Jpn.*, 1972, **45**, 1860–1863.
46. T. L. Ross, J. Ermert, C. Hocke and H. H. Coenen, *J. Am. Chem. Soc.*, 2007, **129**, 8018–8025.
47. Z. Gao, V. Gouverneur and B. G. Davis, *J. Am. Chem. Soc.*, 2013, **135**, 13612–13615.
48. J.-P. Meyer, P. Adumeau, J. S. Lewis and B. M. Zeglis, *Bioconjugate Chem.*, 2016, **27**, 2791–2807.
49. S. Verhoog, C. W. Kee, Y. Wang, T. Khotavivattana, T. C. Wilson, V. Kersemans, S. Smart, M. Tredwell, B. G. Davis and V. Gouverneur, *J. Am. Chem. Soc.*, 2018, **140**, 1572–1575.
50. W. R. Gutekunst and P. S. Baran, *Chem. Soc. Rev.*, 2011, **40**, 1976–1991.
51. G. Yuan, F. Wang, N. A. Stephenson, L. Wang, B. H. Rotstein, N. Vasdev, P. Tang and S. H. Liang, *Chem. Commun.*, 2017, **53**, 126–129.
52. E. E. Gray, M. K. Nielsen, K. A. Choquette, J. A. Kalow, T. J. A. Graham and A. G. Doyle, *J. Am. Chem. Soc.*, 2016, **138**, 10802–10805.

53. S. J. Lee, A. F. Brooks, N. Ichiishi, K. J. Makaravage, A. V. Mossine, M. S. Sanford and P. J. H. Scott, *Chem. Commun.*, 2019, **55**, 2976–2979.
54. K. B. McMurtrey, J. M. Racowski and M. S. Sanford, *Org. Lett.*, 2012, **14**, 4094–4097.
55. W. Chen, Z. Huang, N. E. S. Tay, B. Giglio, M. Wang, H. Wang, Z. Wu, D. A. Nicewicz and Z. Li, *Science*, 2019, **364**, 1170–1174.
56. D. M. Jewett, *Int. J. Radiat. Appl. Instrum. Part A*, 1992, **43**, 1383–1385.
57. K. A. Frey, R. A. Koeppe, M. R. Kilbourn, T. M. Vander Borght, R. L. Albin, S. Gilman and D. E. Kuhl, *Ann. Neurol.*, 1996, **40**, 873–884.
58. G. Antoni, in *Radiopharmaceutical Chemistry*, eds. J. S. Lewis, A. D. Windhorst and B. M. Zeglis, Springer International Publishing, Cham, 2019, DOI: 10.1007/978-3-319-98947-1\_11, p. 207–220.
59. Y. Andersson and B. Långström, *J. Chem. Soc., Perkin Trans. 1*, 1995, 287–289.
60. Y. Andersson, A. Cheng, B. Langstrom, K. Zetterberg, B. Nilsson, C. Damberg, T. Bartfai and Ü. Langel, *Acta Chem. Scand.*, 1995, **49**, 683–688.
61. M. Pretze, P. Grosse-Gehling and C. Mamat, *Molecules*, 2011, **16**, 1129–1165.
62. K. Takahashi, T. Hosoya, K. Onoe, H. Doi, H. Nagata, T. Hiramatsu, X.-L. Li, Y. Watanabe, Y. Wada, T. Takashima, M. Suzuki, H. Onoe and Y. Watanabe, *J. Nucl. Med.*, 2014, **55**, 852–857.
63. D. Le Bars, M. Malleval, F. Bonnefoi and C. Tourvieille, *J. Label. Compd. Radiopharm.*, 2006, **49**, 263–267.
64. D. Soloviev and C. Tamburella, *Appl. Radiat. Isot.*, 2006, **64**, 995–1000.
65. R. B. Workman and R. E. Coleman, in *PET/CT: Essentials for Clinical Practice*, eds. R. B. Workman and R. E. Coleman, Springer New York, New York, NY, 2006, DOI: 10.1007/978-0-387-38335-4\_1, p. 1–22.

66. P. Som, H. L. Atkins, D. Bandoypadhyay, J. S. Fowler, R. R. MacGregor, K. Matsui, Z. H. Oster, D. F. Sacker, C. Y. Shiue, H. Turner, C.-N. Wan, A. P. Wolf and S. V. Zabinski, *J. Nucl. Med.*, 1980, **21**, 670–675.
67. Y. Lin, W. Y. Lin, J. A. Liang, Y. Y. Lu, H. Y. Wang, S. C. Tsai and C. H. Kao, *Korean J. Radiol.*, 2012, **13**, 760–770.
68. S. Bastawrous, P. Bhargava, F. Behnia, D. S. W. Djang and D. R. Haseley, *RadioGraphics*, 2014, **34**, 1295–1316.
69. D. A. Weber, E. J. Greenberg, A. Dimich, P. J. Kenny, E. O. Rothschild, W. P. L. Myers and J. S. Laughlin, *J. Nucl. Med.*, 1969, **10**, 8–17.
70. H. Jadvar, B. Desai and P. S. Conti, *Semin. Nucl. Med.*, 2015, **45**, 58–65.
71. L. Wahl and C. Nahmias, *J. Nucl. Med.*, 1996, **37**, 432–437.
72. D. Skovgaard, A. Kjaer, K. M. Heinemeier, M. Brandt-Larsen, J. Madsen and M. Kjaer, *PLOS ONE*, 2011, **6**, e16678.
73. W. E. Klunk, H. Engler, A. Nordberg, Y. Wang, G. Blomqvist, D. P. Holt, M. Bergström, I. Savitcheva, G.-F. Huang, S. Estrada, B. Ausén, M. L. Debnath, J. Barletta, J. C. Price, J. Sandell, B. J. Lopresti, A. Wall, P. Koivisto, G. Antoni, C. A. Mathis and B. Långström, *Ann. Neurol.*, 2004, **55**, 306–319.
74. C. A. Mathis, Y. Wang, D. P. Holt, G.-F. Huang, M. L. Debnath and W. E. Klunk, *J. Med. Chem.*, 2003, **46**, 2740–2754.
75. M. Yoshimoto, A. Waki, Y. Yonekura, N. Sadato, T. Murata, N. Omata, N. Takahashi, M. J. Welch and Y. Fujibayashi, *Nucl. Med. Biol.*, 2001, **28**, 117–122.
76. I. Grassi, C. Nanni, V. Allegri, J. J. Morigi, G. C. Montini, P. Castellucci and S. Fanti, *Am. J. Nucl. Med. Mol. Imaging*, 2012, **2**, 33–47.
77. C. Spick, K. Herrmann and J. Czernin, *J. Nucl. Med.*, 2016, **57**, 30S–37S.
78. S. Ceysens, K. Van Laere, T. de Groot, J. Goffin, G. Bormans and L. Mortelmans, *Am. J. Neuroradiol.*, 2006, **27**, 1432.

79. C. L. Welle, E. L. Cullen, P. J. Peller, V. J. Lowe, R. C. Murphy, G. B. Johnson and L. A. Binkovitz, *RadioGraphics*, 2016, **36**, 279–292.
80. G. Elisabetta, L. Patrizia, M. Amalia, G. Maria Chiara and C. Andrea, *Curr. Pharm. Des.*, 2015, **21**, 121–127.
81. I. GBD 2015 Disease, Incidence and Prevalence Collaborators, *Lancet*, 2016, **388**, 1545–1602.
82. I. S. Mackenzie, S. V. Morant, G. A. Bloomfield, T. M. MacDonald and J. O’Riordan, *J. Neurol. Neurosurg. Psychiatry*, 2014, **85**, 76–84.
83. E. M. Visser, K. Wilde, J. F. Wilson, K. K. Yong and C. E. Counsell, *J. Neurol. Neurosurg. Psychiatry*, 2012, **83**, 719–724.
84. L. E. Mokry, S. Ross, O. S. Ahmad, V. Forgetta, G. D. Smith, A. Leong, C. M. T. Greenwood, G. Thanassoulis and J. B. Richards, *PLoS Med.*, 2015, **12**, e1001866.
85. L. Steinman, *Annu. Rev. Immunol.*, 2014, **32**, 257–281.
86. A. Verkhratsky and A. Butt, in *Glial Physiology and Pathophysiology*, John Wiley & Sons, Ltd, Chichester, 2013, p. 245–319.
87. E. M. Frohman, M. K. Racke and C. S. Raine, *N. Engl. J. Med.*, 2006, **354**, 942–955.
88. A. Compston and A. Coles, *Lancet*, 2008, **372**, 1502–1517.
89. A. J. Thompson, B. L. Banwell, F. Barkhof, W. M. Carroll, T. Coetzee, G. Comi, J. Correale, F. Fazekas, M. Filippi, M. S. Freedman, K. Fujihara, S. L. Galetta, H. P. Hartung, L. Kappos, F. D. Lublin, R. A. Marrie, A. E. Miller, D. H. Miller, X. Montalban, E. M. Mowry, P. S. Sorensen, M. Tintoré, A. L. Traboulsee, M. Trojano, B. M. J. Uitdehaag, S. Vukusic, E. Waubant, B. G. Weinshenker, S. C. Reingold and J. A. Cohen, *Lancet Neurol.*, 2018, **17**, 162–173.
90. M. Filippi, M. A. Rocca, O. Ciccarelli, N. De Stefano, N. Evangelou, L. Kappos, A. Rovira, J. Sastre-Garriga, M. Tintorè, J. L. Frederiksen, C. Gasperini, J. Palace, D. S. Reich, B. Banwell, X. Montalban and F. Barkhof, *Lancet Neurol.*, 2016, **15**, 292–303.

91. R. S. Shaikh, S. S. Schilson, S. Wagner, S. Hermann, P. Keul, B. Levkau, M. Schäfers and G. Haufe, *J. Med. Chem.*, 2015, **58**, 3471–3484.
92. T. Sanchez and T. Hla, *J. Cell Biochem.*, 2004, **92**, 913–922.
93. T. Mutoh, R. Rivera and J. Chun, *Br. J. Pharmacol.*, 2012, **165**, 829–844.
94. C. Jaillard, S. Harrison, B. Stankoff, M. S. Aigrot, A. R. Calver, G. Duddy, F. S. Walsh, M. N. Pangalos, N. Arimura, K. Kaibuchi, B. Zalc and C. Lubetzki, *J. Neurosci.*, 2005, **25**, 1459–1469.
95. H. Mattes, K. K. Dev, R. Bouhelal, C. Barske, F. Gasparini, D. Guerini, A. K. Mir, D. Orain, M. Osinde, A. Picard, C. Dubois, E. Tasdelen and S. Haessig, *ChemMedChem*, 2010, **5**, 1693–1696.
96. A. D. Hobson, C. M. Harris, E. L. van der Kam, S. C. Turner, A. Abibi, A. L. Aguirre, P. Bousquet, T. Kebede, D. B. Konopacki, G. Gintant, Y. Kim, K. Larson, J. W. Maull, N. S. Moore, D. Shi, A. Shrestha, X. Tang, P. Zhang and K. K. Sarris, *J. Med. Chem.*, 2015, **58**, 9154–9170.
97. J. L. Gilmore, J. E. Sheppeck, S. H. Watterson, L. Haque, P. Mukhopadhyay, A. J. Tebben, M. A. Galella, D. R. Shen, M. Yarde, M. E. Cvijic, V. Borowski, K. Gillooly, T. Taylor, K. W. McIntyre, B. Warrack, P. C. Levesque, J. P. Li, G. Cornelius, C. D'Arienzo, A. Marino, P. Balimane, L. Salter-Cid, J. C. Barrish, W. J. Pitts, P. H. Carter, J. Xie and A. J. Dyckman, *J. Med. Chem.*, 2016, **59**, 6248–6264.
98. W. Hur, H. Rosen and N. S. Gray, *Bioorg. Med. Chem. Lett.*, 2017, **27**, 1–5.
99. K. Chiba, Y. Yanagawa, Y. Masubuchi, H. Kataoka, T. Kawaguchi, M. Ohtsuki and Y. Hoshino, *J. Immunol.*, 1998, **160**, 5037–5044.
100. A. J. Rosenberg, H. Liu, H. Jin, X. Yue, S. Riley, S. J. Brown and Z. Tu, *J. Med. Chem.*, 2016, **59**, 6201–6220.
101. C. Braestrup and R. F. Squires, *Proc. Natl. Acad. Sci. U.S.A.*, 1977, **74**, 3805–3809.
102. F. Li, J. Liu, N. Liu, L. A. Kuhn, R. M. Garavito and S. Ferguson-Miller, *Biochemistry*, 2016, **55**, 2821–2831.

103. V. Papadopoulos, M. Baraldi, T. R. Guilarte, T. B. Knudsen, J. J. Lacapere, P. Lindemann, M. D. Norenberg, D. Nutt, A. Weizman, M. R. Zhang and M. Gavish, *Trends Pharmacol. Sci.*, 2006, **27**, 402–409.
104. J. J. Lacapere and V. Papadopoulos, *Steroids*, 2003, **68**, 569–585.
105. A. J. Filiano, S. P. Gadani and J. Kipnis, *Brain Res.*, 2015, **1617**, 18–27.
106. S. Venneti, B. J. Lopresti and C. A. Wiley, *Prog. Neurobiol.*, 2006, **80**, 308–322.
107. D. Hanahan and Robert A. Weinberg, *Cell*, 2011, **144**, 646–674.
108. A. G. Mukhin, V. Papadopoulos, E. Costa and K. E. Krueger, *Proceedings of the National Academy of Sciences*, 1989, **86**, 9813–9816.
109. K. Morohaku, S. H. Pelton, W. R. Butler, V. Selvaraj, D. J. Daugherty and W. Deng, *Endocrinology*, 2014, **155**, 89–97.
110. V. Papadopoulos, *Endocrinology*, 2014, **155**, 15–20.
111. V. Papadopoulos, J. Fan and B. Zirkin, *J. Neuroendocrinol.*, 2018, **30**, 10.1111/jne.12500.
112. B. Mahata, J. Pramanik, L. v. d. Weyden, G. Kar, A. Riedel, N. A. Fonseca, K. Kundu, E. Ryder, G. Duddy, I. Walczak, S. Davidson, K. Okkenhaug, D. J. Adams, J. D. Shields and S. A. Teichmann, *bioRxiv*, 2018, DOI: 10.1101/471359, 471359.
113. M. N. Tantawy, H. Charles Manning, T. E. Peterson, D. C. Colvin, J. C. Gore, W. Lu, Z. Chen and C. Chad Quarles, *Mol. Imaging Biol.*, 2018, **20**, 200–204.
114. P. Charbonneau, A. Syrota, C. Crouzel, J. M. Valois, C. Prenant and M. Crouzel, *Circulation*, 1986, **73**, 476–483.
115. F. Chauveau, H. Boutin, N. Van Camp, F. Dollé and B. Tavitian, *Eur. J. Nucl. Med. Mol. Imaging*, 2008, **35**, 2304–2319.
116. S. Lavisse, D. García-Lorenzo, M.-A. Peyronneau, B. Bodini, C. Thiriez, B. Kuhnast, C. Comtat, P. Remy, B. Stankoff and M. Bottlaender, *J. Nucl. Med.*, 2015, **56**, 1048–1054.

117. D. R. Owen, A. J. Yeo, R. N. Gunn, K. Song, G. Wadsworth, A. Lewis, C. Rhodes, D. J. Pulford, I. Bennacef, C. A. Parker, P. L. StJean, L. R. Cardon, V. E. Mooser, P. M. Matthews, E. A. Rabiner and J. P. Rubio, *J. Cereb. Blood Flow Metab.*, 2012, **32**, 1–5.
118. D. R. J. Owen, R. N. Gunn, E. A. Rabiner, I. Bennacef, M. Fujita, W. C. Kreisl, R. B. Innis, V. W. Pike, R. Reynolds, P. M. Matthews and C. A. Parker, *J. Nucl. Med.*, 2011, **52**, 24–32.
119. A. Blair, F. Zmuda, G. Malviya, A. A. S. Tavares, G. D. Tamagnan, A. J. Chalmers, D. Dewar, S. L. Pimlott and A. Sutherland, *Chem. Sci.*, 2015, **6**, 4772–4777.
120. A. Blair, L. Stevenson, D. Dewar, S. L. Pimlott and A. Sutherland, *MedChemComm*, 2013, **4**, 1461–1466.
121. L. Qiao, E. Fisher, L. McMurray, S. Milicevic Sephton, M. Hird, N. Kuzhuppilly-Ramakrishnan, D. J. Williamson, X. Zhou, E. Werry, M. Kassiou, S. Luthra, W. Trigg and F. I. Aigbirhio, *ChemMedChem*, 2019, **14**, 982–993.
122. A. A. S. Tavares, J. Lewsey, D. Dewar and S. L. Pimlott, *Nucl. Med. Biol.*, 2012, **39**, 127–135.
123. P. J. Riss, S. Kuschel and F. I. Aigbirhio, *Tetrahedron Lett.*, 2012, **53**, 1717–1719.
124. M. D. Morrison, J. J. Hanthorn and D. A. Pratt, *Org. Lett.*, 2009, **11**, 1051–1054.
125. D. T. Racys, S. A. I. Sharif, S. L. Pimlott and A. Sutherland, *J. Org. Chem.*, 2016, **81**, 772–780.
126. J. Lindley, *Tetrahedron*, 1984, **40**, 1433–1456.
127. C. Sambigao, S. P. Marsden, A. J. Blacker and P. C. McGowan, *Chem. Soc. Rev.*, 2014, **43**, 3525–3550.
128. S. Mondal, *ChemTexts*, 2016, **2**, 17.
129. Z. J. Kamiński, *J. Pept. Sci.*, 2000, **55**, 140–164.

130. S. L. Cockroft, J. Perkins, C. Zonta, H. Adams, S. E. Spey, C. M. Low, J. G. Vinter, K. R. Lawson, C. J. Urch and C. A. Hunter, *Org. Biomol. Chem.*, 2007, **5**, 1062–1080.
131. D. T. Racys, C. E. Warrilow, S. L. Pimlott and A. Sutherland, *Org. Lett.*, 2015, **17**, 4782–4785.
132. M. A. B. Mostafa, E. D. D. Calder, D. T. Racys and A. Sutherland, *Chem. Eur. J.*, 2017, **23**, 1044–1047.
133. M. Tredwell, S. M. Preshlock, N. J. Taylor, S. Gruber, M. Huiban, J. Passchier, J. Mercier, C. Génicot and V. Gouverneur, *Angew. Chem. Int. Ed.*, 2014, **53**, 7751–7755.
134. A. V. Mossine, A. F. Brooks, K. J. Makaravage, J. M. Miller, N. Ichiishi, M. S. Sanford and P. J. H. Scott, *Org. Lett.*, 2015, **17**, 5780–5783.
135. N. Miyaura and A. Suzuki, *Chem. Rev.*, 1995, **95**, 2457–2483.
136. M. Fujinaga, R. Luo, K. Kumata, Y. Zhang, A. Hatori, T. Yamasaki, L. Xie, W. Mori, Y. Kurihara, M. Ogawa, N. Nengaki, F. Wang and M.-R. Zhang, *J. Med. Chem.*, 2017, **60**, 4047–4061.
137. P. G. Gildner and T. J. Colacot, *Organometallics*, 2015, **34**, 5497–5508.
138. A. L. Casalnuovo and J. C. Calabrese, *J. Am. Chem. Soc.*, 1990, **112**, 4324–4330.
139. F. Lo Monte, T. Kramer, J. Gu, M. Brodrecht, J. Pilakowski, A. Fuertes, J. M. Dominguez, B. Plotkin, H. Eldar-Finkelman and B. Schmidt, *Eur. J. Med. Chem.*, 2013, **61**, 26–40.
140. A. Leo, C. Hansch and D. Elkins, *Chem. Rev.*, 1971, **71**, 525–616.
141. R. N. Waterhouse, *Mol. Imaging Biol.*, 2003, **5**, 376–389.
142. D. E. Clark, *Drug Discov. Today*, 2003, **8**, 927–933.
143. S. Ong, H. Liu, X. Qiu, G. Bhat and C. Pidgeon, *Anal. Chem.*, 1995, **67**, 755–762.

144. C. Y. Yang, S. J. Cai, H. Liu and C. Pidgeon, *Adv. Drug Deliv. Rev.*, 1997, **23**, 229–256.
145. K. Valkó, *J. Chromatogr. A*, 2004, **1037**, 299–310.
146. W. M. Meylan and P. H. Howard, *Perspect. Drug Discovery Des.*, 2000, **19**, 67–84.
147. J. Zhang, X. Zhang, Y. Li and J. Tian, *Molecules*, 2012, **17**, 6697–6704.
148. J. A. Dodge, M. G. Stocksdale, K. J. Fahey and C. D. Jones, *J. Org. Chem.*, 1995, **60**, 739–741.
149. R. S. Mali, A. R. Manekar and S. G. Tilve, *Org. Prep. Proced. Int.*, 1992, **24**, 52–54.
150. T. Nakanishi and M. Suzuki, *Org. Lett.*, 1999, **1**, 985–988.
151. J. Nowicki, *Molecules*, 2000, **5**, 1033–1050.
152. Z. Zhang, H. Wang, P. Liu and Y. Guan, *J. Nucl. Med.*, 2009, **50**, 1960.
153. X. Tang, G. Tang and D. Nie, *Appl. Radiat. Isot.*, 2013, **82**, 81–86.
154. M. Kovac, T. Miklovicz, L. Li, J. Russell, R. Canales Candela, F. Aigbirhio and I. Boros, *J. Label. Compd. Radiopharm.*, 2019, **62**, 190–197.
155. S. S. Tanzey, X. Shao, J. Stauff, J. Arteaga, P. Sherman, P. J. H. Scott and A. V. Mossine, *Pharmaceuticals*, 2018, **11**, 136.
156. T. Kikuchi, K. Minegishi, H. Hashimoto, M.-R. Zhang and K. Kato, *J. Label. Compd. Radiopharm.*, 2013, **56**, 672–678.
157. M. J. Adam, S. Jivan, J. M. Huser and J. Lu, *Radiochim. Acta*, 2000, **88**, 207–210.
158. C. Harrison and J. R. Traynor, *Life Sci.*, 2003, **74**, 489–508.
159. N. W. DeLapp, W. H. Gough, S. D. Kahl, A. C. Porter and T. R. Wiernicki, in *Assay Guidance Manual*, eds. G. S. Sittampalam, A. Grossman and K. Brimacombe, Eli Lilly & Company and the National Center for Advancing Translational Sciences, Bethesda, 2012, p. 217–228.

160. X. Zhao, M. Wu, Y. Liu and S. Cao, *Org. Lett.*, 2018, **20**, 5564–5568.
161. T. Niwa, H. Ochiai and T. Hosoya, *ACS Catal.*, 2017, **7**, 4535–4541.
162. T. Chanda, R. K. Verma and M. S. Singh, *Chem. Asian J.*, 2012, **7**, 778–787.
163. M. Fieser, *Fieser and Fieser's Reagents for Organic Synthesis*, Wiley, New York, 1967.
164. F. Shah, S. P. Hume, V. W. Pike, S. Ashworth and J. McDermott, *Nucl. Med. Biol.*, 1994, **21**, 573–581.
165. A. Bredihhin and U. Mäeorg, *Org. Lett.*, 2007, **9**, 4975–4977.
166. T. Imaeda, Y. Hamada and T. Shioiri, *Tetrahedron Lett.*, 1994, **35**, 591–594.
167. J. Pawlas, P. Vedsø, P. Jakobsen, P. O. Huusfeldt and M. Begtrup, *J. Org. Chem.*, 2000, **65**, 9001–9006.
168. L. S. Monteiro, M. M. A. Pereira-Lima, S. Pereira and J. N. Machado, *Arkivoc*, 2014, **5**, 170–180.
169. A. Blair, PhD Thesis, University of Glasgow, 2014.
170. L. Stevenson, A. A. S. Tavares, A. Brunet, F. I. McGonagle, D. Dewar, S. L. Pimlott and A. Sutherland, *Bioorg. Med. Chem. Lett.*, 2010, **20**, 954–957.
171. L. Stevenson, PhD Thesis, University of Glasgow, 2010.
172. A. Combes, *Bull. Soc. Chim. Fr.*, 1888, **49**, 89.
173. R. H. Bradbury, C. P. Allott, M. Dennis, E. Fisher, J. S. Major, B. B. Masek, A. A. Oldham, R. J. Pearce and N. Rankine, *J. Med. Chem.*, 1992, **35**, 4027–4038.
174. A. Cappelli, M. Anzini, S. Vomero, P. G. De Benedetti, M. C. Menziani, G. Giorgi and C. Manzoni, *J. Med. Chem.*, 1997, **40**, 2910–2921.
175. E. Valeur and M. Bradley, *Chem. Soc. Rev.*, 2009, **38**, 606–631.

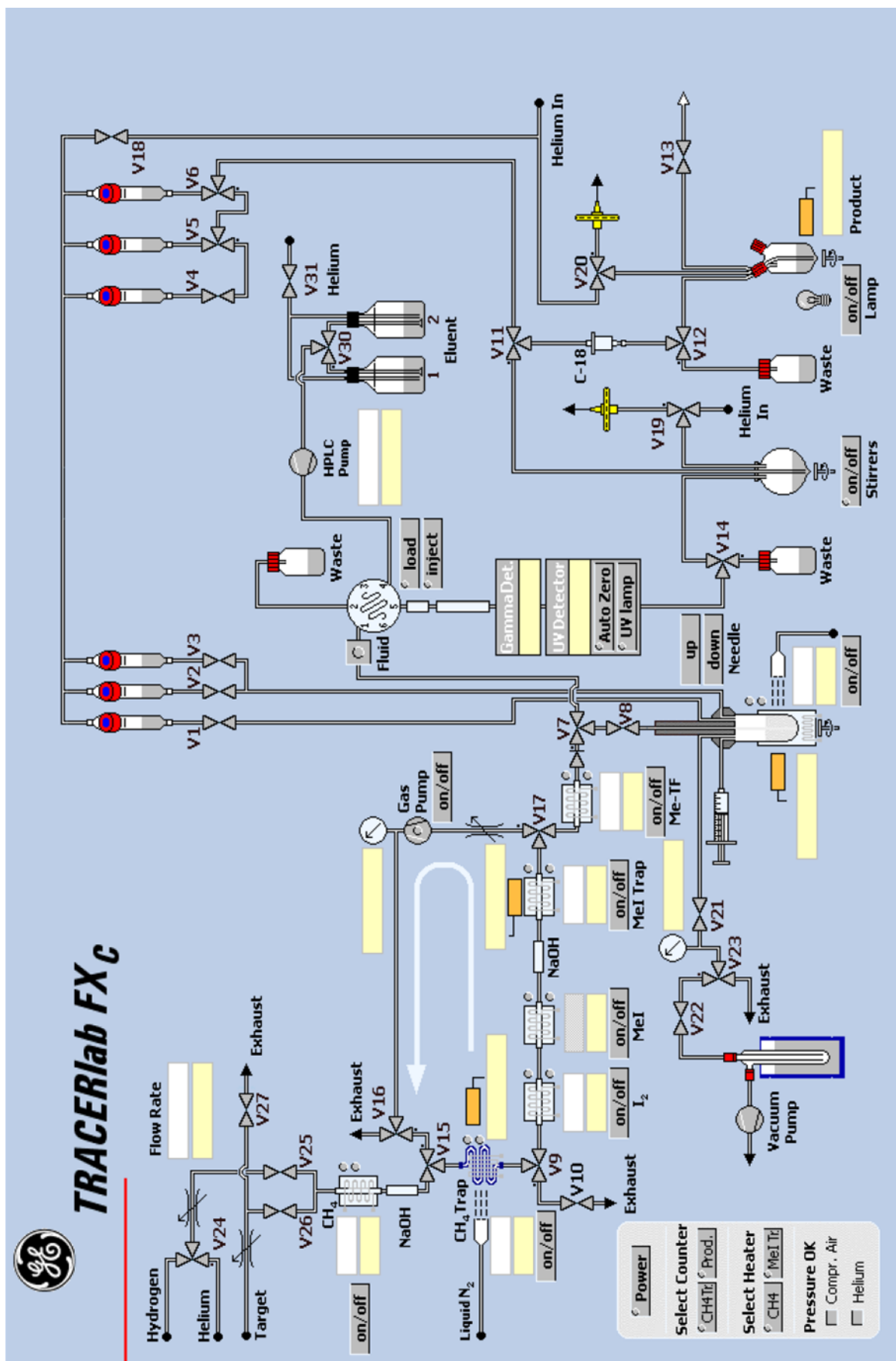
176. A. Sidduri, J. W. Tilley, K. Hull, J. Ping Lou, G. Kaplan, A. Sheffron, L. Chen, R. Campbell, R. Guthrie, T.-N. Huang, N. Huby, K. Rowan, V. Schwinge and L. M. Renzetti, *Bioorg. Med. Chem. Lett.*, 2002, **12**, 2475–2478.
177. C. Djerassi, *Chem. Rev.*, 1948, **43**, 271–317.
178. M. Geffe, L. Andernach, O. Trapp and T. Opatz, *Beilstein J. Org. Chem.*, 2014, **10**, 701–706.
179. G. W. Gokel, S. Negin and R. Cantwell, in *Comprehensive Supramolecular Chemistry II*, ed. J. L. Atwood, Elsevier, Oxford, 2017, p. 3–48.
180. A. Fafalios, A. Akhavan, A. V. Parwani, R. R. Bies, K. J. McHugh and B. R. Pflug, *Clin. Cancer Res.*, 2009, **15**, 6177–6184.
181. V. D. Filimonov, M. Trusova, P. Postnikov, E. A. Krasnokutskaya, Y. M. Lee, H. Y. Hwang, H. Kim and K.-W. Chi, *Org. Lett.*, 2008, **10**, 3961–3964.
182. N. L. Sloan, S. K. Luthra, G. McRobbie, S. L. Pimlott and A. Sutherland, *Chem. Commun.*, 2017, **53**, 11008–11011.
183. N. L. Sloan, PhD Thesis, University of Glasgow, 2017.
184. F. Jiang, J. Bupp, S. Rhee, L. Toll and N. T. Zaveri, *J. Label. Compd. Radiopharm.*, 2012, **55**, 177–179.
185. R. E. Damschroder and W. D. Peterson, *Org. Synth.*, 1940, **20**, 16.
186. F. Shi, J. P. Waldo, Y. Chen and R. C. Larock, *Org. Lett.*, 2008, **10**, 2409–2412.
187. J. Zhou, J. He, B. Wang, W. Yang and H. Ren, *J. Am. Chem. Soc.*, 2011, **133**, 6868–6870.
188. R. J. Faggyas, N. L. Sloan, N. Buijs and A. Sutherland, *Eur. J. Org. Chem.*, **0**.
189. L. S. Fowler, D. Ellis and A. Sutherland, *Org. Biomol. Chem.*, 2009, **7**, 4309–4316.
190. L. Gilfillan, R. Artschwager, A. H. Harkiss, R. M. J. Liskamp and A. Sutherland, *Org. Biomol. Chem.*, 2015, **13**, 4514–4523.

191. A. H. Harkiss, J. D. Bell, A. Knuhtsen, A. G. Jamieson and A. Sutherland, *J. Org. Chem.*, 2019, **84**, 2879–2890.
192. N. Buijs, MSci Thesis, University of Glasgow, 2018.
193. S. R. Chhabra, A. Mahajan and W. C. Chan, *J. Org. Chem.*, 2002, **67**, 4017–4029.
194. M. S. Egbertson, J. J. Cook, B. Bednar, J. D. Prugh, R. A. Bednar, S. L. Gaul, R. J. Gould, G. D. Hartman, C. F. Homnick, M. A. Holahan, L. A. Libby, J. J. Lynch, R. J. Lynch, G. R. Sitko, M. T. Stranieri and L. M. Vassallo, *J. Med. Chem.*, 1999, **42**, 2409–2421.
195. V. J. Huber, T. W. Arroll, C. Lum, B. A. Goodman and H. Nakanishi, *Tetrahedron Lett.*, 2002, **43**, 6729–6733.
196. F. D. Bellamy and K. Ou, *Tetrahedron Lett.*, 1984, **25**, 839–842.
197. L. F. Tietze, C. Eichhorst, T. Hungerland and M. Steinert, *Chem. Eur. J.*, 2014, **20**, 12553–12558.
198. G. G. Stokes, *Phil. Trans.*, 1852, **142**, 463–562.
199. M. C. Henry, H. M. Senn and A. Sutherland, *J. Org. Chem.*, 2019, **84**, 346–364.
200. Y. Yamaguchi, Y. Matsubara, T. Ochi, T. Wakamiya and Z.-i. Yoshida, *J. Am. Chem. Soc.*, 2008, **130**, 13867–13869.
201. G. Chelucci, M. Falorni and G. Giacomelli, *Synthesis*, 1990, **1990**, 1121–1122.
202. J. Zhao, Y. Wang, Y. He, L. Liu and Q. Zhu, *Org. Lett.*, 2012, **14**, 1078–1081.
203. I. Islam, G. Brown, J. Bryant, P. Hrvatin, M. J. Kochanny, G. B. Phillips, S. Yuan, M. Adler, M. Whitlow, D. Lentz, M. A. Polokoff, J. Wu, J. Shen, J. Walters, E. Ho, B. Subramanyam, D. Zhu, R. I. Feldman and D. O. Arnaiz, *Bioorg. Med. Chem. Lett.*, 2007, **17**, 3819–3825.
204. G. J. Smith, *Color. Technol.*, 1999, **115**, 346–349.
205. L. Biczók, P. Valat and V. r. Wintgens, *Phys. Chem. Chem. Phys.*, 1999, **1**, 4759–4766.

206. S. H. Habenicht, M. Siegmann, S. Kupfer, J. Kübel, D. Weiß, D. Cherek, U. Möller, B. Dietzek, S. Gräfe and R. Beckert, *Methods Appl. Fluoresc.*, 2015, **3**, 025005.
207. A. M. Thooft, K. Cassaidy and B. VanVeller, *J. Org. Chem.*, 2017, **82**, 8842–8847.
208. A. Bose and P. Mal, *Tetrahedron Lett.*, 2014, **55**, 2154–2156.
209. F. Mongin and M. Schlosser, *Tetrahedron Lett.*, 1996, **37**, 6551–6554.
210. M. Anzini, A. Cappelli and S. Vomero, *Heterocycles*, 1994, **38**, 103–111.
211. S. Moore, R. P. Patel, E. Atherton, M. Kondo, J. Meienhofer, L. Blau, R. Bittman and R. K. Johnson, *J. Med. Chem.*, 1976, **19**, 766–772.
212. M. Mąkosza, T. Lemek, A. Kwast and F. Terrier, *J. Org. Chem.*, 2002, **67**, 394–400.



# Appendix II



# Appendix III

